ANNUAL REPORT 1995

Institut Max von Laue
Paul Langevin
Grenoble - France

ANNUAL REPORT 1995

Institut
Max von Laue
Paul Langevin

Grenoble - France

The High Flux Reactor of the Institut Laue-Langevin, with the European Synchrotron Radiation Facility on the same site, represents a "landmark" at the confluence of the rivers Drac (left) and Isère (right).

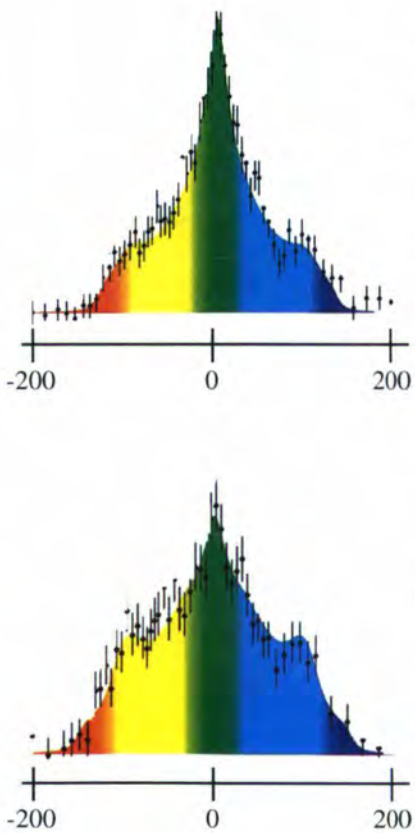

Front cover and Figs. aside.

Following neutron capture in a ^{48}Ti-nucleus, imbedded in a $SrTiO_3$ single crystal, a recoiling ^{49}Ti-atom is produced by the emission of a primary γ-ray from the nucleus. The Ti-atom is slowed down by collisions with the surrounding atoms. During the slowing down process, the still excited Ti-nucleus emits a secondary γ-ray which is measured with the High Resolution Crystal Spectrometer "GAMS". Whenever the secondary γ-ray is emitted in flight, its energy is Doppler shifted in the laboratory system. This is called: Gamma-Ray Induced Doppler Broadening (GRID), see "Blue Box" page 35.

The primary recoils are isotropically distributed. The front cover shows many superimposed trajectories of a recoiling Ti-atom in $SrTiO_3$, as calculated by Molecular Dynamics simulation.

The results, given aside for two different crystal orientations with respect to the spectrometer, show dramatically different spectra. Nevertheless the theoretically predicted profiles are an accurate reproduction of those observed experimentally.

The colour code in the theoretical profiles and in the trajectories (front cover) is correlated to the recoil directions (blue towards the spectrometer) of the Ti-atom.

Such measurements make it possible to deduce information about the repulsive part of interatomic potentials.

CONTENTS

CONTENTS

Associates of the ILL

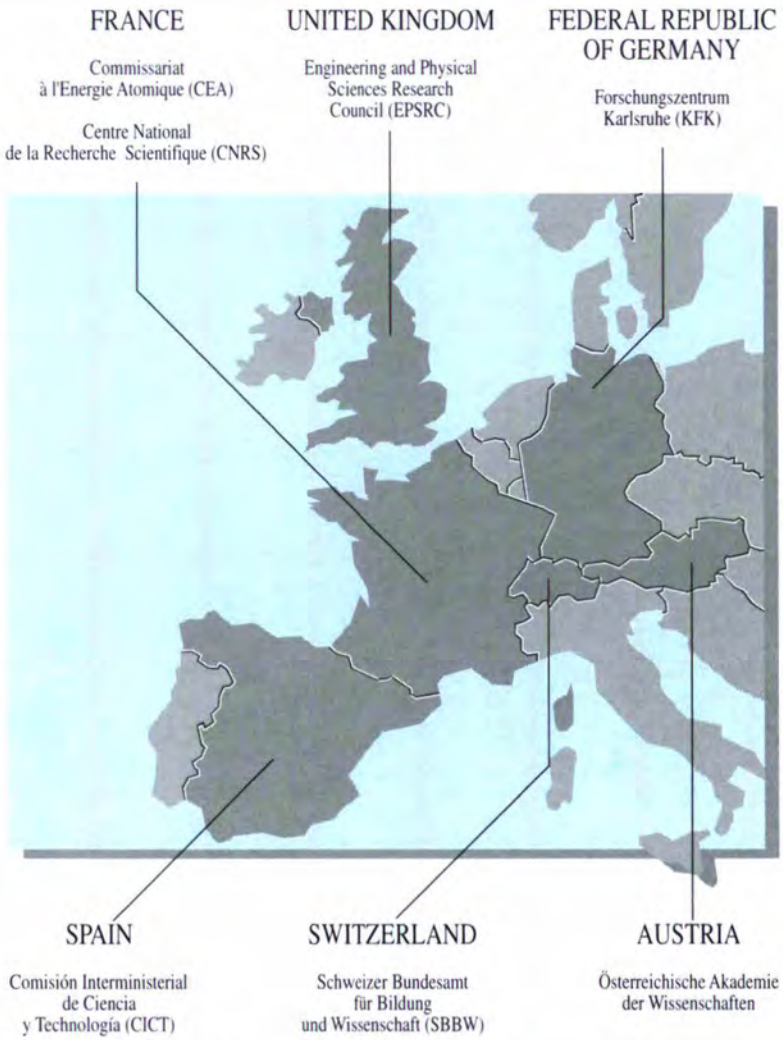

Countries with scientific membership

Steering Committee

Members
(at its last meeting)

❍ Freytag (BMBF)	❍ Cesarsky (CEA)	❍ Hughes (EPSRC)
❍ Hennies (KFK)	❍ Hammer (CEA)	❍ Taylor (RAL)
❍ Schunck (BMBF)	❍ Comès (CNRS)	❍ Ward (EPSRC)
❍ Steiner (HMI, Berlin)	❍ Rigny (CNRS)	❍ Wilkins (EPSRC)
Observers		
❍ Martinez (Spain)	❍ Reiter (Austria)	❍ Zinsli (Switzerland)

Scientific Council

(15 members; Chairman: Stirling; Vice-chairman: Bienfait)

Plenary Session	**8 Subcommittees**
26 participants	76 members

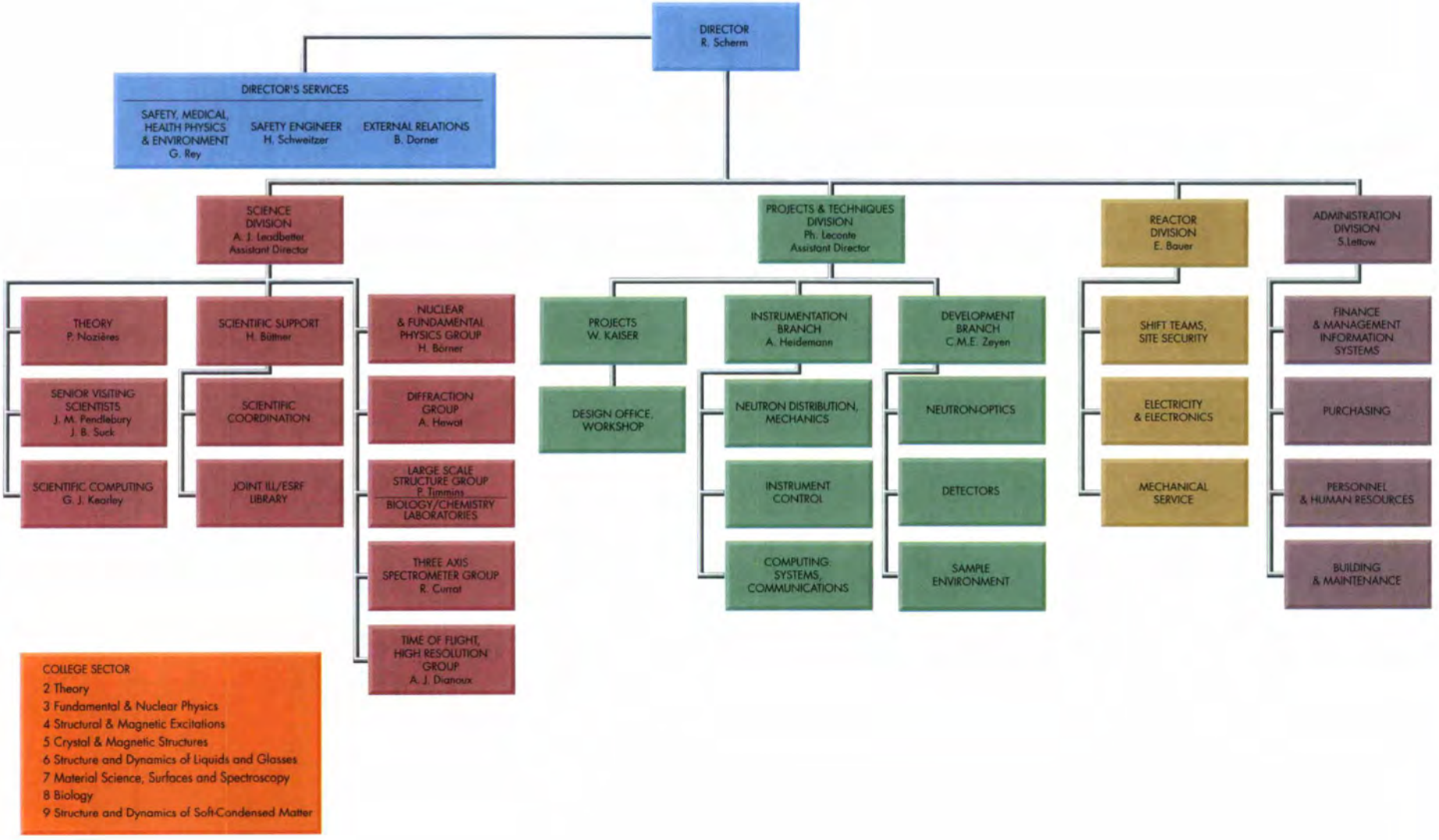
DIRECTOR
R. Scherm
DIRECTOR'S SERVICES
SAFETY, MEDICAL, HEALTH PHYSICS & ENVIRONMENT
G. Rey
SAFETY ENGINEER
H. Schweitzer
EXTERNAL RELATIONS
B. Dorner
SCIENCE DIVISION
A. J. Leadbetter
Assistant Director
PROJECTS & TECHNIQUES DIVISION
Ph. Leconte
Assistant Director
REACTOR DIVISION
E. Bauer
ADMINISTRATION DIVISION
S.Lefrow
THEORY
P. Nozières
SENIOR VISITING SCIENTISTS
J. M. Pendlebury
J. B. Suck
SCIENTIFIC COMPUTING
G. J. Kearley
SCIENTIFIC SUPPORT
H. Büttner
SCIENTIFIC COORDINATION
JOINT ILL/ESRF LIBRARY
NUCLEAR & FUNDAMENTAL PHYSICS GROUP
H. Börner
DIFFRACTION GROUP
A. Hewat
LARGE SCALE STRUCTURE GROUP
P. Timmins
BIOLOGY/CHEMISTRY LABORATORIES
THREE AXIS SPECTROMETER GROUP
R. Currat
TIME OF FLIGHT, HIGH RESOLUTION GROUP
A. J. Dianoux
PROJECTS
W. KAISER
DESIGN OFFICE, WORKSHOP
INSTRUMENTATION BRANCH
A. Heidemann
NEUTRON DISTRIBUTION, MECHANICS
INSTRUMENT CONTROL
COMPUTING: SYSTEMS, COMMUNICATIONS
DEVELOPMENT BRANCH
C.M.E. Zeyen
NEUTRON-OPTICS
DETECTORS
SAMPLE ENVIRONMENT
SHIFT TEAMS, SITE SECURITY
ELECTRICITY & ELECTRONICS
MECHANICAL SERVICE
FINANCE & MANAGEMENT INFORMATION SYSTEMS
PURCHASING
PERSONNEL & HUMAN RESOURCES
BUILDING & MAINTENANCE
COLLEGE SECTOR
2 Theory
3 Fundamental & Nuclear Physics
4 Structural & Magnetic Excitations
5 Crystal & Magnetic Structures
6 Structure and Dynamics of Liquids and Glasses
7 Material Science, Surfaces and Spectroscopy
8 Biology
9 Structure and Dynamics of Soft-Condensed Matter

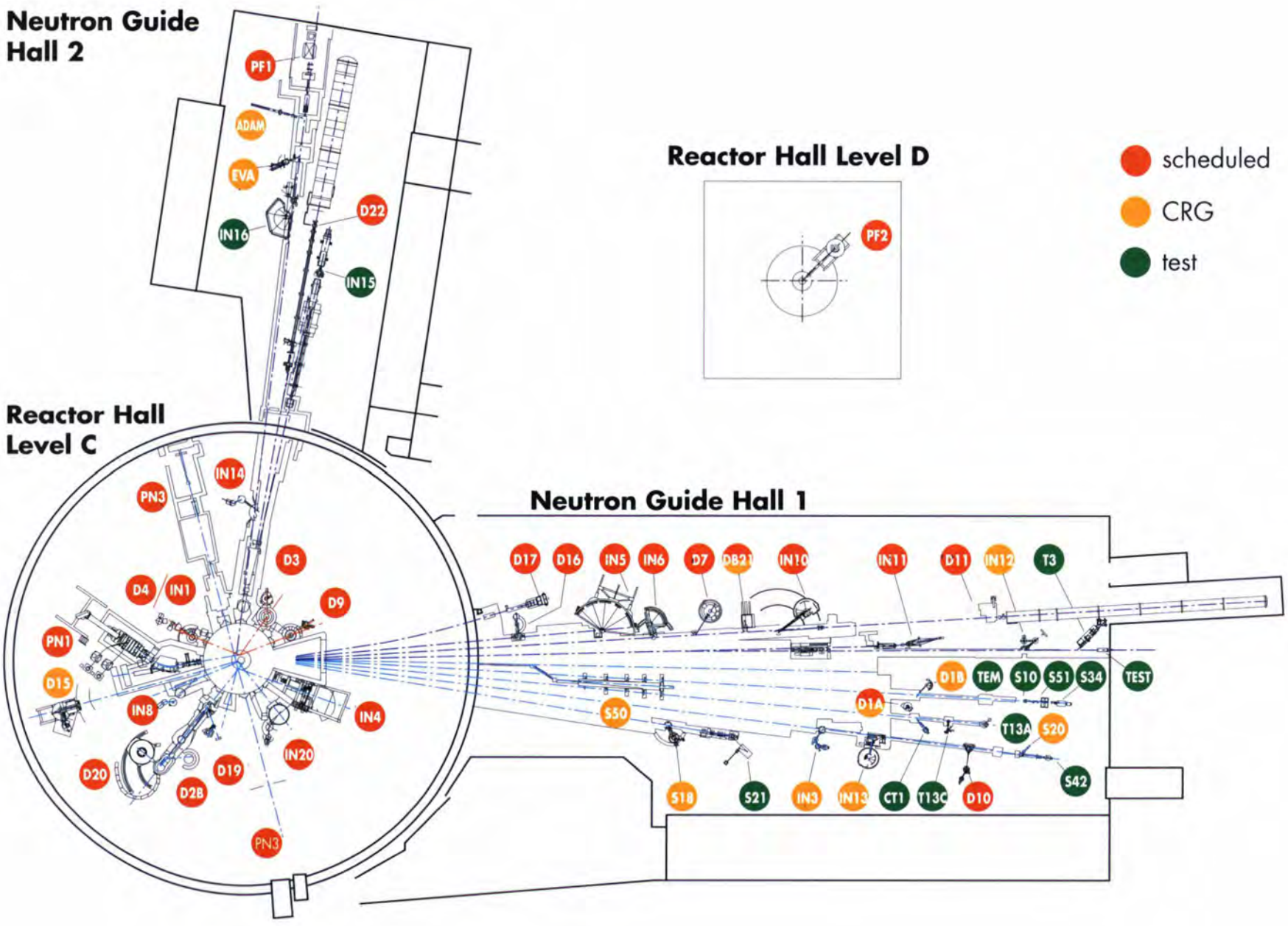
Neutron Guide Hall 2
PF1
ADAM
EVA
D22
IN16
IN15
Reactor Hall Level D
PF2
scheduled
CRG
test
Reactor Hall Level C
IN14
PN3
D3
D4
IN1
D9
PN1
D15
IN8
IN4
IN20
D20
D19
D2B
PN3
Neutron Guide Hall 1
D17
D16
IN5
IN6
D7
DB21
IN10
IN11
D11
IN12
T3
D1B
TEM
S10
S51
S34
TEST
D1A
S50
T13A
S20
S42
S18
S21
IN3
IN13
CT1
T13C
D10

LA LUMIERE BLEUE
Saynette pour la fête de la Renaissance
(Philippe LECONTE)

Trois sorcières vont se retrouver (ou bien 3 fées).
La première est très jeune et parle allemand (SA), la seconde est déjà d'âge moyen et parle français (SF), la dernière est beaucoup plus vieille et parle anglais (SB).

L'obscurité se forme lentement dans la salle. Musique Paul DUCAS, "l'apprenti sorcier" ou MOZART, "la flûte enchantée". Apparaît dans le coin droit de la scène une lueur bleue émanant d'une bulle translucide représentant l'ILL. On devine à peine les visages des 3 femmes.

SB Dear sisters, have you seen the light ? Many moons have passed since we beheld it last. Men have resumed their guessing and checking play searching for the laws of nature. Shall we, sisters, let them go alone on this path ?
(Les deux sœurs font signe que non).
Then, I suggest that each of us expresses again the wishes we made at the first shining of this blue light.

SF Ma sœur dit vrai, nous devrions à nouveau prononcer des vœux pour cette nouvelle naissance, il y a tant de lunes que la lueur bleue ne s'était pas manifestée.

SA Geliebte Schwestern! Gerne will auch ich im Anblick dieses blauen Lichts mir etwas wünschen. Doch sollten's, ist die Zeit neu, nicht die alten Wünsche sein. Es sollten Wünsche sein wie für ein neues Leben: neue Wünsche.

SF Des vœux nouveaux pour une Renaissance.

SB Entirely new wishes, I like the idea.

SA Dann, meine Schwestern, sage von uns jede,
was sie wünscht.

SB Then, my sisters, as I am the eldest, I shall speak first.
Let me think about my wish... I wish that by using properly this light and by using all possible bits of cleverness, the men will gain a deeper and deeper understanding of the laws of nature, that they may harness and organize its forces and thus create themselves great wealth.

SA Dies also ist der erste Spruch. Du, Schwester, nimmst mit deinem Wunsch die Menschheit in die Pflicht, mit aller Geisteskraft noch tiefer der Natur Gesetze zu versteh'n und mit den Kräften der Natur zu schalten und zu walten in der Art, die aller Menschen Wohlstand mehrt.

SB It is what I meant.

SA Ein grossherziger Wunsch! Die Menschheit wird das Wirken der Natur verstehen und zu nutzen lernen. Nicht aber ohne harte Prüfungen! Hört meinen Willen nun: die Forschung soll nicht ohne ernstliches Bemühen glücken. Dafür wird dann zum Ende auch sich selbst der Mensch erneuert haben.
Und wird dein Wunsch, geliebte Schwester, ihm den Wohlstand bringen, wird er nach meinem Willen neue Eigenschaften, Lebensformen und ein neues Weltbild finden.

SF Mes sœurs, c'est à mon tour de prononcer le vœu qui accompagnera la renaissance de cette lueur. Grandes sont les richesses matérielles et spirituelles promises aux hommes par vos vœux. Grandes aussi seront les épreuves.
Ma sœur aînée a promis aux hommes la maîtrise des lois de la nature par leur travail autour de la lueur bleue. Cette maîtrise les rendra puissants et riches. Est-ce bien cela ?

SB True, my sister.

SF En rendant cette entreprise très difficile ma sœur cadette leur a promis une transformation d'eux-mêmes. L'effort demandé fera naître un homme nouveau regardant autrement le monde.

SA Genau, meine Schwester.

SF J'ajoute maintenant une épreuve nouvelle.
Aucun homme ne sera capable de progresser seul dans ses recherches. De nombreux talents seront nécessaires. Et si les hommes refusent de travailler ensemble, alors les promesses de mes deux sœurs ne pourront se réaliser. En retour, mon cadeau sera précieux. Les hommes progresseront dans l'art le plus difficile pour tous : l'art de vivre ensemble et de se comprendre.
Tel est mon vœu.

SA Geliebte Schwester, dieser Wunsch zwingt alle Forscher fortan zur Gemeinsamkeit. Zusammenarbeit nur kann ihnen Fortschritt und Erfolge bringen. Doch eben dies ist eine harte Prüfung, denn beim Denken sind sie ganz mit sich allein!
Gleichwohl ist dein Geschenk auch wahrhaft großherzig: nichts ist begehrenswerter für die Menschen als ein friedliches Zusammenleben.

SB My dear sisters, you have increased by far the difficulty of the way which I proposed to the users of the light. But you promised them great treasures in exchange.
My youngest sister promised to reward men with a greater mind, a greater spirit after the effort of discovering the laws of nature. And my other sister promised a progress in the art of living together by the obligation to help each other. But, would they refuse the challenge, she threatened them with failure. These are great, great trials... Let us watch on them from our retreat to see how they perform along these whishes.

SA Ja! Ziehen wir uns jetzt zurück ins Unsichtbare. An den Menschen laßt uns sehen, was aus unsren Wünschen wird.

SF Et maintenant, place aux hommes et à leurs aventures.
Notre regard et nos vœux les accompagnent depuis notre retraite.

At the celebration of the Renaissance of ILL, several speakers addressed the guests:

Robert Comes, Chairman of the ILL Steering Committee.

Cliff Shull, Nobel Prize winner "The Early Days of Neutron Scattering".

Norman Ramsey, Nobel Prize winner "Neutron Spin Reorientation Experiments".

Reinhard Scherm, Director of ILL

The multitude of distinguished guests at the ceremony to celebrate the Renaissance of ILL.

Bill G. Stirling, Chairman of the ILL Scientific Council.

Alan Leadbetter, British Associate Director, Master of Ceremonies.

Madame Elisabeth Dufourcq, Ministre Chargé de la Recherche Scientifique, visited the large-scale scientific installations in Grenoble on 23 June. From left to right: Michel Destot, Mayor of Grenoble, Elisabeth Dufourcq, Richard Casenave, City Councillor for the opposition, Jean-Paul Watteau, Recteur de l'Académie de Grenoble, listening to an introductory presentation by Reinhard Scherm.

Madame Elisabeth Dufourcq coming out of the air-lock accompanied by Michel Destot and Ekkehardt Bauer.

On the level of reactor operation. From left to right, Richard Casenave, Michel Destot, Elisabeth Dufourcq, Jean-Paul Watteau, Ekkehardt Bauer and Reinhard Scherm.

Visit by Hans Zehetmair, Deputy Minister-President and Minister for Education, Culture, Science and Art in Bavaria, on 14 and 15 September. Here at the press conference together with Reinhard Scherm, Director of ILL. In the background Philippe Leconte, French Associate Director and Sigurd Lettow, Head of the Administration Division.

Visit by Hans Zehetmair. Wolfgang Gläser, Technische Universität Garching, former Director of ILL, talking to Ekkehardt Bauer, Head of the Reactor Division.

Hans Zehetmair talking to Michel Destot, Mayor of Grenoble, with Reinhard Scherm and Philippe Leconte looking on.

Visit by Hans Zehetmair. From left to right: Daniel Bois, Directeur du CNET, Grenoble, Jean Paul Watteau, Recteur de l'Académie de Grenoble, Philippe Leconte and YvesPetroff, Director General of the ESRF.

Workshop: "New Tools for Neutron Instrumentation", Les Houches, 6-9 June. Coffee break in front of the lecture theatre.

Workshop: "New Tools for Neutron Instrumentation". A. Heidemann, P. Böni, W. Heil, U. Schmidt and R. Scherm.

Workshop: "Quantum Atomic and Molecular Tunnelling in Solids", Seyssins, 4-7 October. Discussion in front of the "Maison d'Hôtes, La Baume".

Workshop: "Quantum Atomic and Molecular Tunnelling in Solids". S. Clough , A. Heidemann and G. Kearley.

Zum Jahresende 1995 bietet sich das altvertraute Bild. Überall drängen sich die user, Experimente werden durchgeführt, erste Ergebnisse diskutiert: "business as ususal". Dabei ist es gerade erst ein Jahr her, daß nach fast vier Jahren Stillstand der Reaktor wieder anfuhr. Nach der Betriebsgenehmigung am 3. Januar 1995 "divergence" am 6. Januar, am 7. volle Leistung. Nach wenigen Wochen Probebetrieb wurde dann Ende Februar der offizielle user-Betrieb aufgenommen.

Natürlich gab es während dieser Einfahrtzeit Schwierigkeiten zu meistern: gelegentliche Probleme mit einer neuen Elektronik oder einem neuen Steuerprogramm oder die Kinderkrankheiten eines neu gelieferten Multidetektors; einmal bedurfte es sogar der Aufmerksamkeit eines prominenten Gastes, um einen tief versteckten logischen Fehler in der Ausleseelektronik zu entdecken. Unseren "friendly users" sei gedankt, die Verständnis zeigten und mitanpackten. Alle unsere Wissenschaftler, Ingenieure und Techniker leisteten hierbei ihr Bestes.

Nach diesem ersten Jahr im "2. Leben des ILL" sind 24 der nominellen 25 ILL-Instrumente in vollem Betrieb. Hierzu sind im Laufe dieses Jahres von Seiten der selbständigen CRG Gruppen noch 6 CRG-Instrumente hinzugekommen. Das wissenschaftliche Leben mit Ideen, Experimenten, Diskussionen und Seminaren ist wieder intensiv erblüht. Dies mögen einige Zahlen belegen: 3958 offizielle Strahltage im Jahr 1995. Insgesamt besuchten 1244 Experimentatoren das ILL (bei 2261 Besuchen) und verbrachten hier 23100 Tage.

Im Jahr 1995 erlebten wir endlich wieder "real time" Sitzungen des Wissenschaftlichen Rates. Während an den Instrumenten Messungen und Experimente laufen, diskutieren die subcommittees die neuen proposals für die kommenden Monate. Angesichts einer Überbuchung von 2 bis 3 werden Weichen gestellt und manchmal Schicksale gelenkt.

In seiner neuen Form, mit dem vom Lenkungsausschuß ernannten Vorsitzenden, hat der Rat deutlich an Gewicht gewonnen. Aus seinen Reihen sind den verschiedenen Projekten Paten zugewiesen, die in der Sitzung berichten. Deren direkter Kontakt mit den Projektverantwortlichen trägt dazu bei, das ILL enger mit der Außenwelt zu vernetzen. Lange diskutiert wurde die Frage des "juste retour scientifique". Wie im Vereinbarungsprotokoll zum Regierungsabkommen festgeschrieben ist die wissenschaftliche Qualität nicht das einzige Auswahlkriterium. Vielmehr sollen die vergebenen Meßzeiten auch das finanzielle Engagement der Partnerländer widerspiegeln. Diese Forderung stieß weder bei den subcommittees noch im Wissenschaftlichen Rat auf große Gegenliebe, sodaß es der Direktion vorbehalten bleibt, nach den Empfehlungen der subcommittees noch korrigierend einzugreifen. Der Traum vom "open access" setzt eben auch freigebige Finanzierung voraus.

Die erste Sitzung des Wissenschaftlichen Rats bot Anlaß und Rahmen, die Wiedergeburt des wissenschaftlichen Lebens nach der Renovierung zu feiern. Drei Hexen brachten ihre Wünsche dar, und die Nobelpreisträger N. Ramsey und C. Shull, beide alte Freunde des Hauses, verliehen dem Fest ésprit und Würde. In Jamben wünschten die Hexen den Wissenschaftlern nach der Mühe Erfolg und gedeihliches Zusammenwirken. Norman Ramsey berichtete aus dem Inneren des Neutrons und natürlich auch über den bisher kleinsten Wert des elektrischen Dipolmoments, Cliff Shull erzählte von den ersten heroischen Experimenten mit Neutronen, damals als Zählraten noch von Hand notiert wurden.

Da Forschung mit Neutronen zu Fragestellungen aus den unterschiedlichsten Fachgebieten beiträgt, werden ihre Ergebnisse in erster Linie auf Fachkonferenzen vorgestellt. Gerade wegen dieser Multidisziplinarität hat das ILL es sich schon immer zur Aufgabe gemacht, als ein Zentrum des internationalen Austauschs den Zusammenhang der heterogenen Neutronen-community durch workshops mit speziellen wissenschaftlichen und methodischen Themen zu fördern.

Der workshop "Quantum Tunneling of Atoms and Molecules in Solids" behandelte ein typisches Neutronengebiet: Tunnelbewegungen in Festkörpern bei tiefen Temperaturen, eine Thematik, die eng mit der hochauflösenden Spektroskopie verknüpft ist. In Les Houches fanden 60 Teilnehmer zu einem von der EC geförderten workshop "New

Tools for Neutron Instrumentation" zusammen. Diese Veranstaltung zeigte überdeutlich, daß in der Kunst der Instrumentierung bei weitem noch nicht alle Möglichkeiten ausgeschöpft sind. So wird zum Beispiel eine vielversprechende neue Methode der Polarisationsanalyse sichtbar und neue Entwicklungen beim Bau von Multidetektoren oder optischen Elementen nehmen konkrete Gestalt an.

Was wäre ein wissenschaftliches Gebiet ohne die Neugier der Studenten und jungen Wissenschaftler? Die Universität Grenoble und INPG veranstalten jährlich den Kurs HERCULES : Neutron and Synchrotron Radiation for Condensed Matter and Biology. Seit 1995 können die Studenten - die user von morgen - endlich wieder an den Geräten am ILL erste konkrete Bekanntschaft mit der Neutronenstreuung machen.

Eine weitere Veranstaltung verdient besondere Erwähnung. In den ersten Januartagen 1996 fand in Autrans ein workshop "Scientific Prospects for Neutron Scattering with Present and Future Sources" statt. Unter dem Siegel ESF, weiter unterstützt von EC, ENSA und ILL animierte G. Lander 80 Teilnehmer in 10 Gruppen, über die Gegenwart nachzudenken und über die Zukunft zu spekulieren. Dabei waren mehr als 1/3 der Teilnehmer "neutrale" Wissenschaftler, die nicht auf Neutronen angewiesen sind. Die abschließende Paneldiskussion, geleitet von H.Curien, ließ mehrere Tendenzen erkennen:

• Auch angesichts der märchenhaften Fortschritte der Synchrotronstrahlung stellt sich nicht so sehr die Frage X oder n, sondern weit öfters das komplementäre X und n.

• Neutronenstreuung ist eine etablierte Technik geworden. Die Nachfrage wird weiter zunehmen. Ihre Anwendung wird in die Breite gehen und noch in weitere Fachgebiete vordringen.

• Statt der einfachen Probe von gestern finden sich auf dem Probentisch immer komplexere Systeme (wie z.B. soft matter, komplizierte Werkstoffe).

• Die Meßtechnik und Instrumentierung können und werden noch große Fortschritte machen.

• Man nutze die bestehenden Hochflußquellen voll aus.

• Langfristig sollte man eine Quelle der 3. Generation vorbereiten. Hier hat wohl die gepulste Spallation die besten Chancen, den Fluß von heute noch einmal zu übertreffen.

Die Niederschrift dieses workshops wird bei den anstehenden Diskussionen um das zukünftige wissenschaftliche Profil des ILL noch oft zu Rate gezogen werden.

Eigentlich gäbe es mit dem Betrieb von Reaktor und Instrumenten und bei der täglichen Auseinandersetzung mit den wissenschaftlichen Ergebnissen schon genug zu tun. Trotzdem sollten wir uns von finanziellen und personellen Beschränkungen nicht ganz entmutigen lassen, sondern ständig versuchen, Methodik und Instrumentierung weiter zu verbessern. Hierzu vom Lenkungsausschuß ausdrücklich ermutigt, sind jetzt für die kommenden fünf Jahre Projekte im finanziellen Rahmen von etwa 7 MF pro Jahr geplant: D17 soll endlich zum Reflektometer umgebaut werden des weiteren sollen die Instrumente D16, IN5, D4 und IN8 wesentlich verbessert werden.

Ein langjähriger Begleiter und steter Freund des Instituts wurde am 8.August 1995 auf dem Friedhof Montparnasse begraben. Seit den Anfängen des Instituts vertrat Dr.Jules Horowitz (1921 - 1995) das CEA über 20 Jahre im ILL-Lenkungsausschuß. Seine Weisheit, seine Weitsicht und sein Engagement prägten zutief die Entwicklung des Instituts.

Des weiteren beklagt die internationale Gemeinde der Neutronenforscher den Verlust von T. Riste (Kjeller) und A.R. Mackintosh (Risø).

Am Rande der Sitzung des Lenkungsausschusses wurde im November ein Vertrag unterzeichnet, mit dem zum 1. Januar 1996 die Rolle des deutschen Gesellschafters vom Forschungszentrum Karlsruhe (KfK) auf das Forschungszentrum Jülich überging. Das ILL bedankt sich von Herzen bei KfK, vor allem natürlich bei den Herren Greifeld†, Klose und Hennies für die langjährige treue Unterstützung und heißt seinen neuen Gesellschafter herzlich willkommen.

Reinhard Scherm

At the end of 1995, life at ILL paints a familiar picture. Everywhere you turn, there are users milling around, experiments being conducted, results being discussed: it is business as usual. Yet it was just one year ago that the reactor was restarted after a shutdown lasting almost four years. On 3 January 1995, authorisation to restart was received, three days later the reactor went critical and by 7 January it had reached full power. After a few weeks of testing, user operation was then officially launched at the end of February.

Of course, there were a number of difficulties to be overcome during the restart period, such as occasional problems with a new piece of electronics or a new control program or the teething troubles of a new multidetector. On one occasion, it even needed the keen powers of observation of a prominent guest to discover a logic error hidden away deep within the readout electronics. We are grateful to our "friendly users" for the understanding they showed during this period and their willingness to lend a hand. Our scientists, engineers and technicians all gave their very best.

One year into ILL's "second life", 24 of the 25 official ILL instruments are fully operational. A further 6 CRG instruments were added to this total during the course of the year by the independent Collaborating Research Groups. Scientific life with its ideas, experiments, debates and seminars is once again flourishing. The figures speak for themselves: there were 3958 official beam days in 1995. A total of 1244 experimentalists visited ILL (2261 visits) and spent some 23,100 days at the Institut.

In 1995, we were finally able to hold "real-time" meetings of the Scientific Council again. While measurements and experiments were being carried out on the instruments, the Sub-committees were already discussing the new proposals for the coming months. Faced with a demand which exceeds supply by a factor of between two and three, it is at these meetings that decisions are taken which orientate scientific activity and sometimes influence personal destinies.

Following its reorganisation, the Council, whose Chairman is now appointed by the Steering Committee, has clearly gained in importance. Each project is assigned a so-called "godfather" from among the Council's ranks, who reports to the meeting. This gives the Council direct contact with those responsible for the projects, thereby helping to create closer links between ILL and the outside world. The question of the "juste retour scientifique" has been discussed at great length. As stipulated in the Memorandum of Understanding on the Intergovernemental Convention, scientific merit is not the only criterion for selection. Allotted beam time should also reflect the financial commitment of the individual member countries. As neither the Sub-committees nor the Scientific Council welcomed this requirement with very much enthusiasm, it is left to the Management to make adjustments after the Sub-committees have put forward their recommendations. The truth is that the dream of "open access" also requires generous funding.

The first meeting of the Scientific Council provided a perfect opportunity and an ideal setting to celebrate the rebirth of scientific life at ILL following the refurbishment of the reactor. Three witches were on hand to wish the ILL well, as were Nobel prize winners N. Ramsey and C. Shull, both old friends of the Institut, whose presence brought a spirit of wit and dignity to the festivities. Speaking in iambic verse, the witches hoped that the efforts of the scientists would be rewarded with success and that their cooperation would be fruitful. Norman Ramsey gave a talk on the inside of the neutron and, of course, also on what continues to be the smallest value of electric dipole moment ever obtained, while Cliff Shull spoke about the first heroic experiments with neutrons back in the days when the count rate was still noted by hand.

Because neutron research contributes to solving problems in a wide variety of fields, the results are presented primarily at specialist conferences. It is precisely because of the multidisciplinary nature of its activities that ILL, as a centre for international exchange, has always made it its business to foster links between the different members of the neutron research community by organising workshops on specific science and methodology-related topics.

The workshop "Quantum Tunnelling of Atoms and Molecules in Solids" explored a typical area of interest for neutron researchers, that of tunnelling movements in solids at low temperatures, a topic which is closely related to high-resolution spectroscopy. At Les Houches, 60 delegates gathered

to take part in a workshop supported by the EC entitled "New Tools for Neutron Instrumentation". This event demonstrated only too clearly that, in the art of instrumentation, the possibilities are far from exhausted. For example, we are seeing the emergence of a promising new technique for polarisation analysis and new developments in the construction of multidetectors and optical elements are beginning to take shape.

What would a scientific field be without the curiosity of students and young scientists? Every year, the University of Grenoble and the INPG organise a course known as HERCULES: Neutron and Synchrotron Radiation for Condensed Matter and Biology. In 1995, the students taking part in the programme, who are after all tomorrow's users, were finally able once again to have their first real taste of neutron scattering using ILL instruments.

Another event deserves particular mention. At the very beginning of January 1996, a workshop entitled "Scientific Prospects for Neutron Scattering with Present and Future Sources" was held in Autrans. This event was organised under the auspices of ESF, with additional support from the EC, ENSA and ILL. Under the guidance of the workshop's moderator, G. Lander, the 80 participants, who were divided into 10 groups, were encouraged to think about the present and speculate on the future of neutron scattering. More than one-third of those taking part were "neutral" scientists who do not rely on neutrons for their work. The concluding round table debate, led by H. Curien, revealed a number of trends:

- Even in view of the spectacular progress being made in the field of synchrotron radiation, it is rarely a matter of choosing either X-rays or neutrons but far more often a question of making complementary use of X-rays and neutrons.
- Neutron scattering has become an established technique. Demand is set to increase. Its field of application will grow as it breaks into still more specialist areas.
- The straightforward samples of yesterday are being replaced by increasingly complex systems (such as soft matter and complicated materials).
- Further major progress can and will be made in the field of measuring techniques and instrumentation.
- The capacity of existing high-flux sources ought to be used to the full.
- In the long term, we should be preparing the way for a 3rd generation source. In this context, pulsed spallation is the technique most likely to produce the next flux increase.

We can expect the proceedings of this workshop to be consulted frequently during the forthcoming discussions on the scientific profile of ILL.

We may feel that we already have quite enough to do with the running of the reactor and instruments and our daily confrontation with scientific results. However, we must not be completely disheartened by financial and staff restrictions and must constantly try to improve methods and instruments still further. To this end and with the full support of the Steering Committee, a programme of projects to be carried out over the next five years has been elaborated within the framework of an envelope worth some 7 million francs per year: D17 is finally to be converted into a reflectometer, while substantial improvements will be made to instruments D16, IN5, D4 and IN8.

On 8 August 1995, a long-standing ally and devoted friend of the Institut was laid to rest in the Montparnasse cemetery. Since the early days of the Institut and for more than 20 years, Dr. Jules Horowitz (1921-1995) represented the CEA on the ILL Steering Committee. His wisdom, foresight and commitment have had a profound influence on the Institut's development.

The international community of neutron scientists was also saddened by the death of T. Riste (Kjeller) and A.R. Mackintosh (Risø).

On the fringe of the November meeting of the Steering Committee, a contract was signed to mark the transfer, on 1 January 1996, of the role of German Associate from Forschungszentrum Karlsruhe (KfK) to Forschungszentrum Jülich. ILL would like to take this opportunity to thank KfK, and in particular, of course, Messrs. Greifeld†, Klose and Hennies for their loyal support over the years, and to welcome its new Associate.

Reinhard Scherm

Fin 1995, l'Institut a retrouvé son image habituelle. Partout des utilisateurs pressés, les expériences sont réalisées, les premiers résultats discutés : "business as usual". Et pourtant, il n'y a qu'un an que le réacteur redémarrait, après un arrêt de presque 4 années. Suite à l'autorisation de remise en service le 3 janvier 1995, le réacteur divergeait le 6 janvier et atteignait sa puissance nominale le 7 janvier. Après quelques semaines de contrôles et de tests, la fin février marquait l'arrivée officielle des utilisateurs.

Bien entendu, cette période de reprise ne s'est pas faite sans quelques difficultés : un nouveau matériel électronique, un nouveau programme de contrôle à mettre au point, un "défaut de jeunesse" d'un multidétecteur nouvellement livré à corriger ; il a même fallu l'attention d'un invité éminent pour découvrir une erreur logique dissimulée dans l'électronique de sortie. Nous tenons ici à remercier nos "friendly users" qui se sont montrés compréhensifs et n'ont pas hésité à mettre la main à la pâte. Nos scientifiques, ingénieurs, et techniciens ont tous donné le meilleur d'eux-mêmes.

Après cette première année dans la "deuxième vie" de l'ILL, 24 des 25 instruments officiels de l'ILL fonctionnent à plein. De plus, 6 instruments CRG appartenant à des Groupes de Collaboration Scientifique indépendants sont venus s'y ajouter. La vie scientifique, avec ce qu'elle représente d'idées, d'expériences, de discussions et de séminaires, est de nouveau en plein essor. Quelques chiffres le prouvent : 3958 jours de faisceau officiellement programmés en 1995. Au total 1244 expérimentateurs sont venus à l'ILL (2261 visites) et y ont séjourné quelque 23 100 jours.

En 1995, nous avons enfin pu revivre "en temps réel" les réunions du Conseil Scientifique. Pendant que, sur les instruments, les mesures et les expériences se poursuivaient, les Sous-Comités discutaient les nouvelles propositions pour les mois à venir. Les demandes d'expériences étant de 2 à 3 fois supérieures aux possibilités, ces instances fixent des orientations scientifiques et influencent parfois des destins.

Dans sa forme actuelle, avec le Président nommé par le Comité de Direction, l'importance du Conseil Scientifique s'est considérablement renforcée. Chaque projet est parrainé par un membre du Conseil, qui fait un rapport lors de la réunion. Des contacts directs sont ainsi créés avec les responsables des projets, ce qui contribue à établir des relations plus étroites entre l'ILL et le monde extérieur. La question du "juste retour scientifique" a été longuement discutée. Comme il est stipulé dans le Protocole d'accord à la Convention Gouvernementale, la qualité scientifique n'est pas le seul critère de sélection. Les temps de mesures accordés doivent également refléter l'engagement financier des pays membres. Cette exigence n'ayant été accueillie avec enthousiasme ni par les Sous-Comités ni par le Conseil Scientifique, il revient donc à la Direction d'effectuer quelques corrections après les recommandations des Sous-Comités. Le rêve du "libre accès" a bien pour condition un financement généreux.

La première réunion du Conseil Scientifique a été l'occasion de fêter la renaissance de l'activité expérimentale de l'ILL suite à la rénovation du réacteur. Trois sorcières ont présenté leurs voeux, et la présence de N. Ramsey et C. Shull, Prix Nobel de Physique, tous deux amis de longue date de notre Institut, a conféré à cette fête Esprit et Dignité. Sous une forme poétique, les sorcières ont souhaité aux chercheurs de voir leurs efforts couronnés de succès et de réussir à établir des collaborations fructueuses. Norman Ramsey a fait un exposé sur l'intérieur du neutron et naturellement sur la plus petite valeur du moment dipolaire électrique obtenue jusqu'à présent. Cliff Shull nous a parlé des premières expériences héroïques réalisées avec des neutrons, du temps où les taux de comptage étaient encore notés à la main.

La recherche neutronique contribue à résoudre des problèmes dans les domaines les plus divers, c'est pourquoi les résultats obtenus sont en premier lieu présentés dans le cadre de conférences d'experts. C'est en raison de cette pluridisciplinarité que l'ILL, en tant que centre d'échange international, a toujours eu à coeur d'encourager les relations au sein de la communauté hétérogène des chercheurs neutroniques en organisant des workshops sur des thèmes scientifiques et méthodiques bien spécifiques.

Le workshop "Quantum Tunnelling of Atoms and Molecules in Solids" traitait d'un thème typique de la neutronique : mouvements tunnels dans les corps solides à basses températures, une thématique étroitement liée à la spectroscopie à haute résolution.

Aux Houches, 60 scientifiques ont pris part à un workshop subventionné par la CE intitulé "New Tools for Neutron Instrumentation". Cette manifestation a clairement démontré que, dans l'art de l'instrumentation, toutes les possibilités étaient loin d'être épuisées. Par exemple, une nouvelle méthode d'analyse de polarisation se dessine, qui semble tout à fait prometteuse pour l'avenir, et de nouveaux développements dans la construction de multidétecteurs ou des éléments optiques se concrétisent.

Que serait un domaine scientifique sans la curiosité des étudiants et des jeunes chercheurs ? L'Université de Grenoble et l'INPG organisent chaque année le cours HERCULES : Neutron and Synchrotron Radiation for Condensed Matter and Biology. Depuis 1995, les étudiants, qui sont les utilisateurs de demain, ont à nouveau accès aux instruments de l'ILL et peuvent faire connaissance de manière concrète avec la diffusion neutronique.

Il convient également de mentionner une autre manifestation importante. Dans les premiers jours de janvier 1996 a eu lieu à Autrans un workshop intitulé "Scientific Prospects for Neutron Scattering with Present and Future Sources". A l'initiative de l'ESF et avec le soutien de la CE, de l'ENSA et de l'ILL, cette réunion, animée par G. Lander, a rassemblé 80 participants, répartis en 10 groupes, qui ont réfléchi sur le présent et spéculé sur l'avenir de la diffusion neutronique. Plus d'un tiers de ces participants était des scientifiques "neutres", c'est-à-dire dont les travaux ne dépendent pas directement des neutrons. La table ronde finale, dirigée par H. Curien, a permis de distinguer plusieurs tendances :

- Face aux progrès fabuleux du rayonnement synchrotron, la question qui se pose actuellement n'est pas tant le choix entre rayons X et neutrons, mais bien plus la complémentarité rayons X et neutrons.
- La diffusion neutronique est maintenant une technique reconnue. La demande continuera à augmenter. Son domaine d'application s'élargira, d'autres spécialités y auront recours.
- Les échantillons simples d'hier sont remplacés par des systèmes de plus en plus complexes (par exemple matière molle, matériaux compliqués).
- Les techniques de mesure et l'instrumentation peuvent encore se développer et feront des progrès importants.
- Les sources à haut flux actuellement existantes doivent être exploitées à pleine capacité.
- Il faudrait à long terme préparer une source de la troisième génération. La spallation pulsée semble la mieux placée pour surpasser le flux dont nous disposons actuellement.

Le compte rendu de ce workshop sera encore souvent consulté au cours des discussions qui auront lieu prochainement sur le futur profil scientifique de l'ILL.

Le fonctionnement du réacteur et des instruments ainsi que la confrontation quotidienne aux résultats scientifiques pourraient nous sembler une tâche suffisante. Nous ne devons cependant pas nous laisser décourager par les limitations financières et les restrictions de personnel, mais devons constamment essayer d'œuvrer pour améliorer les méthodes et les instruments. Le Comité de Direction nous a formellement encouragés à travailler dans ce sens, et, pour les cinq années à venir, des projets ont été élaborés dans le cadre d'une enveloppe financière de 7 MF par an : D17 doit enfin être transformé en réflectomètre, les instruments D16, IN5, D4 et IN8 feront l'objet d'améliorations substantielles.

Un ami fidèle, qui a accompagné l'ILL pendant de nombreuses années, nous a quittés et repose depuis le 8 août 1995 au cimetière Montparnasse. Depuis l'origine de l'Institut et pendant plus de 20 ans, le Dr. Jules Horowitz (1921-1995) a représenté le CEA au Comité de Direction de l'ILL. Sa sagesse, sa vision à long terme et son engagement ont eu une influence profonde et positive sur le développement de l'Institut.

La communauté internationale des neutroniciens a été également tristement marquée par le décès de T. Riste (Kjeller) et A.R. Mackintosh (Risϕ).

Parallèlement à la réunion du Comité de Direction, un contrat a été signé en novembre portant sur le remplacement, à dater du 1er janvier 1996, du Forschungszentrum Karlsruhe (KfK) par le Forschungszentrum Jülich en tant qu'Associé allemand. L'ILL remercie vivement le KfK, en particulier M. Greifeld†, M. Klose et M. Hennies pour le soutien qu'ils ont apporté au cours des années à l'Institut, et souhaite la bienvenue à son nouvel Associé.

Reinhard Scherm

Relations with ESRF and EMBL

The relations with ESRF have continued to develop at the management level through direct contacts between the Director-General of ESRF and the Director of ILL, and in regular meetings between the two Heads of Administration.

ILL and ESRF together went on pressing for much-needed improvements in the provision of International Schooling for the children of their non-French staff in local schools. Apart from a certain progress in creating a more original and open teaching system (Charter for international schooling in Grenoble) the problem of premises remains unsolved. This unacceptable situation has lasted for years and promises proved to be hollow ones. Both ILL and ESRF raised the question of international schooling with Mme Dufourcq, French Secretary of State for Research, during her visit to the Institutes on 23rd June. The latest developments deserve particular attention. The Mayor of Grenoble has recently proposed the setting up of an international school complex ("Cité Scolaire Internationale") with all the necessary facilities (reception offices, sports facilities, library, canteen etc.) on an easily accessible site located close to the science pole. This proposal is supported by the local authorities. The Managements of ILL and ESRF will follow very carefully these new ideas in order to ensure that this project is more than just an empty promise.

ILL and ESRF receive a large number of visitors from countries (Northern Europe, Germany etc.) having better airline connections with Geneva airport than with Lyon-Satolas airport. It is consequently important to have good railway connections between Geneva and Grenoble to avoid long waiting times for these visitors. ILL and ESRF therefore jointly approached the SNCF (French Railways) to request the improvement of the connections. The SNCF, acknowledging our common arguments, finally decided to add a new connection from 24th September onward.

The extension of the jointly-used building ILL20 has been completed. ILL acted as the secretariat of the "Comité de gestion de l'extension de l'EMBL", and managed the financing received from the French Ministries, the "Région Rhône-Alpes" and the "Département de l'Isère". A new agreement is now being discussed between ILL and EMBL in order to redefine the rights and duties of each institute regarding the enlarged building.

ILL, ESRF and EMBL have a common computer network for accessing INTERNET. In order to protect this network against intrusion, the three institutes decided to install a joint "firewall". This was done in June 1995. ILL has also signed, in its own name and for ESRF and EMBL, the Security Charter for the use of the French network RENATER.

COLLEGES

The scientific life of the ILL is organised through the Colleges. The Colleges are the forum for scientific contacts and exchanges. The College Secretaries organize seminars and meetings.

The scientists have their hierarchical positions defined in the Science Division. In this respect, they are instrument responsibles and have the duty of dealing with more technical topics. As regards their scientific activities on the other hand, they are left with the utmost freedom, to choose individually their main fields of interest.

The College Secretaries are elected in June each year for a term of one year, which can be renewed for a second year.

College Secretaries in 1995

		Spring	**Autumn**
College 2:	Theory	P. Bares	A. Pimpinelli
College 3:	Nuclear and Fundamental Physics	G. Fioni	U. Mayerhofer
College 4:	Structural and Magnetic Excitations	J. Kulda	N. Pyka
College 5:	Crystal and Magnetic Structures	G.J. McIntyre (5a) C. Ritter (5b)	S. Mason (5a) C. Ritter (5b)
College 6:	Structure & Dynamics of Fluids and Glasses	I. Anderson	H. Fischer
College 7	Material Science, Surfaces and Spectroscopy	H. Lauter	H. Lauter
College 8:	Biological Structures and Dynamics	L. Vuillard	P. Langan
College 9:	Structure & Dynamics of Soft-condensed Matter	H.J. Lauter C. Lartigue	B. Frick

The Colleges (except Theory) correspond one-to-one to the Subcommittee of the Scientific Council. The College Secretaries (with help from the Scientific Coordination Office, H. Büttner) prepare the meetings of the Subcommittees. They classify the proposals by subjects and collect advice on their technical feasibility from the College members. In the meetings of the Subcommittees they act as secretary to the Chairperson. One experienced ILL scientist (if possible a Visiting Senior Scientist) per Subcommittee also attends the meetings.

Theory

Members of the College

Internal Members

P.-A. Bares
S. Brazovski
Yu.A. Bychkov
N. Cooper
T. A. Costi
I. Dzyaloshinski
B. Fourcade
F. Gebhard
A. Gogolin
K. Kassner
T. Martin
P. Nozières
A. Pimpinelli
A. Würger

External Members

M. Altarelli (ESRF)
O.K. Andersen (ESRF)
P. Carra (ESRF)
P. Johansson (ESRF)
H. König (ESRF)
N. Manini (ESRF)
D. Núñez-Regueiro (ESRF)
M. Papoular (ESRF)
B. Thole (ESRF)
M. Van Veenendaal (ESRF)

Scientific activity in 1995

The scientific activity of the Theory College during 1995 has focused on condensed matter. The major topics examined were: strongly correlated systems (with and without impurities), mainly in low dimensionality, dissipative systems, surface properties, crystal growth and membranes. As always, the composition of the Theory College has varied greatly during the year. P.-A. Bares left for Switzerland, I. Dzyaloshinski moved back to his home institution, A. Gogolin left for the Imperial College in London, K. Kassner left for Germany, while N. Cooper, T.A. Costi and F. Gebhard joined the College last November. A number of active scientists visited our College for short periods: C. Caroli, B. Clements, M. Kagan, E.I. Kornilov, B. Toperverg and A. Tanguy.

P.-A. Bares has continued his research on a class of one-dimensional strongly correlated models with impurities. In particular, he found that a solvable t-J model with impurity has zero resistivity due to the fact that only forward scattering occurs. This is very exceptional and probably true for the whole class of solvable models. In collaboration with K. Kassner, he investigated the possibility of exact solutions in a spin system coupled to a boson field. The original motivation was to assess the effect of correlations on the transition of the single-mode radiation field to the superradiant state.

S. Brazovski has studied the role of intrinsic defects in density wave systems and layered superconductors. These systems are connected by a common subject which may be called: "equilibrium and induced plasticity of electronic and vortex crystals" or "anomalous plasticity, sliding and melting in fragile superstructures". This work was the continuation of the programme followed by S. Brazovski during his previous long stay at ILL in 1992-93. Applications are expected to the joint ILL-ESRF-CRTBT and ILL-LPS (Orsay) experiments on scattering by charge density waves. The completed stages address the experimental studies in CRTBT - Grenoble and LPS - Orsay. Metastable plastic deformations of sliding electronic crystals determine their low frequency response, long-time relaxation and nonlinear I-V characteristics. The author presents a theory of plastic deformations due to the pinning-induced dislocation loops which cause the local metastable state. Within the same model, two remarkable features commonly observed in charge and spin density waves are described. Both the anomalous peak of the response at a frequency-dependent temperature and the characteristic I-V curve with a second threshold field in the sliding regime appear. The features of the response result from a competition between the local relaxation and the collective pinning caused by freezing of the Coulomb screening. The upper critical field in I-V curves is reached when the shortest life time configurations are accessed by the fast moving density waves. S. Brazovski has also developed a theory related to the NMR experiments in layered superconductors, which reveal an unexpectedly large concentration of highly diffusive thermally activated defects: interstitials and vacancies proliferate below melting and indicate the presence of unbound 2D dislocations above it. Also the observed critical 2D regime of freezing is interpreted as a fluctuation enhancement effect.

Yu.A. Bychkov has investigated the existence of topological defects, known as skyrmions, within the spin exciton band of a 2D electron gas in a strong magnetic field at a filling factor equal to 1. The Hartree-Fock approximation was used. In the linear momentum representation, it was shown that the inhomogeneity created in the system by a charged skyrmion can be described by a nonuniform rotation of the spin density operators in a condensate of spin excitons. In the limit where the spatial dependence is very smooth over the magnetic length, it was found that the winding number of created skyrmions is equal to the number of particles injected into, or removed from, the system.

N. Cooper arrived at ILL in November, and since this time he has predominantly focused on the continuation and completion of certain projects initiated during his previous post-doctoral position at Harvard University. This included the revision of a paper concerning the theory of photoluminescence in the Wigner crystal regime of two-dimensional electron systems, which has been submitted for publication; the preparation of a subsequent paper on the same subject; and the conclusion of a long-term project, started in collaboration with a post-doc at Harvard, concerning the luminescence spectrum of two-dimensional electron systems at filling fractions close to one. He also prepared a seminar on the results of this last activity which was presented as part of the Nozières seminar series.

T. A. Costi also arrived in November. He has completed earlier work on the equilibrium dynamics of the dissipative two-state system, started in Karlsruhe with a diploma student, C. Kieffer. In this work they showed that the two-state system coupled to ohmic dissipation is equivalent to the anisotropic Kondo model for the whole range of dissipation strengths, α, between 0 and 1. They considered the dynamics of the two-state system by calculating the spin response of the anisotropic Kondo model using Wilson's momentum shell renormalization group method. The results are of relevance for interpreting the tunneling of protons and muons in solids as well as for understanding the role of dissipation in macroscopic quantum coherence experiments in rf SQUIDs. This work is being extended to calculate non-equilibrium correlation functions for the two-state problem by analogy to the calculation of response functions in the x-ray problem. Preliminary results for the spin-boson model reproduce the expected behaviour for weak and strong dissipation. The approach can be applied to correlated transport through small devices.

I. Dzyaloshinski spent two and a half months at ILL, as part of a period of sabbatical leave from the University of California, Irvine. During his stay in Grenoble, he was concerned with the anomalous behaviour of 2D Fermi liquids when the Fermi level lies close to a van Hove singularity. The density of states then displays a logarithmic singularity, corresponding to the constant energy hyperbolae. This Log adds up to the usual Cooper singularity. It is then possible to collect systematically all terms of order Log^2, thereby constructing a new scaling analysis. It is then found that momentum and energy are equally singular and that they are characterized by non-trivial, coupled scaling equations. As the temperature falls, when the Fermi level lies exactly at the van Hove point, the Fermi velocity changes sign at a critical T_c, marking the breakdown of the Fermi liquid regime. As it stands, the theory ceases to be valid at this point, and cannot predict what happens when $T< T_c$- but does clearly identify the nature of the singularity.

B. Fourcade has worked on soft condensed matter problems, involving membrane shapes and instabilities. Besides his research activities, he taught four courses at the University Joseph Fourier. With one of his students, Thierry Charitat, he has investigated the physical properties of membranes with complex topologies. These systems are non-trivial and they are experimentally observable. Their analysis was based on a complete analytical approach supported by numerical calculations. The main points to note are: ''passages'' between membranes can repel or attract depending on the geometry; these systems are not sensitive to shear deformations; two types of phases can exist depending on the concentration of passages. With the same student, he is presently studying the physics of an elastic toroidal rope. Because of a spontaneous curvature, they have shown that there exists a non-trivial bifurcation from a planar state to a helicoidal state. This problem may have interesting relations to the elastic properties of D.N.A. With another student, Norbert Kern, he has studied the effect of ferrofluid particles on the shape of a membrane. They mainly concentrated on the case where the ferrofluid is a thin layer stuck to the membrane. This allows the response of a membrane to a magnetic field to be studied. This work was motivated by experimentalists (J. Baccry, from Paris). Finally, B. Fourcade has drafted a preliminary version of his lecture notes for the Classical Mechanics course.

F. Gebhard was at ILL for six months in 1993/94 and rejoined the Theory Group in November 1995 after he had obtained his Habilitation from the Philipps-Universität of Marburg, Germany. His thesis work concerns the Mott metal-insulator transition, which is governed by electron correlations. Its English translation, which he is presently working on, will appear in the textbook series *Springer Tracts in Modern Physics* in 1996. After completion of the Habilitation procedure, F. Gebhard was concerned with the optical absorption of tight-binding electrons in half-filled Peierls-distorted chains, both for weak and strong electron-electron interactions. Together with his collaborators at Marburg University, he scrutinized the structure of the current and the dipole operator for one-dimensional electrons and gave explicit analytical results for the linear optical absorption for the case of non-interacting electrons. They also provided analytical results for the case of strongly correlated electrons when the Hubbard interaction U is large compared to the energy scale for spin excitations J. Including the Peierls deformation and a nearest-neighbor interaction V, they obtained an exact solution for the optical absorption for the case of an incoherent spin background, and Simpson's exciton bands were recovered. The more realistic case of a definite ground state could be treated within a "no-recoil" approximation. The spectra now display single exciton lines whose intensity depends greatly on the spin structure of the ground state. The results will subsequently be applied to the optical absorption of charge-transfer salts and, tentatively, to conjugated polymers such as polydiacetylene.

A. Gogolin has studied, in collaboration with Michele Fabrizio, how non-trivial boundary conditions can affect the behavior of a one-dimensional electron gas. In this work, a general "open-boundary bosonization" method was formulated, which made it possible to obtain all the correlation functions of the electron fields and to study various physical processes (e.g. electron tunneling between a quantum wire and a superconductor). A. Gogolin has also analyzed the influence of electron-phonon coupling on the orbitally degenerate impurity ions and found that this coupling may be relevant and result in an interesting interplay between the Kondo and the Jahn-Teller effect. He has furthermore proposed a solvable model for an impurity spin embedded into a superconductor.

K. Kassner has investigated the linear stability of a sandwich structure (ABA) consisting of two elastically different solids submitted to uniaxial stress. This work,

which was carried out in collaboration with Chaouqi Misbah from U.J.F., resulted in a strong discrepancy with similar calculations by Grilhé et al. for epitaxially grown materials. Grilhé et al. found that whether a "strangulating" or a "meandering" mode was unstable for a thin layer of material B depended on whether or not B was softer than A, whereas according to calculation by Kassner and Misbah the strangulating mode was always more unstable for large wavelengths. This discrepancy was traced back to the use of different boundary conditions for the elastic fields used by the two groups. However, neither set of boundary conditions is entirely satisfactory. The issue has not yet been clarified. K. Kassner has also devoted time to two other projects, one with P. Metzener from EPF Lausanne, the other with C. Misbah. In the first project, the authors were concerned with the question of wavelength selection of stationary patterns in directional solidification and its relation to symmetry breaking of either a spontaneous nature or as imposed by an external flow. They found that whenever both the basic pattern and the equations of motion exhibit parity symmetry, there is no wavelength selection. In travelling waves this symmetry is broken, so there is a fixed wavelength at fixed velocity. However, since the velocity itself is a new degree of freedom, the wavelength is still not strictly selected, because the velocity can vary, leading to different wavelengths. In the second project, the authors studied the coupling of diffusional and elastic instabilities in directional solidification. The presence of a temperature gradient in directional solidification (and in almost all industrial processes involving the casting of alloys) leads to a strong modification of typical wavelengths to be expected in the Asaro-Tiller-Grinfeld instability (the temperature gradient provides an effective "gravitational field" that is increased by several orders of magnitude). They can become of the same order of magnitude as the lengthscales arising from the Mullins-Sekerka instability. Thus a strong coupling between the two instabilities can be inferred. Linear stability analyses as well as a weakly nonlinear analysis have been performed. They show that the upper and lower thresholds of the Mullins-Sekerka instability are shifted by an order of magnitude by internal stresses as weak as 0.1 bar (and these thresholds disappear altogether for larger stresses).

T. Martin has investigated the crossing time of a tunnel barrier using Feynman path integrals. The average time can be expressed as the derivative of the transmission coefficient for any barrier. The feasibility of defining a real and positive crossing time has been considered. It has been concluded that only higher-order moments give a reasonable answer. T. Martin has also extended the wave-packet approach used for computing shot noise in mesoscopic conductors to the description of normal-superconducting junctions. At low temperatures, and for an applied voltage smaller than the superconducting gap, a formula is obtained which reflects the suppression of shot noise. The transmission probability is replaced by the Andreev reflection probability, and the elementary charge is twice the electronic charge. Until October 1995, T. Martin was in charge of the ILL and the joint ILL-ESRF seminars. Since last summer, he has been busy organizing the XXXI Moriond Meeting in condensed matter, that took place on 20-27 January 1996. He has chosen the title: "Correlated fermions and transport in mesoscopic systems". The main topics were: normal-superconducting junctions, Luttinger liquids, fractional quantum Hall effect, persistent currents, 1D systems, quantum boxes, and localisation.

P. Nozières took his sabbatical year from Collège de France in 1995. He has thus attacked several items. Together with C. Caroli, he has investigated "solid on solid" friction. The phenomenological laws governing friction were already known to Leonardo da Vinci, and were stated explicitly by Coulomb two centuries ago. Tabor, around 1950 pointed to the role of plasticity in the geometry of local contacts. Recent developments concern the "stick-slip" relaxation, and find their motivation in the geophysical problem of the motion of fault edges. Superb experiments by the group at the Ecole Normale Supérieure show the existence of logarithmic precursors and scaling laws relating static and dynamic friction. A 1/f noise spectrum is also observed, and one would wish to explain this phenomenon. A semi-microscopic model has been constructed to describe the gliding of a skate on a substrate. The existence of asperities on both surface is assumed. This creates a *trapping potential* V when the skate touches the substrate. Each active trap is characterised by a configuration variable ρ_i which measures the distance between two asperities. The potential V can be attractive or repulsive. In the dynamic regime all ρ_i between $-\infty$ and $+\infty$ are scanned. A time average must be taken. In the static regime, only the configurational average has to be taken. Every trap reacts *elastically* to the potential V, which generates a coupling between traps. If traps are far apart, this interaction is weak and can be neglected in first approximation. The "one site" problem is nevertheless still non-trivial. For "soft" materials, it can lead to a *multistable* regime, and thus to *hysteresis*. It is easy to show that for a monostable system in the quasistatic regime, the average friction vanishes (in local equilibrium energy dissipation is not possible). Friction is indeed caused by the discontinuities due to hysteresis. The dynamic friction coefficient μ_d is directly connected to the *area of the hysteresis cycle*, much in the same way as in the magnetic hysteresis of a ferromagnetic material. If the pulling velocity is low enough, one can expect an anticipated jump due to thermal activation. This partly explains the observed logarithmical transients. In the static regime, the skate recoils to compensate on average the traction force. The coefficient μ_s needed to restart is thus equal to μ_d: the stationary distribution of the configuration variables ρ_i must be recreated. To explain the observation $\mu_s > \mu_d$, a plastic relaxation of the traps must be invoked. Another logarithmic correction is thus introduced, and scaling laws between μ_s and μ_d are observed, as suggested by the experiments. Although weak, the interaction between traps plays an important role because of its long range. For multistable traps in the static regime, it creates a *screening length* λ_D,

which limits the range of all elastic perturbations. The screening effect disappears in the dynamic stationary regime. In this case, the effect of all sites which break is to create a *noise* of the configuration variables ρ_i and this, in turn, causes other sites to break - whence the idea of an ''avalanche of breakdowns'' which is likely to be responsible for the observed noise spectrum. The theory of such avalanches is still sketchy, because a careful analysis of time correlations is necessary to avoid divergences. Similarly, it must still be shown that the intersite coupling may induce multistability for ''hard'' materials which are monostable at the single site level (a minimum size for multistable clusters would naturally appear). The essence of the model is in any case established: solid friction is an hysteresis phenomenon, with all associated complexities coming from activated jumps and interactions.

P. Nozières has also explored the often neglected role of elasticity in crystal growth. Last year, evidence of a step-bunching instability driven by elastic coupling between steps and adatoms was discovered. More generally, a step is seen to create on the substrate a non-vanishing *resultant force* when a uniaxial stress is exerted on the surface. Two steps at a distance d experience an interaction varying as $\ln d$. This interaction may destroy facets, which are replaced by two exponential profiles joining at an angle. This effect may explain a number of observations of the silicon surface by electron microscopy. Another question which attracted Nozières' attention was the Mott metal-insulator transition in a repulsive, half-filled Hubbard band. The transition corresponds to the Bose condensation of hole-electron pair triplets at the zone boundary (antiferromagnetic ''SDW'' state). The problem is identical to the superconducting transition in the attractive case. Is the symmetry breaking unavoidable ? Can one have bosons which are not superfluid ? Can one have an insulator (with gap) without SDW ordering ? The classical counterexample is the 1D chain. Indeed, this example proves nothing, for the disappearence of long-range order (superconducting or SDW) is, in this case, due to the continuous nature of the broken symmetry (the phase of the order parameter ''rotates'' slowly, without affecting its magnitude, which fixes the gap). This analysis is confirmed by the exact solution of the Hubbard model with finite magnetization, and also by the direct examination of macroscopic phase fluctuations (for a bosonic chain, for instance). Finally, P. Nozières considered the case of an antiferromagnet in an external field B_z. This system exhibits a ''spin-flop'' transition when z is an easy axis. Both sublattices at first orient themselves perpendicular to z, then they close continuously until a critical field is reached, where magnetization jumps to its saturation value. The problem becomes richer if an exchange anisotropy opposes the crystal field anisotropy. If the latter favours the (xy) plane, and the exchange favours the z axis, a region of values of B_z exists, where ferromagnetic ordering in the (xy) plane spontaneously appears. This unexpected effect should be observable.

A. Pimpinelli has worked on three main topics during 1995. With C. Misbah and O. Pierre-Louis in Grenoble, previous work on a diffusional instability of the Si(111) vicinal surface sublimating under DC or AC resistive heating has been extended to cover the very high temperature limit (of the order of 90% of the bulk melting temperature). In this temperature domain, surface vacancies are created which contribute to the movement of the steps. Assuming that the electric current biases the diffusion of both adatoms and vacancies (electromigration hypothesis), the stability diagram of the sublimating surface can be computed. Qualitative agreement is found with experiments. Secondly, together with J.C. Arnault, J.L. Bubendorff and J.P. Bucher in Strasbourg, A. Pimpinelli has investigated the kinetics of surface cavities on $NbSe_2$ during exposure to ambient atmosphere. The cavities have monolayer depth and their radius is seen to vary as t^{α} as a function of the time t. The exponent $\alpha \approx 0.4$ at small t, then it changes to 1 at larger times. This crossover is interpreted in terms of a characteristic diffusion length of the chemical agent responsible for the cavity formation (chemical etching). Using a simple diffusion model it is possible to find the observed behaviour analytically and to estimate the potential energy barriers which rule the kinetics. Thirdly, in collaboration with P. Peyla in Grenoble, A. Pimpinelli has investigated the growth of a crystalline vicinal substrate by atom deposition, as a model for molecular beam epitaxy on stepped substrates. In particular, the authors have studied the scaling behaviour of the density of atom clusters in the submonolayer as well as in the thick-film regime. They have performed extensive Monte Carlo simulations and have solved a simple mean-field model based on rate equations for the cluster densities. The model clarifies some puzzling numerical results and even makes it possible to derive analytically the crossover scaling function, in excellent accord with the simulations. Finally, A. Pimpinelli has worked on the completion of the English version of the book *Physique de la croissance cristalline*, which he has written together with J. Villain, and which was published early this year in French by Editions Eyrolles, Paris. The English edition will appear with Cambridge University Press.

A. Würger joined the College in April 1995 and has since been working on dissipative dynamics of two-level systems and tunneling of substitutional defects in alkali halide crystals. The findings of a mode-coupling approach to tunneling in amorphous solids have been compared with data observed for several oxide glasses (SiO_2, GeO_2, Be_2O_3), polycristalline metals (Ag, Al, Cu, Nb, Pd, Pt, and Ta), and polystyrene. There is strong evidence that the enhanced relaxation at about 5 K and the linear temperature dependence of sound velocity arises from incoherent tunneling. This theory, which implies that the tunneling systems become overdamped above 5 K, proved to fit the data much better than the thermally activated process. Dissipative tunneling in a double-well potential with a phonon heat bath has been tackled in several approaches, using diagrammatic perturbation theory, path integral

methods, and mode-coupling theory, with contradictory results as to the high-temperature dynamics. (In a real-time path integral calculation, Leggett et al. claimed that the dynamics would not become overdamped, in contradiction with mode-coupling and perturbation theory.) Several aspects of this superohmic spin-boson model are closely related to the diffusion of the small polaron coined by Holstein and others. Starting from the two-state polaron Hamiltonian and applying a simple equation-of-motion method, the dissipative two-state dynamics has been derived by means of a cumulant expansion of the resolvent operator. The first-order approximation yields a pair of complex poles; it is identical to the *non-interacting blip approximation* (NIBA) developped by Leggett et al., and others. The second-order terms give rise to an additional relaxation pole on the imaginary axis whose residue increases as a function of temperature from zero to unity. Rigorous upper and lower bounds for the high-temperature rate are established and the discrepancy with the path-integral approach is resolved. Lithium impurities in KCl crystals occupy off-center positions on the crystal axes, 0.7 Å from the original potassium site. At low temperature, thermally activated barrier crossing is inhibited and the motion between the eight off-center positions occurs by tunneling. At low density, most impurities may be considered as isolated from each other; yet there are a few nearby pairs which interact strongly. The dipolar interaction J of two impurities on nearest-neighbour sites is by orders of magnitudes larger than the bare tunnel energy $\Delta_o \approx 1$K, resulting in coherent motion of the two ions. Using degenerate perturbation theory with respect to the small parameter Δ_o/J, it is possible to calculate both the energy spectrum and response function of such a coupled pair. Since dipole moment p, distance R and tunnel energy Δ_o are known, there is no free parameter. The results describe quantitatively rotary echoes obtained from resonant microwave spectroscopy. For the two stable isotopes ^{6}Li and ^{7}Li tunnel energies of $^6\Delta_o$= 1.6 K and $^7\Delta_o$ = 1.1 K are found respectively. Comparing data on samples doped with ^{6}Li, ^{7}Li, or a mixture of both, yields an isotope effect which agrees with theory to within a few percent. This suggests the surprising fact that the tunneling states of a Lithium ion are not affected significantly by the dipolar interaction, which is of the order of 100 K. Substitutional defects in alkali halides (such as Li^+, BN^-, OH^- in KCl, NaCl, LiF...) provide a model system for the study of quantum tunneling in a crystalline environment. The dynamics is determined by the tunnel energy Δ_o and the dipolar interaction p^2/R_{ij}^3. In the dilute case (< 100 ppm), most impurities may be considered as non-interacting; yet a few of them are sufficiently close to form strongly coupled pairs, which are observed by rotary echoes. With increasing number density n = N/V of impurities, the average interaction np^2 exceeds the tunnel energy and drives a cross-over from coherent tunneling to collective relaxation where the dimensionless coupling parameter $m = np^2/\Delta_o$ is equal to unity (at an impurity concentration of about 1000 ppm). In two-state approximation, the Hamiltonian for N impurities reads

$$H = \frac{1}{2}\Delta_o \sum_i \sigma_x^i + \frac{1}{2}\sum_{i<j} J_{ij}\sigma_z^i\sigma_z^j$$

where $\sigma_z^i = \pm 1$ denotes two localized states for the defect at site i. Applying Mori's reduction method, the dynamical susceptibility has been calculated as a function of the known quantities Δ_o, number density n, and dipole moment p; there is no free parameter. Comparison with observed data for various defect systems with concentrations between 4ppm and 4000 ppm shows a quantitative agreement for frequency and temperature dependence of the susceptibility. The essential result is that there is cross-over from coherent tunneling to incoherent relaxation at $m \approx 1$. For $m > 1$ the susceptibility *decreases* with rising concentration.

Secretary: Alberto Pimpinelli

Nuclear and Fundamental Physics

Members of the College at ILL

Börner H.G.
Drexel W.
Faust H.R.
Fioni G.
Friedrichs T.
Geltenbort P.
Jentschel M.
Last J.
May D.
Mayerhofer U.
Nesvizhevsky V.
Oed A.
Oliver R.
Pendlebury J.M.
Stellmach C.
Weber M.
Williams A.
Zimmer O.

External Members

Groß M. (ISN)
Bao Z. (CIAE, Beijing)
Doll C. (TU München)
Hesse M. (Univ. Tübingen)
Köster U. (TU München)

Guests

Ageron P. (ILL)
Baessler S. (Univ. Heidelberg)
Chibane Y. (Univ. Sussex)
Fujimoto H. (NRLM, Japan)
Green K. (RAL, Oxford)
Grossmann J. (Univ. Osnabrück)
Harris P. (RAL, Oxford)
Iaydjiev P. (INRNE, Sofia)
Keller F. (UJF, Grenoble)
Liaud P. (LAPP Annecy)
Metz C. (Univ. Heidelberg)
Müller A. (TU Vienna)
Müller T. (Univ. Heidelberg)
Piboule M. (UJF, Grenoble)
Smith K. (Univ. Sussex)
Vatin-Perignon N. (UJF, Grenoble)
Van der Grinten M. (University of Sussex)

CRG

Kaufmann F. (PTB Braunschweig)
Nistler W. (PTB Braunschweig)
Weirauch W. (PTB Braunschweig)

Summary

At last the neutronless time of ILL can be regarded as history. With the neutrons, the normal scientific life of the College has restarted. All four instruments assigned to College 3 are operating in their normal mode. The cold polarised neutron beam facility PF1 as a new construction became operational at the beginning of this year and the major components of the project GAMS5, a high resolution gamma-spectrometer, were achieved.

The College was marked by the departure of its Senior Scientist Mike Pendlebury. Two Instrument Responsibles, W. Drexel and J. Last, left ILL. Two new Instrument Responsibles, V. Nesvizhevski and O. Zimmer, started their activities at PF1.

Four thesis students joined the College: T. Friedrichs (PN1), C. Stellmach (PF2) and M. Weber (PF2) as members, C. Doll (PN3) as external member.

Scientific Highlights in 1995

At PN1 Lohengrin

During the reactor shutdown period a modernization program on the PN1 spectrometer was completed with the help of our external user groups. In particular a new focusing magnet is now operating on the exit slit of the instrument and the high tension regulation was partly improved. The first cycle of the year was used to test the high tension stability with a fission fragment beam and the beam optics of the reconstructed spectrometer with inclusion of the new magnet. The measurements showed that the focusing magnet behaved according to the calculation. The new set-up, together with a new ionization chamber, proved to be especially useful for yield measurements in ternary fission. Here, during the year, the Tübingen group (F. Gönnenwein) completed measurements of heavy particles from tripartition for the compound system ^{241}Am(2n,f), and could detect nuclei at masses up to A = 35.

ILL-Munich (T. von Egidy) experiments concentrated on the search of fission yield of very exotic neutron-rich isotopes from ternary splits. From several fissile compound systems ^{11}Li and ^{14}Be could be detected, which are nuclei situated at the edge of nuclear stability near to the neutron drip line. Fig. 1 shows the ^{11}Li results in the reaction ^{239}Pu(n,f). The measurements shed light on the excitation for light charged particles emitted in the fission process. ^{11}Li is known to be bound by only 320 keV and is considered to be a halo nucleus where the last two neutrons occupy orbits located very far from the ^{9}Li center. If ternary particles were strongly excited during fission, ^{11}Li would decay before having left the target. The observation of a non-perturbed gaussian shape for ^{11}Li emission demonstrates that this is not the case. Our conclusions are that the heavier ternary

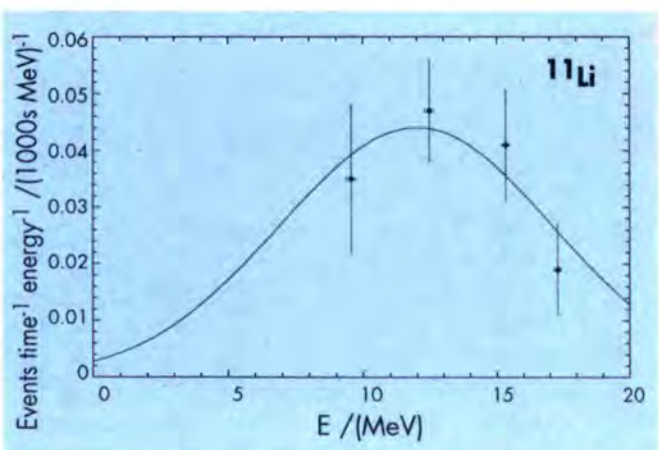

Fig. 1: Emission of ^{11}Li particles in ternary fission of ^{239}Pu(n,f)

particles are unlikely to stem from a neutron-rich region in a stretched configuration of the fissioning system, in which case they would contain considerable excitation energy.

To understand the ternary fission process on theoretical grounds, calculations were performed on the basis of the Boltzmann model, developed formerly for binary mass splits [1]. Under the assumption that the same fission mode is active for ternary and binary fission, the calculation of the yield of ternary particles can be performed almost parameter free [2]. It has been recognized, however, that a term describing the loss of pairing during the fission process in the case of light particle emission is very important. Fig. 2 shows the results for the system ^{236}U and demonstrates that the calculations perfectly reproduce the abundance of light charged particles. Similar agreement was found for other compound systems. A remarkable feature of the model is that the Coulomb-energy of the three-particle configuration has to be calculated from a compact scission configuration, and not a stretched one. This is in agreement with the above arguments for the observation of only low excited ^{11}Li fragments.

The investigation of the binary fission process for thermal neutron induced reactions, from a theoretical and experimental view point, continued during the year. The Boltzmann formulation of fission was applied to a couple of compound systems. In this model only a few terms aim at the description of yield from fission at low excitation energies. The relevant parameters entering into the calculations are the reaction Q-value, the Coulomb energy of two touching fragments, an energy term connected to a distinct fission mode, and some correction for loss of pairing correlations during the process. We calculated the yield of fission fragments from thermal neutron induced fission of 229Th and found the fission mode to be located at the same state as in 236 U, see Fig. 3. This observation points to a fission mechanism where fission modes are the same for a limited number of neighboring actinides.

On the experimental side, measurements on PN1 for binary splits were centered on the investigation of far asymmetric distributions from fission of ^{233}U(n,f), ^{241}Pu(n,f) and ^{245}Cm(n,f) (H. Faust, ILL,U. Keyser, Univ. Braunschweig). For this last compound system, fission around the most probable yield was also investigated. Former data from experiments on the Curium isotopes, done elsewhere, showed pronounced fine structure in the yield. The PN1 data do not confirm these measurements and demonstrate that results on yield in 246Cf fit nicely into a systematic where odd-even effects disappear when proceeding from 230Th to 250Cf (Fig. 4).

The installation of the focusing magnet made it possible to install a new He-jet system operating with aerosol clusters to collect fission products in an efficient way on the new focal plane (U. Keyser, PTB Braunschweig). The set-up was tested for different operating conditions: pressure, flow, cluster size and cluster density. Transport efficiencies of up to 80% have been recorded for specific fission products with transport times well below 1s. The new system will be used for spectroscopy of neutron-rich isotopes, especially in the region of refractory elements where no thermal ion source can operate.

Excitation and de-excitation of fission fragments were investigated on the basis of a statistical model description. The basic assumptions for excitation are that fission fragments are brought, at the very end of the fission process, to a nuclear temperature kT_f. From the calculations it was seen that this temperature can be assumed to be almost constant, independent of the actual mass split or the specific compound system. Applying standard statistical arguments, excitation and de-excitation of fission fragments were

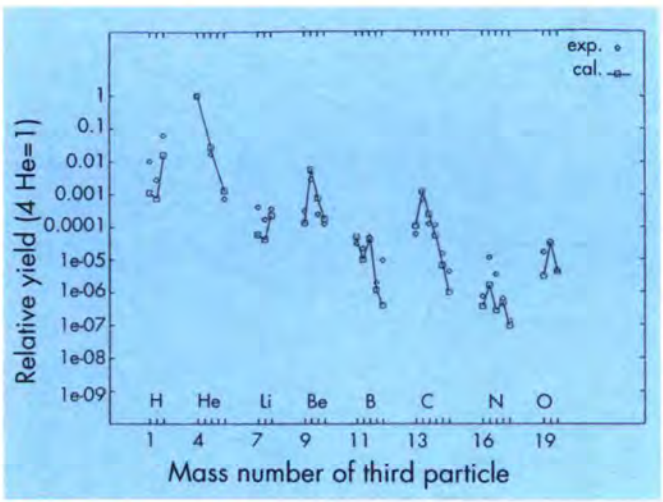

Fig. 2: Calculation of light particle yield from ^{236}U following thermal neutron capture. Squares with full line represent the calculated yields, rhombi represents experimental data.

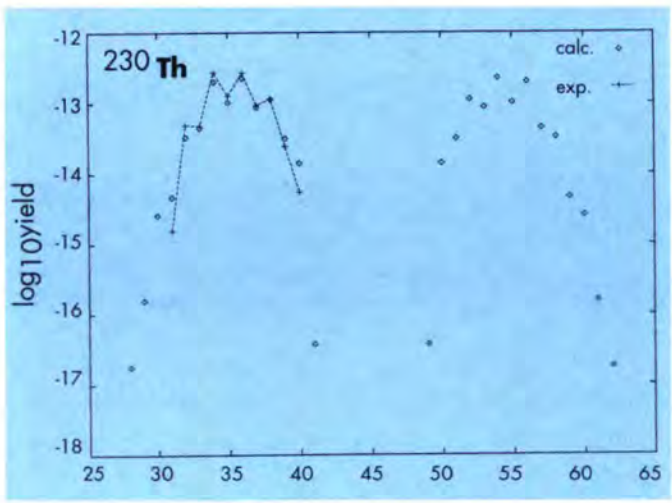

Fig. 3: Calculation of elemental yield for ^{230}Th(n,f) on the basis of Boltzmann model. Experimental data are shown by crosses connected by a dashed line. The calculations reproduce nicely the odd-even structure in the yield.

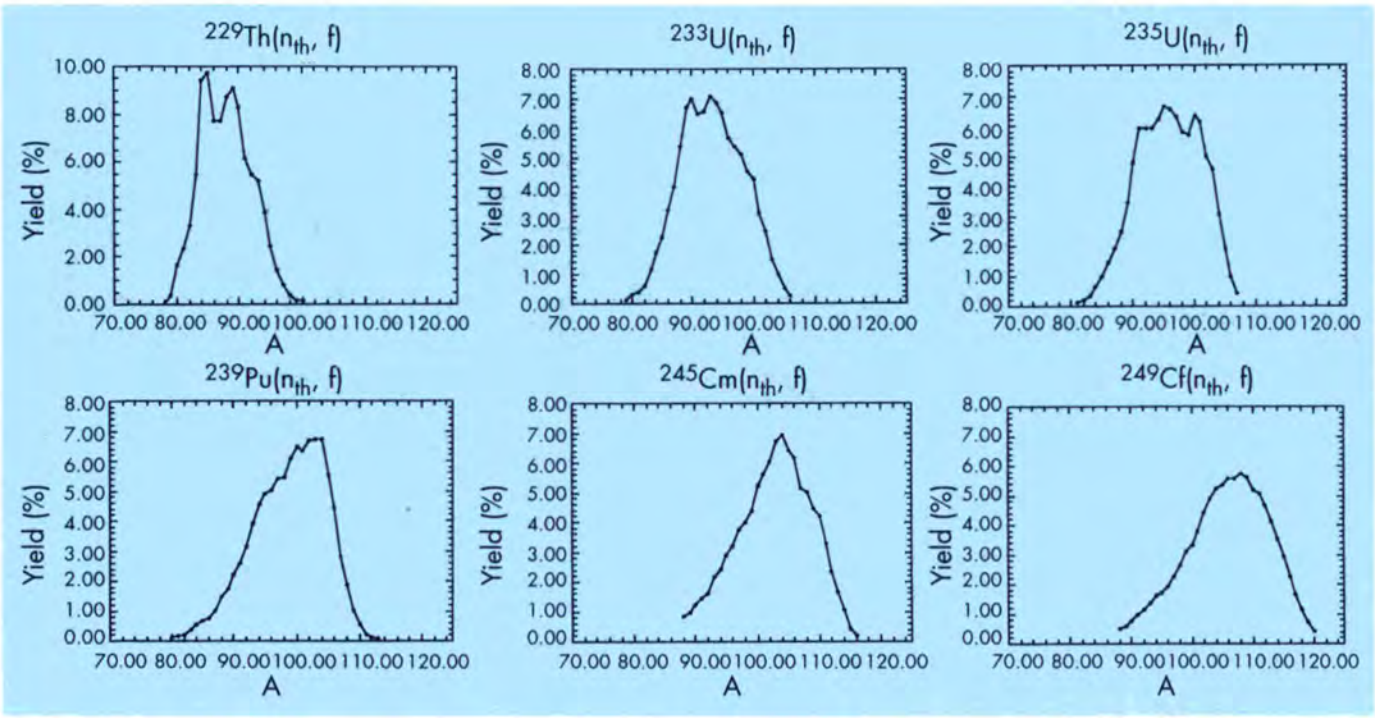

Fig. 4: Systematic of yield measurements carried out at Lohengrin for compound nuclei between ^{230}Th and ^{250}Cf. The decrease of time structure towards higher compound nuclei is clearly visible.

calculated. The resulting excitation energies and their systematic behaviour with fragment mass and compound nucleus mass are in agreement with the observations. The results for fragment excitation were used to investigate the de-excitation process of the fission products in a statistical model. It is assumed that de-excitation by neutron and gamma emission follows the pattern of the decay of an equilibrated compound nucleus. The results agree with a picture of decay where the entry state is depopulated by neutron emission and a few gamma quanta, with almost no loss of angular momentum. Once the Yrast line is reached, a couple of stretched E2 transitions lead to the ground state. The calculation showed values on γ and neutron-multiplicity, anisotropies and alignment of the decay products, and the population of high spin isomeric states can only agree with the experimental data when fairly high entry spins of about 6h to 7h are assumed. Examples for a selected mass split in ^{252}Cf-spontaneous fission are shown in Fig. 5.

At PN3 - GAMS

The physics emphasis on PN3 was centered on two principal areas of application of the GRID technique: the continuing attempt to understand the nature of vibrational states in deformed nuclei and the application of the GRID method (see also "blue box") to topics which allow one to study in detail the dynamics of atoms in solids.

An example of the nuclear structure measurements is given by ^{168}Er where previous experiments had shown [3] that the double gamma vibration in deformed nuclei is of a collective nature (by measuring lifetimes of the $J^{\pi} = 4^{+}$ and 5^{+} members belonging to the $K^{\pi} = 4^{+}$ band at 2055 keV). Now the interest was centred on the study of the nature of the low-lying $K^{\pi} = 0^{+}$ bands in this nucleus (J. Jolie,

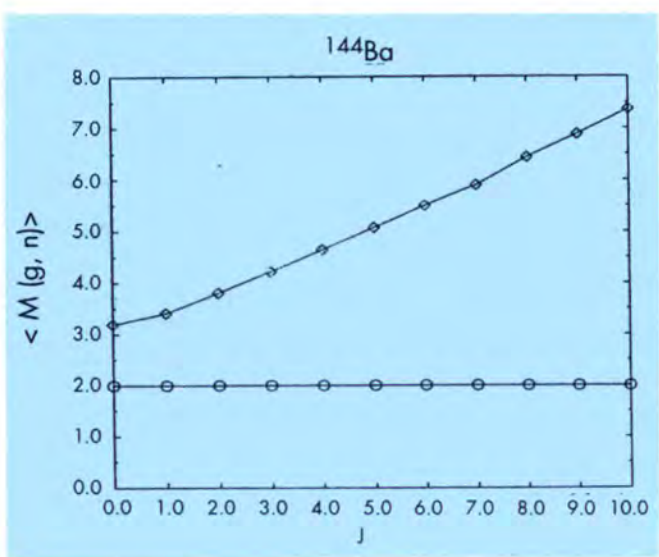

Fig. 5: γ- and n-multiplicities in the deexcitation of ^{144}Ba in dependence of the entry spin. Experiemental values are matched at spin I=6.

Fribourg, R.F. Casten, Brookhaven, H.G. Börner, ILL). Such studies are very important due to different theoretical interpretations of the so-called beta vibration: In ^{168}Er two low-lying $K^{\pi} = 0^{+}$ bands were observed. Whether these bands are related to the collective "beta vibration" is still an open question due to the lack of absolute transition rates for decays out of these $K^{\pi} = 0^{+}$ bands. Therefore lifetimes and/or lifetime limits for some of those states were investigated. The evaluation is currently in progress and quite tedious as these lifetimes appear to be relatively long (ps-region), situated at the limit of the GRID sensitivity.

The aim of the first Crystal-GRID [4] measurements was to prove experimentally the predicted dependence of the form of the measured lineshapes on the orientation of a single crystalline target with respect to the spectrometer, and to establish the sensitivity of the lineshape on potential and lifetime variations. For these reasons, the well-investigated 1498 keV transition of ^{49}Ti was chosen. The primary γ-quanta, resulting from transition from the 8142 keV capture state to the 3260 keV level, induce recoils with a kinetic energy of 261 eV. The Doppler broadening of the following γ transition to the 1762 keV level (E_{γ} = 1498 keV) was then measured.

For this study single crystals of SrTiO3, which exhibit the cubic perovskide structure, were selected. Simulations, carried out prior to the measurement, had shown the <100>, <110>, <111> orientations to be of interest experimentally. For the measurement of each crystal orientation, pairs of target crystals were used. For each orientation, one ligned pair was used, with both crystals placed one behind the other in the in-pile target facility, such that the orientation of interest was in the axis of view of the two-axis flat-crystal spectrometer GAMS4. The change of the target crystal orientation was realized simply by changing the targets. Fig.1 shows the first experimental results obtained with these crystals.

In the experiment cited above, the kinetic energy of the recoil is largely sufficient to allow the atom to leave its lattice site. In contrast to that, the recoil produced in K-capture in ^{152}Eu → 152 Sm delivers (due to the neutrino which leaves the nucles: p + e^{-} = n + ~) to the atom only about 3 eV of extra kinetic energy, such that the atom cannot leave permanently its lattice position allowing the response of the lattice to the desequilibrated atom to be directly studied. To this end we have studied (A. Kuronen, Helsinki, H.G. Börner, ILL, J. Jolie, Fribourg) the slowing down of 0.02 -eV/amu ^{152}Sm recoils in EuF_2, EuF_3, $EuCl_3$ and Eu_2O_3, produced in K-capture of ^{152}Eu. The Doppler broadened 842- and 963-keV γ-ray line shapes were simulated by molecular dynamics technique using empirically derived interatomic pair potentials. The results [5] show that the slowing down of the recoiling ion is sensitive to the potential well it experiences in the host lattice. Also, a strong dependence of the slowing-down of the ion on the charge state was observed. Fig. 3 shows the magnitude of the recoil velocity as a function of time. The attenuating oscillatory motion of the recoiling atom is clearly demonstrated.

At the cold polarized neutron beam facility PF1

The first two experiments this year at PF1 were devoted to studies of neutron beta-decay and can be considered as continuation of a scientific program which already has some tradition at ILL.

As the most elementary of the semi-leptonic weak hadron decays, the beta-decay of the free neutron, $n \rightarrow p + e^{-} + \bar{\nu}$, continues to represent one of the essential sources of experimental information about the structure of the weak interaction. Believing the V-A-theory to be the appropriate description of weak processes between quarks and leptons, the weak vector and axialvector coupling constants G_V and G_A may be extracted out of experimental data: measurements of neutron lifetime and beta-asymmetry (i.e. the ratio of probabilities for the decay electron to be emitted parallel or antiparallel to the spin of the decaying neutron) may be expressed as different functions of the ratio $\lambda = G_A/G_V$ from which the coupling constants themselves can be deduced and enter into a consistency check with experimental values from superallowed nuclear decays (see for example the overview [6]).

"In-beam" measurements of neutron lifetime presently seem to have reached their limit in obtainable accuracy (the required absolute neutron beam flux calibration is very difficult) and have been replaced by experiments with bottled UCN. So several research groups are now concentrating on beta-asymmetry and different angular correlations in cold neutron decay and have used the long reactor shutdown to prepare a new generation of dedicated experiments.

The first beam-time at PF1 was devoted to a precision measurement of the electron asymmetry coefficient A and allocated to the Heidelberg group of D. Dubbers for "PERKEO II", the successor of a well-known neutron decay spectrometer of the same name [7]. The main principle of this device is 4π-detection of the decay electrons by means of a strong magnetic field superimposed on a polarized neutron beam instead of using a 4π detector array: the charged decay particles gyrate along the magnetic field lines and eventually become detected by one of two scintillation detectors at which the field lines are pointing. The electron asymmetry shows up as a difference in countrates of these detectors when the neutron polarization becomes inverted relative to the magnetic field.

Compared to the old PERKEO set-up the new apparatus was designed to cope better with the main systematic errors within the measurement of A. The magnetic mirror effect, by which electrons may become reflected in a magnetic field gradient and thereby hit the "wrong" detector, has been reduced by use of a split pair superconducting coil which imposes a much more homogeneous transverse magnetic

field over the decay volume of the spectrometer. Background conditions were improved in this configuration by introducing a greater distance between the scintillation detectors and the beam. The third main systematic error is insufficient knowledge of the neutron beam polarization, which is a particular problem for supermirror polarizers. It was intended to reject this error well below the previously reached limit in the percent region obtained by the standard method, involving one analysing supermirror polarizer, which relies on the fact that the error in polarization is limited by the difference between its value and 100%. Different schemes exist for obtaining a more precise measurement involving two analysing supermirror polarizers. Discussions about which method should be applied for PERKEO II gave a clear picture of the specific problems of each method. A new method was invented and applied [8], which does not require any permutation of polarizers to remedy the inrealistic assumption that their polarizing efficiency remains exactly the same after changing their order in the beam.

PERKEO II has already successfully finished taking data. They now need to be evaluated in detail.

The second experiment by the Sussex group of J. Byrne at PF1 is still under way. Instead of looking at the decay electrons, it focuses on the protons: the aim is to get for the first time a value of λ by measuring the asymmetry in the emission direction of the decay protons relative to the neutron spin. The experiment also involves 4π detection via a strong magnetic field. As the maximum kinetic energy of the decay protons is lower by a factor of 1000 compared with the decay electrons, detection of the protons is more sophisticated and involves application of a strong electric field of about 30kV to accelerate them onto a surface barrier detector in order to pull the signal out of thermal noise. A very good vacuum is required to avoid electrical breakdown. An ingenious method has been invented to fully get rid of the magnetic mirror effect for the decay protons. It is based on the fact that one can reflect them by an electrostatic potential of only 1kV [9]. The experiment is just beginning to take serious data and will continue until the end of the first cycle in 1996.

At the Ultracold Neutron (UCN) and Very Cold Neutron (VCN) Facility PF2

Even though very shortly after the restart of the reactor and the inevitable and detailed safety checks of the different experimental installations at the PF2 facility, the first users arrived and an extensive, versatile and ambitious research program came successfully into operation, last year was above all marked by staff departures: after nearly a quarter of a century of remarkable and loyal duties in different important positions at ILL, Winni Drexel left at the end of November. With the departure of Mike Pendlebury in September, we lost not only a distinguished and very collaborative physicist but also the institution of "Senior Scientists" is now part of the Institut's history.

The major research topics with UCNs are the electric dipole moment (EDM) and the lifetime of the free neutron, while VNCs are used for interferometry.

For particles to have EDMs, the forces concerned in their structure must be asymmetric with regard to space-parity (P) and time (T). P-violation is a well-known intrinsic feature of the weak interaction, but CP- (and hence T-) violation, which is believed to be responsible for the baryon asymmetry of the universe, has so far been found only in the neutral kaon system. Such limited information leaves open a wide range of possibilities for competing theories attempting to explain the origin of T-violation. Experimental measurements of particle EDMs, and in particular that of the neutron, are providing one of the strongest additional constraints on these theories. The Standard Model of the electroweak interaction gives a contribution to the neutron EDM of the order of 10^{-31} to 10^{-33} e·cm, while the most recent result from our Sussex-RAL-ILL-Harvard-Washington-collaboration (M.J. Pendlebury, K. Smith, K. Green, P. Geltenbort, N. Ramsey, B. Heckel,. S Lamoureaux) is $(3\pm2\pm4)\times10^{-26}$ e·cm. However, extensions to the Standard Model, such as additional Higgs Fields, right-handed currents or supersymmetric partners, give rise to larger dipole contributions which are in the order of 10^{-25} to 10^{-27} e·cm. That is why our collaboration is trying to improve upon this critical measurement. To achieve this, significant changes have been made to the hardware, and we are now once again on the verge of data taking. Amongst other things it may be noted that a new, large storage cell, machined in Russia from a single fused quartz boule has been installed for both the neutrons and the polarised mercury atoms from the magneometer. Using this bottle, the first ever co-storage of hot polarised atoms with ultracold polarised neutrons has been demonstrated, and excellent spin relaxation times of 170 s for the neutrons, and over 200 s for the mercury have been achieved. The most important milestone, however, has been the convincing demonstration that the resonant frequencies of neutrons and mercury follow one another as the magnetic field drifts. This allows the measured precession frequency of the mercury atoms to be used to calculate the expected (i.e. zero EDM) frequency of the neutrons on a cycle-by-cycle basis, and then the neutron counts to be fitted to a "mobile" Ramsey lineshape which moves in the appropriate way as the magnetic field drifts (e.g. if the big crane on level D is in action). This is shown in Fig. 6. The net effect is to fit the ratio of the two precession frequencies; it is this ratio which will be directly sensitive to the neutron EDM.

It is believed that by these upgrades the systematic errors will now contribute only about 2×10^{-27} e·cm to the uncertainty of the measurement of the neutron EDM, and that several years' running will be needed before the statistical uncertainty can be reduced to a comparable level.

The accurate measurement of the free neutron beta-decay lifetime (τ_β) allows one to determine parameters of the electroweak interaction, which in combination with other

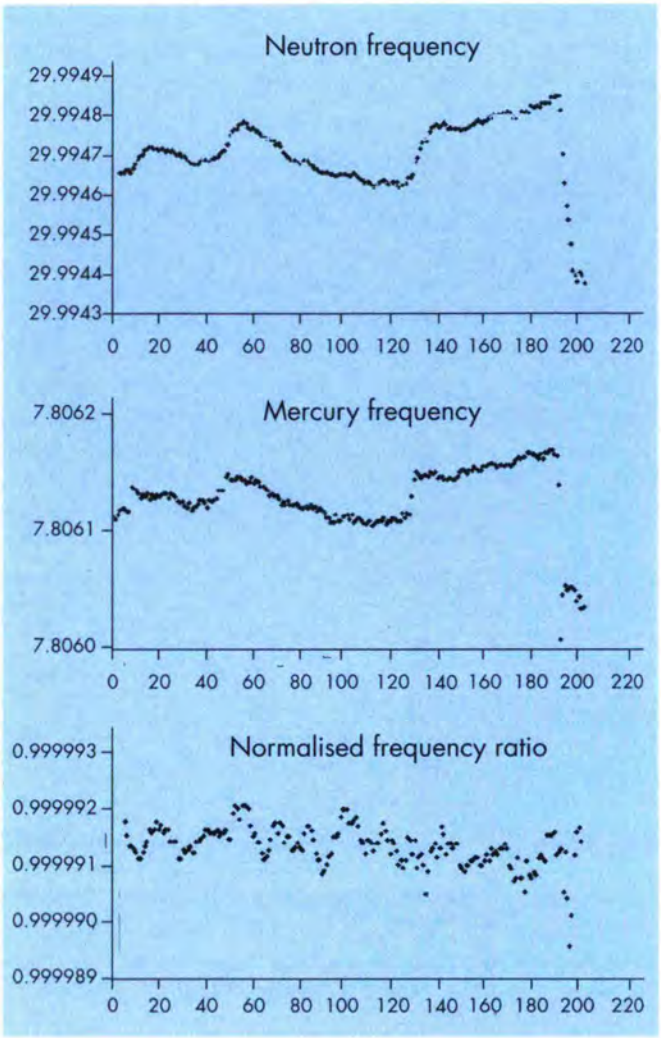

Fig. 6: Graphs showing how the precession frequencies of neutrons and mercury change as the magnetic field drifts. Each point represents a counting time (cycle of approximately 3 minutes). The point-to-point fluctuations are seen in the mercury by a 4-cycle integration period. The ration of frequencies (normalised to the ratio of gyromagnetic ratios) stays constant to within a few parts in 10^7, corresponding to field shifts at the nanogauss level.

exprimental data can provide a test of the Standard Model. Additionally, a precise knowledge of τ_β is important for questions concerning particle physics, neutrino induced reactions and cosmology. E.g. in the cooling of the big bang fire ball τ_β influences the relative amounts of ^{2}H, ^{3}He and ^{4}He produced compared to ^{1}H; the longer the free neutron lives, the more there is of the heavier species compared to ^{1}H. The calculated ratios using experimentally determined τ_β can be compared with the measured ratios from astronomical observations.

For these reasons several collaborations are continuing their efforts to try to measure in storage experiments using UCNs the lifetime with an overall precision smaller than 1 s (about 0.1 %). The first experiment was performed by

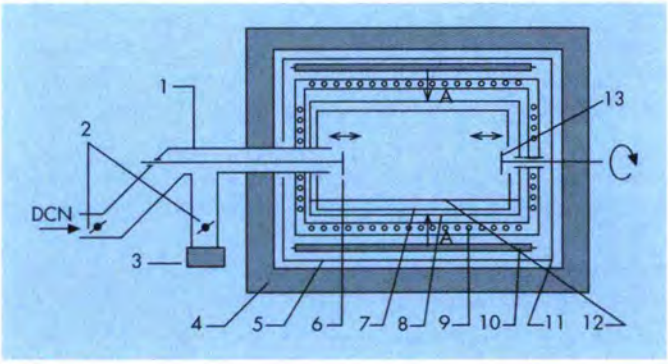

Fig. 7: 1 - UCN guide, 2 - shutters, 3 - UCN detector, 4 - polyethylene shielding, 5 - cadmium housing, 6 - plate shutter, 7 - inner storage vessel, 8 - outer storage vessel, 9 - cooling coil, 10 - thermal neutron detector, 11 - vacuum housing, 12 - oil puddle, 13 - plate shutter.

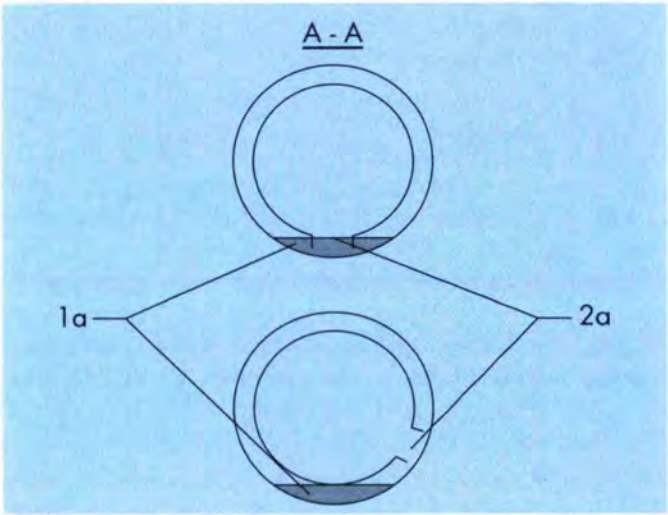

Fig. 8: 1a - oil puddle, 2a slit.

L. Bondarenko, V. Morozov, RRC Kurchatov Institute, Moscow, W. Drexel, P. Geltenbort, ILL. Its experimental set-up is shown in Fig. 7 and Fig. 8. In this approach not only are the number of UCNs at the beginning and at the end of a storage cycle measured but also the number of up-scattered (and therefore lost) UCNs at thermal energies during the storage cycle. The storage vessels had walls of Al coated (refreshable) with Fomblin oil. Moveable plate shutters made it possible to change the wall surface area exposed to the UCNs, and hence the number of collisions of UCNs with the walls. Besides changes of surface area, measurements were carried out at room temperature as well as at -8°C and -26°C. For each choice of surface area and each temperature, an independent set of data was obtained which, when combined, yields the lifetime. The statistical precision achieved is about 0.8 s while the final value of τ_β will be obtained after a careful analysis of possible systematic errors based on additional test experiments.

Crucial and common to all types of storage experiments with UCNs using material walls is the reduction of wall losses and as good an understanding as possible of the

underlying physics for later corrections to the experimentally determined number of surviving neutrons. Two different experiments have aimed at a better understanding of these loss mechanisms, especially in the case of a Be-surface. A RRC Kurchatov Institute - ILL collaboration used neutron activation analysis, following the capture of UCNs, to analyse the isotopic content of the surface at room temperature. The use of a high resolution Ge-detector close to the sample under investigation made it possible to distinguish captured UCNs by the characteristic γ-energy of the corresponding (n, γ)-reaction from up-scattered UCNs, which are determined by 477 keV gammas from ^{7}Li. Additional UCN detectors allowed finally the determination of the different loss factors. For the UCN-Be interaction a preliminary upper limit of the loss factor of 1.5×10^{-6} per reflection from the surface has been determined while the theoretical one is about 2×10^{-7}. In a PNPI (Gatchina) - JINR (Dubna) - ILL collaboration (A.P. Serebrov, A.V. Strelkov, P. Geltenbort, V. Nesvizhevsky) a prestorage volume is used to determine the UCN spectrum before they interact with an enlarged Be-surface which can be cooled down by means of liquid nitrogen. UCNs and up-scattered UCNs are detected in gaseous ^{3}He-detectors with variable ^{3}He pressure and, hence, variable detection efficiencies for up-scattered (i.e. thermal) neutrons. This experiment is still at the data taking stage.

For the sake of completeness two more experiments have to be mentioned which are being carried out in collaboration with Heidelberg (H. Abele, D. Dubbers, C. Stellmach, P. Geltenbort), and which are both still in an initial stage.

The first one looks for anomalous spin precession. With UCNs this effect can only be controlled in a spin-echo type set-up, as UCNs are difficult to monochromatize and, in a high magnetic field, make many precessions even over short distances. A spin-echo signal, however, can be measured using a broader velocity distribution and is nevertheless sensitive to small differences in the precession frequency.

The second experiment looks for coherent effects with UCNs in disordered media. The backscattering of neutrons is expected to be enhanced by up to 100 % within a narrow cone centered on the backscattering direction.

The VCN beam position is for the time being exclusively used by A. Zeilinger (Innsbruck), R. Gähler (Munich), W. Drexel, P. Geltenbort, M. Weber (ILL) for VCN interferometry. The interferometer consists of three quartz plates with etched phase gratings with 500 lines per mm, which can in principle be seperated by a distance of up to 2 m, thus allowing a Mach-Zehnder interferometer to be built for neutrons with an overall length of up to 4 m. It uses just a small part of the VCN beam which is reflected by a Ni-coated mirror at an angle of 10° to cut off neutrons faster than 40 m/s. As for all interferometers, vibration isolation is one of the keystones for precise and reproducable results. After a major redesign during the reactor shutdown the instrument is again operational and interference fringes with a visibility (contrast) of about 26% could already be observed. In these measurements one of the three gratings has to step tilt-free horizontally about 1 mm in steps of several tenths of a micron. For this purpose a prototype of a translation stage without the usual ball bearing mechanism but elastic metal junctions serving as hinges has been constructed. Initial tests show very promising results.

It should be pointed out that on request a bender which consists of a stack of refelecting curved Ni-coated glass plates can be placed beside the above-mentioned Ni mirror. It serves as a side deviator of the VCN beam and branch off half of the beam for other experiments using VCNs with a cut-off wavelength of about 60 Å.

Another Innsbruck - Munich - ILL collaboration (A. Zeilinger, J. Felber, K. Raum, P Geltenbort) measured the effective mass enhanced deflection of neutrons by gravity inside an Si-crystal. This is one of the few experiments which, for its interpretation, involves both quantum mechanics and the equivalence principle of relativity theory. The experiment was not carried out at one of the standard fundamental physics installations but at the instrument T13A (merci!) as monochromatic neutrons with wavelengths around 2.35 Å were needed. The set-up consists of two silicon single crystals on a common base cut from one crystal, several diaphragmas and a position-sensitive neutron detector. As the experiment is extremely sensitive to a bending of the crystal under its own weight it was placed in a fluid of equal density. As shown in Fig. 9 a deflection as high as ±4.7 mm was observed due to the minute effective mass of a neutron propagating under diffraction conditions in a crystal. This deflection is enhanced by more than 5 orders of magnitude over the expected deflection in free space. A remarkable feature of the experiment is that there are two effective mass states inside the crystal, one with a positive and one with a negative effective mass. The

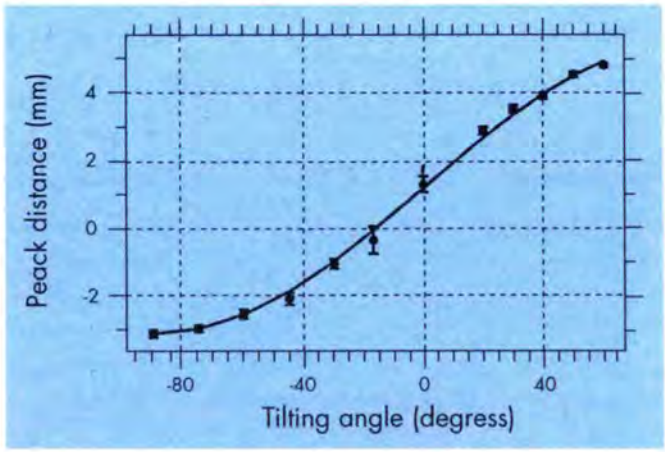

Fig. 9: Deflection as a function of the tilting angle. The deflection at zero tilting angle is caused by prism refraction of slightly missaligned walls of the container for the fluid and an intrinsic bending of the crystal, which was also observed in former experiments with the same crystal.

neutrons with a negative effective mass fall upwards. Furthermore, experiment and theory agree within the errors of about 1.5 %.

At PIAFE

The project at Grenoble/France aims at the production, ionization and acceleration of exotic isotopes using an in-pile fission source at the ILL High-Flux reactor. Phase-1 of the project deals with the fission source, the extraction of the neutron-rich isotopes and the mass separation. In a second step a planned Phase-2 comprises the beam transport to the nearby 'Institute des Sciences Nucleaires' and the acceleration of the ions to energies above the Coulomb barrier.

In autumn 1995 the PIAFE collaboration submitted a first technical report to ILL to be examined by the services concerned, the reactor and the technical divisions. The report contains already detailed investigations concerning heat charges and temperatures on different in-pile parts located in a neutron flux of $3 \cdot 10^{13}$n/cm·s, and reactivity responses of the source on the reactor. In parallel to the calculations, experimental tests are under way investigating the behavior of source confinement by a rhenium envelope under various conditions and isolators at high temperatures. For the beam line design and mass separators situated in the reactor hall, optical calculations are now available allowing the most suitable implantation scheme to be chosen.

The project was presented to the Scientific Council (SC) at its spring and autumn meetings. On the basis of the report 'PIAFE project-Physics case' (Lecture Notes in Physics, in print), the reports of three referees, and following extended discussions, the SC recommended to proceed with studies on the technical implantation of the source. The item was taken up in the November meeting of the ILL Steering Committee, which authorized the collaboration between ILL and PIAFE organisation for this project study, it being understood that the realisation of the project will require a further formal decision.

At the beginning of 1996 the collaboration is convened to Grenoble to discuss the organisational aspects of the CRG (collaborating research group) which has to be established, and to coordinate further steps of fund raising at national level.

At the S10 facility

During the past decade, several (n,p) and (n,a) reactions of importance to stellar nucleosynthesis have been investigated (C. Wagemans, P. Geltenbort) with thermal neutrons at the S10 position in ILL and with resonance neutrons at the linear accelerator facility GELINA at the IRMM in Geel, Belgium. These measurements are very complementary as illustrated in the neutron induced reactions of ^{36}Cl and ^{41}Ca.

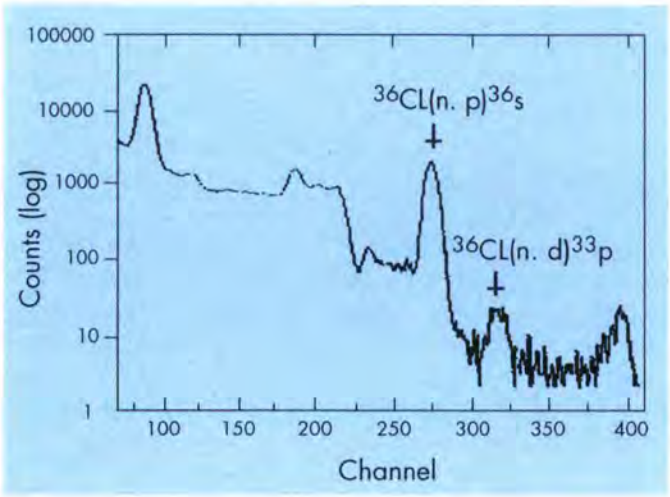

Fig. 10: Pulseheight of the ^{36}Cl(n,p) and (n,α) reactions.

The ^{36}Cl(n,p) ^{36}S reaction is one of the keys to understanding the abundance of the very rare isotope ^{36}S in terms of nucleosynthesis processes. Shortly before the reactor was shut down in 1991, its thermal cross-section was determined accurately to (47±2) mb. In the meantime, this reaction has also been studied with resonance neutrons, revealing the presence of a significant (n,a)-component in some of the resonances. This is a hint at a non-neglible thermal ^{36}Cl(n,a)^{33}P cross-section. Using a suitable experimental set-upat S10 and AgCl targets enriched with ^{36}Cl it has been measured in the last experimental campaign to be (0.59±0.07) mb and a typical pulseheight spectrum is shown in Fig. 10.

In the case of ^{41}Ca, however, prominent a_0 and a_1 transitions, but no (n,p) transitions were observed with thermal neutrons in previous experiments. Again the detection of a significant (n,p)-component in some resonances pointed to the existence of such thermal (n,p) transisitons. In a recent experiment we found that these 1.2 MeV protons were completely hidden in the tail of ^{10}B(n,a)-background particles. With a special set-up a preliminary value of (7±1) mb for the ^{41}Ca(n_{th},p) cross-section has been determined.

At S50

The investigation of the quotient h/m_n was continued. The experimental set up is described in [10]. From h/m_n the value of the fine structure constant α can be derived. The value of h/m_n measured so far leads to α^{-1} = 137,03601082(524) [10].

At the S51-INAA facility for geological studies

Activity by the geology fraction (M. Piboule, UJF, Grenoble) has been somewhat curtailed this year due for the most part to the fact that R. Oliver presented a thesis at the University Joseph Fourier, Grenoble, entitled "The geology and geochemistry of the intrusive rocks of the Valsenestre region, and their context within the magnetic province of the Haut Dauphiné". However, analysis performed in the previous year allowed the completion of on-going studies, notably of the Permian Island arc of the Briançonnais.

Secretary: Ulrich Mayerhofer

References

[1] H. Faust, Proceedings of the Seminar on Fission, Pont d'Oye III, May 1995

[2] Faust and Z. Bao, Proceedings of the Seminar on Fission, Pont d'Oye III, May 1995

[3] H.G. Börner et al., Phys. Rev. Lett. 66 (1991) 691

[4] M. Jentschel et al., NIM B, accepted for publication

[5] A. Kuronen et al., Phys. Lett. B

[6] J.Byrne, Physica Scripta, Vol T59, 311-322, 1995

[7] J.Döhner et al., Nucl. Instr. Meth. A284 123-126, 1989

[8] S.Bässler et al., to be published

[9] J.Byrne et al;, to be published

[10] E. Krüger, W. Nistler and W. Weirauch, Metrologia, 1995, 32, 117-128

Crystal-GRID: A new method for the investigation of atomic interaction in solids

Michael Jentschel

The question of atomic interaction in solids at energies below 1 keV has become more and more relevant for a number of experimental techniques, like for instance the ion beam modification of materials or the measurements of nuclear state lifetimes. The GRID (**G**amma **R**ay **I**nduced **D**oppler-broadening) method gives a unique opportunity to compare the measured effect, which is directly related to the interatomic potentials in solids, to simulations.

In 1995 a very important step in order to improve the GRID method applied to the investigation of interatomic potentials in solids has been done: For the first time there were carried out Crystal-GRID experiments using single crystalline targets.

The GRID method [1] uses the fact that, following neutron capture, a recoiling excited nucleus is produced by emission of a high energetic primary γ-quanta γ_1. The recoil velocity is determined by momentum conservation:

$$v_o = E^0_{\gamma_1} / Mc, \qquad (1)$$

where $E^0_{\gamma_1}$ is the energy of γ_1, M the mass of the nucleus and c the velocity of light. The recoil energies are in the order of 10 eV up to 1000 eV, depending on the mass and $E^0_{\gamma_1}$. The atoms loose this energy by collisions with the surrounding lattice atoms and are thermalized within a certain time. Meanwhile the still excited nuclei continue to deexcite by secondary γ_2 emission, where the emission probability is defined by the lifetime τ of the intermediate nuclear state, being populated by the γ_1 emission

$$P_{\gamma_2} = \frac{1}{\tau}\exp(-t/t) \quad . \quad (2)$$

Since these quanta are emitted in flight, their energy is Doppler shifted in a laboratory system

$$E_{\gamma_2} = E^0_{\gamma_2}\left(1+\frac{\vec{v}(t)\vec{n}}{c}\right) \quad (3)$$

where $\vec{n}$ is a unit vector parallel to the axis of observation (spectrometer axis). The measurement of γ_2 leads to a Doppler-broadened line shape, the intensity distribution of which is given by

$$I(E)dE = \sum_i \int_o^\infty dt\ \exp(-t/t)\,\delta\left[E-E^o_{\gamma_2}\left(1+\frac{\vec{v}_i(t)\vec{n}}{c}\right)\right]dE \quad (4)$$

where $v_i(t)$ is the velocity of the i-th recoiling atom at time t The time t is counted after each recoil moment and the summation is done over all obtained recoil events.

The main advantage of using single crystalline targets is, that the measured line shape contains all available information on both, the lifetime (nuclear time scale) and the slowing down (atomic time scale). In the case of polycrystalline targets one has to average over all $\vec{n}$ and only an effective slowing down velocity $\langle v(t) \rangle$ enters. Therefore in this case important information on the slowing down is lost, but on the other hand the extracted nuclear lifetimes do not depend so strongly on details of the potentials.

For single crystalline targets the projection $\vec{v}(t)\vec{n}$ depends on the alignment of the target with respect to the spectrometer axis. This results in different line shapes for different target-spectrometer alignments. Each of these line shapes has a characteristic structure, which is more sensitive to the details of the potentials than the line shapes from polycrystalline targets. This has been shown by MD-simulations of the recoiling atoms and calculations of line shapes using (4) [2].

The first Crystal-GRID measurements, carried out in 1995, had the aim to prove experimentally the predicted dependence of the line shapes on the spectrometer-target alignment. Further they allow to establish criteria on resolution and intensities needed to be sensitive to interatomic potentials. For this purpose it was decided to use a nucleus, which is well investigated from the nuclear physics point of view. As an good candidate ^{49}Ti was chosen, the level scheme of which is shown in Figure 1. The lifetime of the 3260 keV state has been carefully studied by a row of GRID measurements with different chemical compounds and the value of $\tau = 17.5^{0.8}_{1.7}$ fs was adopted [3]. The level is populated to 95% by a primary γ-transition from the capture state, leading to a sharp distribution of the recoil energies around 261 eV. The 1498 keV line, depopulating this level, is strongly Doppler-broadened due to the short lifetime and the strong recoil. Further the 1498 keV transition induces again a recoil to the nucleus which leads to a Doppler broadening of the subsequently emitted 1768 keV line. The moment of this second recoil depends on the lifetime of the 3260 keV state, and consequently this 1762 keV line may be used as a secondary test, whether or not the Doppler broadening of the 1498 keV is well understood. As the target compound $SrTiO_3$ was chosen, crystals of which are commercially available. For them the <100>, <110> and the <111> directions were expected to show strongly different structure.

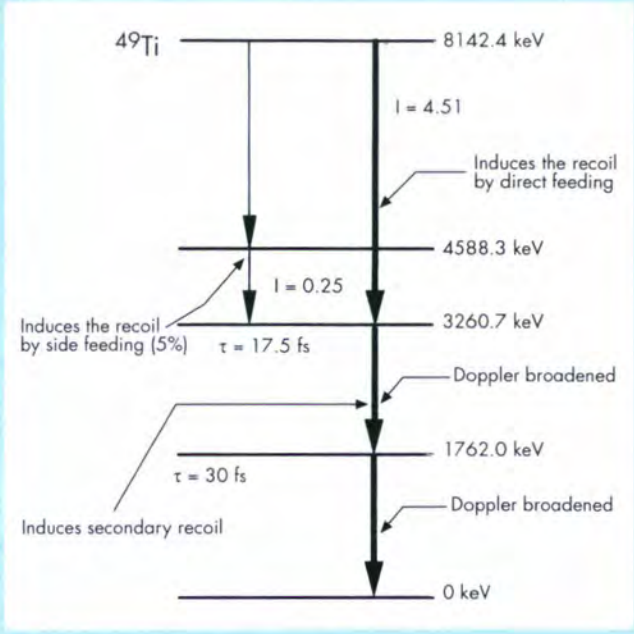

Fig. 1: Nuclear level scheme of ^{49}Ti after thermal neutron capture. The 3260.7 keV level is mainly feeded by a strong primary transition, wich results in a nearly monoenergetic recoil of the excited nucleus. The lifetime of this state is expected to be short enough to measure a strong Doppler-broadening of the 1498 keV transition.

The experimental result of the 1498 keV line for the <100> and the <111> directions are shown in Fig. 2, together with the instrumental response function (dashed line). A comparison of both line shapes shows clearly that the predicted dependence on the crystal direction could be verified experimentally.

A first comparison of the experimental data to profiles resulting from MD-simulation has been done. Here two approaches were used, which give a first idea of agreement/ disagreement in between simulation and experiment: One way is to use a potential, fitted to reproduce in simulations the equilibrium properties of solid $SrTiO_3$ and then to extrapolate it to higher energies. The other way is to take potentials, valid for high energetic collisions (> 1 keV), successfully used in simulations of high energetic ion-solid interaction and to extrapolate them to lower energies. The extrapolations might be in both cases only bad approximations, but they give a starting point to correct the potentials in such a way that they describe the behaviour from lower up to very high energies correctly.

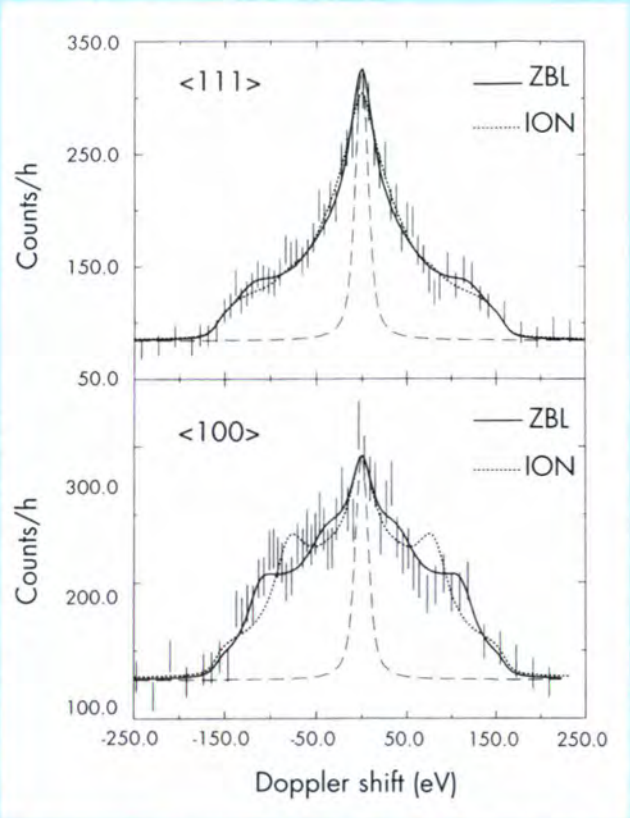

Fig. 2: The measured lineshapes of the 1498.keV obtained from the <111> and the <100> directions of single crystals of $SrTiO_3$. The thick solid and dotted lines result from MD-simulations of the recoiling ^{49}Ti atoms based on the ZBL- and a ionic potential, ION, respectively. ION does clearly not reproduce the data for the <100> direction. The dashed line corresponds to the instrumental response function.

For the first approach a potential developed by Kawamura et.al. [4] was used, which gives correct atomic positions and elasticity constants of $SrTiO_3$ in MD simulations. This is an ionic potential with Born-Mayer repulsion, which describes the low energy behaviour, but has not been tested for higher energies. The best fit to the experimental data from a simulation with this potential results in lifetimes τ = 5.4±0.6 fs for the <100> and τ = 8.6±1.1 for the <111> directions, respectively (Fig. 2, thick dotted line). It is evident that these values are by far shorter than the adopted value. From that one can conclude that the repulsive part of the potential is too steep above 10 eV.

In the second approach one assumes that during the time scale, which is relevant for the slowing down, the lattice appears to be static for the recoiling atom. That means that the binding part of the potential and the dynamic of the surrounding lattice is less important for the slowing down. In this case it is sufficient to calculate the full collision dynamics only in a close sphere surrounding the recoiling atom. Only this approximation enables one to use pure repulsive potentials, resulting from Hartree-Fock or similar calculations [5] of neutral atom pairs. Line shape fits to the experimental data based on such simulations are shown in Fig. 2 as a thick solid line. The corresponding lifetime values are τ = 12.8±1.2fs and τ= 17.2±1.3fs for the <100> and the <111> directions, respectively. These values are in much better agreement with the expectations, but they are still too different for each direction.

Exactly this fact must be used as the basic criterion for the further modification of the potentials, since the lifetimes must be the same for arbitrary directions. As free parameters for the modification one should use in a first step the ionic charge number of the recoiling atom and the corresponding screening length of the electron cloud. This is motivated by the fact, that the Ti-atom has an ionic charge number of *+4* before the recoil happens. This enters also in the potential of Kawamura. However, as the simulation seems to indicate, a neutral atom gives better results. The question of charge transfer during the recoil acceleration and/or during further collisions is a point, which has now to be further investigated by this method.

As additional criteria for the potential study the agreement/disagreement of the line shapes resulting from correlated fits of all measured directions can be taken.

Once the potential is determined such that all lifetimes are equal for arbitrary directions, one will have extracted the lifetime and the potential from the same target. This is a qualitatively new step in the GRID-technique.

References

[1] H.G.Börner, J.Jolie, J.Phys.G: Nucl. Part.Phys. 19 (1993) 217-248

[2] K.H.Heinig, D.Janssen, ILL Internal Report 92HGB16T

[3] A. Kuronen, J. Keinonen, H.G.Börner, J.Jolie, S. Ulbig, Nuclear Physics A549 (1992) 59-83

[4] K. Kawamura in F. Yonezawa 'Molecular Dynamics Simulations' Springer Series in Solid State Science 103

[5] F.J. Ziegler, J.P. Biersack and U. Littmark, The Stopping and Ranges of Ions in Matter Vol1, New York Pergamon, 1985

Structural and Magnetic Excitations

Members of the College

Internal members

K. Andersen
T. Baumbach
J. Bossy
T. Chattopadhyay
R. Currat
Ch. Doll
B. Dorner
B. Fåk
B. Farago
W. Henggeler
M. Johnson
J. Kulda
H.J. Lauter
A. Magerl
G. McIntyre
A.P. Murani
H. Mutka
S. Pouget
N.M. Pyka
O. Randl
H. Requardt
B. Roessli
J. Saroun
O. Schaerpf
W. Schmidt
H. Schober
C.M.E. Zeyen
M. Zolliker

External members

M. Alba (CENG)
G. Dolino (UJF)
C. Filippini (CNRS)
P. Monceau (CNRS)
L.P. Regnault (CENG)
M. Vallade (UJF)
Ch.Vettier (ERSF)

Introduction

The early starting of the reactor meant that, for the first two months of this year, the attention of all the instrument staff was focused on testing the instruments and aligning the spectrometers and all the equipment, electronics and new software under 'real' conditions. This commissioning phase was successfully completed within the time schedule for almost all instruments, and scheduled experiments from the proposal round in October 1994 began end of February. Considerable time was also spent to make some crucial improvements to safety aspects. During this first year of renewed reactor operation, most ILL scientists in the College were unable to spend as much time as they would have wished on their own scientific interests, since they devoted considerable efforts to removing many of the 'bugs' occurring during operation of the instruments. The aim was to achieve further progress in increasing the power of the instruments and support external users, helping them to make their stay a most successful one.

During the past three proposal rounds, College-4 instruments have attracted an increasing number of proposals of high and, in some cases, excellent quality covering exciting new subjects as well as more traditional ones. The proposed experiments on the triple-axis and time-of-flight instruments ranged from general spin and lattice dynamics to magnetism in high-T_c and classical superconductors, heavy fermions in Uranium compounds and rare-earth cuprates, critical scattering at phase transitions, magnetism in non-Fermi liquids, the inorganic Spin-Peierls system $CuGeO_3$,which was programmed on several instruments, fullerenes (C_{60} molecules and related compounds) and quasielastic scattering. The spectrometers were heavily overloaded, with excess demand at a factor of 2-4. In particular demand were the cold neutron TAS and TOF instruments. Some results are presented below.

We have had the pleasure of welcoming some new scientists, among them CRG instrument responsibles. Herwig Requardt already started his thesis work at the end of 1994 in the TAS-group in collaboration with the CRTBT. Markus Zolliker, PSI-Würenlingen, joined in October 1994 as the Swiss responsible for CRG-IN3. Wolfgang Henggeler, PSI-Würenlingen, started his thesis work in January 1995. Wolfgang Schmidt, from ISIS, took responsibility for the German (KFA-Jülich) CRG-IN12 in August 1995. His coresponsible is Björn Fåk (CENG). Subsequent to some shorter stays, Ian Saroun, University of Prague, joined us in September for a two-year stay. He is in charge of the installation and development of dedicated resolution programs for focused neutron beams and of neutron optical elements on IN20.

Magnetic excitations in a half-metallic ferromagnet: NiMnSb

Spin wave measurements have been carried out [1] on the semi-Heusler ferromagnet NiMnSb (T_c = 730 K), using the IN8 spectrometer over a wide range of energy transfers (1 - 70 meV).

Band structure calculations [2] indicate that in the ordered state of NiMnSb the electronic Fermi level falls in a gap of the minority spin (down spin) density of states. Thus only electrons with up spins are present at the Fermi level, a situation referred to as a "half-metallic"state. As a consequence of this, the single-particle excitation spectrum (Stoner continuum) is expected to exhibit a temperature-dependent low-frequency gap.

The low-temperature magnetic excitation spectrum of such a system is thus characterised by gaps in both the collective spin wave spectrum (the usual anisotropy gap) and a gap in the single-particle spectrum. Direct information on the magnetic excitation spectrum by inelastic neutron scattering is thus essential in order to understand the macroscopic thermal behaviour of the compound (magnetisation, resistivity, magnetoresistance).

Fig. 1 shows a summary of the room temperature results for the magnon and phonon dispersion curves. The anisotropy gap, not visible in the figure, is estimated at 1.0 ± 0.2 meV. The observed magnon lineshapes broaden dramatically above 50 meV, due to the interaction of the

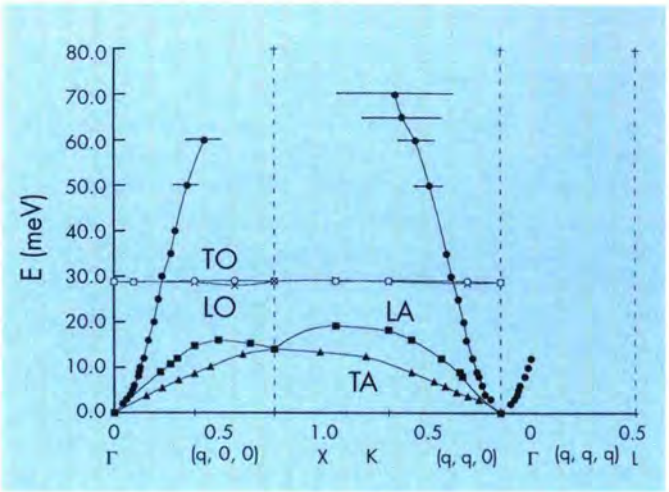

Fig. 1: Room-temperature phonon and magnon dispersion curves in NiMnSb. Magnon widths, as observed in constant-E scans, are shown as horizontal bars. Above 50 meV these widths are much larger than the instrumental widths.

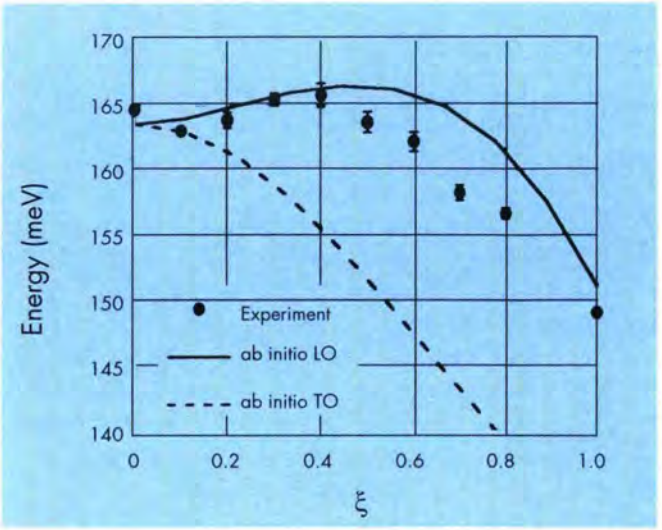

Fig. 2: Observed and calculated [100] LO phonon frequencies in diamond.

spin waves with the Stoner continuum. This result is at variance with the value of the Stoner gap (150 meV) estimated from band calculations. Additional measurements at higher energies and at higher temperatures are in preparation.

Optical phonons in diamond

The lattice dynamics of the group IV elements (and of the III-V compounds) provides important tests for the *ab initio* computational methods permitting the calculation of the band structure and of the lattice properties of the crystals from first principles. In addition, some of these elements exhibit curious features such as the negative thermal expansion in the case of silicon or a sharp peak in the second order Raman spectra in the case of diamond, about 2 cm^{-1} ($\approx$ 0.25 meV) above twice the zone centre optic phonon frequency.

Known experimentally since the late 40s, this peak has given rise to a number of speculations including two phonon bound states. The most straightforward explanation - a maximum of the longitudinal optic (LO) phonon dispersion appearing within the Brillouin zone rather than at the Γ-point (origin) - has found initial confirmation in the recent results of *ab initio* calculations [3], predicting a maximum of the longitudinal optic phonon frequencies at [0.5, 0, 0], some 25 cm^{-1} ($\approx$ 3 meV) above the zone centre frequency.

As the available neutron scattering data for the optic phonon branches from the 60s are incomplete and exhibit error bars around 3-5 meV, too large to permit any conclusions, this problem was revisited during a recent experiment on the IN1 three-axis spectrometer. The required accuracy of the order of 0.5 meV at an energy transfer of 165 meV represented in itself a challenge and necessitated

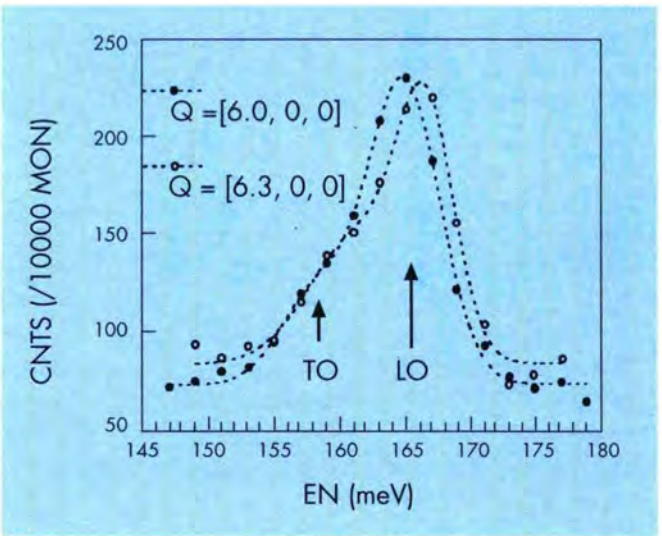

Fig. 3: Example of neutron groups from diamond observed in the (6, 0, 0) Brillouin zone; the LO component is systematically shifted towards higher energy at ξ ≈ 0.25-0.4 when compared to the zone origin data.

extensive efforts to optimise the energy resolution and to eliminate all possible sources of spurious signal. The observed phonon frequencies are displayed in Fig. 2, the values for ξ = 0, 0.3 and 0.5 being averages over several scans. These data as well as a direct comparison of the profiles from different scans given in Fig. 3, support the conclusion that the mean frequency in the range of $0.25 \leq \xi \leq 0.4$ with 165.5(5) meV is above the mean observed Γ-point frequency of 164.7(4) meV [4]. This difference of the order of 0.5-1.0 meV is mid-way between the results of optical measurements and the calculated dispersion curve.

Electron-phonon coupling in superconducting quarternary boro-carbides

Research into intermetallic superconductors has recently been revived by the discovery of a number of tetragonal alloys of the formula RNi_2B_2C (R = Y or rare-earth element) [5]. They form an interesting layered crystal structure series of space group I4/mmm [6]. For YNi_2B_2C with a T_c = 15.2 K, electronic structure calculations indicate that it is a strongly three-dimensional metal with all atoms contributing to the metal character, completely unlike the cuprate high-temperature superconductors [7]. By incorporating resistivity data, Pickett et al. [7] further deduced a very strong electron-phonon coupling (λ = 2.6), which they relate to an unusual combination of states at the Fermi level, and expect substantial contributions especially from the vibrations of the light atoms (roughly 50 % B and 30 % C) but also from the Ni atoms (~ 20 %). They also suggest an additional soft-mode behaviour from the heavier atoms.

From heat capacity measurements in comparison to the specific heat anomaly at T_c, the magnetic susceptibility and the calculated bandstructure, Carter et al. [8] found these compounds to be in the weak-to-intermediate coupling limit with λ = 0.5 to 1.0 and also conclude that the electron pairing is of dominant phonon-mediated character. In addition, structural studies [9] have shown a surprising flattening of the NiB_4 tetrahedra, which are embedded within the Ni-B double layers of the structure, when going from superconducting YNi_2B_2C to non-superconducting $LaNi_2B_2C$. Including these findings, Mattheiss et al. [10] performed tight-binding calculations and, in combination with bandstructure results near the Fermi level, proposed that the mechanism for superconductivity in these boro-carbides is based on high-frequency boron $A_g(1)$ optical phonons that dynamically modulate the NiB_4 tetrahedral bond angles.

Generalized phonon densities of states (GDOS) can be deduced from inelastic neutron scattering (INS) experiments on powdered samples for which we have used two multidetector time-of-flight (TOF) spectrometers, the high-flux IN6 instrument at ILL with an incoming energy of E_o = 3.12 meV and the DN6 spectrometer at the SILOE reactor at the CEN-Grenoble with E_o = 17.4 meV. Measurements were carried out on Y $(Ni_{1-x}Co_x)_2B_2C$ with x = 0; 0.15; 0.30 (with T_c = 15.2 K; 3 K, no T_c, respectively) and $Lu(Ni_{1-x}Co_x)_2B_2C$ with x = 0; 0.30 (with T_c = 16.5 K; no T_c, respectively) at room temperature and partially at 80 K and 30 K, all in the energy-gain mode. Because of the extreme high absorption cross-section of B^{10}, all samples were prepared with the boron isotope B^{11}.

INS experiments could help elucidate whether strong electron-phonon interactions leading to anomalous frequency shifts (i.e. for example involving the boron vibrations of the A_g (1) mode) and / or to soft-mode behaviour of certain dispersion branches (i.e. for example low-frequency Ni involved vibrations) are taking place in these systems.

In order to check what we could learn from determining the GDOS deduced from INS experiments on powder samples, we performed a Born-von-Karman (BvK) analysis for these systems. The result for YNi_2B_2C is shown in Fig. 4. Because of the strong differences in mass between the metal and non-metal atoms, the phonon spectrum decomposes into two well-separated parts, the low-frequency part of predominantly Y + Ni vibrations (up to 38 meV) and a series of optic branches due to the vibrations of the light elements. The interactions between the light atoms will probably be of short range, therefore the optical branches will be relatively flat, which should give us the unique possibility to classify them and observe their individual behaviour when going from superconducting to non-superconducting systems. At the Γ point, the 18 phonon frequencies decompose according to $\Gamma = A_g(1) + B_g(1) + 4A_u + 2E_g + 4E_u$ which are indicated in Fig. 4a. Fig. 4b shows the partial DOS for the individual kinds of atoms.

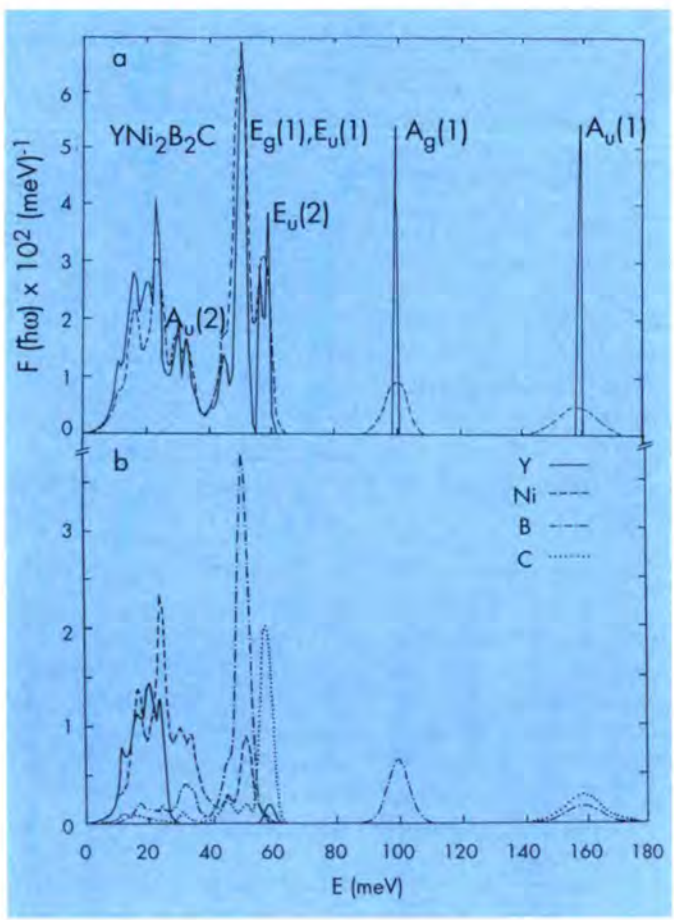

Fig. 4: Born-von-Karman model calculation for YNi_2B_2C
a. True phonon density of states (PDOS) - solid line and generalized PDOS folded with resolution of spectromter - dashed line.
b. Partial PDOS for the individual kinds of atoms.

The energetically lower part (below 40meV) of the PDOS is made up of 3 acoustic and 4 optic modes, i.e. B_g (1) (Ni only), one A_u (Ni + R), one E_g (Ni + B) and E_u (1) (Ni + R). The remaining bands, i.e. A_g (1) (B only), two A_u-, one E_g-, and two E_u-modes are representative of the high-frequency excitations. The largest A_u vibration is expected to be the highest frequency of the spectrum. There, the two boron atoms vibrate in antiphase with the carbon atom. Our BvK-model calculation further predicts that the corresponding Davidov partner, the A_g (1) mode, has a considerably lower frequency with only the boron atoms vibrating and the carbon atoms being at rest. The high in-plane modes, represented by an E_u-E_g Davidov pair of Ni-B bondstretching vibrations, are expected to be very close in energy. The C-contribution to the E_u (1) intensity is small and zero for E_g (1). The two remaining bands involve motions of the carbon atoms. The E_u (2) mode is essentially a R-C bondstretching mode and for the A_u (2) intensity, the B-C-B unit vibrates almost as an entirety against the heavy R component.

In Fig. 5 we compare the GDOS for superconducting YNi_2B_2C with non-superconducting Y $(Ni_{.7}Co_{.3})_2B_2C$ and register:

i. The A_g (1) mode (insert in Fig. 5) lies at the same energetical position for both compounds.

ii. A significant shift towards higher energies takes place for in-plane vibrations of the light atoms in the energy band between 40 and 70 meV when Co is substituted and T_c is suppressed. This is mainly due to the in-phase and out-of-phase boron excitations, i.e. the E_g (1) and E_u (1) frequencies. The E_u (2) carbon contributions leading to a peaked shoulder at 61 meV show little change, a fact which is underlined from the measurement of Y $(Ni_{.15}Co_{.85})_2B_2C$ with a T_c of 3 K (dashed line in Fig. 5). These results are in good agreement with measurements of the boron (^{10}B-^{11}B) isotope effect in YNi_2B_2C by D.D. Lawrie et al. [11], who determined the partial boron isotope exponent to be: $\alpha_B = 0.25 \pm 0.04$ and also stated that preliminary investigations of the carbon (^{12}C-^{13}C) isotope effect did not show a change in T_c. From their results, however, it cannot be decided whether the boron excitations based A_g (1) mode, which modulates the NiB_4 tetrahedra, is involved in the electron pairing mechanism or not. This prediction is strongly favoured by theory [10,7].

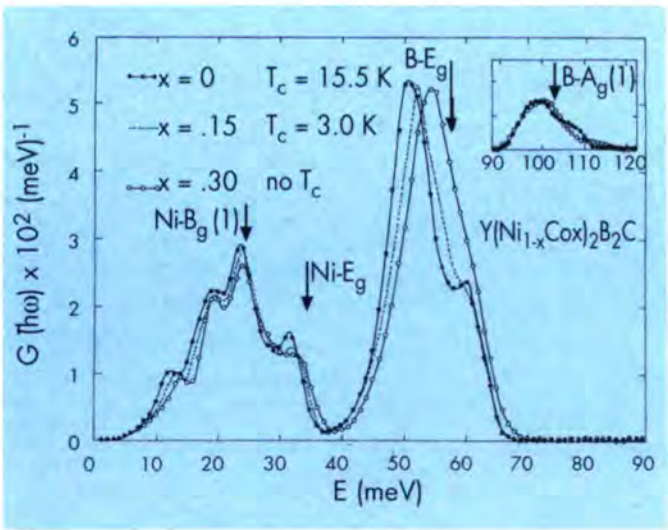

Fig. 5: Generalized PDOS for $Y(Ni_{1-x}Co_x)_2B_2C$. Arrows indicate Raman active Γ-point frequencies as determined by Hadjiev et al [13].

iii. Due to the smaller neutron scattering cross section of Co in comparison to Ni, we can explain the decrease in peak intensities at 20, 24 and 32 meV as "trivial" nicely scaling with neutron scattering power and Co-content. In this metal-atom dominated low-energy part of the spectrum there are, however, changes which are larger than the difference in scattering power would allow, i.e. a hardening of vibrations for the Co-doped compounds between 34 and 38 meV and a very pronounced shift towards larger frequencies between 6 and 18 meV.

The GDOS derived for a sample with a Co-content of 45 % (no T_c, but still metallic) showed no further increase in the dramatic frequency shifts discussed above [12].

In order to clarify whether the soft-mode behaviour of the superconductor displayed between 9 and 13 meV, as shown in Fig. 5, is caused by Y vibrations, we also investigated Lu $(Ni_{1-x}Co_x)_2B_2C$ which for x = 0 has a comparable T_c (= 16.5 K). Due to the heavier mass of Lu, one then expects a "trivial" frequency shift towards smaller energies from 12 meV to 8.5 meV. The measurement of the GDOS of $LuNi_2B_2C$ verified this prediction exactly and upon substituting 30 % of the Ni atoms with Co (compound has no T_c), these now well-separated Lu-excitations hardened by 1 meV [12].

At the IN6 we also carried out temperature-dependent measurements on $LuNi_2B_2C$. With good statistics, we could cover the energy range between 0.25 and 12 meV for 300 K and 80 K as displayed in Fig. 6. Upon cooling we observed an increase in intensity between 3 and 6 meV and a softening of the Lu-caused lattice excitations from 8.5 meV to almost 8 meV. The statistics of an additional measurement at 30 K was poor, but good enough to show that there was no further strong increase in this behaviour.

In conclusion we find:

i. The A_g (1)-phonon mediated electron pairing mechanism predicted by theory [6] is not reflected in the GDOS of the superconducting quarternary boro-carbides when compared to non-superconducting reference systems.

ii. The dramatic frequency shifts between 40 and 70 meV suggest appreciable electron-phonon coupling of in-plane boron vibrations.

iii. Changes in the GDOS energy interval between 20 and 38 meV, which is dominated by Ni-B_g (1) and Ni-E_g excitations, indicates that in-plane Ni vibrations are participating substantially in this coupling mechanism.

iv. Our results below 14 meV demonstrate the strong influence of Y and / or Lu on the electron-phonon coupling of the superconductors by either displaying dramatic energy shifts when compared to non-superconducting reference compounds or soft-mode behaviour upon cooling.

Relaxation of a crystal field excitation in $Ho_{0.1}Y_{0.9}Ba_2Cu_3O_7$

Nuclear relaxation techniques (NMR and NQR) have been used extensively to probe certain aspects of the microscopic nature of the cuprate superconductors, in particular the temperature variation of the relaxation rate and frequency shift, in order to extract the symmetry of the superconducting order parameter. A similar type of experiment can be performed by neutron spectroscopy of a crystal field transition whose position and line width are analogous to the nuclear relaxation time and Knight shift, and depend on the real and imaginary parts of the susceptibility associated with the CuO_2 planes.

We have studied the 0.5 meV crystal field transition of Ho^{3+} in $Ho_{0.1}Y_{0.9}Ba_2Cu_3O_7$ ($T_c \approx 94$ K) on IN5. Our measurements cover the temperature range 2 K to 135 K, and so extend from the superconducting into the normal state. We have extracted the line widths and peak shifts by convoluting the residual peak shape at 2 K with a single Lorentzian broadening function. Figures 7(a)-(c) display the temperature variation of the width Γ (HWHM), the peak shift relative to 2 K, and the integrated intensity normalised to unity at absolute zero. The relaxation rate ($\propto \Gamma$) is seen to increase very slowly with temperature at first, then more rapidly up to $T_m = 105$ K, where the variation becomes roughly linear. Compared with the curve expected for a normal metal, shown by the line in Fig. 7(a), the line width is considerably reduced in the superconducting state. The peak shift towards higher energies shows a more marked initial increase with T than does Γ, but eventually flattens out at T_m.

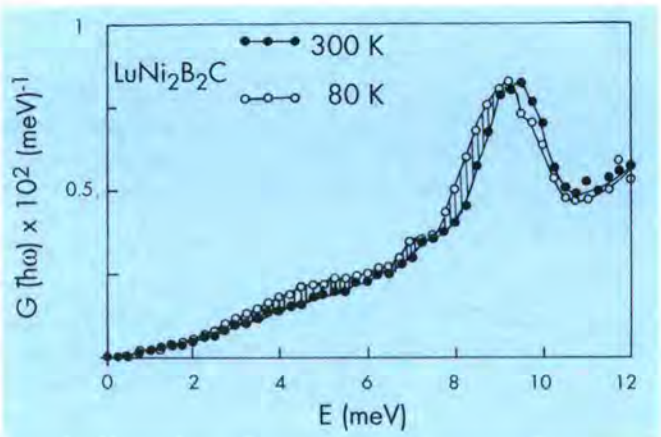

Fig. 6: Low-frequency soft-mode behaviour of the $LuNi_2B_2C$ superconductor upon cooling.

The decrease in the integrated intensity with temperature, Fig. 7(c), is due to thermal depopulation of the ground state and closely follows the curve calculated from the known CF level scheme. This suggests that any scattering from transitions between thermally excited CF levels separated by ~0.5 meV is too small to have influenced the result.

There is considerable debate concerning the orbital pairing state in the cuprate superconductors. The type of pairing affects the anisotropy of the superconducting energy gap, and this in turn determines the number of quasiparticle excitations in thermal equilibrium available to relax the crystal field transition. As a consequence, information on the pairing state can be inferred from the temperature variation of the line width and peak position. For instance, an isotropic gap 2Δ leads to an initial variation of the form $\exp(-\Delta/k_BT)$. As is evident from Fig. 7(b), however, the data show larger effects at low temperatures than would be expected for an exponential rise, and this suggests there exists a significant density of quasiparticle excitations present at low temperatures. We conclude from this that the gap may be highly anisotropic.

Dispersion of the $\Gamma_6^{(1)}$-$\Gamma_6^{(2)}$ Nd crystal field excitation in Nd_2CuO_4

Nd_2CuO_4 has been recognised to be the parent compound of an electron superconductor with heavy fermion-like behaviour. Upon doping with Ce and subsequent annealing in reducing atmosphere, superconductivity is achieved in $Nd_{2-x}Ce_xCuO_{4-d}$ for $0.13 \leq x \leq 0.18$ with a highest T_c of ~ 22 K. For $x > 0.18$, the system becomes a normal metal. For $x > 0.15$ and temperatures $T \leq 0.3$ K, the system shows a specific heat linear in temperature with a huge Sommerfeld coefficient and a corresponding large effective mass, indicating heavy fermion behaviour.

The investigation of the exchange interactions plays a key role in the understanding of this heavy fermion-like behaviour and the interplay between both superconductivity and antiferromagnetism. One approach to determining the

coupling constants is a measurement of the dispersion of the crystalline electric field (CEF) excitations in the paramagnetic state. We therefore performed inelastic neutron scattering experiments with a single crystal to determine this dispersion for the $\Gamma_6^{(1)}$-$\Gamma_6^{(2)}$ CEF transition at ~ 21 meV [14].

The experiments were performed on the triple-axis spectrometers IN8 and IN3 at the high-flux reactor of the Institute Laue-Langevin (ILL) in Grenoble. On IN8, we used a Cu111 monochromator and PG002 analyser, both vertically bent. In the case of IN3, we used a vertically bent Cu111 monochromator and a horizontally bent PG002 analyser. The sample was mounted in an orange-type He cryostat and kept at a temperature of 4 K. This temperature is well above the Nd ordering temperature of ~ 1.5 K.

To describe the data we made use of the random phase approximation (RPA) model. In this model, the excitations are given by the following expression:

$$E(q) = [\Delta^2 - 2M^2\Delta(J(q) \pm |J'(q)|)]^{1/2}$$

where Δ is the crystal field splitting, M the transition matrix element, and J(q) and J'(q) the Fourier transformed coupling constants between ions of the same and of different sublattices, respectively.

The + sign corresponds to acoustic, the - sign to optical branches. The scattering intensity of the two branches is proportional to $1 \pm \cos(q)$ with q = tr-j where t: reciprocal lattice vector, r: vector connecting the two sublattices and j = arctan(Im(J'(q)/Re(J'(q))).

In Fig. 8 we show the measured dispersion of the crystal field excitation. The lines give the best fit of the random phase approximation model. Observed intensities are

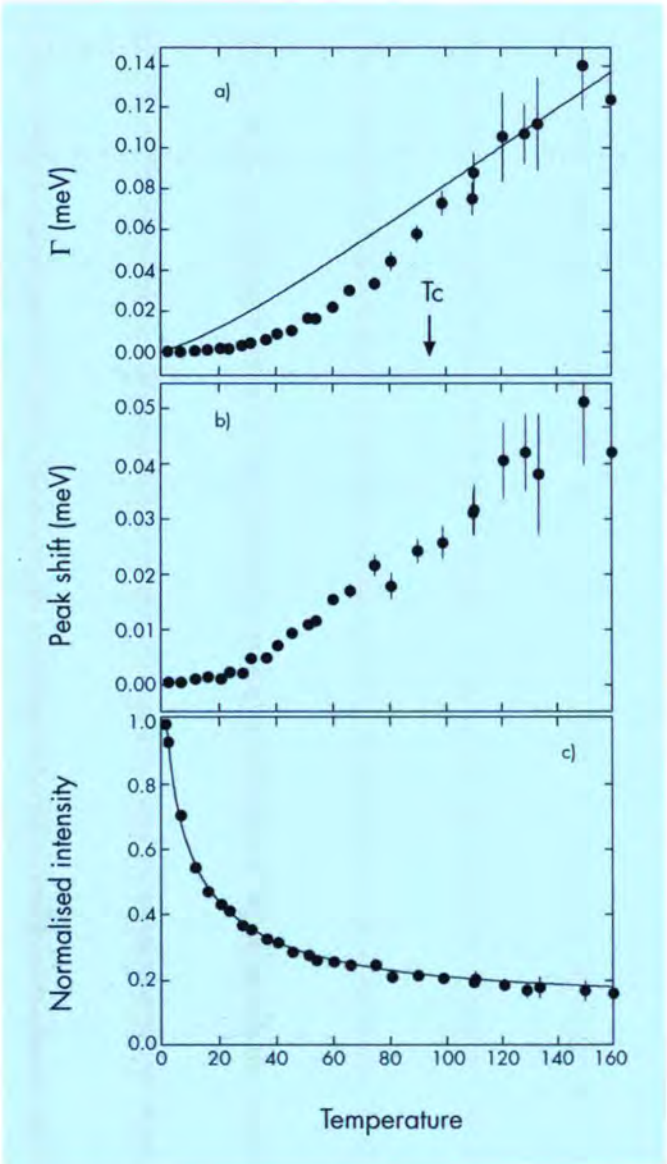

Fig. 7: The temperature-dependence of (a) the line width Γ, (b) the peak position, and (c) the integrated intensity (normalised to 2 K) of the 0.5 meV crystal field excitation of Ho^{3+} in $Ho_{0.1}Y_{0.9}Ba_2Cu_3O_7$. Anomalies in the line width and peak position near $T_m \approx 105$ K suggest the opening of a gap in the CuO_2 plane excitation spectrum, and the initial temperature variation implies that the gap is highly anisotropic.

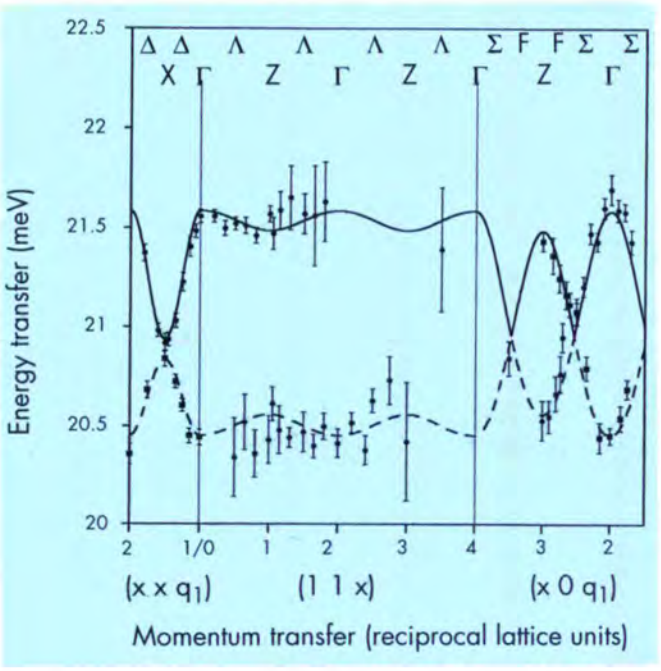

Fig. 8: Measured dispersion of the $\Gamma_6^{(1)}$-$\Gamma_6^{(2)}$-Nd crystal field excitation in Nd_2CuO_4 at 4 K (circles: $q_l = 0$, squares: $q_l = 2$). The lines correspond to the RPA model calculation. (- - -: acoustic branch, —: optical branch).

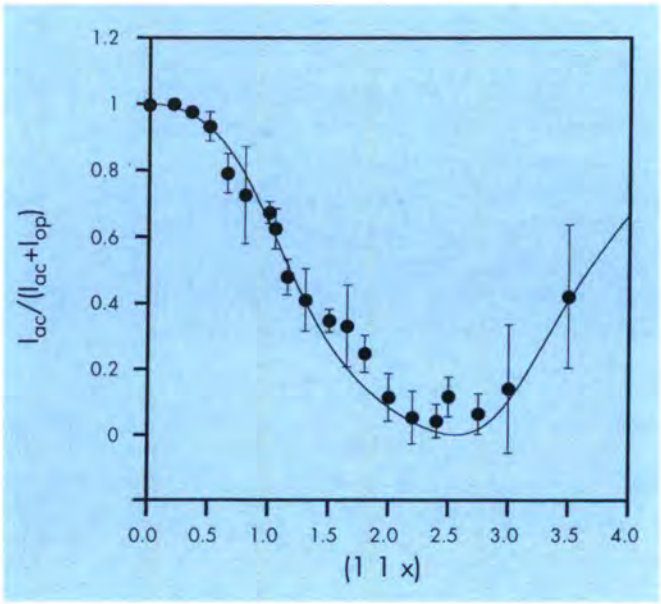

Fig. 9: Measured intensity of the acoustic branch, normalised to the total magnetic scattering. The line corresponds to the RPA model calculation.

depicted in Fig. 9, normalised to the total magnetic scattering, together with the result of our model (solid line). The outstanding correspondence inspires confidence in the coupling constants thus deduced.

Secretary: Niels Pyka

References

[1] C. Hordequin, J. Pierre and R. Currat, submitted to J.M.M.M.

[2] S.J. Youn and B.I. Min, Phys. Rev. **B51,** 10436 (1995).

[3] P. Pavone, K. Karch, O. Schütt, W. Windl, D. Strauch, P. Giannozzi and S. Baroni, Phys. Rev. B 48 (1993), 3156 and 3164.

[4] D. Strauch, J. Kulda, B. Dorner, Th. May, H. Sterner, B. Roessli, in preparation.

[5] R.J. Cava, H. Takagi, H.W. Zandbergen, J.J. Krajewski, W.F. Peck, jr., T. Siegrist, B. Batlogg, R.B. van Dover, R.J. Felder, K. Mizukashi, J.O. Lee, H. Eisaki, and S. Uchida, Nature **367**, 252 (1994)

[6] T. Siegrist, H.W. Zandbergen, R.J. Cava, J.J. Krajjewski, and W.F. Peck, jr., Nature **367**, 254 (1994)

[7] W.E. Pickett and D.J. Singh, Phys. Rev. Lett.**72**, 3702 (1994)

[8] S.A. Carter, B. Batlogg, R.J. Cava, J.J. Krajewski, W.F. Peck, jr., and H. Takagi, Phys. Rev. B **50**, 4216 (1994)

[9] T. Siegrist, R.J. Cava, J.J. Krajewski, and W.F. Peck, jr., J. Metals and Alloys (in press)

[10] L.F. Mattheiss, Phys. Rev. B **49**, 13279 (1994)

[11] D.D. Lawrie and J.P. Franck, Physica C **245**, 159 (1995)

[12] F. Gompf, W. Reichardt, H. Schober, B. Renker, and M. Buchgeister, to be published

[13] V.G. Hadjiev and L.N. Nozukov, to be published

[14] W. Henggeler, T. Chattopadhyay, B. Rössli, D.I. Zhigunov, S.N. Barilo, A. Furrer, Z. Phys. B, in press.

Paramagnetic Spectral Response of $CePd_3$: towards possible resolution of a controversy

A.P. Murani

Magnetic properties of ions of the rare earths, the elements forming the 4f series of the periodic table, are usually amenable to descriptions within well-established physical models, particularly in insulating compounds and ionic salts. Standard theories hold to a great extent even in metallic environments, such as their pure elemental state, as well as in alloys and intermetallic compounds. This is because the magnetic 4f electrons are well localised and shielded by the electrons in the outer higher energy shells which participate in the ionic, covalent or metallic bonds. Some *metallic* rare earth systems, however, particularly those containing Ce and Yb at the ends of the rare earth series, often show very unusual physical properties resulting from the interaction (or hybridisation) of the localised 4f electrons with the freely moving conduction electrons. This interaction has the effect of inducing temporal fluctuations between two or more valence states of such rare earth ions, hence these alloys or compounds are commonly referred to as valence fluctuation systems. The hybridisation with conduction electrons is equivalent, within certain limits, to the interaction of the spin (magnetic moment) of the ion with the conduction electron spins which gives rise, for negative (or antiparallel) coupling, to the famous Kondo effect. Hence, a classic valence fluctuation compound such as $CePd_3$ in which Ce ions form a regular lattice is sometimes also referred to as the Kondo-lattice.

Kondo effect and valence fluctuation phenomena in rare earth systems have been investigated theoretically and experimentally with considerable interest during the last two decades. While some progress in understanding the physical origin of the underlying mechanisms has been made, considerable work, both experimental and theoretical, still remains to be done especially since the subject has often been clouded by controversies in a number of domains such as, for example, photoemission, inverse photoemission or Bremstrahlung Isochromat Spectoscopy (BIS) as well as neutron scattering, amongst others. It is, of course, important to address these controversies with a view to reaching consensus on reliable experimental facts so as to provide impetus for further understanding and development of the subject.

Several years ago Galera and co-workers [1,2] investigated the magnetic scattering from polycrystalline $CePd_3$ at ILL using the time-of-flight technique (IN4) as well as polarised neutrons on the three-axis spectrometer D5. They found the spectral response could be well represented by a broad Lorentzian centered on ~ 55 meV,

The Kondo Effect:

A very interesting phenomenon was discovered a few decades ago in which the electrical resistivity of an alloy of a noble metal such as Cu, Ag or Au formed with a small concentration of a magnetic metal e.g. Fe, Mn, etc. was found to increase with decreasing temperature. This behaviour contrasts with the decreasing electrical resistivity with decreasing temperature of pure metals, as well as of alloys formed with non-magnetic metals.

An explanation of the phenomenon was first proposed by the Japanese theoretician J. Kondo as due to the coupling (or exchange interaction) between the spin angular momentum of the magnetic ion (Fe, Mn) and the spin of the conduction electrons. The observed logarithmic increase in the resistivity with decreasing temperature results if this coupling has the negative sign. It followed from this that as the temperature decreases below a certain characteristic (or Kondo) temperature, which depends on the strength of the interaction, a correlated cloud of conduction electrons begins to form around the magnetic impurity with spins aligned antiparallel, thus compensating out the magnetic moment of the ion at low temperatures. Some of the interesting consequences of the formation of such a demagnetised low-temperature state are claimed to have been observed in the magnetic susceptibility as well as the specific heat of these dilute alloys.

The concept of a compensating cloud of conduction electrons surrounding each magnetic site is, however, an oversimplification or perhaps not even accurate when applied to a whole lattice of magnetic ions such as Ce in the intermetallic compounds like $CePd_3$. However, the idea of a characteristic energy scale (often referred to as the Kondo temperature) which is a measure of the spin fluctuation rate of the local moment remains a central parameter in the physical interpretation of many interesting phenomena associated with these systems. The characteristic Kondo energy (Kondo temperature) T_K can be inferred from inelastic neutron scattering measurements via the (half) width Γ of the magnetic quasi-elastic distribution ($T_K \sim \pi/2 * \Gamma$) or identified with the centroid ω_o of the broad inelastic response ($T_K \sim \omega_o$). The latter form is usually observed when the ground state degeneracy is high (≥ 6), implying that crystal field splittings are quenched.

which represents its characteristic or Kondo energy. A subsequent investigation using a three-axis spectrometer by Shapiro, Stassis and Aeppli [3] on a single crystal of $CePd_3$ close to the zone center at Q = (0, 1.1, 1.1), however, claimed to find magnetic scattering *only* at low energies corresponding to *two low-energy scales* of ~ 3 and ~ 16 meV. These results were rather surprising,- especially since Shapiro and co-workers claimed that their measurements *"over a wide range of q's including some at the zone boundary have failed to reveal the high energy feature (reported by Galera et al.)"*.

The form of the spectral response from a classic valence fluctuation compound like $CePd_3$ is central to our understanding of these systems. Theoretically in the limit of large degeneracy N of the 4f state (N = 2J + 1, with J representing the total angular momentum), and given that conduction electron hybridisation dominates over intersite interactions, the magnetic response from a lattice of such ions is well approximated by that from a collection of isolated impurities with a *single, dominant* characteristic energy [4 , 5]. The discrepancy between the two reported studies is, therefore, rather serious and needs to be resolved. It is important to establish clearly whether or not $CePd_3$ belongs to the same class of valence fluctuation systems as, for example, the isostructural (cubic) compound $CeSn_3$ [6] and many others.

This has motivated us [7] to undertake a comparative neutron inelastic scattering reinvestigation of this compound, performed just prior to the long reactor shutdown, using the time-of-flight spectrometer IN4B on the same single crystal sample of $CePd_3$ as used earlier by Shapiro and co-workers (and kindly loaned to us by them) as well as on a polycrystalline powder of $CePd_3$. The latter was packed, using thin aluminium foil, into a cylinder of similar dimensions as the single crystal, viz. 5 mm diameter and ~ 40 mm length, in order to keep the geometrical shape-dependent effects such as multiple scattering closely similar for both. This is important since, as discussed below, multiple scattering processes in the large samples dominate the observed non-magnetic response at low angles. This conclusion is supported by another experiment performed some two years later [8] at ISIS on the high energy transfer (HET) time-of-flight spectrometer, where steps were taken to reduce multiple scattering using neutron absorbing slats to subdivide the polycrystalline samples of $CePd_3$ and YPd_3 into smaller elements.

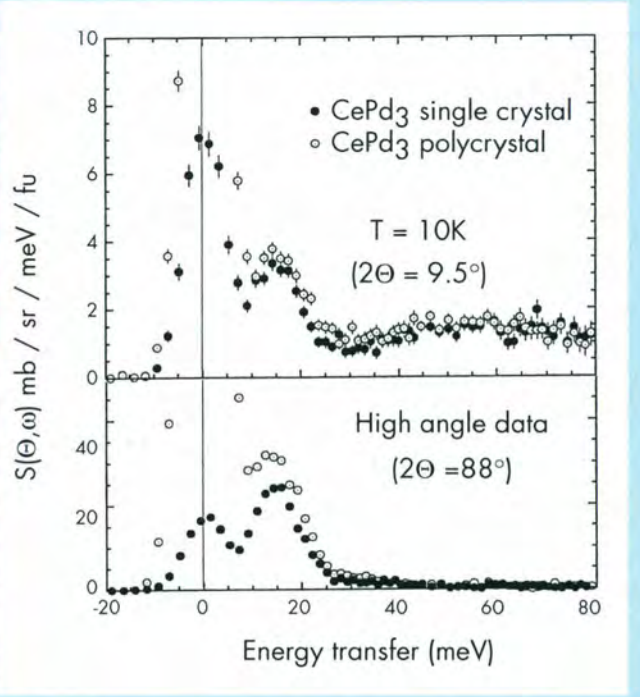

Fig. 1: Observed scattering, using the time-of-flight (TOF) technique, at 10 K from single crystal and polycrystalline samples of $CePd_3$ using neutrons of incident energy 115 meV; a) the scattering at low angles, $2\Theta = 9.5^o$ and b) at high angles, $2\Theta = 88^o$.

In Fig. 1a we show the low angle ($2\Theta = 9.5^o$) time-of-flight data taken on the thermal-beam spectrometer IN4B for both the single crystal and powder samples of $CePd_3$ after a one-to-one background subtraction. The results for the high angle bank ($2\Theta = 88^o$) are shown in Fig. 1b. The form of the inelastic scattering is similar for both samples, albeit slightly weaker for the single crystal, while the elastic scattering is very much stronger for the polycrystal compared with the single crystal.

The stronger elastic scattering at high angles in the case of the polycrystalline powder is due mostly to the fact that the scattering triangles for $\omega = 0$ 'cut' several Debye-Scherrer rings for some of the detectors making up the high angle bank (average angle = 88^o), while for the single crystal none of the detectors within the same angular range satisfied the Bragg condition. At low angles ($2\Theta = 9.5^o$), however, few Debye-Scherrer rings were cut. The enhanced *elastic* scattering in this case results partly from the higher (elastic) multiple scattering as well as increased surface scattering from a polycrystalline powder possibly contaminated by moisture. The *inelastic* scattering at high energies,

represented by the broad hump centred on ~ 50-60 meV in the low angle bank is, however, closely similar for both samples. It should be noted that this high energy scattering is practically non-existant in the high angle data while the lower energy component centered on ~ 10 - 15 meV is similar in spectral shape but stronger in intensity by roughly a factor of 8 to 9 compared with the low angle data.

As shown in Fig. 2b, except for the high energy response, centered on ~50-60 meV, closely similar inelastic scattering is observed below 30 meV from the isostructural non-magnetic compound YPd_3, suggesting clearly that this low energy inelastic scattering must be non-magnetic in origin. Also, it is interesting that the *shape* of the low energy *inelastic* scattering from the single crystal is so similar to that from the polycrystalline sample. Our use of broad angular detector groups and no input collimation implies measurements with relaxed Q-resolution. We did, however, observe sharp peaks appearing and disappearing with increasing scattering angle and as the crystal orientation was changed. These sharp peaks are superposed on a broad inelastic structure (resembling phonon density of states), which increases in intensity with increasing scattering angle. This may be seen from the high angle data at 88° where sharp phonon modes are absent for this particular orientation of the single crystal.

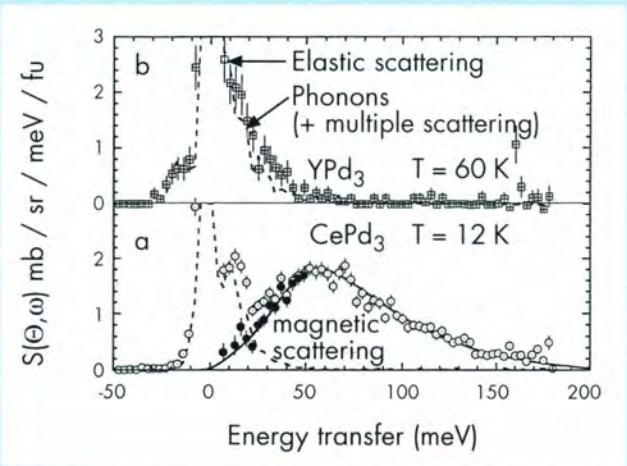

Fig. 2: Observed low angle scattering at $2\Theta = 5^o$ from a) $CePd_3$ at 12 K and b) YPd_3 at 60 K using neutrons of incident energy 200 meV on the TOF spectrometer HET at ISIS. The dashed curves in the figures represent high angle scattering scaled down by a factor 11.8. For $CePd_3$ this represents the estimated non-magnetic contribution. The filled circles in a) show the difference signal, i.e. the magnetic contribution obtained by subtracting off the dashed curve from the as-measured data. They fall closely on the continuous curve which represents a least-squares fit to data above 30 meV to the Kuramoto -Müller-Hartmann single-ion spectral function.

At low angles the cross-section of a phonon mode, proportional to Q^2, is rather low compared with other contributions discussed below, due to the low value of Q (~1.2 $Å^{-1}$), hence the scattering appears to remain practically invariant with crystal orientation. The question of the form of the observed scattering aside, intensity considerations alone suggest that if only single phonon processes contribute to the observed low energy inelastic scattering at low angles, its intensity is anomalously high relative to the high angle bank. From the Q^2-variation for single phonon events, we expect an intensity ratio of ~ 70 for the two scattering angles of 9.5° and 88°, whereas the observed ratio of between ~ 8 to 9 for the polycrystal and single crystal respectively indicates much higher scattering at low angles than expected. We thus conclude that the observed *low energy inelastic* scattering *at low angles* (observed also in non-magnetic YPd_3) must originate, to a large extent, from non-magnetic *multiple scattering* processes. The dominant contribution to this scattering originates from processes in which the first scattering event is along the axis of the cylindrical sample, since this provides the longest path and hence the highest probability for a second event through a similarly large angle into the low angle bank. The similarity of the low energy scattering for the single and polycrystalline samples (of similar geometrical shape) provides the clearest demonstration that, in experiments using thermal and high energy neutrons, multiple scattering occurs in a fairly similar manner in both types of samples.

In a later experiment on HET at ISIS, we have attempted to reduce multiple scattering by subdividing the large rectangular slab-shaped polycrystalline samples (of $CePd_3$ and YPd_3) into smaller elements using neutron absorbing slats [8]. With the adopted configuration the multiple scattering contribution was reduced by ~ 60 %. Note that the peak-heights of the low and high energy inelastic components are roughly similar, i.e. 1:1 in Fig. 2a, whereas in previous measurements, Fig. 1, the ratio of the peak-heights was > 2:1 in favour of the lower energy (non-magnetic) structure.

The observed scattering at low angles ($2\Theta = 5^o$) for the non-magnetic reference, YPd_3, measured at 60 K using identical sample configuration are shown in Fig. 2b (squares). The dashed curve in the figure represents high angle data scaled down by a factor ~12. As mentioned earlier, whereas the observed low energy inelastic structure is very similar for both $CePd_3$ and YPd_3 samples, the high energy response is not observed in YPd_3. The non-magnetic contribution within the low

angle data of $CePd_3$ may be estimated by assuming that the ratio of the non-magnetic contribution relative to the high angle scattering (which is essentially non-magnetic due to the relatively small magnitude of the magnetic form-factor at high Q-values) is the same as that for the observed scattering from the non-magnetic reference YPd_3 for the same two scattering angles [6]. This does not require that phonon frequencies be exactly the same for the two compounds, but only that the overall scattering and absorption cross-sections should not be grossly different [6]. The method has been found to work well for two non-magnetic iso-structural compounds and has also been justified by Monte Carlo simulations recently [9]. The non-magnetic contribution thus estimated for $CePd_3$ is shown by the dashed curve in Fig. 2a. The spectral fit using the single-ion spectral form proposed by Kuramoto and Müller-Hartmann [10] is indistinguishable from a Lorentzian fit over the energy range covered and returns a characteristic energy T_K of ~50 meV, fully consistent with the results of Galera and co-workers[1,2]. With the help of the spectral fit to the high energy magnetic signal, we have evaluated the form-factor corrected integrated magnetic cross-section to be ~280 mb sr^{-1} fu^{-1} corresponding to a 4f occupancy $<n_f>$ ~ 0.9. We have also evaluated the static susceptibility from the magnetic response and found it to be consistent with the bulk susceptibility of $CePd_3$.

From our comparative time-of-flight measurements on the single and polycrystalline samples of similar geometrical shape, Fig. 1, it is evident that relatively strong (and very similar) contribution from non-magnetic multiple scattering processes occurs at low energy transfers in both types of samples when measurements are performed using thermal and high energy neutrons. Thus, we believe, a good fraction of the low energy scattering in the three-axis measurements at low q (zone center) from the single crystal could be accounted for by such processes. We believe also that the failure to observe the high energy response in the latter measurements could, quite plausibly, be associated with the high background conditions of the three-axis spectrometer, particularly at high energy transfers.

Finally, we have taken advantage of the high energy neutrons available from a spallation source to investigate $CePd_3$ with neutrons of incident energy 900 meV using the same time-of-flight spectrometer HET. These high energy data, shown in Fig. 3, are corrected for non-magnetic scattering using YPd_3 as the non-magnetic reference measured under identical conditions. We have fitted the resultant response (over the range $100 < \omega < 250$ meV) to the Kuramoto - Müller-Hartmann spectral form convoluted with the broad energy resolution function fixing the two characteristic parameters (T_K and α) to their values determined more accurately from the low energy data (Fig.2). The resultant fit shown in Fig. 3 describes the high energy data fairly well *except for the broad residue*, shown on an expanded vertical scale in the inset. This signal, we believe, *represents the excitation to the* $^2F_{7/2}$ *spin-orbit state*. A Lorentzian fit yields a half-width of ~ 60 meV, centrered on ~ 360 meV. The rather low intensity of the excitation relative to the main response is, however, consistent with the magnitudes of the respective matrix elements of the transitions [11]. The observation of the broad 'spin-orbit' excitation at ~ 360 meV compared with the spin-orbit energy of the isolated Ce^{3+} ion of ~ 270 meV [12] suggests that the Kondo energy of the upper ($^2F_{7/2}$) spin orbit state is ~ 90 meV, almost twice that for the ground state ($^2F_{5/2}$). The higher magnitude of the Kondo energy of the upper spin-orbit level can be justified theoretically [13].

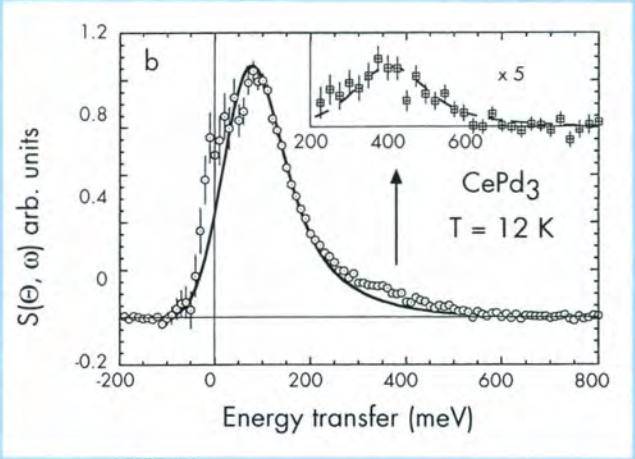

Fig. 3: The magnetic spectral response from $CePd_3$ at 12 K measured with the TOF technique using high energy neutrons (E_i = 900 meV), obtained by subtracting off the non-magnetic contribution with reference to YPd_3 measured under identical conditions. The solid curve represents a fit (over the range $100 < \omega < 250$ meV) to the Kuramoto - Müller-Hartmann spectral form convoluted with the energy resolution, fixing the parameters T_K (the Kondo energy) and α (= $\sin(\pi < n_f > /N$, with $<n_f>$ representing the occupancy and N the degeneracy of the 4f state) to their values determined more accurately from the low energy, high resolution data (Fig. 2) and varying only the vertical amplitude. The apparent difference in the fitted curves in the two figures, particularly at low energies, is due to the broad energy resoltion of the present high energy experiment. The inset shows the difference signal relative to the fitted curve on an expanded vertical scale and using a doubled energy bin-width on the horizontal axis.

In conclusion, we have shown that the paramagnetic scattering from the ground ($^2F_{5/2}$) state of the lattice of Ce ions in the compound $CePd_3$ has essentially the single ion form with a high characteristic or Kondo energy of ~ 50 meV, confirming the expectation that a Kondo lattice such as $CePd_3$ with conduction electron hybridisation as the dominant interaction is well approximated by a collection of isolated impurities. Our data allow us to put an upper limit of 2% of the main response to possible additional or deviational scattering (at finite, non-zero q's) associated with low-temperature coherence effects such as evidenced in the electrical resistivity, for example. The enhanced high energy excitation to the $^2F_{7/2}$ spin-orbit state suggests that the characteristic Kondo energy of this state is even higher, viz. ~ 90 meV. Finally, the fact that localised, single-ion character of the 4f state, with occupancy ~ 90%, persists in $CePd_3$, as in αCe [14] and a number of αCe-like compounds, suggests that 4f-band formation [15] (as distinct from quasi-particle states or bands) in such systems may, in fact, be a relatively rare phenomenon.

References

[1] R.M. Galera, D. Givord, J. Pierre, A.P. Murani, C. Vettier and K.R.A. Ziebeck, J. Magn. Magn. Mater. **47&48**, 139 (1985).

[2] R.M. Galera, A.P. Murani, J. Pierre and K.R.A. Ziebeck, J. Magn. Magn. Mater. **63&64**, 594 (1987).

[3] S.M. Shapiro, C. Stassis and G. Aeppli, Phys. Rev. Lett. **62**, 94 (1989).

[4] T.V. Ramakrishnan and K. Sur, Phys. Rev. B **26**, 1798 (1982).

[5] R.M. Martin, Phys. Rev. Lett. **48**, 362 (1982).

[6] A.P. Murani, J. Phys. C **33**, 6359 (1983).

[7] A.P. Murani, A. Severing and W.M. Marshall, Phys. Rev. B (to appear).

[8] A.P. Murani, R. Raphel, Z.A. Bowden and R.S. Eccleston, Phys. Rev. B (to appear).

[9] E.A. Goremychkin and R. Osborn, Phys. Rev. B **47**, 14280 (1993).

[10] Y. Kuramoto and E. Müller-Hartmann, J. Magn. Magn. Mater. **52**, 122 (1985).

[11] E. Balcar and S.W. Lovesey, J. Phys. C **19**, 4605 (1986).

[12] W.T. Carnall, G.L. Goodman, K. Rajnak and R.S. Rana, J. Chem. Phys. **90**, 3443 (1984).

[13] N.E. Bickers, D.L. Cox and J.W. Wilkins, Phys. Rev. B **36**, 2036 (1987).

[14] A.P. Murani, Z.A. Bowden, A.D. Taylor, R. Osborn and W.G. Marshall, Phys. Rev. B **48**, 13981 (1993).

[15] B. Johansson, Philos. Mag. **30**, 469 (1974).

Crystal and Magnetic Structures

Members of the College at ILL

T. Baumbach
P.J. Brown
T. Chattopadhyay
(MPI Stuttgart)
A. Christensen
J. Cole
P. Convert
R. Cubitt
F. Fauth (PSI)
M.-T. Fernández-Díaz
A. Filhol
H.E. Fischer
B. Hamelin
T. Hansen
A.W. Hewat
J. Kulda
P. Langan
M.S. Lehmann
E. LeLièvre-Berna
A. Magerl
S.A. Mason
G.J. McIntyre
A.P. Murani
B. Ouladdiaf
M. Portes de Albuquerque
P. Radaelli
M. Reehuis
E. Ressouche (CENG)
C. Ritter
J. Saroun
O. Schärpf
E. Suard
F. Tasset
P. Timmins
R. Wimpory
C. Zeyen

External Members

M. Anne (CNRS)
R. Arons (CENG)
M. Bacmann (CNRS)
J. Baruchel (ESRF)
E.F. Bertaut (CNRS)
M. Bonnet (CENG)
J.X. Boucherle (CENG)
F. Bourdarot (CENG)
P. Burlet (CENG)
A. Fitch (ESRF)
D. Fruchart (CNRS)
D. Givord (CNRS)
A. Hiess (CENG)
C. Janot (UJF)
Å. Kvick (ESRF)
M. Marezio (CNRS)
J.C. Marmeggi (CNRS)
J. Pannetier (Pechiney)
E. Pebay-Peyroula (IBS)
P.L. Regnault (CENG)
C. Riekel (ESRF)
M. Schlenker (CNRS)
J. Schweizer (CENG)
D. Schmitt (CNRS)
J.L. Soubeyroux (CNRS)
Tranqui Duc (CNRS)
C. Vettier (ESRF)
C. Wilkinson (EMBL)
G. Zaccaï (IBS)

Introduction

Neutrons at last ! Travel to other neutron centres and to conferences was much reduced. The few administrative hitches were soon out of the way, and exciting experiments started. New software interfaces, new commands, new measuring techniques could be tested with real neutrons. For some, it was a somewhat painful introduction to the field, for others, the main effort was to remember the sequences of calibrations, systematic tests, sample mounting procedures, spurion hunts... that had worked so well "before". Techniques learned at other sites were even tried. Most instruments used by College members were in full flight before the summer, though a few users and local contacts had forgotten some of the hard facts about sample quality, statistics...

It was particularly pleasing to see the new depths reached with the single-crystal four-circle cryostat on D10: a truly unique instrument, the more so as it is now controlled by Unix. An increasing proportion of beam time on D19 is used for fibre diffraction. D2B and D1B are the workhorses for increasingly sophisticated powder experiments, with D20 eagerly awaited. The CRG instruments are coming into play, and are a vital component in the life of the ILL. The new CRG teams increasingly make their presence felt: they are very welcome and already contribute to the scientific life of the ILL - many are of course old friends - and to experiments where continuity and careful preparation and analysis are needed.

Claire Wilson and Jason Buckley left the ILL during the year, as did Jean Pannetier to take up a research management position at Pechiney. We welcomed back Jacqui Cole, as well as Robert Wimpory to continue support for the materials science and industrial use of neutrons, in particular on D1A, and Thomas Hansen to help commission D20. The College was saddened to learn of the death of Alan Mackintosh.

As the instruments reached steady state operation, the new ILL scientists ask how they can cooperate with others to achieve synergy in their chosen areas. But many diffractionists are near their limit in local contact work; for some it is a choice, others find it hard to refuse. Users need to be conscious of the demands they make.

Proposal quality was high, and by the October 1995 round it was clear that the level of interest in neutrons was at least as high as before the shutdown; typically 75 proposals in College 5a (crystallography) and more than 100 in College 5b (magnetic structures). Proposals requiring extreme sample environments are often very demanding on scientists and technical services, but continue to be hallmarks of the ILL, and we fully support all efforts to optimise technical support. The scientific interests of the College are very wide, as is reflected in the brief reports below. The subject of this year's blue box, giant - or even colossal - magnetoresistance was very fruitful, and is yet another occasion, following high temperature superconductors and fullerenes, for the special virtues of neutrons, of course aided by complementary techniques, to be exploited.

Scientific Highlights in 1995

Crystallography

The atomic decoration of quasicrystalline $Al_{70}Pd_{20}Mn_{10}$

The structure of a quasicrystal may be described in a six-dimensional (6-D) space where translational periodicity is recovered. The 6-D periodic lattice is divided into two 3-D spaces: the physical space, also called parallel space, and the

complementary perpendicular space. The 6-D lattice is decorated by a set of 3-D atomic objects lying in perpendicular space. The problem of quasicrystal structure determination is then the location of these 3-D atomic objects and the determination of their shapes.

Despite the considerable progress made in understanding the atomic structure of quasicrystals since their discovery ten years ago, none of the proposed models give agreement with observation anywhere near that usually obtained for 'conventional' 3-D periodic structures. This is due to the difficulty in tailoring the atomic objects in specific structures, and more generally to the lack of a general modelling procedure; indeed the modelling of the 3-D objects requires in principle an infinite number of parameters. To complement the current extensive theoretical efforts on this problem, there is a need for more experimental data, in particular reflections corresponding to high values of Q_{perp}, the momentum transfer in perpendicular space.

The coarse structure of the $Al_{70}Pd_{20}Mn_{10}$ icosahedral phase has previously been determined by powder diffraction by isomorphous replacement of Mn with FeCr, and from contrast of the different relative scattering factors of Pd and Mn in X-ray and neutron single-crystal diffraction there is evidence for strong chemical order [1]. This results in a model consisting of quasiperiodic packing of two atomic clusters, identical topologically but with different chemical decoration. The neutron single-crystal data collected thus far however extend to just $Q_{perp} \sim 1$ Å^{-1}, this limit being due mainly to the dramatic fall-off in intensity which is roughly proportional to Q_{perp}^{-6}.

Two measurements on D19 (Garry McIntyre in collaboration with UJF, Grenoble) in 1995 have greatly extended the experimental data for $Al_{70}Pd_{20}Mn_{10}$. Taking advantage of the large 2-D position-sensitive detector (PSD), complete asymmetric volumes of reciprocal space were recorded to $Q_{parallel} = 11$ Å^{-1}, at room temperature, and just above the structural transformation observed between 550° and 770° C. Since a volume of reciprocal space is scanned with the 2-D PSD, rather than individual reflections as with a conventional diffractometer, the range scanned in Q_{perp} is infinite and the observational limit is determined by the counting time or the instrumental resolution. Such systematic data collections are the first on quasicrystals, and in the seven days available for each measurement gave observed reflections to $Q_{perp} \sim 1.6$ Å^{-1}, giving roughly five times the number of unique reflections previously recorded, over a dynamic range of more than four orders of magnitude. Fig. 1 shows one reciprocal lattice row with reflections near the limits of this range. Also evident is diffuse scattering due to phason disorder, and which is clearly different for the neighbouring reflections 15/24 and 16/24 which otherwise have similar integrated intensities.

These data are presently being analysed by Patterson techniques. A first analysis of the room temperature data has revealed significant deviations from the crude spherical

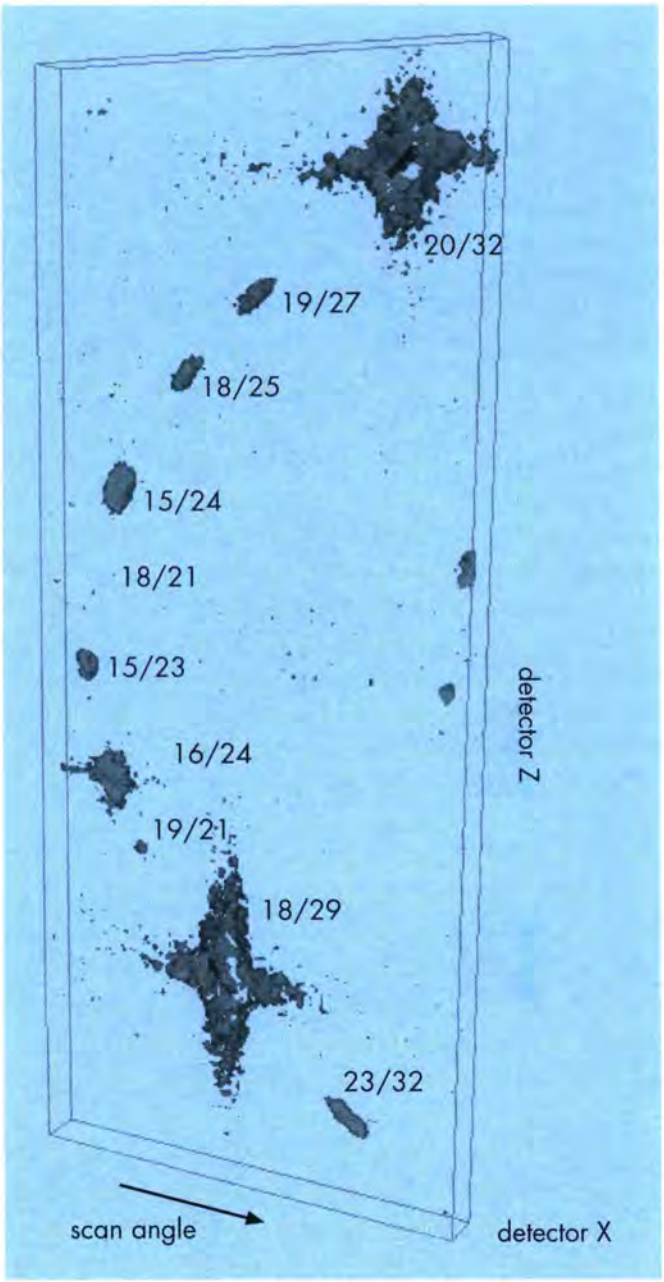

Fig. 1: A scan through the reciprocal lattice row of icosahedral $Al_{70}Pd_{20}Mn_{10}$ with the two-dimensional detector of D19. The reflections span four orders of magnitude in intensity. The extended tails in the scan direction for the reflections 18/29, 16/24 and 20/32 are due to phason disorder.

model that was previously derived for the shape of the decorating atomic object (Fig. 2). With allowance for the different overall Debye-Waller factors, there are also large differences between the room-temperature and high-temperature data for about 30% of the reflections; the structures at the two temperatures are thus similar but by no means identical. The room-temperature data will be complemented by synchrotron X-ray data collected on the same crystal to $Q_{perp} \sim 3.0$ Å^{-1} near the Pd absorption edge.

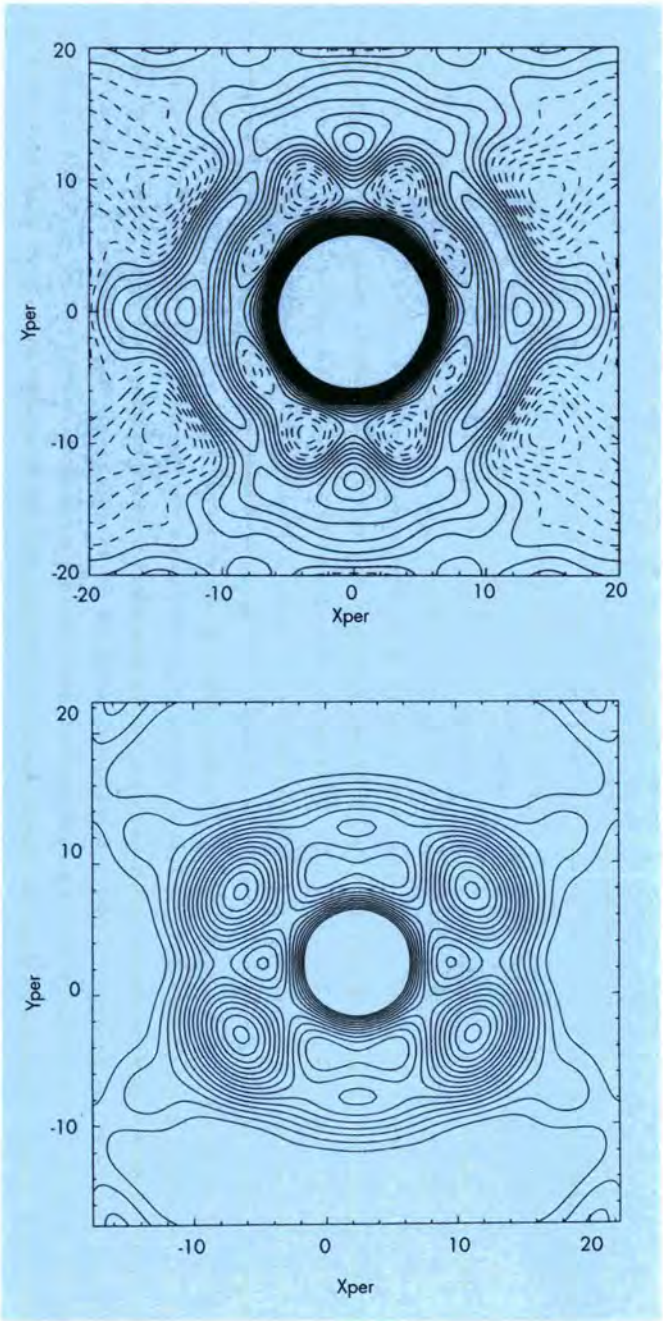

Fig. 2: Difference Patterson syntheses based on the superlattice reflections of the atomic decoration in icosahedral $Al_{70}Pd_{20}Mn_{10}$: Sections in perpendicular space at, a) the origin, and b) the body centre of the 6-D cube.

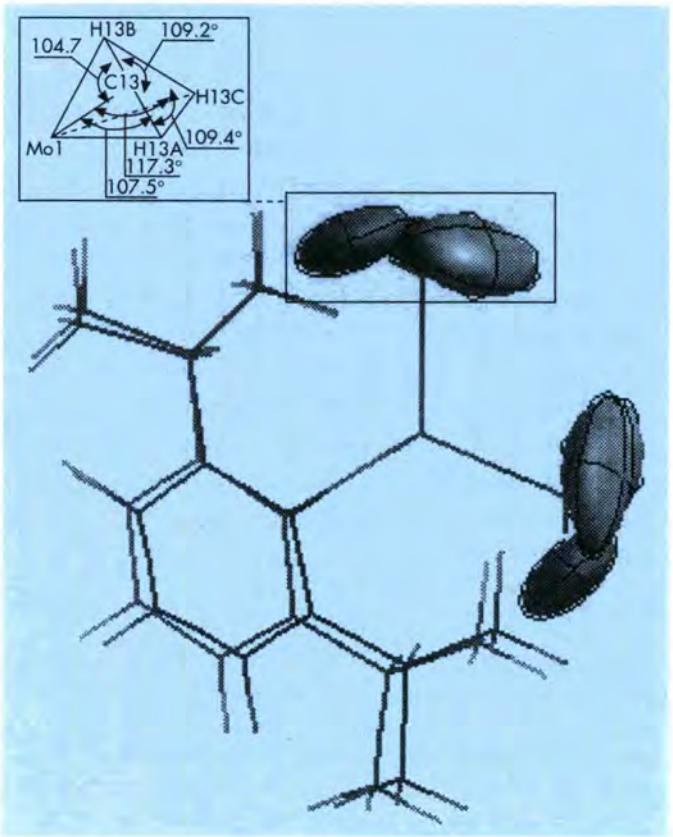

Fig. 3: The molecular structure of $Mo[Me]_2[NC_6H_3(^i\text{-}Pr)_2]_2$, illustrating (a) the distortion of the methyl groups from regular tetrahedral geometry, and (b) the sense of the librational effects of the methyl hydrogen atoms. The two alpha-Mo methyl groups are symmetry equivalent so values are given for only one of the groups.

Multiple α-agostic interactions in $Mo[Me]_2[NC_6H_3(^i\text{-}Pr)_2]_2$ *

Three-centre M-C-H α-agostic interactions have been proposed to play an important role in polymerisation catalysis, in particular of the Ziegler-Natta variety. Simple agostic interactions have been known for some time now and many of these compounds have been characterised by single crystal X-ray diffraction but only a very few by neutron diffraction. Furthermore, compounds exhibiting *multiple* agostic interactions are very rare. Results from recent work in Durham (De Silva D., Gibson V.C., Howard J.A.K., Walker G.L.P., unpublished work) had indicated the presence of such multiple α-agostic interactions in the compound, $Mo[Me]_2[NC_6H_3(^i\text{-}Pr)_2]_2$. Neutron studies were deemed necessary in order to unambiguously confirm (or otherwise) their presence.

A single crystal neutron diffraction experiment was carried out on D9 (Jacqueline Cole in collaboration with the University of Durham) to study $Mo[Me]_2[NC_6H_3(^i\text{-}Pr)_2]_2$ at T = 150K. Best results so far obtained indicate that α-agostic interactions do indeed exist; each methyl's coordination is markedly distorted from regular tetrahedral geometry and of special note is the angle Mo-C13-H13B which is particularly low (104.7°). A large amount of librational motion ensues, thus disguising the exact positions of the hydrogen atoms; however, this thermal motion appears to be directed towards the Mo atom. Figure 3 illustrates this directed libration and further, one can see that two of the hydrogen atoms lie distinctly closer to the Mo atom than the other. The average distances (considering librational effects) between the Mo

atom and H13A and H13B respectively are 2.627 Å and 2.604 Å (compared to 2.756 Å for Mo H13A), thus confirming the presence of α-agostic interactions. We suppose that both of these two hydrogens take part in this type of interaction with the Mo atom; although not both to the same extent but such that the overall effect results in the obeyance of the $18e^-$ rule.

* ^{i}-Pr = isopropyl (a 2-methyl-ethyl group).

Diffraction from polymeric gratings

One of the first successful experiments on the new small-angle scattering facility D22 of the ILL was on Bragg diffraction from laser-induced gratings in polymers.

Using photo-inducers, one can create regions of higher density in a thermally prepolymerised deuterated polymer matrix by polymerising additional monomers in a holographic light-interference field.

The density modulation, which is very weak, creates a three-dimensional lattice with a lattice constant of about 800 nm in this example and a thickness of some mm in the polymer. The grating is able to diffract slow neutrons with a high yield.

Fig. 4 (page 158) shows the diffraction pattern obtained at the ILL (Romano Rupp and colleagues, University of Osnabrück, Germany together with Roland May, ILL) at D22 using neutrons of about 4.1 nm. What is seen is the direct beam at x = 0, a strong first order reflection about 12 channels to the right, a weak first order reflection to the left, and a weak second order peak at the right. The relative intensities can be changed by turning the grating in front of the beam. As can be seen in the profile below, the first-order peak is significantly stronger than the transmitted beam. The inclination of the diffracted spots is due to the fact that neutrons with larger wavelengths contained in the wavelength distribution of 10% (fwhm) also fall further down before they reach the detector.

In a second experiment on D11, the same team was able to demonstrate for the first time the existence of the interference of cold neutrons (wavelength 1.5 nm) with a contrast of up to V = 0.2.

Ultimately, such experiments can serve two purposes: They allow one to build neutron-optical components, and they can serve to study the relaxation of laser-induced patterns in polymers by means of combined neutron and light interferometry.

Thermally induced redistribution of residual stress in high temperature components

The failure of engineering components which are subjected to steady loading at elevated temperatures can occur over a period of time by creep rupture, (which occurs when the creep durability of the material is exhausted), by creep crack growth or some combination of both processes [2]. Creep rupture is most likely to occur in structures that do not contain stress concentrations and which are defect-free, whereas failure by crack growth is most likely to take place in components which contain a sharp defect from which a crack can propagate. With the increasing use and sensitivity of non-destructive inspection techniques, defects are more readily detected than previously and there is a growing need for methods of assessing their significance, especially in components which operate at elevated temperatures.

In order to produce reliable estimates of the lifetimes of high temperature equipment, such as steam pipes and pressure vessels in electrical power and chemical process plants, procedures are needed for reliably predicting the rate of growth of any defects that may be present. Models have been produced for describing these cracking rates in terms of creep damage accumulation in a process zone ahead of a crack tip using creep fracture mechanics concepts and a knowledge of the loading conditions applied to a component. However, components such as steam pipes and pressure vessels typically contain residual stresses, which are introduced during fabrication by bending and welding operations, and these will contribute to the overall stress. It is necessary to determine to what extent these stresses influence component lifetimes. Also, because of creep, these residual stresses will relax with time. It was the purpose of this investigation to examine the residual stress redistribution caused by creep in a low alloy steel steam pipe material.

The 'C', half thick pipe section, geometry was chosen because a crack can subsequently be propagated along the plane XX (see Fig. 5) to represent the behaviour of an axial defect in a steam pipe. It had an inner radius 25 mm and outer radius 50 mm. The thickness was restricted to 12.5 mm to limit neutron beam attenuation. The material was a 1% CrMoV ferritic steel that had been taken from a rotor forging. The sample was pre-stressed in tension at a load of

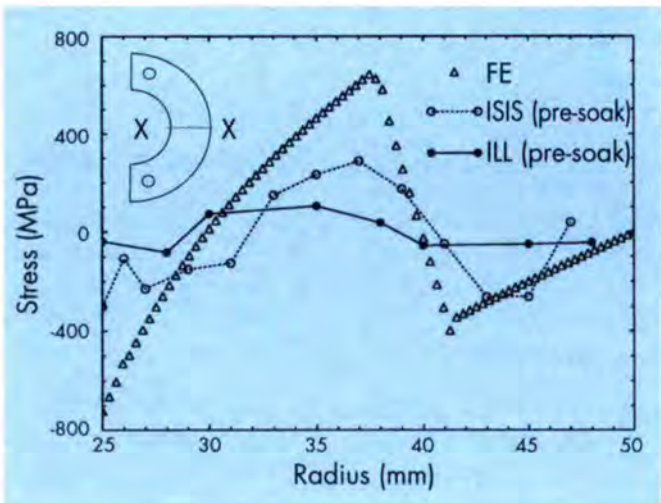

Fig. 5: Calculated and measured residual stresses across section X-X

51 kN, so that yielding occurred at the bore resulting in a compressive residual stress field at the bore and a balancing field across the ligament XX. The predicted residual stress field, which was calculated using a finite element code, is shown in Fig. 5 together with the original stress distribution, which had been measured during a previous investigation at ISIS. The original measured stresses were, in general, not as high as those predicted by the FE model.

To simulate typical high temperature service the sample was soaked in a furnace at 550°C for 250 hours. The redistributed residual stress field, determined from data obtained using D1A (collaboration with G.A. Webster, Imperial College & P.J. Webster, Salford University) and the (211) reflection, is also shown in Fig. 5. It is evident that the treatment caused relaxation, by creep, of most of the residual stresses, particularly the peak stresses at the centre of the sample ligament. Comparisons are being made with finite element predictions of the relaxation process. It is anticipated that the magnitude of the changes observed will have a significant effect upon lifetime predictions.

The crystal structure and optical activity of tellurium

The elements tellurium and selenium have a crystal structure made up of spiral chains of bonded atoms packed in an hexagonal array. The spiral chains may be of either hand and consequently the symmetry of the structure is enantiomorphic. The right-handed form belongs to space group $P3_121$ and the other to $P3_221$. Crystals of tellurium exhibit strong optical rotatory power, the two enantiomorphs having opposite senses for the rotation. It has not yet been possible to determine experimentally which particular enantiomorph gives which sense of optical rotation since the normal methods of crystal structure determination cannot distinguish between enantiomorphs, nor is this straightforward using anomalous dispersion. The sense of the spiral chains can be obtained in a diffraction experiment only through the anisotropy of the electron density due to bonding which combined with anomalous dispersion can produce small differences in the intensities of Friedel pairs of reflections. However the intensity differences expected are only a fraction of a percent so that their measurement is hardly feasible.

It has been shown in previous experiments that the polarisation dependence of the neutron spin-orbit (Schwinger) scattering is a sensitive probe of the asymmetry of the electron density in acentric structures. This property of the Schwinger scattering has now been used to determine the sense of the structural spiral in tellurium. In an order of magnitude calculation made to estimate the feasibility of the experiment, the asymmetry of the electron density was modelled by a bond charge of 0.05 electrons (the value determined from Schwinger scattering experiments of GaAs) placed at the mid points of the Te-Te bonds. This calculation showed that there should be no polarisation dependence of the intensity of {h0l} reflections due to charge asymmetry; but that for more general reflections including the form

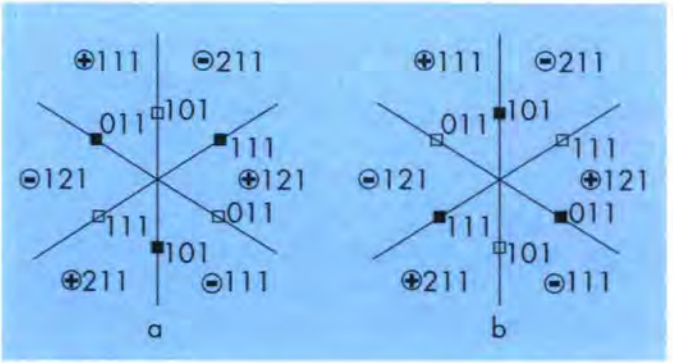

Fig. 6: Diagram of the hk1 plane of reciprocal space for the two enantiomorphs of Te. The positions of the 101 and 111 reflections are indicated. In the point group $P3_121$ the 12 101 reflections are divided into two groups of 6 which for Te have very different structure factors. For enantiomorph (a) the squares marking the sets with strong (s) or weak (w) structure factors are filled or open respectively. The positions of the 111 reflections are marked with positive or negative signs indicating the expected sign of R-1. It can be seen that for enantiomorph (a) the sequence on rotating the diagram clockwise from 111 is - w + s - w + s... whereas for (b) it is - s + w - s + w.....

{hhl} a polarisation dependence amounting to a few parts in 10^{-4} should be observed. Furthermore, the calculations show that there is a characteristic sequence of positive and negative differences, shown in Fig. 6, which distinguishes between enantiomorphs. Measurement of such a small effect is possible only with a large crystal and a high intensity polarised neutron source, since some 10^8 neutrons per reflection must be counted to obtain 25% accuracy in the difference from unity (R-1) of the polarised neutron flipping ratio estimated in the model calculation.

Measurements of 4 sets of {hhl} reflections were made (Jane Brown in collaboration with Bruce Forsyth, RAL) on the polarised neutron diffractometer D3 with $\lambda = 0.84$ Å, two of these were remeasured with $\lambda = 0.51$ Å. The results are shown in Table 1. The differences R-1 are consistent with those calculated for the space group $P3_121$. They show an asymmetry which is due to the imaginary part of the Te scattering length. The actual values of R-1 lead to a value of the bonding charge in the simple model outlined above of 0.032(15) electrons.

The optical rotation of the crystal was measured using an infra-red Fourier transform spectrometer. The wavelength dependence of the rotatory power had the same functional form as that of previous measurements. Its sense showed that our crystal was laevo-rotatory: it rotates the light to the left as seen by an observer looking through the crystal towards the light source.

These experiments show conclusively that the plane of polarisation of light transmitted along [001] rotates in the same sense as the spiral chains of bonded tellurium atoms.

The simple principles based on the polarisable ion model, which have proved successful in determining the sense of optical rotation in quite a number of compounds, predict that the plane of polarisation in Se and Te should rotate in the opposite sense to the structural helix in contradiction with our observation. It is probable that this disagreement is due to the inadequacy of a single ionic polarisability to describe the highly anisotropic, covalent structure of tellurium.

Table 1

The differences from unity of the observed flipping ratios R, and their signs ± calculated for the space group $P3_121$ for different members of the forms {hhl}.

{hkl}	hkl	hk-l	-h-kl	-h-k-l
λ=0.84	(R-1)×10^6 ±	(R-1)×10^6 ±	(R-1)×10^6 ±	(R-1)×10^6 ±
1 1 0	-9(7)	-		10(4) +
1 1 1	35(11)	+ 31(12)	+ -16(10)	-9(11) -
0 0 3	2(5)	+ -1(5)	+	
1 1 2	14(11)	- -2(11)	--31(17)	+ -4(15) +
λ=0.51				
1 1 1	-55(21)	+ 40(20)	+ -59(26)	- -31(21) -
0 0 3	14(6)	+ 9(6)	+	

Superconductors produced under high pressure

Until their crystal chemistry is understood, many interesting compounds can only be prepared in very small quantities and often under extreme conditions. This is the case of some high temperature superconductors, such as $Ca_2Sr_2Cu_3GaO_9$. This structure was studied and published by Roth [3] on D1A shortly before the long reactor shutdown, but the material was prepared under normal conditions and was non-superconducting.

Recently a group from the Japanese Institute for Research in Inorganic Materials (F. Izumi, Tsukuba) succeeded in producing small quantities of superconducting material (Tc = 73K) at 1250°C and 6 GPa. The structure (Fig. 7, page 158) of a very small sample of the superconducting material was obtained on D2B by Khasanova et al. [4]. It was found that only at high pressure was the Ca^{2+} site completely occupied (Sr^{2+} and Ca^{2+} are completely ordered on two different sites). This permits sufficient hole doping of the CuO_2-layers for superconductivity, with the formal oxidation state of copper 2.33.

This work is an excellent example of how the increasing efficiency of neutron powder diffractometers (the new D20 will be able to study milligramme samples) contributes to the understanding of the crystal chemistry of new materials prepared under extreme conditions.

Structural analysis of $CuGeO_3$: relation between nuclear structure and magnetic interaction

One-dimensional spin-1/2 structures have been studied extensively both experimentally and theoretically, but, until recently, spin-Peierls (SP) transitions were known in only rather complicated metal-organic structures. Therefore the announcement by Hase et al [5] of a SP transition at 14 K in the rather simple inorganic compound $CuGeO_3$ triggered a lot of interest in this compound. The observed magnetic phase diagram and excitation spectrum followed the expectations from the organic SP compounds, but the structural component of the SP transition remained subject to controversy. Eventually a combined X-ray and neutron study positively identified a superlattice with space group Bbcm giving rise to very weak reflections of the type (h/2 k l/2) in the room-temperature Pbmm cell.

The importance of the nuclear structure for the magnetism in $CuGeO_3$ is suggested by several macroscopic observations: the SP transition is accompanied by a spontaneous strain along b, and by large anomalies in the ultra-sound velocities, and even above T_{SP} the crystal structure is rather anharmonic. Our knowledge of the nuclear structure in the SP phase, and its relation to the higher-temperature structure is however limited by the very low intensity of the superlattice reflections, the strongest being some four orders of magnitude smaller than the strongest reflection in the high-temperature structure. This lack was rectified by a very careful diffraction measurements on D10 to determine the structure of $CuGeO_3$ at room temperature, at 20 K and at 4 K [6]. The number of unique superstructure reflections measured reliably was increased sevenfold over earlier studies.

The $CuGeO_4$ structure consists of CuO_6 octahedra and GeO_4 tetrahedra stacked along c (Fig. 8). A pronounced temperature dependence of the atomic positions in the high-temperature phase was observed. The major deformation on cooling from room temperature to 20K is a rotation of the $Cu(O_2)$ ribbons around the c axis, accompanied by a

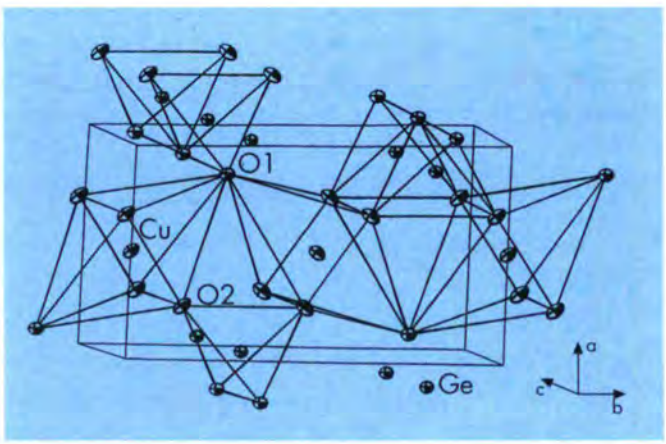

Fig. 8: The room-temperature structure of $CuGeO_3$. The ellipsoids represent 40% probability density. The lines indicate the Pbmm cell.

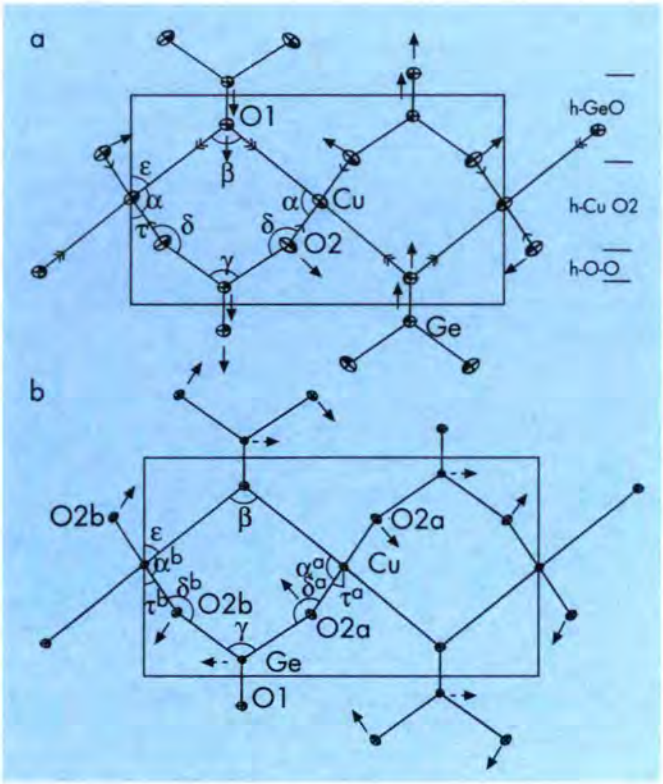

Fig. 9: a) Projection of the $CuGeO_3$ structure at room temperature on the a,b plane; the arrows indicate qualitatively the shift of the atomic positions on cooling to 20 K.
b) Projection at 4 K in the spin-Peierls phase; the arrows indicate the displacements with respect to the high-temperature phase.

translation of the tetrahedra. The reason for this behaviour might be an internal mismatch between the sizes of the octahedra and tetrahedra, and the volumes of the cavities. The rotation is similar to the distortion observed below the spin-Peierls transition, with the important difference that the displacement of neighbouring octahedral edges are displaced in the same direction above the transition, while below the transition they are displaced in opposite senses to result in a twist distortion (Fig 9.). The rotation of the $Cu(O_2)$ ribbons has an impact on the magnetic interaction parameter J; computation of J shows that its splitting in the spin-Peierls phase is dominated by the modulation of the Cu-O-Cu angle.

Crystallography and Magnetism

Measuring natural Sm on D1B, the magnetic structures of $SmMn_2Ge_2$

Giant magnetoresistance (GMR) phenomena (see also Blue Box) have first been found in artificially produced thin film Layered Metallic Magnetic Structures (LMMS). A spin flop transition can be induced by a field, destroying thereby the antiferromagnetic ordering between successive layers. Later it was found that these GMR effects can also be expected in bulk LMMS.

The intermetallic compounds RMn_2X_2 (R = Rare-Earth, X = Ge or Si) crystallise in the $ThCr_2Si_2$ type structure. It is made up of atomic layers stacked along the c-axis direction with sequence R-X-Mn-X-R.

Magnetisation measurements on $SmMn_2Ge_2$ revealed already in 1985 an interesting sequence of phase transitions from paramagnetism at high temperatures through ferromagnetism between 350 K > T > 140 K to antiferromagnetism for 140 K > T > 105 K and finally back to ferromagnetism below 105 K. This compound was of special interest due to its reentrant behaviour at low T and due to the GMR present in the antiferromagnetic phase between 105 K and 140 K.

Later a plenitude of RMn_2X_2 compounds was studied with magnetic measurements and neutron diffraction; an overview of the neutron results is given in [7]. However, although being in a certain sense the prototype of the RMn_2X_2 compounds the exact magnetic structure of $SmMn_2Ge_2$ has never been studied by neutron diffraction due to the very large absorption cross-section of Sm.

In a collaboration with the University of St Andrews (C. Ritter, G. Tomka, C. Kapusta, P.C. Riedi) it was planned to perform the measurement on an isotopically enriched sample with less absorption. Unluckily, however, the supplier of the isotope could not honour his engagement and we had to try the 'impossible': Powdering the sample very finely and diluting it with Al-powder in a ratio of 1:10, a natural sample of $SmMn_2Ge_2$ was measured on D1B with $\lambda = 2.52$ Å. Figure 10 shows a spectrum as obtained after 1 h measuring time, peaks at $2\Theta = 66°$ and 77° stem from the added Al-powder, the peaks at 72° from the vanadium sample holder. The high absorption still present is mirrored in the behaviour of the background which decreases strongly when going to low 2Θ values. Its effect on the peak intensities can be corrected for by introducing an absorption coefficient into a modern Rietveld refinement program such as FULLPROF.

Data were collected at several selected temperatures: 1.5 K, 80 K, 120 K, 220 K, RT and 415 K. The profile refinement resulted in the magnetic structures and values of magnetic moments listed in table 1.

The 4 manganese atoms which are present in the unit cell are labelled in sequence, Mn1 at 1/2 0 1/4, Mn2 at 0 1/2 1/4, Mn3 at 1/2 0 3/4 and Mn4 at 0 1/2 3/4. A sequence ++++ in table 1 means obviously a ferromagnetic alignment of the 4 spins whereas ++— or -++- are antiferromagnetic couplings of the 1-4 labelled Mn spins. The numbers give the values of the component in the particular direction.

Although called ferromagnetic from the magnetisation results the phases at T < 105 K and at T > 140 K comprise a strong antiferromagnetic contribution, the magnetic structure is spin canted. This antiferromagnetic -++- coupling in the a-b plane is in fact the only exchange coupling present over the whole temperature range. The ferromagnetic coupling

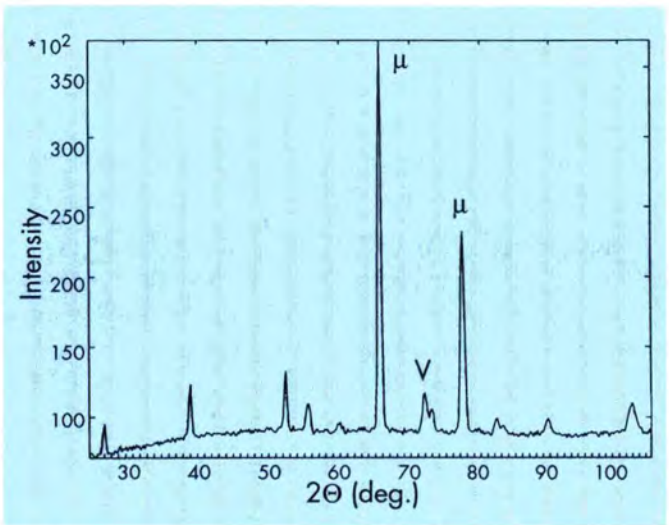

Fig. 10: Neutron diffraction pattern of $SmMn_2Ge_2$ at 1.5 K as measured on D1B in 1 hour

not only disappears in the intermediate phase 105 K < T < 140 K but changes the spin direction from parallel to the c-direction at high temperatures into the a-b plane at low temperatures.

Figure 11 displays the magnetic structures as found at 2 K, 120 K and 220 K. The existence of a Sm moment at 220 K must surprise when compared to similar RMn_2Ge_2 compounds. We believe it to be real and induced by the strong molecular field of the Mn sites.

Temperature		a-direction	b-direction	c-direction	total moment (μ_B)
1.5 K	Mn	++++ 2.1(1)	-++- 1.7(2)	/	2.7(2)
	Sm	++ 0.75(2)	/	/	0.75(2)
80 K	Mn	++++ 1.8(1)	-++- 1.5(2)	/	2.3(2)
	Sm	++ 0.5(3)	/	/	0.5(3)
120 K	Mn	/	-++- 0.8(2)	++— 1.5(2)	1.7(2)
	Sm	/	/	/	/
220 K	Mn	/	-++- 1.4(2)	++++ 1.6(2)	2.1(3)
	Sm	/	/	++ 0.45(3)	0.45(3)
300 K	Mn	/	-++- 1.4(1)	++++ 1.3(1)	2.0(2)
	Sm	/	/	++ 0.13(2)	/
415 K	Mn	/	/	/	/
	Sm	/	/	/	/

Comparing these results with data gathered in a collaboration with the University of Zaragoza on $Nd_{1-x}Tb_xMn_2Ge_2$ compounds a further phase transition should take place in $SmMn_2Ge_2$ between RT and T_N. In fact it was shown for compounds of the $Nd_{1-x}Tb_xMn_2Ge_2$

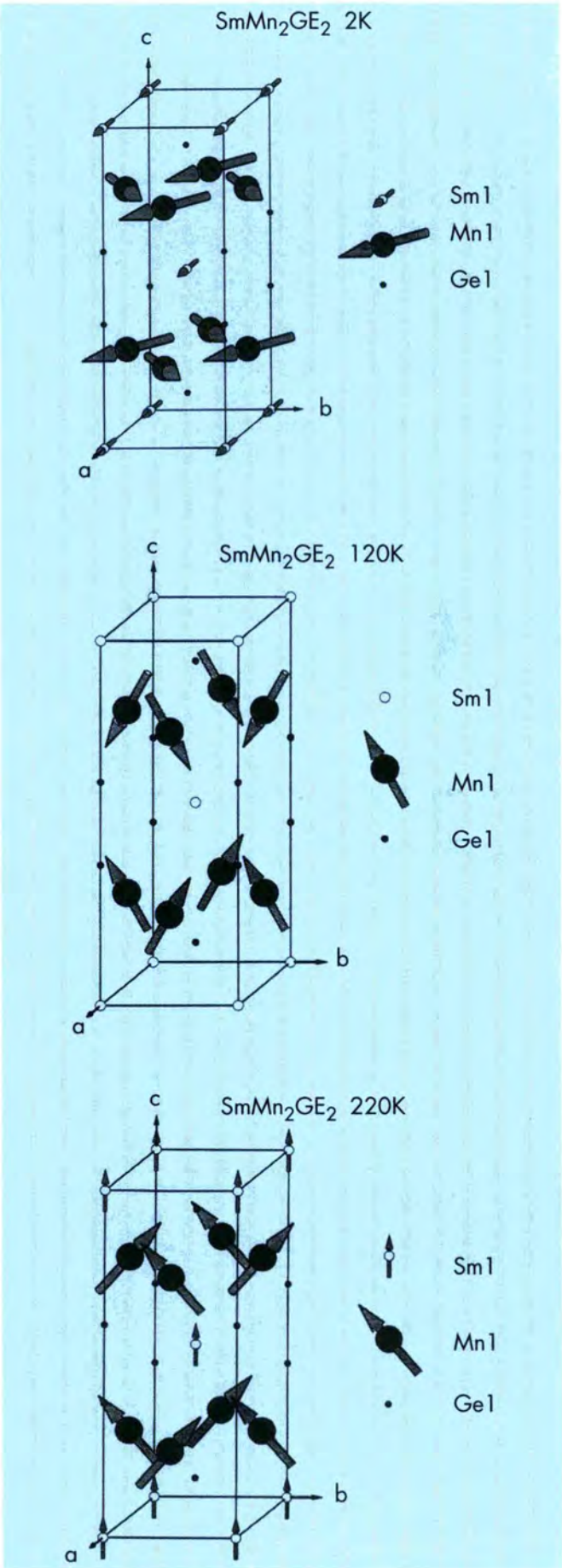

Fig. 11: Magnetic structure of $SmMn_2Ge_2$ at 2 K, 120 K and 220 K

system that have a similar canted antiferromagnetic structure at about RT the ferromagnetic component always disappeared at lower temperatures than T_N.

Spin-glass state in $(Tb_{1/3}La_{2/3})_{2/3}Ca_{1/3}MnO_3$

The giant magnetoresistance (GMR) effects found recently in some of the $A_{1-x}A'_xMnO_3$ compounds (where A is a rare earth ion and A' is a divalent alkali) are at the origin of sudden increase of interest of the scientific community in these compounds (see as well the Blue Box).

Magnetoresistance ratios ($MR(\%) = 100 \times (\rho(0)-\rho(H))/\rho(H)$) greater than 10^7 in polycrystalline $A_{0.7}A'_{0.3}MnO_3$ have especially attracted researchers' attention. $\rho(H)$ is the field-dependent electric resistivity. It seems that the largest GMR ratios appear around this composition and special effort is currently being devoted to these particular compounds. Hwang et al. [8] recently proposed universal behaviour of $A_{0.7}A'_{0.3}MnO_3$ compounds. The so-called tolerance factor ($t = d_{A-O}/(2d_{Mn-O})$), a geometrical quantity involving the bond lengths d, is the important parameter to determine the magnetic and transport state of this kind of compounds.

Until now, only ferromagnetic behaviour has been reported in $A_{0.7}A'_{0.3}MnO_3$ compounds but susceptibility and magnetisation measurements strongly indicate spin-glass (SG) behaviour for terbium rich $(TbLa)_{2/3}Ca_{1/3}MnO_3$ compounds. With the help of the $(Tb_xLa_{1-x})_{2/3}Ca_{1/3}MnO_3$ series the universal phase diagram was mapped out from t = 0.916 to t = 0.887. For $x > 1/3$ ($t < 0.906$) the SG state sets in due to the competition between the ferromagnetic double-exchange interaction and antiferromagnetic superexchange interaction, which prevents the occurrence of long range magnetic order.

Neutron diffraction was the last proof needed to confirm the absence of long range magnetic order and the presence of a spin-glass state at low temperatures. In a collaboration with the University of Zaragoza (the above mentioned magnetic measurements were performed there) data were collected on D1B on $(Tb_{1/3}La_{2/3})_{2/3}Ca_{1/3}MnO_3$ [9]. Figure 12 shows a plot of scattering intensity versus temperature in the 2Θ range from 2.5° to 41°. The first nuclear peak at 2Θ = 39° shows no extra magnetic contribution and no additional Bragg peaks appear as the temperature is lowered. This indicates the absence of long range magnetic ordering. However, the low-angle diffuse magnetic scattering increases from 95 K downwards. Both features are hallmarks of the random freezing of spins.

In figure 13 is plotted the electronic and magnetic phase diagram of $(Tb_xLa_{1-x})_{2/3}Ca_{1/3}MnO_3$ plotted as a function of t. At high temperatures all the compounds are paramagnetic insulators (PMI). At low temperatures there are two possibilities. For $x < 1/4$ ($t > 0.908$) a ferromagnetic metallic state (FMM) sets in. At and beyond $x = 1/3$ ($t = 0.906$) a spin-glass insulator state (SGI) takes place. The correlation between magnetic and transport properties is evident. If the

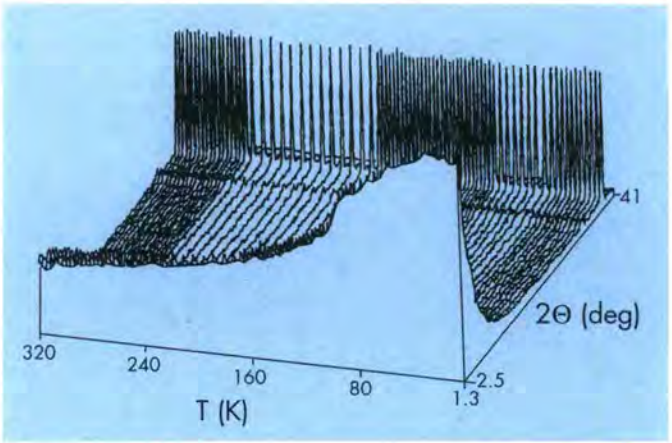

Fig. 12: Temperature and angle dependence of the intensity of the neutron scattering of $(Tb_{1/3}La_{2/3})_{2/3}Ca_{1/3}MnO_3$

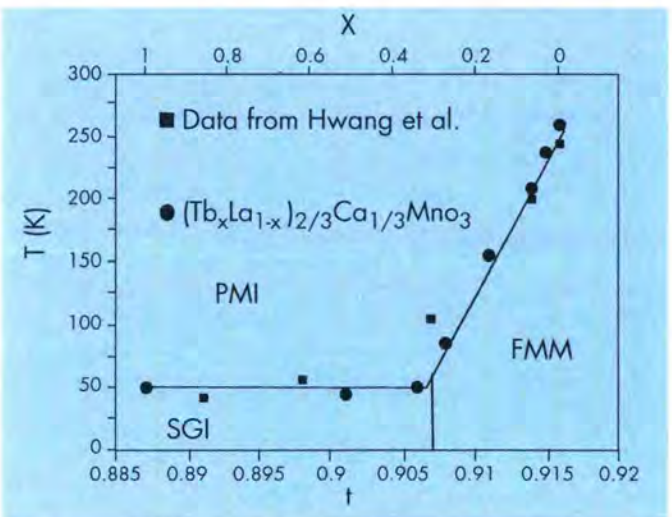

Fig. 13: Electronic and magnetic phase diagram of $(Tb_xLa_{1-x})_{2/3}Ca_{1/3}MnO_3$ as function of x and t

compound has long range magnetic order it will undergo a spontaneous insulator-metal transition at T_C. If a spin-glass state emerges the compound will remain an insulator.

3-D Magnetic Structure of ErF_3

Binary rare-earth fluorides are known to undergo magnetic phase transitions but due to their low ordering temperatures their magnetic structures are often not yet known. These fluorides are orthorhombic and crystallise in space group Pnma with Z=4. Among them, the magnetic structures of TbF_3 (T_C = 3.96 K), HoF_3 (T_C = 0.53 K) and DyF_3 (T_C = 2.8 K) were already determined. A collaboration with the University of Bern and the PSI [10] looked now at the magnetic structure of ErF_3. Neutron diffraction patterns

at low temperatures were recorded on the D1B spectrometer using a dilution cryostat. The magnetic ordering point was determined to T_N = 1.05 K. A diffraction pattern recorded at 0.25 K was used to determine the magnetic structure. It is characterised by the vector k = (0, 0, 0) and Pn'm'a' has been found to be the correct magnetic space group. The magnetic moments of Er^{3+} lie within the a-c plane at an angle of 60° from the a-axis, almost parallel to the long Er-F distance of 2.503 Å as shown in figure 14. Within the a-c plane ErF_3 behaves as a canted ferromagnet and therefore similar to TbF_3 and HoF_3. However, along the b-axis, the magnetic moments of ErF_3 are antiferromagnetically coupled along the b-direction. ErF_3 is thus an antiferromagnet whereas TbF_3 and HoF_3 are canted ferromagnets.

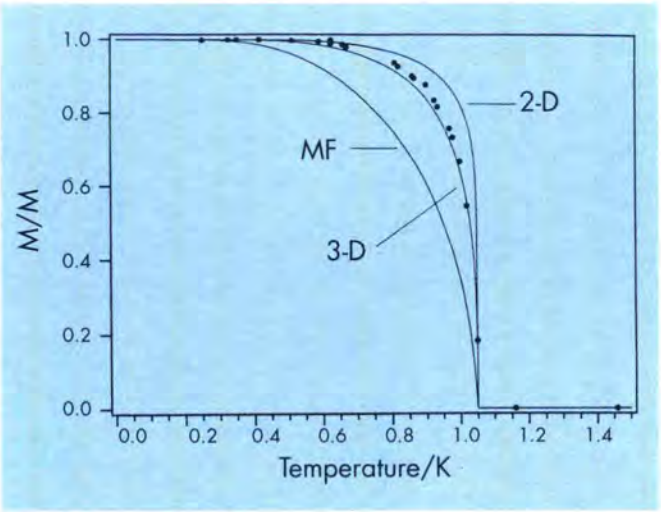

Fig. 15: Temperature dependence of the magnetisation of ErF_3 derived from magnetic Bragg peak intensities. The lines show calculations for the mean field model (MF), the 3-D and 2-D Ising spin 1/2 model.

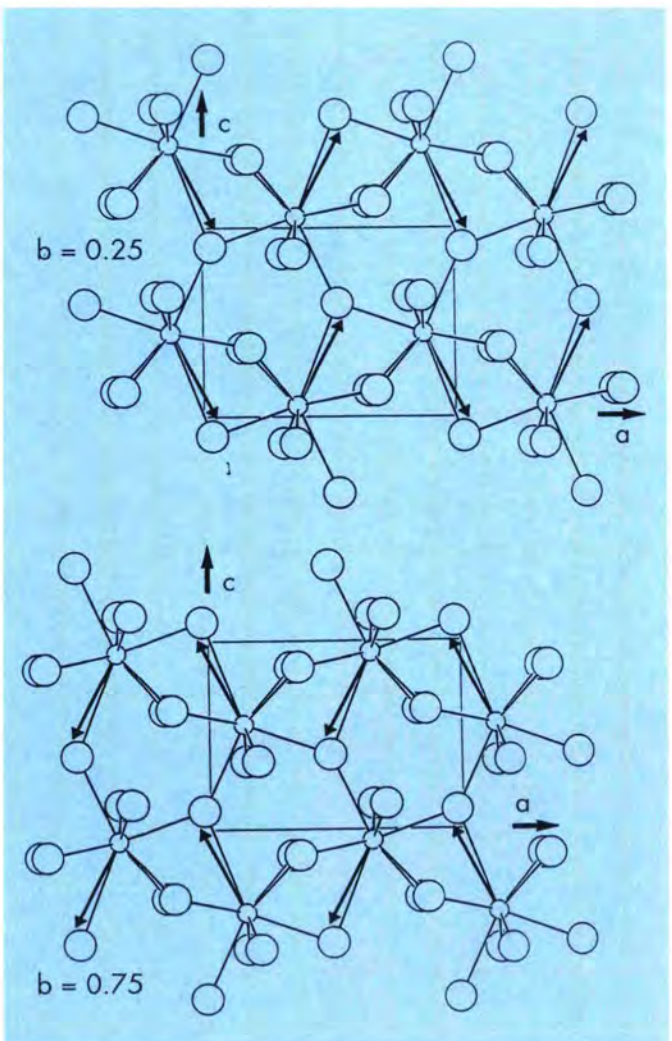

Fig. 14: Crystal structure of ErF_3 at 0.25 K, the small cycles represent the Er atoms. The orientation of the magnetic moments is indicated by arrows.

It is at first sight surprising to find such differences in the magnetic behaviour of the YF_3 type fluorides which are quite similar from a chemical point of view. The interactions that lead to three dimensional magnetic order are very weak for these compounds as can be seen from the low ordering temperatures; exchange interactions are of the same order of magnitude as magnetic dipole interactions. The magnetic structure is the result of a complicated balance of forces which depend on the crystal structure as well as on the magnetic moment of the rare earth ion and its anisotropy, and are thus sensitive even to minor changes.

Three different theoretical curves of the spontaneous magnetisation M vs. T have been calculated: the mean field (MF) solution, the two dimensional quadratic Ising lattice (2-D) using the solution of Onsager and a three dimensional simple cubic Ising lattice (3-D) using a Pade approximation (see figure 15). The 3-D curve yields the best agreement with the data, suggesting that a three dimensional, spatially quite isotropic interaction is more likely than a planar or chain interaction.

Observation of two length scales in critical scattering in the Kondo compound $CeAl_2$

The cubic Laves phase compound $CeAl_2$ is perhaps the best example of a Kondo lattice and has been investigated quite intensively. The Kondo temperature T_K = 5 K is of the order of the Néel temperature T_N = 3.8 K and therefore there is a competition between the demagnetising tendency of the Kondo effect (see blue box of College 4) and the moment-stabilising tendency of the RKKY interaction.

$CeAl_2$ orders at T_N to an incommensurate phase with the wave vector k = (1/2-δ, 1/2+δ, 1/2). In this sine-wave modulated structure the amplitudes of the magnetic moments are modulated along [-δ, δ, 0] (δ = 0.110) which is perpendicular to the moment direction [111]. Recently two modulations corresponding to the wave vectors (1/2-δ, 1/2+δ,1/2) and (1/2-δ,1/2+δ,-1/2) have been observed. They are coupled together and present in a single-domain $CeAl_2$ single crystal which had been produced by the application of a magnetic field.

This shows that the magnetic structure of $CeAl_2$ is actually a double-k spiral structure. The origin of such a complicated magnetic ordering in $CeAl_2$ must be related to the competition of the Kondo effect and the RKKY interaction. It is to be noted that the other $REAl_2$ (RE = rare-earth element) compounds order ferromagnetically.

Magnetic diffuse scattering above T_N can give valuable information about the magnetic interaction as well as the critical experiment. We (T. Chattopadhyay, G. McIntyre) have therefore performed such an investigation on $CeAl_2$ on D10.

Fig. 16 shows the scans as function of temperature around the reciprocal point 3/2, 3/2, 1/2 passing through the two satellite reflections 3/2-δ, 3/2+δ, 1/2 and 3/2+δ, 3/2-δ, 1/2 (δ=0.11). At T = 3.6 K two relatively strong satellite Bragg peaks are observed at the above-mentioned reciprocal positions. The satellite Bragg peaks have been fitted by Gaussian functions. The half width at the half-maximum (HWHM) of the satellite reflections is 0.0037 reciprocal lattice units and is resolution limited.

At T = 3.90 K broader diffuse scattering peaks are observed at about the same positions where magnetic Bragg reflections appear below T_N. The diffuse scattering consists of two components: a broad component corresponding to a relatively short correlation length and a narrow component corresponding to a much larger correlation length. The broad component has been fitted with a Lorentzian convoluted with the Gaussian resolution function. The narrow component has been fitted with a Gaussian but can as well be fitted by the square of a Lorentzian.

The broad component observed above the ordering temperature is due to the spin correlations and gives the average short range ordered domain size. The temperature dependence of this correlation length which diverges at the ordering temperature gives the critical exponent. In our case the presence of the additional narrow component complicates the analysis of the critical phenomena.

The existence of two length scales has also been observed in other magnetic systems by x-ray and neutron scattering. The longer length scale (the narrow component) has been attributed to random strain fields localised at or near the sample surface. But the observed ratio of the intensities of the narrow and broad components does not support such interpretation. We believe that the existence of the two length scales in diffuse scattering should be further investigated.

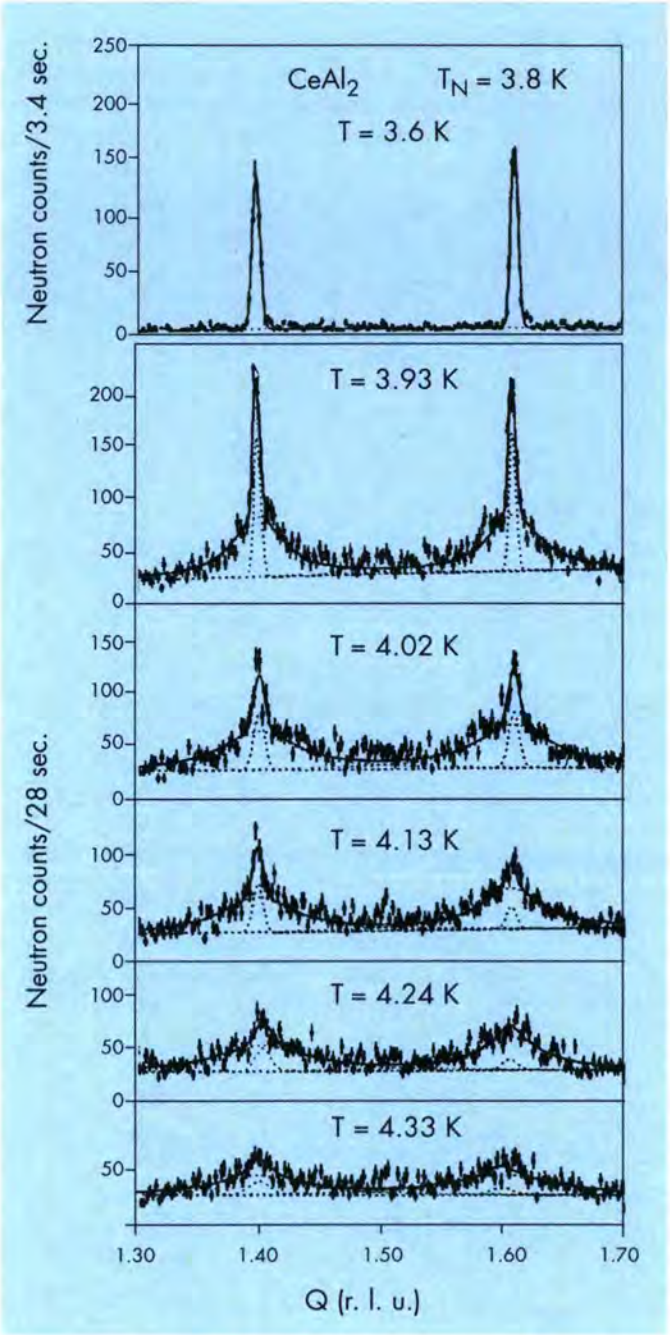

Fig. 16: Temperature variation of the integrated intensity of the 3/2-δ, 3/2+δ, 1/2 satellite reflection.

Phase transitions in rare-earth manganites

Rare-earth manganites, when doped with divalent ions on the rare-earth site, exhibit a variety of magnetic and structural transitions as a function of temperature, which in turn lead to large changes in conductivity. When a magnetic

field is applied to such a material the conductivity may be further enhanced to produce a giant magnetoresistance (GMR) effect. Compounds such as $La_{1-x}(Sr/Ca)_xMnO_3$ and $Pr_{1-x}Sr/Ca_xMnO_3$ exhibit such effects, and are the subject of intense current investigation (See the blue box for further information).

The parent compounds, $LaMnO_3$, $PrMnO_3$ and $CaMnO_3$ are all antiferromagnetic insulators. Doping with divalent ions such as Sr, Ca or Ba, produces Mn^{3+} and Mn^{4+} ions which results in competition between the antiferromagnetic and the ferromagnetic exchange interactions, so far best described by the so-called double-exchange mechanism. This mechanism is now being severely tested by new results from $Pr_{1-x}Sr/Ca_xMnO_3$ which exhibits 'charge ordering', i.e. a regular arrangement of Mn^{3+} and Mn^{4+} in a 1:1 ratio for a limited range of x. In fact in $Pr_{0.5}Sr_{0.5}MnO_3$, the transition to the charge-ordered state occurs at the ferromagnetic to antiferromagnetic transition. The doped La compounds also undergo a structural transformation from rhombohedral to orthorhombic symmetry as the temperature is lowered, with transition temperature being extremely sensitive to the value of x. This transition recently generated a lot of excitement when it was demonstrated that it may also be brought about by the application of a magnetic field at fixed temperature [11]. The magnetic-field-induced switching of the crystal structure is most effective when the structural transition temperature (T_s) is close to the ferromagnetic ordering temperature (T_c).

As occurred after the first observations of high-temperature superconductivity in the perovskite cuprates, much of the early characterisation of these compounds and the mapping of their phase diagrams, is being done by powder diffraction, and justifiably so. However, for more accurate investigation of particular compounds, and closer scrutiny of the magnetic structures, single-crystal studies should follow. The Warwick group was one of the first in Europe to grow single crystals of a number of these compounds, and two of these, $Pr_{0.5}Sr_{0.5}MnO_3$ and $La_{0.83}Sr_{0.17}MnO_3$, were investigated in experiments on D10 with unpolarised neutrons and on D3 with polarised neutrons [12].

All crystals tried of each compound turned out to be made up of several crystallites, which may be due simply to the present methods of crystal growth, but which could also suggest symmetry-lowering phase transitions between the growth temperature and room temperature.

The room temperature structure of $Pr_{0.5}Sr_{0.5}MnO_3$ proved to be monoclinic, very similar but obviously not identical to the orthorhombic structure reported earlier. The structure remains monoclinic through the ferromagnetic transition at $T_c \sim 270$ K, but a splitting of the reflections is observed at the antiferromagnetic transition at $T_N \sim 140$ K, suggesting simultaneous lowering of the nuclear symmetry at this transition. The brief search for evidence of the charge ordering at T_N was inconclusive.

$La_{0.83}Sr_{0.17}MnO_3$ was investigated in zero and applied magnetic fields to attempt to observe switching of the nuclear structure in a magnetic field, and by polarised-neutron diffraction to map out the magnetisation density in the different structural phases. It turned out however that at this value of x, T_s (~ 183 K, Fig. 17) is below T_c (~ 283 K, Fig. 18), which precludes switching of the nuclear structure in a field. We have since learned that reducing x to just 0.165 is sufficient to give $T_c < T_s$. Nevertheless the high-temperature rhombohedral and the low-temperature orthorhombic structures at x = 0.170 could be investigated in detail. The symmetry lowering at T_s results in twinning of the structure with six domain orientations. This does

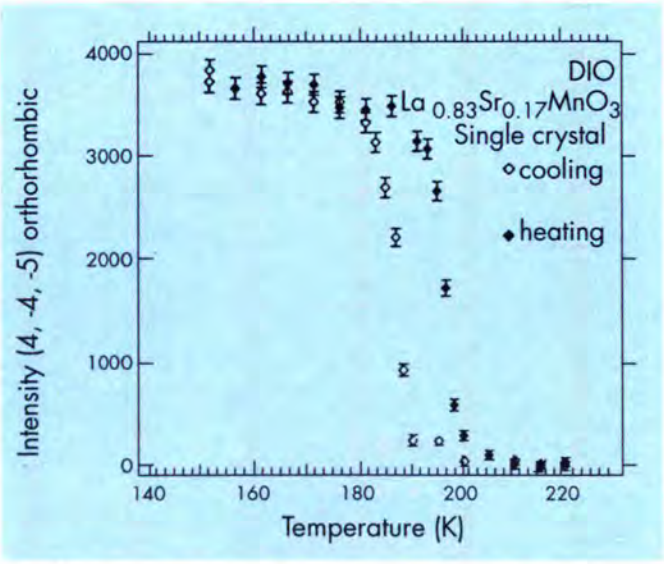

Fig. 17: Temperature variation of the orthorhombic (4,-4,-5) reflection in $La_{0.83}Sr_{0.17}MnO_3$ through the first-order structural transition at $T_s \sim 183$ K.

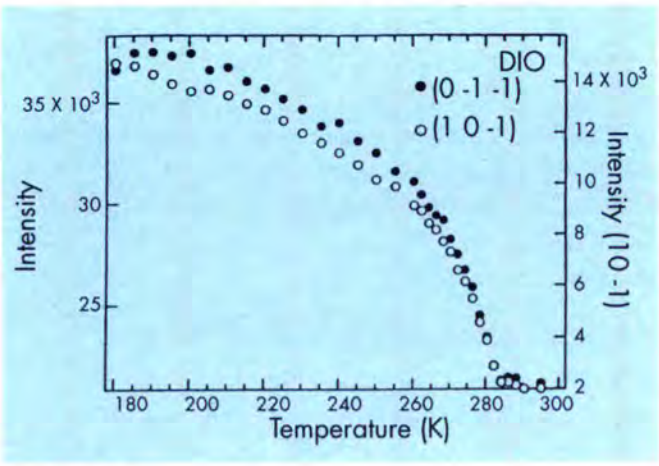

Fig. 18: Temperature variation of two low-angle reflections in $La_{0.83}Sr_{0.17}MnO_3$ through the ferromagnetic transition at $T_c \sim 283$ K.

complicate the analysis, particularly of the polarised-neutron data, although some reflections do correspond to just one domain alone.

It is clearly early days yet in the elucidation of the many structures and transitions in doped rare-earth manganites, but with the variety and power of the neutron techniques available they will not long remain obscure.

Secretaries: Sax A. Mason (5a)
Clemens Ritter (5b)

References

[1] M. Boudard, M. de Boissieu, C. Janot, G. Heger, C. Beeli, H. Nissen, H. Vincent, R. Ibberson, M. Audier and J.M. Dubois, J. Phys. Cond. Matter 4 (1992) 10149.

[2] G.A. Webster & R.A. Ainsworth 'High temperature component life assessment'. Chapman and Hall, London 1994.

[3] G. Roth, P. Adelmann, G. Heger, R. Knitter and Th. Wolf (1991) J. Phys. I 1, 721.

[4] N.R. Khasanova, F. Izumi, E. Takayama-Muromachi, A.W. Hewat (1996) J. Phys. C (in press).

[5] M. Hase, I. Terasaki and K. Uchinokura, Phys. Rev. Lett. 70 (1993) 3651.

[6] M.Braden, G. Wilkendorf, J.Lorenzana, M. Aïn, G.J. McIntyre, M. Beruzzi, G. Heger, G. Dhalenne and A. Revcolevschi, submitted to Phys. Rev. B.

[7] G.Venturini, R.Welter, E.Ressouche, B.Malaman, J.Mag.Mag.Mat. 150 (1995) 197.

[8] H.Y.Hwang, S.-W.Cheong, P.G.Radaelli, M.Marezio, B.Batlogg, Phys.Rev.Lett. 75 (1995) 914.

[9] J.M.DeTeresa, M.R.Ibarra, J.Garcia, J.Blasco, C.Ritter, P.A.Algarabel, C.Marquina, A.del Moral, subm. Phys. Rev.Let.

[10] K.Kraemer, H.Romstedt, H.U.Guedel, P.Fischer, A.Murasik, M.T.Fernandez-Diaz subm. Eur. J. Solid State Inorg. Chem.

[11] J.Knizek, Sol.State Chem. 100 (1992) 292.

[12] A.Asamitsu, Nature 373 (1995) 407.

Giant magnetoresistance: structural "tuning" of magnetism in $AMnO_3$ manganese perovskites

Paolo G. Radaelli

Introduction

Manganese perovskites with the general formula $A_{1-x}A'_xMnO_3$ (A = La, Pr, Y...; A' = Ca, Sr, Ba...) have been the subject of renewed interest, due to the giant magnetoresistance (GMR) exhibited near the ferromagnetic (FM) spin ordering temperature T_C. For the electronic hole doping concentration of x~0.30, the high-temperature paramagnetic state is a poor electrical conductor, whereas the low-temperature FM state is metallic (Fig. 1). The critical temperature of the coupled magnetic and metal-insulator (M-I) transitions is raised upon application of an external magnetic field, thereby producing, at constant temperatures near T_C, large changes in the electrical resistivity, an effect known as magnetoresistance. For this reason, manganese perovskites are presently being evaluated as a possible alternative to magnetic multilayers for a new generation of magnetoresistive sensors. It has been shown that magnetoresistive ratios up to 11 orders of magnitude can be attained by adjusting the relative sizes (ionic radii) of the metal ions [1,2] (see below). Furthermore, it appears that the properties of these materials improve when they are grown as thin films, probably due to substrate-film interactions [3,4]. At present, however, these extreme values of the magnetoresistive ratios can only be reached at low temperatures (~30 K), which are not ideal for most foreseen applications. The main goal of the applied research on these compounds is to improve their room-temperature magnetoresistances, which, for bulk materials, are now typically of the order of 100% in a 5 Tesla field. In a completely separate area, manganese

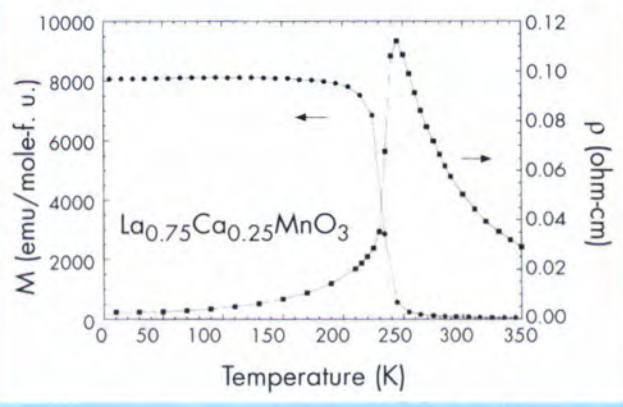

Fig. 1: Magnetic and electrical properties of a typical manganese perovskite: magnetisation M (H = 0.1T) and electric resistivity ρ (H = 0) vs temperature for $La_{0.75}Ca_{0.25}MnO_3$ (reprinted from Ref. 13).

perovskites have also attracted attention as cathode materials for high-temperature solid oxide fuel cells, due to their high oxygen ionic conductivity [5].

In addition to their exciting potential for industrial applications, manganese perovskites are also of great interest for fundamental research. Shortly after the discovery of these compounds some forty years ago [6], the concept of double exchange was developed to describe the essential aspect of the magnetic interactions between the Mn ions, which, due to the divalent substitutions for La on the *A* site, are in a mixed-valence state (+3/+4) [7]. The double exchange theory considers the interaction between itinerant electrons and the localised Mn moment, in the presence of strong on-site Hund's rule coupling, as the main contribution to the scattering of charge carriers in the paramagnetic state. More recently, however, it has been pointed out that this mechanism may not be sufficient to explain the magnitude and the behavior of the resistivity [8]. For this reason, an additional important aspect, first introduced by Goodenough [9] in the fifties, has been reevaluated as a possible key element for the physics of manganites: lattice distortions due to the different ionic size of Mn^{+3} and Mn^{+4} in general, and Jahn-Teller (J-T) type distortions of the oxygen octahedra around Mn^{+3} in particular [8]. For instance, the crystal structure of the parent compound $LaMnO_3$ [5] can be interpreted in terms of a J-T distortion of the $Mn^{+3}O_6$ octahedra. These developments, prompted both by experimental [10,11] and theoretical work [8], have emphasised the interplay between crystal structure and physical properties, and assigned a primary role to crystallographic techniques. As both long-range and short-range structural distortions appear to be present in this system, both the average and the local structure need to be studied in detail as a function of the thermodynamic and chemical parameters (temperature, pressure, magnetic field, chemical substitutions).

By studying the fundamental physics of these materials, we hope to learn how their relevant properties (Curie temperature and magnetoresistive ratio) can be improved so much that they become appealing for industrial applications. In this article, some recent diffraction experiments on manganese perovskites will be described. Far from giving a comprehensive picture of this complex system, they nonetheless provide some useful "pieces of the puzzle" toward a better understanding of these compounds.

Structure and Magnetism in $La_{0.5}Ca_{0.5}MnO_3$

By varying the nominal Mn valence between Mn^{+3} and Mn^{+4} with divalent substitutions on the perovskite *A* site, the low-temperature magnetic and transport properties of manganese perovskites can be changed from FM insulator to FM metal to AFM insulator [12,13], as the relevant magnetic interaction changes between double exchange and superexchange. A variety of magnetic structures, some of which have already been studied in the past [9,14], are displayed. $La_{0.5}Ca_{0.5}MnO_3$ is a particularly interesting example, since, upon cooling, it first becomes FM (at T~225 K) and then AFM (at T~155 K). The low-temperature AFM structure of this compound, first studied by Wollan and Koehler in 1955 [14], can be described by means of two manganese magnetic sublattices (nominally Mn^{+3} and Mn^{+4}) having two different propagation vectors.

The structural properties of this compound were studied by high-resolution x-ray synchrotron and high-resolution neutron powder diffraction, using the X7A diffractometer at Brookhaven National Laboratory and the D2B diffractometer at ILL, respectively. It was determined that significant structural changes occur in the region between the FM and AFM transitions [10]. In this temperature range, a large anomaly of the lattice parameters (Figure 2) is associated with the onset of a strong Jahn-Teller distortion of the MnO_6 octahedra.

To study the low-temperature AFM structure of $La_{0.5}Ca_{0.5}MnO_3$, D2B was employed in a new configuration, which yields instrumental FWHM of ~0.2° in the angular range $0° \leq 2\Theta \leq 100°$. Coupled with the use of a rather long wavelength (2.4 Å), this option allows an excellent resolution to be attained in the angular range where magnetic Bragg reflections are

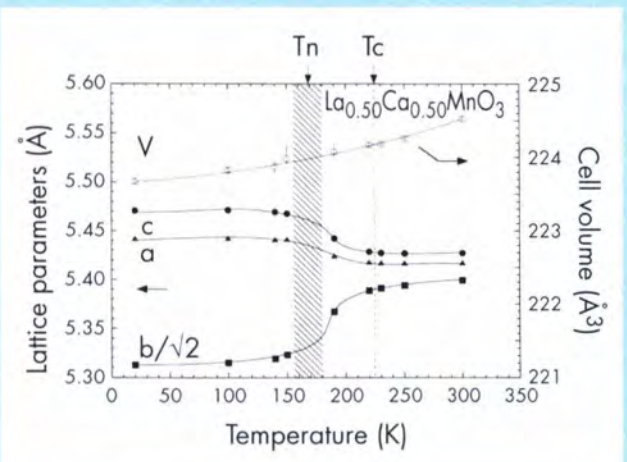

Fig. 2: Lattice parameters and cell volume as a function of temperature for $La_{0.5}Ca_{0.5}MnO_3$, measured on cooling, using high-resolution x-ray synchrotron diffraction at the X7A beamline (Brookhaven National Laboratory). Error bars are smaller than the symbols. Lines through the points are guides to the eye. The shaded area represents the width of the magnetisation hysteresis loop.

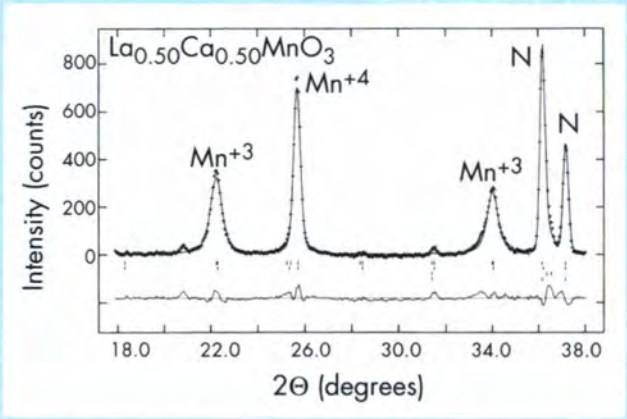

Fig. 3: Selective coherence length effects on the magnetic structure of $La_{0.5}Ca_{0.5}MnO_3$. Portion of a full-pattern Rietveld refinement profile of neutron powder diffraction data obtained on D2B (λ = 2.4 Å) using a 10 mm secondary collimator. The instrumental FWHM is ~0.2°. Note how the magnetic Bragg reflections associated with the Mn^{+3} sublattice are much broader than either the nuclear reflections or the Mn^{+4} magnetic reflections.

stronger. A portion of the Rietveld plot for $La_{0.5}Ca_{0.5}MnO_3$ at 1.5 K is shown in Fig. 3. It is clear from the figure that the magnetic Bragg peaks associated with the Mn^{+3} sublattice are much broader than either the nuclear peaks or the Mn^{+4} magnetic peaks. Such a selective peak broadening can be modeled by assuming that the Mn^{+3} magnetic sublattice has a very short coherence length (~300 Å), whereas the crystal structure and the Mn^{+4} magnetic sublattice are long-range ordered. The most peculiar aspect of this result is that the two intertwined magnetic sublattices appear to have different ordering lengthscales. This effect can be explained with the presence of domain walls (magnetic "twins") which break the coherence of the Mn^{+3} sublattice while leaving the Mn^{+4} sublattice unperturbed.

The Role of the Ionic Radius

Recently, it has been shown that a very complex phase diagram can be obtained at constant electronic doping (i.e. at constant Mn^{+3}/Mn^{+4} ratio), by simply varying the average ionic radius $\langle r_A \rangle$ of the species on the *A*-site [1]. This is accomplished by appropriate mixtures of "small" ions (Pr, Y, Ca) with "large" ions (La, Sr, Ba). As the perovskite structure distorts through several space group symmetries, T_C displays a non-monotonic behavior, being depressed both at small $\langle r_A \rangle$ and, to a lesser extent, at very large $\langle r_A \rangle$. In general, low T_C are associated with high values of the resistive jump at the M-I transition, and, as a consequence, of the magnetoresistance. This general trend can be understood by considering that the M-I transition occurs between a generic "semiconducting" state (the resistivity of which *increases* exponentially with decreasing temperature) and a generic "metallic" state (which shows a linear resistivity *decrease* with decreasing temperature). Below a critical value of $\langle r_A \rangle$, the properties change from FM metal to canted FM insulator, the highest values of the magnetoresistive ratios being attained in the vicinity of this phase boundary [2].

Using D2B, the structural phase diagram of $A_{0.7}A'_{0.3}MnO_3$ (*A* = La, Pr; *A'* = Ca, Sr, Ba) as a function of the average *A*-site ionic radius $\langle r_A \rangle$ was determined at a constant value x = 0.3 of the electronic doping (Fig. 4). In particular, it was found that, in addition to the well-known orthorhombic and trigonal phases (with space group symmetries Pnma and $R\bar{3}c$, respectively), a new orthorhombic structural allotype (with space group Imma) is present for large values of $\langle r_A \rangle$ at low temperature, and transforms into the $R\bar{3}c$ phase with increasing temperature through a first-order transition [15]. These phases can be derived from the ideal cubic perovskite through different tilt distortion of the MnO_6 octahedra (Fig. 5 p.158). Analysis of the internal structural parameters as a function of $\langle r_A \rangle$ has revealed very interesting correlations with the physical properties. The average Mn-O bond length <Mn-O>, the average Mn-O-Mn bond angle and the degree of octahedral distortion are shown in Fig. 6 (bottom, center and top panels, respectively). <Mn-O> has a *minimum* which

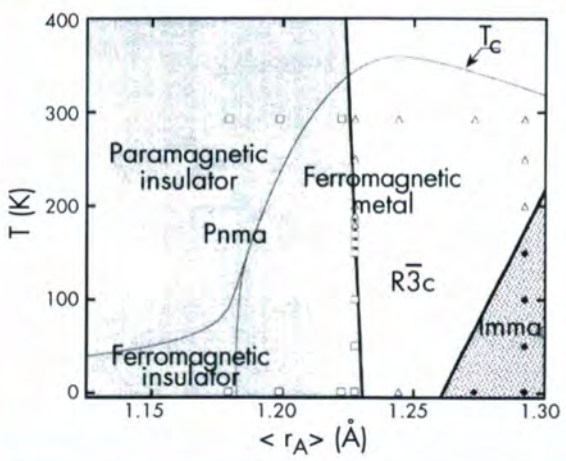

Fig. 4: Structural phase diagram of the $A_{0.7}A'_{0.3}MnO_3$ system (A = La, Pr; A' = Ca, Sr, Ba) as a function of $\langle r_A \rangle$. The three crystallographic phase regions are represented with different shadings and separated by thick lines. The T_C and M-I transition curves (from Ref. [1]) are shown as thin lines (note the maximum of T_C at $\langle r_A \rangle \approx 1.244$). Neutron diffraction data sets are shown as symbols (squares: Pnma; triangles: $R\bar{3}c$, diamonds: Imma).

coincides with the *maximum* of the Curie temperature, indicating that T_C is very sensitive to subtle structural changes. The Mn-O-Mn bond angle increases monotonically, a factor that may further contribute to the general enhancement of T_C for large $\langle r_A \rangle$ [1]. For small $\langle r_A \rangle$, the loss of metallic behavior is associated with a measurable distortion of the MnO_6 octahedra. In particular, a sample with composition $Pr_{0.7}Ca_{0.3}MnO_3$, which never undergoes the M-I transition, was found to display a strong distortion of the MnO_6 octahedra, associated with a very complex canted magnetic structure [16-18]. Temperature-dependent data on this compound, obtained using D2B and D1B, have shown that, upon cooling, this sample becomes first AFM at ~150 K. At lower temperatures (~110 K), an FM component is then added to its magnetic structure (see also D1B instrument report).

Structural Anomalies at Tc

Considerable attention has lately been devoted to the possible role of structural distortions in the charge carrier localisation process itself. By means of high-resolution synchrotron x-ray powder diffraction, it was determined that a significant lattice contraction ($\Delta V/V \approx 0.13$ %) occurs at T_C upon cooling [10]. The large volume change at T_C is highly unusual and cannot be attributed simply to the development of FM spin order because lattice parameters for ferromagnetic 3d transition metals and their compounds at T_C change typically by 10-100 ppm. Neutron diffraction experiments are currently been performed at several sources around the world in order to determine which internal structural parameters are responsible for this effect. Preliminary results indicate that, in addition to a contraction of the average Mn-O distance due to the formation of metallic bonds, a significant reduction of the distortion of the MnO_6 octahedra occurs at T_C upon cooling [17-19]. Furthermore, anomalies of the Debye-Waller factors at T_C suggest that the local structural distortions may also play a role in the charge localisation process [11,17]. It has to be pointed out that these effect are rather subtle, and may require larger powder samples (in order to employ high-resolution configurations), or, even better, single crystals, to be properly examined.

Conclusions

In the last few months, there has been a surge of interest in manganese perovskites as promising materials for magnetoresistive sensors. We have learned that the physical properties of these materials can be "tuned" by adjusting electronic doping and cation sizes. Diffraction techniques, and powder diffraction in particular, have been at the leading edge of the research effort in this field. The future will see an even more extensive use of these techniques, applied to the study of samples in special environments (high temperature, high pressure, applied magnetic field), with the goal of obtaining a better understanding of the fundamental properties of these compounds.

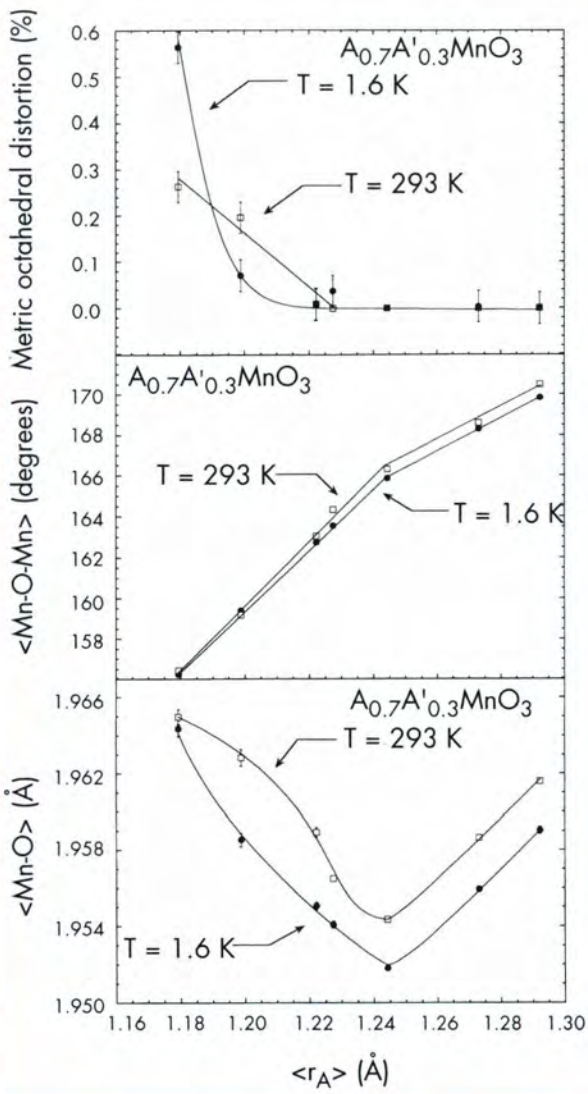

*Fig. 6: Evolution of the internal structural parameters as a function of $\langle r_A \rangle$ for $A_{0.7}A'_{0.3}MnO_3$. **Lower**: Average Mn-O distance; **Center**: Average Mn-O-Mn bond angle; **Top**: percent metric distortion of the MnO_6 octahedra. Filled circles and empty squares indicate 1.6 K and 293 K data, respectively.*

References

[1] H.Y. Hwang, S-W. Cheong, P.G. Radaelli, M. Marezio and B. Batlogg, Phys.Rev.Lett. **75**, 914 (1995).

[2] A. Maignan, C. Simon, V. Caignaert and B. Raveau, unpublished (1995).

[3] R. von Helmolt, J. Wecker, B. Holzapfel, L. Schultz and K. Samwer, Phys.Rev.Lett. **71**, 2331 (1993).

[4] S. Jin, T.H. Tiefel, M. McCormack and R.A. Fastnacht, Science **264**, 413 (1994).

[5] P. Norby, I.G.K. Andersen, E.K. Andersen and N.H. Andersen, J Solid State Chem **119**, 191 (1995).

[6] G.H. Jonker and J.H.V. Santen, Physica **16**, 337 (1950).

[7] C. Zener, Phys. Rev. **82**, 403 (1951).

[8] A.J. Millis, P.B. Littlewood and B.I. Shraiman, Phys Rev Lett **74**, 5144 (1995). A.J. Millis, B.I. Shraiman and R. Mueller, unpublished (1995).

[9] J.B. Goodenough, Phys. Rev. **100**, 564 (1955).

[10] P.G. Radaelli, D.E. Cox, M. Marezio, S-W. Cheong, P.E. Schiffer and A.P. Ramirez, Phys. Rev. Lett. **75**, 4488 (1995).

[11] P. Dai, J. Zhang, H.A. Mook, S.-H. Liou, P.A. Dowben and E.W. Plummer, unpublished (1995).

[12] A. Urushibara, Y. Morimoto, T. Arima, A. Asamitsu, G. Kido and Y. Tokura, Phys. Rev. B **51**, 14103 (1995).

[13] P. Schiffer, A.P. Ramirez, W. Bao and S-W. Cheong, Phys.Rev.Lett. **75**, 3336 (1995).

[14] E.O. Wollan and W.C. Koehler, Phys. Rev. **100**, 545 (1955).

[15] P.G. Radaelli, M. Marezio, H.Y. Hwang and S-W. Cheong, submitted to J. Sol. St. Chem. (1995).

[16] Z. Jirák, S. Krupicka, Z. Simsa, M. Dlouhá and S. Vratislav, J.Mag.Mag.Mat. **53**, 153 (1985).

[17] P.G. Radaelli, M. Marezio, H.Y. Hwang, S-W. Cheong and B. Battlog, submitted to Phys. Rev. Lett. (1995).

[18] V. Caignaert, E. Suard, A. Maignan, C. Simon and B. Raveau, unpublished (1995).

[19] D.N. Argyriou, J.F. Mitchell, C.D. Potter, D.G. Hinks and J.D. Jorgensen, submitted to Phys. Rev. Lett. (1995).

Structure and Dynamics of Liquids and Glasses

Members of the College at ILL

K. Andersen
T. Baumbach
M. Bée
H.G. Büttner
J.C. Cook
A.J. Dianoux
C. Doll
F. Dugain
B. Farago
M. Ferrand
H. Fischer
B. Frick
P. Girard
M.A. González
C. Hayes
A. Heidemann
C. Janot
G.J. Kearley
A. Kollmar
H.J. Lauter
V. Lauter-Pasyuk
P. Lindner
A. Magerl
N.-D. Morelon
H. Mutka
B. Nicolai
S. Pouget
G.Pratesi
C. Ritter
O. Schärpf
P. Schleger
H. Schober
J.-B. Suck (until 31/10/95)
A. Tölle
C. Zeyen

External Members

M. Anne (CNRS)
F. Bley (INPG)
J. Bouvaist (Pechiney)
A. Chamberod (CENG)
J.-P. Cohen Addad (UJF)
J. Dupuy (U. Lyon)
B. Fåk (CENG)
P. Guyot (INPG)
J.-F. Jal (U. Lyon)
C. Lartigue (UJF)
F. Livet (INPG)
Y. Maréchal (CENG)
J.-P. Morlevat (CENG)
J.-M. Piau (UJF)
M. Pineri (CENG)
C. Poinsignon (INPG)
C. Riekel (ESRF)
P. Terech (CENG)

Introduction

The year 1995 witnessed the restart of the ILL reactor and the resumption of normal scientific activity in the colleges. More than 4 reactor cycles were devoted to users' experiments, and the subcommittee meetings gave evidence of tough competition among the submitted proposals. The result was the production of much good science in 1995, as testified by this annual report.

Concerning College 6, the renewed scientific participation after a relatively long hiatus allowed a further clarification of the scientific scope of the college, which will now include the following sections:

6-01) Monatomic liquids and gases
6-02) Molecular liquids and gases (including aqueous solutions)
6-03) Liquid alloys and molten salts
6-04) Glass transition (only) in polymeric glasses
6-05) Glasses and amorphous materials (non-polymeric)

All other amorphous polymer studies not dealing specifically with the glass transition will be covered by College 9. Note that the College 6 categories make no distinction between structural (diffraction) and dynamical (inelastic) studies. In 1995, approximately 2/3 of the College 6 proposals were for inelastic spectrometers (for the most part instruments IN5, IN6, IN10, IN11 and IN16), and the remaining 1/3 for diffractometers (mostly D4, followed by D11, D16 and D17, the detector of D22 having been under repair).

The following scientific highlights appear in no particular order.

Scientific Highlights

Structure of liquid metals and semiconductors

The electronic properties of poorly conducting liquids are still insufficiently understood. For example, the nature of the electronic states and their contribution to the electronic conductivity remains a highly controversial subject. Recent studies of the electronic properties of liquid semiconductors have revealed a rich variety of unusual and often contradictory behaviour as the transition from a dominantly electronic to a dominantly ionic contribution to the conductivity takes place. This is equivalent in liquid semiconductor systems to a metal-insulator transition. Recently it has also been suggested that the mobility of the underlying ions may have a significant effect on the electronic contribution to the total conductivity [1].

An important requirement in the study of these materials is a knowledge of the structure of the liquids. A material of particular interest is liquid Ag_2Se. This shows very anomalous properties immediately after melting (most notably, a negative temperature coefficient for its conductivity) which may be related to the high silver ion mobility observed in the superionic phase. By using isotopic

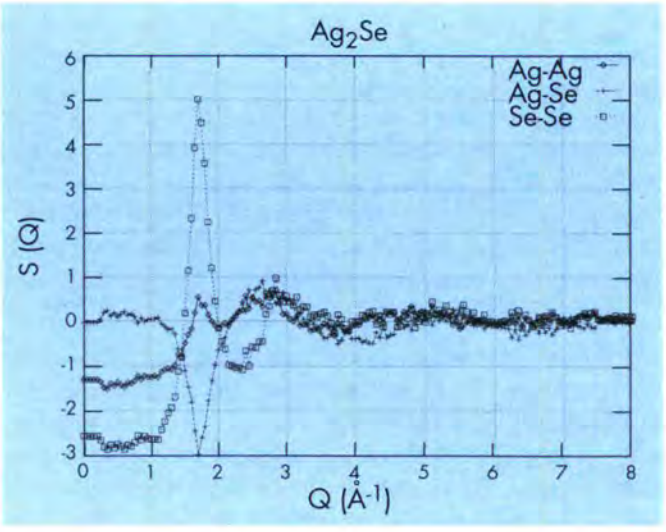

Fig. 1: Measured partial structure factors for Ag_2Se.

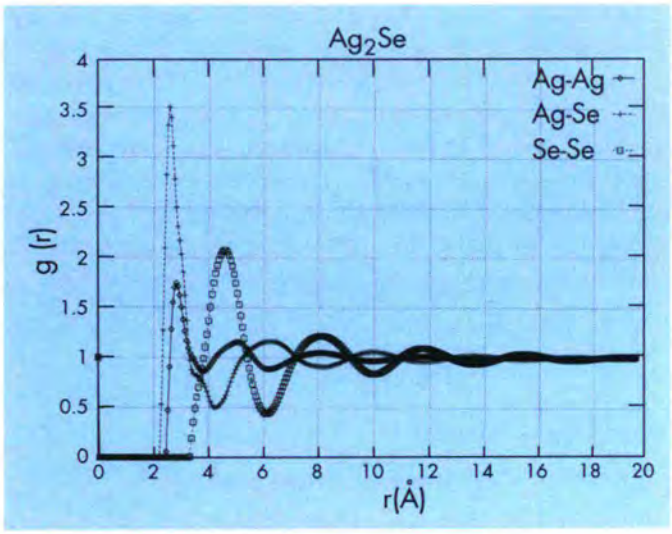

Fig. 2: Pair-pair correlation functions for Ag_2Se, calculated from the data of Fig. 1 through Fourier transform.

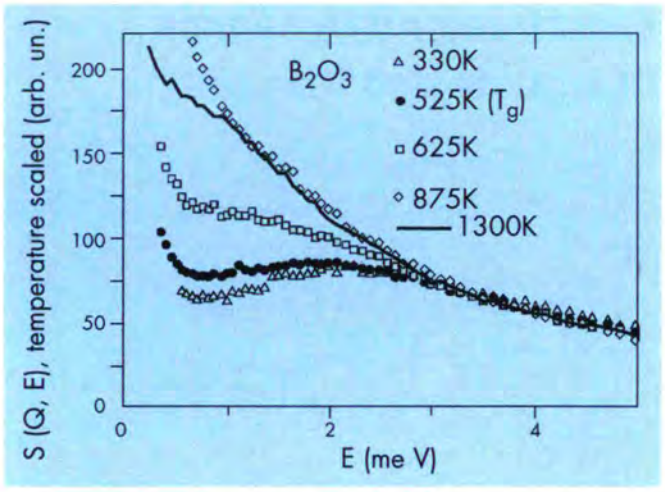

Fig. 3: The dynamic structure factor of B_2O_3 as a function of temperature for Q_{el} = 2.1 Å^{-1}.

substitution of both Ag and Se, an experiment to study the structure of this material to the partial structure factor level has been carried out at the D4 instrument by S. Lague and A.C. Barnes (U. Bristol), P. Salmon (U. East Anglia), and H. Fischer (ILL). Figures 1 and 2 show the partial structure factors obtained from the experiment and the corresponding partial g(r)'s. Although the diffraction data extended to 16 Å^{-1}, we have presented only the lower-q data for clarity. The results show that the local coordination structure is very similar to that of the superionic (solid) phase. The results also show good agreement with recent Ab Initio Molecular Dynamics calculations [2] and conventional molecular dynamics calculations using ionic potentials [3].

Dynamics of the strong glassformer B_2O_3

IN6 spectra of the strong glassformer B_2O_3, obtained by L. Börjesson, D. Engberg and L. Torell (CIT Göteborg), U. Buchenau and A. Wischnewski (KFA-IFF), A. Sokolov (MPI Mainz) and A.J. Dianoux (ILL), reveal a surprising feature at temperatures well above the glass transition temperature T_g = 523 K. At low temperatures, the Bose- and Debye-Waller scaled spectra in Fig. 3 behave as in many other glass formers: a well-pronounced boson peak at a few meV which gets covered by a quasielastic contribution as the temperature is raised above T_g. Further heating, however, *reduces* the quasielastic contribution and reveals again a boson peak, in good agreement with recent light scattering data of Torell et al.

The results clearly show the existence of a crossover temperature T_c for the glass-forming liquid, above which the fast dynamics becomes nearly temperature independent. Such behaviour is one of the essential predictions of the mode coupling theory, but has not been directly observed for the more fragile glassformers investigated so far, due to the fact that the slower α-relaxation merges with the fast

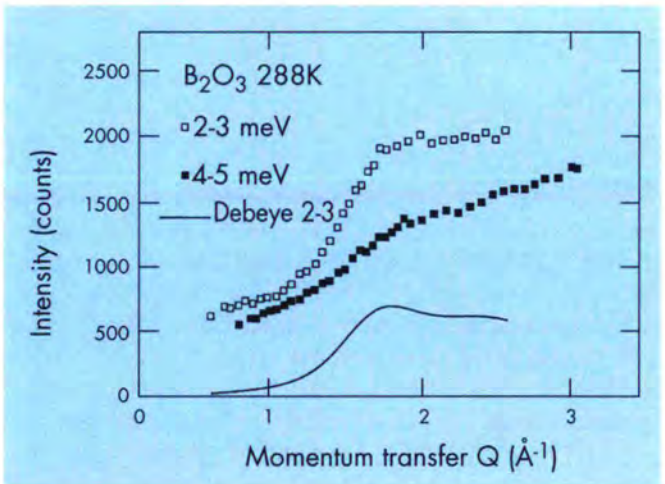

Fig. 4: The q dependence of the boson peak signal (2 to 3 meV) in B_2O_3 compared to that expected from the Debye model for sound waves.

dynamics above T_c. Therefore, only such a strong glass former as B_2O_3, having an extremely slow α-relaxation, can show this behaviour so clearly. However, by adopting this interpretation, one is forced to conclude that the crossover temperature is *above* the melting point (T_m = 725 K) in this substance.

The nature of the motions responsible for the so-called boson peak, typical of glasses and disordered materials, is presently a 'hot topic'. In B_2O_3, there is a fair chance of unravelling the eigenvectors of the motion from the q dependence of the spectra. This is shown in Fig. 4, which compares the q dependence of the signal at the boson peak (2 to 3 meV) to the one at a higher frequency and to the expectation of the Debye model for sound waves. The latter is calculated from the elastic intensity and known data for

sound velocities and the density at that temperature. The measurements corroborate earlier measurements of Hannon et al. They show that at the boson peak, one still sees the signature of the sound wave contribution, which then disappears at higher frequencies. Thus, the comparison with the Debye expectation supports an interpretation of the boson peak as a crossover in the dynamics from sound wave to a different kind of vibration, possibly localised.

Structure of cyclohexane in confined geometries

Liquids in confined geometry show markedly different properties from liquids in the bulk phase and there is a growing interest in the study of phase transitions for the systems. Previous investigations by the University of Kent at Canterbury group (J.C. Dore, J.B.W. Webber, et al.) have shown that cyclohexane in porous silicas exhibits a very large change in nucleation temperature (~35°C) and significant structural modification in the plastic crystal phase. It was decided that studies could be usefully extended by making SANS measurements using H/D substitution methods and investigating the equilibration process by adding the liquid to the top of the powered dry silica sample and allowing it to diffuse. The results were surprising and have revealed an interesting new phenomenon.

As the vapour enters the lower porous particles and begins to condense, there is a distinct development of an orange coloration in transmitted light suggesting the presence of critical fluctuations in the metastable fluid. This feature also corresponds to enhanced SANS intensity for D-cyclohexane but not for H-cyclohexane. The first observation was made for 60 Å pores on D17 (with H. Fischer and R. Cubitt of the ILL) and then confirmed in a test run for 500 Å pores on D11 (with L. Vuillard of the ILL). The D11 results are shown in Fig. 5, where the C_6D_{12} liquid front had not yet reached the neutron beam, although the vapour phase had. The corresponding results for C_6H_{12} at $\rho \sim 0$, by contrast, are almost identical to the profile for the dry silica, showing that the enhanced SANS intensity is indeed intrinsic to the cyclohexane. It is unclear why the critical phase is formed in the pores. The orange colour is strongest after several hours (when the C_6D_{12} vapour has diffused throughout most of the sample container volume and partially condensed in the silica pores) and fades over a period of several days. It is completely reproducible.

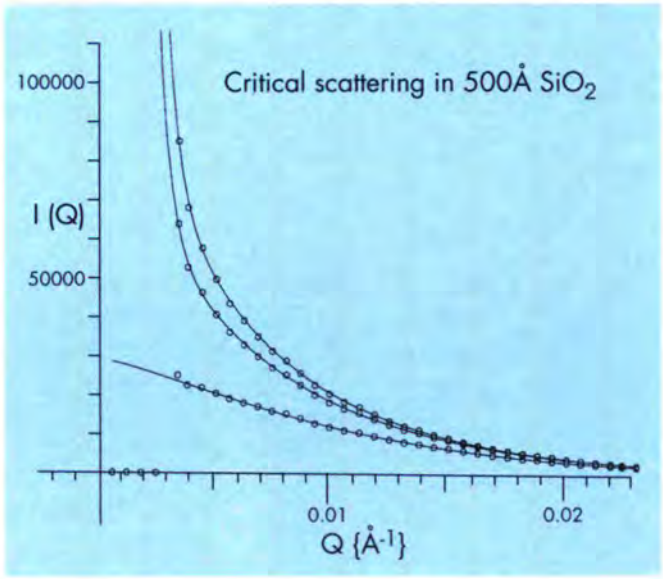

Fig. 5: Critical scattering of C_6D_{12} in 500 Å porous SiO_2. Adding C_6D_{12} to the dry silica (lower trace) increases the scattering markedly at low q, even in advance of the liquid front. The middle trace is after 10 min, the upper one after 15 min. The liquid front takes some hours to reach this part of the sample, and hence has not yet entered the neutron beam.

Inelastic light and neutron scattering of an amorphous polymer

The inelastic neutron scattering (INS) of poly(methyl methacrylate) (PMMA) was measured from a temperature T = 10 K up to 470 K above T_g (= 395 K) by E. Duval and A. Mermet (U. Claude Bernard, Villeurbanne), J.-F. Jal and J. Dupuy-Philon (U. Lyon), and A.J. Dianoux (ILL). At temperatures lower than T_g the density of states (DOS), $g(\omega)$, deduced from INS can be separated into two parts: one, temperature independent, resulting from harmonic vibrations and including the boson peak, referred to as HDOS; and the other, temperature dependent, due to anharmonic or relaxational motions and centred around the elastic peak, called RDOS. As the RDOS is negligible at low temperature (< 50 K), the RDOS at higher temeperature is obtained by subtracting the HDOS at low temperature from the high temperature DOS.

The intensity of Raman scattering $I(\omega)$ is:

$$I(\omega) = \frac{C(\omega)}{\omega}\, g(\omega)[n(\omega) + 1]$$

where $h\omega/2\pi$ is the energy transfer, $C(\omega)$ the light vibration coupling coefficient, $g(\omega)$ the DOS and $n(\omega)$ the Bose factor. $I(\omega)$ is the sum of $I_h(\omega)$ from harmonic vibrations and $I_{ah}(\omega)$ from anharmonic or relaxational motions. In Fig. 6, $I_h(\omega)/[(n(\omega)+1)\omega)]$ divided by $HDOS/\omega^2$ gives $C(\omega)$, plotted log-log. The slope of the straight line is 1.3. This implies that, from the above equation, $C(\omega) \sim \omega^{1.3}$. It should be noted that there is a "swelling" at the position of the boson peak.

In Fig. 7, $RDOS/\omega^2$ is compared with $I_{ah}(\omega)/[(n(\omega)+1)\omega]$. Both curves are very similar, which implies that the light vibration coupling coefficient for the relaxational motions is frequency independent.

We must emphasise that RDOS or $I_{ah}(\omega)$ do not correspond to quasi-elastic scattering due to diffusion. More information can and will be obtained from neutron data, such as the mean square displacement, quasielastic scattering, etc.

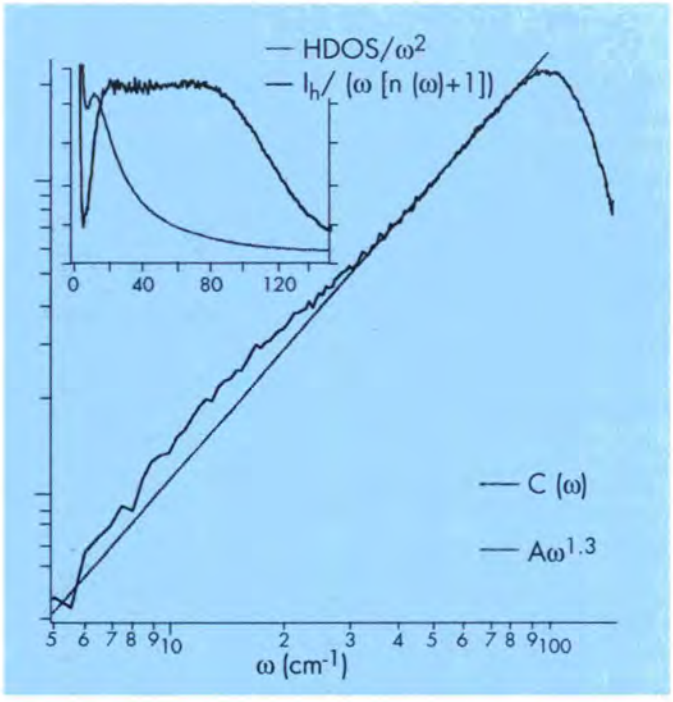

Fig. 6: The two curves $I_h(\omega)/[(n(\omega)+1)\omega)]$ and $HDOS/\omega^2$ for PMMA (insert), and their ratio C(w) plotted log-log, showing that $C(\omega)\sim\omega^{1.3}$.

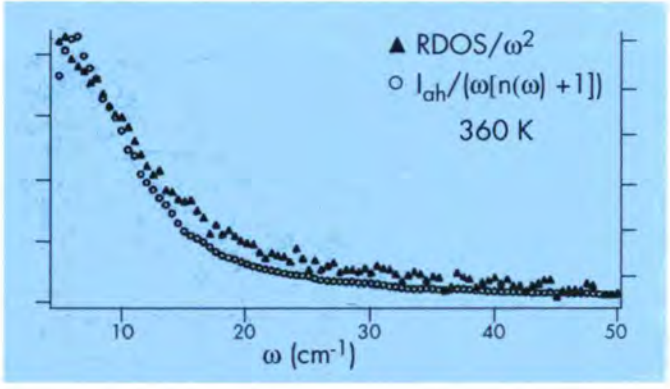

Fig. 7: $RDOS/\omega^2$ and $I_{ah}(\omega)/[(n(\omega)+1)\omega]$ for PMMA at 360 K. The similarity of the two curves suggests that the light vibration coupling coefficient for the relaxational motions is frequency independent.

Structure of Molten Salts

Simple binary molten salts have been extensively studied both experimentally and through computer simulation in recent years. More recently there has been renewed interest in the study of molten salt mixtures. This has arisen from fundamental questions concerning the nature of the interactions in these liquids and also from commercial interests: for example, $NaF\text{-}AlF_3$ mixtures used in aluminium smelting.

$ZnCl_2$ and the alkali halides show markedly different structures in the molten phase. Studies of the pure materials have shown that in $ZnCl_2$, the zinc is 4-fold coordinated to the chlorine, and there is a tendency to form a covalent-like network [4]. On the other hand, sodium chloride, for example, retains the essentially 6-fold coordination of the rocksalt structure. Earlier studies of alkali halide (NaCl or KCl)/zinc chloride mixtures have shown that the characteristic tetrahedral coordination of Zn is little affected by adding the alkali halide. Surprisingly, it even appears to enhance it. It is only when the concentration of the alkali halide reaches 80% that the local zinc coordination is significantly disrupted.

It has been postulated that a larger alkali ion (for example Rb or Cs) could have a greater effect in disrupting the zinc chloride structure [5]. An experiment to test this hypothesis has been carried out at the D4 instrument by M. Durell and A. Howe (U. Leicester) and H. Fischer (ILL) by measuring the total structure factor of $ZnCl_2$/CsCl mixtures at various concentrations. The total structure factors for the four concentrations are shown in Fig. 8. The characteristic intermediate-range order peak (indicative of long-lived $ZnCl_4$ tetrahedra) in $ZnCl_2$ is clearly observed at 1 $Å^{-1}$. On adding CsCl it is observed that this peak becomes narrower and higher indicating a strengthening of the intermediate range order. This is very similar to the behaviour observed in the $KCl/ZnCl_2$ mixtures, which suggests that the size of the alkali ion has no bearing on the stability of the Zn-Cl coordination in these mixtures.

Glass transition phenomenon under pressure: Dynamical structure factor of the compressed fragile liquid orthoterphenyl

Although the structural glass transition is a long-standing problem, our understanding of the phenomenon is still very

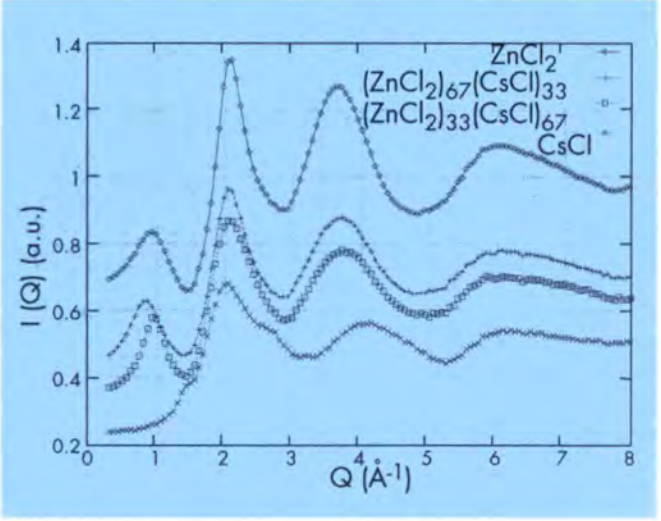

Fig. 8: Neutron diffraction intensity for molten salts $(ZnCl_2)_x(CsCl)_{1-x}$

incomplete. The particular dynamical features associated with the glassy state cannot be expressed in the framework of critical phenomena near second order transitions.

A new approach to the glass transition problem was initiated when mode coupling theory (MCT) for the first time provided an approximation scheme which allows the evolution of time correlations to be calculated from a microscopic equation of motion. It is based on the existence of a subtle singularity causing anomalies on microscopic length scales and mesoscopic time scales. Inelastic neutron scattering (INS) is the most advanced experimental tool for exploring the space time region relevant for the theory. In the simplest case, correlations in a viscous liquid are found to decay in two steps, which are identified as α- and β-relaxation and described by a set of scaling laws.

Up to now, temperature alone was used as a parameter to drive the glass transition in INS experiments, where indeed a two-step relaxation process was observed. The fast relaxation processes are found to follow the scaling law predictions of the MCT β-process.

As density and its fluctuations are the central quantities of MCT, the most direct way of testing the theory consists of using pressure as a control parameter. It is, therefore, of particular interest to determine whether the evolution of β–relaxation dynamics with varying temperature and varying pressure follow a similar pattern, and whether the MCT can be applied to both cases. The aim is to answer the following question: Is density the dominant parameter for the liquid-to-glass transition dynamics or do thermal effects also play an important role?

Recently, several reasearch groups (C. Alba-Simionesco of LLB, A. Tölle and H. Schober of ILL), have undertaken INS measurements on compressed fragile glass formers.

For our investigations we chose the molecular liquid orthoterphenyl (OTP) for several reasons:

- OTP is a fragile glass and consists of rigid molecules which are weakly linked by non-directional van der Waals interactions.
- OTP is easy to handle since the melting temperature T_m and the glass transition temperature T_g are not to far from ambient temperatures.
- OTP has been extensively studied in the literature by many spectroscopic methods; in particular, we have already performed a huge variety of INS experiments on the temperature dependence of the incoherent and coherent dynamical structure factors.

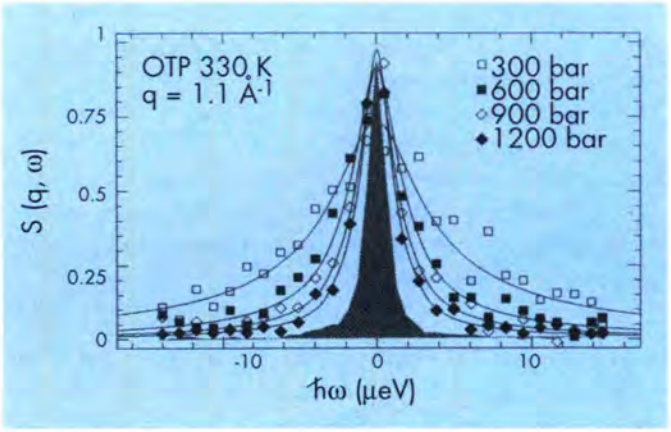

Fig. 9: Representative isothermal BS-spectra at different pressures. Lines are fits with a KWW function (stretched exponential) having its exponent fixed to 0.65.

- OTP shows the highest observed dT_g/dP (25 K/kbar) for molecular liquids, so that we can hope to observe drastic effects with relatively small pressure changes.

Our experiments were performed on the time-of-flight (TOF) spectrometer IN6 and on the backscattering (BS) spectrometer IN10. Standard ILL neutron scattering high pressure cells have been used to obtain pressures up to 300 MPa (3 kbar) at temperatures around 320 K.

On the backscattering instrument we obtain microscopic information on the slowing down of the structural α-relaxation. Figure 9 shows representative isothermal (330 K) spectra at q=1.1 $Å^{-1}$. As expected, the quasielastic broadening increases when the pressure is released.

For a first estimation of α-process relaxation times, the spectra were fitted by a Kohlrausch law having a fixed stretching parameter derived from previous investigations at atmospheric pressure. The relaxation times obtained in this way, when compared with isothermal viscosity data, seem to scale with viscosity as they do in isobaric experiments (at atmospheric pressure). Hence, the α-relaxation process is controlled by temperature and pressure in the same way as viscosity.

Experimental tests of MCT are best perfomed in the cross-over region between the α- and β-processes, which is accessible by neutron TOF scattering.

In this range, self correlations of tagged particles as obseverd by incoherent scattering are predicted by MCT to obey a scaling law. A Fourier transform of this implies a factorisation of the scattering law in a purely q-dependent and a frequency-dependent term:

$S(q,\omega)=h(q)*G(\omega)$.

This property is found to be valid for our TOF data as shown in Fig. 10. Because G(ω) is treated as an unknown, we impose an abitrary normalisation h(q=1 Å^{-1}) = 1. The rescaled spectra are then compared as functions of ω and q for one representative pressure of 1200 bar, but this factorisation is found to be true for all pressures measured in our experiments. Although this is a prerequisite for any mode coupling analysis, it by no means excludes other interpretations of the data.

Since the dynamical range of one instrument is not nearly sufficient for a complete MCT analysis, we have only been able to compare variable temperature and variable pressure measurements. For this purpose we have to use the dynamical susceptibility.

In Fig. 11 we show scaled susceptibilities at q=1.8 Å^{-1} at atmospheric pressure (lines) for temperatures of 290, 293, 306 and 312 K, as well as at 316 K (symbols) for pressures of 300, 600, 900 and 1200 bar. As can be seen, the dynamical susceptibility at 290 K, 0 bar coincides with that at 316 K, 1200 bar. The densities, 1.085 g/cm^3 and 1.124 g/cm^3 respectively, are quite different. Therefore, the susceptibility can be quite similar for different densities. In other words, the same density does not necessarily lead to the same dynamical response (e.g. the density at 316 K, 300 bar is 1.081 g/cm^3, which is approximately the same as that at 290 K, 0 bar, mentioned above).

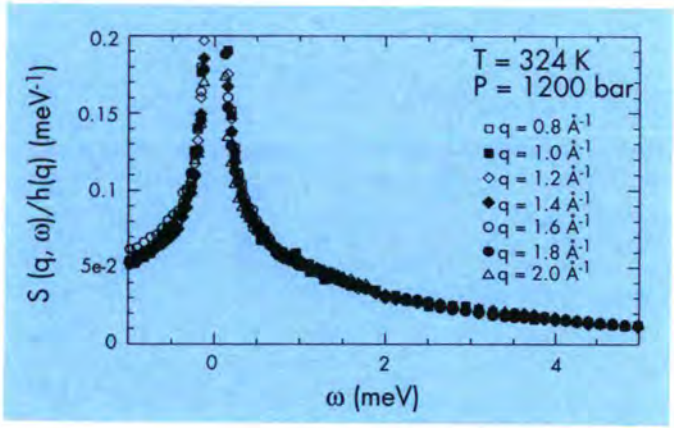

Fig. 10: Test of factorisation hypothesis (see text). Data are from IN6 at 324 K and 1200 bar. Seven spectra are shown for the q values indicated, each spectrum being rescaled by a factor h(q).

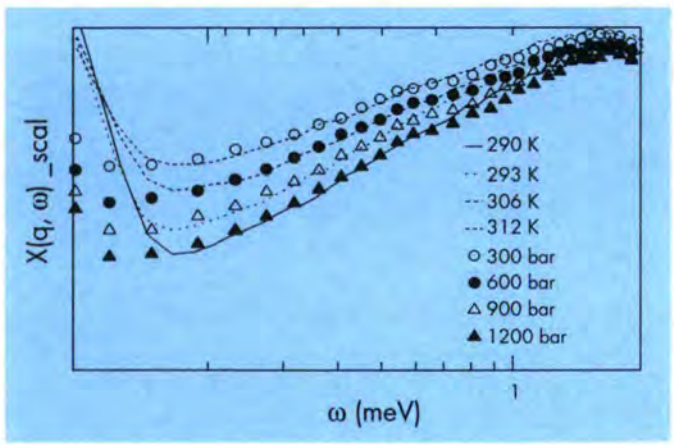

Fig. 11: Scaled (onto the value at ≈ 4 meV) isobaric and isothermal suceptibilities at q = 1.8 Å^{-1}.

This comparison of variable temperature and variable pressure measurements indicates that density cannot be the only relevant parameter for the liquid-glass transition dynamics. The effect of temperature is more than just changing the density via thermal expansion and has its own direct effect on the relaxation dynamics. These findings are in agreement with recent light-scattering results. Further investigations are required to quantify our results.

Structure of $^{113}Cd^{2+}$ surface complexes on hydrous ferric oxide by anomalous neutron scattering

The mobility, biodisponibility and toxicity of cadmium in the environment are largely controlled by chemical reactions which take place at the solid particles/water interface. A thorough understanding of surface assisted chemical reactions is needed to assess and predict more effectively its behaviour in natural systems. Among natural particles, hydrous Fe oxide (HFO) has long been recognized as playing an important role in controlling the fate of trace metals, including cadmium. This role is mainly due to its high natural abundance, structural disorder, and small particle size of typically 30 Å. Such a nanocrystalline, near amorphous structure makes HFO an ideal sample for study at the D4 diffractometer for fluids and glasses.

The sorption mechanism of Cd on HFO particles has been investigated by solution chemistry, EXAFS spectroscopy, wide-angle (WAXS) and anomalous wide-angle X-ray scattering (AWAXS), and anomalous ^{113}Cd neutron scattering. Solution chemistry experiments indicate that cadmium is a poorly hydrolysable cation and does not form multinuclear surface complexes on mineral surfaces. This unique property makes cadmium a particularly well-suited structural probe, as it allows the identification of the nature of surface sites to which heteroatoms bond, together with their binding mechanism [6]. Due to the small size of HFO particles, as much as 10 weight % Cd may be sorbed before reaching the monolayer surface coverage. Two Fe coordination shells are detected by EXAFS at 3.25 Å and 3.5 Å. No Cd-Cd interaction is detected, in agreement with solution chemistry, i.e. the absence of Cd polymers. Based on Cd-Fe distances, Cd-centered $Cd(O,OH)_6$ octahedra are assumed to share edge(s) and double corner(s) with Fe-centered $Fe(O,OH)_6$ octahedra at the surface of the particles (Fig. 12).

EXAFS analysis of disordered systems can, in some cases, yield results which exclude the full distribution of interatomic distances. This possible loss of neighbours may

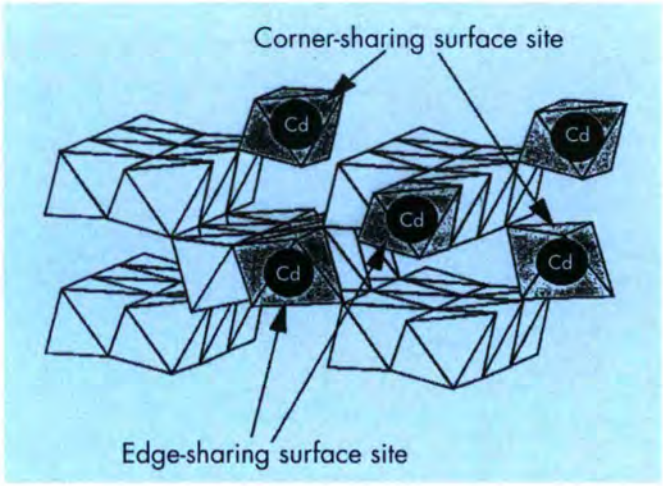

Fig. 12: Structural model for the sorption mechanism of Cd on hydrous ferric oxide (HFO).

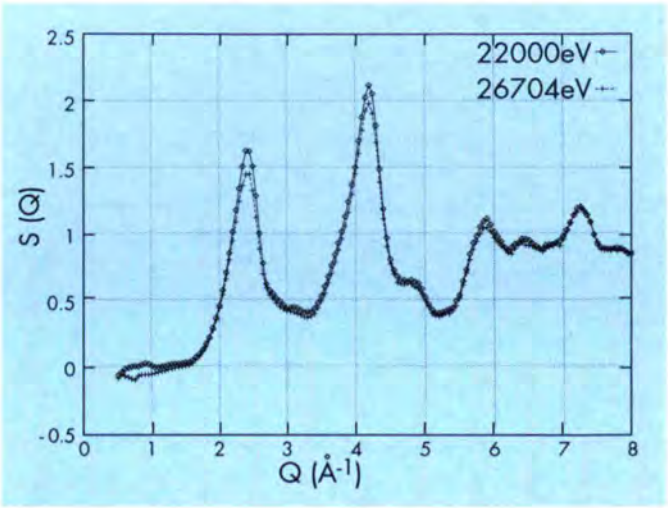

Fig. 13: X-ray diffraction data for $Cd_{0.014}Fe_{0.14}O_{0.423}D_{0.423}$ at two different wavelengths.

lead to the inaccurate determination of coordination numbers and, hence, to errors in the quantification of the relative density of surface sites. X-ray and neutron scattering experiments are less sensitive to disorder effects than EXAFS, and provide a better estimate of the number of Fe atoms around cadmium. Chemical selectivity may be achieved by anomalous scattering experiments. The X-ray scattering amplitude of Cd atoms in the vicinity of the K absorption edge (26711 eV) is expressed in a complex form as b=b_0+b'+ib", where b_0 is the nonresonant coherent scattering amplitude, b' is the real and b" the imaginary resonant increment. Since b' and b" vary with the X-ray energy, the local order around Cd can be accessed by tuning the wavelength in the vicinity of the scattering resonance (the X-ray experiment having been performed at LURE, Orsay, with B. Bouchet-Fabre). A comparison of structure factors S(q) for Cd-HFO (approximate stoichiometry: $Cd_{0.014}Fe_{0.14}O_{0.423}D_{0.423}$) at 22000 eV and 26704 eV is given in Fig. 13. The difference between the two curves (about 3% or 4%) is weak. Analyses are in progress to obtain the differential scattering cross-section and then the differential pair correlation function $\Delta G_{Cd}(r) = a*\Delta G_{CdO}(r) + b*\Delta G_{CdFe}(r)$, where G_{CdCd}=0 due to the lack of Cd polymerisation.

Chemical selectivity may also be achieved with neutrons by using ^{113}Cd as it presents a strong neutron resonance scattering at a wavelength of 0.68 Å. Figure 14 shows reduced neutron diffraction data for a sample of $^{113}Cd_{0.014}Fe_{0.14}O_{0.423}D_{0.423}$ at wavelengths of 0.60 Å and 0.82 Å. The experiment was performed by A. Manceau and L. Spadini (UJF) with H. Fischer and P. Palleau (ILL) at the D4 instrument. These two wavelengths were chosen so as to give the maximum change in coherent scattering length for ^{113}Cd while having roughly the same absorption (b"). The difference between these two curves (roughly 20%) is

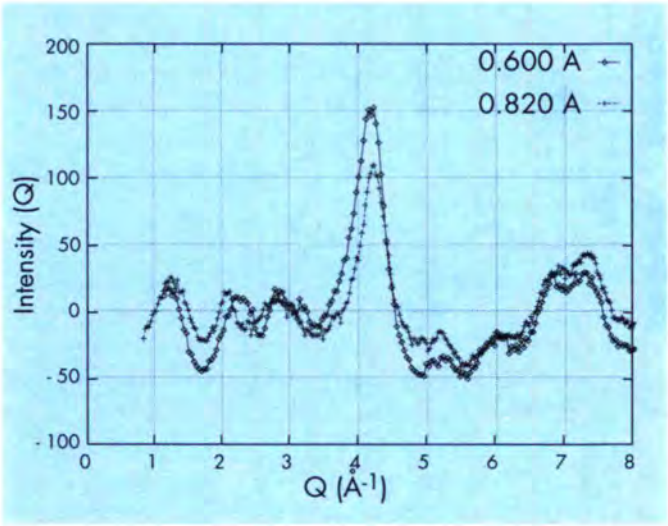

Fig. 14: Neutron diffraction data for $^{113}Cd_{0.014}Fe_{0.14}O_{0.423}D_{0.423}$ at two different wavelengths.

more marked than that for the X-ray data. This neutron scattering contrast is also independent of q since neutron scattering lengths are (nearly) constant in q. The absence of an atomic form factor for neutrons represents a noticeable advantage since in X-ray experiments the scattering contrast is greater than ≈7% only for q>10 $Å^{-1}$ and the damping of oscillations at high q results in a drastic decrease in the signal-to-noise ratio. Both the X-ray and neutron data were taken up to q values of about 20 $Å^{-1}$, but only the lower-q results are shown here, in the interest of clarity. Differential structure factors obtained with neutrons and X-rays will be ultimately compared and then simulated for different structural models.

Measurements of the ^{4}He roton lifetime using neutron backscattering

A direct measurement of the roton line width in ^{4}He II at the roton minimum as a function of temperature below 1.1 K has been possible using neutron backscattering with a measured inelastic resolution of 1.0μeV. The temperature-dependence of the roton lifetime can be understood in terms of the 4-quasiparticle decay process first introduced by Landau and Khalatnikov [7] and refined by Bedell, Pines and Zawadowski (BPZ) [8]. The roton excited by the neutron decays by combining with a thermally excited roton and then decaying into two other quasi-particles. Both theories predict a deviation from the near pure exponential temperature dependence of the line width just below T_λ (2.17 K) to a more rapid decrease below $T \approx 1.3$ K. The roton wave-vector at the roton minimum is $Q_R = 1.925$ Å^{-1}. At $Q=Q_R$ the roton energy is around $\hbar\omega_R = 8.610$ K = 741.9 μeV. Up to now, the only technique that has been used for resolving the anticipated line widths below $T \approx 1.2$ K has been the neutron spin-echo (NSE) technique [9]. Recent developments on the neutron backscattering spectrometer IN10 [10,11] (configuration IN10B), allow a *direct* measurement of the roton peak. IN10B accesses the roton minimum region of (Q,ω) space by using a NaF(111) - Si(111) monochromator-analyser crystal combination oriented in backscattering; such an experiment was carried out by J.C. Cook, K.H. Andersen and J. Bossy of the ILL. Energy transfer scans through the roton peak were performed by varying the temperature of the monochromator. Because of the need to measure in a restricted Q-range around Q_R, it was necessary to improve the default Q-resolution of IN10. This was done by restricting the scattering angles f at the analyser to the rings (similar to Debye-Scherrer rings for a polycrystal) in the range $123° < f < 128°$, resulting in a Q-acceptance $Q=Q_R \pm DQ$ where $DQ \approx 0.02$ Å^{-1}. Measurements of the line shape were performed at 4 temperatures (880±10 mK, 970±10 mK, 1040±10 mK and 1100±10 mK). By assuming that the dispersion in the roton region is described by the usual parabolic expression

$$\hbar\omega(Q) = \hbar\omega_R + \frac{\hbar^2(Q-Q_R)^2}{2\mu_R} \qquad (1)$$

where μ_R is the effective roton mass, the measured peaks were fitted to the following expression,

$$S(Q_R,\omega) = \frac{Z_0\Gamma_0}{\pi}\int_{Q_R-\Delta Q}^{Q_R+\Delta Q}\frac{dQ}{\Gamma_0^2+\hbar^2\left(\omega-\omega_R-\hbar(Q-Q_R)^2/2\mu_R\right)^2} \qquad (2)$$

where the integral has to be calculated numerically. In equation (2), Γ_0 is the roton peak half-width at Q_R, Z_0 is an intensity scaling factor and we have assumed that the quasi-particle weight and half-width $Z(Q)$ and $\Gamma(Q)$ are independent of Q over the measured Q-region. The resolution width $2\Gamma_{res}$ was obtained from a fit of equation (2) to the lowest temperature data (T=0.88K). Equation (2) gives excellent agreement with the measured line shapes. Fig. 15 shows the best-fit roton half-widths, $\Gamma_R(T)$, which are in very good agreement both with the theory of Bedell *et al* and with the NSE measurements of Mezei. It is clear also from the magnitude of the error bars that the present measurement constitutes a significant improvement over the NSE results. Further measurements using IN10B are planned at even higher Q-resolution and over an extended temperature range.

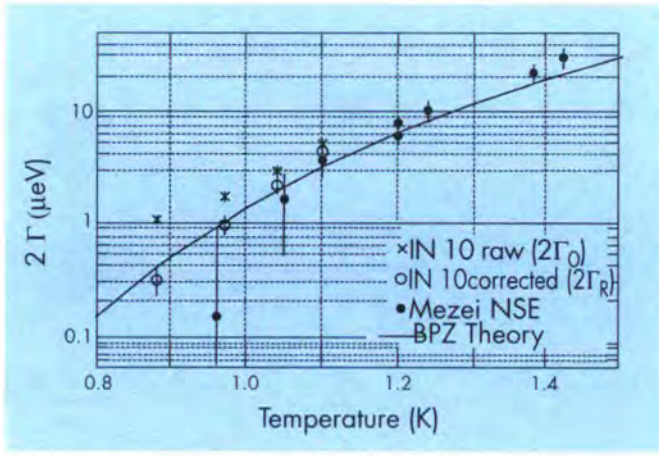

Fig. 15: Roton widths $2\Gamma_R$ from the present measurement, from the Mezei NSE data and as predicted by the theory of Bedell et al.. From the present work, both the best-fit $2\Gamma_0(T)$ and the extracted roton widths $2\Gamma_R(T) = 2\Gamma_0(T) - 2\Gamma_{res}$, corrected for the instrumental energy-resolution, are shown.

Structure of glasses using the second order difference method of isotopic substitution

Glassy materials containing silver often show unusual properties. An important and fundamental question that arises when trying to understand these properties concerns the way in which the silver enters the glass structure, especially as silver often serves as a mobile ionic species. From measurements of the total structure factor it is not possible to determine the coordination environment of the silver ions. Partial structure factors are much more useful and, accordingly, a D4 experiment has been done by P.S. Salmon, S. Xin (U. East Anglia) and H. Fischer (ILL) to measure the silver-silver partial structure factor, and related difference functions, for the glassy fast-ion conduction compound $AgPS_3$. Silver is a convenient element for making this second order difference experiment owing to the relatively large scattering length contrast of the ^{107}Ag and ^{109}Ag isotopes. The first order difference function obtained

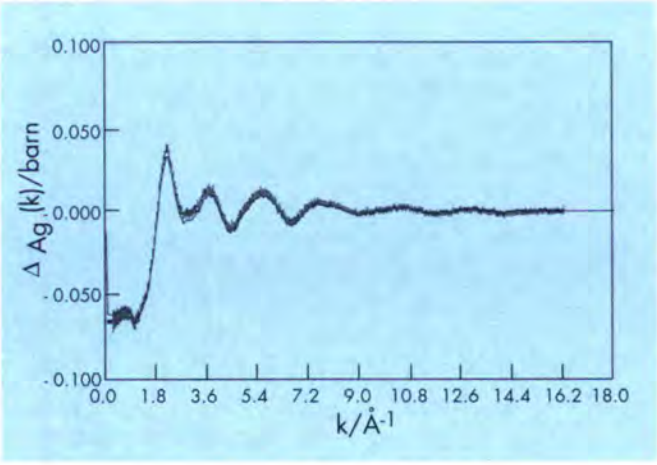

Fig. 16: First order difference for glassy $AgPS_3$, showing the diffraction intensity due to Ag correlations: $\Delta_{Ag}(q) = {}^{107}S(q) - {}^{109}S(q)$. The solid curve shows the Fourier back-transform of the corresponding r-space function (Fig. 17) after the unphysical low-r features have been set to their calculated limiting value.

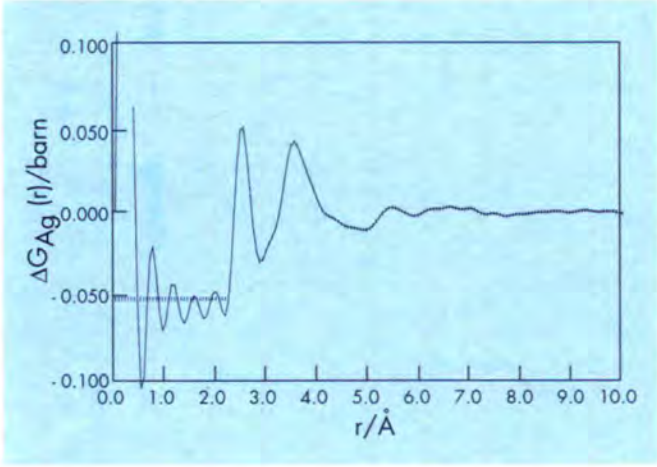

Fig. 17: The solid curve is the Fourier transform $G_{Ag}(r)$ of the $\Delta_{Ag}(q)$ data of Fig. 16. The Hashed curve suppresses the unphysical low-r features and was used for the Fourier back-transform shown in Fig. 16.

from two of the three measured total structure factors (ie. for $^{107}AgPS_3$, $^{109}AgPS_3$ and $^{Nat}AgPS_3$), and which comprises only silver ion correlations, is illustrated in Fig. 16 as $\Delta_{Ag}(q) = {}^{107}S(q) - {}^{109}S(q)$, with the corresponding Fourier transform G(r) shown in Fig. 17. There is evidently a clear contrast between the measured scattering patterns used for this first order difference and, at present, the full data sets are being carefully analysed to determine the second order difference and the precise nature in which Ag enters the glass structure.

Generalised vibrational density of states and dynamic structure factor of the (bulk) metallic glass $Zr_{65}Cu_{17.5}Ni_{10}Al_{7.5}$

The generalised vibrational density of states (GVDOS) and the dynamic structure factor of the metallic glass $Zr_{65}Cu_{17.5}Ni_{10}Al_{7.5}$, which belongs to one of the very few alloy systems within which **bulk** metallic glasses can be produced, were determined. For this investigation, performed at 294 K with a melt-spun sample, we used the thermal-neutron TOF spectrometer KARTOFFEL of the Institut für Nukleare Festkörperphysik (FZK), situated at the reactor Siloë of the CEN-G, as well as the cold-neutron time-focusing spectrometer IN6 at the ILL; the experimental team included J.-B. Suck (then at ILL), H.J. Güntherodt (U. Basel) and H. Schober (ILL). The incident energy from the thermal-neutron beam was E_o = 17.4 meV, and that from the cold guide 4.76 meV, where we used the highest energy accessible on IN6 in order to achieve the best possible averaging in reciprocal space of the predominantly coherently scattered intensity from this sample. The energy resolution of these investigations with thermal and cold neutrons was 0.7 meV and 0.125 meV (at E_o) respectively.

The GVDOS of $Zr_{65}Cu_{17.5}Ni_{10}Al_{7.5}$ (not shown here) consists essentially of one very broad band with a pronounced maximum at 22.6 meV, and it extends out to very high energies of $\omega_{max} \approx 60$ meV, compared with the GVDOS of the metallic glass $Zr_{54}Cu_{46}$ which ends already at $\omega_{max} \approx 36$ meV. The GVDOS increases at the lowest resolvable energies (> 0.8 meV on IN6, > 1.8 meV on KARTOFFEL) with an ω-exponent of 1.5 (instead of 2) due to the **very large amount of low energy modes (LEM)** found in the spectra of this glass, which even **exceeds** the amount of LEM found in the GVDOS and the dynamic structure factor of $Zr_{54}Cu_{46}$. The thermal-neutron data (KARTOFFEL) are shown in Fig. 18, normalized to the vanadium calibration run so that $S(q=\infty) = 1$.

These low energy modes, which can be studied in more detail in the total dynamic structure factor, show surprisingly **little dependence on momentum transfer**, even though the Q-region of the very pronounced first peak (occuring near 51 degrees) of the static structure factor is completely covered by the experiment performed with thermal neutrons. This is in strong contrast to the observations made with other metallic glasses, where the intensity of the LEM as a function of momentum transfer normally mimics the general shape of the static structure factor. This lack of Q-dependence can be understood if one assumes that a large part of the vibrational modes (especially of the LEM) in this metallic glass is **localised**. It is interesting to note that in this

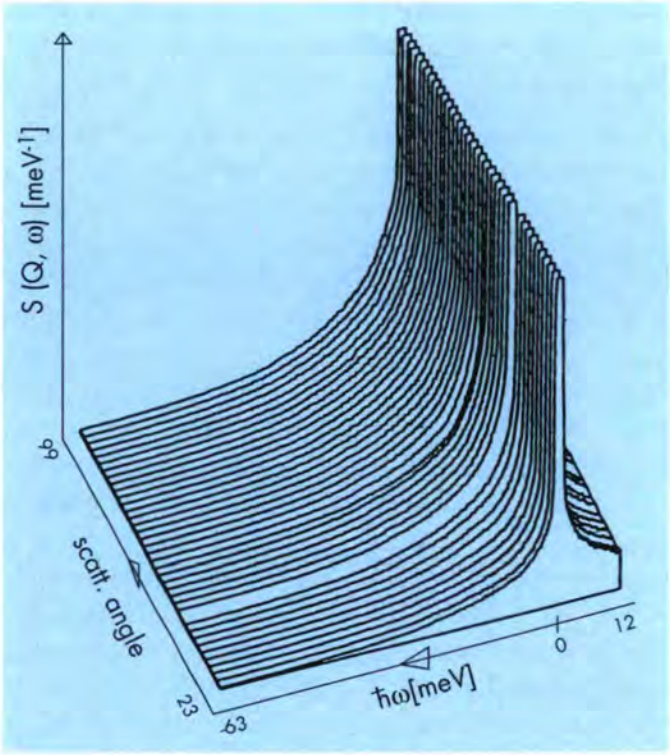

Fig. 18: Series of 37 cuts through the dynamic structure factor of the metallic glass $Zr_{65}Cu_{17.5}Ni_{10}Al_{7.5}$ at constant scattering angle Θ in steps of 2 degrees for $23 \leq \Theta \leq 99$ degrees, measured with thermal neutrons ($E_0 = 17.4$ meV) for $-63 \leq \hbar\omega \leq 12$ meV. The vertical scale has been enhanced to emphasize the inelastic part of $S(Q,\omega)$, the peaks of the elastically scattered neutrons being therefore off-scale in this plot. The Q-range corresponding to the scattering angles spans the static structure factor up to the second maximum of $S(Q)$ at $\Theta \approx 91$ degrees (the first pronounced peak of the static structure factor occurs at $Q = 2.57$ Å^{-1}, near 51 degrees). This figure clearly demonstrates that the low energy part of the spectrum does not show the variation with Θ that is usual for other metallic glasses, suggesting that a large part of the low energy modes in this glass are localised.

metallic glass, which forms nearly as easily as nonmetallic glasses and much more easily than other metallic glasses, the **tendency for mode localisation seems to be as pronounced as for nonmetallic glasses**.

Secretary: Henry Fischer

References

[1] S. Ramasesha, J. Solid State Chemistry **41** (1982) 333-357.

[2] F. Kirchhoff, J.M. Hollender and M.J. Gillan, submitted to Phys. Rev. (1995).

[3] J.P. Rino, Y.M.M. Hornos, G.A. Antonio, I. Ebbjso, R.K. Kalia and P. Vashishta, J. Chem. Phys. **89** (1988) 7542-7555.

[4] D.A. Allen, R.A. Howe, W.S. Howells and N.D. Wood, J. Chem. Phys. **94(7)** (1991) 5071-5076.

[5] Y.S. Badyal and R.A. Howe, J. Phys. Condensed Matter **5(39)** (1993) 7189-7202.

[6] L. Spadini, A. Manceau, P.W. Schindler and L. Charlet, "Structure and Stability of Cd2+ Surface Complexes on Ferric Oxides. I. Results from EXAFS Spectroscopy", Journal of Colloid and Interface Science **168** (1994) 73-86.

[7] L.D. Landau and I.M. Khalatnikov, Zh. Eksp. Teor. Fiz. **19** (1949) 637.

[8] K. Bedell, D. Pines and A. Zawadowski, Phys. Rev. **B29** (1984) 102.

[9] F. Mezei, Phys. Rev. Lett. **44** (1980) 1601.

[10] J.C. Cook, W. Petry, A. Heidemann and B. Frick, ILL internal report No. 91CO06T (1991).

[11] J.C. Cook, W. Petry, A. Heidemann and J.-F. Barthélémy, Nucl. Inst. and Methods **A312** (1992).

Study of the Johari-Goldstein β-relaxation regime in a glass-forming polymer

A. Arbe[1], U. Bucheneau[1], L. Willner[1], D. Richter[1], B. Farago[2], J. Colmenero[3]

It is well known that in glass-forming liquids, in addition to the primary α-relaxation, a secondary relaxation process, the so-called Johari-Goldstein β-relaxation, always appears at low temperatures. Although both relaxational processes have been studied exhaustively by relaxational methods, their molecular nature is still unknown. For further progress, a combination of conventional relaxation techniques with quasielastic neutron scattering methods, which provide spatial information, is necessary.

By combining neutron spin-echo (NSE) and dielectric spectroscopy, we have investigated the molecular dynamics of 1-4 polybutadiene in the α-β relaxation regime. NSE measurements (ILL) were performed over a large momentum transfer (Q) range, reaching even the second maximum of the static structure factor S(Q) (Q=2.7 $Å^{-1}$). An initial analysis of the dynamic structure factor S(Q,t)/S(Q) in terms of Kohlrausch-Williams-Watts (KWW) functions

$$\frac{S(Q,t)}{S(Q)} \propto \exp\left[-\left(\frac{t}{\tau_{KWW}}\right)^{\beta}\right]$$

showed that, while at the first peak of S(Q) the relaxation times follow the temperature dependence of the viscosity, near the second peak they follow the Arrhenius law corresponding to the dielectric β-relaxation,

$$\tau_{KWW} = \tau^{o}_{KWW} \exp\left(\frac{E_A}{kT}\right)$$

where E_A=0.41 eV (see Fig. 1). This result indicates that the process dominating the dynamics in the first maximum of S(Q), reflecting interchain correlations, is the α-relaxation (process related to the viscous flow), whereas at the second maximum of S(Q), which is dominated by intrachain correlations, the β-relaxation plays the most important role.

At low temperature (T ≤ 210 K), the α-relaxation becomes so slow that it virtually cannot be detected in the NSE-window. In this temperature region the NSE data are dominated by the β-relaxation - a localised relaxational process. The simplest elemental motion one can imagine for such a relaxation is a jump between two equivalent sites separated by a distance d. The atom jumps with a characteristic time τ, whose temperature dependence will be given by an Arrhenius law, $\tau = \tau_0 \exp(E/kT)$, where E is the potential barrier of this elemental process. For this kind of hopping process, the incoherent scattering function reads

$$S^{hop}_{inc}(Q,t) = 1 - \frac{1}{2}\left[1 - \frac{\sin(Qd)}{Qd}\right] + \frac{1}{2}\left[1 - \frac{\sin(Qd)}{Qd}\right]\exp\left(-\frac{2t}{\tau}\right) =$$

$$1 - A^{hop}(Q,d) + f^{hop}(Q,d,\tau,l)$$

Let us assume that the atoms perform their jumps independently of each other or that the distance between correlated jumps is much larger than the jump distance d. Then we can approximate the inelastic part of the coherent scattering function by the incoherent inelastic part. The interference terms from the average atom distribution remain, giving rise to the presence of S(Q) in the coherent scattering function. The normalised coherent scattering function can then be written as

$$\frac{S^{hop}_{coh}(Q,t)}{S(Q)} = 1 - \frac{A^{hop}(Q,d)}{S(Q)} + \frac{f^{hop}(Q,d,\tau,t)}{S(Q)}$$

From dielectric measurements of the β-relaxation performed on the same polymer, we have determined the distribution function of the potential barriers of the elemental processes involved in this relaxation, g(E). NSE data were fitted by assuming the same distribution of barrier heights as observed by dielectric spectroscopy. We found a very good agreement between this model and the experimental data for all Q values and temperatures investigated for a jump distance of 1.5 Å. We also obtained the following surprising and not yet understood result: the timescale of the relaxation of the density fluctuations, as measured by neutrons, and the

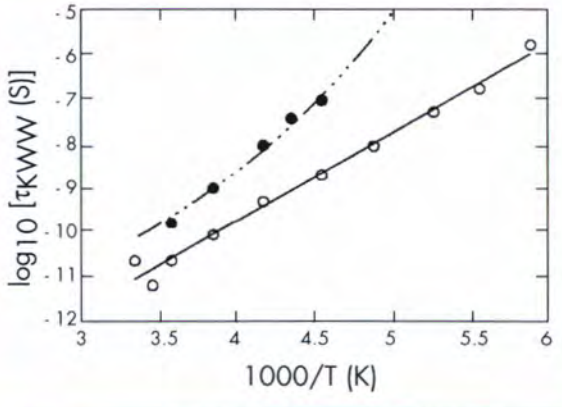

Fig. 1: Temperature dependence of the characteristic times τ_{kww} at Q = 1.48 $Å^{-1}$ (•) and Q = 2.71 $Å^{-1}$ (o). Dashed dotted line corresponds to the Vogel Flucher-like temperature dependence of the viscosity and the solid line to the Arrhenius-like temperature dependence of the β-relaxation.

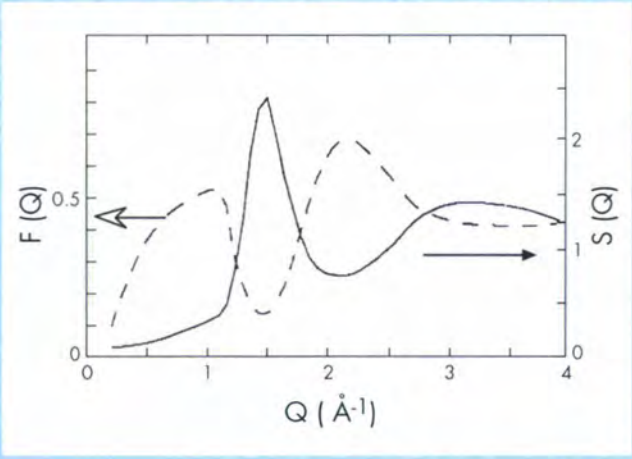

Fig. 2: Amplitude F(Q) of the relative quasielastic contribution of the β-process to the coherent scattering function obtained from the hopping model as a function of Q (dashed line). The static structure factor S(Q) at 160 K is shown for comparison (solid line).

timescale of the relaxation of the electric dipoles, as determined from dielectric spectroscopy, differ by approximately two orders of magnitude.

Figure 2 shows the Q-dependence of the relative inelastic contribution F(Q) of the β-relaxation to the dynamic structure factor as deduced from the hopping model:

$$F(Q) = \frac{1}{S(Q)} \int_0^{\infty} g(E)\, A^{hop}\, (Q,d)\, dE$$

This contribution is large in the neighbourhood of the minimum and the second maximum of S(Q), and quite small close to the first maximum of S(Q). This behaviour qualitatively clarifies the experimental results shown in Fig. 1. In the neighbourhood of the first peak of S(Q), where interchain correlations dominate the dynamics, the α-relaxation plays the most important role, whereas at the second peak, the intrachain maximum, the dynamics are mainly due to the local β-relaxation.

[1] KFA Jülich
[2] ILL
[3] U. País Vasco

Liquid-glass transition under high pressure

C. Alba-Simionesco, CPMA, Université Paris Sud, Orsay

At normal pressure the liquid-to-glass transition has been widely studied as a function of temperature. Several techniques exploring relaxation times from the picosecond to the calorimetric structural arrest around 1000 sec at Tg have been combined, allowing considerable progress to be made in the description of the freezing processes down to Tg indicated by discontinuities of the thermodynamic susceptibilities (expansion coefficient α, compressibility χ_t, heat capacity Cp). Considering an empirical thermodynamic approach, with an extrapolated phase transition below Tg, or a dynamical approach as introduced by the Mode Coupling Theory (MCT), with a Tc well above Tg, a better understanding of the decoupled temperature and density effects on realistic molecular liquids is required. Bearing in mind the properties of the supercooled liquid at atmospheric pressure, the thermodynamic, structural and dynamical properties are now investigated in the overcompressed regime under high pressure along isobaric, isothermal and isochoric paths down to the glassy state. The density rather than the temperature becomes the single driving parameter of the phenomenon.

The liquid chosen in the present report is m-toluidine classified as «fragile»[(1)] by Angell. For fragile liquids the viscosity has a strong non-Arrhenius behaviour. This system, an aromatic ring plus two substituted groups, $-CH_3$ and NH_2 in the meta position, offers many advantages: the supercooled regime is easily accessible by several techniques (Tg≈186 K); it is a rigid molecular liquid for which crystallisation can be controlled and avoided, while at the same time it is possible to encounter interesting metastable crystalline phases. Detailed relaxational processes can be examined, since a non-negligible dipolar moment exists and weak hydrogen bonds develop, which stabilise and reveal the effects on local order while the fragile character of this system remains close to a van der Waals type of liquid such as toluene. Last but not the least, it is possible to compare with Monte-Carlo simulations using a potential due to Jorgensen[(2)].

Pressure and temperature limits of the supercooled and overcompressed liquid: the Pg definition

On a macroscopic time scale, when the phenomenon is extended in the P-T phase diagram, some boundaries as well as thermodynamic properties (volume V) must be known. Apart from the melting line, other characteristic lines are required, such as the isochronic glass transition

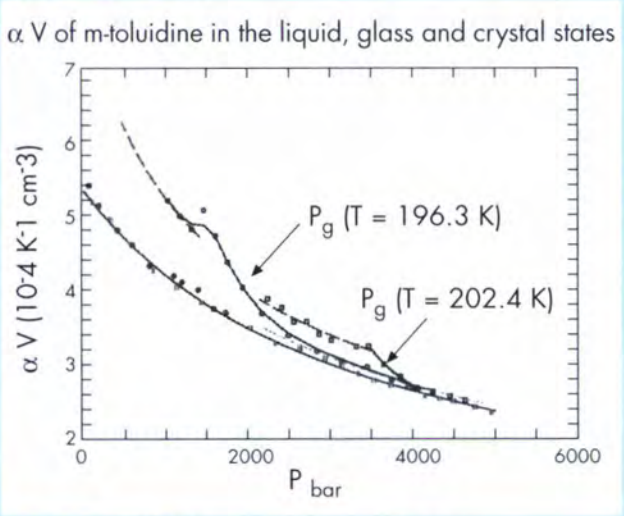

Fig. 1: Total (αV) data of m-toluidine at 196.3 K (○,●) and 202.4 (□,■). Open and solid marks represent the results for liquid, glass and for crystal, respectively.

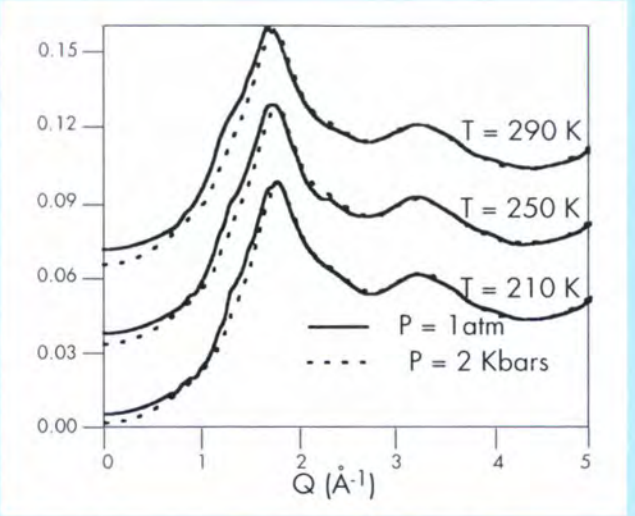

Fig. 2: Experimental structure factors $S_M(Q)$ of liquid and supercooled m-toluidine along isothermal paths.

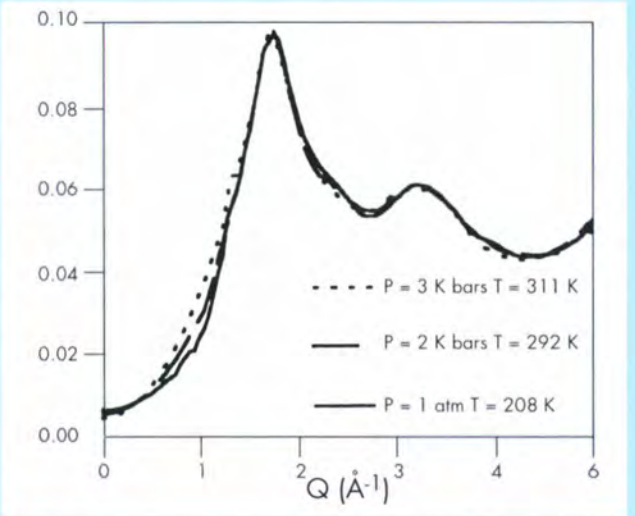

Fig. 3: Experimental structure factors $S_M(Q)$ of liquid and supercooled m-toluidine along isochoric path.

line. As a rule, Tg(P) or Pg(T) is taken at a mean relaxation time of 1000 sec, provided by adiabatic or isothermal calorimetry. The jump of the product αV between the metastable liquid and the glass at constant temperature defines the calorimetric Pg[3], as shown in Fig. 1. From our experiment we derive a liquid-glass transition line of Tg with P to be dTg/dP ≈ 4.5° per kbar in this pressure range. The knowledge of this phase boundary, at a given relaxation time (here 1000 sec), is necessary for further investigations on density and temperature dependence of all relaxational processes encountered in the supercooled regime.

Structural changes accompanying glass formation under pressure

Elastic neutron scattering experiments on a deuterated sample were performed for the first time in the supercooled and overcompressed m-toluidine through glass transition. The measurements[4], carried out on the spectrometer 7C2 at LLB, were performed up to 5 kbar with an incoherently scattering cell made of TiZr. The liquid structure factor $S_M(Q)$ is proportional to the total coherent elastic part of the differential scattering cross-section. For a molecular liquid, it may be split into the product of a molecular form factor $f_l(Q)$ and a function $D_M(Q)$ containing all the intermolecular contributions. The intermolecular pair correlation function $G_l(r)$ is related to the Fourier transform of $D_M(Q)$. This composite function is a linear combination of partial atomic radial distribution functions $g_l(r)$ weighted by the atomic coherent scattering lengths. Simulations of m-toluidine have been performed in the canonical ensemble (N,V, T) at different temperatures and densities.

Fig. 2 and Fig. 3 give the density and temperature dependence of the experimental structure factor in the liquid, metastable liquid and glassy state. The increase in density is characterised by a displacement of the main peak position (1.8 $Å^{-1}$) to larger Q values and a decrease in intensity of a shoulder around 1.3 $Å^{-1}$. When cooling the system at constant density, Fig. 3, the width of the main peak decreases, the position of this peak remaining constant.

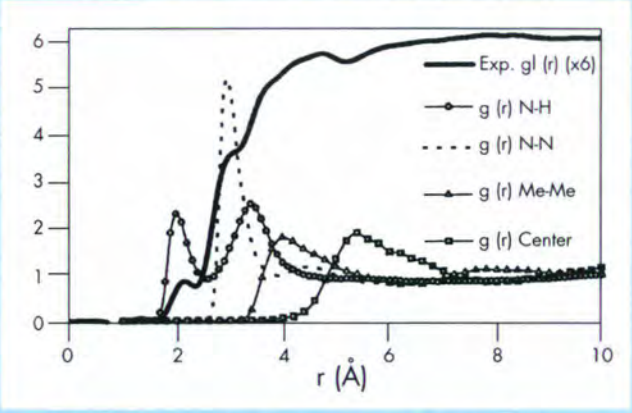

Fig. 4: Experimental gl(r) and simulated partial radial distribution functions of liquid m-toluidine at atmospheric pressure and room temperature.

From the experimental structure factors we derived radial distribution functions $g_l(r)$, see Fig. 4, and find a good agreement between the experimental and the simulated radial distribution function $g_l(r)$. This allows us to attribute the origin of the shoulders at 2 Å and 3 Å in the experimental $g_l(r)$ to the partial $g_{N\text{-}H}(r)$ and $g_{N\text{-}N}(r)$ obtained from simulations related to the hydrogen bond (N-H...N). On the one hand, the local order at constant density (at different temperatures and pressures) is defined through these partial radial distribution functions. We observe that the packing of the molecules is essentially unchanged while local ordering of the molecules is changing due to variations in the hydrogen bonding. At constant temperature on the other hand (at different pressures and densities), the density dependence on the packing is illustrated by the displacement of the position of the first peak in the methyl-methyl and the center-center radial distribution functions. It is clear that the local structure and the way such an order can or cannot extend is a key to understanding the transition. However, careful systematic exploration along isochoric lines in several temperature domains is required to derive the corresponding partial correlation functions before any conclusions concerning the role of molecular reorientation in addition to the translational displacements can be drawn.

Inelastic neutron scattering of m-toluidine as a function of pressure

From the above analysis, averaged positions are deduced but the liquid structure is dynamic: the environment about each molecule or group of molecules is therefore time-dependent and controls the rates of diffusion and reorientation. This can be studied by inelastic neutron scattering as measured using time-of-flight and backscattering methods. The first step was to build a new kind of high pressure cell suitable for inelastic neutron scattering experiments made from Niobium. Comparing the results with those obtained in an aluminium cell at atmospheric pressure, we have concluded that the new cell is satisfactory because of the weak elastic intensity provided by the material (Nb) and the weak multiple scattering contribution at low frequencies due to the conception of the cell. The results of several measurements of the incoherent dynamical structure factor at different pressures along an isotherm (T=277 K) well above the calorimetric glass transition temperature and at different temperatures along an isobar at P=2 kbar are now available. A series of spectra measured on IN6 (with λ = 5.1 Å) is shown in Fig. 5 for different pressures at Q=1.92 $Å^{-1}$. At P=3 kbar, the quasielastic part of the intensity disappears within the resolution of IN6 (whereas the calorimetric glass transition Pg is around 20 kbar), the remaining part of the spectra being referred to the phonon-like contribution. The disappearance of the quasielastic part of the intensity can be related to a 2 step relaxation process. At lower densities, i.e. lower pressures, a broadening of the central quasielastic line is observed. The greatest change of this contribution is concentrated between 2 and 3 kbar, which corresponds to a density increase of only 1% ! The disappearance of this extra intensity is a crucial point for the description of the fast processes in the glass formation and must be systematically explored as a function of the density. Such exploration concerns two major questions about the origin of the «Boson peak» around 2-3 meV: the extension of the MCT and the coupling of vibrational to relaxational contributions[5].

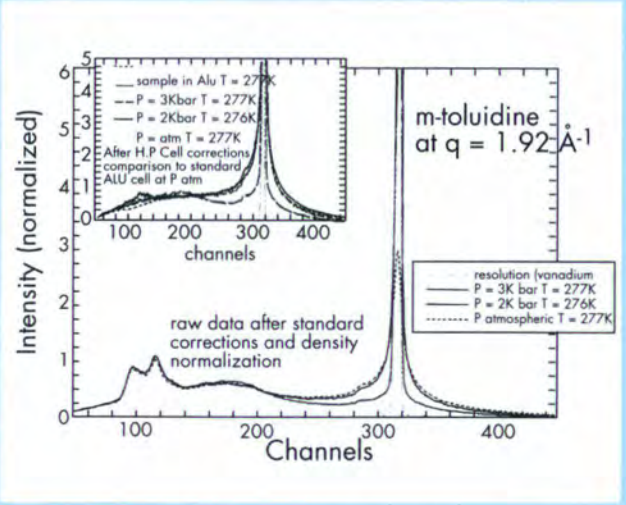

Fig. 5: Isothermal T.O.F. spectra of m-toluidine at T = 277 K as a function of pressure.

In a first approximation, the T-P dependence of a 2-step relaxation process from isothermal and isobaric experiments would be 15°/kbar, higher than the slope of the liquid glass transition line. Of course different isochoric lines in a T-P diagram are not expected to be parallel and the lowest must be the calorimetric one at very long relaxation times.

To explore this, we used the better resolution of IN10 and performed elastic scans at several pressures as a function of temperature and also elastic scans at constant temperature, as a function of pressure. Scans of the former kind are plotted in Fig. 6: almost no temperature dependence of the elastic intensity is observed in the glassy regime at high pressure but an important decrease starts around 250 K, well above Tg (at 3 kbar Tg = 202 K). Note that the slope decreases as P increases.

The experiments under high pressure constitute a new approach to glass transition allowing the distinction to be made between temperature and density effects. With future experiments in the extended T-P space we will check whether the experimentally observable phenomena stay the same and whether the liquid state theories remain valid. This is questionable since the competition with crystalline phases increases considerably at high temperature and high pressure. However, in view of the large number of experiments required for the T-P exploration, we must select certain ranges and carry out comparisons for a given system and between one system and another, given that a density temperature-relaxation time normalisation is not yet available.

During the last few years, many people have contributed significantly at various levels to the work presented here and therefore deserve mention: M.C. Bellissent-Funel, G. Coddens, A.J. Dianoux, B. Frick, H. Fujimori, V. Krakoviack, M.F. Lauthié, D. Morineau, R. Pellenq with the technical assistance of F. Milliou, J. Jaffré, R. Millet and N. Ratovelomanana.

References

[1] C.A. Angell, C. Alba-Simionesco, J. Fan, J.L. Green, NATO, ASI Series C, *Mathematical and Physical Sciences*, **435** (1994), M.C. Bellissent-Funel, J. Dore ed.; C. Alba-Simionesco, J. Fan, C.A. Angell, in preparation.

[2] W.L. Jorgensen, T.B. Nguyen, *J. Comput. Chem.* **14**, 2, 195-205 (1993).

[3] C. Alba-Simionesco, *J. Chem. Phys.*, **100**, 2250 (1994) C. Alba-Simionesco, H. Fujimori (to be published).

[4] C. Alba-Simionesco, D. Morineau, R. Pellenq, M.C. Bellissent-Funel, M.F. Lauthié, in preparation; D. Morineau, R. Pellenq, C. Alba-Simionesco, in preparation

[5] C. Alba-Simionesco, M. Krauzman, J. *Chem. Phys.*, **102**, 6574 (1995); V. Krakoviack, C. Alba-Simionesco, M. Krauzman, Conference Proceedings Pisa, Sept. 1995

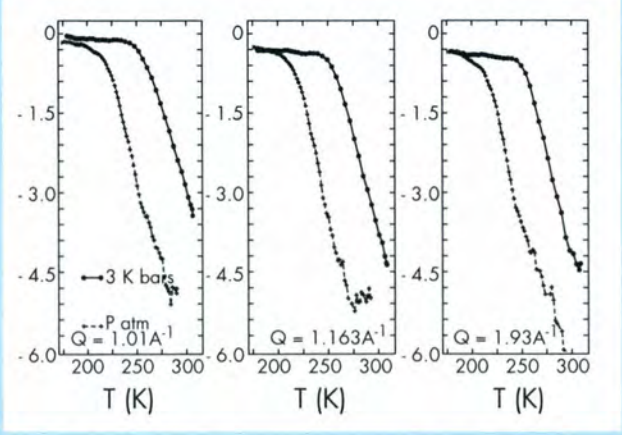

Fig. 6: Elastic scans at constant pressure of m-toluidine as a function of temperature.

Material Science, Surfaces and Spectroscopy

Members of the College

I. Anderson	A. Kollmar
H. Büttner	H. Lauter
R. Cubitt	V. Lauter
A.Dianoux	P. Lindner
C. Doll	A. Magerl
B. Farago	H. Mutka
B.Frick	S. Pouget
A.Heidemann	C. Ritter
M. Johnson	O. Schaerpf
G. Kearley	

This is the first report of College 7, a college which was created following a redistribution of topics between College 6, 9a and 9b. College 7 deals with the subjects **Material science, Surfaces and Spectroscopy**. The majority of proposals came from spectroscopy side.

Material science

Ordered Vacancies in Ni_3Sb

The origin of the anomalously high Ni diffusivity in the high-temperature DO_3 phase of Ni_3Sb has been a mystery since its discovery in the late sixties. A set of complementary measurements using different neutron scattering techniques has allowed us to eliminate several possible explanations: QNS measurements on IN10 have shown that the diffusion mechanism is far from exotic, whereas phonon measurements [1] have demonstrated that 'phonon enhancement' cannot be the only explanation either. A series of diffraction measurements carried out recently on D1B has demonstrated [2] that fast diffusion in Ni_3Sb is due rather to a high amount of vacancies in the Ni sublattices. In fact, when one compares the powder diffraction pattern of $Ni_{1-x}Sb_x$ alloys ($0.26<x<0.29$) to that of an ideal DO_3 structure, it turns out that a whole class of superlattice peaks is much less intense than expected. Rietveld refinement has shown that this effect is due to the appearance of ordered vacancies: The Sb excess in $Ni_{1-x}Sb_x$ alloys is compensated by the creation of vacancies in the two Ni sublattices, α and γ, the α sites being favoured (see Fig.1). The vacancy concentration on the different sites is practically independent of temperature. As the stoichiometric composition is approached, the vacant sites are continuously filled; at the composition $Ni_{74}Sb_{26}$ there are no more vacancies on the γ sites, which also determines the limit of phase stability. Of course, these high vacancy concentrations favour fast diffusion, as the diffusing atoms always find an empty neighbouring site to jump onto.

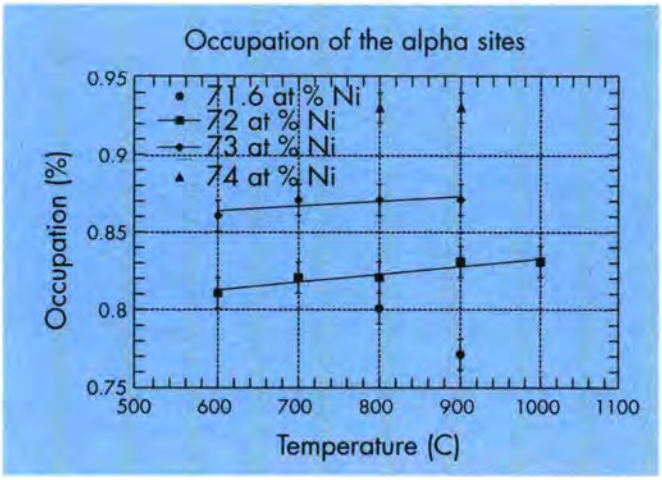

Fig. 1: Occupation of the α sites of Ni_3Sb as a function of temperature and alloy composition.

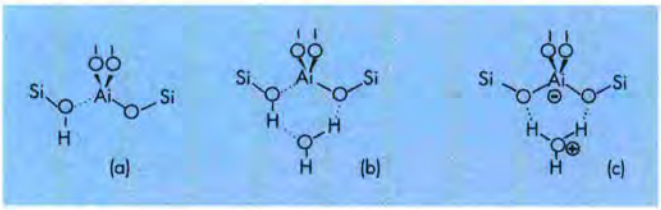

Fig. 2: The active sites of the zeolites are formed by bridging hydroxyl groups. Three possibilities are depicted.

Surfaces

Interaction of water with hydroxyl groups in ZSM-5

Zeolites in the proton form are extensively used in acid catalysis. The active sites are formed by the bridging hydroxyl groups (Brönsted sites) as depicted in Fig. 2a. A question much debated at the moment is whether the Brönsted acidity of these solids is high enough to protonate molecules, as in super acids.

There is conflicting evidence on the formation of hydronium ions (H^3O^+) in several zeolites, after water adsorption. It is also difficult to choose between structures (b) or (c) in Fig. 2.

Ab initio calculations performed on small clusters are not, at present, entirely unambiguous.

Inelastic neutron scattering (INS) has been used to follow water adsorption in the H-ZSM-5 zeolite [3]. The INS spectrum of the dehydrated zeolite is shown in Fig. 3a between 80 and 2000 cm^{-1} (10-250 meV). The most prominent peaks correspond to the in-plane and out-of-plane bending modes of the Brönsted OH groups, as in related systems [4]. After water adsorption (about 1 molecule per acidic site), the spectrum shown in Fig. 3b was obtained. Because the 2 spectra were recorded under the same experimental conditions, a difference spectrum, shown in

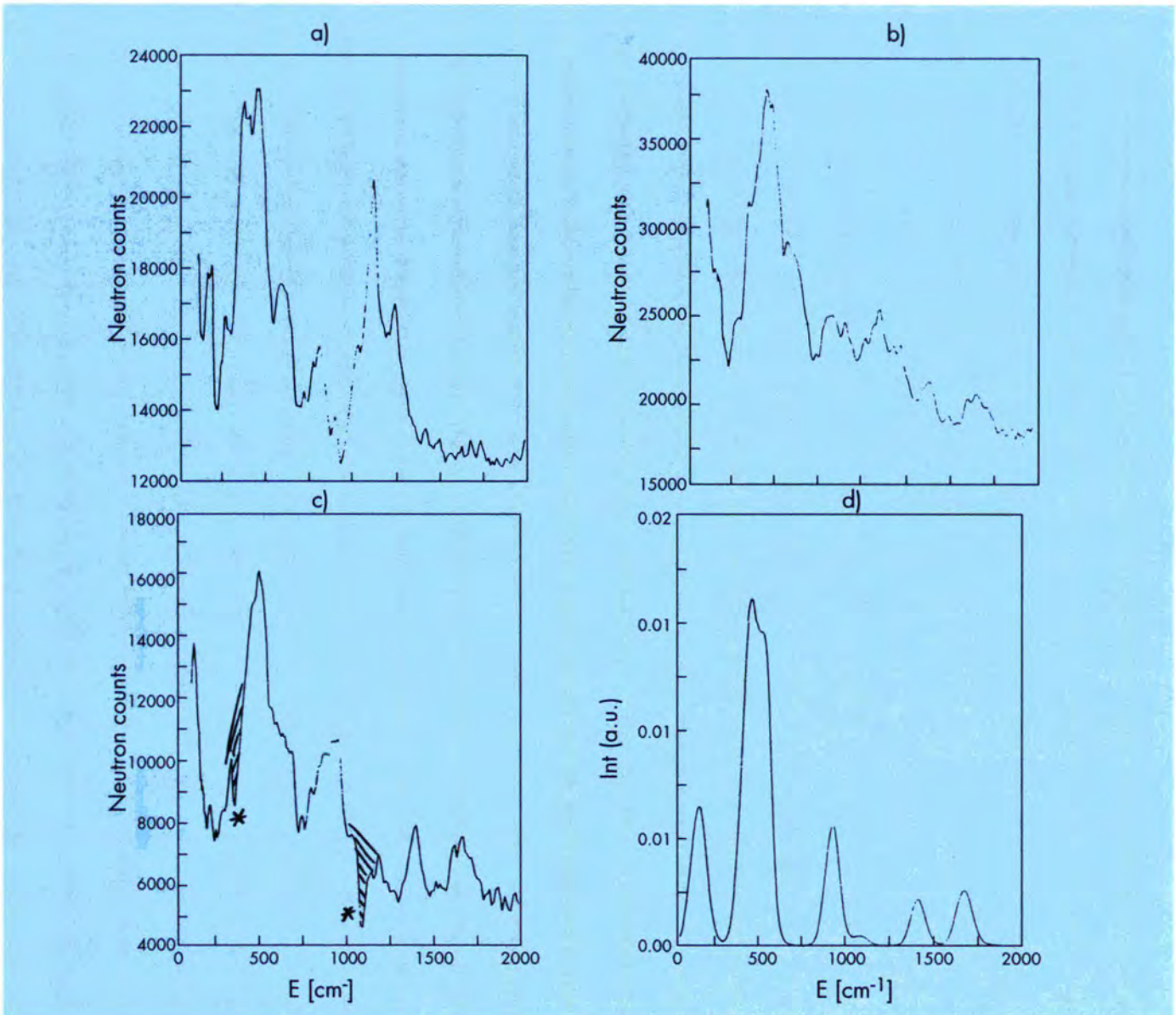

Fig. 3: INS spectra of a) dehydrated zeolite, b) after water adsorption, c) the difference spectrum between a) and b), and d) the simulation of the H^3O^+ ion bond spectrum bonded to the zeolite.

Fig. 3c can be calculated. This spectrum contains 2 negative bands (*), at the position of the OH bending modes, proving the interaction of water with the Brönsted sites. The positive bands can be better simulated with an H^3O^+ ion bonded to the zeolite (Fig. 3d) than with an H-bonded H_2O molecule. This experimental result contradicts the recent quantum mechanical calculations.

INS of para-nitroaniline chains in $AlPO_4$-5 molecular sieve

Zeolite-like molecular sieves are nanoporous oxidic crystals, e.g. aluminosilicates, aluminophosphates, or silicates, that can recognise and discriminate among molecules. Increasingly, molecular sieve crystals serve as hosts, organising organic and inorganic guest atoms, molecules, and supramolecular compounds in their pores, which results in composite materials with novel optic, optoelectronic, and electrochemical properties [5].

In addition to its function as a dispersing and stabilising medium, a molecular sieve crystal can incorporate guest molecules in a geometry that is related to its pore structure (self-assembly of semiconductor quantum dots or wires, in-situ synthesising of polymer chains...). It has recently been found that $AlPO_4$-5 crystals loaded with para-nitroaniline (pNA) exhibit second harmonic generation. The occurrence of nonlinear optical effects of second order proves that, in addition to the alignment of the molecules,

the adsorbed molecules must have a preferred direction in the pores, at least for regions longer than the wavelength of the light (Fig. 4).

The orientation of pNA in large single crystals of $AlPO_4$-5 has been checked by vibrational optic spectroscopy. The presence or absence of certain modes indicated that the molecules were aligned as in Fig. 4. This good alignment of the dipolar pNA molecules is a result of the restricted space in the pores and of both the electrostatic forces and intermolecular H-bonds in the dipole chain. However, only some bands are visible in the optical spectra: the Raman bands are superimposed by a strong background and the adsorption of the host lattice in infrared makes the detection of guest bands impossible in certain spectral regions.

The inelastic neutron scattering (INS) spectrum of pNA adsorbed in $AlPO_4$-5 has been measured on IN1BeF between 10 and 250 meV (Fig. 5) [3]. All the observed peaks are due to pNA, the scattering from $AlPO_4$-5 being negligible. The total amount of sample was only 2g, including 0.3g of pNA, and the spectrum was obtained in 12 h. The spectrum of pNA in the solid phase was also recorded within the same running time (see Fig. 5). The statistics are much better than in the adsorbed phase because 2 g of pNA were used. A comparison of the 2 spectra shows substantial changes below 100 meV. Assignments for the adsorbed molecule are not complete and a normal coordinate analysis is required to understand the modifications of the intra and intermolecular interactions induced by adsorption.

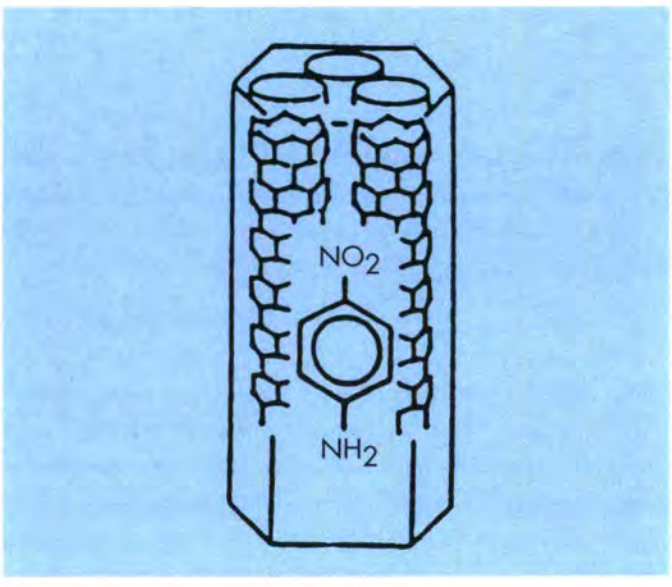

Fig. 4: Para-nitroaniline (pNA) in $AlPO_4$-5

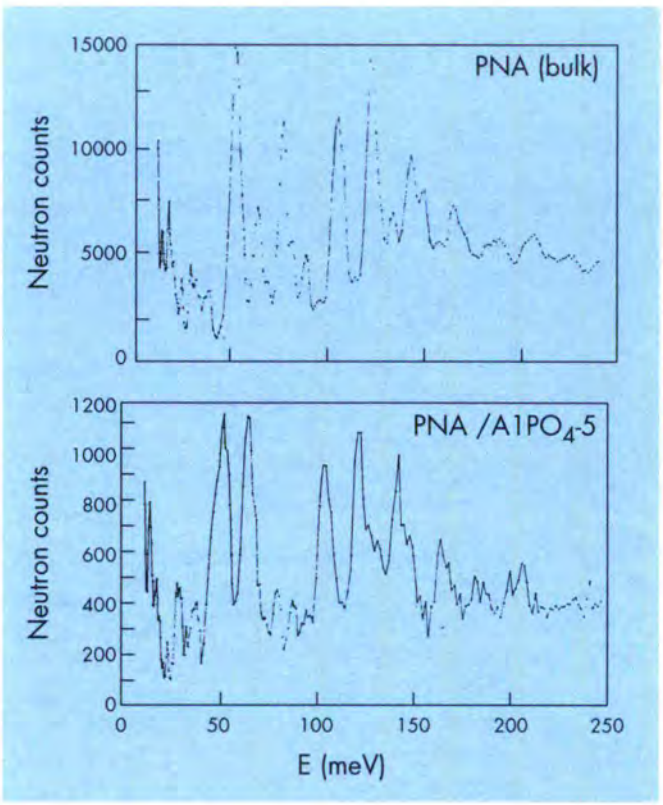

Fig. 5: INS spectra of pNA adsorbed in $AlPO_4$-5 and of bulk pNA

Spectroscopy

Temperature Dependence of the Vibrational Density of Statesof Decagonal Al_{70} Co_{15} Ni_{15}

The temperature dependence of the generalised vibrational density of states (GVDOS) of a decagonal alloy (and of crystalline variants) was determined for the first time using the cold neutron time-focusing time-of-flight spectrometer IN6 [6]. The highest incident energy (4.76 meV) accessible on this instrument was chosen in order to achieve the best possible averaging in reciprocal space of the intensity coherently scattered from this sample.

After annealing the sample for several hours at 1100K and then quenching it in liquid N_2 in order to freeze-in the high temperature decagonal phase, the sample was measured at 294, 473, 1100, 970, 870, 670 and 294 K. At all temperatures the GVDOS consists essentially of two broad bands and extends to surprisingly high energies of $\omega_{max} \geq 60$ meV (for pure Al, the lightest of the 3 elements, $\omega_{max} \geq 42$ meV) (see Fig. 6). The first band between 0 and approximately 40 meV has a sharp maximum at 22.5 meV (at 294 K), which shifts to slightly lower energies with increasing temperature. It is the dominant band already at room temperature. The very broad second band, starting

approximately just below 30 meV, has a strong overlap with the first band. Thus this second one appears more as a shoulder at the upper slope of the first band. On heating one observes a strong intensity transfer from the upper to the lower band, which therefore dominates even more strongly the shape of the frequency distribution. At the same time this band shifts slightly to lower energies. *Thus a considerable softening of the vibrations* is observed. As the increase of intensity in the lower band is, within a reasonable approximation, linear with temperature, the observed softening is not assumed to be caused by either phase changes or by simple anharmonicity. Instead this intensity transfer is more likely to be related to an *anisotropic expansion of the two-dimensional lattice*, suggesting that the expansion within the quasiperiodic plane is different from that along the periodic (c)-axis.

Most of the observed facts are strongly supported by a model calculation of the vibrational properties of decagonal-AlCoNi using the modified Burkov model (Mihalkovic and Henley) *with a priori* pair potentials and the real-space recursion method up to 40 recursion levels. On the basis of these model calculations, the lower band is dominated by the vibrations of the TM-atoms. This band appears to be on top of a very broad band due to Al-atom vibrations, the upper part of which forms the upper band of the observed GVDOS. As observed in the experiment, these Al-atom vibrations also extend out to 60 meV in the model calculation, supporting the conclusion drawn from the experiment that quite short atomic distances must be present in this decagonal phase and that the strong interaction potentials leading to the observed high frequency Al-atom vibrations are due to the many Al-TM nearest neighbours.

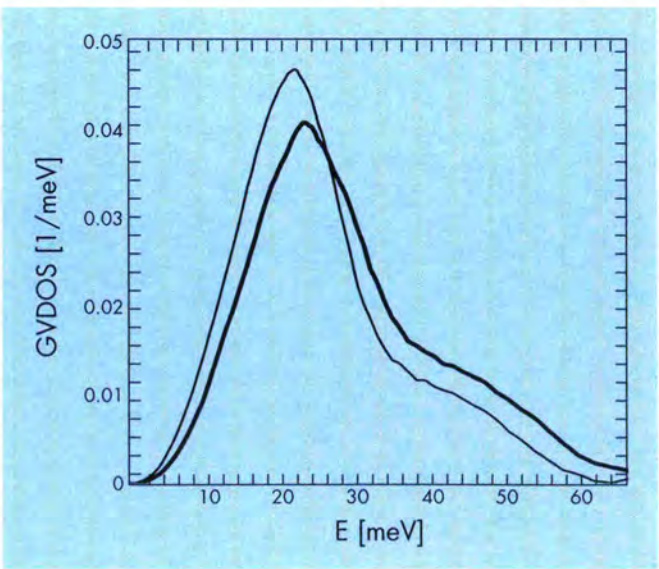

Fig. 6: Experimental DOS of the sample [$Al_{70}Ni_{15}Co_{15}$] at room temperature (thick line) and at 1100 K (thin line).

Dynamics of the NH^-_2 anion in potassium amide KNH_2

Three phases of potassium amide are known from diffraction experiments: *monoclinic* ($T \leq 326$ K, space group $P2_1/m$), *tetragonal* (326 K $\leq T \leq$ 348 K, P4/*nmm*) and *cubic* ($T \geq 348$ K, $Fm\bar{3}m$, NaCl structure) as depicted in Fig. 7. The amide anion NH^-_2 has a geometry similar to that of the water molecule: N-H distance 1.04 Å, bonding angle 105°.

The amide anions NH_2 are orientationally ordered in the monoclinic phase and orientationally disordered in the other two phases: in the tetragonal phase there are 4 equivalent equilibrium positions for the two H atoms and in the cubic phase even 8. On IN5, we have investigated the dynamics of the amide anion in all three phases in a temperature range 265 K $\leq T \leq$ 415 K with different resolutions (λ_0 = 3 Å, 5 Å, 6.5 Å) [7].

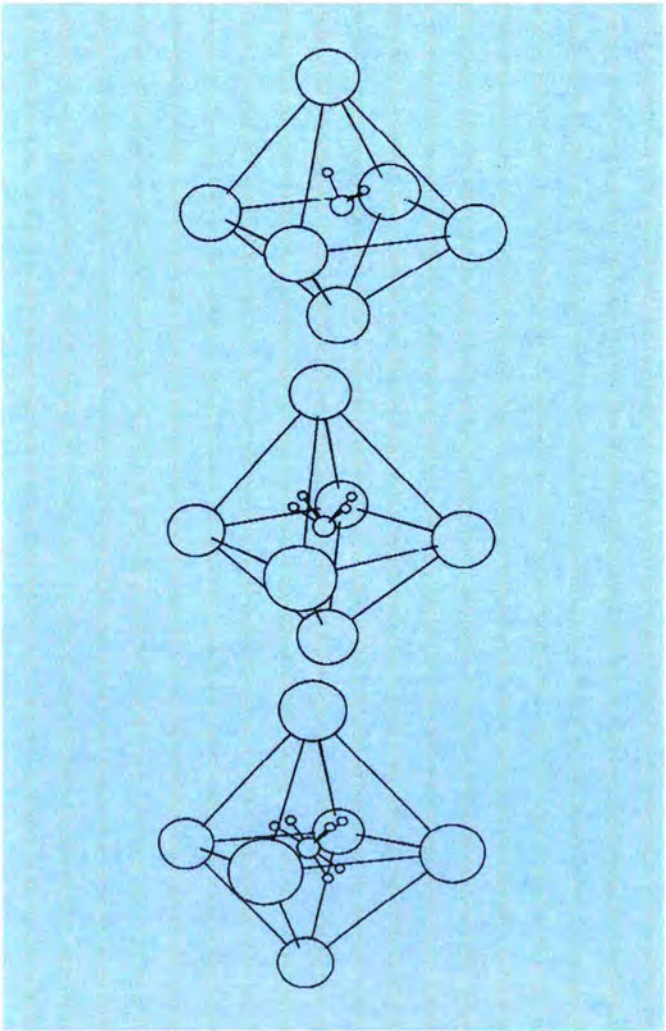

Fig. 7: The three phases of potassium amide from top to bottom: monoclinic, tetragonal and cubic.

Fig. 8 shows a typical spectrum in the *monoclinic* phase at 320 K. It shows a significant broadening of the elastic line. A single Lorentzian is sufficient to fit the quasielastic part of the spectrum. Both the elastic and quasielastic intensities can be explained by a two site jump model with a jump distance $\rho = 1.47$ (1) Å.

Fig. 9 shows observed and calculated structure factors; the parameters of the fit are listed in Tab. 1. The value for τ agrees with the H-H distance within the NH_2 group (1.6 Å) and shows that the quasielastic scattering in the monoclinic phase is due to 180° reorientational jumps around the twofold symmetry axis of the amide anion. These 180° reorientations have a large activation energy $E_A = 208 \pm 9$ meV as determined from an Arrhenius plot of the mean residence times (Fig. 10). Below $T = 265$ K the quasielastic broadening could no longer be resolved further.

The dynamics of the amide anion accelerates by more than one order of magnitude in the *tetragonal* phase (see Fig. 10) but almost no changes are observed at the phase transition tetragonal-cubic. In both phases the quasielastic distribution may be described by the sum of two Lorentzians with widths differing by a factor of 2. The temperature dependence is weak in the *cubic* phase ($E_A < 40$ meV). The EISFs in these two phases do not show significant differences either. So the conclusion is that the dynamical process is the same in the tetragonal and cubic phases: 90° jumps about the (twofold) amide symmetry axis. The observed structure factors for the cubic phase ($T = 360$ K)

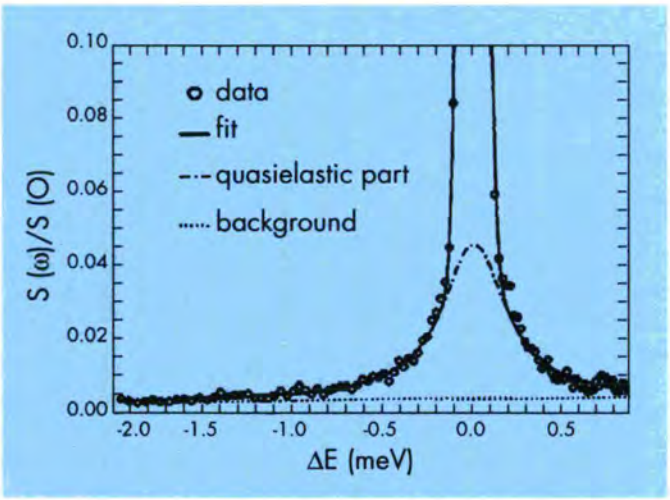

Fig. 8: Spectrum in the monoclinic phase of KNH_2, 320 K ($\lambda_0 = 5$Å). It is well described by the sum of an elastic line, a quasielastic part (Lorentzian, FWHM = 428 μeV) and a linear background.

	Reorientations about twofold axis	
	ρ (Å)	1.47(1)
	FWHM(μeV)	428(16)
320 K	τ (s)	$3.87(15).10^{-11}$
	$(u^2)_H$ (Å^2)	0.080(5)
	Reorientations about fourfold axis	
	2ρ (Å)	1.90(2)
	FWHM (meV)	2.25(4)
360 K	τ (s)	$1.83(3).10^{-12}$
	$(u^2)_H$ (Å^2)	0.093(2)

Table 1: Model parameters obtained from the fit. For the monoclinic phase (320K) the jump distance ρ, the quasielastic broadening (or mean residence time τ) and mean square displacement $\langle u^2 \rangle_H$ of the H atoms are determined. For the cubic phase (360K) the corresponding values for 180° reorientations are shown, the 90° jumps are twice as fast for a jump distance of $\sqrt{2}\rho$.

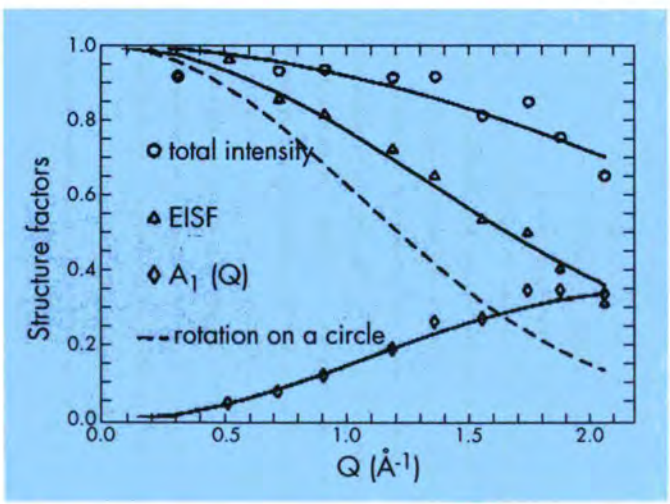

Fig. 9: EISF, quasielastic structure factor $A_1(Q)$ (FWHM = $4\tau^{-1}$) and total intensity in the monoclinic phase of KNH_2 at 320 K. The parameters (see Tab. 1) are obtained by a simultaneous fit of the spectra with the model of 180° reorientations.

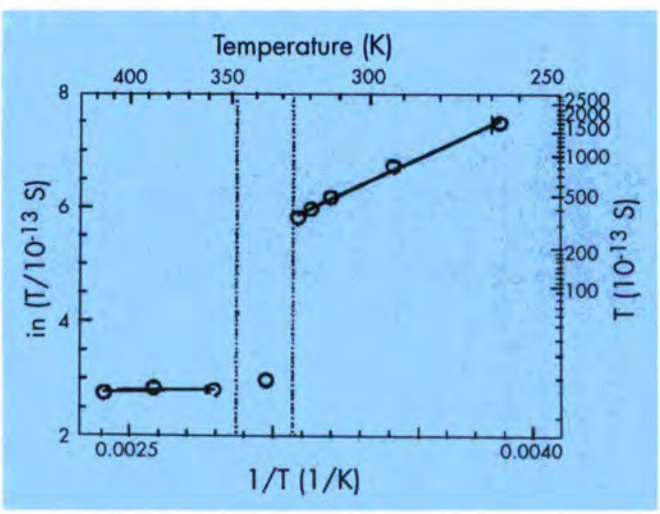

Fig. 10: Arrhenius plot of the mean residence times τ between 180° jumps in all three phases of KNH_2. The mean residence time between 90° jumps in the tetragonal and cubic is $\tau/2$.

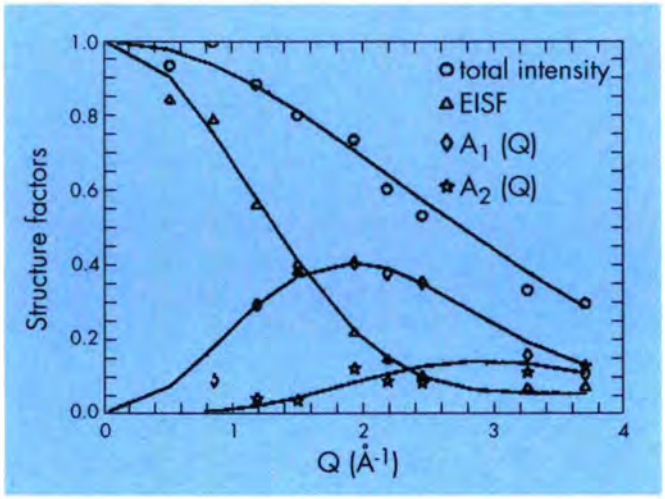

Fig. 11: EISF, quasielastic structure factors $A_1(Q)$ (FWHM τ^{-1}), $A_2(Q)$ (FWHM $2\tau^{-1}$) and total intensity in the cubic phase of KHN_2 at 360 K. The parameters (see Tab. 1) are obtained by a simultaneous fit of the spectra with the model of reorientations about a fourfold axis.

are shown in Fig. 11 and compared to the strucutre factors calculated on basis of the 90° jump model. For the parameters of the fit, see Tab. 1. The increase of the jump distance is in agreement with diffraction results. For the tetragonal phase a jump distance of 2ρ = 1.76 Å with a mean square displacement $\langle u^2 \rangle_H$ = 0.089 Å was observed. Both these values lie between those obtained for the monoclinic and cubic phase, respectively.

Neutron scattering studies of linear chains in an organic inclusion compound

The nitroxide $C_9H_{16}NO_2$ (tano) forms channel inclusion compounds with a large range of linear chains or slightly branched molecules. All of them present disorder phenomena of the guest species in the channels of the structure, but also of the host matrix molecules from one chiral form to the other. The evolution of this disorder as a function of the temperature is accompanied by one or two phase transitions above 100 K, depending on the length of the included chain [8] . The first transition is strongly of first order. Its temperature depends on the number, n, of the carbons of the chain. Upon heating from the low-temperature phase, a strong hysteresis of 50-80 K is observed. It is accompanied by the appearance of superstructure Bragg peaks indicating a 3D ordering of the alkane guest species (Fig. 12). The matrix parameter along the direction of the channels becomes commensurate with the chain length. Together with the ordering of the alkane in the channels, a reorganization of the tano matrix occurs, resulting in less disorder.

Because of the presence on the matrix molecule of a nitroxide group, a precise study of the molecular dynamics in these systems is very difficult by NMR. On the contrary, the neutron scattering technique is able to provide reliable information. Therefore the dynamical disorder of these systems was extensively investigated by Incoherent Quasielastic Neutron Scattering (IQNS) [9-11]. The motions of the chains and of the tano molecules for the tano/heptane, tano/octane, tano/1-bromohexadecane and tano/1-bromodecane systems were studied in their low, intermediate and high-temperature phases. The experiments were carried out on polycrystalline samples using several neutron spectrometers (IN6, IN16, D7) with a temperature ranging from 103 K to 300 K. An analysis of the results in terms of the general model proposed in the earlier IQNS study of the tano/alcane compounds with short included chains pointed out original features associated to the chain length [11]. The studies with longer included chains in particular evidenced a direct influence of the chain length

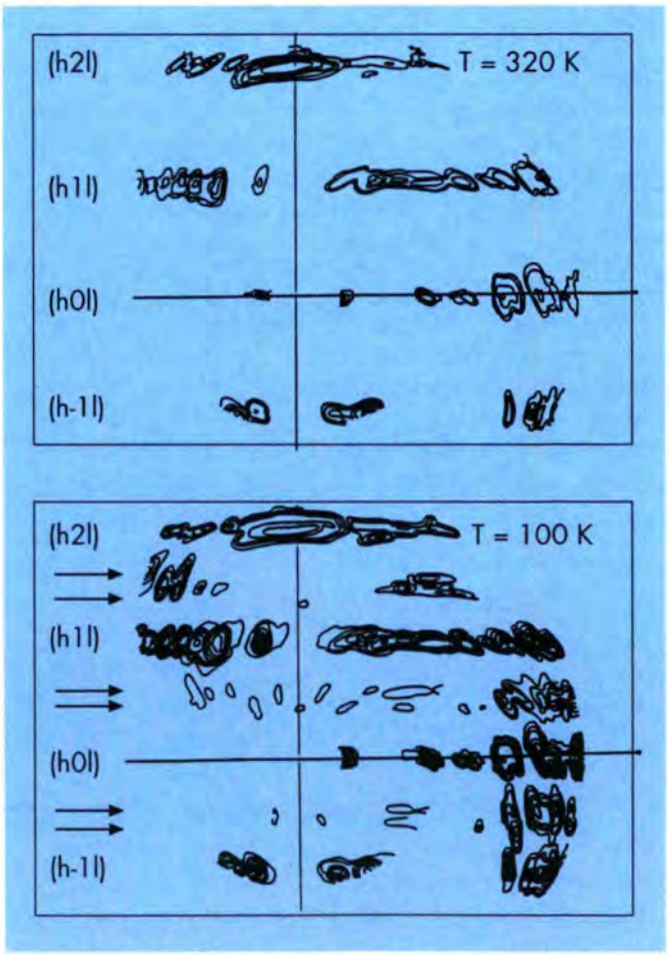

Fig. 12: Neutron diagram of tano/octane obtained with the spectrometer D7 at the Institut Laue-Langevin. At T = 320 K the intermediate diffuse planes have disappeared. Superstructure Bragg peaks are clearly visible at T = 100 K.

on the motions of the molecules of the matrix, only a part of which appeared mobile. Simultaneously, the values of the correlation times for the motions of the methyl groups were found to be slightly smaller than with the tano/heptane and the tano/octane systems. Actually, in the interpretation of the earlier IQNS experiments, all the CH_3 groups were considered as dynamically equivalent. The number of "fixed" methyl groups increases slightly with the length of the included chain and another analysis of the earlier data for tano/heptane and tano/octane would perhaps yield a small portion of immobile methyl groups and, subsequently, a smaller value of the correlation time for the mobile part. The activation energies for the methyl jumps deduced from the present experiments (ΔH = 12.6 kJ.mol^{-1}. for tano/BrC_{16} and ΔH = 13.9 KJ.mol^{-1}. for tano/BrC_{10}) are consistent with the earlier value (ΔH = 12 KJ.mol^{-1}) and support the attribution of the inelastic bands near 34 meV to the torsional excitations of the methyl groups, with a barrier height of 13 kJ.mol^{-1}. A very extensive inelastic neutron scattering study of a series of systems with various guest chains, together with Raman light scattering experiments on the same compounds, provided information about the conformational behaviour of the included chains [12].

In recent years it has been demonstrated that calculations based on empirical energy functions could be very useful for investigating the physical properties of molecules. Such calculations were performed in the case of the tano molecule, using the program CHARMM [13], in order to evaluate the heights of the potential barriers associated with the ring inversion of the tano molecules and the rotation of the methyl groups about their threefold axis.

The empirical energy function comprising internal energy terms (bond potentials, bond angle potentials, dihedral torsion potentials and improper torsion terms) together with nonbonded interactions (Van der Waals interactions and an electrostatic potential) was built from force constants obtained from the literature concerning similar molecules. Geometric constants were derived from crystallographic data.

The refinement of the molecular structure by minimizing its potential energy yielded a geometry close to the conclusions of X-ray diffraction analyses. The energy barriers against intramolecular deformations were evaluated in two ways, using the adiabatic method and the rigid method respectively.

Concerning the rotation of the methyl groups, both methods yielded similar results, the values of the potential barrier being 19 kJ.mol^{-1} and 18 kJ.mol^{-1}, respectively. The deviations with respect to the experimental value measured from IQNS (12 kJ.mol^{-1}) can be explained as due to an incorrect distribution of the charges of the nitroxide group and a coupling with the chain motions experienced by the methyl groups. In spite of the lack of information about the actual intermediate conformations, the evaluation of the energy barrier in relation to the ring inversion yielded a value of 33.5 kJ.mol^{-1}, in good agreement with the estimation of the earlier IQNS studies.

It must be pointed out that several aspects are neglected in the potential energy function. The harmonic form employed for the internal coordinate energies is a local approximation to the potential near minima. Cross-coupling between internal coordinate energies are neglected. The force field neglects charge-induced dipole terms and three-body polarizations effects. Nevertheless, the molecular simulations are very promising approaches for future developments of IQNS. It is intended to carry out such calculations first on the pure tano, then on the inclusion compounds in order to evaluate the vibrational spectra and the scattering functions.

The nature of the Rh-H_2 bond in a dihydrogen complex stabilized only by nitrogen donors. An inelastic neutron scattering study of $Tp^{Me2}RhH_2(\eta^2\text{-}H_2)$ (Tp^{Me2} = Hydrotris(3,5 dimenthylphyrazolyl)borate).

Since the original discovery by Kubas et al. [14] of transition metal complexes containing coordinated molecular hydrogen, these compounds have attracted increasing attention as they are likely to provide a better understanding of the nature of dihydrogen-metal interactions and, therefore, of the fundamental process of dihydrogen activation at a metal centre and of the role of dihydrogen complexes in homogeneous catalysis. Schematic representations of the $M(H_2)$-and MH_2-interactions in their complexes are shown in Figure 13.

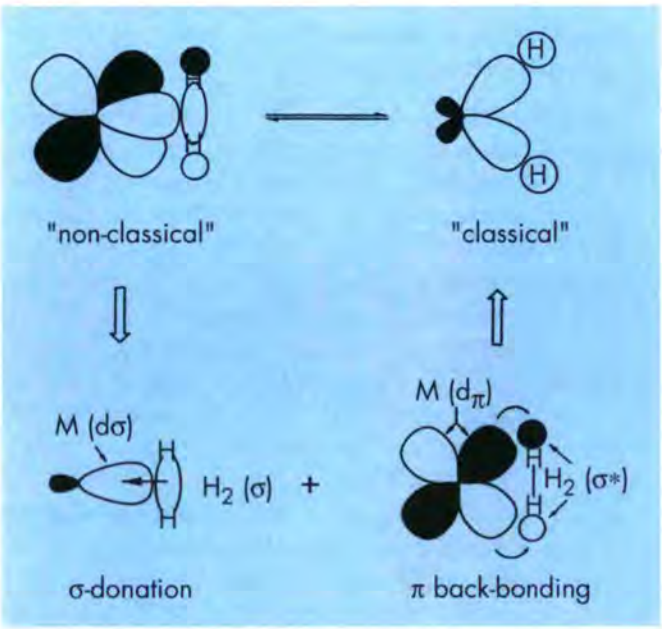

Fig. 13: Schematic representation of the MH_2- and $M(H_2)$-interactions

Most of these complexes contain phosphine, cyclopentadienyl or organometallics donors as co-ligands, and it has been assumed that the high electron density at the metal centre induced by the presence of these ligands strengthens the $M(H_2)$ bond by π-bacdonation. The structure of **1** is shown in Fig. 14.

INS measurements of the rotational and vibrational transitions of the dihydrogen ligand in **1** were performed in order to carry out a detailed study of its rotational barrier.

The data collected on the spectrometer IN5 at a temperature of 5K, yielded the tunnel splitting of the librational ground state of the coordinated dihydrogen. Another set of data, obtained at 15K, on the FDS instrument at the Los Alamos National Laboratory provided vibrational data including transitions to the excited librational states (" torsions ") of the dihydrogen ligand.

The vibrational spectra were obtained with the aid of a "difference technique" using two samples, one of the hydride and the other of the corresponding complex, in which the two H- and the H_2-ligands were replaced by D- and D_2, respectively.

The rotational tunneling spectrum, obtained on IN5 at 5K, is shown in Figure 15a and the two peaks at ± 6.7 cm^{-1} are assigned to the rotational tunneling of the bound dihydrogen. The vibrational difference spectrum of the $RhH(H_2)$-fragment is shown in Figure 15b.

The two peaks at *ca.* 120 and 200 cm^{-1} are assigned to the dihydrogen torsions because of their high intensities and the weaker peaks at higher frequencies to the skeletal deformation modes involving the $(H)_2/(H_2)$ motions. Data from both experiments are summarized in Table 2.

The barrier height can be calculated using the equation for a hindered rotor:

$$[-B(\delta^2/\delta\phi^2) - + \Sigma V_n(1-\cos n\phi)]\psi = E\psi$$

where ϕ is the angle of rotation about the N-Rh-H_2 axis and B is the rotational constant ($B = h^2/2I \times r$, and $I \times r$ = moment of inertia) under the assumption of planar rotation and negligible coupling with vibrational modes [15].

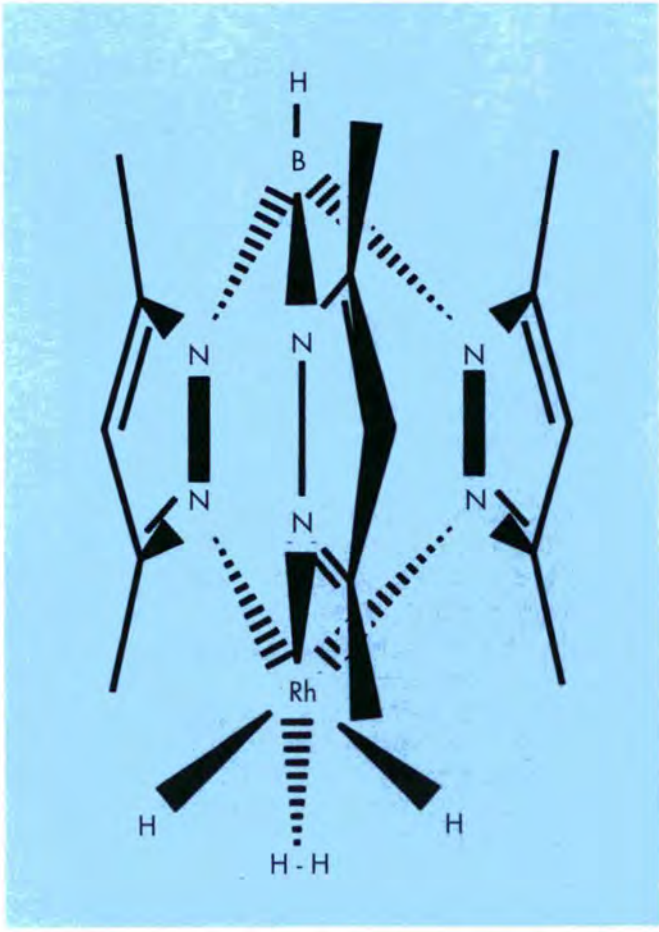

*Fig. 14: Structure of $Tp^{Me2}RhH_2(\eta^2\text{-}H_2)$ (**1**) (Tp^{Me2} = hydrotris(3,5-dimenthylphyrazolyl)borate)*

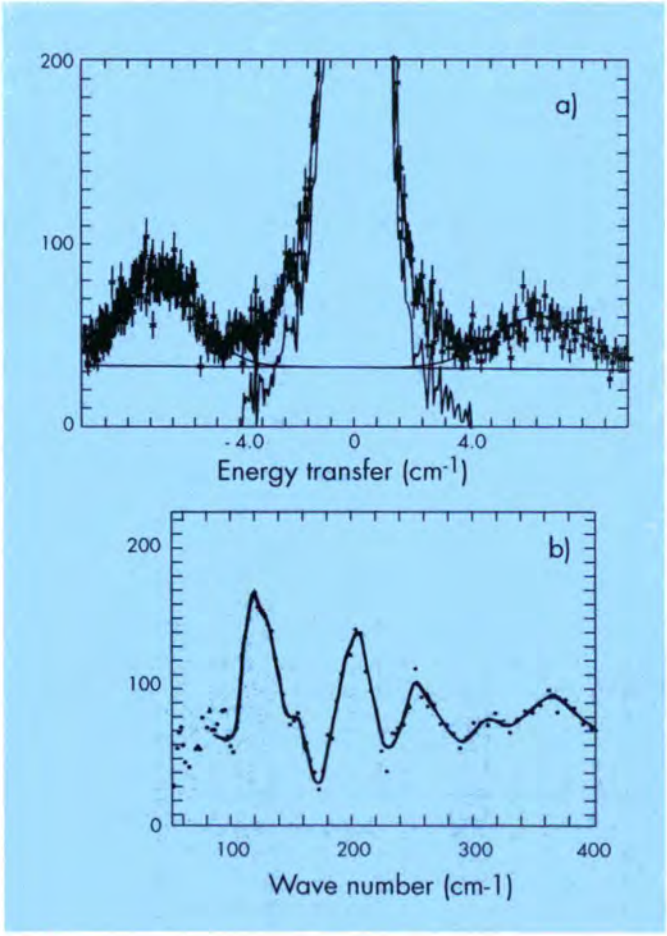

*Fig. 15: INS spectra of $Tp^{Me2}RhH_2(\eta^2\text{-}H_2)$, **1**: (a, top) Low frequency spectrum collected at T = 5K, on IN5 at ILL using an incident neutron wavelength of 5 Å; (b, bottom) Sample difference spectrum, at T = 15K, obtained on FDS at LANSCE.*

ω_t	ε(obs.)		ε(calc.)	
		$V_2 = 1.1$ $B = 49.7$	$V_2 = 0.68$ $B = 37.1$	$V_2 = 0.60$ $V_4 = 0.26$ $B = 37.1$
6.7(5)				
	118, 126	-	121	123
	194	188	180	195
	203	255	219	204

Table 2
Tunneling frequency $\omega_t(cm^{-1})$, observed and calculated rotational transitions, ε, (cm^{-1}) and barrier heights V_n, (kcal/mol) for dihydrogen in $[Tp^{Me2}RhH_2(\eta^2\text{-}H_2)]$.

The rotational constant B, and, consequently, the H-H distance, was allowed to vary. This approach is reasonable as both the chemistry and the spectroscopic data for compound **1** indicate that the H-H distance in the coordinated dihydrogen is significantly longer than 0.81 Å. Much better agreement was obtained using a potential where $V_2 = 0.60$ and $V_4 = 0.26$ kcal/mol. This potential had a maximum well depth of 0.56(2) kcal/mol and a set of secondary minima at 90° to those of the equilibrium orientation of the dihydrogen. The resulting rotational constant was 37.1 cm^{-1} giving an H-H distance of 0.94 Å. This value is qualitatively in accord with the fact that **1** is a fairly stable dihydrogen complex, i.e. that the M-H interaction is rather strong and the H-H interaction weak. The latter conclusion is also consistent with the assignment of the very low energy IR band at 2238 cm^{-1} to ν(HH).

It should be noted that the rotational tunneling peaks and some of the torsional peaks appear to be split; a further discussion of this is found in [16]. The very low value obtained for the barrier to rotation of dihydrogen in this compound would appear to be somewhat surprising in view of the spectroscopic evidence for a weak H-H interaction with its attendant enhanced Rh-H interaction. The most plausible explanations for this low value are: (i) the strong metal-H_2 bond is mainly due to a σ-interaction which does not directly contribute to the barrier to rotation and (ii) the direct interaction of dihydrogen with the *cis*-hydrides has the effect of lowering the barrier to rotation.

Workshop on "Quantum Tunnelling of Atoms and Molecules in Solids"

The workshop, financed by the ILL and CNRS, took place on October 4 to 7, 1995 at the Château de la Baume, Seyssins, on the outskirts of Grenoble. The organisers were F. Fillaux, LASIR-CNRS Thiais, H. Büttner and G. Kearley, ILL Grenoble, and J. Meinnel, University of Rennes. The workshop attracted over 50 people, presenting papers within the following main topics:

- study of rotational tunnelling using neutrons (inelastic and elastic), NMR and other techniques such as light-scattering.
- quantum proton-transfer along hydrogen bonds using neutrons and NMR
- mobile protons in solids, such as metals, proton conductors, etc.

Inelastic neutron scattering (INS) was the most popular single technique, accounting for almost half of the talks and posters. Hot topics were: rotational translational coupling proposed by several groups, motion of protons in H-bonds being independent (or not) of other molecular motions, tunnelling of mixed isotope rotors, and use of single crystals. The proceedings will be published in Physica B.

Secretary: Hans-Jochen Lauter

References

[1] G.Vogl, O.G. Randl, B. Sepiol, ILL Annual report 1994, blue box, p. 67.

[2] O.Randl, G.Vogl, Kaisermayr, Bührer, Pannetier, to be published.

[3] H. Jobic, to be published.

[4] H. Jobic, M. Czjzek and R.A. van Santen, *J. Phys. Chem.* **96** (1992) 1540.

[5] G.A. Ozin, *Adv. Matter* **4** (1992) 613; G.D. Stucky and J.E. McDougall, *Science* **247** (1990) 669.

[6] F. Dugain, M. Mihalkovic, J.-B- Suck, to be published.

[7] M. Müller, B. Asmussen, W. Press, to be published;

[8] M. Le Bars-Combe and J. Lajzérowicz-Bonneteau, *Acta Cryst.* B **43** (1987) 386 and 393.

[9] M. Bée, A. Renault, J. Lajzérowicz-Bonneteau and M. Le Bars-Combe, *J. Chem. Phys.* **97,** 10 (1992) 7730.

[10] M. Bée, J. Lajzérowicz-Bonneteau and A. Renault *Physica B* **180/181**, (1992) 653.

[11] M. Bée, J. Combet, F. Guillaume, N-D Morelon· M. Ferrand· D. Djurado and A.J. Dianoux· *Physica B* in press, (1996).

[12] J. Combet, F. Guillaume and M. Bée, *Mol. Phys.* submitted (1996).

[13] B. Brooks, R. Bruccoleri, B. Olafson, D. States, S. Swaminathan and M. Karplus, *J. Comput. Chem.* **4**, 2 (1983) 187.

[14] Kubas, G.J.; Ryan, R.R.; Swanson, B.I.; Vergamini, P.J.; Wasserman, H.J. *J. Am. Chem. Soc.***106**, (1984), 451.

[15] Eckert, J.; Kubas, G.J. *J. Phys. Chem.* **97**,(1993), 2378.

[16] Juergen Eckert, Alberto Albinati, Urs E. Bucher, and Luigi M. Venanzi, to be published.

Biological Structures and Dynamics

Members of the College at the ILL

C. Bon
E. Bellet-Amalric
P. Chenavas
A.J. Dianoux
S. Egelhaaf
M. Ferrand
P. Langan
M.S. Lehmann
P. Lindner
S.A. Mason
R. May
O. Randl
E. Pebay-Peyroula
S. Penel
P.A. Timmins
L. Vuillard
G. Zaccaï

External members

EMBL

A. Åberg
A. Barge
F. Baudin
G. Bec
H. Belrhali
C. Berthet
D. Birse
F. Borel
K. Brown
S. Cusack
M.T. Dauvergne
C. Elster
M.L. Ferri
H. Härtlein
U. Kapp
T. Kawashima
K. Larsen
R. Leberman
S. McSweeney
S. Monaco
S. Price
B. Rasmussen
R. Ruigrok
L. Seignovert
C. Taupin
A. Thompson
M. Tukalo
C. Wilkinson
A. Yaremchuk

IBS

G. Arlaud
J. Chroboczek
C. Cohen-Addad
O. Dideberg
A.M. Di Guilmi
C. Ebel
J.C. Fontecilla
E. Forest
J. Gagnon
B. Jacrot
R. Margolis
D. Marion
M. Van der Rest
R. Wade

ESRF

C. Branden
A. Hammersley
A. Kvick
C. Riekel
M. Saad

Introduction

The reactor restart at the beginning of this year signalled the end of a period of interruption for projects which are dependent on the unique facilities offered by the ILL. It also brought to light new projects which had been developing during the long shutdown. The important role played by neutron scattering techniques in the study of Biological structure and dynamics is mainly due to their complementarity to other techniques such as x-ray diffraction. During the shutdown the scientific life of the College had continued in these complementary areas with collaborations strengthened and established between a number of research facilities and institutes. Some of these scientific programmes are associated with projects for developing new instrumentation and techniques. This year, College members and their colleagues were involved in realising these developments.

A number of instrument development programmes were of particular relevance to studies of the structure and dynamics of Biological systems. In April the first experiments were carried out on the new small-angle neutron scattering, SANS, diffractometer, D22. Because of an interruption for repairs to the position sensitive detector, PSD, commissioning of this instrument will continue into 1996. The PSD on the single crystal diffractometer D19 was refilled with gas to restore it to its design efficiency. A new PSD on the time-of-flight spectrometer IN5 was commissioned. With appropriate samples, it is now possible to measure correlated motions on length scales from 20Å to 100Å. The quasi-Laue diffractometer, Ladi, was tested at the end of cold neutron guide H142. Detailed status reports of these projects are given under the relevant instrument groups.

College members represented these developments at conferences and workshops throughout the world. Their efforts were rewarded by a record number of proposals being submitted to the Biology subcommittee. The College received fifty-five proposals for the use of ten different instruments in the October proposal round (D7, D11, D16, D17, D19, DB21, D22, IN5, IN6 and IN10). A number of trends were identified from these proposals and those submitted at the previous two rounds.

Many proposals concerned the use of inelastic scattering instruments. Progress in structure determination, e.g. of trans-membrane proteins, and methods of biotechnology, such as replacement of amino acids at particular sites in a protein, now allow specific questions to be asked about protein dynamics in relation to its biological function. In recognition of this trend and the need to develop procedures for data analysis, a workshop "Inelastic Neutrons in Biology" will be organised by the ILL and held in October 1996.

Some of the other trends and scientific highlights of this year are presented below in no particular order.

Scientific Highlights

Microtubule self-organisation

Self-organisation and morphogenesis are important in a number of Biological processes. Microtubules in solution can, under appropriate conditions, self-organise and form macroscopic structures. When assembled in spectrophotometric cells, uniformly spaced stripes form which reflect periodic variations in microtubule orientation. It has been proposed

that the self-organising properties of this system are due to chemically dissipative reaction-diffusion mechanisms. If present, these mechanisms should also lead to variations in microtubule concentration. As opposed to optical methods SANS can unambiguously and simultaneously measure both microtubule concentration and orientation independently of one another.

Measurements carried out on D11 involved scanning along the length of a striped microtubule sample (J. Tabony, CENG and L. Vuillard, ILL). Figure 1 shows the variation, as a function of position, of the intensity of the radially averaged microtubule scattering curve. The scattering intensity is proportional to microtubule concentration. The changes in concentration coincide with changes in orientation. This result is an important element of proof that chemically dissipative processes are responsible for the systems' self-organising properties.

Non detergent sulfobetaines (NDSB)

NDSB agents for protein solubilization and stabilisation featured in last year's annual report. NDSB's were developed during the long shutdown through a collaboration with a Grenoble based CEA-INSERM lab. This year new applications were found for these agents, notably for the stabilisation of halophilic proteins [1] and for increasing the yields in protein renaturation [2]. A possible explanation for the function of NDSB is that the solubilisation is caused by attachment to the protein. In order to prove or disprove this explanation SANS experiments were carried out on D11 on two commonly used proteins in the presence of NDSB (L. Vuillard and M.S. Lehmann, ILL).

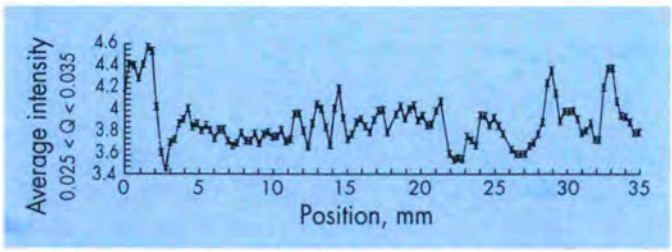

Fig. 1: The variation in microtubule scattering intensity as a function of position along a flat cell of 2mm optical path length. The beam size was 1x0.3mm.

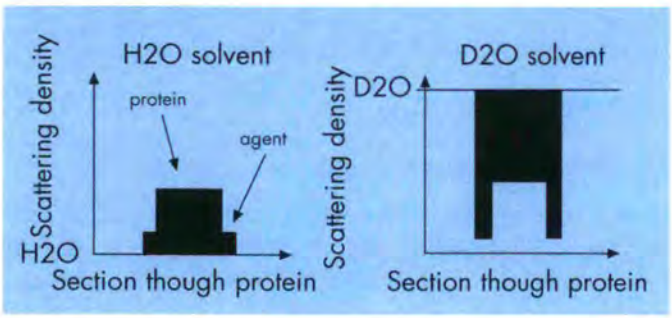

Fig. 2: The scattering density profile of a protein in H_2O and D_2O environments with the solubilising agent NDSB prefentially bound.

Figure 2 shows that if NDSB is preferentially bound to the protein, then the scattering density profile is very different for the sample in H_2O and D_2O environments. Consequently the radius of gyration in the two cases will be different. Preliminary results suggest that there is no binding or exclusion of NDSB at the surface of the protein. Since NDSB can have a significant effect on the solubilisation by detergents of membrane bound proteins, the action of NDSB on the size of detergent micelles was also investigated. This showed that the size of micelles was modified in the presence of NDSB but the variations observed could not be correlated to the changes observed in extraction yields.

Membrane/protein/detergent interactions

The solubilisation of membrane proteins by detergents is at present the only way in which such proteins can be prepared for crystallisation and high resolution crystallographic studies. (The only exception is the naturally crystalline purple membrane of halophilic bacteria). For this reason the study of membrane protein/detergent interactions both in crystals and in solution is important. The characterisation and determination of the geometrical parameters of detergent micelles of potential use in crystallisation is also of major interest. A number of projects are underway in this field. Data collection has been almost completed on crystals of the porin/C8E4 complex from *Rhodobacter capsulatus* (W.Welte, Freiburg/Konstanz, E.Pebay-Peyroula, S.Penel and P.Timmins, ILL) and the same complex has been studied in solution by SANS (W.Welte, Freiburg/Konstanz and P.Timmins, ILL). A comparison between the crystal and solution complexes should give important information on the crystallisation process as well as on the detergent binding surfaces of the protein which in turn are relevant to lipid/protein interactions in the real membrane. A similar study on the trigonal Ompf porin from E.Coli is underway (T. Schirmer, Basel, E.Pebay-Peyroula, S. Penel and P. Timmins, ILL) to complement the study on the tetragonal form recently pulished [3]. The distribution of detergent around a trimer of the OmpF porin is shown in figure 3 page 159.

A number of novel detergents of potential use in membrane protein crystallisation have been studied (J. Hovers, Konstanz, P. Timmins, ILL) and attempts are being made to correlate micelle size and shape with the efficacity of these detergents. In another set of experiments novel non-ionic detergents which form vesicles and are of potential use as drug delivery systems have been studied (D. Barlow, Kings College, London). Detailed information on molecular conformation is being obtained by specific deuteration of the detergent heads and acyl chains.

Bacteriorhodopsin

Neutron diffraction studies of purple membranes from Halobacterium halobium mutants have been extended to functional mutants. We recall that the membrane contains one protein, bacteriorhodopsin, BR, which functions as a light driven proton pump. The membrane studied in a collaboration between the IBS (M. Weik and J. Zaccai) and MPI Biochemie, Martinsried, (H. Patzelt and D. Oesterhelt) contained BR mutated in an amino acid of the proton pathway. This mutant shows a significantly reduced pumping rate. The neutron amplitude difference density map with the wild type membranes has significant peaks in the lipid areas, strongly suggesting modifications in the mutant lipid composition. This totally unexpected observation has stimulated a new interest in the functional role of the membrane lipids.

Location of cholesterol sulfate in phospholipid membranes

Cholesterol and cholesterol sulfate, CS, are steroids present in natural membranes, such as those found in skin lipids and in the head of spermatozoa. The presence of the sulfate moiety seems to greatly affect the steroid properties. In particular, CS has been shown to induce a greater hydration of the lipid interface in dimyristoylphosphatidylcholine (DMPC) membranes as well as less ordering of the lipid chains. One possible explanation is that there is a difference in the vertical location of the two steroids in the membrane. In order to prove or disprove this explanation neutron lamellar diffraction experiments were carried out on D16 (C.Faure and E.J.Dufourc, CNRS and E.Bellet-Amalric, ILL).

Orientated model membranes were made of DMPC mixed with either protonated or deuterated, d^5-(2,2,4,6,6), CS (30%). Up to ten orders of diffraction with a mosaic spread of $<1^{\circ}$ were observed. The scattering amplitudes were combined with phases, determined by repeating the experiments in different H_2O/D_2O concentrations, allowing the detailed scattering density across the DMPC membrane to be imaged. Data treatment is still in progress but initial comparisons with similar work carried out on the location of cholesterol in DMPC [4] indicates that the two steroids are both well embedded in the membrane.

Conformational changes and spatial arrangements of the Escherichia coli chaperones GroEL and GroES

Molecular chaperones are proteins which can be found in all three kingdoms of organisms, eucaryots, eubacteriae and archebacteriae. They bind unfolded, e.g. heat-denatured, polypeptides preventing aggregation, and then mediate their folding or refolding in an ATP dependent (energy-consuming) process. The chaperone system consists of the main protein GroEL (relative molecular mass M_r = 798kDa) and of the helper protein GroES (M_r = 70kDa). GroEL and GroES form a complex that interacts with the denatured substrate protein.

SANS experiments were carried out on D11 (R.May, ILL) and at the HMI on the E.coli chaperone system Hsp60 in complex with citrate synthase mutant as a substrate model protein (collaboration with R. Stegmann and H. Heumann, MPI für Biochemie, Martinsried, R. Plückhun, ETH Zürich and A. Wiedenmann, HMI). The scattering of isolated GroEL can be interpreted as originating from two stacked heptameric rings. When citrate synthase is bound in the absence of MgATP, GroEL seems to dissociate into two rings with one substrate molecule bound. In the presence of MgATP, GroEL apparently remains a 14-mer upon binding substrate protein.

Another series of experiments was conducted to investigate structural changes of GroES upon binding to GroEL. For this purpose a complex of deuterated GroES and natural (protonated) GroEL was formed. The scattering curves of the isotope-chimerical complex were measured at different levels of D_2O in the solvent ("contrast variation"). Comparing the scattering curve of isolated GroEL with that calculated for GroEL-bound GroES for a H_2O/D_2O mixture where GroEL becomes "invisible", it appears that the bound GroES has a 15% smaller radius of gyration than the isolated one.

Protein-nucleic acid interactions: elongation factors

In bacteria, elongation factor EFTu carries aminoacyl-tRNA to the ribosome during the translational process. EFTu is a G protein associated with one molecule of GDP in its inactive state, a state in which it does not bind aminoacyl-tRNA. The protein is activated by GTP-GDP exchange facilitated by an intermediate association with another elongation factor named EFTs. In its GTP bound form, EFTu.GTP binds aminoacyl-tRNA. Recently, crystallographic studies have provided high resolution information on the structures of EFTu.GDP [5], EFTu.GTP [6, 7] and the EFTu.GTP.aminoacyl-tRNA complex from thermophilic bacteria [8] and the EFTu.EFTs complex from E.coli [9]. Very interesting complex structures and conformational changes have come to light. Because of the power of SANS for the study of protein-nucleic acid interactions, this has stimulated a number of ILL proposals to examine the solution properties of the complexes as a function of solvent composition and make the link between the very different crystal conditions and conditions in which the biochemical reactions have been characterised. Scientists from laboratories in Sweden, Denmark, Russia, France and EMBL are involved in these studies that have started in 1995 and are continuing into 1996.

Dynamics in short peptides

Hydrogen bonding is the key feature in the Biological information transfer mechanisms. In studies of the dynamics of chains of hydrogen-bonded peptide groups anomalies have been observed; the vibrations of the -NH...OC- atoms are anharmonic and show unexpected splittings. These anomalies have been assigned to a number of origins including conformational substates of the amide proton, dynamic proton transfer along the hydrogen bond, and localised modes resulting from coupling between different oscillators. However, hydrogen-bonding patterns in linear peptides and amino acids have not yet been studied systematically. Studies have therefore been initiated to investigate the temperature dependence of the vibrational density of modes and the quasi-elastic broadening in simple amino acids and short polypeptides (M. Barthes, Montpellier, J. Eckert, Los Alamos and V. Helenius, Jyvaskyla, Finland).

In initial experiments the vibrational density of states of a small (O.2g) sample of Tryp-$(Ala)_{15}$ polypeptide has been studied at 4K on IN1 with a Be filter, and compared to the data collected with crystalline alanine and two deuterated derivatives of alanine, in order to assign the main features. The spectrum of the peptide is shown in Fig.4, together with the spectrum of alanine-D4 (or H_3N-C_2D_4-COO).

The spectrum of the peptide consists of wide bands, indicating for each oscillator a large frequency distribution, due to the low rate of crystallinity. The main features in the peptide spectrum are assigned to modes of the methyl group, (the methyl torsion is observed around 33 meV), while in alanine-D4, the NH3 torsion is the most intense peak at about 65meV. The hydrogen bond deformations, which are around 16meV for alanine, are not observed in the peptide spectrum. They should be shifted to lower energy as a result of the soft peptide structure.

Normal modes analyses of the alanine crystals are now underway, to compare neutron scattering data to the results of computer simulations, in order to make progress in the understanding of the peptide dynamics.

Neutron fibre diffraction studies

Over the years neutron diffraction has been used to study a number of Biological polymers which do not form single crystals but can be prepared as fibres. One of the most

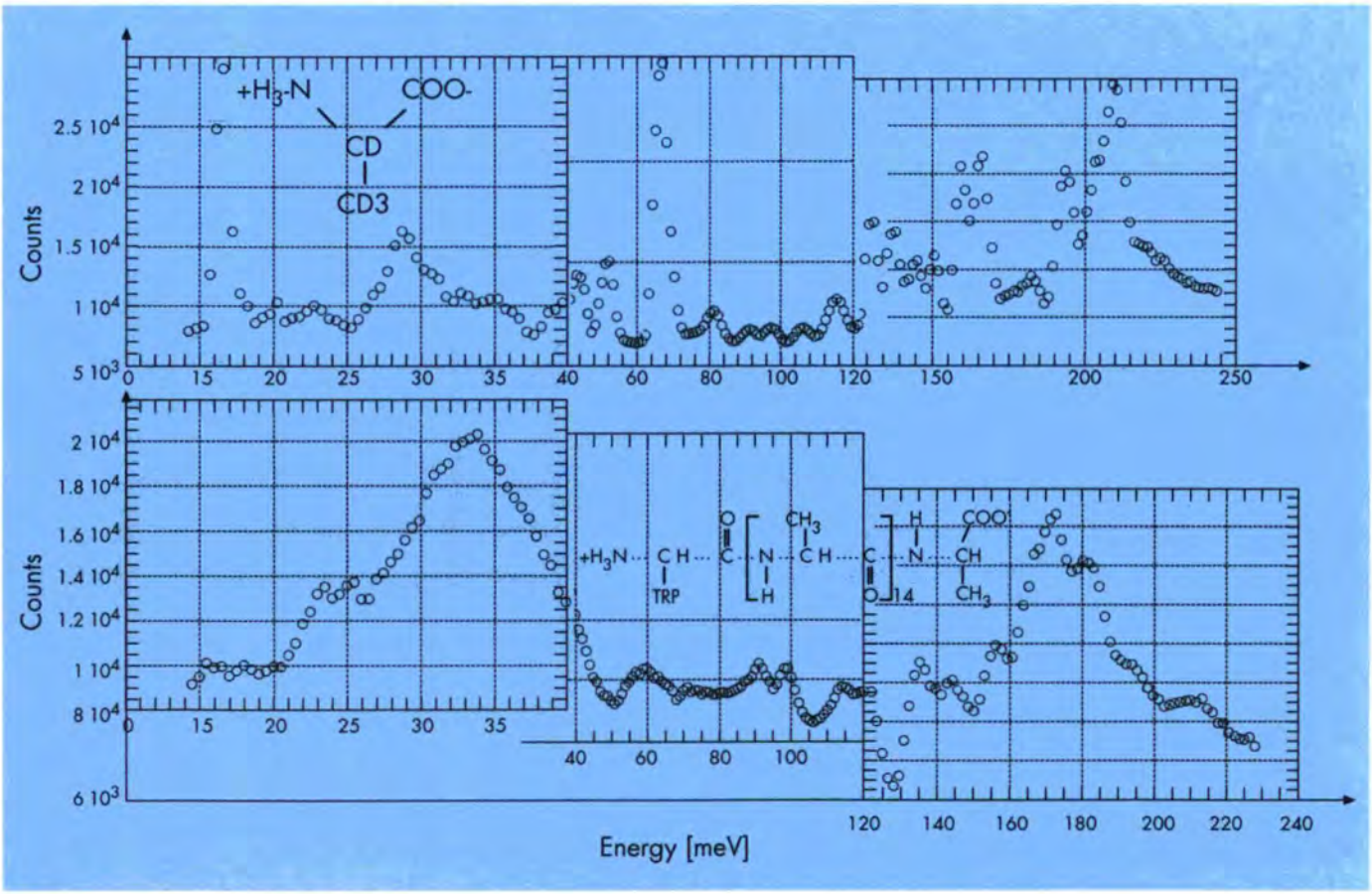

Fig. 4: The spectra, collected on IN1 with a Be filter, from alanine-D4 (top) and Tryp-(Ala)15 polypeptide (bottom).

significant recent advances in this field has been the development of techniques commonly used in studies of single crystals now applied to high resolution fibre diffraction studies (W. Fuller, V.T. Forsyth and A. Mahendrasingam, Keele and P. Langan and S.A. Mason, ILL). This followed the availability of large PSD's on high flux instruments, which allowed the efficient coverage of large continuous volumes of reciprocal space simultaneously. One such instrument is D19. Although D19 is often used as a single crystal diffractometer, since the reactor restart more of the beam-time has been taken up by fibres. Developments on D19 which have accompanied this trend are reported under the Diffraction group. Some of the fibre diffraction experiments are described below.

The highly successful investigation being carried out by Keele (W. Fuller, V.T. Forsyth and A. Mahendrasingam) into the hydration of DNA has continued. DNA is a double helical polymer which has been shown by x-ray fibre diffraction to assume a number of distinct conformations depending on hydration, ionic environment and base pair sequence. These studies have provided detailed molecular models for the A, B and C forms of naturally occuring DNA as well as the D and S forms of synthetic polynucleotides. The possibility that these conformations have different functional roles makes the relationship between DNA conformation and ordered water and ions of particular biological importance. The arrangement of water around the A and D forms of DNA was investigated using neutron diffraction techniques on D19 before the long shutdown [11-12] and featured in the 1989 annual report (W. Fuller, V.T. Forsyth and A. Mahendrasingam, Keele and P. Langan and S.A. Mason, ILL). During the shutdown these studies were extended to investigate the hydration of the B and perdeuterated A forms of DNA on SXD at ISIS (W. Fuller, V.T. Forsyth and A. Mahendrasingam, Keele, C. Wilson, ISIS and P. Langan and S.A. Mason, ILL) [13]. This year studies have restarted on D19 with data being collected from the perdeuterated A and B forms (W. Fuller, V.T. Forsyth, A. Mahendrasingam and M. Whalley, Keele and P. Langan and S.A. Mason, ILL).

In these studies of DNA hydration the ability to replace H_2O by D_2O is used in order to exploit the difference in scattering length between H and D. In addition to the isotopic substitution of water there exists the possibility of isotopically substituting H covalently bound to DNA, except for H bound to nitrogen which are not exchanged when water is substituted. In a collaborative project between ILL (P. Langan) and EMBL (R. Leberman) the triphosphate components from which polynucleotides are synthesised are now being produced in their deuterated form. This makes possible the synthesis of polynucleotides with short repeating sequences of deuterated and protonated nucleotides. In this way selected components of the system can be highlighted in a manner which is not possible with x-rays. Another application of this exciting development will be in neutron diffraction studies of DNA triplexes and DNA-protein complexes in which specific strands are highlighted.

Hyaluronic acid is a Biological polymer found in the intercellular matrix of mammalian connective tissue and the capsules of some bacteria. X-ray fibre diffraction studies have shown that this linear polysaccharide is a double helix which, like DNA, can assume a number of conformations and packing arrangements depending on hydration, ionic environment and temperature. Data were collected from samples corresponding to the polysaccharide being surrounded by H_2O and then D_2O so that Fourier difference techniques could be used to image the localised water (A. Deriu, F. Cavatorta, D. Di Cola, M. Oscar, Parma, A. Rupprecht, Stockholm and P. Langan, ILL). The long term aim of this project is to collect H_2O/D_2O data sets at a number of different humidities so that the role of water in facilitating the observed conformational transitions can be determined.

Natural cellulose, cellulose I, is used in the textile industry, usually after undergoing some form of treatment with NaOH. This mercerisation process involves a structural conversion to cellulose II with associated improvements in strength, appearance and reception to dye. In this study high angle data were collected from a sample prepared using NaOH and then from a sample prepared using NaOD (A. Mahendrasingam, A. Jaber, Keele and P. Langan, ILL). The difference in scattering length between H and D is being exploited in Fourier difference analysis to determine the positions of hydrogen atoms which are substituted on the cellulose during mercerisation. This experiment was also used to test a new fibre precession data collection geometry (P. Langan, ILL).

Laue and quasi-Laue diffraction

The development of quasi-Laue techniques continues to promise considerable expansion of neutron crystallography studies of biomolecules and make possible new types of study relating structure to function. A description of tests carried out with the large cylinder image plate detector (constructed at the EMBL) at the end of cold neutron guide H142 appears under "Small Projects in DS" (Lehmann, ILL and Wilkinson, EMBL). The first Laue diagram, recorded from triclinic lysozyme, is shown in Fig. 5 page 159. Quasi-Laue data have now been collected from a number of biomolecules, inlcuding triclinic lysozyme (collaboration with P. Oleinek, Müchen), Concanavalin-A (collaboration with G. Habash and J. Helliwell, Manchester), tetragonal lysozyme

(collaboration with N. Niimura, JAERI) and cobolamin, a derivative of vitamin B12 (collaboration with C. Kratky and G. Jogl, Graz and P. Langan, ILL). Further tests are planned for 1996.

Secretary: Paul Langan

References

[1] Vuillard, L. et al., Analytical Biochemistry, (1995), 230, 290-294.

[2] Goldberg, M. et al., Folding and Design, (1996), 1, 21-27.

[3] Pebay-Peyroula, E., Garavito, R.M., Rosenbusch, J.P., Zulauf, M. and Timmins, P., (1995), Structure 3, 1051-1059.

[4] Léonard, A., Thése, (1993), Université de Bordeaux I, France.

[5] Kjeldgaard, M. and Nyborg, J., (1992), J.Mol.Biol. 223, 721-742.

[6] Kjeldgaard, M., Nissen, P., Thirup, S. and Nyborg, J., (1993), Structure 1, 35-50.

[7] Berchtold, H., Reshetnikova, L., Reiser, C.O.A., Schirmer, N.K., Sprinzl, M. and Hilgenfeld, R., (1993), Nature 365, 126-132.

[8] Nissen, P., Kjeldgaard, M., Thirup, S., Polekhina, G., Reshetnikova, L., Clark, B.F.C. and Nyborg, J., (1995), Science 270, 1464-1472.

[9] Kawashima, T., Berthet-Colominas, C., Wulff, M., Cusack, S. and Leberman, R., (1996), Nature, in press.

[10] Fuller, W., Forsyth, V.T., Mahendrasingam, A., Pigram, W.J., Greenall, R.J., Langan, P., Bellamy, K. Al-Hayalee, Y. and Mason, S.A., (1989), Physica B 156-157, 468.

[11] Forsyth, V.T., Mahendrasingam, A., Pigram, W.J., Greenall, R.J., Bellamy, K., Fuller, W. and Mason, S.A., (1989), Int. J. Biol. Macr. 11, 236.

[12] Langan, P., Forsyth, V.T., Mahendrasingam, A., Pigram, W.J., Mason, S.A. and Fuller, W., (1992), J.Biomol. Str. Dyn., 10, 489.

[13] Langan, P., Forsyth, V.T., Mahendrasingam, Giesen, U., Dauvergne, M-Th., Mason, S.A., Wilson, C.C. and Fuller, W., (1995), Physica B, 213-214.

Structure and Dynamics of Soft-Condensed Matter

Members of the College at ILL

B. Alefeld
E. Amalric-Bellet
R. Cubitt
S. Egelhaaf
B. Farago
B. Frick
M.A. Gonzalez
C. Hayes
A. Kollmar (KFA Jülich)
C. Lartigue
H. Lauter
P. Lindner
P. Timmins

External Members

M. Alba (CENG)
R. Borsali (UJF)
E. Geissler (UJF)
A. Guillermo (UJF)
A. M. Hecht (UJF)
J.F. Legrand (ESRF)
D. Quenard (CSTB)
C. Riekel (ESRF)
F. Rieutord (CENG)
M. Rinaudo (UJF)
C. Rochas (UJF)
P. Terech (CENG)
G. Vignaud (ESRF)

Introduction

The year 1995 was a very busy year for all college members, mainly because all had to restart their instruments. After the long shutdown period the users come back and this stimulates the scientific live at ILL. Certainly the service to the users and restarting instruments did occupy the major part of time for most college members, sometimes leaving nearly no time to do own research work. We all hope this will change next year, in spite of the reduction of staff.

We are all aware that the race for scientific results on the instruments has started and we have seen last year globally good new proposals in the two subcommittee sessions. Detailed data evaluation and interpretation of course cause some delay and continuation experiments are often necessary. Thus many scientific projects are still going on and only preliminary answers to the tackled questions can be given. In the following we present some selected projects.

Influence of architecture on the aggregation of hetero-arm star polymers in a selective solvent

The aggregation star polymers in solution was studied on D11 by M. Prager, A. Ramzi, D. Schneiders, M. Monkenbusch, D. Richter and B. Farago. PE-PEP diblock polymers dissolved in the selective solvent decane form lamellar sheets with a crystalline PE-core and a swollen PEP-corona. This rather complex shape was identified using small angle neutron scattering (SANS) in combination with the contrast variation technique (H-D exchange) [1]. In extending this work the question is asked how a more complex architecture of the polymer, $(PE)_n(PEP)_m$ with pairs (n,m) = (2,2), (2,1) and (1,2) and varying molecular weight, influences the aggregation behavior.

The SANS diffractograms show that the micellar shape is almost independent of concentration c in the low c regime. Further, at room temperature almost all polymers are contained in the micelles which dissolve around T = 60° C. Based on these observations 2 % solutions of the materials were studied in detail at room temperature. For all samples the PE was partially deuterated and had a constant molecular weight (M_w) of 7000 while that of the protonated PEP varied from 5000 to 15000. Fig. 1 presents the results for five different contrasts and the sample with M_w of PEP of 8000. The spectra look similar to those of diblocks. Thus in analogy to the diblock copolymers the heteroarm star system was modeled by a polymer brush. With a flat dense crystalline PE core of thickness d and a soft corona of PEP hairs sticking out on both sides of the core. Rectangular density profiles were assumed for both, the core and the corona. Their surfaces were smoothed by a convolution with a Gaussian. In the final analysis partial structure factors of the pure core and the pure corona were derived from the original data and the two constituents fitted individually. In core-contrast (Fig. 1 ◊) the intensity decreases at large Q only, in brush contrast (Fig. 1 *) at low Q. Thus like in the diblocks, the PE-layer is remarquably thinner than the brush. The extension L of the PEP hairs into the solvent increases with the molecular weight of the PEP arms from ~ 150 Å at M_w = 5000 to ~ 400 Å at M_w = 15000 while the thickness d ~ 40 Å of the core is almost constant. The analysis of the spectra at very low Q shows that the sheets are large laterally

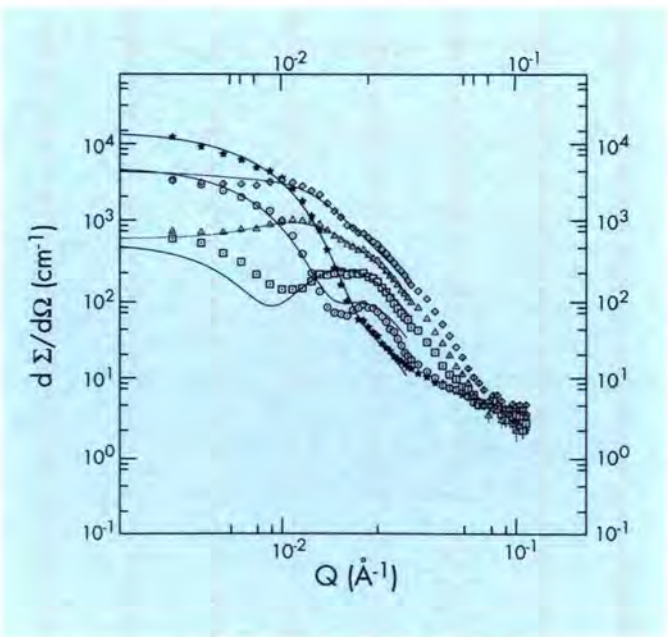

Fig. 1: SANS data of a 2 % solution of $(PE)_2(PEP)_2$ 7K/8K in decane for various degrees of deuteration of the solvent (= 1.0, O = 0.75, ❑ = 0.50, Δ = 0.25, ◇ = 0.025).*

and they form a finite stack of a few (~ 5) layers. From the lattice parameter of crystalline PE and the core thickness the grafting density of PEP hairs emerging from the surface can be derived for the PEP molecular weights used. In the confined environment the PEP brush is significantly stretched.

In the most simple approach, when considering just a single micelle, one can try to explain the geometrical parameters on the basis of the balance of entropic and enthalpic terms: the cristallisation energy of the core is strongly determined by the folding of the PE chains at the surface. Its minimisation would leed to thick sheets. Contrary, to minimise the deformation energy of the PEP hairs in the brush, a large surface of the lamella has to be offered. The compromise between these two contradictory requirements yields the geometrical parameters of the system. Such theories [1,2] predict a simultaneous change of both the core and the brush thickness, while the experiment shows that the core thickness is almost constant. A qualitative explanation of this observation may follow from the fact that PE made from PB contains about 1 sidegroup every 50 bonds. To incorporate such defects into the crystal costs energy and the system might try to locate them at the surface. In agreement with experiment this behavior would stabilise a lamella thickness defined almost purely from the PE properties. Experiments and calculations along this line are under the way.

Thixotropy of clay suspensions: investigation by small-angle neutron scattering

Clay suspensions under shear flow were investigated on D11, a collaboration between UJF, CEA-Rhône-Poulenc and ILL (A. Mangin, B. Cabane, P. Lindner). An area which is attracting much attention in the rheology of colloidal suspensions is the relation between the behaviour of these materials at macroscopic scale and their structure at mesoscopic scale. Materials of this type have many interesting properties, and particular research is being carried out into their thixotropic behaviour. Thixotropy may be defined as follows: at rest, the material has a high consistency. When it is shaken, its consistency decreases and its structure is modified until it reaches another state of organization. When the material is no longer shaken, it gradually returns to the consistency and structure it had at rest. Thixotropy is a reversible process.

Clay suspensions represent a major field of investigation, in terms of both fundamental research and industrial applications. They are considered as model materials for studying thixotropic behaviour. The materials selected for such studies were a synthetic clay of the hectorite type (Laponite), consisting of disk-shaped particles of nanometric size, and a natural clay of fibrous texture with micron-sized particles (Sepiolite).

Small-angle neutron scattering is an excellent technique for examining particle interactions and organisation in a suspension of this kind when it is subject to shear-type flow. The sample is placed in a small gap between two coaxial cylinders (i.e. a Couette cell), one of which rotates with respect to the other and thus produces a constant shear rate in the suspension. Otherwise, rheometric measurements by F. Pignon, A. Mangin and J.M. Piau allowed to correlate the structural changes with the variation of the shear stress over time.

Results with suspensions at rest

With the aqueous suspension of Laponite, there is a marked deviation from the Q^{-2} type relation for scattering intensity at the largest wave vectors (Fig. 2). This demonstrates an increase in particle interactions that is due to short-range ordering [3]. This behaviour ends at the smallest wave vectors in a Q^{-3} dependence, which can be explored by light scattering measurements. This new Q-dependence appears to be due to the formation of tactoids in the suspensions, i.e. small groups of two to four particles separated by a few layers of water.

Results with sheared suspensions

The scattering diagram for a sheared suspension of Laponite remains isotropic, but a disturbance of the short-range order was detected. The straight section between the Q^{-2} and Q^{-3} type behaviours becomes steeper.

The scattering diagram for a suspension of Sepiolite, which was initially isotropic at rest, becomes strongly anisotropic under shear (Fig. 3). The particles are clearly oriented in the direction of flow.

These studies are being carried out under the contract for the "Behavior of thixotropic materials" programme involving the DIMAT and various industries. They are to be

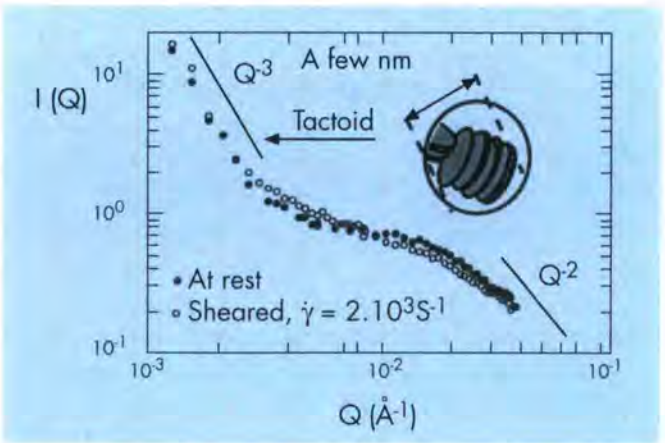

Fig. 2: Scattering intensity vs. wave vector for a suspension of Laponite at rest or sheared. Volume fraction = 1.6 %, [NaCl] = 10^{-3} mol.l^{-1}

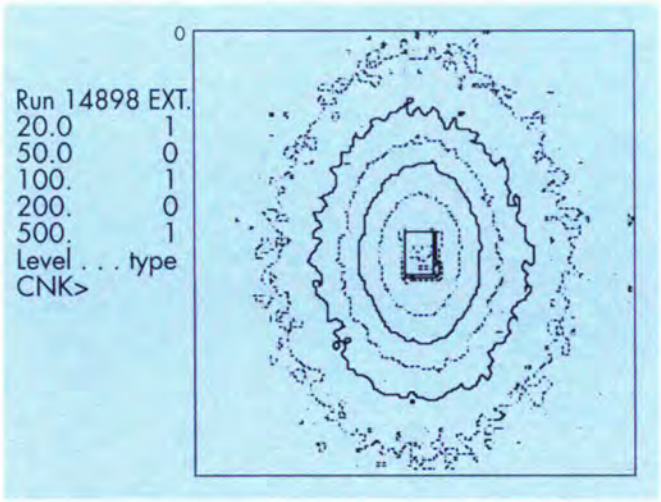

Fig. 3: Contour plot of scattering intensity for a sheared suspension of Sepiolite. Volume fraction = 2 %, shear rate = 10^3 s^{-1}

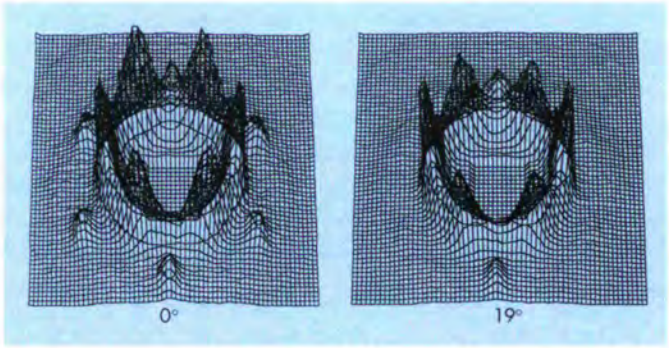

Fig. 4: Hexagonal SANS scattering pattern for a latex suspension ordered under shear a) at normal incidence, b) after rotation of the sample by 19.47° about the vertical axis.

pursued next year by systematically exploring the effect of physical and chemical parameters and shear on thixotropy and on the associated structural state.

Charge stabilized colloidal suspensions under shear

Concentrated dispersions can develop hexagonal scattering patterns under shear, which persist as the shear is turned off. Recently deviations from the hexagonal scattering pattern were observed [4] after the sample was rotated with respect to the neutron beam, indicating more complex structures than hexagonal layers. A first experiment was carried out on latex suspensions on D11 (H. Versmold, C. Dux from RWTH Aachen, V. Reus, P. Lindner from ILL) to investigate the intensity distribution along the Bragg rods in reciprocal space. Deviations from ordered hexagonal layers should show up in an intensity redistribution along the rods. From such an investigation information concerning close packing of the layers and the stacking order can be expected. Fig. 4 shows the first results of this study. The scattering pattern for the shear ordered dispersion with hexagonal symmetry and its change to a lower symmetry, when the sample is rotated by 19° about the vertical axis is shown. Preliminary results of the investigation of several inclination angles indicate a random stacking of the hexagonal layers and that the layers are not closed packed [5].

Strain amplification in model-filled rubbers by SANS

Fillers have a reinforcing effect on the medium in which they are embedded and it is a challenge to predict the effect of fillers on the viscoelastic behaviour of rubbers. Whereas phenomenological approaches have been presented, direct experiments testing the microscopic strain as a function of the volume fraction of fillers are still lacking. SANS at D11 was employed (St. Westermann, M. Kreitschmann, W. Pyckhout-Hintzen, E. Straube, D. Richter (KFA Jülich) and B. Farago (ILL)) to improve our understanding for the major mechanisms by which rubber-reinforcement is believed to take place.

A filled rubber can be defined as a two-phase system of rigid particles, surrounded by an elastomeric network matrix. The effect of the dispersed filler phase on the viscoelastic behaviour is described by an empirical reinforcement or strain amplification factor $f = (1 + 2.5\,\phi + 5.0\,\phi^2)$ causing $\lambda_{mic} = (\lambda - 1) * f + 1$. In these equations ϕ is the volume fraction of filler, the linear term arises from the Einstein equation and the empirical quadratic term takes interactions into account. λ is the macroscopic, λ_{mic} the microscopic extension ratio. Empirical reinforcement factors were until now determined from the relative viscosity changes between a filled and unfilled matrix. A simple semi-microscopic model for evaluating the micorscopic strain with rigid, undeformable particles of concentration ϕ would yield:

$$\lambda_{mic} = \frac{\lambda - \sqrt[3]{\phi}}{1 - \sqrt[3]{\phi}}$$

Block-copolymers, in the strong segregation limit, may be considered as model systems for filled rubbers. Typical conditions can be achieved by a careful synthesis, like: particle sizes due to microphase separation around 100-200 Å, chains that are chemically bound to the surface of the filler particle and bound or occluded rubbers may be produced and fixed upon crosslinking.

The investigated block-copolymer of polyisoprene-polystyrene-polyisoprene (PI-PS-PI), where PS served as filler with a volume fraction ϕ (PS) = 0.17 was designed to phase-match the superstructure of the filler by appropiately mixing H- and D-isoprene monomers during anionic

polymerisation. Further composition-matching with a homopolymer mixture permitted to study the conformation of bulk chains under strain for different invisible filler concentrations. The structure of the triblock-co-polymer was characterised by synchroton radiation and neutron scattering (Fig. 5) and corresponded to spherical PS-domains of about 140 Å in diameter with sharp boundaries ($\chi N \approx 80$; χ being the Flory-Huggins parameter and N the polymerization index).

Three different filled blends with identical chemical crosslinking densities (ϕ (PS) = 0, 0.09, 0.15) were measured at different elongations. The non-ideally matched intensity of the triblock-co-polymer was then subtracted after an affine transformation of the peak position. The scattering patterns for the matrix chains were fitted with a tube model, considering a non-affine and deformation-dependent tube diameter (Fig. 6a). The results allowed a comparison of the microscopic strains λ^{β}, relative to the measured macroscopic strain at different filler contents. The fit parameter β is ideally 1 for long, moderately crosslinked chains with vanishing free dangling chain ends. With increasing filler concentration an increase of the tube diameter is observed from 43 Å at ϕ (PS) = 0 to 52 Å at ϕ (PS) = 0.15. This can be explained by a stretching and disentangling of chains near the PS-surface. Furthermore β increases from 0.42 to 0.83 with increasing filler concentration, which reflects the increase of the effective microscopic strain. In Fig. 6b the experimental overstrain $f^{*exp} = \lambda^{\Delta\beta}$ is plotted as a function of ϕ_{PS} for $\lambda = 1.7$ in comparison to the theoretical predictions mentioned above.

In contrast to the semi-microscopic model, which clearly overestimates the effect of the filler, the empirical approach describes the experimentally observed overstrain quite well. The study shows how a comparison of SANS and mechanical moduli may help to provide a better microscopic understanding of widely used filled rubber materials.

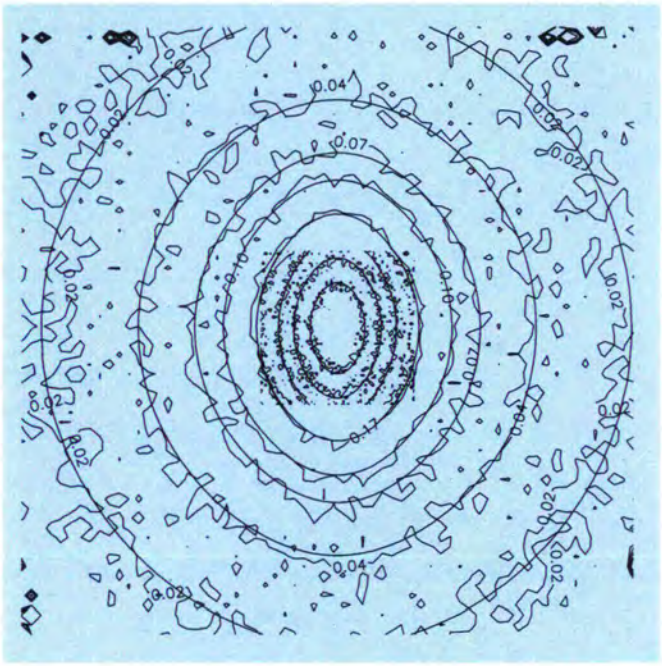

Fig. 6a: Iso-contour intensities for the sample filled with $\phi_{PS} = 0.15$ at a macroscopic strain of $\lambda = 1.70 \pm 0.05$. A higher anisotropy with respect to the unfilled samle is found for the network containing the triblock-co-polymer, i.e. filler particles. The strain is applied in the horizontal direction.

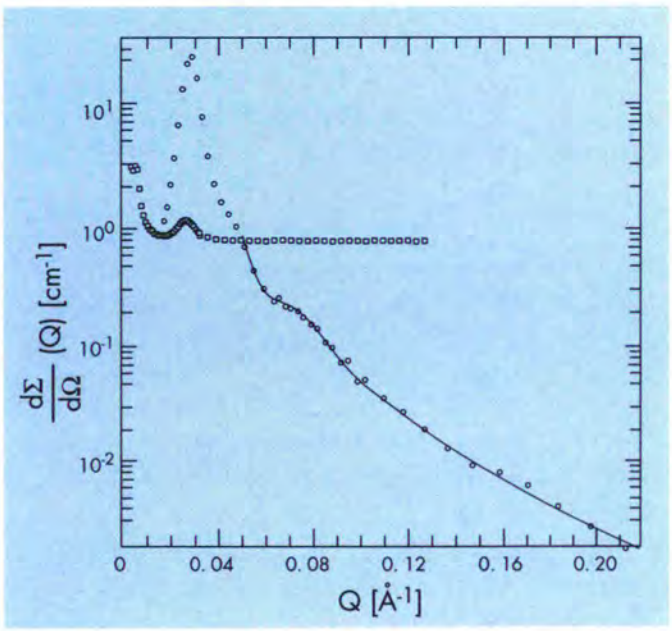

Fig. 5: Filler morphology by Synchroton radiation (circles) and SANS (squares), showing the contrast-matching.

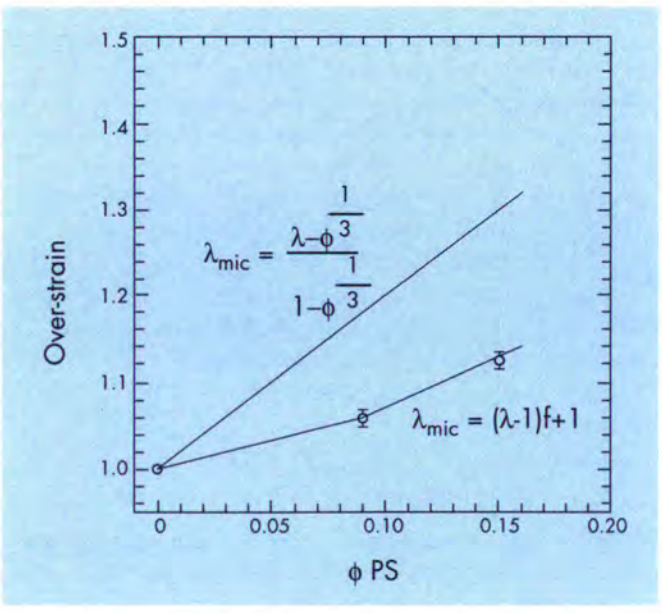

Fig. 6b: Comparison of the experimentally derived over-strain to the theoretical predictions mentioned in the text.

The effect of solvent quality on the local unfolding of swollen polymer networks

The small angle neutron scattering spectra of polymer gels differ from those of liquid polymer solutions in that they display extra intensity at the lower wave vector end of the spectrum. In the liquid, the polymer concentration becomes smooth for wave vectors $Q < 1/\xi$, where ξ is the thermodynamic correlation length. Gels, however, have random elastic strains that extend over long distances, with a characteristic length Ξ: the resulting static variations in concentration generate the extra scattering at lower Q.

The spectra of isotropically swollen gels are usually separable into a dynamic and a static part [6,7] of the form

$$I(Q) = \frac{A}{\left(1 + Q^2\xi^2\right)} + \frac{B}{\left(1 + Q^2\Xi^2\right)^2} \quad (1)$$

For a gel at a fixed degree of swelling, the correlation length ξ with a good solvent is shorter than with a theta solvent, where the polymer chains obey Gaussian statistics. The amplitude of the static concentration fluctuations depends on the relative strength of the elastic perturbation and the restoring osmotic pressure in the gel. This ratio depends on the degree of swelling. In fully swollen gels, where these pressures are equal, the static scattering is most intense.

The present experiment was intended to detect the effect of solvent quality on the shape of the scattering function (E. Geissler, A.M. Hecht and C. Rochas). Two types of networks were used, poly(dimethyl siloxane) and poly(vinyl acetate). These were swollen, respectively, in octane and toluene, and in acetone, toluene and isopropyl alcohol. The order of these solvents is in decreasing quality, acetone being an excellent solvent for PVAc and isopropyl alcohol being a theta solvent at 52° C.

For both gels contrast variation measurements were made to check the chemical homogeneity of the sample, thereby ensuring that the cross-links do not contribute to the signal at low Q. Several samples were investigated at different degrees of swelling, both under isotropic and anisotropic swelling. For the isotropic gels, the correlation length Ξ of the second term is practically independent of swelling in a given solvent, but ξ decreases roughly as c^{-1}, c being the polymer concentration. Now the mean square end-to-end distance of a network chain, R_t^2 is expected theoretically to vary as R_x^3/ξ, where R_x is the mean distance between cross-links (i.e. $R_x^3 \propto c^{-1}$). The present experimental results suggest that Ξ can be identified with R_t. This result, which needs to be confirmed, is interesting, since the end-to-end distance R_t is not an easily accessible quantity experimentally.

On stretching a swollen gel uniaxially, a figure-of-eight ("butterfly") isointensity pattern is generally observed [8,9]. This happens if the static fluctuations are sufficiently decoupled from the liquid-like fluctuations: the static scattering then belongs to an invariant, i.e. its second moment is independent of angle. If the characteristic length scale Ξ of the elastic perturbation becomes anisotropic under stretching, then the condition of invariance ensures a figure-of-eight isointensity pattern [10].

In the present experiment, it was found, for a given degree of swelling and at fixed overall strain, that the scattering pattern was solvent dependent (Fig. 7a): the standard butterfly pattern appeared only with toluene (Fig. 7b). This surprising result shows that the strain configuration is a result of local chain unfolding and is hence sensitive to the solvent.

Decomposition of the anisotropic spectra using the same function (1) yields good fits for PVAc/toluene (Fig. 8), which allow the microscopic Poisson ratio to be determined.

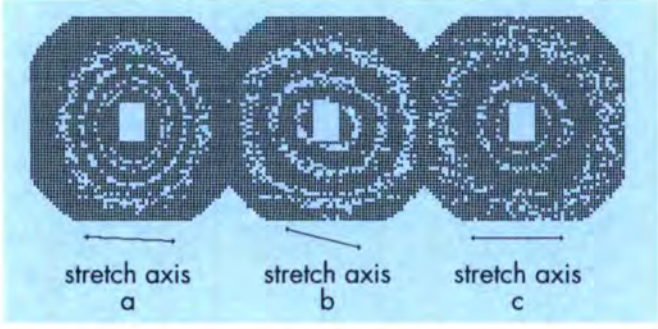

Fig. 7: Isointensity plots at the 20 m detector position on D11 (6 Å incident neutrons) for the same PVAc gel swollen anisotropically (axial ratio 0.73) to the same degree in three different solvents: a) acetone (excellent), b) toluene (good), and c) isopropyl alcohol (theta). The standard "butterfly" response is visible only in the second case.

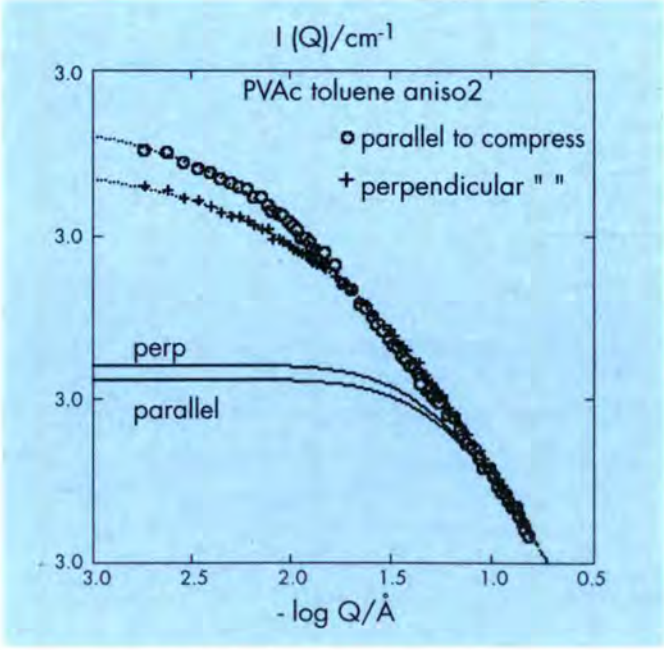

Fig. 8: Fits of Eq. 1 to the data along the parallel and perpendicular axes for a PVAc gel swollen in toluene with an axial ratio of 0.55. Continuous lines are the dynamic components of the spectra in each direction.

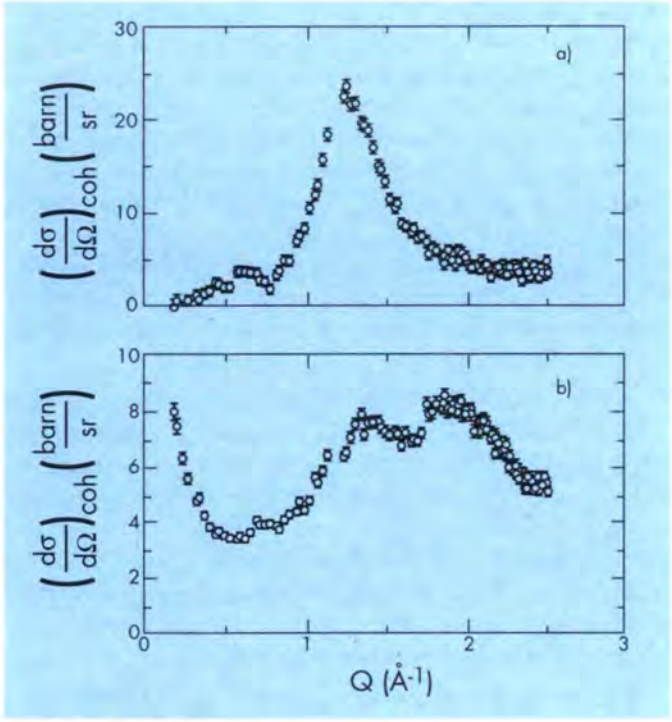

Fig. 9: Coherent scattering cros-sections of (a) H-BPA-PC and (b) perdeuterated BPA-PC-(d_{14}).

The quality of the fits of Eq. 1 is poorer for the anisotropic PDMS samples, stronger scattering being observed in the parallel direction. The discrepancy probably comes from a different local structure introduced by the cross-linking mechanism. To allow a model-independent analysis and extract the effective Poisson ratios, these scattering spectra must be analysed in terms of their anisotropic density correlation functions.

Determination of the static structure factor of amorphous polymers by polarisation analysis

There is considerable interest in the investigation of polymer structures at a local scale, corresponding to higher Q values. The main difficulty is the separation of intra- and intermolecular contributions which play a role near the first structure factor peak (below about 3 = Å^{-1}).

Spin polarisation analysis on D7 was used to determine the static structure factors of differently deuterated polycarbonate samples (J. Eilhard, J. Zirkel, D. Richter and O. Schärpf). Only polarisation analysis enables the separation of coherent and incoherent scattering contributions [11]. In combination with the deuteration of specific monomeric parts correlations of inter- as well as intramolecular origin were detected. Fig. 9 shows the coherent structure factor measured on fully protonated and fully deuterated bisphenol-A-polycarbonate (BPA-PC). In Fig. 9a the "amorphous halo" at Q = 1.3 = Å^{-1} can be seen, which is the result of correlations between neighbouring chains. Fig. 9b shows a second peak at 1.9 = Å^{-1}, corresponding to intramolecular correlations, whereas the intensity of the halo is strongly reduced.

Improved computer simulations on polycarbonates are in progress and should reveal the details of the partial structure factors.

Secretary: Bernhard Frick

References

[1] L. Leibler, H. Orland and J.C. Wheeler, J. Chem. Phys. **79**, 3550 (1983).

[2] T. Vilgis and A. Halperin, Macromolecules **24**, 2090 (1991).

[3] J.D.F. Ramsay, and P. Lindner, J. Chem. Soc. Faraday Trans. **89,** 4207 (1993).

[4] H. Laun et al., J. Rheol. **36**, 743 (1992).

[5] (see exp. report 9-10-147).

[6] E. Geissler, F. Horkay, A.-M. Hecht, C. Rochas, P. Lindner, C. Bourgaux,G. Couarraze, submitted to Polymer.

[7] F. Horkay, A.M. Hecht, S. Mallam, E. Geissler, A.R. Rennie, Macromolecules **24**, 2896 (1991).

[8] R. Oeser, in Polymer motion in dense systems, Springer Proc. in Physics **29**, 104 (1988).

[9] J. Bastide, F. Boué, M. Buzier in Molecular Basis of Polymer Networks, Springer Proc. in Physics **42**, 65 (1989).

[10] E. Geissler, F. Horkay, A.M. Hecht J. Chem. Phys. **102**, 9129 (1995).

[11] O. Schärpf, B. Gabrys, D.G. Pfeiffer, ILL-Report 90SC26T (1990).

ILL is finally building its own dedicated neutron reflectometer, in addition to the two CRG instruments EVA and ADAM. This is an ideal opportunity to report on an interesting aspect of the application of neutron reflectometry to polymers.

Neutron reflectometry at interfaces between incompatible polymers

D.W. Schubert and M. Stamm,
MPI für Polymerforschung, Mainz, Germany

Incompatible polymer blends are characterised by narrow interfaces and generally exhibit poor mechanical properties. Nevertheless they are important for many applications [1, 2] and much work has been done to optimise these polymer blends in order to design materials with properties tailored to specific use. An understanding of microstructures and polymer-polymer interactions is, however, still largely lacking. One essential parameter for obtaining good mechanical properties is good cohesion between phases; different materials must interpenetrate at the interface. This interpenetration is of the order of several nanometers and difficult to determine experimentally. For most incompatible materials, the interface is not very wide and typically in the range of 1 to 20 nm, depending on compatibility. This situation is schematically shown in Fig. 1.

If two incompatible polymers are brought into contact with one another, some interpenetration will occur when materials are heated above the glass transition. The interface width increases with time reaching an equilibrium value a_I, which according to mean field theory [3, 4], is determined by the Flory-Huggins interaction parameter χ.

$$a_I = \frac{2b}{\sqrt{6\chi}} \qquad (1)$$

where b is the characteristic segment length. The corresponding volume fraction profile is given by

$$\phi = \frac{1}{2}\left(1 + \tanh\frac{2z}{a_I}\right) \qquad (2)$$

Neutron reflectometry (NR) is, in many cases, the only technique for investigating the interfaces between immiscible polymers with the necessary accuracy. It first provides optimal resolution typically of the order of 0.2 nm for the interface width a_I in the range of a_I = 1 to 20 nm [5]. It can also be applied to virtually all polymeric systems, provided one component can be deuterated to achieve a contrast at the interface. On the other hand, it requires a dedicated sample preparation, where relatively large (typically 5 x 10 cm^2) thin films have to be deposited on top of each other. Interfacial roughness (typically 1 nm) also limits the resolution in some cases. Non-uniqueness of data analysis, which might be a problem in some complicated cases for the application of the technique, is not a problem for the analysis of a double layer system (Fig. 2) of two incompatible polymer films, since the starting situation is very well defined. Information is obtained on both interface width a_I and form of the profile $\phi(z)$. X-ray reflectometry as an alternative technique is largely

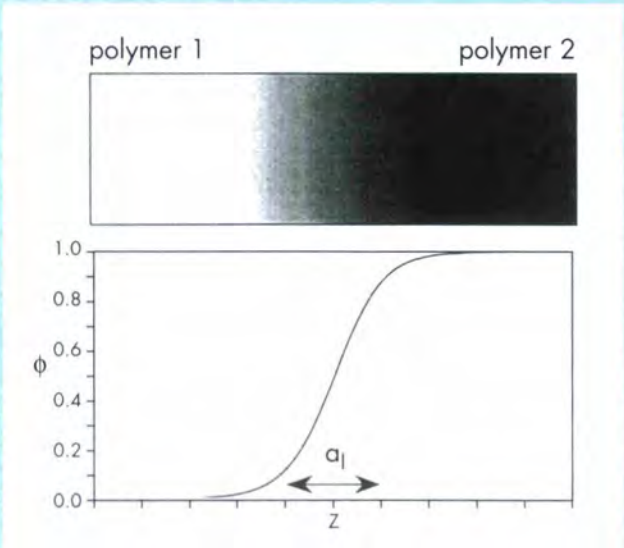

Fig. 1: During annealing an equilibrium interface is formed between two incompatible polymers and a particular profile for the volume fraction ϕ perpendicular to the interface exists.

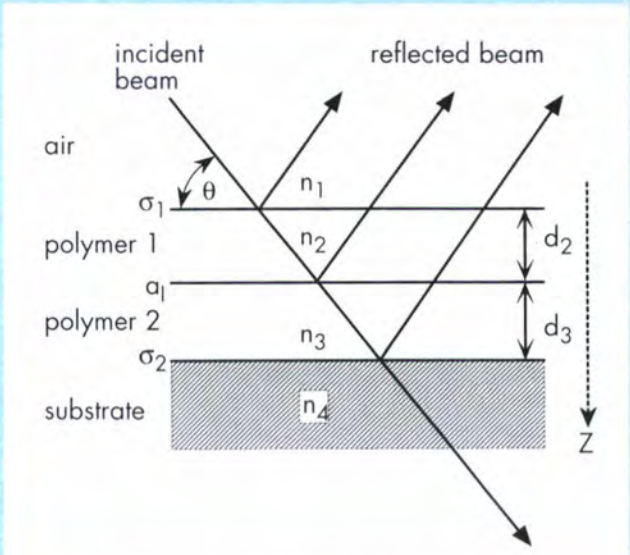

Fig. 2: Schematics of the neutron reflection experiment indicating the parameters used in the fits of experimental data as explained in the text. n_i are indices of refraction, d_i thicknesses and σ_i and a_I roughness or interfacial width parameters, respectively.

limited in its application to polymeric systems, since for most polymer pairs the contrast at the interface is not sufficiently large.

Analogous to optics, a refractive index can be specified for neutrons [5, 6]

$$n = 1 - \frac{\lambda^2}{2\pi} b\rho_n - i\frac{\lambda}{4\pi}\mu_n \qquad (3)$$

where $b\rho_n$ is the neutron scattering length density (b is the scattering length, ρ_n the particle number density), μ_n the linear absorption coefficient for neutrons, and λ the wavelength. Note that $b\rho_n$, and μ_n, are defined for a specific atomic species and that for the application to a particular material, the mean values involving the macroscopic mass density and the mass of the monomer must be calculated. Interaction between matter and neutrons is generally weak and the refractive index n is very close to 1 ($\sim 1 - 10^{-6}$). For neutrons absorption is negligible in many cases. To illustrate the contrast problem, the scattering densities for the neutrons of some materials are compiled in Table I.

It is evident from a comparison of the deuterated and protonated materials that a large contrast can be obtained for neutrons by deuteration. It should, of course, be borne in mind that deuteration also changes thermodynamics slightly, although for strongly incompatible systems this is usually negligible. Figure 2 shows a schematic diagram of an NR experiment and characteristic parameters which define the refractive index profile.

The reflectivity of a multilayer system is determined by the profile of refractive index n assumed to vary only in the direction z perpendicular to the interfaces. Error functions characterised by their variances σ_1 and σ_2, respectively, are used to describe the roughnesses of the interfaces air/polymer 1 and polymer 2/substrate. A refractive index profile according to Eq. (2) with the characteristic parameter a_I is used between polymer 1 and polymer 2. The refractive index profile n(z) can be approximated by a sequence of thin homogenous layers. The reflectivity as a function of the angle of incidence θ of such a multilayer system can be calculated [6] using a matrix formalism [7]. A fit to the experimentally observed reflectivity curve gives information about the refractive index profile. Minimising the deviation between experimental and calculated curves yields values for interfacial profiles and thicknesses of the individual layers with an accuracy of up to 0.1 nm.

Examples:

PS/Poly(n-butylmethacrylate) (PnBMA)

The temperature dependence of the interface width of PS/PnBMA has recently been investigated by NR [8]. Neutron reflection curves are shown in Fig. 3, together with best fits based on a simple two-layer model, where parameters as indicated in Fig. 2 are used.

The PS-film is deuterated to achieve good sensitivity for the interface between the two polymer films. Since the interface width can be determined with an accuracy of ±0.2 nm, the temperature dependence of a_I is resolved (Fig. 4) and can be correlated on the basis of Eq. (1) to a temperature dependent χ-parameter.

Compounds	Chemical formulas	ρ [g cm^{-3}]	$b\rho_n$(H/D) [10^{10} cm^{-2}]	μ_n(H/D) [cm^{-1}]
air/vacuum		0	0	0
PS	$(C_8H_8)_n$	1.03	1.41/6.46	3.9/0.6
PMMA	$(C_5H_8O_2)_n$	1.15	1.06/7.02	4.5/0.6
PVC	$(C_2H_3Cl)_n$	1.38	1.56/5.76	3.3/0.5
PBrS	$(C_8H_7Br)_n$	1.57	1.76/5.58	4.0/0.6
quartz	SiO_2	2.3	4.20	0.2
silicon	Si	2.33	2.15	0.1
nickel	Ni(^{58}Ni)	8.91	9.25 (12.9)	2.6
gold	Au	19.32	4.48	3.3

Table 1: Comparison of characteristic data for the reflection of neutrons at interfaces: mass density ρ, neutron scattering length densities $b\rho_n$ for protonated (H)/deuterated (D) compounds, and linear absorption coefficient for neutrons, μ_n (λ = 0.1 nm). The two values in certain columns correspond to H- and D-materials, respectively.

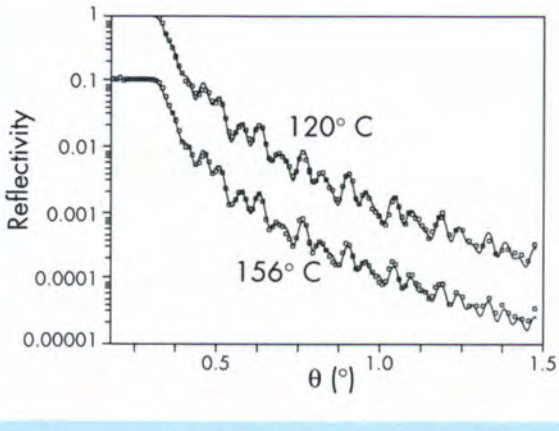

Fig. 3: Neutron reflectivity curves of the incompatible polymer system PS(D)/PnBMA(H) on a glass substrate showing the different interface widths at different annealing temperatures. The solid lines represent fits assuming an interface width of a_I = 6.4 nm (120°C, upper curve) and a_I = 8.6 nm after annealing at (156°C, lower curve).

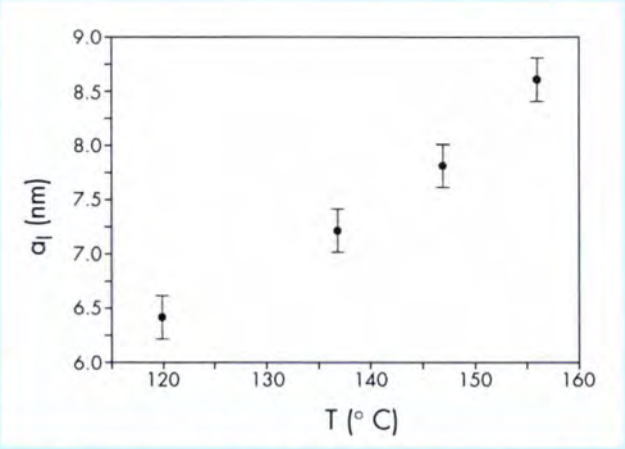

Fig. 4: Temperature dependence of the interface width of PS/PnBMA as determined by neutron reflection experiments.

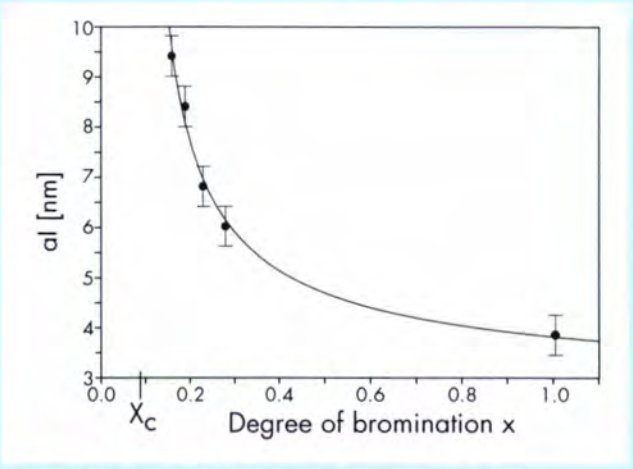

Fig. 5: Dependence of interface width a_I on the degree of bromination x for the blend system PS(D)/PBr$_x$S(H). By a variation of x the compatibility of this blend system changes from compatible (small x) to strongly incompatible (large x), which is also reflected in the interface width.

The data agree well with small-angle neutron scattering (SANS)-data from compatible blends of PS with a statistical copolymer of PnBMA and poly(cyclohexylacrylate) of different compositions [8].

PS/poly(styrene-stat-para bromo styrene) (PBr$_x$S)

The blend system of PS and the statistical copolymer poly(styrene-stat-para bromo styrene) was chosen for a systematic investigation of the dependence of interface width on compatibility, since the compatibility between components can be easily tuned from completely compatible to highly incompatible by a change in the degree of bromination x. A systematic study of the change of the interface width with the degree of bromination has been performed by NR [9] and results are shown in Fig. 5.

At low x the interface width diverges, since the system becomes compatible. The functional form is fitted by a composition dependent χ-parameter, which contains the concentration-weighted individual segment-segment interaction parameters of components. Starting from two well-separated films, the segmental diffusion across the interface can also be followed [9] and detailed power laws are obtained. For incompatible polymers, an equilibrium interface width is formed at large diffusion times. In blends of such polymers, polystyrene is enriched at the surface [10], which is a consequence of the lower surface energy of this component. This effect may be used for a dedicated surface modification of thin films, where surface and bulk properties can differ significantly and are tailored for specific use.

Neutron reflectometry thus provides a powerful technique to determine the segment interaction parameter χ of strongly incompatible polymer systems also, which is otherwise difficult to obtain. The resolution is good enough to resolve details such as time, molecular weight or temperature dependences and information on the functional form of the interfacial profile may also be obtained. This research can thus serve as a basis for understanding polymer blends in general.

References

[1] O. Olabisi, L.M. Robeson, M.T. Shaw, Polymer-Polymer Miscibility. New York, Academic Press (1979).

[2] L. Utracki, 1989. Polymer Alloys and Blends. München. Hanser Publishers (1989).

[3] E. Helfand, Y. Tagami, J. Chem. Phys. 56 (1971) 3592.

[4] D. Broseta, G.H. Fredrickson, E. Helfand, L. Leibler, Macromol. 23 (1990) 132.

[5] M. Stamm, D.W. Schubert, Annu. Rev. Mater. Sci. 25 (1995) 325.

[6] M. Stamm, Physics of Polymer Surfaces and Interfaces, ed. I.C. Sanchez, Boston, Butterworth-Heinemann (1992) 163.

[7] J. Lekner, Theory of Reflection, Martinus Nijhoff, Dardrecht (1987).

[8] D.W. Schubert, V. Abetz, T. Hack, M. Stamm, W. Siol, Macromol. 28 (1995) 2519.

[9] B. Guckenbiehl, M. Stamm, T. Springer, Physica B 198 (1994) 127.

[10] B. Guckenbiehl, M. Stamm, T. Springer, Colloids and Surfaces A: Physicochen. Engin. Aspects 86 (1994) 311.

DIRECTORATE SERVICE

Public Relations

The H.F.R. started up on 6 January at 10.29 hrs and reached full power on 7 January at 21.15 hrs. The start-up itself created much enthusiasm both inside and outside ILL. Outside specialists were astonished that the reactor needed just 35 hours to reach full power, a fact which points to faultless technical preparation.

The countless congratulatory telegrams received from all over the world were a clear indication of the level of interest generated by ILL's "Renaissance".

On Friday, 28 April 1995, on the afternoon following the Scientific Council Meeting, ILL organised a ceremony to celebrate the restart of the reactor and of the experimental programme.

Two Nobel Prize winners honoured the "Renaissance" by giving lectures.

- Norman Ramsey:
"Neutron Spin Reorientation Experiments"
- Cliff Shull:
"The Early Days of Neutron Scattering".

The ceremony opened with a sketch written by Philippe Leconte. To the surprise of the audience, three witches appeared and delivered their wishes to ILL. The text of this sketch is reproduced on page 8 of this report.

The ceremony was followed by a buffet dinner.

Madame Elisabeth DUFOURCQ, Ministre chargé de la Recherche Scientifique, visited the large-scale scientific installations in Grenoble on 23 June 1995. The visit took place only a few weeks after the formation of the new government in Paris and revealed Mme Dufourcq's particular interest in international research. At ILL she was welcomed by the Management and went on to visit the reactor in operation and the experimental halls. She expressed her appreciation of the scientific activity in progress, with many users on the instruments, and gave her full support to multinational scientific research at ILL.

Herr Hans ZEHETMAIR, Deputy Minister-President and Minister for Education, Culture, Science and Art in Bavaria, came to ILL on 14 and 15 September 1995 to learn about the Institut's activities. He was accompanied by a delegation of 10 high-ranking officials representing the Universities of Munich and Bavarian Industry.

The ILL Director, R. Scherm, explained ILL's highly diversified scientific activity, based on the High Flux Reactor, and the wide variety of experimental facilities. R. Scherm pointed out that Europe was at the forefront of neutron-based research. The activities were based on a network of complementary neutron sources, each specialised in the development of a number of particular disciplines. Together with the High Flux Reactor at ILL, the national sources played an important role because of their greater flexibility and easier access. In this context, R. Scherm acknowledged especially the project to construct a new reactor, FRM-II, at Garching near Munich.

Herr Zehetmair confirmed that FRM-II would contribute to Europe's network of sources by providing complementary capacity. In particular, it would open up new possibilities for applied research in materials science and medical therapy. Herr Zehetmair recalled the considerable contribution made by Bavarian scientists to the success of ILL, in particular Prof. H. Maier-Leibnitz.

Collaborating Research Groups (CRGs)

With the restart of the experimental programme, instruments with a special status - known as CRGs - appeared on the scene. The name Collaborating Research Group Instrument is new to ILL, but not this type of operation. Some CRGs emerged from former S-instruments. In addition, due to the reduction of the number of scheduled ILL instruments to 25, several former ILL instruments were transformed into CRG's.

The programme to create CRGs is progressing well. The "General Conditions", which have been approved by the ILL Steering Committee and form the basis for specific contracts, distinguish between three different kinds of CRGs:

- CRG-As are instruments which were built by ILL and remain the property of ILL. The CRG must maintain the instrument in good working order, if necessary upgrade it and provide 50% of the beam-time for ILL use.
- CRG-Bs are instruments of general interest, built and paid for by an outside group. Former ILL instruments which have been purchased by a CRG come under this category. 30% of the beam-time is requested for ILL use.
- CRG-Cs are experiments rather than instruments. Only a well-defined group is interested in setting up the experiment and in running it. There is little interaction between ILL and these groups, apart for safety matters.
- The operation of CRG instruments has to be cost-neutral for ILL. During the time of "ILL use" the CRG remains responsible for all technical and safety matters and provides a "local contact" service. Recurrent costs generated during this time are borne by ILL.

Specific contracts have been concluded for operating instruments:

CRG-A

- D1A (for one half of the time) Powder Diffractometer, Paul Scherrer Institut, Villingen/Switzerland
- IN3Three-Axis Spectrometer, Paul Scherrer Institut, Villingen, Switzerland

CRG-B

- D15 Diffractometer with Lifting Counter purchased by CEA Grenoble, France
- IN12 Three-Axis Spectrometer, purchased by Forschungszentrum Jülich, Germany
- EVA Evanescent Wave Diffractometer, Bergische Universität Gesamthochschule, Wuppertal/Germany

CRG-C

- S-50 h/m_n, Physikalisch Technische Bundesanstalt, Braunschweig/Germany.

Instruments under construction or in the process of being commissioned:

CRG-B

- D23 Diffractometer with Polarized Neutrons, CEA Grenoble/France
- S20 Topography and Diffractometer, CNRS Grenoble/France
- IN22 Three-Axis Spectrometer with Polarisation Analysis, CEA Grenoble/France
- ADAM (Advanced Diffractometer for the Analysis of Materials) Reflectometer, Ruhr-Universität, Bochum/Germany

CRG-C

- S-18 Interferometer, Atominstitut, Vienna/Austria.

These 11 instruments, 9 of which provide time for ILL users, increase the experimental potential and variety of ILL considerably. They are all due to be operational by the end of 1996.

Bruno Dorner

Scientific Secretary

Safety, Radioprotection, Medical and Environment Group (Health Physics)

Activities of the "Délégué"

- CHSCT (Committee for Health, Safety and Working Conditions):
organisation of 5 plenary meetings and 6 building inspections.
- CIS (Internal Safety Committee):
organisation of a committee for each of the following topics:
– Conditions for use of isobutane gas on the PN1 experiment
– Experimentation with viruses at EMBL.
- Acceptance of instruments: examination of the instrument safety files (DSI) of all instruments currently in operation.
- Environment: Supervision of the installations covered by:
– the ministerial orders authorising the disposal of liquid and gaseous radioactive waste,
– the order of the prefect authorising the use of infrastructure for drawing and discharging water from and into the River Drac, as well as ground water, waste water and rain water, and preparation of the relevant documents.
- Document management:
Drafting of a catalogue of the statutory documentation (internal and external) currently in force at ILL, with a view to incorporating information into a specialised computer file.

Safety

Various measures have been taken as regards safety:

- Drafting of safety forms for the instrument safety files (DSI).
- Drafting of prevention plans for work carried out by external firms.
- Safety analysis of experiment proposals.
- Safety training for ILL staff.
- Organisation of various statutory inspections (pressure vessels, electrical controls, lifting equipment).
- Continued renewal of fire alarm equipment (outside the reactor building).

Radioprotection

The SPR (Radioprotection Service) has been very closely involved in work on restarting the reactor and experimental facilities. In this area, its most important activities were:

- Carrying out radiology checks on the various reactor sites to ensure that the radiological situation was consistent with the pre-shutdown state,
- Verifying the radiological efficiency of all beam shutters connected with neutron distribution,
- Carrying out radiology checks on all instruments before they were put into normal operation.

During 1995, the SPR also resumed its routine tasks in line with normal ILL operating conditions, namely:

- Activities connected with the running of the reactor and instruments,
- Its role in providing assistance, in particular to the experimenters, in the field of radiological safety,
- Analysis of experiment proposals from the viewpoint of radiological safety.

In addition, the unit has continued its statutory activities, including:

- Providing training to ILL staff and, in particular, visiting researchers, on radioprotection,
- Inspecting and designating work areas according to the risk of radiation,
- Monitoring radioactive waste,
- Inspecting the shielding of X-ray tubes and devices containing radioactive sources,
- Radioactive source management,
- The transport of radioactive materials.

Finally, the SPR has performed shielding calculations for instruments ADAM on beam line H53, and D23 and IN22, which are to be installed on beam line H25.

Joint Works Medical Service

In accordance with French Labour Law, the Joint Works Medical Service (SMTC) acts as health advisor, providing information on hygiene, safety and how to adapt to working conditions. It is also responsible for monitoring the health of individual members of staff at ILL, ESRF and EMBL in relation to their work activities, as well as looking after sick or injured persons throughout the joint site.

Gérard Rey

SCIENCE DIVISION (DS)

The great event of the year has clearly been our return to normal operation. After a gap of almost four years the user programme restarted on schedule on February 27 for the last third of the first cycle and by the end of the year we completed a further four cycles of operation. The details of the user programme and scientific highlights from the different Colleges are reported elsewhere. Suffice it to say here that the ILL is again looking and feeling like the ILL I knew as a user, buzzing with activity, ideas, users, seminars and "joie de vivre". Thanks to the hard work of all the scientific and technical staff the instruments came into operation on schedule. The nominal profile of ILL instruments is 25, comprising 23 full and 4 'half' instruments (the diffractometer D4 and triple-axis instrument IN1 share a beam line and the operation of two instruments is shared with outside institutions: the biological diffractometer DB21 with the European Molecular Biology Laboratory and the powder diffractometer D1A with the Paul Scherrer Institut (as a CRG)). One instrument is the new thermal time-of-flight spectrometer (IN4) which will not be operational until later in 1996 but another new instrument, the second high-resolution backscattering spectrometer (IN16), was gradually brought into user operation during the year. The large microstrip detector for the high intensity powder diffractometer D20 (to replace D1B) is expected to be completed early in 1996, after which the instrument will be commissioned as quickly as possible.

After the long shutdown and the many changes and improvements, the performance and reliability of the instruments has in general been very good indeed and the total time delivered to users was very close to what was originally scheduled: the details are given later. There were however two unfortunate exceptions to the generally good news: the new detector on the new small-angle diffractometer D22 failed in June after only a brief period of operation and although it has now been repaired by the ILL detector group and is awaiting on-line tests, three cycles of operation were lost. Secondly, more than a cycle was lost on the GAMS spectrometer (PN3) because of problems with the target changer.

The restart of operations has also been accompanied by the arrival of Collaborating Research Groups (CRG's), either operating their own user instruments or operating ILL instruments on lease. By the end of the year, five and a half such instruments were operating with at least five more in the pipeline. In addition to extra scientific capacity and output, the presence of these outside groups brings scientific and technical stimulation and already appears to be a great success.

The world has not stood still during our long shutdown and further stimulation and competition is provided not only by advances in neutron scattering techniques on other sources but also by our neighbour the ESRF. It is therefore important to be able to report that ILL is continuing its tradition of technical innovation and development. The new spin-echo spectrometer (IN15) built as a joint project with HMI Berlin and Forschungszentrum Jülich is under commissioning. The construction of the new γ-ray spectrometer GAMS-V (an addition to PN3) has been completed on schedule and under budget, and commissioning has begun. Two development projects which have been under way for several years have reached successful milestones. First, equipment for producing ^{3}Helium polarising filters is under construction and the filters will be tested in 1996 on two instruments. Secondly, a prototype quasi-Laue detector (LADI) for protein crystallography has been constructed and tests on a variety of crystals have begun and will continue through 1996 with the aim of reaching a definite conclusion about the effectiveness of this technique before the end of the year. Lastly but very importantly, the Steering Committee has approved, following strong endorsement by the Scientific Council, a programme of new instrument projects extending over the next five years. These are the straightening and rebuilding of two guides and the movement of D17 and D16 so as to give these instruments, together with IN5, end positions viewing the whole of a guide; the conversion of D17 to a dedicated reflectometer; the upgrade of D16, IN5, D4 and IN8. In all cases the potential improvement is at least an order of magnitude compared to current performance. This is a highly cost-effective programme and, with ILL's reduced manpower, a challenging one but we are confident of achieving it – given continued funding. In conclusion therefore the scientific prospects for 1996 are excellent – a full user programme, a growing CRG activity and exciting new projects.

Alan Leadbetter

Members

Scientific Coordination

Brigitte Aubert
Herma Büttner
Diana Dijoux
Katja Mayer-Jenkins

Joint ESRF/ILL Library

Maryvonne Alexandre (ILL)
Christine Castets (ILL)
Maria Da Silva (ESRF)
Virginie Teissier (ESRF)

Scientific Coordination Office (SCO)

Workshops

The Scientific Coordination Office was involved in the organisation of the following workshops:

Workshop	Organisers
New Tools for Neutron Instrumentation Les Houches, 6-9 June 95	F. Tasset, ILL H.G. Büttner, ILL
Quantum Atomic and Molecular Tunnelling in Solids Seyssins, 4-7 October 95	F. Fillaux, CNRS H.G. Büttner, ILL G. Kearley, ILL J. Meinnel, Rennes

Statistics of the Scientific Programme

The reactor restarted on the 6th of January 1995. After several weeks of reactor tests, safety checks and commissioning of instruments the ILL welcomed the first users on the 27th of February. It was even possible to accommodate the 'Hercules' course at the end of the first cycle. There are many new safety features and operational procedures and this year we all, users and ILL staff, had to get used to the procedures.

In 1995 the ILL welcomed some 1500 visitors, 70% coming from the member countries (386 French, 354 German and 331 British).

The Scientific Council of October 1994 had allocated 115 days and a further 84 days could be allocated in April 1995, i.e. about 200 days beam time were allocated in 1995. Figure 1 shows the beam-time request and allocation by instrument for the year 1995. The backscattering instrument IN16 started to accept users during its commissioning period in summer 1995. Several CRG instruments became operational and therefore ILL users also received beam time on D1A, D15, EVA, IN3, IN12 in the second half of 1995, allocated by the Scientific Council in April 1995.

Unfortunately, D22 had to be taken out of user operation for the last three cycles of the year because of a breakdown of the new multidetector. A sample changer problem also stopped PN3 for more than a cycle. The full statistics are given in table 1 which summarises the performance of all the scheduled instruments. Overall about 600 days of the total available beam-time was lost due to various malfunctions. However, most of this time was not lost to users because time for minor breakdowns, tests, calibrations and scheduling difficulties is normally allowed for by initially scheduling about 80% of the total available beam-time. The result is that the total number of days delivered to users was 3397 compared with the 3467 originally scheduled - a loss of 70 days (this excludes the 3 cycles for which D22 was taken out of operation).

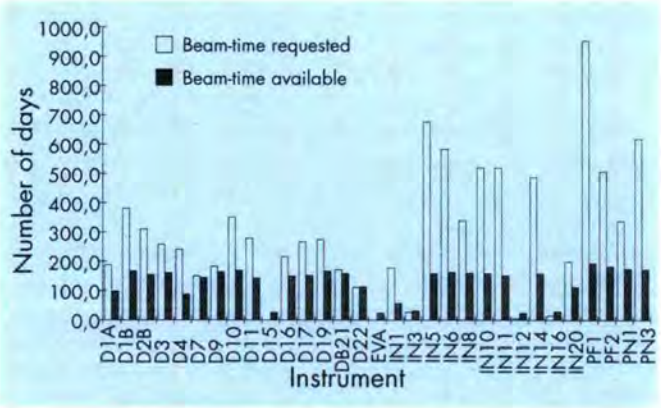

Fig. 1: Beam-time request and allocation on the instruments in 1995.

instr.	days lost	% lost	sched. days	days used	instr.
D1A	14	13,5%	86	100	D1A
D1B	9	4,8%	153	152	D1B
D2B	9	4,8%	153	155	D2B
D3	12	6,4%	146	140	D3
D4	16	15,7%	87	73,5	D4
D7	6,5	3,5%	166	175	D7
D9	15	8,0%	154	162	D9
D10	17,9	9,5%	162	147	D10
D11	16	8,5%	127	121	D11
D16	17,5	9,3%	135	130	D16
D17	4	2,1%	127	153	D17
D19	17	9,0%	150	170	D19
DB21	9	4,8%	131	153	DB21
D22	152,5	81,1%	52	20	D22
IN1	2,8	3,3%	58	70,5	IN1
IN5	20,2	10,7%	150	136,5	IN5
IN6	16,5	8,8%	149	158	IN6
IN8	7,3	3,9%	151	160	IN8
IN10	12,15	6,5%	142	157,25	IN10
IN11	15,5	8,2%	156	158	IN11
IN14	31,5	16,8%	154	134	IN14
IN16	9	9,6%	26	38	IN16
IN20	29,5	15,7%	129	134	IN20
PF1	58,5	31,1%	185	127	PF1
PF2	12	6,4%	*	*	PF2
PN1	15,7	8,4%	175	164,5	PN1
PN3	66,5	35,4%	163	107,5	PN3
total	612,55		3467	3396,75	total

Table 1: Performance of instruments.
** PF2 consists of several long-term experiments so comparison of days scheduled and used is not meaningful.*

The distribution of beam-time amongst the colleges is shown in Figure 2.

Table 2 shows the beam-time request and allocation for ILL's member countries and the pie-chart in Figure 3 illustrates the beam-time allocation in percent for 1995 (scientific council October 1994 and scientific council April 1995). The same principle as described in last year's annual report was used as basis for the statistical breakdown. Italy is cited amongst ILL's member countries, since it receives beam time as a result of specific instrument contracts.

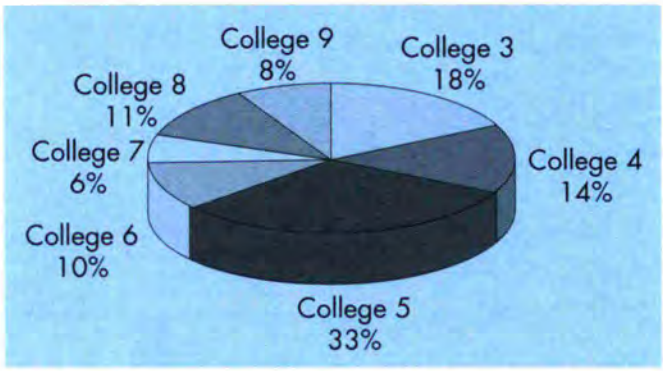

Fig. 2: Beam-time allocation amongst the colleges in 1995.

Beam-time request and allocation
Scientific Council Oct. 94 & April 95
ILL Member Countries

Country	Requested days	Requested in %	Allocated days	Allocated in %
AUT	185,9	1,9%	87,5	2,2%
CH	506,8	5,2%	196,5	5,0%
D	3406,7	35,2%	1324,6	33,4%
E	306,3	3,2%	98,4	2,5%
F	2409,4	24,9%	1050,9	26,6%
ITA	145,5	1,5%	48,0	1,2%
UK	2721,6	28,1%	1151,9	29,1%
Total	9682,2	100,0%	3957,8	100,0%

Table 2: Requested and allocated beam-time amongst the ILL member countries for 1995.

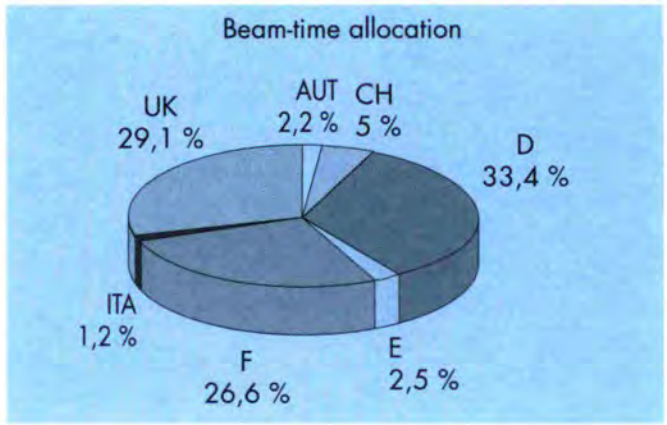

Fig. 3: Beam-time allocation amongst the ILL member countries for 1995 (SC Oct. '94 + SC Apr. '95).

Joint ILL-ESRF Library

Librarian: Christine Castets

During this year, further progress was made in the service given to users, in particular as regards the consultation possibilities in the library:

- A client-server version of the library software was implemented on a special consultation post in the library allowing user friendly consultation of the library catalogues (books, ILL and ESRF publications).

- Highly appreciated, the CD-ROM station 'libre service' is now widely used and a second stand-alone station equipped with two towers of 7 readers each was installed beginning 1995. This brings to 26 the total number of discs loaded permanently allowing to search major scientific databases as
  - INSPEC
  - Medline
  - Science Citation Index

- Current Contents on Diskette with Abstracts (Physical, Chemical and Earth Science) is still loaded on the Appletalk network and can be searched from scientists' offices and, since 1995, from a consultation post in the library.

Improvements are still needed to the facilities for consultation from scientists' offices of the library catalogues (this is in progress) and of the databases on CD-ROM (this is more difficult to undertake as regards technical, personnel and financial implications).

This year was also the year of the Internet which came into force in all areas of library science.

The library used some Internet services as

- Electronic version of scientific journals as Physical Review Letters online, Applied Physics Letters online, free of charge in 1995 for subscribers to paper copy

- Electronic version of catalogues of publishers, libraries, booksellers

- Electronic preprints in full text available from many research institutes

This use will certainly increase in the next years.

Concerning the day-to-day library work, in 1995:

- 900 books were processed
  - 300 for ESRF Departments or Divisions (275 in 1994)
  - 150 for ILL Departments or Divisions (140 in 1994)
  - 450 for the Joint Library (same as in 1993)
- 800 volumes were bound (650 in 1994)

In addition, a lot of time had to be spent on the library management software and it is now clear that this item will always be time consuming, which we did not know before.

The high increase in journal costs led us to discontinue some subscriptions in 1995. The decisions were made in agreement with the Users' Committee.

Allocation of literature costs

According to the agreement on "the Operation and Maintenance of a Joint ILL-ESRF Library" all library costs are shared equally by the two Institutes. The estimate of expenditure at 1.11.1995 was about 1 560 KFF excl. taxes which gives for the ILL share a cost of 780 KFF, excl. taxes.

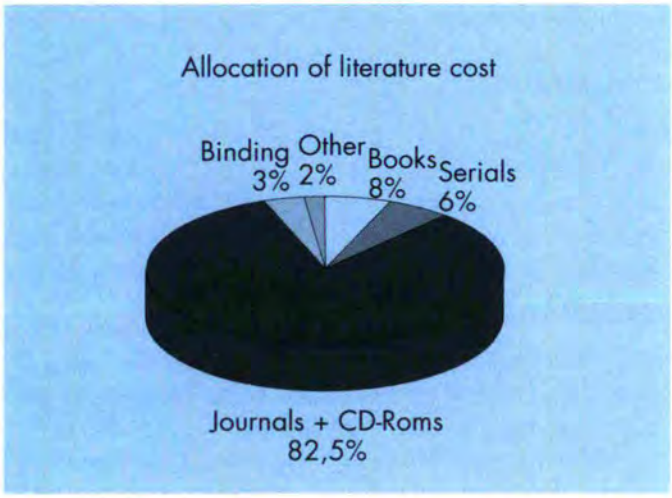

Publications

The number of publications from ILL staff and users remained at a low level, not exceeding 250. Results of experiments performed in 1995 were not yet published and scientists were very busy this year with the starting of the experimental program.

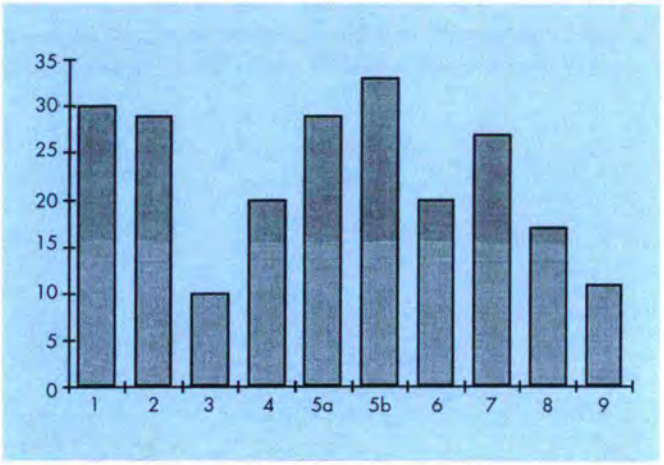

Publications received in 1995 by subject:

1 - Instruments and Methods
2 - Theory
3 - Fundamental and Nuclear Physics
4 - Structural and Magnetic Excitations
5a - Crystallographic Structures
5b - Magnetic Structures
6 - Structure and Dynamics of Liquids and Glasses
7 - Material Science, Surfaces and Spectroscopy
8 - Biology
9 - Structure and Dynamics of Soft-Condensed Matter

Herma Büttner

Scientific Computing

Members of the Group
Alain Filhol
Ron Ghosh
Don Kearley
Christian Lacaille-Desse
Beatrice Nicolai (Thesis student)
Didier Richard
Steven Fayers (Long-term stagiaire, Univ. Surrey)

Visitors

A. Navarro (Univ. Jaen), K. Knowles (ISIS), M. Neumann (Univ. Grenoble), Y. Raoul (interim), R. Joufrey (interim)

Introduction

The scientific computing group was formed during the reactor shutdown, and 1995 was the first year for the group under normal operating conditions. At the time of the restart, some groups at ILL were using exclusively UNIX systems for data reduction and analysis whilst others were either using exclusively VMS or at some intermediate stage between the two. Given this mixed system, changes in data format, and software which was used in-action for the first time, the start-up was an exciting time for the entire scientific computing group.

It has been easy to attract students and trainees to work on specific projects for the group on a temporary basis. Not only do they help reduce the general workload, but they also have a fresh outlook and bring new ideas. Because our group is small, they integrate rapidly and their contributions make a significant impact on the output of the group as a whole.

Development of Hardware

Since the group was formed, it has been our policy to concentrate mainly on the systems most commonly used at the ILL. At present we test and develop software mainly under UNIX (HP and SGI),and Macintosh. Next year we hope to include PC and DEC Alpha which are targeted more at visitors than ILL scientists. The workstations which the group uses for development are now shared (via network access) with users who have specific hardware or software requirements which, for various reasons, are not available within their instrument group. In addition, we provide two basic workstations and some special-purpose peripherals for semi self-service use.

Development of Software

The small angle neutron scattering (SANS) programs have been completely overhauled with the aid of K. Knowles (ISIS) and a student doing an "industrial year". This project has followed the principle of using standard transportable programs, enhanced by the use of graphical user interfaces (GUI) built with public domain software (Tk/Tcl) (see Figure 1, page 159).

Similarly, PGPLOT (a public domain plotting library) is available for all common platforms at the ILL, and has become the basis for simple plotting throughout the Science Division.

The LAMP project, which offers a very high level for data inspection and analysis, has matured into a popular standard on many instruments. In contrast to the SANS project above, the principle here is to use the best available commercial product to develop powerful in-house software at low cost in man-power. Nevertheless, LAMP can be exported to those who have a licence to run IDL (the language used by LAMP), and versions already exist at HMI (Berlin), IPNS (Argonne) and Julich. Much of our recent effort has been in developing interfaces which allow simple installation for various data-types and data-bases found at different institutes.

Many existing programs for the TOF/HR and TAS groups have been constantly modified, improved and documented since the reactor start-up. Many of the Macintosh programs now have native code to fully exploit the Power/PC, which is becoming a *de facto* standard at the ILL.

Data

The change to ASCII data format has simplified many aspects of accessing raw data, and treated data too is now principally stored in text form. Internal annotation of data is also increasing since this is straightforward for ASCII files. A data-base browser, TOUCH_BASE, has been written in IDL and incorporates LAMP (see Figure. 2, page 160). This allows data-bases to be scanned via snap-shots of the data themselves viewed as surfaces, contours, etc., with automatic restore into a lamp "work-area" if desired.

Participation at Workshops

Software developed by the group was presented at the "New Tools For Neutron Instrumentation" workshop at Les Houches and resulted in other institutes becoming interested in ILL software. The group also participated in the "Soft Ness" meeting at NIST in the USA to assist with the definition of a standardised data format. As a result, converters to and from an intermediate HDF format (a standardised interchange format for treated data) are now being studied.

The group has also collaborated with the ESRF in organising an international workshop to examine new developments in better user-group software (NOBUGS). This will take place in early 1996 and it is hoped that this will lead to better ties between computing groups in different centres.

Documentation

The WWW overview of computing for science at ILL has evolved during the year into a repository of general information of facilities, data treatment, data formats and programming aids. The use of hypertext for documentation within the ILL has started, and there is little doubt that with the new tools for creating hypertext, this form of documentation will increase.

Gordon Kearley

Nuclear and Fundamental Physics (NFP) Group

PN1 Fission product separator LOHENGRIN on beam tube H9 (H.R. Faust, G. Fioni, I. Gartshore)

PN3 Curved and flat-crystal spectrometers GAMS2/3, GAMS4, GAMS5 (project) on the through-tube H6-H7 (H. Börner, T. Eaton (part-time), U. Mayerhofer (part-time), A. Williams, R. Oliver)

PF1 Cold polarized neutron beam PARSIFAL at the end position of guide H53 (U. Mayerhofer (part-time), V. Nesvizhevsky, O. Zimmer, A. Trouillon)

PF2 Ultra-cold neutron source and distribution system on level D using the vertical guide from the cold source and neutron turbine (W. Drexel, P. Geltenbort, H. Just)

PN1 Fission product separator

The spectrometer, which underwent major modifications during the reactor shutdown period, was fully tested and brought back into normal operation. A particular effort was necessary to stabilize the electric field; several insulators, a H.V. connector and a full resistor chain needed to be replaced. Part of the H.V. stabilization chain also had to be modified. These units, which now constitute the older and weaker part of the spectrometer, will be completely replaced in 1996, when a new PC-computer driven system will be available. A new reference voltage unit to control the first magnet was installed and several other electronics units were replaced and tested.

To operate the PN1 detectors (high-resolution ionization chambers), a completely new gas supply system - compliant with new safety regulations - was designed and installed. Now the alternative use of two different gases is possible, providing the users with an increased flexibility to satisfy the most varied experimental needs.

The new PC-based multiparameter 8-ADCs data acquisition system (by FAST-Electronics, Munich - Germany) was installed and successfully used in most of the experiments. The data can be transferred by FTP to any ILL computer for further analysis. A completely new set of data analysis programs was developed on UNIX workstations (ILL Scientific Computing Group, using the IDL library, with help of T. Friedrichs, PN1 thesis student). Very accurate and fast data analysis is now possible for nuclear fission experiments. In this context, a new HP 712/80 workstation (known as "Wendy") and severeal X-Terminals were installed. The programs provide the following features: coloured scatterplots, cut and projections along all axes, one-dimensional gaussian fits (up to 5), parameter fixing while fitting, background treatment (gaussian background), error analysis of the fit, Motif look and feel.

The program was designed for fission yield analysis but may also prove interesting for other groups that have to analyse two-dimensional spectra.

The ion-optical characteristics of the improved spectrometer were determined, confirming the calculations carried out for the RED (Reverse Energy Dispersive)-magnet. Only a shift of about 6 cm in the position of the focal point in beam direction was observed (Fig. 1). This was probably due to an imperfect knowledge of the previous focal position and was easily corrected with an adaptation piece.

In addition, the new ionization chamber to be used in correlation with the RED-magnet was tested and the preliminary results on the determination of the fission-fragment incoming angle were very satisfying (Fig. 2).

PN3 Gamma ray spectrometers

The double flat-crystal spectrometer GAMS4 (NIST-ILL collaboration) was re-installed on level C of the reactor. The new anti-vibration systems furnished by NIST, and some additional improvements to the damping of the

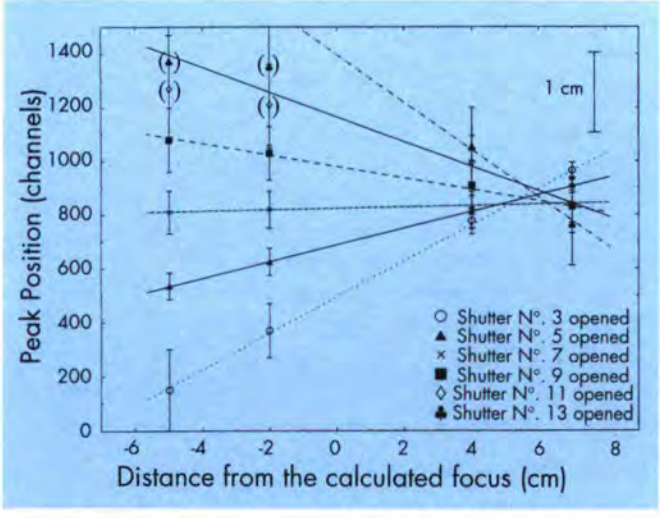

Fig. 1: Measured trajectories near the calculated focal position of the RED magnet for heavy ions passing through different shutters placed along the energy dispersion direction of the parabola of the Lohengrin spectrometer. Each point corresponds to the peak position of the beam measured with a position sensitive detector and the error bars correspond to the FWHM of the particle distribution. While the beam size is in perfect agreement with the calculations, a shift of about 6 cm is observed and it is probably due to a displacement of the original focal point caused by a modification of the Condenser fringing field.

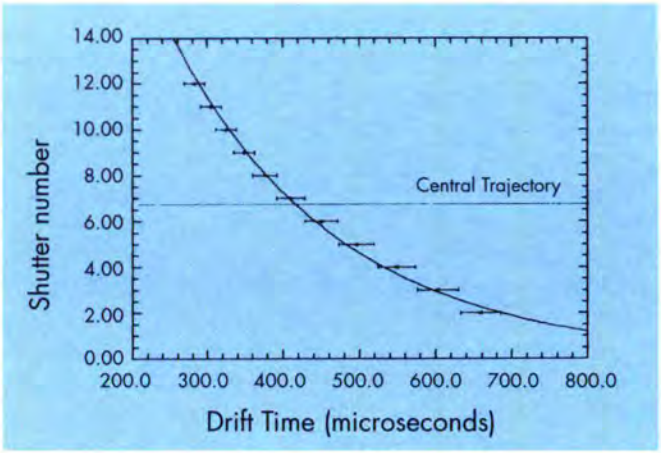

Fig. 2: Drift-time difference between signals from the two parts of the anode of the new ionisation chamber for PN1 for ions coming from different shutters placed along the energy dispersion direction of the parabola of the Lohengrin spectrometer. It is evident how the trajectories of ions coming from different shutters can be determined by measuring the drift time; this will enable the determination of the ion nuclear charge by the ΔE-E method together with the benefit of an increase of a factor of seven in the particle density due to the RED magnet.

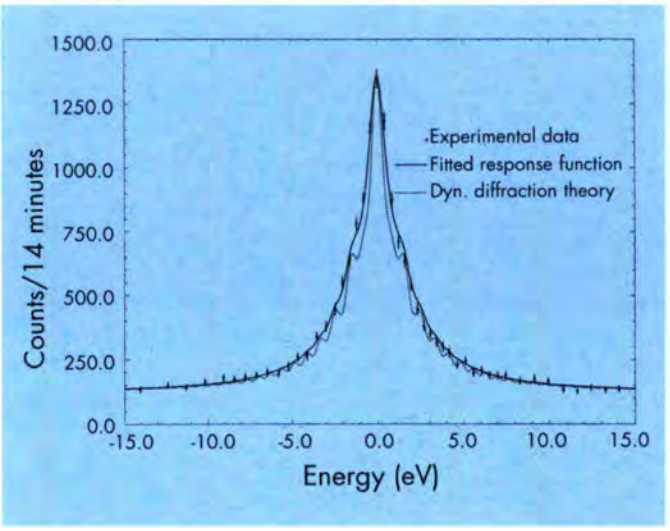

Fig. 3: Theoretical (dashed line) and experimental response function, obtained for a 472 keV transition in non-dispersive mode. The fitted response function is obtaind by folding the theoretical one, obtained from dynamical diffraction theory, with a gaussian distribution width ("excess-width") of $\Delta E/E = 1.3 \cdot 10^{-6}$. This is also the current limit which can be achieved for the resolving power.

spectrometer, resulted in an improvement in the so-called "excess width", e.g. the instrumental contribution to the resolution as predicted by dynamical diffraction theory (Fig. 3).

On the bent-crystal spectrometer GAMS23 the old Michelson interferometers were completely replaced by two-frequency laser interferometers. Heterodyne interferometers are used with two different frequencies, with linear polarisation, orthogonal to each other. The recombined laser beam produces beats with a frequency of about 1.8 MHz. The phase of these beats measured with respect to a reference signal depends on changes in the optical path length in the interferometer. These phase changes can be determined with very high precision. This permits a more accurate and reliable determination of the rotation angle of the crystals and thus a more reliable measurement of the gamma-ray energies. This measure also goes towards standarisation of the components of the three crystal spectrometers GAMS23, GAMS4 and the new GAMS5.

The construction of the new GAMS5 instrument has been taken to a point where test runs with the instrument in a double flat-crystal configuration are possible. These tests should elucidate the final performance of the spectrometer as regards the precision which can be achieved. Tests of the interferometers with respect to the phase non-linearity (relative angle between two interference fringes) have already been carried out very successfully using a pressure cell in one of the interferometer arms. Measurements using γ-transitions in different reflection orders should now yield the final parameters concerning the calibration constants of the instrument as well as their reproducibility. The next and final step will then be to equip the spectrometer with bent crystals.

PF1 Cold polarised beam facility

1995 saw the inauguration of PF1 as a scheduled instrument with two experiments devoted to neutron decay (see "Scientific highlights in College 3").

Due to some changes in the H53 beam line during the reactor shutdown, a decrease in neutron capture flux at the PF1 position compared to its previous value of 10^{10} $cm^{-2}s^{-1}$ was expected. A new measurement gave the present value of $7.4 \cdot 10^{9}$ $cm^{-2}s^{-1}$.

Severe background problems at the beginning were solved by the reconstruction of the main beam shutter of PF1, as well as by careful shielding of the neutron polariser in the casemate.

The polariser is mounted in its lead housing such that it can be adjusted externally by means of stepping motors driven by a PC with a program in Visual Basic (A. Trouillon). The polariser can be displaced in a reproducible manner which allows for quick switching between the polarised and the unpolarised beam. Presently a supermirror polariser of O. Schärpf is used, which allows for a beam size of 46 mm in height and 33 mm in width. Its polarising efficiency was measured to be about 98%.

During the setting-up of the "PERKEO" experiment (see "Scientific highlights in College 3"), a set of magnetic guide fields were constructed to maintain the neutron

polarisation between polariser and spectrometer. With their different sizes they are well adapted to the varying circumstances at PF1

A number of simple current-sheet spin flippers proved to be rather inefficient for the full polarised beam size and were improved to produce in a flipping efficiency of about 99.5%.

A general problem encountered for most of the experiments scheduled for PF1 up to now (i.e. all experiments which investigate correlation coefficients in polarised neutron decay) is, that a knowledge of the neutron beam polarisation is required to a precision of a few parts in a thousand. Unfortunately the polarising efficiency of a supermirror polariser is not known a priori and can only be determined by a rather complicated measuring procedure involving three supermirror polarisers together with several spin flippers. A compact device to fulfill this task was recently bought by ILL from Gatchina and tested over the last few weeks. This device consists of two sputtered supermirror polarisers (cross-section 5 mm high, 50 mm wide), which are rigidly mounted onto a support, together with an intermediate neutron guide section and two radio frequency spin flippers. The whole unit can be rotated to change the position of the two analysing polarisers in the beam (which allows partial self-consistency checks within the method). Systematic investigations turned out to be rather promising: preliminary results indicate the analysing accuracy of the device to be below $2 \cdot 10^{-3}$, see Fig. 4.

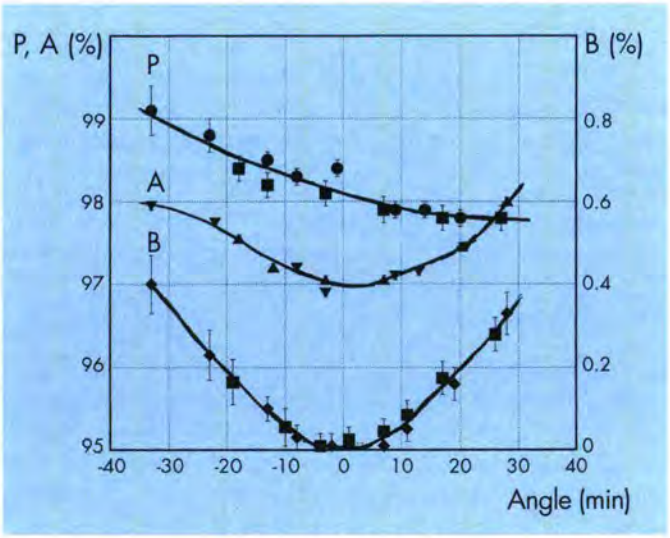

Fig. 4: The results of polarisation measurements with two different analysing devices (one is the mirror image of the other). P - ●● angular distribution of beam polarisation (the angle is measured between the beam axis and the analysing device). A - ▲▼ the analysing efficiency of these devices (as measured in this experiment). B - ■◆ the probability of spin flip at the supermirrors of the analyser.

PF2 Very cold and ultracold neutron source

Constant efforts are being made to improve the infrastructure at the PF2 installations on level D. Oil-containing vacuum pumps on the turbine - to minimise oil contaminations within the turbine house and on the neutron reflection blades - have been replaced. Furthermore, on all exit tubes from the turbine which feed the different experimental installations, thin Al windows have been installed to separate the experiment from the turbine itself. The experiments are automatically controlled and in case of any irregularities the valves to the turbine are closed immediately. On the turbine itself all bearings and the universal joint have been replaced and should now run as long and as reliably as before.

A VCN-bender has been constructed and successfully tested. Its schematic layout is shown in Fig. 5. This set-up allows - if required - a more efficient use of the UCN beam which bypasses the turbine. This device was described in last year's report. The transmitted wavelength band peaks around 60 Angstroem and its brightness is shown in Fig. 6.

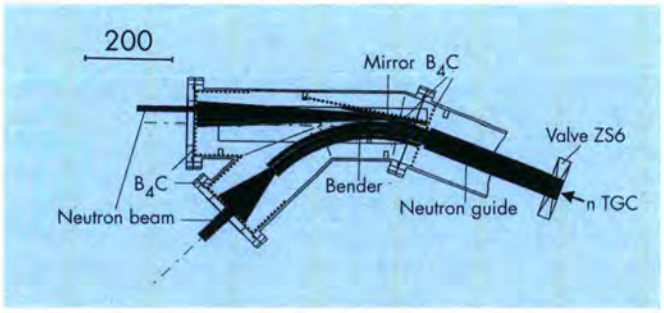

Fig. 5: Principal layout of the new VCN exit port ('V-tube').

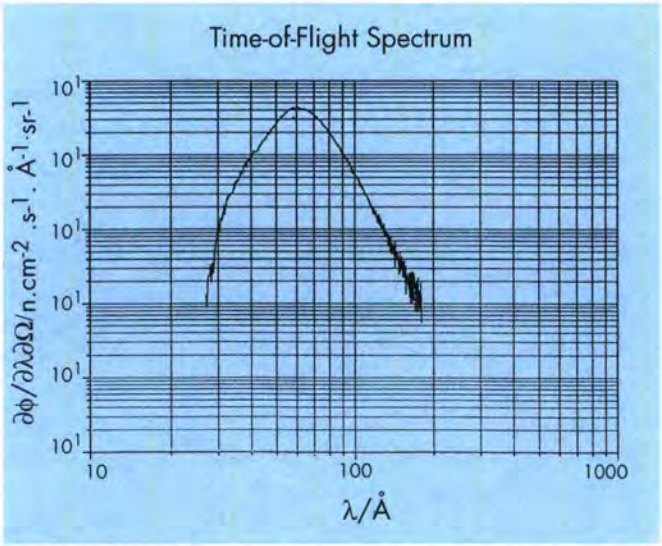

Fig. 6: Brightness of the neutron beam after passing through the new bender at the position of the highest flux. The TOF data set (TOF3') has been corrected for detector efficiency and absorption losses in air and He (see text).

At the reflected VCN beam an interferometer has been installed in collaboration with the University of Innsbruck. The VCN interferometer, which has been redesigned during the long shutdown, consists of three quartz plates with etched phase gratings with 500 lines per mm. They can be separated by a distance of up to 2 m, thus allowing to build a Mach-Zehnder interferometer for neutrons with an overall length of up to 4 m.

The EDM collaboration (University of Sussex, RAL, ILL, Harvard, University of Washington) has completed most of the significant changes to the hardware of the experiment and is now once again on the verge of taking data. To summarise, a new large storage cell machined in Russia from a single fused quartz boule, has been installed. This provides a cell suitable for containing both the ultracold neutrons and the polarised mercury atoms from the magnetometer, whilst acting as an excellent insulator for the applied high voltage. A new set of HV electrodes, designed and built at RAL, has also been installed. It is hoped to apply up to 250 kV without breakdown. A technique to coat the electrodes with Teflon has also been developed. Teflon has a considerably higher Fermi potential than aluminium and is thus better able to contain the neutrons. The PCbased data aquisition system written using the LabView software package has been considerably upgraded. It is believed that, with all these efforts, systematic errors can be reduced to a point where they will contribute only about 2×10^{-27} e cm to the uncertainty of the measurement of the neutron EDM. Several years' running will be needed before the statistical uncertainty can be reduced to a comparable level.

At another UCN beam position an experiment has been set up, in conjunction with colleagues from the RRC Kurchatov Institute, Moscow, to determine the neutron lifetime by storaging UCNs and simultaneously detecting inelastically scattered neutrons. The set-up consists of two storage vessels made of aluminium, which are coated with a thin layer of Fomblin oil to reduce the losses of UCNs when interacting with the walls. The vessels are surrounded by 24 thermal neutron detectors to determine the number of upscattered neutrons experimentally. Measurements were carried out for different ratios of storage volumes to wall area and different temperatures. Both a group from the RRC Kurchatov Institute and a PNPI Gatchina/JINR Dubna collaboration have performed independent experiments aimed at a better understanding of the unomalous losses of UCNs when interacting with material walls (see AR 1993). Finally, a group from the University of Heidelberg has set-up two experiments on a UCN beam. The first looks for anomalous spin precession, the second studies coherent effects with neutrons in disordered media.

CRG C: Determination of h/m_n (PTB)

The main objective of the work done in 1995 concerned a systematic experimental study of possible sources of error. After the long shutdown, the instrument had first to be repaired and readjusted. First measurements were then devoted to studies of reproducibility and very good agreement was obtained with respect to the data taken before shutdown. Then a new very pure Si-crystal was installed (to determine precisely the wavelength of the neutrons), as the one previously used contained a rather high carbon concentration which meant that the lattice constant was smaller than usual (relative difference: 2.8×10^{-7}). Before a final evaluation of h/m_n can be carried out for the measurements with the new crystal, its lattice constant has to be determined with high precision. This will be done in early 1996 at the PTB. A preliminary analysis led to the results expected for a pure Silicon crystal.

Hans Börner

Diffraction (DIF) Group

D1A	High Resolution 2-Axis Diffractometer ($^1/_2$ CRG - A.W. Hewat, F. Fauth, P. Cross, Ph. Decarpentrie)
D1B	High Efficiency PSD Diffractometer (Future CRG - B. Ouladdiaf, C. Ritter, K. Ben Saïdane)
D2B	High Resolution Powder Diffractometer (P. Radaelli, E. Suard, P. Cross)
D3	Polarized neutron diffractometer (E. Lelièvre-Berna, F. Tasset, E. Bourgeat-Lami)
CRYOPAD	Cryogenic Polarization Analysis Device (F. Tasset, P.J. Brown, E. Bourgeat-Lami)
D4	Disordered Materials and Liquids Diffractometer (H. Fischer, P. Palleau)
D9	Four-circle diffractometer (C. Ritter, M.-T. Fernandez-Diaz, J. Archer)
D10	Four-circle 3-Axis Diffractometer (G. McIntyre, B. Ouladdiaf, G. Schmidt)
D15	Two-Axis Diffractometer with Lifting Counter (CRG - P. Burlet, F. Bourdarot, J. Brown, B. Vettard)
D19	High-flux single crystal multidetector diffractometer (S.A. Mason, P. Langan, J. Archer)
D20	High-flux multidetector (P. Convert, Th. Hansen, J. Torregrossa)

1995 saw the return of normal operation of all instruments with the restart of the ILL reactor. D1A after its return from Saclay was upgraded with 25 new collimators, detectors, pre-amplifier electronics, pyrolytic graphite filter, stress goniometer etc. and serves half time as a Swiss CRG. D1B continued as a fully scheduled instrument awaiting the completion of D20, when it will become a CNRS CRG. D2B received a new monochromator, pyrolytic graphite and beryllium filters, and collimation systems. D3 started its conversion to Unix control. D4 prepared for the D4c project. D9 improved its sample environment. D10 was converted to Unix control, with a Silicon Graphics computer replacing the DEC Vax. D15 became a CRG, owned and operated by the CENG. D19 cured some problems with its old PSD detector while awaiting its new detector. And D20 finally appeared to be approaching completion ! All of these instruments (except D20), while being modified and improved, continued to support a full work load of experiments.

Problems remain with many instruments. On D1A/D1B 40% of the beam is lost due to a defect that has developed in the thermal guide (to be corrected in March 1996). A new monochromator for D1A will be constructed using the old D2B monochromator. The D1B pre-amplifiers are noisy and must be replaced. D3 needs a new cryomagnet to ensure that the instrument will not be disabled if its 20+ year old cryomagnet fails (but we cannot afford this in 1996). D4 has a project for a new detector to make full use of the available beam, and a prototype will be built in 1996 if we can find extra money and manpower. D9 needs new cryomagnet hardware to compensate for the loss of D15. D10 will hopefully have a small 2D position sensitive detector in 1996. D19 awaits the larger position sensitive detector that was ordered from CERCA in 1990, and will hopefully be finished by ILL in 1996. And D20 is still waiting for its large PSD detector (which is now almost complete). In 1996 several more instruments will be converted to new VME electronics and control by Silicon Graphics UNIX computers, which are already used for data reduction on all diffractometers.

D1A High Resolution Powder Diffractometer on thermal guide H23

A major improvement to D1A was completed in 1995 with the replacement of the old 10-detector bank by a new bank of 25 detectors and collimators covering 150° (Fig. 1, page 160). This increases the efficiency of the machine to 250% and means that a full diffraction pattern can be obtained with a single short scan of 6°. The quality of the diffraction pattern is identical to that obtained with the old detector bank.

With 25 detectors, the pre-amplifier electronics were replaced by the new ILL design, which is much less sensitive to electronic noise. Tests with electric drills and over-head crane operation produced no noise in the detector chain - a big improvement over the old electronics.

A pyrolytic graphite filter was provided by the PSI CRG-partner, so that a very clean 2.9Å beam can now be obtained with little loss of intensity. This is important for measurements on magnetic materials, zeolites and other structures with large d-spacings. The temporary replacement of the monochromator broken at Saclay gives a clean profile, but the beam is poorly focussed. Early in 1996 we will produce a new monochromator using material from the old D2B monochromator, which is adequate for D1A resolution: this will provide better focussing for small samples, but also more intensity, since the whole height of the guide tube will be used.

A second major developement on D1A was the installation of a heavy duty XYZ-translator for neutron strain scanning (Fig. 2, page 160). The stress/strain option on D1A will be further developed in 1996 with new VME electronics and Unix computer control of the XYZ-translator as well as the detector and monochromator. A small position sensitive detector will be installed to speed up data collection for such

experiments. Robert Wimpory, a Ph.D. student from Loughborough is working on stress, and has been assisted by Terry Eaton and of course Peter Cross. Early in 1996, an EU-HCM fellow will finally arrive to further develop stress measurements on D1A. The plenary meeting of the international VAMAS meeting on neutron strain scanning will be hosted at ILL in January.

D1B High Efficiency PSD Powder Diffractometer on thermal guide H23

After the reactor restart, D1B continues to be in a very high demand. In 1995, 63 scheduled experiments were carried out successfully. A variety of interesting experiments were performed. Besides the standard experiments using the normal cryostat and furnace, several studies in the mK range using a dilution cryostat and in the high temperature range (1800K) with the special furnace as well as pressure studies, were performed.

A large number of experiments were dedicated to real time diffraction studies such as in-situ chemical reaction, physisorption. A time-dependent study of a polar molecular liquid in an electric field has also been performed. An exotic type of experiment dealt with the study of the alignment of clay particle in fluid flows. This experiment required a novel set-up of D1B. A syringe pump was used to obtain steady flow of the clay. The pump was connected to the CAMAC electronics to allow counting to be inhibited when the pump reached the end of its travel and began to reverse. The large success of this experiment has initiated further use of similar techniques e.g. to study not only the steady but also turbulent flows. A nose cone (conical collimation) was made for D1B to allow small incident beam sizes.

An effort has also been done to complete the data reduction programs on the SGI workstation such as fild1b, xrfit (for cyclic refinement). The Lamp program, which is a graphical user interface for visualization of 2D and 3D data as in line-plots, contour-plots or surfaces is also installed.

D2B High Resolution Powder Diffractometer on thermal beam H11

D2B has been considerably upgraded through a series of modification to the neutron optics, the data acquisition and analysis system and the special environment options:

A new Ge 335 monochromator (Fig. 3), constructed using the multiblade technique, has been installed and tested. The Bragg peaks obtained using the new monochromator can be fitted using theoretical lineshapes, without any appreciable flux reduction at the sample position. One of the benefits of the improved peak profiles is the possibility of obtaining high-quality data in the high-resolution mode (5' primary collimation).

Two sets of automated slits have been installed on the instrument. The first, positioned about 20 cm from the sample position, allows the beam to be precisely defined both in the vertical and in the horizontal directions. The second, located inside the concrete shielding at ~15 cm from the monochromator, controls the horizontal divergence of the monochromatic beam, and, as a consequence, the resolution function of the instrument. A typical high-resolution configuration, with a 1 cm slit opening, yields experimental FWHM $\Delta 2\Theta \leq 0.25°$ in the angular range $0° \leq 2\Theta \leq 100°$ (Fig. 4). The reduction in flux (about a factor of 3) is partially compensated by a much better signal-to-background ratio. Since it affects mainly the lower-to-intermediate angular range, this option is complementary to the 5' primary collimation, which is most effective in "focusing" geometry ($2\Theta = 135°$).

A 300×60×30 mm highly-oriented pyrolitic graphite filter has been installed in the primary beam (Fig. 5, page 161). An hydraulic translation mechanism allows the filter to be removed at the push of a button. With the filter in place, the 2.4 Å wavelength can now be used with less than 0.3% $\lambda/2$ and $\lambda/3$ contamination. This option has been extensively employed by the users during cycles 954 and 955.

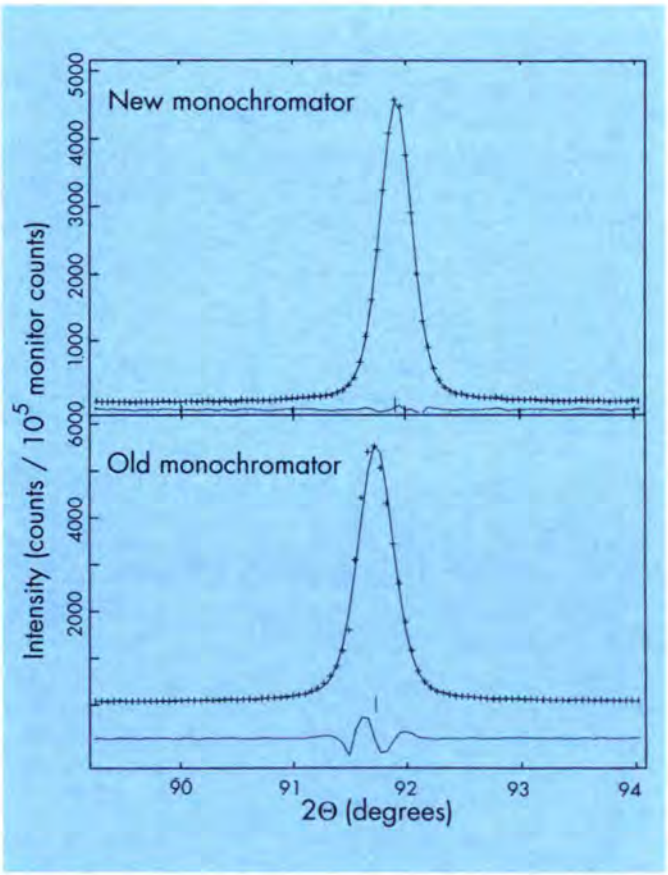

Fig. 3: Almost perfect fit to a single peak obtained with the new D2B monochromator, compared to the less good fit obtained with the old monochromator.

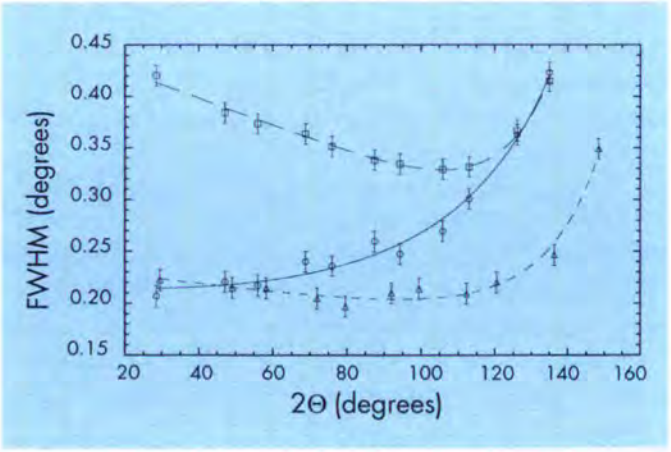

Fig. 4: Experimantal D2B resolution functions measured on standard samples (Si or Ge) for three instrument configurations. ***Squares****: high-intensity mode.* ***Circles****: high intensity mode with a 1 cm slit in front of the monochromator.* ***Triangles****: high-resolution mode (5' primary beam collimator) with a 1 cm slit in front of the monochromator. The lines represent fits obtained using the Cagliotti function.*

The secondary beam tube has been modified to house a liquid N_2-cooled beryllium filter as well as other future "insertion devices". Using the Be filter, a clean 6.05 Å beam can now be obtained. This option allows extremely high resolution to be attained on Bragg reflections with d>3 Å, and should be ideally suited for studying the effect of coherence length and strain on magnetic structures.

Most of the data treatment is now performed on a dedicated Silicon Graphics Indy workstation, which is also equipped with on-line data visualization. Standard files are produced for the popular Rietveld programs FULLPROF and GSAS.

The sample table has been equipped with an automated lifting mechanism, with a maximum load of 300 kg. This device allows the heaviest sample environment equipment (including the 10 Tesla cryomagnet) to be safely installed.

D3 Polarized Neutron Diffractometer on hot beam H4

From after the restart of the reactor, the instrument has been tested, aligned and calibrated using Heusler and CoFe polarizing monochromators/samples for both channels A and B. Calibrations were made directly with the 4.6 Tesla cryomagnet and the directions and amplitudes of the magnetic guide fields were set, leading to an optimized flipping efficiency. The dead-time of the detector is taken into account which allows count-rate up to 70.000 counts/s. Using the in-shield carousel system for automatic insertion of resonance filters, very weak $\lambda/2$ contamination is measured for both CoFe and Heusler monochromators. First experiments scheduled at the end of February were performed successfully, and the instrument has been running smoothly since then.

Printers and workstations are now installed in an adjacent area which is shared with Cryopad. The data reduction programs are available on the Silicon Graphics workstation d3sgi. 3D-visualization of the magnetization density can be done using a specific Explorer 3.0 based program. We plan to increase the RAM of d3sgi in order to better visualize magnetization density in large unit cells.

Next year, we plan to exchange the Camac/RSX aging data acquisition system for a VME/UNIX system with the help of the DPT group. We also plan to add a graphical user interface to the data reduction programs written by J. Brown.

CRYOPAD for Spherical Neutron Polarimetry (SNP) on IN20

The whole of the August-September cycle on IN20 was devoted to Spherical Neutron Polarimetry (SNP). The beam-time was divided into two periods, the longest, initial one being used for scheduled experiments compatible with Cryopad-I.

The Cryopad data acquisition system was restarted smoothly except for the two encoding systems on the nutation units (MicroControle) which have not been reliable for very long. The communication between the PDP11 computer and the new DEC-alpha of IN20 was quickly established by J. Allibon. The first experiment which dealt with manipulation and detection of magnetic domains in Cr_2O_3 (a unique capability of SNP) started right away. It was not seriously impeded by the recurrent blockage (every 24 hours) which developed on the variable temperature insert after a few days. After two long weeks struggle - a difficult summer holiday period! - we overcame the problem by changing all of the O-rings in the helium gas injection circuit. This was accomplished just in time to conduct the 1.5 K measurement on $CeAl_2$ (Other experiments had suffered from lost beam time and lack of good temperature control but did not fail completely since they did not require the lowest temperature). This last measurement was quite interesting as it showed qualitatively for the first time a small rotation of the magnetic interaction vectors resulting from the temperature variation of the "non-chiral $CeAl_2$ magnetic structure". Technically, the high sensitivity of the SNP technique to such very small magnetic changes is unique and due to its capability to observe transverse components of the final polarization. (Only the longitudinal component is accessible to Uniaxial Polarization Analysis in a magnetic guide field).

The final 10 days of the cycle were devoted to the first neutron test with the recently built Cryopad-II. The combination of a 20 cm diameter, widely accessible, cylindrical zero-field sample chamber with low stray-field nutators is a complete success, the so-called "nutation waves" being magnificent from the beginning. As regards the brand new, monolithic design of the precession coils, we could validate the computer design (M. Thomas) comprising a very unusual combination of toroïdal superconducting

coils sandwiched between two cylindrical Meissner shields. Overall, we may say that these tests were extremely satisfactory up to the point where we were stopped from finalizing the calibration and conducting the TbAlO3 "friendly test experiment" as we discovered that it was not possible to drive the precession currents from the computer because of faulty electrical insulation of the superconducting coils combined with a non-floating computer-interface. At the time we write this report the coils are being carefully rewound with a thin insulating layer of Al_2O_3 deposited on the bobins to cure the grounding problem, a variable temperature Orange Cryostat has been delivered which will fit in the R.T. chamber of Cryopad-II for low temperature work, the nutation encoders are being replaced with Heidenheim ones and a Silicon Graphics computer/Hytec Camac Interface has been acquired to replace the obsolete PDP11/Schlumberger data acquisition system.

D4 Fluids and Glasses Diffractometer on the hot beam H8

The recommissioning of D4, after the nearly 4-year ILL shutdown, encountered very few difficulties. In fact, a gain of about 10% in flux was found (normalized to the true reactor thermal power), believed due to the installation of a new doigt de gant and a slightly improved configuration of the monochromator. In addition, the detector cells previously damaged by the direct beam, constituting 1/8 of the total counts of the detectors, successfully "healed themselves" during the shutdown, presumably due to their not being under high tension for several years.

A very large user demand for D4 resulted in an overall beamtime division of 61% D4 / 39% IN1 for 1995 (i.e. including test time but not including commissioning time). The rejection ratio (in days) for the first semester was 118/59 = 2 to 1, and for the second semester 133/30 = 4.4 to 1. The recent round of proposals for the first semester of 1996 witnessed a 123/45 = 2.7 to 1 rejection ratio for D4.

Of the total amount of beam time given to D4 users (i.e. not including test time), a full 16% was lost due to instrument problems, the large majority being malfunctioning electronics (Camac) and associated software that caused scans to stop - very often during the night. These problems were finally resolved in early December 1995.

Although no experiments had to be postponed or were judged as failures due to instrument problems, some of the cryostat experiments had their data compromised by large temperature gradients across the length of the sample, especially for sample temperatures near 300 K. This problem was subsequently mitigated, and there are also plans to construct another sample environment for the bell jar which will function for temperatures between approximately -20 C and 150 C.

Of the 22 experiments performed at D4 in 1995, 16 came from college 6, 4 from college 5, and 1 each from colleges 7 and 9. Concerning sample environment for these experiments, 8 were carried out under ambient conditions, another 8 using the cryostat, 5 using the oven, and 1 using an external setup (high pressure).

Improvements to the instrument continued throughout 1995, including a new and slightly longer vanadium cryostat tail for the sample calorimeter, a better alignment of the detector collimation, a new "ensemble de pompage" for evacuating the bell jar which increases the convenience and security of this operation for the users, and the installation of data reduction and plotting software on the Silicon Graphics workstation. A new "alimentation four" will arrive in early 1996 to replace the antiquated version used until its failure point was reached, and a new set of vanadium sample cans is planned for purchase.

The D4c project received the Steering Committee's green light for funding to begin early in 1997, and we plan to begin work on a prototype in 1996. D4c will replace the present multi-wire detectors with micro-strip detectors similar to those recently developed for D20, increasing the detector area (and hence the count rate) by a factor of 10. Much of the detailed planning is contingent on performance tests of D20's detector, scheduled for early 1996.

D9 Four-Circle Diffractometer on the hot beam H3

24 single crystal experiments were successfully performed on D9 during 1995. Apart from minor problems with the stability of the multidetector (6 days were lost alltogether) the machine ran smoothly. Most of the experiments used the classical displex cooler (routinely down to 16K) or the 4-circle furnace from D9.

For one experiment the displex cooler was modified so as to allow the sample to be irradiated by an external laser at low temperatures. After adapting the large D10 goniometer table to D9, a pressure experiment using a standard orange cryostat was performed.

The project of building a 4-circle helium flow cryostat advances slowly but surely (cryogenics people were heavily demanded in 1995 for setting up dilution cryostat and cryomagnet experiments). Various pieces are already ordered, and the cryostat should be ready for testing in the first half of 1996.

In order to allow the use of cryomagnets, pressure cells, dilution cryostats and special furnaces in a more routine way the group is discussing the possibility of inclining the detector out of the equatorial plane on both D9 and later D10, as is already done on the now CRG instrument D15.

D10 Four Circle 3-Axis Diffractometer on thermal guide H24

D10 was up and running very shortly after the reactor restart, with just a few minor corrections to the control program and to the safety interlocks. The commissioning period was then spent successfully on real experiments to test the many configurations that D10 may adopt:

conventional diffraction data collection with the Eulerian cradle, measurement of phonons and magnons in four-circle geometry, and elastic and inelastic measurements with heavy sample environment, in this case study of the spin-Peierls compound $CuGeO_3$ at high pressure. The first scheduled experiment, on the incommensurate magnetic phases of Nd, was also a great success, despite the demanding schedule of sample and pressure cell changes. We especially thank Ted Forgan, Bill Nuttall, Paul Sokol and Dave Watson for their accepting to be our first external users, and for their untiring efforts to keep the instrument running efficiently during the experiment.

For the rest of the year D10 gave its habitual sterling service, with experiments covering a wide range of problems in structural and magnetic crystallography. Two of these were on the phase transitions in the perovskite manganites that exhibit giant magnetic resistivity and whch have recently triggered a flurry of activity in many laboratories. The new four-circle dilution cryostat (Fig. 6, page 160) has been used four times during the year, twice for scheduled experiments. Thanks to the dedicated efforts of Serge Pujol, the initial problems with excessive torsional flexibility in the ϕ shaft have now been rectified, and temperatures down to 0.11 K have been achieved and maintained in full four-circle geometry (Fig. 7). Two experiments exploited the computer control of the goniometer stage, used for heavier cryostats and furnaces, to access reflections in several reciprocal lattice planes. It is disconcerting to see a cryostat tilting through 20° seemingly of its own will, but the reflections appeared to prove that it works!

The conversion to control by Unix on a Silicon Graphics Indy workstation was begun in September, and two experiments in the last cycle were performed in this mode, both successfully. This required upgrade of the CAMAC controllers, and a complete rewrite and modernisation of the control program MAD by John Allibon, with emphasis initially on the commands and routines which are common to all diffractometers. Side-by-side with this work Franck Cecillion has begun constructing a common graphical user interface for all diffractometers. Full conversion to Unix and control by the graphical interface should be achieved by the first cycle of 1996, when refurbishment of the D10 cabin will leave no space for the trusty but old-fashioned microVax.

D19 High-Flux Single Crystal Multidetector Diffractometer on the thermal beam H11

Although D19 is often used as a Single Crystal Diffractometer its high flux and large position sensitive detector (PSD) make it suitable for High Angle Fibre Diffraction studies as well. Since the reactor restart more of the scheduled beam time on D19 has been taken up by fibres. Visitors performing experiments with single crystals expect to go home with structure factor amplitudes or even a refined structure, having made use of established procedures in the areas of data collection, display and processing. For the growing number of neutron fibre diffractionists the past year has marked a period of development: D19 visitors can now collect fibre data in the most efficient way and leave with processed data.

An optimum data collection strategy has been determined which involves precessing the fibre axis around the instrument axis so that the whole of reciprocal space is scanned. Data acquisition on D19 is controlled by a Vax running standard ILL software, MAD. Data display and processing for fibre diffraction is carried out on a Silicon

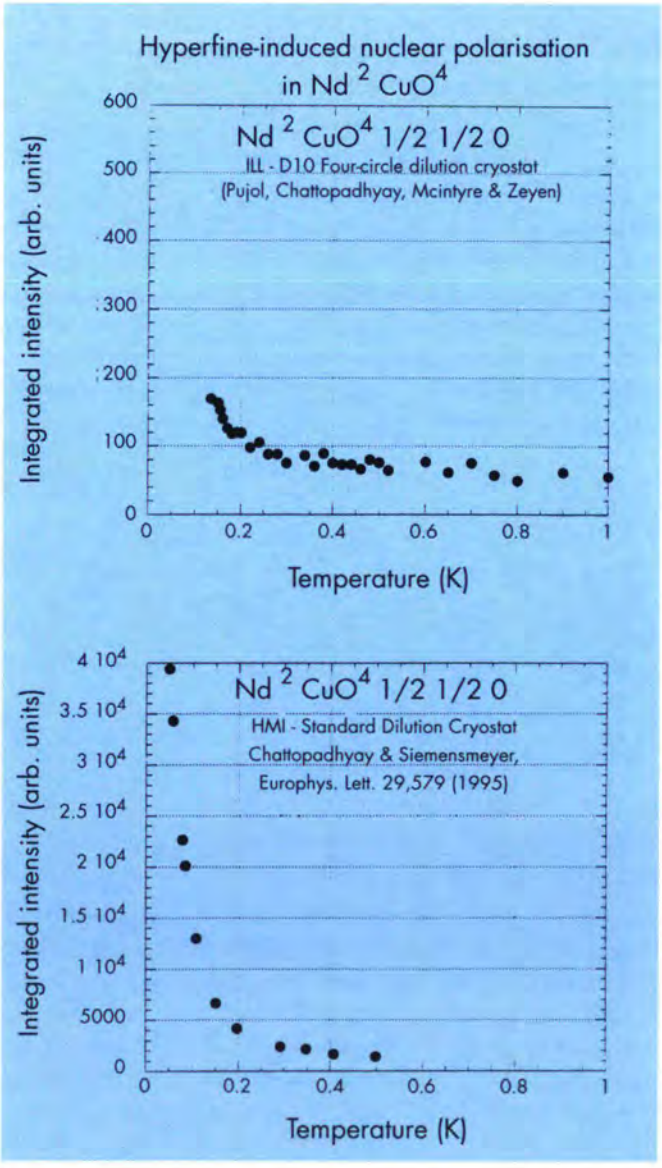

Fig. 7: Temperature variation of the superstructure reflection (1/2, 1/2, 0) due entirely to nuclear polarisation of Nd in Nd_2CuO_4, as measured with the D10 four-circle dilution cryostat and with a conventional dilution cryostatat HMI.

Graphics Indy. A suite of programmes for processing the data and binning it into reciprocal space has been written by Paul Langan. During the summer Mark Shotton, a long term visitor from Keele University, wrote a Graphics Interface for these programmes in Metacard, called mcFibre. McFibre accesses the new ASCII data base and visualises data using Pgplot graphics. The use of push buttons, menus and dialogue boxes minimises the amount of typed input required. These programmes have been made compatible with intensity integrating programmes from the BBSRC funded CCP13 project. Together MAD, mcFibre and CCP13 cover the full range of requirements for data collection and analysis using Fibre Precession geometry.

Some neutron diffraction studies require the amount of water in the sample under investigation to be controlled. This is usually achieved by regulating the relative humidity, RH, of the sample's environment. The traditional approaches to this problem are to enclose the sample in a cell and to either seal it with an appropriate saturated salt solution or to pass through it a gas, humidified to the desired RH by bubbling it through an appropriate salt solution. However in order to change the RH in a controlled manner over a wide range, salt bottles must be changed and the flow rate through these bottles carefully monitored and adjusted. These studies require constant attention and are often irreproducible. To circumvent these problems a system has been built for automatically controlling the RH: the D19 Automatic Humidity Control system (AHC). The AHC consists of a sample cell which is fed a mixture of wet and dry compressed air. The proportions of this mixture are adjusted by an electronic valve to obtain the desired RH inside the cell. The valve is operated by a controller unit which can respond in a programmed way to changes in RH as detected by a probe in the sample cell.

Software development is now concentrated on processing and displaying single crystal data. Many of the D19 utility programs already run on the Diffraction Group Unix cluster, as do the standard crystallographic packages, Shelxl, Xtal, etc; conversion of the main single crystal data processing program, Retreat - to access the Unix ASCII data base directly - is nearly done. Garry McIntyre has adapted Retreat for integration of peaks from incommensurate and quasicrystal structures. In Autumn 1995, the D19 PSD, which had been gradually losing He since 1986, was emptied, and purified gas added up to the design pressure of 6 atm. The design efficiency was thus fully restored. We thank Dominique Feltin and colleagues for their expert care in this delicate operation. Instrument development in 1996 will hopefully be concentrated on commissioning a new PSD. A brief description of D19 can be found on the World Wide Web (http://www.ill.fr/).

D20 High-Flux Multidetector on the thermal beam H11

Parallel activity on several items is continuing to make the whole D20 instrument available for users as soon as possible after the end of the detector construction. For details see "Projects and Techniques Division" (DPT).

After completion of the instrument, many tests have to be performed before the instrument will become ready for external users during summer 96.

Jean Pannetier has left ILL and D20. A young German scientist, Thomas Hansen, arrived on December 1st to complete the D20 team with Jacques Torregrossa and Pierre Convert.

A.W. Hewat

Large Scale Structures (LSS) Group

D11 Small-angle scattering diffractometer on the cold guide H15 (P. Lindner, L. Vuillard, P. Timmins, A. Polsak)

D16 Four-circle diffractometer on cold guide H16 (J. Zaccai, E. Bellet-Amalric, S. Wood)

D17 Reflectometer and small-angle scattering diffractometer on the cold guide H17 (H.-J. Lauter, R. Cubitt, M. Bonnaud)

DB21 Diffractometer for very large unit cells on cold guide H15 (E. Pebay-Peyroula (IBS; until 31.3.95), M.S. Lehmann, C. Wilkinson (EMBL), S. Wood)

D22 New small-angle scattering diffractometer on cold guide H512 (R. May, S. Egelhaaf, P. Timmins, P. George)

EVA Evanescent wave diffractometer on cold guide H53 (CRG-B, S. Odenbach, R. Günther, F. Adams)

The restart of the ILL reactor in January 1995 was an event of great excitement both for the ILL staff and for external users of the instruments. The dedicated and conscientious effort made by the technicians and scientists of the LSS group, with the very active collaboration of the technical services, allowed the instruments to come on line with an absolute minimum of commissioning. Indeed D11 was the first ILL instrument to receive users, on February 10th, only 5 weeks after the reactor start. The only major problem for the group was the unexpected failure of the D22 multidetector shortly after the beginning of the user program. Thanks, however, to the enthusiastic and highly competent work of the ILL detector group supported by the other services of the DPT the detector was able to be repaired in-house and will be ready for operation again early in 1996.

Apart from preparing the instruments for restart the major work of the shutdown had been the transformation of the computing facilities from the centralised VAX VMS system to a distributed UNIX system. In the LSS group this has been carried out under the guidance of Roland May and is now almost complete as far as data treatment facilities are concerned.

The LSS group now owns 6 Silicon Graphics workstations; 5 Indies and one Iris Indigo (D11, D17, DB21, D22 and two for general use). Ron Ghosh and colleagues from the Scientific Computing Group have upgraded and converted to Unix the suite of programs for treatment of small-angle scattering data and these are currently under test. Regrouped data are saved as single ASCII files in a newly defined standard ILL format. Information on the use of these programs is available from the ILL Home Page on the World Wide Web. In parallel, Didier Richard and colleagues furnished a SANS version of LAMP, a program for inspecting and treating on-line raw data and data stored in ILL's ASCII database.

On the instruments, the data acquisition program MAD worked well although the program for the creation of parameters (PARAME) for experimenters using the automatic sample changers on the small angle instruments proved to be too unwieldy to use efficiently. A summer student, Barbara Pfeifer, with the help of Michel Roure, wrote an interface program (SACHA) that replaces PARAME and simplifies the use of MAD for experiments with a sample changer.

D11 Small-Angle Scattering Diffractometer on the cold guide H15

First tests of the instrument after the restart of the HFR have immediately revealed a 100% increase in neutron flux using the new light-weight velocity selector CONSTANZE which had been installed in 1994. The new selector turns between 1900 and 8800 min^{-1}, corresponding to wavelengths between 20 and 4.5 Å. The wavelength spread is $\Delta\lambda/\lambda$ = 10.4 % at 4.5 Å, 11.2 % at 6 Å and 12.4 % at 10 Å as determined with TOF measurements (compared to $\Delta\lambda/\lambda$ = 10 % at 10Å with the old selector BRUNHILDE).

The beginning of the first cycle in 1995 was used for a systematic testing and, where necessary, improvement of all the components of the instrument. The new VME electronics worked reliably except for a problem with the TOF channel card which now seems to have been resolved. The new instrument control program MAD has been constantly improved and is operating well. A new program (SACHA) is now available for programming run sequences with the sample changer.

Concerning the sample environment, the sample table has been realigned with respect to the neutron beam height and direction. A vacuum sample changer using the horizontal rack plate is under construction and will soon be available.

Having been out of operation for 3 years and 11 months, D11 was made again available for users on the 10 February 1995. Since then the experimental program has been carried out routinely without major difficulties. 138 days of beamtime were used at D11 in 1995 for 73 different experiments, thus 1.89 days on the average per experiment. During the first year of operation after the restart a lot of "old" friends came back to measure at D11 but we also had the pleasure to welcome new users.

D16 Four-Circle Diffractometer on cold guide H16

Following its complete overhaul in 1994, D16 functioned smoothly throughout 1995 with a requested to available day ratio close to 2. Experiments on D16 require a very good

Q-resolution over a wide Q-range and include studies on lipid bilayers and their interactions with various molecules, two dimensional ordering in biological membranes and on graphite or MgO adsorbed layers, surface reflectometry in mixed liquids, magnetic ordering, polymers and clays.

The overall radiation background which is rather high around D16 was greatly reduced following a better protection both of the H16 guide and of the instrument itself.

During the whole year efforts were made in order to improve the performance of the instrument as a reflectometer, with a new boron nitride slit with a precision of a few µm, a translation table for the positioning of the sample and a sample holder for vertical samples. All these changes were optimised during an experiment performed at the end of the year and concerning the interaction of a peptide with a model membrane deposited on a Si substrate.

For data collection, the new MAD version, common to the diffractometers was implemented. It allows computer control of the slits, the beam stop and the new sample translations.

The reorganisation of the D16-D17-IN5 experimental area of the guide hall has been approved and will take place over the next 2 - 3 years. Concerning the D16 move to a new position, planning is in progress for improvements involving a guide three times the present height, a focusing monochromator, and a larger detector.

D17 Reflectometer and High Resolution Small-Angle Scattering Diffractometer on the cold guide H17

D17 runs both as a reflectometer and still as a small-angle scattering diffractometer. As soon as D22 is operating satisfactorily after its detector repair the main activity of D17 will be shifted towards reflectivity experiments. Several major improvements to the instrument were made in 1995. A variable slit system is in place for reflectometry. The data acquisition electronics was changed to VME during the October - November shutdown and subsequent tests have shown it to be operating satisfactorily. A Silicon Graphics Indy workstation operating under UNIX has been installed in the instrument cabin for data analysis.

The instrument can be used at constant wavelength with a 5% wavelength selector, a 10% wavelength selector or with a chopper for TOF. A first TOF reflectometry experiment was carried out, but it is still too early to run it as a TOF instrument for users.

D17 can be used for the investigation of magnetic films in the reflectivity mode although the polarisation of neutrons has still to be improved.

The start of a project to convert D17 into a dedicated and optimised reflectometer was agreed. It will take up to 1998 to straighten the H17 and H18 guides, which will have D16 and D17, respectively, on their end positions. Thus IN5 on H16 will have also a full guide at its disposal, because D16 will have moved out of H16. The new D17 reflectometer will run in TOF in the main mode and will make use of a greatly increased neutron flux in the H18 guide in the range of at least 3 to 30 Å. For this reason the H18 guide will have supermirrors for the upper and lower surfaces and a focussing end-piece in front of the sample position. The spectrometer itself will also be redesigned. To take advantage of the vertically focusing guide the instrument will be used for investigating vertical surfaces. D17 will be flexible in resolution in order to adapt to the requirements of the various kinds of samples and thus to give optimised signal intensities. An option with a multilayer monochromator is planned mainly for the use of polarised neutrons.

DB21 Diffractometer for Very Large Unit Cells on the cold guide H15

At the start-up the new Vax-station installed during the long shut-down was tested successfully before being put into operation. Since then it has worked well, but problems are appearing on the level of the electronics, which in a few cases have briefly stopped the measurements. This should be handled next year when the instrument - as planned - will be transferred to VME electronics under the control of a Unix workstation.

Apart from this the instrument has worked well with a healthily growing demand, and to help in the analysis a Silicon Graphics Workstation belonging to the LSS group has been installed in the instrument cabin and equipped with a CD-ROM disk reader.

Work on automatisation of the detector movement on air-pads has progressed, and the system will be tested at the end of the year.

The instrument still uses the Anger camera as two dimensional area detector, but the leak problems of the new detector have now been fixed, and the assembly has been started (D. Feltin, A. Rambaud).

D22 New Small-Angle Scattering Diffractometer on cold guide H512

The construction of D22 was completed during the long shutdown and commissioning was begun as soon as the reactor restarted. User operation commenced at the beginning of the second cycle with the first experiment taking place on April 5th 1995.

Several experiments were carried out successfully, but unfortunately soon after the start of the experimental programme the detector showed signs of malfunctioning. They did not disappear even when the high tension was lowered to a value which jeopardized correct addressing by the coincidence unit of the detector electronics. Therefore, the decision was taken to open the detector for inspection and repair. Several reasons were identified that explain the electrical discharges which apparently were at the origin of the problems. The ILL detector group, with the help of other services, repaired the detector, and first tests with a neutron source indicated a successful completion at the end of the year.

The access to the sample zone was simplified after a revision of the safety procedure. The sample zone is now enlarged in order to allow users to take advantage of the high maximal flux of the instrument. According to gold foil activation and calibrated-monitor measurements, the flux at D22 exceeds 10^8 $s^{-1}cm^{-2}$ on the sample position for optimal collimation and wavelength conditions (selector at $\Delta\lambda/\lambda$ = 10% FWHM). The sample environment was extended by a vacuum vessel with dimensions largely similar to those of the D11 "cloche". A new shorter aperture holder was constructed for the exit side of the collimation box, and also a new silicon entrance window into the detector will soon help to facilitate experiments with bulky devices.

The instrument control program MAD (Michel Roure) is performing in a very satisfying way. A manual for its use, as well as other information about the instrument is available on-line on D22's Power Macintosh in the World-Wide Web standard format HTML. Xavier Claeys, a summer student, worked on a program under Windows for controlling the Dornier velocity selector. This task was continued by a programmer staying at the ILL in the framework of an educational contract, Cathérine Misse. The aim of this exercise is the integration of the selector control into the instrument control program.

EVA Evanescent Wave Diffractometer at the cold guide H 53 (CRG-B)

The upgrading of the instrument control for the reflecto-diffractometer EVA was completed in 1995. The newly installed 486 PC running the SPEC software package under LINUX directly controls all important instrument components such as stepper motors, the monitor counter and detectors and additional devices such as e.g. the air cushions on the 2θ-arm. With the help of SPEC's macro programming, all these processes can be easily combined into user-defined scans. This enables external CRG-B users to implement scanning routines which are well-suited for their specific experimental problem. After completion of the basic instrument control, further options and improvements were developed:

- The polarization system, consisting of CoTi-multilayers (provided by Prof. Schärpf, ILL), spin-flippers and magnetic guide fields, was finished and set in operation at the end of 1995.
- In addition to the position sensitive detector (PSD) on the 2θ-arm, a second PSD was installed in the forward direction. This detector will allow the simultaneous measurement of reflectivity and surface-sensitive Bragg diffraction of a sample.
- Close collaboration with the radioprotection group throughout 1995 made possible a reduction of the gamma-noise mainly produced by air-scattering inside the casemate down to ca. 10% of the starting value in January.

The new UHV sample environment for temperature dependent evanescent Bragg scattering and reflectivity measurements under the influence of external magnetic fields was built at the home institute in Wuppertal. It is expected to be installed at EVA in the beginning of 1996.

The performance of the instrument has been tested since last summer by measurements on free Ni (110) surfaces. We studied the reflectivity of these samples down to ca. $4*10^{-5}$ at an angle of incidence of 3.7°, corresponding to ca. 7*the critical angle. We thus found surface roughness values of less then 10 Å. Grazing incidence diffraction on Ni(110) was performed for the first time and allowed the characterization of two different samples with regard to their surface and bulk mosaicity and the misalignment of their surface with respect to the (110)-direction.

Within the framework of the new CRG-B status of EVA, a first external user (T. Baumbach, ILL) performed measurements on various layered systems, e.g. GaAs/GaInAs superlattices. Apart from strong reflectivity and diffuse scattering in the forward direction, first evidence of grazing angle diffraction on this kind of samples was found. Further CRG-B beamtime has been requested by several external groups for the beginning of 1996.

Laboratories

The Chemistry and Biochemistry laboratories of ILL, located on the 2nd floor of ILL20, are available for sample preparation for users of the neutron beam instruments. In 1995 the ILL signed an agreement with the ESRF for a reciprocal use of the two institutes' Chemistry facilities which broadens significantly the range of equipment available to users. For Biochemical users facilities are also available in the laboratories of EMBL.

Chemistry Laboratory

(P. Lindner, P. Chenavas, M. Romero)

The Rheometrics RFS II fluids spectrometer has successfully been put into operation. It served already to four different user groups for rheological characterisation of their samples.

A new PAAR DMA 58 density meter with an automatic sample changer (min. sample volume 2 ml) has been purchased and installed in the chemistry laboratory.

Biochemistry Laboratory

(L. Vuillard, P. Chenavas, M. Romero)

The biochemistry laboratory provides biochemical users with facilities complementary to those available in the EMBL laboratories. In 1995 these facilities were enhanced by the provision of a fully operational HPLC system and a new ultra-violet and visible spectrophotometer. The laboratory was also used in a collaborative project with the ESRF on protein isolation and purification.

Peter Timmins

Three-Axis Spectrometers (TAS) Group

IN1, IN1Be	3-axis and Be-filter spectrometers on the hot source beam tube H8 (B. Roessli, B. Dorner and P. Palleau)
IN8	3-axis spectrometer on the thermal beam tube H10 (J. Bossy, B. Dorner and D. Puschner)
IN14	3-axis spectrometer on the cold guide H53 on the horizontal cold source (N. Pyka, R. Currat and A. Brochier)
IN20	3-axis spectrometer for neutron polarisation analysis and spin-echo option (TASSE) on the thermal beam tube H13 (J. Kulda, T. Baumbach and P. Flores; C.M.E. Zeyen for the TASSE option)
IN3	3-axis spectrometer on the thermal guide H24 (CRG-A, M. Zolliker, W. Bührer, P. Decarpentrie)
IN12	3-axis spectrometer on the cold guide H142 (CRG-B, W. Schmidt, B. Fåk, J. Previtali)

1995 was the first year of normal experimental activity after the extended reactor shutdown. For the TAS Group, it came after a period of intense instrumental activity, with reassembly, reinstallation and major electronic upgrading work on 3 out of 4 machines. Thus the January startup provided a crucial opportunity to check the performance of the newly upgraded spectrometers, through extensive test and recalibration campaigns scheduled during the first reactor cycle, and on real experiments, thereafter. In general the instruments performed very satisfactorily. Details may be found below, under the relevant instrument heading.

The instrument control hardware and software (programme TASMAD) was almost completely renewed on all 4 instruments during the reactor shutdown. On three of them - IN1, IN8 and IN20 - VME electronics in an autonomous crate is used to handle the low-level control and data collection tasks. As the reliability of the new system proved excellent, plans are underway to convert IN14, the last instrument in the group still on the CAMAC standard, to VME by the end of 1996. The new control system of each instrument is completed by a dedicated DEC-α workstation (operating under Open VMS for the time being), connected to the VME crate via ethernet. An additional X-terminal and Macintosh is available on each instrument for on line data treatment. This set-up has operated satisfactorily, particularly for instruments using the VME electronics, after some initial adjustments.

The group is actively engaged in a program of software developments, concerning both the spectrometer control programme TASMAD and the data reduction programmes, in collaboration with DPT-SCI (A. Barthélémy) and DS-SC (A. Filhol, D. Richard, G. Kearley), respectively. This work includes the implementation of the general purpose resolution programme RESTRAX (J. Saroun, J. Kulda), the development of a data visualisation programme under IDL (D. Richard, G. Kearley) and further work on the data analysis programme PKFIT (A. Bouvet, A. Filhol).

IN1 and IN1Be: 3-axis and Be-filter spectrometers on the hot source beam tube H8

The 3-axis spectrometer IN1 shares the H8 hot-beam position with the Be-filter spectrometer IN1Be and the liquid diffractometer D4. The three instruments operate on a time-sharing basis with a common monochromator and primary protection.

Most of the current effort aims at reducing the instrument's background, by installing additional B_4C shielding elements inside the analyser and detector drums and by using suitable combinations of resonance filters. IN1 is often used at low scattering angles, when air scattering in the sample area and scattering from the sample container are major sources of background. In this context a large (Ø 100 cm) vacuum box has been designed, which can be used as the primary vacuum chamber for cryostats and ovens. This set-up provides for a longer neutron beam path in vacuum and reduces the amount of aluminium in the incident and scattered beams. As a result of this, together with improvements in the beam stop positioning mechanism, useful measurements can now be performed with scattering angle values as low as $2\theta = 2.5°$ (compared to 5° previously).

Several tests were carried out using horizontally focusing analysers, pyrolytic graphite and perfect, elastically bent Si(111), with fixed vertical and variable horizontal curvature (see blue box below). These preliminary measurements confirmed that significant intensity gains can be achieved on IN1 through the use of horizontal focusing, with no (or minimal) costs in terms of instrumental resolution and signal-to-noise ratio. In the case of the Si(111) analyser an additional bonus is the suppression of the $\lambda/2$ contamination. Further consideration will thus be given to optimising such an analyser for specific use in the IN1 wavelength range.

In order to verify the performance of the instrument, a one-day test experiment with a sapphire (Al_2O_3) sample was performed. The same sample was examined in March 1991, a few weeks before the reactor shutdown. As a first observation, the lattice parameter turned out to be the same as four years ago within less than $1^o/oo$. This gives the confirmation, that the wavelength alignment of IN1 is as good as before. Then 12 inelastic scans were repeated with the same monochromator Cu(220) and analyser Cu(200) crystals and with the same collimation 25-20-40-40 throughout the spectrometer. In Fig. 1 one old and one new scan is presented, where each measured point is normalized to 100 sec counting time. This seems to be the best way to compare the results. The new scan is 10 to 20% higher than

the old one. Similar ratios were obtained for 9 out of the 12 scans, while 3 scans - along the 3-fold axis of Al_2O_3 had a lower ratio with 10 to 20% less intensity. In most cases, the background scales with the signals. In conclusion, the intensity of IN1 appears to be about 10% higher than before the reactor refurbishment. The main reason is probably a reduced water gap between the hot source and the thimble.

A number of molecular spectroscopy experiments using the IN1/Be-filter spectrometer have been performed. The spectrometer was used in the low-resolution mode, i.e. without the graphite filter option. The results showed that the instrument's high luminosity can be of great interest for experiments where flux is preferred to resolution (weak scatterers) or when only a selected energy transfer range is of interest. Further experiments and tests using the Be-filter/graphite-filter combination are planned.

IN8: 3-axis spectrometer on the thermal beam tube H10

The IN8 spectrometer has been operational for scheduled experiments since the February reactor startup. A total of 21 scheduled experiments were performed during the year with only 5 days lost due to instrument failure.

During the March-April shutdown, a new pyrolytic graphite analyser was installed with fixed vertical curvature and adjustable horizontal curvature. The new 36-piece composite analyser is used in conjunction with a 5-bar cylindrical ^{3}He counter mounted with its axis vertical. This set-up replaces a smaller vertically focusing unit used with a horizontal axis 3-bar counter. Here again significant intensity gains (up to a factor 5) have been obtained, with little effect on the observed instrumental resolution widths and signal-to-background ratios.

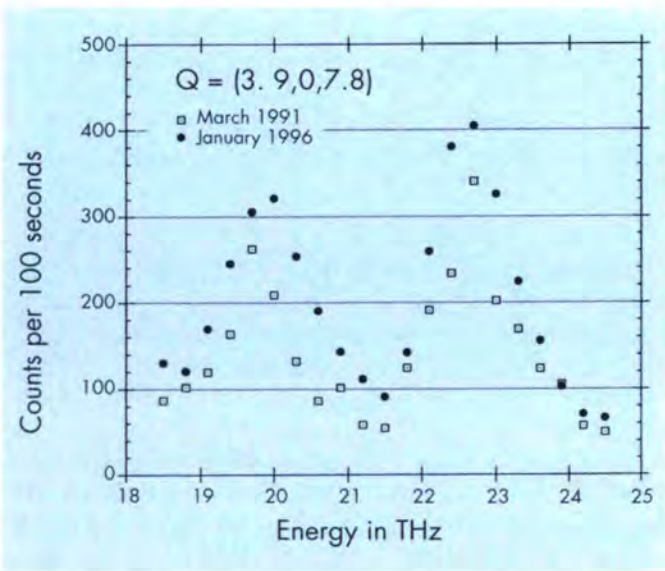

Fig. 1: Two identical inelastic constant-Q scans performed before and after the reactor shutdown on IN1 with the same sample of sapphire (Al_2O_3). The data points are individually normalized to 100 sec counting time.

The detailed performance of the new analyser will be given in a forthcoming report [1]. The best use of horizontal focusing arises in the case of weakly dispersive excitation branches and small (<1 cc) sample volumes. A situation of that type was encountered in spin wave measurements on a 240 mm^3 single crystal of neptunium bismuthide [2]. In that case the intensity gain associated with the use of the focusing analyser proved crucial to the detection and characterisation of the unusual magnetic excitation spectrum of this exotic compound.

IN14: 3-axis spectrometer on the cold guide H53 on the horizontal cold source

During the extended reactor shutdown the IN14 monochromatic beam geometry has been modified in order to reduce the monochromator-to-sample distance from 270 to 210 cm. The secondary beam shutter and the Soller collimator (or polarising bender) is now integrated into the primary protection. As a result, the monochromatic neutron flux at the sample position has increased by a factor of 1.3 and the 'beam–off' γ-background in the experimental area is now acceptable.

A number of modifications have been implemented in connection with instrument safety. New biological shielding, stationary and mobile, has been installed at the periphery of the experimental area; the software in the electronic module controlling the positions of the monochromator protection blocks has been rewritten; safety procedures have been redefined and/or clarified.

Current efforts are devoted to improving the instrument's performance in the polarised beam mode of operation. The users' demand for polarised beam inelastic scattering is considerable and only limited by the large intensity loss associated with the process of spin-polarisation on the incident neutron beam and of spin-analysis on the scattered beam. In the thermal neutron range this loss typically amounts to a factor of 9 to 15, depending upon the polarising technique used. Since the measurement of both spin states adds another factor of 2, the total loss factor is of the order of 25, compared to a classical inelastic set-up.

The situation is not quite as catastrophic in the cold neutron range, because of the good reflectivity of Heusler crystals at long wavelengths. On IN14 Heusler crystals are used in the analyser position but, given the upstream position of the instrument on guide H53, the use of a highly absorbing Heusler monochromator is precluded. The spin-polarisation of the beam incident on the sample is therefore achieved by mounting a FeCo/V supermirror bender in the monochromatic beam. Two different benders are now available, one optimised for 14 meV neutrons, with a 25% up-spin transmission, and one optimised for neutron energies in the range 2 to 5 meV, with an up-spin transmission of the

order of 50% in that range. Both have polarisation characteristics in the range 90 to 95%, which is more than adequate for inelastic scattering work.

Recent measurements have been performed in order to test the performance of the Heusler analyser in the horizontal focusing mode (see Fig. 2, page 161). Although this possibility had been foreseen at the design stage, the focusing and polarisation properties of the Heusler analyser have only been tested recently. Tests were performed on a small vanadium sample with the α_3 and α_4 Soller collimators, normally mounted before and after the analyser, replaced by appropriate diaphragms. The results show an intensity gain of a factor 4 to 5, depending on neutron energy, with an energy resolution equivalent to a α_3/α_4 = 40'/60' configuration at 14 meV (α_3/α_4 = 40'/40' at 2 meV). The measured energy resolution width as a function of neutron energy is shown in Fig. 3. Additional measurements showed that the use of a broad diverging beam at the analyser position produces only minor beam depolarisation.

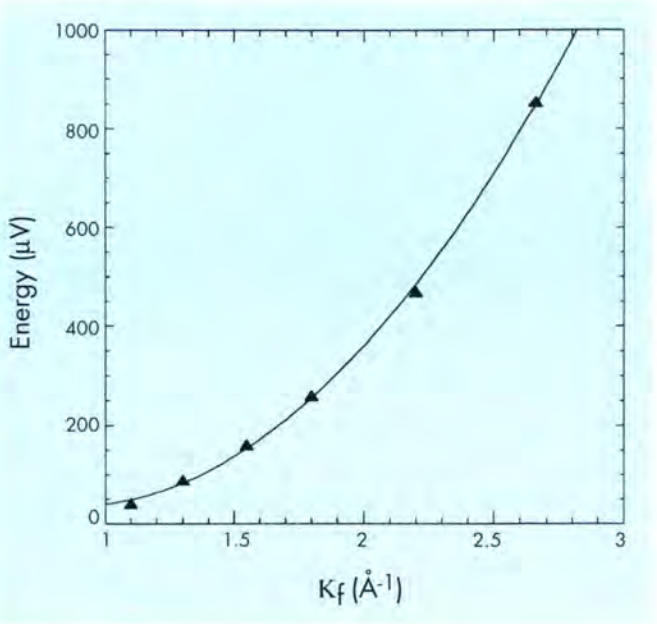

Fig. 3: Focusing Heusler analyser: Energy resolution (μeV) vs k_f (Å^{-1}) with α_2 = 40'.

IN20: 3-axis spectrometer for neutron polarisation analysis on the thermal beam tube H13

The reinstallation of IN20 was completed in early January, in time to begin the instrument alignment and calibration using the very first neutrons available after the reactor restart. Part of the commissioning experiments, in the unpolarised mode, was devoted to tests of the newly installed elastically bent perfect Si 111 monochromator and analyser. The characteristics of these new generation devices are presented in more detail in the following "blue box". To summarize: the IN20 silicon monochromator used in an open geometry provides a monochromatic flux at the sample position (k_i = 3-4 Å^{-1}) about twice as intense as that of Cu 111 (with α_2 = 40' Soller collimation) at essentially the *same* resolution. Similarly the Si 111 analyser provides, in an open geometry, a resolution comparable to PG 002 (with α_3 = 40') but the count rate in the detector is 3-5 times higher depending on sample size. At the same time the second order of the Si 111 reflection is forbidden so that the neutron energy can be varied freely without restrictions imposed by the use of a PG filter.

Tests in the polarised mode were performed during the second half of February. Reasonable values (85-90%) were obtained for the beam polarisation, under a variety of experimental conditions (Helmholtz coil, cryomagnet 0-6 Tesla) and for a wide range of thermal neutron energies. At the end of the first reactor cycle the overall performance of the instrument was verified in the course of two polarised beam experiments involving external users.

The regular exploitation of the instrument for scheduled experiments started at the beginning of April and since then IN20 has worked reliably, most of the time in the polarised mode, either with the 6 Tesla cryomagnet or with the 3D Helmholtz coil. The entire cycle of August/September was devoted to experiments with CRYOPAD (zero field neutron polarimetry) including the first successful operation of the new CRYOPAD II. On the other hand, the installation of the TASSE spin-echo option had to be postponed until the following year due to problems with the cooling system of the superconducting coils (see below). The other major event scheduled for 1996 is the test of the ^{3}He polarising filter which, in case of a positive outcome, should provide a substantial gain in polarised neutron flux at higher thermal energies.

TASSE: Spin-echo option on the polarised beam 3-axis spectrometer IN20

The IN20 neutron tests of the superconducting spin-echo coils had to be postponed due to cryogenic problems with the three-stage cryocooler systems developed at the SBT/CENG. The origin of the trouble has now been identified. The Joule-Thomson stages were in fact overheating and cracking the lubrification oil. The cracked hydrocarbons having a wide range of low temperature melting points were then periodically blocking the system. The cure is a simple increase of the oil throughput of the compressors. We hope that the cryogenics will run smoothly for the next beam test-time in May 1996.

Meanwhile, following successful experiments on a simple and inexpensive spin-echo option based on the same **O**ptimal **F**ield **S**hape principle (OFS) on the Japanese Spectrometer PONTA of ISSP Tokyo, the future of this technique looks even more promising. With an investment of 100 k$ it has been possible to build optimised resistive precession OFS coils which improved the energy resolution

from the classical 1 % to 10^{-5} (0.15 μeV FWHM at 16 meV incident energy). The OFS coils being very short, no significant intensity loss from the normal polarised mode of the spectrometer could be observed. They are designed to accept large beam divergencies without loss of spin-echo quality.

Although even better energy resolution can be obtained with the super-conducting OFS coils at the ILL (a factor of 50 better expected), this extremely high resolution is really useful for quasielastic scattering at high momentum transfer. This represents a very spectacular extension of the (hω,Q) range accessible to neutron spectroscopy and not covered by other techniques such as backscattering.

However, for inelastic work, for example the investigation of the lifetimes of elementary excitations, the resolution obtained with resistive OFS coils can for the moment be considered sufficient. This is due to reasons inherent to NSE: for typical TAS momentum and energy distributions, the relation between the energy transfer and the spin-echo phase becomes non linear with increasing energy transfer and better energy resolution, i.e. larger precession number. The practical upper limit lies at about 1000 precessions, a number which can be obtained for thermal neutrons with resistive OFS coils.

Resistive coils of the type of those built on PONTA are ideally suited for phonon work because they allow the best possible use of the neutron flux available on a TAS. Their short construction and nevertheless large inner diameter cause no intensity loss (distances monochromator-sample-analyser only slightly increased) and allow all possible focusing tricks compatible with the experiment to be performed to maximise the intensity.

With these ideas it could be judicious at the ILL to build a second set of resistive OFS coils, together with gradient coils necessary for phonon focusing, for a high intensity ILL three-axis spectrometer to specialise on phonon work. The present IN20 TASSE with the superconducting OFS coils could then efficiently cope with quasielastic scattering at high momentum transfer and nanoeV resolution and flat branch (nondispersive) spectroscopy.

The short resisistive OFS coil TASSE option, which just as the Japanese set could be built at low cost, will have to be designed to yield maximum neutron intensity. The ILL three-axis spectrometer best suited for this will have to be determined based on intensity calculations.

IN3: 3-axis spectrometer on the thermal guide H24

The 3-axis spectrometer IN3 was one of the first generation instruments of the ILL. Since then, more powerful machines like IN8 and IN20 have been built, and IN3 has become a second priority instrument. Already before the reconstruction of the reactor it was operated as a CRG instrument. In December 1994 a 3-year CRG-A contract was signed between ILL and the Laboratory of Neutron Scattering (ETH Zurich & PSI Villigen; local representative: M. Zolliker). Following the terms of the contract, 50% of the beam time is allocated to the contracting CRG group and 50% to ILL users.

After the long shutdown the electronics, the mechanics and the floor had to be revised. The good collaboration with technical and scientific staff at the ILL made it possible for the spectrometer to be ready by the time the first neutrons arrived on the monochromator. After a four week test period normal experiments have been performed, since March 1995. Due to a project in the neighbourhood of IN3, a short interruption was necessary in August for a recabling of the instrument. Thanks to the effort of the electronic staff of ILL, the work could be finished in the shortest possible time, with a beam time loss of three days only.

In a step by step process, the instrument was tuned to higher intensity and better reliabilty:

- The copper monochromator was revised (it was operated with only two well focused lamellas instead of five in the first cycle).
- A converging guide (Fig. 4, page 161) with supermirrors has been installed to increase neutron flux at the sample position. For low energy transfer at the standard configuration (K_F = 2.662 $Å^{-1}$) the integrated intensity is about 80% higher with practically the same energy resolution [3].
- The minimal distance sample-analyser has been reduced from 110 cm to 84 cm to increase the integrated intensity by a factor 1.7, with almost no loss in energy resolution (focusing analyser).
- The motor-positioning software has been modified in order to reduce problems when driving the spectrometer arms.
- A parasitic peak (Si 220 reflection) on the graphite analyser has been eliminated. Cadmium sheets were mounted to cover the silicon support. (A similar problem remains on the graphite monochromator).

Another insufficiency remains in the positioning of the monochromator shielding blocks. The safety circuit shut the primary beam on several occasions, due to positioning errors on one block, as a result of which several nights of beam time were lost. Nevertheless, the overall loss of beam time caused by instrument failures was less than 3%.

IN12: 3-axis spectrometer on the cold guide H142

IN12 is operated as a CRG-B instrument by KFA-Jülich in collaboration with CEA/Grenoble with 30% of the beam time being used by the ILL. Scheduled experiments have been performed under normal conditions since April 1995. The modifications of the secondary beam shutter and of the support for the optical bench in the incident beam, carried out during the shutdown, have proved very useful and it is now easier to change the collimator between monochromator and sample as well as to align the

supermirror bender. The magnetic parts of the sample table have been replaced by non-magnetic materials to allow the use of the 12 Tesla vertical field superconducting magnet of CEA/Grenoble. The installation of a permanent guide field before the analyser has improved the flipping ratio in polarised mode. We have obtained a flipping ratio of 85 at a wave vector of 2.0 $Å^{-1}$ from a Bragg peak of a standard sample, using the IN12 supermirror bender and Heusler analyser. A modern programmable logic control has replaced the old relay control system for the monochromator shielding blocks. With this change we have achieved a much higher standard for safety and reliability.

Roland Currat

References

[1] J. Bossy, "Use of IN8 with a horizontally focusing analyser", ILL Technical Report (in preparation).

[2] F. Bourdarot, P. Burlet, L.P. Regnault, B. Fåk, J. Bossy, G. Lander, J. Rebizant, J.C. Spirlet, "Magnetic excitations in NpBi" (to be published).

[3] See: "Realisation of a horizontally focusing guide on IN3" by J. Mesot, W. Bührer, M. Zolliker, P. Böni, M. Koch and P. Decarpentrie, ILL experimental reports 1995.

Experience with the elastically bent silicon monochromator and analyser on IN20.

Jiri Kulda, Institut Laue-Langevin, Grenoble

Vertically focusing monochromators and analysers composed of arrays of mosaic crystal slabs were proposed in the early 70s [1] and soon became a standard at ILL. Horizontal focusing [2], although tried out shortly after, is less common due to a more complicated mechanical design as well as the more intriguing influence of the curvature on the spectrometer resolution. Well-documented experience with fully focusing TAS set-ups is much more recent [3, 4] and exists in a few laboratories only; most recently such a pyrolitic graphite analyser became available on the IN8 spectrometer. In all these cases the focusing assemblies are composed of mosaic crystals (PG, Cu), whose misorientation widths η about 30' enable sufficient reflecting power to be achieved, but on the other hand they introduce an additional divergence of the order of 2η into the monochromatic beam, which relaxes the energy resolution and smears considerably the focal spot at larger distances. In this contribution we would like to report on the first experience obtained with a vertically and horizontally focusing monochromator and analyser installed on IN20 and using elastically bent perfect Si 111 crystals [5].

To understand the two-fold effect of the elastic deformation, which provides horizontal focusing and creates an effective "mosaic spread" in the crystal at the same time, an elastically bent crystal can be imagined as a pack of thin lamellas [6]. If the focusing condition is met, the local misorientation of each thin lamella is such that the beam diffracted at any place on its surface would pass through the same focal point. By adding more layers one extends the focal point in the transverse direction and augments the flux through a sample of finite volume (Fig. 1a). As a consequence, one may expect a focal spot size comparable to the thickness of the bent crystal with little dependence on the distance found with diverging beams from mosaic crystals (Fig. 1b).

The bending holders of the silicon monochromator and analyser of IN20, whose photograph is displayed in Fig. 2, page 161, use a four-point bending scheme which allows one to achieve a good approximation of cylindrical bending between the two inner supports. In the course of their design we have extensively benefited from the experience obtained at NPI Rez near Prague and at PTB Braunschweig [7] with the construction of similar prototypes of focusing monochromators using elastically bent silicon crystals. The final realisation differs, however, profoundly from its predecessors. The

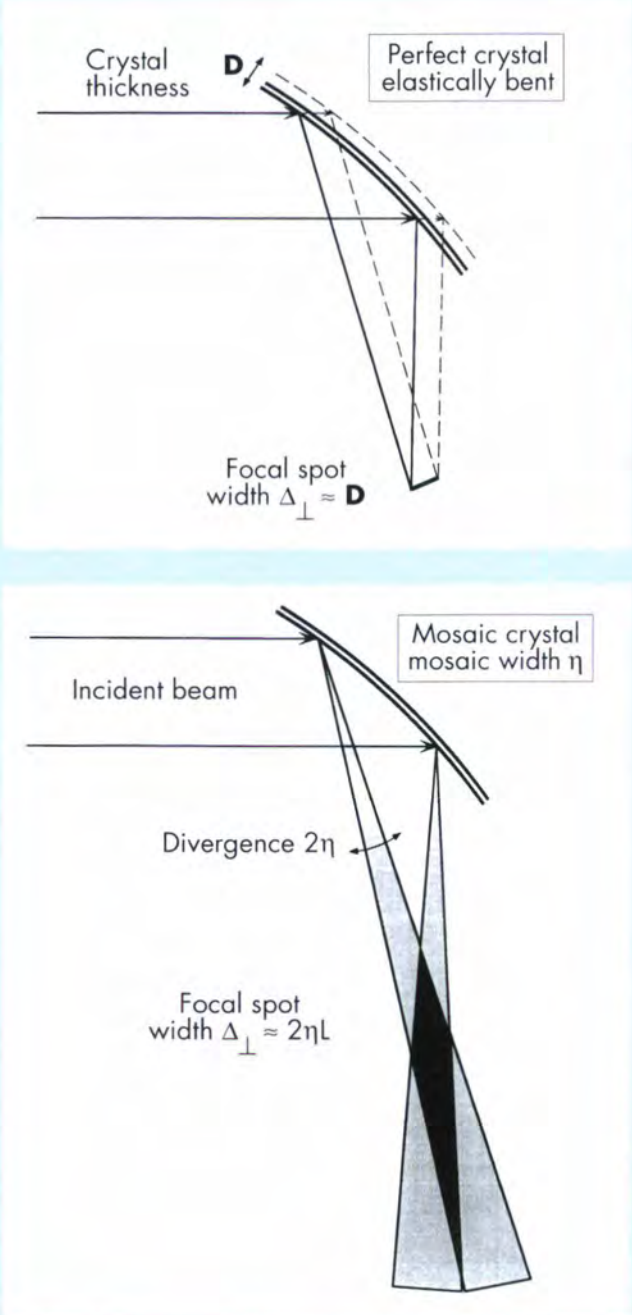

Fig. 1: Horizontal focusing of an incident parallel polychromatic beam by an elastically bent perfect crystal (a) and by a mosaic crystal (b). In the case of negligible absorption, the focal spot width depends essentially on the thickness of a perfect bent crystal, while the mosaic spread introduces an additional beam divergence which smears the focal point proportionally to the focusing distance L.

horizontal bending force is transmitted from a remotely controlled step motor by a worm gear, camshafts and levers instead of the screw with differential threading in the original design. All the crystals are mounted with their front faces parallel and the fixed vertical focusing is brought about by an inclination of the reflecting planes in the top and bottom plates by means skew cuts. In order to achieve crystal curvatures needed for real space focusing (bending radii down to about 5 m) and to keep sufficient reflecting volume at the same time, single silicon plates were replaced by packs of 2 or 3 plates of 200 mm length and 40 mm height with an overall thickness of 10 mm. In the course of cutting special care had to be taken to preserve the parallelism of the crystal faces so that mutual misorientation of the plates in the final assembly was kept below 2' of arc as checked by γ-diffractometry. Only in a few cases additional Al spacer foils had to be introduced between the plates to correct their orientation.

The output fluxes of the different IN20 monochromators, measured at sample position with a calibrated monitor having a circular aperture of 10 mm diameter, can be compared in Fig. 3. The results were obtained with a 40' Soller collimator after the mosaic monochromators PG 002 and Cu 111, with 60' in the case of the Heusler 111 and without collimator in the case of Si 111, as would correspond to their routine use. The data are corrected for the second order contamination, being important for all of the PG, Cu and Heusler monochromators at k_i below 4.5 Å^{-1}. The output flux of the silicon monochromator reaches about 1/2

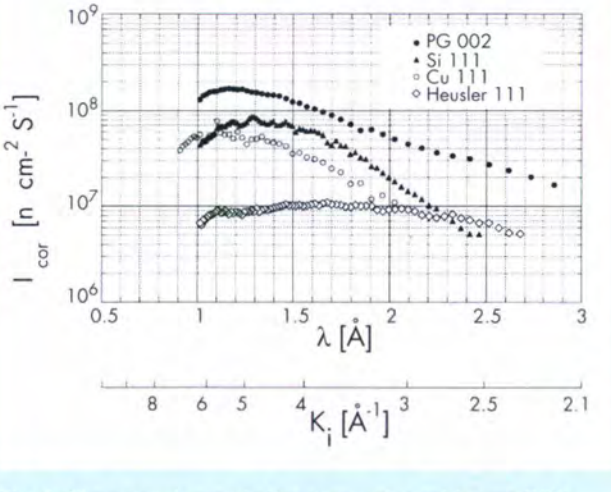

Fig. 3: The monochromatic flux at sample position on IN20 measured with a calibrated monitor with an aperture diameter of 10 mm. The data are corrected for higher order contamination; vertical focusing of the mosaic monochromators as well as horizontal focusing of Si 111 is optimised for each wavelength.

of the flux with PG 002 in the range of k_i between 3 Å^{-1} and 5 Å^{-1}, for which the fixed vertical curvature was optimised. Such performance is interesting from a practical point of view as the beam has a smaller energy spread (as we shall see later) and can be considered as free of second order contamination thanks to the fact that the 222 reflection is forbidden in the diamond structure. Moreover its performance can be significantly improved in a next generation device by using a more suitable vertical focusing scheme with a larger number of crystal plates and, possibly, with a variable curvature.

The vanadium scan data obtained with a cylindrical sample of 15 mm diameter and 20 mm height and displayed in Fig. 4 permit a comparison between the luminosity *and* energy resolution of the Si 111/Si 111 combination in open geometry and of the PG 002/PG 002 with and without Soller collimators. The peak intensity of the silicon set-up exceeds by several

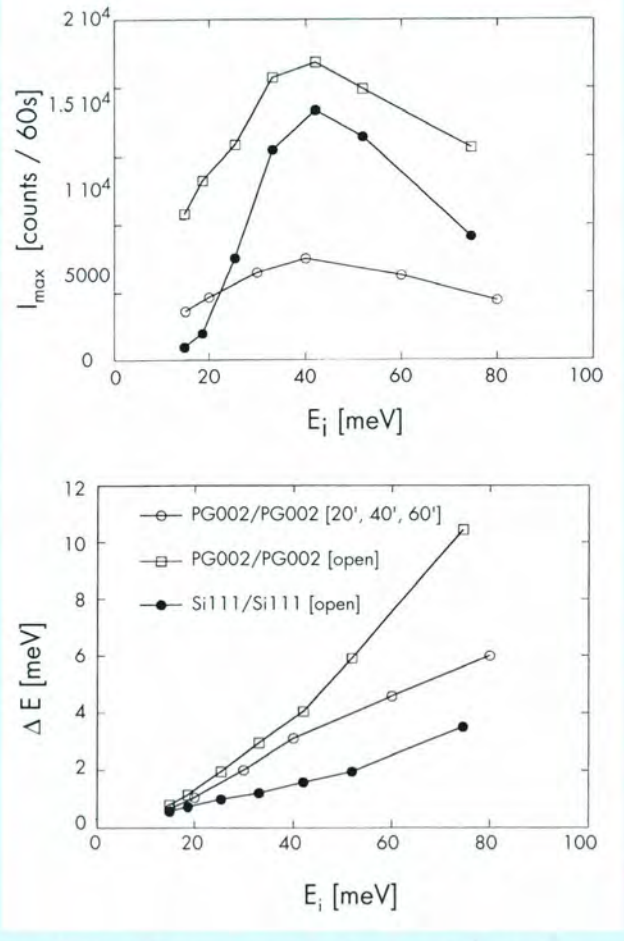

Fig. 4: The peak intensities (a) and energy widths (b) of the vanadium scan profiles obtained with a sample of Ø15x20 mm^3 dimensions; the solid lines are a guide to the eye.

times the intensity provided by the pyrolitic graphite with collimators and approaches that of PG in the open geometry, which on the other hand has a 2-3 times worse energy resolution. The drop of the peak intensity when approaching both ends of the thermal energy range is due to the above-mentioned lack of vertical focusing on the monochromator side. It follows that the performance of the horizontally focusing silicon analyser is in the whole thermal range significantly better than that of its flat PG counterpart. Indeed, replacing just the PG 002 analyser (with 40' Soller collimators before and after) by an Si 111 analyser in an open geometry brings typical gain factors of the order of 3-5 in intensity; this gain is reduced by 30% - 40% if a 60' collimator is used with the Si analyser to avoid the risk of parasitic scattering by a cryostat as in Fig. 5. The increase in intensity obtained with the silicon analyser is similar to the values reported for horizontal focusing set-ups with PG crystals [3, 4]; in such a comparison the advantage of silicon would be better resolution, absence of second order contamination and a low cost.

The basic theory needed to understand the behaviour of the elastically bent focusing monochromators is quite simple. The integrated reflecting power of an elastically bent perfect crystal can be calculated, unlike the case of mosaic crystals, in an exact manner using dynamical diffraction theory [8, 9] and for the present purpose the general solution can be largely simplified. In fact, it is safe to assume that the rocking curve of a perfect crystal plate of thickness D bent with a radius R has a rectangular box-like shape so that the integrated reflectivity ρ is given simply by the product of its width $\delta\theta$ and height r. In the case of a symmetric reflection geometry and of a negligible absorption, we obtain

$$\rho = \delta\theta \; r = \frac{D}{R}\cot\theta\left[1 - \exp\left(-Q_{kin}R/\cos\theta\right)\right] \quad (1)$$

where θ is the Bragg angle and $Q_{kin} = \dfrac{F_G^2\lambda^3}{v_0^2 \sin 2\theta}$ is the usual expression for the kinematic reflectivity. The expression (1) corresponds to a simplified case of one-dimensional cylindrical bending, in the case of need it can be extended to cover completely any known three-dimensional strain field in the crystal in a general diffraction geometry.

The performance of a monochromator is measured by the flux delivered at the sample position to which the beams leaving the whole exit surface of a focusing monochromator can contribute. The conditions for real space focusing are governed by the basic equations of the mirror optics (e.g. ref. [6]) and there is no difference

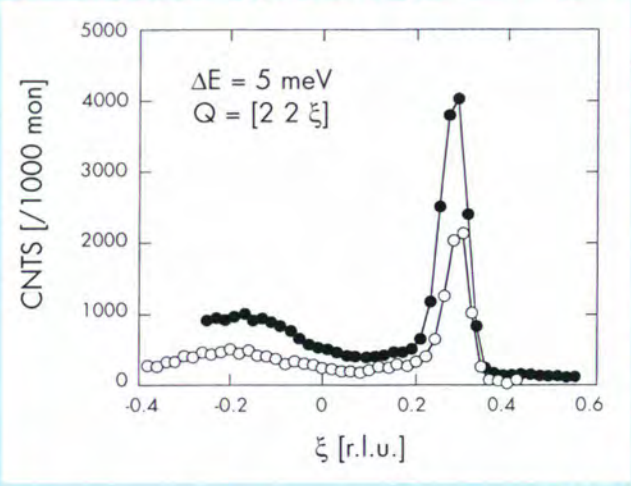

Fig. 5: Transverse acoustic phonon scans in $Sc_{0.1}Ti_{0.9}Fe_2$ measured at $k_f = 4.1$ Å^{-1}. The Cu 111 monochromator is used in combination with either the Si 111 analyser with 60' -∞ collimation (●) or the PG 002 analyser with 40' - 60' collimation (○).

between perfect and mosaic crystals in this respect. In the horizontal plane, there are two cases of particular importance:

- The *monochromatic* (Rowland) *focusing* between a point source and point focus lying at equal distances (symmetric reflection)

$$L_m = R \sin\theta \qquad (2)$$

in this case, the flux concentration in real space is achieved without deterioration of the energy resolution (the focused beam has a spread in wave vector direction only).

- The *parallel beam focusing* at a distance

$$L_p = \frac{1}{2} R \sin\theta \qquad (3)$$

which provides maximum flux for an incident beam emanating from an extended source at a large distance (paid by an increased spread in both wave vector direction and length).

The important difference between the elastically bent and mosaic crystals is that the width of the rocking curve of an elastically deformed crystal depends on the bending radius and hence on the focusing distance via equations (2) or (3). Inserting the bending radius e.g. from eq. (3) into eq. (1), we obtain a formula for the integrated reflecting power of a focusing monochromator of thickness D illuminated by an incident beam of width S as seen by a sample placed at the focal distance L_p,

$$\rho = \frac{S D}{2 L_p} \cot\theta \left[1 - \exp\left(-4\, Q_{kin} L_p / \sin 2\theta\right)\right] \qquad (4)$$

One should notice that the integrated reflectivity ρ, in the case of a strong reflection (vanishing exponential in the brackets), is given simply by the effective "mosaicity" $S\,D/(2L_p)$ which is proportional to the irradiated monochromator volume $S\,D$ and inversely proportional to the focal distance L_p. As a consequence of this coupling between focusing and "mosaicity" the performance of the elastically bent crystals can be optimised by employing compact arrangements with short focusing distances and / or by maximising the irradiated volume of the crystals. For use of large curvatures, as required for short focusing distances, materials such as Ge or Be, exhibiting a high kinematic scattering power Q_{kin} are needed since otherwise the small bending radius would result in a drop of the peak reflectivity given by the exponential terms in eqs. (1) and (4). If a large crystal thickness is preferred, the use of silicon with its excellent transmission properties is favourable. However, as the focal point gets smeared because of the rays coming from different depths in the crystal (cf. Fig. 1a), a thickness of the order of 1 cm, comparable to the typical sample dimensions, appears to be a reasonable choice.

So far we have concentrated on the focusing in real space yielding the maximum monochromatic flux on the sample. Another interesting option is however to sacrifice the maximum flux in favour of reaching the best possible resolution for the study of the line shape of an excitation focused in reciprocal space. The TAS resolution ellipsoid has the form of a relatively flat disk whose thickness (shortest main axis) is determined by the effective mosaicity of all three crystals involved and hence can become very thin if flat perfect monochromator and analyser are used together with a high-quality sample crystal. This point is illustrated by the results shown in Fig. 6, which refer to a recent investigation of the isotopic disorder effects on phonon frequencies and line widths in germanium. By reducing the bending of both monochromator and analyser, the Bragg scan width was brought down to about 0.025 reciprocal lattice units (r.l.u.) and the line width of the TA phonons in the [110] direction approached very closely this value. When converted to the energy scale, the FWHM of the phonon peak in Fig. 6b amounts to about 150 μeV. This resolution limit is given by the mechanical accuracy of the spectrometer, which permits a minimum angular step width of 0.01°; in addition the

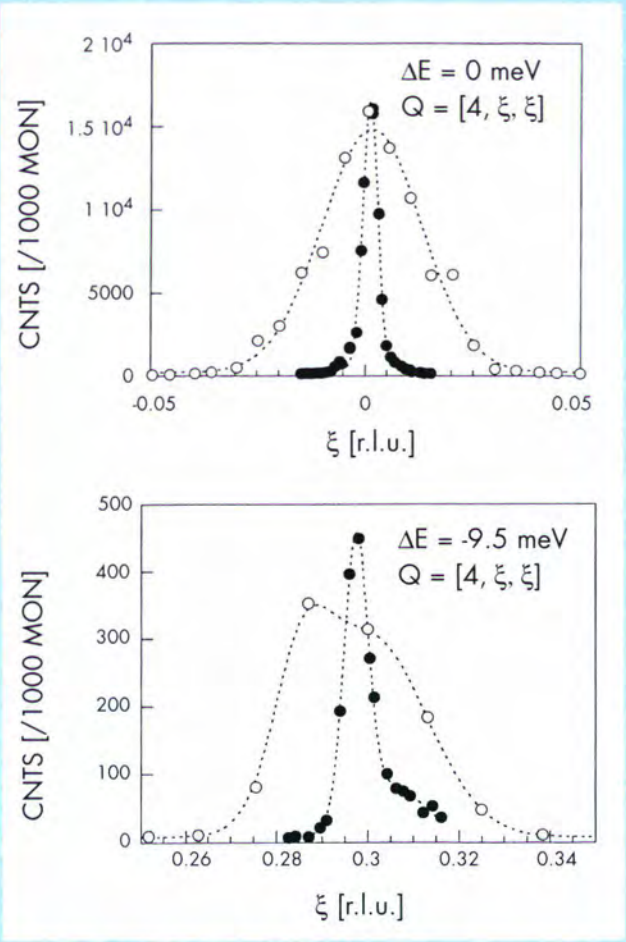

Fig. 6: The profiles of a Bragg scan (a) at [4 0 0] and of a transverse acoustic phonon scan (b) at Q = [4 0.3 0.3] on an isotopic mixture crystal of Ge^{70}/Ge^{76} measured with the Si 111 monochromator and analyser at curvatures optimised for maximum intensity by real space focusing (○; intensity reduced 5x) and for maximum resolution by reciprocal space focusing (●) at $k_f = 4.1$ Å^{-1}.

data in Fig. 6 had to be taken using E = const. scans in order to minimise the influence of spectrometer positioning errors by avoiding the variation of the monochromator and analyser angles.

This last example demonstrates the flexibility offered by the elastically bent crystals, which allow one to optimise the IN20 configuration for maximum scattered intensity as well as for maximum energy resolution. When optimised for real space focusing, the gain in intensity for the same energy and momentum resolution reaches a factor of up to 5 (depending on the sample shape and size) compared to mosaic crystals combined with Soller collimators. On the other hand, about the same gain factor can be obtained in line width when looking for reciprocal space focusing. Besides its direct interest for regular experiments, this set-up provides a point of departure for implementation of the perfect crystal monochromators and analysers on other instruments. In particular the IN20 analyser, thanks to the standardisation of the mechanical design, can already be used on IN1 and IN14.

References.

[1] T. Riste, Nucl. Inst. Meth. **86**, 1 (1970).

[2] R. Scherm, G. Dolling, R. Ritter, E. Schedler, W. Teuchert and V. Wagner, Nucl. Inst. Meth. **143**, 77 (1977).

[3] W. Bührer, Nucl. Inst. Meth. **A338,** 44 (1994).

[4] L. Pintschovius, Nucl. Inst. Meth. **A338,** 136 (1994).

[5] J. Kulda and J. Saroun, Nucl. Inst. Meth. A (1996) in press.

[6] R. Scherm and E. Krüger, Nucl. Inst. Meth. **A338,** 1 (1994). P. Mikula, J. Kulda, P. Lukás, M. Vrána, V. Wagner and R. Scherm, Nucl. Inst. Meth. **A338**, 18 (1994).

[7] V. Wagner, P. Mikula and P. Lukás, Nucl. Inst. Meth. **A338**, 53 (1994).

[8] J. Kulda, Acta Cryst. **A40**, 120 (1984).

[9] J. Kulda and P. Lukás, phys. stat. sol. (b)**153**, 435-441 (1989).

Time-of-Flight and High Resolution (TOF/HR) Group

IN4C	New TOF Spectrometer on the thermal beam tube H12 (project) (H. Mutka, A. Murani, D. Weddle)
IN5	Multichopper TOF Spectrometer on the cold guide H16 (J. Cook, M. Ferrand, S. Jenkins)
IN6	Focusing TOF Spectrometer on the cold guide H15 (H. Schober, A.J. Dianoux, S. Jenkins)
IN10	Backscattering Spectrometer on the cold guide H15 (O. Randl, M. Johnson, P. Joubert)
IN11	Spin-Echo Spectrometer on the cold guide H141 (B. Farago, P. Schleger, E. Thaveron)
IN15	High-Resolution Spin-Echo Spectrometer for long wavelengths on the cold guide H511 (project) (A. Kollmar (KFA), S. Pouget, P. Giraud)
IN16	New Backscattering Spectrometer on the cold guide H53 (project) (B. Frick, M. Johnson, F. La Rizza)
D7	Diffuse Scattering Instrument with Polarisation Analysis on the cold guide H15 (K. Andersen, I. Anderson, R. Rebesco)

Group Engineer: J.F. Barthélemy

Two new scientists were employed at the beginning of the year: K. Andersen and M. Johnson. C. Lartigue left ILL in the middle of the year as a result of which P. Schleger was recruited, who is working on the spin-echo spectrometers IN11 and IN15. B. Alefeld has been seconded since July from KFA Jülich to prepare installation of the focusing mirror option on IN15. C. Hayes (E.U. post-doc) arrived in October and will spend two years at ILL developing this option on IN15.

Besides the activities concerning the instruments, some members of the group have invested a lot of time to the area of Computing for Science. This important topic is the responsibility of M. Ferrand.

Computing for Science

The computing activities of the TOF/HR Group have developed in three main directions: time-of-flight and backscattering on-line data inspection and data analysis, the creation of a new Molecular Simulations activity and, as a consequence, the implementation of a new package for Molecular Dynamics simulations analysis for comparison with results derived from neutron scattering experiments.

• Large Array Manipulation Program (LAMP)

LAMP was developed jointly by the CS & TOF/HR groups [1-2]. It provides a predictable and intuitive graphical user interface, which integrates scientific visualisation with an enhanced data language. Many high-level modules are predefined to enable interactive data analysis and visualisation of 2D and 3D data. Originally, LAMP was designed for time-of-flight and backscattering data examination. Now, with very little effort on the part of LAMP users, it is possible to go beyond data inspection. Fast and relatively accurate on-line data reduction and data treatment can thus be performed.

LAMP is running at the moment on the Silicon Graphics workstations of IN5, IN6, D7, IN10, IN16. LAMP is also running on VMS computers and is currently being developed for Power MacIntosh.

After working with LAMP for a year, the majority of users appear satisfied and extremely interested in this interface.

• Application for General Analysis of Time-of-flight and High-resolution Experiments (AGATHE)

AGATHE is an environment developed especially for the UNIX systems by M. Bée [3]. A user interface makes it possible to graph, inspect and analyse time-of-flight and backscattering experimental data *on the basis of a plausible model for the scattering function*. Indeed, attempts to build programs applicable to numerous different situations generally result in a very complicated code, with a lot of input parameters and options. Even a sophisticated code is unlikely to be so general as to be able to deal with any physical problem. AGATHE provides a midway option. The user is left to write his own model himself, i.e. the relevant scattering function to be compared to experimental data, but he is relieved of the task of writing the code for comparison.

The refinement facility enables the comparison of the same user's scattering function with data obtained from different spectrometers. In fact, different aspects of the same dynamics may be revealed by different instruments measuring on different timescales. It must be pointed out that an important option offered by AGATHE is the ability to refine simultaneously data derived from different neutron scattering experiments (data from different spectrometers and/or data recorded at several temperatures or with various incident energies).

• Ab initio calculations and Molecular Dynamics Simulations

This new activity was initiated by A.J. Dianoux, M. Bée and M. Ferrand. Simulating structural and dynamical properties of molecules for comparison with results obtained by neutron scattering experiments has been found to be of crucial interest.

The simulations make use of semi-empirical potential energy functions that express the potential energy in terms of chemically interpretable interactions. Before any simulations can be performed, the molecular force field must first of all be correctly parameterised. Ab initio quantum chemistry calculations make it possible to obtain a more accurate description of the geometry and energetics of

molecules. The information derived from these calculations is then transferred to the semi-empirical potential energy functions for simulations.

A Ph.D. thesis student (N. D. Morelon, whose supervisors are M. Bée and M. Ferrand) is currently carrying out Molecular Mechanics and MD Simulations on inclusion compounds (system TANO-alkanes). Ab initio calculations are performed in the gas phase, using the program Gaussian 92 on a CRAY at the CENG [4]. Molecular Dynamics Simulations are then due to be performed using the program CHARMM Version 24.b [5], which was bought by the TOF/HR Group in November 1995. Preliminary results have been very encouraging.

• Neutron scattering-oriented analysis of Molecular Dynamics Simulations (nMOLDYN)

This program was written by G. Kneller [6-7] from the Institut für Theoretische Physik, Aachen, Germany and both implemented and tested in collaboration with M. Ferrand in March 1995. nMOLDYN is a modular program package for the analysis of Molecular Dynamics Simulations. It is especially designed for the computation and decomposition of neutron scattering spectra. The structure and dynamics of the simulated systems can be characterized in terms of various space and time correlation functions. To analyse the dynamics of complex systems, rigid-body motions (using quaternions) of arbitrarily chosen molecular subunits can be studied. In the TOF/HR Group, this program should very soon be used extensively for the analysis of the dynamics of inclusion compounds and molecular crystals.

IN4C New TOF Spectrometer on the thermal beam tube H12

The time-of-flight spectrometer on the thermal beam H12 is being built in cooperation with Italian neutron users (CNR-Italy, coordinator F. Sacchetti, Perugia).

The design of all the mechanical components is now finished and orders for their manufacture have been placed. The installation of the primary casemate is for the most part complete. Several sub-assemblies have been delivered or are expected in the first months of 1996. Difficulties in the factory testing of the choppers have delayed the mounting of the primary spectrometer elements. This work is now planned for the first half of 96. Final installation of the spectrometer will take place once the secondary flight path box is available (expected mid 96).

In the organisation of the Institute this project is attached to the Projects and Techniques Division (see relevant chapter for further information).

IN5 Multichopper TOF Spectrometer on the cold guide H16

During 1995, 610 experimental days were requested and 159 days were allocated, corresponding to an over-demand of a factor of around 3.8.

IN5 started up essentially with new acquisition and multidetector electronics, untested with a pulsed neutron beam. The CAMAC time-of-flight unit and chopper control were replaced by their VME equivalents. The first neutrons from the reactor during the instrument recommissioning period quickly revealed inadequacies in the phasing algorithm for the frame overlap chopper (slave) for speeds differing from that of the master chopper. The cause of the problem was rapidly identified and resolved by a temporary modification to the hardware (and subsequently by a permanent signal divider unit developed at ILL). Initial measurements of the incident beam monitor count rate indicated an approximate loss in flux of about 30 % with respect to the value expected. This result was confirmed by a carefully controlled measurement using standard scatterer, as well as by gold foil measurements. The loss of flux was discovered to have been caused by a broken section of guide due to the over-tightening of a screw. Maintenance work could only be carried out on the guide during the subsequent shutdown of the reactor. Some of the user beam time lost as a result was recovered by allocating all available test days to the first visitors. Once the guide had been repaired, the expected incident flux level was re-established. During the shutdown, the parameter setup program interface was improved to help users unfamiliar with the time-of-flight technique to avoid typical errors in the choice of their experimental parameters. This interface has been continually updated and improved throughout the year, to ensure that the instrument configuration setup is as straightforward and meaningful to the user as possible.

Following some calculations of maximum peak and mean neutron arrival rates at the multidetector, it was estimated that the area of the existing beam stop (which was circular) was largely insufficient to eliminate the possibility of electronic saturation both at the data buffering stage and from the point of view of the maximum data processing rate of the multidetector channel card. Estimates showed that all possibilities for saturation could be eliminated for neutron wavelengths greater than 10 Å and so a new beam stop was tailored to the profile of a 10 Å beam (which is clearly rectangular) at the position of the multidetector. This new beam stop allows a minimum Q of approximately $0.14/\lambda$ Å^{-1}. The first Brillouin scattering experiment during the second reactor cycle revealed a serious logic fault on the multidetector channel card, whereby the detector address and the timer word were displaced with respect to each other by one event. This led to TOF spectra in each regrouped zone of the multidetector which resembled the area-averaged spectrum. The problem was rectified on a replacement channel card, whose data processing capacity was also increased by a factor of four compared with the original card. A new high-performance dedicated multidetector channel card is currently being developed at ILL to replace the existing channel card.

Following the third reactor cycle, the disk of the frame overlap chopper (2-slot) was replaced with a single-slotted disk, recently recoated with Gd_2O_3. This meant that the same spectral information could be collected by turning the new disk at double the speed of the old disk. This modification has the clear advantage of increasing the phase stability of the disk at higher speeds (and, most importantly, increasing the stability of the TOF unit triggering), as well as eliminating to an even greater extent the likelihood of contaminant wavelengths leaking through the chopper system.

During the first shutdown, serious subsidence of the floor around the sample area of IN5 was rectified by the high-pressure injection of concrete into the affected zones and a releveling of the sample table support structure. 16 new detectors have been ordered to replace defective units generating unacceptable noise levels.

IN5-TF (Time Focusing)

Replacement of the primary spectrometer is in the project definition stage. The new primary spectrometer will incorporate a dedicated supermirror converging guide and a fundamentally new concept for the chopper system capable of time focusing of the incident neutrons at the detectors. The anticipated gain of neutrons on the sample is typically one order of magnitude over the current IN5 with an increased energy resolution.

IN6 Focusing TOF Spectrometer on the cold guide H15

Instrument IN6 operated according to schedule. Initial problems with the data acquisition electronics were resolved during the commissioning period. An electronic damping device, which further enhances the phase stability, has been added to the chopper control unit. On-line data visualisation using the ILL program package LAMP has proved to be an extremely useful tool for carrying out the experiments. Several components of the instrument are now reaching their natural age limit and will be replaced in succession. In this context, the B_4C shielding has been renewed and the moving collimator refurbished. Test experiments carried out with time-focusing in the inelastic (up-scattering) region have produced very encouraging results (see Fig. 1). However, the actual chopper bearings do not allow this option to be exploited on a regular basis, as their speed is limited to about 10 000 rpm (focusing at 4 meV). If there is sufficient demand from the IN6 user community for higher speeds, efforts to change to magnetic bearings should be undertaken.

Where the sample environment is concerned, IN6 will be equipped with a cryo-furnace at the beginning of 1996, allowing very stable and gradient-free temperature settings in the range from 4 K to 600 K.

IN10 Backscattering Spectrometer on the cold guide H15

No major problems were encountered during the five cycles of 1995. The first cycle after the refurbishment of the HFR has been mainly dedicated to instrument tests.

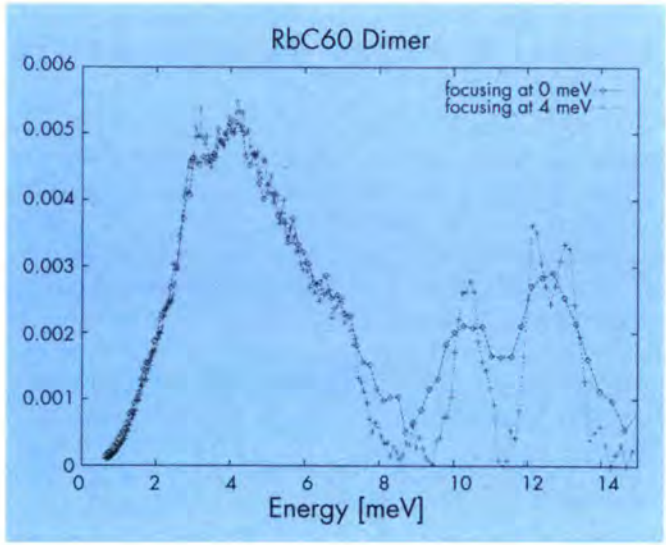

Fig. 1: Comparison of the vibrational density-of-states G(ω) as obtained with the instrument IN6 using a) the elastic time-focusing condition and b) time-focusing at 4 meV (up-scattering). The substance is RbC_{60} in its dimer state (B. Renker, F. Gompt (FZK), H. Schober (ILL)) (only a section of G(ω) is shown). This example shows very convincingly the improvement in resolution at larger energy transfers obtained by time-focusing in the inelastic region.

In particular, the different monochromators for IN10B (BaF_2, KCl, NaF, NaCl, NaBr, NaI) have been calibrated and their intrinsic resolution has been measured. A set of Si (311) analyser plates - financed and manufactured jointly by the University of Vienna (Prof. Vogl) and the TU Munich (Prof. Petry) - has been examined in order to determine the ideal glueing procedure. At the end of this first cycle, scheduled experiments could already be carried out successfully.

Altogether, there were 164 scheduled measuring days on IN10 in 1995. Apart from unscheduled reactor shutdowns, no effective losses were incurred, since buffer time was allocated to users who lost time due to instrument problems.

Some technical progress has been achieved:

IN10B (i.e. the variation of the neutron energy by heating or cooling the monochromator instead of using a Doppler drive) has withstood tests and is now used as a standard option. Fig. 2 shows the results recently obtained on Tribromomesitylene. A huge dynamical range (up to 0.8 meV) can now be covered (see Tab. 1) without significant losses in resolution. Recently, the lifetime of the ^{4}He roton was measured with a resolution better than 1 μeV (NaF monochromator)! The most frequently used IN10B monochromator, KCl, only gave 3 μeV resolution in initial experiments, but it has since been replaced and now shows resolution and intensity values comparable to that of unpolished Si (111). Development work continues: efforts are currently being made to control the Nitrogen flux more

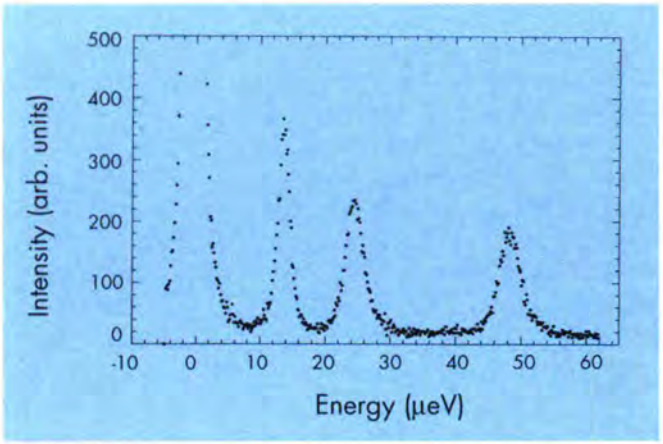

Fig. 2: Tunnelling spectrum of Tribromomesitylene at 1.5 K, measured with the KCl monochromator (resolution approx. 1.5 μeV). The sample was kindly provided by Prof. Meinell (University of Rennes).

Crystal	Reflection	min.energy (μeV)	max. energy (μeV)	Sample flux (arb. units)
Silicon (unpol.)	1 1 1	-14	+14	1
NaF	1 1 1	-813	-602	0.3
NaCl	2 0 0	-534	-339	1.7
NaBr	2 0 0	-252	-80	0.4
BaF_2	2 0 0	-62	+19	0.25
KCl	2 0 0	-16	+128	1.3
NaI	2 0 0	+92	+226	0.5
NaCl	1 1 1	+119	+266	?

Table 1: Energy range and sample flux for the different monochromators used for IN10B. The flux is approximative and can vary according to the crystals available. The corresponding values for unpolished Silicon (used for IN10A only) are given for comparison. The resolution is about 1.5 μeV for KCl, BaF_2 and NaF; it is not yet known for the other monochromators.

automatically, in a similar way to the IN13 setup. Also, a turbo pump has been installed in order to improve the vacuum in the cryofurnace, thereby increasing its lifetime.

As mentioned above, a whole set of **Si (311)** analyser plates has been manufactured by a group of external collaborators and tested on IN10. The whole large-angle region (i.e. all but the small angle rings and arcs) can now be equipped with these analysers. Together with the Si (111) analysers, the new plates make it possible to cover the Q-range from 0.1 to 3.8 $Å^{-1}$. A new oxygen-doped Si (311) monochromator has been supplied by A. Magerl (monochromator group). At the moment, typical count rates are about 2-3 times lower than corresponding values of the Si (111) setup. Preliminary tests have produced a resolution of the order of 3 μeV in 'ideal' backscattering, but the resolution worsens dramatically as soon as the detectors are out of backscattering. Therefore, this option necessitates the use of the multidetector (see below), which allows all the analysers to be in ideal backscattering. Another problem is the existence of parasitic Bragg peaks from the sample environment (furnace or cryostat). It is planned to construct a set of Cd Debye-Scherrer masks to overcome this disadvantage.

The TU Munich has also glued one analyser plate of **Si (111)** crystals. Initial tests have shown that these large crystals (the same as those used on IN16) give better resolution and almost double intensity with respect to the plates currently in use (small crystals). Therefore, it is planned to replace the existing analyser plates in the long run. More systematic tests are scheduled for 1996.

A novel multi-wire ^{4}He **multidetector** - financed by the University of Vienna (Prof. Vogl) - is being constructed jointly by the EMBL (A. Gabriel), the TU Munich (W. Petry) and ILL. The detector housing and most of the surrounding electronics are finished. Tests using a flat prototype have been carried out successfully on D10 in collaboration with the EMBL (F. Cipriani). The multidetector should be ready for tests on IN10 in the first half of 1996.

A new type of **deflector** has been tested in collaboration with A. Magerl. The graphite mosaic crystal was replaced by a perfect Ge crystal stimulated to vibrations by an ultrasound transducer covering about half the beam size. Initial tests have shown that the flux of the deviated neutron beam is about 2/3 of the usual flux with a graphite deflector. We intend to continue these studies in 1996.

The **chopper** has been equipped with an rpm meter and can now be set from the OS9 level. The next step will be to modify the setup program so that the chopper frequency is set automatically depending on the monochromator in use.

The whole instrument (guides, sample position...) has been **realigned** with high precision (A. Cumin, R. Gandelli). An aluminium **ruler** has been installed so that the absolute angle position of the secondary spectrometer can be determined easily.

The **Doppler drive** is old and needs some attention: in particular, it is constantly losing oil. Efforts are being made in collaboration with the Hall d'essais (M. Thomas and M. Locatelli) to modify the piston so that oil losses are reduced.

A new **Silicon Graphics workstation** has been installed, allowing the experimentalists to use sophisticated data visualisation and data treatment routines. The LAMP program now offers a very powerful and user-friendly way of inspecting data. All the relevant programs (SQW, PROFIT, FIRR...) have been adapted to UNIX.

One of the rare components of IN10 that has not been improved or modified in 1995 is the **supermirror guide** between the deflector and the chopper. The possibility of improving the flux at the sample position by replacing this old guide by a supermirror trumpet (similar to the one used on IN3) has been considered. A stagiaire will examine the problem in more detail in early 1996.

IN11 Spin-Echo Spectrometer on the cold guide H141

The new precession coils have confirmed expectations. The magnetic field is more homogenous than before. Together with the better positioning support of the Fresnel coils at a given wavelength, it has been possible to extend the reachable time range by about 30%! At the same time, the phase stability and resolution reproducibility have improved enormously. The compensation coils of the $\pi/2$ flipper were replaced with an asymmetric Helmholtz-type arrangement, which improved flipper efficiency and reduced dependence on the main magnet's residual field (Fig. 3).

The iron neutron guide carter of D11 has been replaced with aluminium. In the high-angle region, it was close to the coils of IN11 and caused serious perturbation of the magnetic field. With the new carters, a gain of at least 50% in resolution is obtained.

The new transmission polariser also gives very comfortable flexibility. The wavelength can be changed without mechanical modification of the instrument (which was not the case with the supermirrors in reflection geometry, where the takeoff angle had to be changed depending on the wavelength). For example, in a recent experiment on glass transition, four different wavelengths were used to measure at a fixed scattering angle. This made it possible to have four different q values at the same time using a different time range (this varies with the third power of the wavelength). The same advantage was also used in the SANS geometry. Here, in general, the scattered intensity drops rapidly with increasing q but at the same time a reduced resolution is sufficient. Changing from 8 to 6 Å increases the incoming flux by almost a factor of 10, while the maximum Fourier time is reduced from 20 ns to 8 ns. In addition, we have a gain factor of about 2 around 5 Å in flux, we break even around 8.5 Å and we lose about 20% at 12 Å. This is explained partly by the absorption of the Si plates of the transmission polariser and partly because of missing divergence arriving on the polariser (long discontinuity of the guide at the selector and a mismatch between the rectangular section of the polariser, the guide in front of the selector and the round guide section between the two). The installation of the prepolariser guide at the same time was delayed, it is planned to replace the ageing velocity selector. This should at least allow us to recover the missing neutrons but we hope for a more substantial gain.

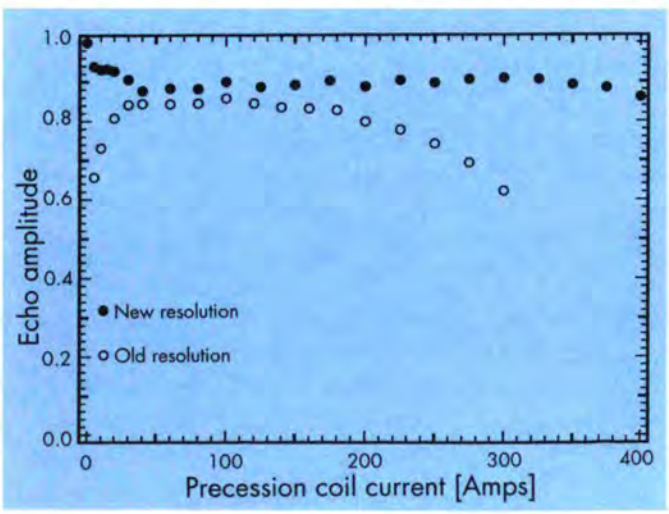

Fig. 3: The best old (empty symbol) and new (full symbol) resolution curve of IN11 at 8.1 Å. At low currents the Helmholtz flipper helped, at high currents the better homogeneity in the main precession field. The 400 Amps correspond to about 20 ns in Fourier time.

IN11C has now about 40% of the necessary supermirrors for the multidetector analysers. At the time of writing, we are just starting the first preliminary measurements with the available supermirrors to test the homogeneity of the magnet. This should allow us to design the necessary correction coils, while the rest of the supermirrors will be produced by our neutron optics group.

IN15 High-Resolution Spin-Echo Spectrometer for long wavelengths on the cold guide H511 (cooperation ILL-HMI-KFA)

The first neutron spin-echo measurements were made on a polymer sample in solution early in 1995. Fourier times of up to 100 ns were achieved. These first measurements were made with the V-shaped transmission polariser in place. This polariser gives a flipping ratio of about 20 and good transmission of neutrons of wavelengths of up to 15 Å. A second polariser is being developed for longer wavelengths. The analyser installed for these first spin-echo measurements does not cover the entire solid angle of the multidetector. It will be replaced next year. Occasional instabilites of the echo phase were recently detected, the origin of which has not yet been identified.

The VME electronics, previously controlled via OS9 by a micro VAX station, is now under the direct control of a Macintosh computer (Mac VEE interface). All the power supplies are controlled via a GPIB bus. Tests of the new acquisition software (Igor Pro, Wavemetrics), similar to that already existing on IN11, are in progress.

A high-quality toroidal focusing mirror was also recently installed on IN15. The focusing mirror is designed to yield a higher intensity at the sample position without degrading the q-resolution at small q values. It will be used for wavelengths above 17 Å. The 4 m long mirror, manufactured by Zeiss, consists of eight identical elements (500 x 150 mm^2). The mirror surfaces are highly polished zerodur substrates coated with a ^{65}Cu layer protected by a thin layer of

aluminium. The surface microroughness is less than 3 Å rms. The mirrors were mounted and optically aligned using a 1 mm diameter light source. The entire mechanics to support and align the mirror was manufactured at KFA Jülich. The neutron focusing properties of the mirror were measured using a small two-dimensional position-sensitive detector with a spatial resolution of 1.5 mm. The detector was placed at one focus (10.7 m from the centre of the mirror) and a circular diaphragm at the exit of the neutron guide tube at the other focus. The wavelength and wavelength distribution of the neutrons, in addition to the diameter and position of the source diaphragm, were varied. Figure 4 shows an isointensity plot and the normalized intensity profile measured for λ = 17.5 Å, $\Delta\lambda/\lambda$ = 15 % and a source diaphragm diameter of 2 mm. The overall width of the image is influenced by the wavelength and the wavelength resolution of the neutrons and also by geometrical factors, such as the great length of the mirror, which gives rise to coma. Image degradation due to the gravitational fall of the neutrons was minimised by lowering the diaphragm below the focus. For this particular configuration, the contrast ratio is of the order of $5 * 10^{-5}$ for $q > 10^{-3}$ Å^{-1} and the minimum resolvable scattering vector is about $5 * 10^{-4}$ Å^{-1}. These results are significantly better than those obtained in previous tests of focusing mirrors (NIST and KFA), which were hampered by poor mirror surface quality. Combination of this neutron focusing option with the standard spin-echo spectrometer configuration will be tested in the coming year.

The mechanical problems associated with the chopper motors for the time-of-flight option have been resolved. Tests with simultaneous rotation of all choppers of the three-chopper ensemble and modifications of the control software are foreseen.

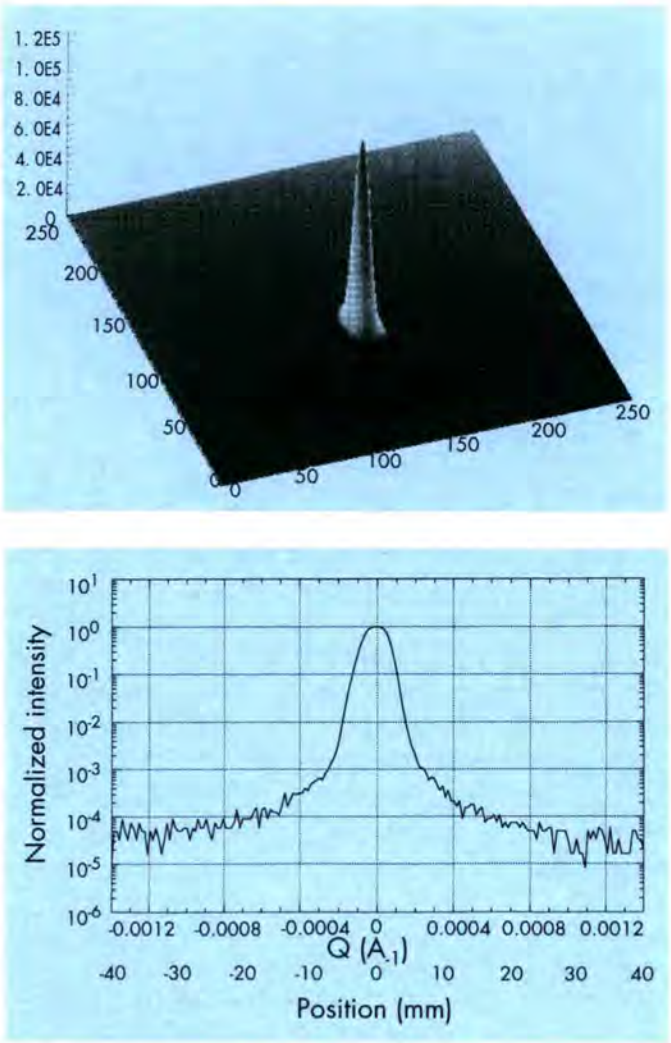

Fig. 4: Isointensity plot (a) and normalised intensity profile (b) of a neutron beam focused using a 4 m toroidal mirror; λ = 17.5 Å, $\Delta\lambda/\lambda$ = 15 %, source diaphragm diameter 2 mm.

IN16 New Backscattering Spectrometer on the cold guide H53 (project)

1995 was an exciting year for everybody involved in the planning, construction and testing of IN16. We were all curious to see how the new backscattering spectrometer would perfom. Would we get more neutron flux with the new focusing concept? Would the deformation of the high energy resolution monochromator and analyser single crystals be too large? *Would the strain distribution on the deformed, low resolution analyser crystals give an energy resolution reasonably distinct from the high resolution setup?* After all, we had assembled the single components of the instrument during the reactor shutdown without being able to test them with neutrons.

On February 4, 1995 we measured, for the first time, the instrumental resolution function with a Si(111) 'deformed crystal' monochromator and analyser. The shape of the resolution function turned out to be close to a Gaussian with a FWHM = 0.9 μeV. The much better defined lineshape in comparison to IN10 was the result of deforming larger silicon wafers, a decision which was taken as a result of multiple tests carried out at LLB and NIST during the reactor shutdown (A. Magerl, B. Frick). These results were encouraging and we continued building the rest of the deformed analyser set, which then was ready in July.

The energy resolution for the undeformed, polished analysers turned out to be FWHM = 0.38 μeV, having a similar shape to the IN10 resolution function. This was not entirely satisfactory. The FWHM was improved to a value of 0.27 μeV (M. Johnson, B. Frick) by using an analyser plate with very thick perfect crystals to avoid deformation during glueing. A new set of thick Si(111) to complete the polished setup has just arrived.

Concerning the neutron flux on IN16, direct monitor comparison and gold foil activation revealed an improvement over IN10 by a factor of 2.5. Under equivalent conditions this extrapolates to a factor of 4-5 more flux on IN16. The signal to background ratio (about 150-200) was

less satisfactory and some improvement was sought. Absorbing shields were included in the deflector chopper, but produced only a minor improvement *because the background occurs during the deflection period of the chopper*. We will try to improve on this during the January shutdown.

Another important improvement was made on the multidetector background. The amplifiers of all detector tubes were replaced with new "Oed amplifiers", which gave a significant improvement. Also preliminary tests were made with Si(311) crystals.

Up to the middle of next year, IN16 is still in the commissioning phase, but the first official users were already received on IN16 in July. In total, 30 days of beam-time were scheduled for users in 1995. They succesfully investigated research areas such as tunneling, anisotropic molecular diffusion in inclusion compounds (see text in College 7 report on TANO), inelastic SANS on liquid crystals, H in nanocystalline Palladium, Oxygen diffusion, lattice dynamics of quasicrystals and dynamics of network glasses.

D7 Diffuse Scattering Instrument with Polarisation Analysis on the cold guide H15

D7 has been running reliably and without technical problems since the startup of the reactor. 1995 has seen a change of instrument responsibles and a gradual transfer of know-how essential for the running of the instrument. In the last round of proposals, D7 was in high demand with a ratio of requested to available beam-time of 2.5. The ability to perform polarisation analysis within a multidetector setup is becoming recognised and is increasing the demand for D7 in the user community. An experiment performed this year on the excitations in liquid H_2, in which the scattering from the $J = 0$ (para-) hydrogen was determined separately from the strong incoherent scattering from the ortho-hydrogen, by using the polarisation analysis option illustrates this trend.

Both diffraction and time-of-flight data from D7 with and without polarisation analysis can now be processed with the new time-of-flight data analysis program LAMP, using IDL macros to manipulate the data. This greatly facilitates both the on-line viewing of data and the later, more detailed data reduction. We are preparing for the planned changeover of the present electronics and instrument control from CAMAC and PDP-11 to VME electronics and a DEC-Alpha workstation running under UNIX. D7 will be the first time-of-flight instrument to run under the new UNIX MAD program and a "point-and-click" graphical interface is being written specifically for D7. The changeover is scheduled to take place between the first two cycles of 1996.

Albert-José Dianoux

References

[1] D. Richard, M. Ferrand, R. Jouffrey and G. J. Kearley The Lamp Book, on http://www.ill.fr. WWW Manual by A.D. Bradley.

[2] D. Richard, M. Ferrand and G.J. Kearley, Journal of Neutron Research (to be published).

[3] M. Bée, ILL internal report 1996 (reference not yet attributed).

[4] M. Frisch, J. Foresman and A. Frisch, Gaussian Inc., Pittsburgh PA15213.

[5] Chemistry at HARvard Molecular Mechanics, B.R. Brooks, R.E. Bruccoleri, B.D. Olafson, D.J. States, S. Swaminathan and M. Karplus, Journal of Computational Chemistry **4**, 187 (1983).

[6] Gerald R. Kneller, ILL internal report ILL95KN02T.

[7] V. Keiner, M. Kneller, M. Schiller and G.R. Kneller Computer Physics Communications (in press).

The Helium-3 neutron polariser

F. Tasset and H. Humblot

With a large absorption cross-section entirely due to antiparallel spin capture, polarised helium-3 is presently the most promising broad-band polariser for thermal and epithermal neutrons. The high density of well-polarised gas which is necessary to achieve a practical device can now be obtained with two different techniques: spin exchange at high pressure through collision with an optically pumped Rb vapor or optical pumping by an LNA laser of metastable ^{3}He atoms in a discharge at low pressure with subsequent compression. While the Rb technique was initially tested at Los Alamos[2] and ILL[3], the metastable ^{3}He technique developped in an intense R&D program at Mainz University[4] has recently improved very quickly.

Encouraged by the HCM program of the European Community*, a collaboration between ILL (F. Tasset), HMI (F. Mezei, M. Steiner), ENS (M. Leduc), and the Johannes Gutenberg Universität in Mainz (E. Otten) was established for the project "Polarised ^{3}He targets as neutron spin filters". Dr. Hubert Humblot, for two years an EC-Research Associate, is now working in Mainz under a contract with ILL. The achievements within this project have been quite remarkable. In the recent Workshop "New Tools for Neutron Instrumentation", Werner Heil[5] (Mainz) has shown how the double-stage Titanium compressor achieves pressures up to 7 bars at 50% ^{3}He polarisation in a 150 cm^3 glass cell. Based on an idea from ENS-Paris[6], the cells were coated with Cesium, resulting in relaxation time of more than 100 hours, and Reinhard Surkau (Mainz) vividly demonstrated how such a cell had been detached from the compressor and transported to the Mainz Triga reactor in order to test its neutron properties. Very recently[7], further such direct neutron tests were carried out with a close-to-optimum configuration for 1 Å neutrons. The filter was 10 cm long, inflated at 4 bars. The neutron polarisation was measured to be 84%, a confirmation for the 50% polarisation of ^{3}He (total transmission was calculated to be 18%).

At the present time, we may say that 50% polarised ^{3}He gas is being produced in detachable containers with long relaxation time on a routine basis in Mainz and that its application to polarised neutron beams can start. ILL now intends to use this technique in Grenoble on short wavelength neutrons beams. In Mainz, we are therefore currently building a duplicate system. The LNA laser is operational and the first stage compressor has been tested. Both the compression ratio and the polarisation transport are satisfactory. The second stage compressor is manufactured and being assembled. In Grenoble, a special laboratory is being equipped in order to host the system by mid-1996. Work has also started on incorporating ^{3}He cells as analysers on the short wavelength diffractometer D3 and the three-axis spectrometer IN20. As a particular example, a fundamental physics experiment on "The study of P- and T-violation in the vicinity of neutron p-wave resonance" is being discussed which requires polarisation analysis capability at.74 eV (.33 Å) on a large 139-La sample.

*EC Grants. Nr. ERBCHRX-CT92-006 and ERBCHRX-CT-93.0122

References

[1] F. Tasset, Physica B, Vol.213&214, p. 935-938.(1995)

[2] K.P. Coulter, T.E. Chupp, A.B. McDonald, *et al*, Nucl. Inst. Meth. **A288**, 463-466(1990)

[3] F. Tasset, T.E. Chupp, J.P. Pique, *et al.*, Physica B **180&181**, 896-898(1992)

[4] G. Eckert, W. Heil, M. Meyerhoff, *et al.*, Nucl.Inst.Meth. **A320**, 53(1992)

[5] J. Becker, M. Ebert, T. Grossmann, *et al.*, to be published in Journal of Neutron Research

[6] W. Heil, H. Humblot, E. Otten, *et al.*, Physics Letters A**201**, 337-343(1995).

[7] W. Heil, private communication, Dec 1995

Quasi-Laue detector

M. Lehmann

In order to speed up data collection on crystals with large unit cells, tests have been done using Laue-methods with a limited wavelength band, the quasi-Laue method, which gives higher flux on the sample than monochromatic techniques. To further increase the count-rate on the detector, and to better resolve the individual Bragg-peaks, the tests were performed with cold neutrons from the end-beam H142 (collaboration with C. Wilkinson, EMBL and P. Oleinek, München).

The most essential part of an improvement of data collection capacity relies however on getting larger detector surfaces, and over the last two years a very large detector based on image plate technology has been constructed at the EMBL (F. Cipriani and J.-C. Castagna). The detector surface is a cylinder with a diameter of 31.8 cm and a length of 40 cm, presently holding 8 million pixels of 0.2 x 0.2 mm^2. The read out time is 5 min., so the detector is well suited for long exposures as is typical for Laue-recordings.

The first step was to carry out complete white-beam detection, and for this purpose a 2 mm^3 crystal of triclinic lysozyme (hen egg-white) was used. The first diagram recorded is now on display in the main entrance hall of ILL 4. These measurements showed, as expected, that due to the overwhelming background it was not possible to go much beyond Bragg reflections with a 3 Å d-spacing, which is far from sufficient for structure analysis at atomic resolution. These observations were confirmed by observations on a crystal of Concanavalin-A (collaboration with G. Habash and J. Helliwell, Manchester).

After an interruption from April to June, while the beam H142 was used by the Nuclear and Fundamental Physics Group, a multilayer monochromator produced at the ILL by P. Høghøj (see report under DPT) was installed, and the reduced 20% bandwidth of the incident beam around 3.4 Å now allowed data collection to d-spacings of 2.4 Å on a crystal of triclinic lysozyme soaked in D_2O, and eventually a resolution of 2.1 Å was reached when the original Siemens image plates (supplied by H. v. Seggern, Siemens) were replaced by plates with higher efficiency made by Fuji (loan from N. Niimura, JAERI, Japan).

Measurements on tetragonal lysozyme grown from D_2O have also been done (collaboration with N. Niimura et al., Japan), and gave 55,000 reflection above 1 σ, leading to 7,200 symmetry-independent observations to 2.1 Å. The internal agreement value (comparing intensities) is 21 %, but detailed studies of symmetry related reflections show many large discrepancies when compared to the counting statistics. At present this is believed to come from the integration procedure, which was designed for a flat-plate instrument, so work is being done to improve the integration model (C. Wilkinson, EMBL).

Other tests have also been made on much smaller systems such as high pressure ices (collaboration with W.F. Kuhs, Göttingen and H. Ahsbahs, Marburg) and vitamin B12 (collaboration with C. Kratky et al., Graz and P. Langan, ILL).

Towards the end of the year tests were also made using a velocity selector with a 15% bandwidth (on loan from NIST, Washington), which showed the two types of monochromatisation to be quite comparable. In further tests the use of multilayers, made at the ILL, will therefore be the normal mode of operation.

Exploitation of data is now under way to get a clearer picture of the capacity of this method for the study of macromolecular problems. As a first step the water structure in triclinic lysozyme crystals will be analysed using a combination of the Quasi-Laue data and X-ray data in order to estimate how much information the neutron data actually bring to the analysis. Further measurements are also planned for completely deuterated systems (collaboration with Brookhaven National Laboratory), as this will much alleviate the problem of high background caused by incoherent scattering from hydrogen atoms in the protein, and thus allow data collection to higher real space resolution.

Finally the time has clearly come to do a few, first studies in collaboration with external biology groups. A search for suitable projects is now under way, and persons who would be interested in making a test measurement are welcome to contact one of the scientists involved (M.S. Lehmann, ILL or C. Wilkinson, EMBL).

"New Tools for Neutron Instrumentation"

H.G. Büttner

The workshop "New Tools for Neutron Instrumentation" was held in Les Houches 6-9 June 1995, in the conference centre of th Ecole de Physique, which is affiliated to the University Joseph Fourier, Grenoble. ENNI, the European Network for Neutron Instrumentation, funded by the EC/HCM programme, a network of 6 laboratories within 6 European countries initiated this workshop. Some 60 people gave presentations on the progress in the areas of:

- data acquisition, visualisation, inversion,
- neutron detection,
- interferometry, diffraction, UCN,
- polarisation,
- optics.

The workshop was organised by Francis Tasset and Herma Büttner, ILL. The proceedings will be published in the Journal of Neutron Research.

PROJECTS AND TECHNIQUES DIVISION (DPT)

After the reactor was successfully restarted at the very beginning of the year, the next challenge facing ILL was to restart the instruments and reestablish normal running. The success of this operation undoubtedly owes much to the skill and dedication of the DPT staff, who played a key role and have every right to be proud of their achievements.

1995 brought some minor changes to the organisation of the Division. Alongside the Instrumentation and Development branches, a new entity, known as the "Project Office", has been set up to deal with long-term developments. As soon as it was created, this new entity, which is headed by W. Kaiser, immediately took charge of producing an accurate evaluation of the group of projects proposed for the next five years. This work has inspired confidence in ILL's ability to complete these projects within the framework of existing resources.

Certain changes have also been introduced within the branches themselves with the aim of simplifying their structure by reducing the number of independent units. The departure of six members of staff from DPT has also allowed us to bring some young blood into the Division.

Several units have experienced heavy workloads. Temporary staff have been brought in to deal with such exceptional loads. In the long term, however, such problems must be resolved either by subcontracting work or finding permanent support, if possible. Otherwise DPT would have to reduce its involvement in supporting the experiments.

The current instrument projects IN4 and D20 have made steady progress. However, delays of a few months have been experienced. Most of these delays were due to our dependence on external industrial subcontractors. Similarly, the new instrument D22 failed to function correctly as a result of a faulty detector delivered by industry. Thanks to prompt action on the part of the detector group, aided by B. Guerra as project manager, the instrument could be repaired while maintaining the high technical standards needed to ensure further reliable operation. However, irrespective of the quality of our internal troubleshooters, we must learn from the difficulties connected with industry's contribution to the development of our instrumentation. It would be quite wrong to conclude that it would be better to prohibit the use of subcontractors for the building of highly sensitive devices. There can be no future in doing it alone. The only way forward is to improve our procedures for subcontracting work. We must always remember that, unlike in the world of sport, there is never a winner and a loser, only two winners or two losers. Subcontracting calls for careful preparation and a gradual building up of trust through the precise definition of needs and requirements.

To conclude, I will briefly mention some of the other highlights of the year:

- The implementation of the first supermirror guide at ILL.
- The delivery of a new monochromator made of mosaicised germanium for the diffractometer D2B.
- Operation of an instrument for the first time under UNIX control.
- The development of a very compact pass band filter with multilayer mirror techniques.
- The Sample Environment laboratory faced successfully an exceptionally high demand for very low temperature experiments.
- The success of the Transuranium experiments.
- The new ILL precision temperature controller is now ready for progressive installation on instruments.

Next year will see the start of operation of the new instruments D20 and IN4C. I firmly believe that, in anticipation of its future successes, ILL will once again move ahead with confidence and the determination to become a leader in the instrumentation field.

Philippe Leconte

Project Office (PRJ)

(W. Kaiser)

With the reorganisation of the Projects & Techniques Division in July 1995, the mechanical design office and the mechanical calculations and engineering science office have been attached to the Project Office, increasing to a staff number of 10. Two staff members of the design office have left during the year, one of them will be replaced in 1996.

In 1995 the investments related to the instruments were 18.4 MF i.e. 6.1 % of the revised budget of 303.1 MF. The two R&D projects of the Science Division (^{3}He Polarizer, Laue Detector) are well advanced. Projects of the Projects & Techniques Division (Neutron Guides, D20 Detector, IN4C) will be reported below.

Detailed project evaluation including ressources has been issued for the proposed 6 new projects with a budget volume of 28 MF over 5 years. The result was presented at the Steering Commitee in November.

Mechanical design office

(Ph. Malbert)

The main activity of the Design Office for 1995 has been the IN4C project. But numerous other studies have been carried out for different instruments. The activities of the mechanical design office are:

New instruments:

- IN4C: -Layout studies, design and drawings of the shieldings.

-Design, drawings and manufacturing of the secondary spectrometer. (two ILL draughtsmen plus subcontractors)

- GAMS5: assembling and settings follow up, complementary studies.
- D20: design and drawings of the mechanics of the 4 faces monochromator. Manufacturing of the mechanics of the HOPG monochromator.
- IID: design work has been stopped by end of April 1995, by decision of the Science Policy Board.

Improvements of existing instruments:

- IN15: design work due to the new focusing mirror, various improvements (mechanical support and adjustment mechanism for Fresnel coils...), design of a polariser.

Preliminary design or layout studies:

- IN8: preliminary design of a new monochromator shielding drum, and of a new set of 3 horizontally and vertically curved monochromators. Preliminary layout of the modified instrument.
- H25: follow up of the design and mounting of the neutrons guide the beam shutters follow up of the layout of the CRG IN22 and D23 instruments.

Tooling or new equipment:

- IN20: design, drawings and manufacturing of a support for Cryopad II.
- X-rays laboratory: studies for the collimation of the generator, design of a double lead diaphragm and of adjustment tables for the detector.
- D11: design, drawings and manufacturing of a sample-changer under vacuum.
- D22: drawings for support of the detector during repair.

Tenders and follow up for the manufacturing of the mechanical pieces.

Mechanical calculations and engineering science office

(M. Thomas)

- PIAFE: Thermal Study of the Source of Exotic Ions

The processes of diffusion and effusion of the fission products of uranium (^{235}U), distributed throughout a porous graphite (Gr) matrix, are at their most efficient at high temperature (2400°C). The heat is produced by fission and by nuclear heating due to the proximity of the reactor core. Radiation is dominant in thermal exchanges with the external environment (D_2O via the beam tube thimble).

We have studied the range of temperatures at equilibrium of the source close to the reactor core (significant nuclear heating) on a simplified model with axisymmetric geometry.

This initial study has allowed us to highlight the considerable emissivity of these materials and, in particular, of the rhenium envelope (Gr/^{235}U).

More recent discussions have prompted the designers to move the source away from the reactor core (constant fission rate = 10^{14} fissions/s, obtained through a higher degree of doping with uranium) and to modify its geometry. The nuclear heating diminishes and, from a purely thermal point of view, the two values governing the temperature of the source are the heat produced by fission and the emissivity of the rhenium.

Both these values must be predetermined before new calculations can be carried out in 1996.

- D22: Elastic Behaviour of the prestressed membrane separating the gases ^{3}He/^{4}He in the multidetector

The membrane separates 2 volumes of different gases (^{3}He/^{4}He) at the same pressure. Under normal operating conditions this pressure does not change. When the detector is filled and/or there is a leak of one of the gases, a low differential pressure Δp causes a considerable distortion of this extremely thin membrane.

We intend to make this membrane less sensitive to pressure variations by prestressing it to make it stiffer.

This is done using the thermo-elastic phenomenon produced by the weld as it contracts.

- IN5: Elastic behaviour of the chopper disks of IN5 (time-focusing)

Each of the 7 disks rotates at 20000 rpm and comprises 4 long slots, which, if possible, must be completely hollowed out in order to prevent neutron absorption and scattering. This rupture of the otherwise axisymmetric rigidity of a full disk produces a significant increase in the stress field around the slots.

It appears that the use of isotropic materials with a high figure of dynamic merit (E / ρ = Young's modulus/density) and high elastic limit (aluminium series 7000) is insufficient to meet the very demanding case of completely hollowed-out slots. On the other hand, if a thin residual membrane can be tolerated, it is possible to optimise its thickness to satisfy the maximum permissible stress criterion.

We are about to begin a study of composite materials with much higher figures of merit than for isotropic materials. This study will be carried out in the context of a possible implementation.

Neutron Guides

H1-H2 Neutron Guides

Neutron capture flux measurements on the refurbished guides were performed in January and showed normal values.

H17-H18 Guides

The project has been suspended due to missing budget.

H25 Guide

The refurbished H25 guide is mounted as supermirror guide over a total length of 52.5 m. Neutron flux measurements performed in October show an increase by a factor of 2.5 compared to the original Nickel guide.

The extension of the guide over 11 m downstream of the S18 CRG-instrument is delivered and will be mounted in 1996.

H511 Guide

The missing 7.5 m FeCo polarizing guide with elements coated by HMI for the IN15 Neutron Spin Echo Spectrometer is under manufacture. Its replacement is foreseen in 1996.

Beam Shutter Replacement

The project was completed in January with the reception procedure for the beam shutters by checks with neutrons. The result was satisfying.

Instrument safety

The authorisation for normal operation of the 25 ILL instruments and the commissionned CRG-instruments was given after approval of the instrument safety and final checks with neutrons at 2 % and full reactor power in February. Additional checks on the safety interlocks were performed in October.

IN4C Thermal Time-of-Flight Project

(H. Mutka)

Collaboration with Istituto di Struttura della Materia, CNR, Italy

A concentrated effort of the Design Office ensured a swift advance in the design work on the mechanics of the secondary spectrometer and of the sample environment. The main components are now completely defined and orders placed. Many of the subassemblies, for example the sample chamber and associated mechanics have been received. The important item conditioning the final installation of the spectrometer is the vacuum flight box whose fabrication will take about five months and is expected to start in the beginning of 1996.

The components for the primary spectrometer are mostly ready. The Italian partner (coordinator Prof. F. Sacchetti) delivered the elements of monochromator goniometer table that has been assembled. The mounting of the crystals on the variable curvature monochromator assembly has been delayed due to priorities on the work of the monochromator group. The graphite crystals will be mounted in the beginning of 1996 and the monochromator will be operational with the graphite face for the first neutron tests of the instrument.

The definitive installation of the primary shielding elements has been completed. Beam elements such as the secondary shutter and the primary diaphragm are ready for mounting but the work has been seriously delayed due to the problems with the factory tests of the choppers. The choppers are mechanically assembled and in running order and are now going through the required endurance tests. After delivery to ILL an extensive test programme for the assessment of the phase control will be carried out at the ILL. Installation and tests of control and acquisition electronics and elaboration of the associated software are in progress.

The Italian partner is constructing the central forward scattering detector with its electronics, according to the concept prepared and defined at the ILL. The mechanical details of the detector tube assembly have now been defined and the mounting can start once the elements have been fabricated.

D20 High Flux Multidetector on the thermal beam H11

(P. Convert)

Parallel activity on several items is continuing to make the whole D20 instrument available for users as soon as possible after the end of the detector construction.

The D20 monochromatic beam is available, and all the major questions related to safety have been solved. A few improvements will be done to have better practical operating conditions. The old 128-wire Position Sensitive Detector is in operation to test the instrument: monochromatic beam, instrument control, data acquisition and data treatment.

The VME data acquisition system for the 1600 cells of the new detector is operational in the reactor hall. The 6 movements, 2θ, ω, χ, ϕ, plus 2 translations, are also controlled by the VME electronics. The Silicon Graphics D20 computer is installed at D20 and can read data and drive the movements. A data treatment system is in preparation with the Scientific Computing Group of ILL.

The new D20 1600-cell Banana (curved linear Position Sensitive Detector) is waiting for the complete delivery of the 50 electrode plates (we have now 7 of these plates) from the external manufacturer IMT. They are expected for mid-february 96. Then the plates have to be precisely cut at ILL, cleaned, and carefully mounted. After outgassing at high temperature, the detector will be filled with gas. The control of operation of the 1600 cells and adjustment of the 1600 amplifiers will be made first in the laboratory, and completed at the D20 position, after remounting of the protection.

After completion of the instrument, many tests have to be performed before the instrument become ready for external users during summer 96.

Jean Pannetier has left ILL and D20. A young German scientist, Thomas Hansen, arrived on December 1st to complete the D20 team with Jacques Torregrossa and Pierre Convert.

Instrumentation Branch (BI)

(A. Heidemann)

Introduction

Two events marked the life of the Instrumentation Branch:

• Several people left the institute:

– R. Klesse, the head of the Electronics Service. The loss of his technical know-how was compensated by the arrival of a young electronics engineer, Ph. Descamps. The departure of R. Klesse enabled us to join the Electronics Service and the Instrument and Networks Computing Service together into a new Service, called the Instrument Control Service (SCI).

– J.J. Tschofen, responsible for the instrument computer maintenance. His position will be used to hire a programmer for instrument control software.

– H. Fertey, technician mainly working in the central workshop. He will be replaced in 1996 by an all-round technician.

• A new Service called ' **S**ervice **M**écanique des **A**ires **E**xperimentales' (**SMAE**) was created under the command of R. Mathieu. This Service regroups the assembly hall, the central and the free access workshop, the vacuum laboratory, the crane operators and the neutron distribution group.

Mechanical Service of the Experimental Halls

(R. Mathieu)

The new Service is responsible for neutron distribution, neutron guide installation and alignment, instrument construction and maintenance, transurania experiments, safety interlocks, the experimental zones, the vacuum group and the general organisation in the experimental halls. In 1995 the main activities were as follows:

• Testing the new beam shutters and control systems which have been fitted on each experiment.

• Testing all the safety interlock systems on the experiments and the introduction of quality assurance management procedures for these systems. The safety interlock systems of machines using mobile protection blocks are being improved.

Three successful transurania experiments were carried out (a total of 27 days measuring time) with the introduction of quality assurance management procedures for these experiments.

Participation in the co-ordination of the construction of the new instruments on the H25 beamline and of IN4C, PF1, ADAM, EVA, GAMS5 and LADI. The assembly hall has installed and aligned the new H25 guide and has assembled the first elements of the new instrument IN4C in the reactor hall. The progress of the construction and testing of IN4C's choppers is followed up. D2B and D11 have also been considerably improved. The first new electrodes for D20's multi-detector have been cut.

The assembly hall maintains and services 6 velocity selectors and 10 choppers.

Co-ordination of general work carried out in the experimental halls: installation of equipment in the experimental zones, building and dismantling of biological protection, fluids, electricity etc., delivery of liquid helium /nitrogen by the "chefs de halls".

This included the co-ordination of the replacement of the roof of ILL7 which required the protection of the instruments, planning the use of the cranes etc.

The vacuum group has a park of 635 pumps and 11 leak detectors to service and maintain. This results in over 1800 oil changes each year, plus the routine replacement of bearings on the rotary and turbo pumps.

To reduce the noise level in the experimental halls 1/3 of the pumping groups have now been sound proofed.

Assistance is also given to users concerning the installation of pumping systems, leak detection problems etc. A lending service for vacuum equipment is also available on a short term basis.

Instrument Control Service

(A. Barthelémy)

The Electronics Service and The Instrument Computing and Networks Infrastructure Service merged on the 1st December 1995.

During 1995 they had three primary objectives for the ILL instruments:

- terminate the reinstallation of the instruments following the reactor refurbishment,
- improve the software and the electronics on the instruments,
- modernisation.

After the first reactor cycle, reserved for tests, all the scheduled instruments were ready for the official scientific schedule with external visitors.

Several instruments were significantly modified during the shutdown:

Three 3-Axis Spectrometers (IN1, IN8 and IN20) now operate with new VME control and acquisition electronics coupled to new DEC Alpha 3000 workstations running under OpenVMS. The instruments IN14 and D4 also have new DEC Alpha workstations, connected to HYTEC Ethernet CAMAC controllers.

The standardisation of scheduled instruments to VME electronics and to the instrument control program MAD is aimed at optimising the technical support and facilitating software developments. The VME electronics on IN5, IN6 and D11 have all given satisfactory performance. D17 migrated from CAMAC to VME, and is now similar to its "sister" instruments D11 and D22.

In October, the first step of the UNIX Plan for the instruments was realised: the diffractometer D10 is now controlled from a Silicon Graphics workstation. The first version of MAD with a new graphical user interface based on OSF/Motif is running (Fig. 1, page 162). This changeover is the beginning of a complete migration of all scheduled instruments to UNIX, which should be completed by the end of 1997.

Complimentary to the VME electronics, it was decided to introduce for the ILL test instruments a new standard, based on "industrial" electronics hardware and PCs with Visual Basic. This standard is already used on instruments in the Nuclear and Fundamental Physics Group.

Several projects were initialised during 1995 for completion during 1996:

Conversion to UNIX:

- with VME and DEC Alpha workstations on the instruments D7, DB21, D16.
- with VME and Silicon Graphics workstations on the instruments D1A, D2B, D3.
- with HYTEC CAMAC and a Silicon Graphics workstation on the Cryopad.
- with a DEC Alpha workstation on IN16.

Additionally, VME development facilities are being completely reviewed and an improved test installation for VME and CAMAC hardware is under construction.

In the local area network domain, many modifications were made during 1995. These were aimed at improving the security, the reliability and the bandwidth of the ILL network.

In order to improve the security of the internal installations against attack from the exterior, a 'firewall' was installed. In this project, common for the three institutes ESRF, EMBL and ILL, the configuration of the external connections (ARAMIS, RENATER and Internet) was modified. Also, a new link through a new Cisco router was installed to connect with the "Polygone Scientifique", CNRS, IBS, ISN, CENG and ENSERG (Fig. 2, page 162).

With the increasing number of connections of acquisition and control electronics to the network, it was necessary to modify the topology of the Ethernet segments to maximise the reliability of the related traffic. Three new segments were installed to separate the "measurement" traffic from the "data treatment" traffic. All the central servers are now connected to a "Gigaswitch" running at 100 Mbits/s giving access to the FDDI ring. A few image treatment workstations have been connected to "Ethernet Commuted Switches" from Siemens UB, giving a dedicated bandwidth of 10 Mbits/s.

A complete recabling of the network of the ILL main building is planned for 1996 in order to give more bandwidth to the users and to prepare for future network needs.

In conclusion 1995 was an important year where a lot of ground-work was done for the future with the initial implementation of the new standards: MAD UNIX with OSF/Motif, PC with industrial cards and the generalisation of VME on all scheduled instruments. The importance of local area networks was confirmed in the continuing decentralisation of the computing environment and with the increasing access of new services on the Internet.

Computing: Systems and Communications Service

(M. Le Sourne)

The activities in 1995 have been dominated by the restart of the scientific experiments and have concerned mainly experimental data collection and archiving, implementation

of new hardware and software facilities for data treatment, and improvement of the communications in a world wide context. An important part of the work has been devoted in helping ILL scientists and visitors to operate in the new computing environment (Fig. 3, page 162).

• UNIX Systems

The 1995 budget has allowed new investments on users equipment and general purpose servers:

– 2 HP workstations for Theory and NFP groups

– 7 SGI workstations for Diffraction, TOF/HR and LSS groups

– 17 X terminals

– new licences for CERIUS (crystal modelling) and IDL (data manipulation and display)

– disk capacity extension to 60 Gbytes on the file server

– new mass storage equipment on the backup server

– new mail server

The Service gives help to users to install software, to provide access to heterogeneous output devices and to standardise both operating systems and file systems on the workstations. The Service has also the responsibility of management of the general purpose servers. The UNIX file server 'IDEFIX' has an important role as it is used for accessing experimental data and also for providing personal disk space. Many public domain programs are available through this server.

This system needs a daily attention and has necessitated a particular technical effort to improve the performance of its operating system and network communications and to set up a better organisation of the file systems.

With the backup server the 50 user workstations and various servers are daily saved over the network. The new Exabyte jukebox allows on-line backups to be kept for 6 weeks. This system has shown his efficiency as it has been possible many times to restore user disk files or to restart users workstations after disk breakdowns.

• VMS Systems

We still offered a VMS service with two DEC ALPHA computers and the old VAX machines. The latter run without an external maintenance service and are planned to be stopped early in 1996. To prepare this step two independent clusters have been created already.

Some applications running on VAX machines have not yet been migrated to the DEC ALPHA machines due to lack of particular graphical libraries nor to UNIX due to lack of manpower. So a VAX station is being configured to run this category of programs for some more time.

With the reactor restart the ALPHA system has been heavily used.

• Microcomputers

The activity on this area consisted of:

– a better integration of MACs and PCs in the UNIX environment by introducing standardised communication facilities, with products like Exodus for X terminal emulation, Eudora for mailing.

– the installation of a phone call back system based on the PPP protocol to allow users to access the ILL network and to get all the UNIX facilities.

• Data Base

Most of the experimental data base has been transferred to the central VMS system and immediately stored in Ascii mode on the UNIX file server. After one year of operation we note that the UNIX data base contains per reactor cycle approximately 100000 files and a total of 6 Gbytes of disk space. A catalogue is permanently updated for accessing the old data.

A part of data treatment is still executed on VMS using the binary data base; this activity is decreasing with the migration of these applications to UNIX.

The data have been archived on optical disks using the compressed mode. Concerning the general archive facility a preliminary study has been done in 1995.

• Communications

A new mail server has been installed on a HP workstation. Progressively users are transferred to this new machine. Most of the ILL people have been registered under the mailing system on UNIX, VMS or EUDORA. A list server has also been implemented.

A dedicated file server on the Internet side of the firewall has been installed to act as an anonymous ftp server for the outside, and to serve as an intermediate staging point for depositing data from ILL for export, or for recovery of data from outside sites. A WEB service has also been implemented on this external server and is accessible from outside without going through the firewall.

• Mathematical libraries and Fortran90

New versions of IMSL library have been installed on the UNIX file server for HP and SGI systems and on the Open VMS Alpha server.

New help facilities are available for the NAG library on UNIX and VMS servers.

The first native Fortran90 compiler has been introduced by DEC. It is available on our VMS Alpha server. We participated in the Beta test operation for the Fortran90 Numerical Recipes library. The Foresys software (Fortran engineering system) which allows translation of Fortran77 to Fortran90 programs is available on the UNIX file server.

Support for the NFP Group

(Ph. Ledebt)

1995 was the second and last year of "UNIX-PLAN" application for the Nuclear and Fundamental Physic Group of the Science Division. We could show that personal

computers are a powerful means of controlling complex, heterogeneous scientific instruments and handling data from the acquisition system. They are equally well adapted of being the direct interface with the electronics of the instruments as well as being a part of a modern, hierarchical network based data handling and evaluation system.

We have implemented a special software PC-DUO, which has the capability, through the network, of taking complete control of the experiment display, keyboard and mouse. In this manner the user can interact with the experiment from anywhere on the network, security being done by means of a password and access lists.

The use of Windows for Workgroup and Visual Basic is very powerful mean to quickly write basic acquisition and control programs. The only difficulty was to really understand and test the electronic itself and for that reason we have developed many tools as well as some special routines in C language or others.

DPT/Development Branch (BD)

(C. Zeyen)

This year the BD had to resume experimental activity with a particularly heavy work load on the Sample Environment Laboratory. M. Frédéric Thomas, a young physicist and cryogenics specialist, joined the Laboratory on December 1st for one year to help with automatising a maximum number of complex tasks connected with dilution cryostats and cryomagnets.

Problems with multidetectors led to a heavy load on the Detector Laboratory too. New glass substrates for the D20 microstrip detector had to be prepared and the large D22 detector repaired. It was operating perfectly on a test bench at the time of writing. A small high-resolution (~ 1 mm) two-dimensional microstrip detector prototype was completed and already tested for a variety of applications. Mr. Jochen Uckelmann a young german engineer will join the Detector Laboratory in February 1996.

The Neutron Optics Laboratory (LON) completed and delivered a number of composite crystal and multilayer systems, the development of which had begun during the reactor shutdown. Mr. Nief left the Optics Laboratory and will be replaced in February 1996 by Mr. Thomas Foltyn.

Mr. B. Guerra, a high temperature expert with industrial experience helped us in a variety of tasks (see Furnaces section in Sample Environment).

Sample Environment Laboratory

(S. Pujol)

P. Dagleish,

P. Andant, M. Brancaleone, A. Bresson, R. Chung, M. de Palma, J.P. Gonzales, P. Keay, P. Martin, L. Mélési, J.L. Ragazzoni, F. Thomas (for 1 year), G. Sirbi (until Dec. 1995).

Cryogenics

About 200 experiments with cryostats or cryofurnaces have been performed since the restart of the reactor. 24 very low temperature (dilution) experiments and 24 experiments with magnetic fields were carried out. Concerning the equipment itself, all cryostats have now been equipped with an automatic cold valve. A new 5 mK refrigerator has been put into operation, as well as an Edwards closed-circuit cooling unit.

Circuits

A second 110 m^3/h Luchard compressor for helium recovery has been put into operation. The ESRF helium recovery system has been connected up to our own.

Furnaces

About 100 high temperature experiments were performed. The 7 pool furnaces and their control consoles have been standardised, and the construction of a new mirror furnace is in the final stages of completion.

New projects in collaboration with B. Guerra:

– Construction and installation of a press-furnace for plastic deformation of monochromator crystals, cf. ILL Technical Report 95GU09T.

– Mirror furnace (for normal and four circle operation). Study and development of a device for the measurement of the sample temperature, cf. ILL Technical Report 95GU08T. Bringing up to European safety standards of electrical equipment, especially those using thyristor control.

– A new SANS (Small Angle Neutron Scattering) furnace which will permit both small and large angle scattering experiments.

– A new 3000 K furnace with the following contractual specifications: continuous operation at maximum operating temperature of 3000 K for a period of up to 30 days; operation at all temperatures up to 3000 K with argon at pressure slightly below atmospheric, maximum of 1700 K if operated under vacuum; useful volume: vertical cylinder of diameter 50 mm and height approximately 100 mm. Availability: 1st half of 1996.

High Pressures

A 5 kbar niobium pressure cell suitable for inelastic TOF experiments has been developed in collaboration with Christiane Alba-Simionesco of the Laboratoire de Chimie-

Physique des Matériaux Amorphes, Orsay. 25 high-pressure experiments were performed, 15 of which also required the use of a cryostat.

Thermometry and sample environment electronics group

The new ILL Sample Environment Controller (ILLSEC) is now working and has been tested in most of its operating modes. Four pre-production units were purchased earlier in the year by the CENG and a further 10 by the ILL for delivery before the end of the year.

The existing liquid helium level monitors for cryostats have been modified to allow them to be used with a new liquid nitrogen gauge developed by the group. This allows them to display either helium or nitrogen level at the flick of a switch.

A new control unit for "T.A.S.S.E." magnets has been developed. This allows the simultaneous monitoring of helium level, 2 current shunts and 4 temperatures.

Detector Laboratory

(A. Oed)

D. Feltin, B. Guérard (since Sept. 1995),
M. Gamon, A. Rambaud,
G. Cicognani (PhD student), N. Vellettaz (PhD student)

After the long reactor shutdown the group had to repair or replace many of the electronics on the various counters and position sensitive detectors of the Institute.

Two important operations shall be mentioned:

In October the gas of the banana shaped detector of the instrument D19 had to be replaced. From 1983 to 1995 the gas pressure was reduced from 6,9 bar to 2.7 bar caused by a leak in the detector housing. With the help of the new gas recovery system of the detector laboratory it was possible to empty and to refill the detector to its nominal pressure in site and without removing the banana out of its protection. The detector has again been in operation since the end of October 1995.

The new detector of the instrument D22 presented such serious defects that it had to be switched off. Before the end of the year it was successfully repaired by the detector group. To do so, it was necessary to design and construct working tools and supports as well as to install a clean room equipped with a filtered laminar air flow system. All the 130 anode-wires have been replaced by thinner ones in order to improve the gain and the stability of the detector. Besides, other minor but essential modifications have been realised. Preliminary measurements with X-rays before and after these modifications using a temporary Plexiglas cover confirmed the improvement. Once the detector was closed it was thoroughly outgased and refilled with a mixture of ^{3}He and CF^{4} at 2.2 bar.

An energy resolution of 15 % for neutrons from a laboratory source was measured for signals of the complete anode wire frame, see Fig. 4 page 162. The repaired detector will be installed at the beginning of 1996 on the instrument which will therefore be available for the first reactor cycle.

Besides these repair activities, three instruments have been equipped with the newly developed amplifiers, namely IN11, IN16 and D1A with 40, 20 and 25 counter tubes, respectively. The amplifiers are installed on a mother board, developed for the D20 instrument. As expected from previous rigorous tests, these amplifiers are unsensitive to perturbations generated by apparatus such as thyristor regulators for choppers or relays that run even close to detector electronics. Problems with so-called earth or ground loops do not exist any more. In the future it is planned to replace all amplifiers and motherboards of all ILL instruments by the new one.

An old multi-wire proportional counter with 64 x 64 cells is presently modified in order to act as a replacement detector for the instrument DB21 which is at the moment equipped with an ANGER- camera.

For the large banana-type detector of the instrument D20, seven micro-strip plates on the new electronic conducting glass substrate (S8900 type SCHOTT, USA) of the 50 plates which have been ordered, have been delivered. Three of these plates will be installed in the existing prototype in order to test their behaviour under operating conditions. The complete delivery is expected for mid-February.

Monochromator Laboratory (up to July)

(A. Magerl)

A. Escoffier, R. Hehn, B. Nief

In the first half of 1995, the group's resources were concentrated on the completion of the D2B Ge monochromator. A new hot press has become available allowing the speedy production of plastically deformed wafers. We opted to build the monochromator from wafers with a thickness of 1 mm and to use Al foils as a bonding agent to build up blocks of sufficient thickness. The essential process parameters for the plastic deformation were finalised by the end of last year, while the procedure for the bonding was retained definitely at the beginning of this year. Fig. 5 shows micrographs at different magnifications of a test stack made from six Ge wafers bonded by an Al foil. The images show the pattern of a secondary precipitation which can be fully understood, including the elemental compositions of all components from the Al-Ge phase diagram near the eutectic point. This bonding can be tuned to provide a strong binding without deteriorating significantly the quality of the crystals at the interfaces.

Together with J. Schefer from PSI, a workshop was organised in June on composite Germanium monochromators to initiate an exchange of expertise. Scientists from seven laboratories and representatives from

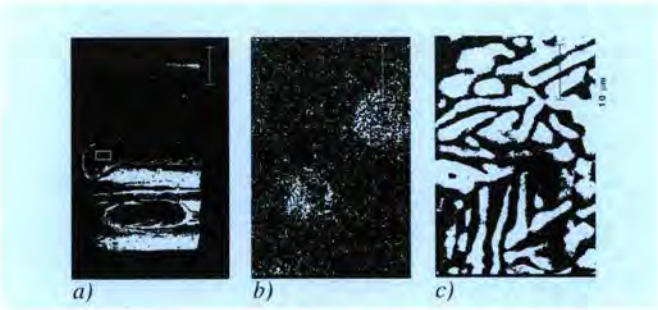

Fig. 5: Micrographs of a test stack of six 1mm thick Ge blades bonded by an Al foil. The rectangles in figs a) and b) indicate the locations of the images in b) and c), respectively. This investigation was performed in collaboration with Dr. Bach from the University of Bochum, Germany.

two industrial companies with hands-on experience of Ge as a neutron monochromator participated in very lively discussions on this subject for two days.

The monochromator for IN4C is a second large-scale project. The production of Cu ingots and crystal conditioning is well under way for the first two faces of the monochromator. This work made progress despite two complete rebuilds of the Bridgman furnace after failures of the stainless steel crucibles due to faulty welds.

In the course of the restart of the reactor, the monochromator laboratory became involved in the improvement and the repair of several monochromators on instruments in use. E.g. the monochromator of D1B was first aligned with new mechanics at LLB. However it needed more attention later in the year due to an incident during the first mounting of the monochromator on site. A new Si 311 made from two pieces of thermally treated Czochralski material on IN10 showed a double peak structure, which could be corrected during an overhaul. Further alignments were done on the graphite analyzers of IN12 and IN8, and assistance was given to DB21 for a new monochromator made from intercalated graphite. In addition, the vertically bent graphite deflector of IN13, damaged during the shut down period, was repaired. Additional work on monochromators was carried out during the reactor shutdown period on the γ-ray diffractometers, such as a re-adjustment of the vertical curvature of the Cu monochromator of IN3.

During the last few years several concepts have been followed which aim in a coherent way to exploit new ways of making higher quality monochromators. The two key issues are, firstly, an understanding of the real defect structures in the crystals and their relation with diffraction properties and, secondly, an engineering of crystals with optimized microstructures. Embedded in this context was a project to make gradient crystals as novel optical elements in neutron diffraction with particular promise for very high quality elements. This idea was followed along various lines of development. However, the project has been significantly reduced because of a lack of resources and a redefinition of priorities and responsibilities. At present it is planned to begin a thesis work on ultrasound excited perfect crystals as the only active part of this program.

Neutron Optics Laboratory

(I. Anderson)

B. Hamelin, P. Høghøj,
M. Berneron, A. Escoffier, W. Graf, R. Hehn, E. Hetzler.

The neutron optics laboratory was formed in July of this year and regroups the activities in monochromators, multilayers and instrumental techniques with the purpose of ensuring a more efficient use of personnel and equipment.

Monochromators

The list of instruments (D2B, IN4C, D20, IN8, D16) for which new monochromators are being constructed or studied demonstrates the continued high demand at ILL.

The D2B Germanium monochromator which was started in 1994 was completed in December 1995 and tested on the instrument during the last week of the cycle. The new monochromator is based on the wafer construction first proposed by Maier-Leibnitz in 1967 [1] and more recently developed at Brookhaven National Laboratory [2]. The method involves the successive bending and flattening of thin single crystal wafers of germanium where the number of cycles is used to determine the final crystal mosaic. It was carried out at high temperature (820 °C) in a new, fully automated, hot press, Fig. 6 page 163, developped by B. Guerra based on specifications from the Monochromator Group [3], and designed to maintain a uniform temperature (± 1°C) within a large zone.

Selected wafers were then welded together using aluminium foil (Ge/Al eutectic at 520 °C) to produce 15 composite blocks each comprising 10 wafers. As shown in Fig. 7 page 163 the blocks have been glued to a support with a fixed vertical radius of curvature. Preliminary tests carried out at the end of the last cycle in 1995 showed that the new monochromator performs well producing the all important symmetric line shape demonstrated in Fig. 8.

The excellent results obtained from D2B have encouraged us to study and develop other monochromators using the wafer technique in the coming year.

The IN4C monochromator is also in production. The basis of the monochromator is a four face support built by the Italien partner. Each face comprises 55 crystals which can be vertically and horizontally focussed automatically. Presently 3 faces have been defined: PG002, Cu220 and Cu111. The PG pieces have been tested by the Italien partner and delivered to ILL ready for mounting at the beginning of 1996.

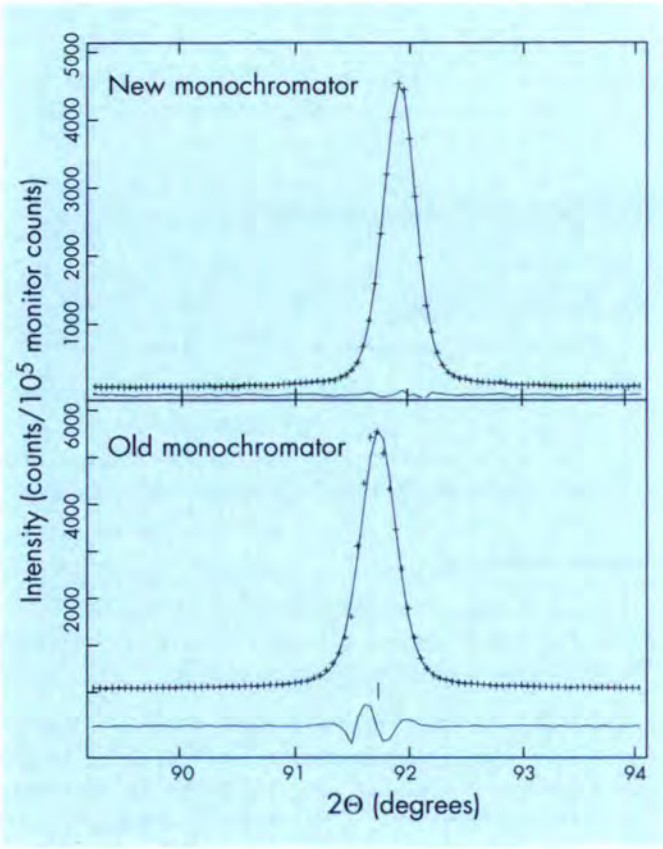

Fig. 8: A comparison of the lineshapes obtained at 2θ = 90° using the the old and the new Ge monochromators on D2B. The peaks have been fitted with a pseudo-voigt profile.

For the Cu220 face 50 out of the 55 crystals have been produced and are in the process of being tested. A further 25 pieces will be produced to ensure a choice for the final mounting.

The ingots required for the remaining monochromators (IN4C: Cu111, D20: Cu200, IN8: Cu111 and Cu220) have been grown though some supplementary ingots will be produced in 1996. A great deal of work remains to be carried out in the deformation, cutting and final mounting of these monochromators.

Multilayers

The Electrotech evaporator was shut down at the end of 1994 to replace the control system with a PC. The project was successfully completed in February of 1995 and since then both evaporators have been dedicated to the fabrication of the IN11C analyser which requires 500 polarizing mirrors. At the end of 1995 approximately 300 of these mirrors have been produced and mounted on the instrument.

The EVRY sputtering facility has also been modified during 1995. The RF generators were replaced with a 5kW DC supply and switching unit allowing us to run 3 cathodes from the same power supply. At the same time the group designed a new magnetron cathode which is better adapted to the new DC power supply than the existing cathodes. The prototype cathode was constructed in the ILL workshops and after installation in September it proved to be a huge success allowing deposition of magnetic materials at low argon pressures.

The sputtering facility has been mainly used during 1995 for the development of multilayer monochromators reflecting a large band width in wavelength. The requirements for such monochromators is best illustrated by the example of the LAue DIffractometer for protein crystallography LADI [4]. First experiments with this instrument using the full spectrum of the H142 neutron guide showed that the long wavelength neutrons did not contribute to the interesting diffraction spots but caused a significant incoherent background which ultimately limited the resolution of the instrument. The results showed that a Quasi-Laue instrument operating at approximately 3.6 Å with a bandwidth $\Delta\lambda/\lambda$ of 20 % would be a significant improvement. A selector device using Ni/Ti multilayers has been developed to produce a neutron beam with the above characteristics. The basic unit of the device is a 748 layer graded d-spacing monochromator with periods ranging from 74 Å to 90 Å deposited onto a 0.5 mm thick silicon wafer. In total 40 such mirrors are stacked together to cover a beam width of 20 mm and the length of the device is only 25 mm (Fig. 9 page 163). The individual monochromators have a reflectivity of 80 % over a band width of 20% $\Delta\lambda/\lambda$, however absorption in the silicon reduces the overall reflectivity of the device to about 75 % as can be seen from Fig. 10

The device has been used on the instrument for a complete reactor cycle and performs well. It is certainly a much cheaper device than the alternative velocity selector which has also been tested on LADI.

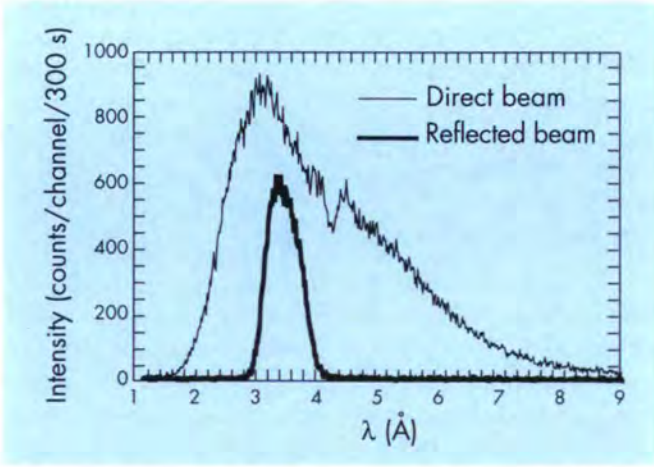

Fig. 10: TOF spectrum of the direct beam at LADI/guide H142 (thin line) and the beam reflected by the large bandwidth multilayer monochromator. The spectra were both recorded through a 1 mm pinhole 3 m from guide exit as required by LADI.

Further developments along these lines are continuing and mononochromators with 30 % $\Delta\lambda/\lambda$ have been produced for other applications.

Instrumental Techniques

The main focus of the activities of this group has been directed toward the installation of the hard X-ray laboratory which will supercede the present gamma-ray facilities in summer 1996. The laboratory is based on a 420 kV generator which will serve several diffractometers. During 1995 the study of a suitable two-dimensional detector was completed and a system using an X-ray intensifier associated with a cooled CCD camera was procured. In addition the plans of the beam collimators were finalised and put into fabrication.

Further activities carried out in 1995 include the construction of a miniature goniometer for use inside cryostats and the study of new mechanical systems for focussing monochromators.

A great deal of effort was also directed towards supporting the work in the development of monochromators.

References

[1] H. Maier-Leibnitz, Ann. Acad. Scien. Fenn. A 267 (1967).

[2] J.D. Axe, Cheung, S. Cox, L. Passell and T. Vogt, J. Neut. Res. **2,3** (1994) 85.

[3] B. Guerra, ILL report 95GU09T.

[4] F. Cipriani, F. Dauvergne, A. Gabriel, C. Wilkinson and M.S. Lehmann, Biophysical Chemistry **53**, 5 (1994).

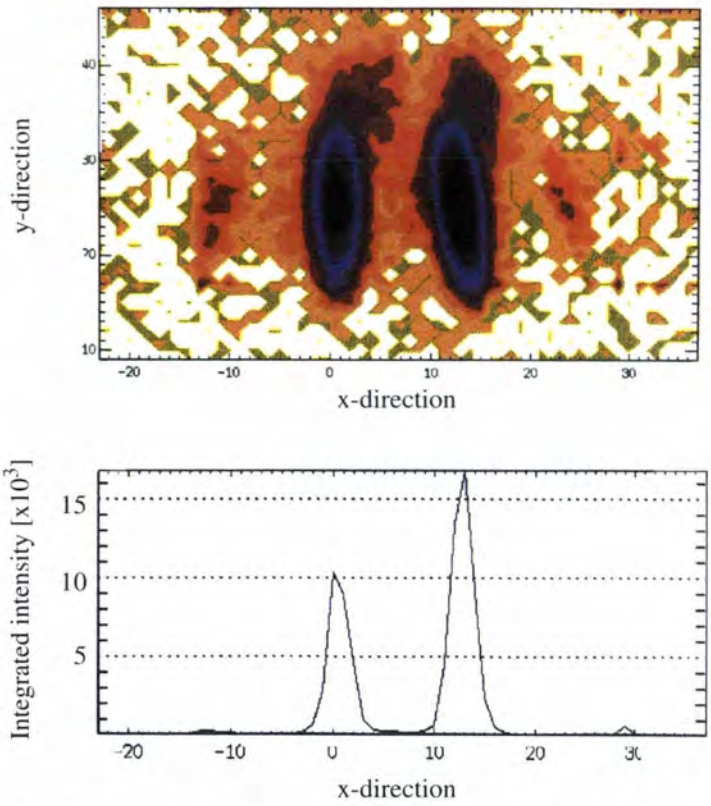

Coll. 5 - Fig. 4: Bragg diffraction of cold neutrons by a holographic grating in D-PMMA.
See report p. 53.

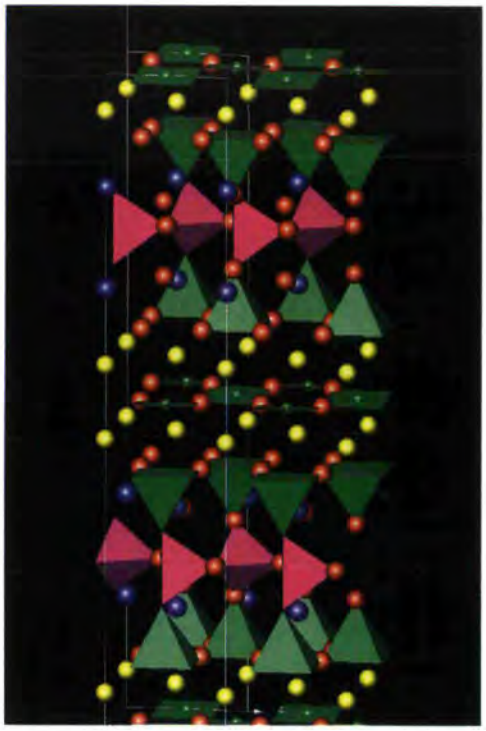

Coll. 5 - Fig. 7: The structure of superconducting $Ca_2Sr_2Cu_3GaO_9$ obtained on D2B from a very small sample prepared at high pressure.
See report p. 55.

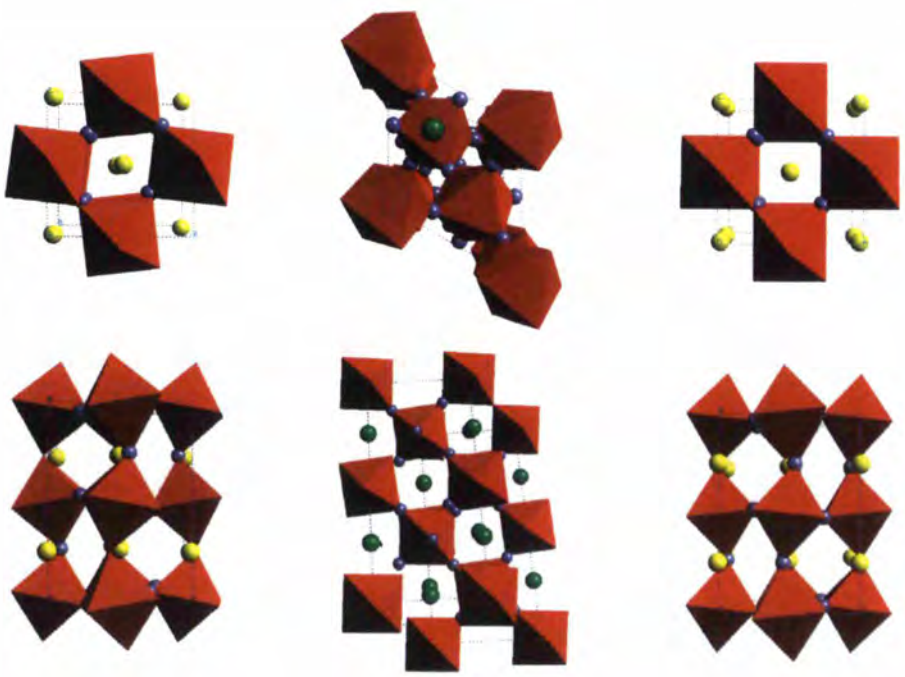

Coll. 5 blue box - Fig. 5: Allotypes of the perovskite structure in the $A_{0.7}A'_{0.3}MnO_3$ system. The three space group symmetries can be described as arising from tilt distortions of the ideal cubic perovskite.
See report p. 64.

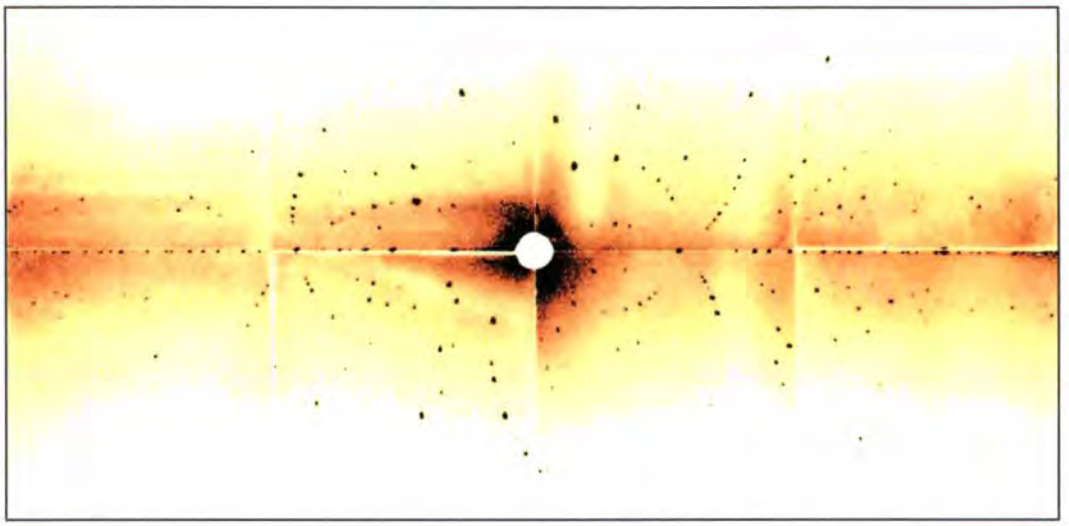

Coll. 8 - Fig. 5: The first Laue diagram recorded from triclinic Lysozyme using the full beam at the end of cold neutron guide H142. The cylinder image plates have now been upgraded.
See report p. 95.

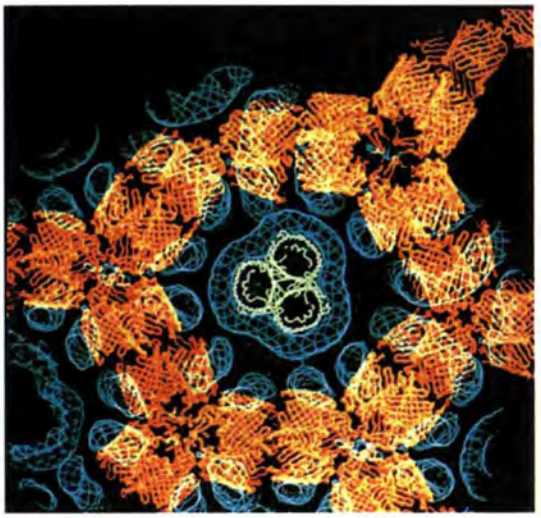

a)

Coll. 8 - Fig. 3: The distribution of detergent around a trimer of the OmpF porin from E. coli. View parallel to the trimer three-fold symmetry axis from crystals containining:
a) ß-octyl glucoside
b) deuterated N, N' methyl decyl amine oxide.
See report p. 92.

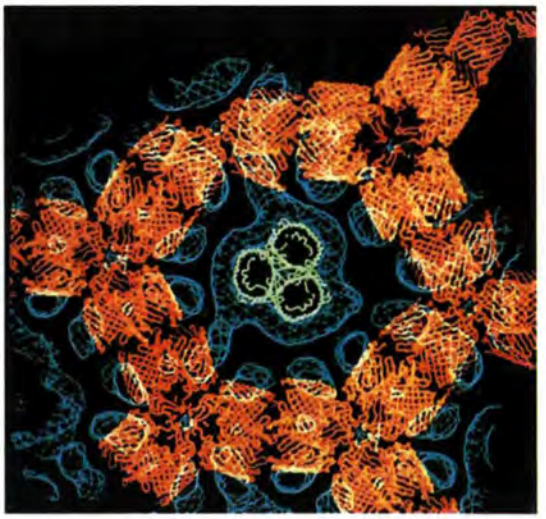

b)

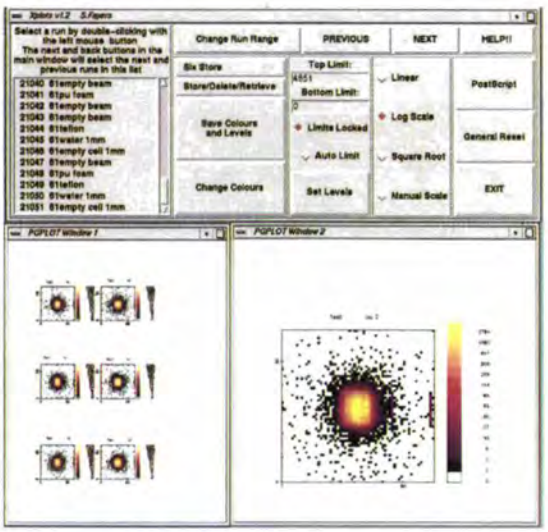

DS - Scientific Computing - Fig. 1: An example application of Tk/Tcl to create an easy to use GUI for plotting raw SANS data.
See report p. 115.

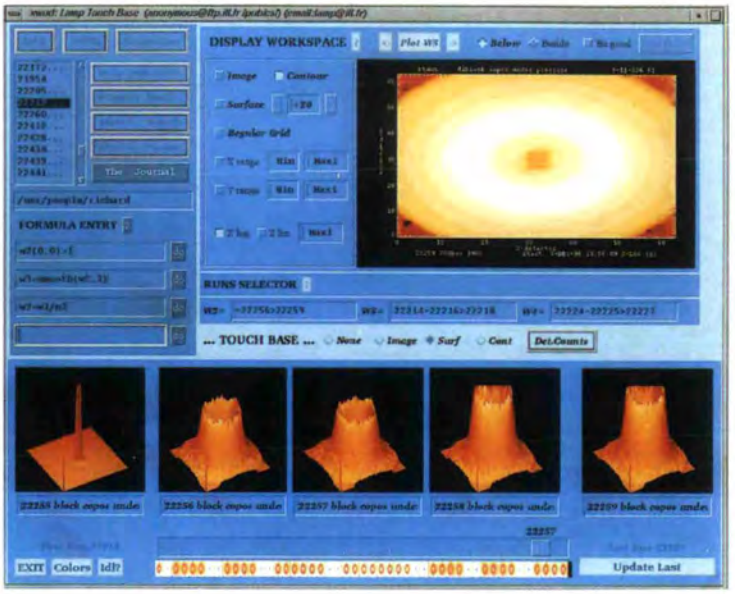

DS - Scientific Computing - Fig. 2: A LAMP interface showing the TOUCH-BASE data-base browser at the bottom.
See report p. 115.

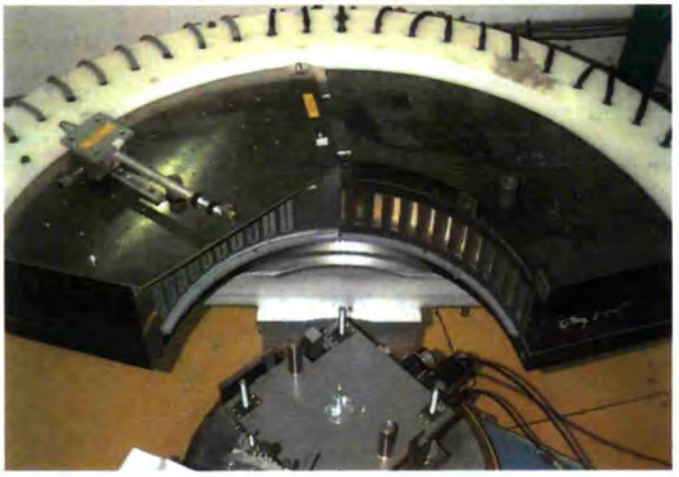

DS - DIF - Fig. 1: New 25-collimator detector covering 150° on DIA.
See report p. 120.

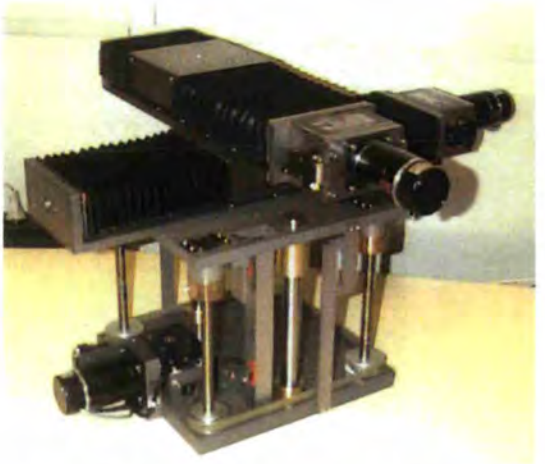

DS - DIF - Fig. 2: X-Y-Z translation table for stress measurements on DIA.
See report p. 120.

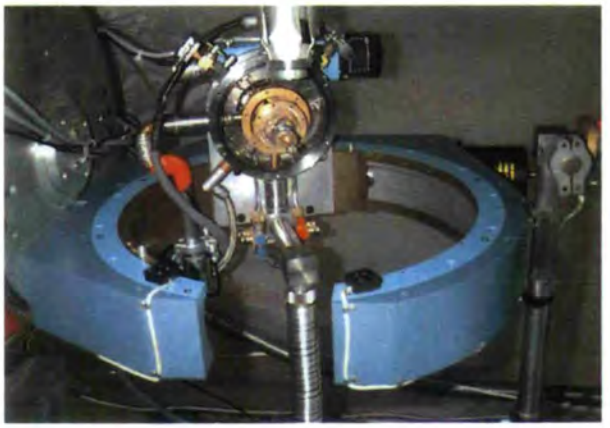

DS - DIF - Fig. 6: A neutron's view of the very low temperature four-circle dilution cryostat of D10.
See report p. 124.

DS - DIF - Fig. 5: The new D2B monochromator, with the large graphite filter for work at 2.4 Å.
See report p. 121.

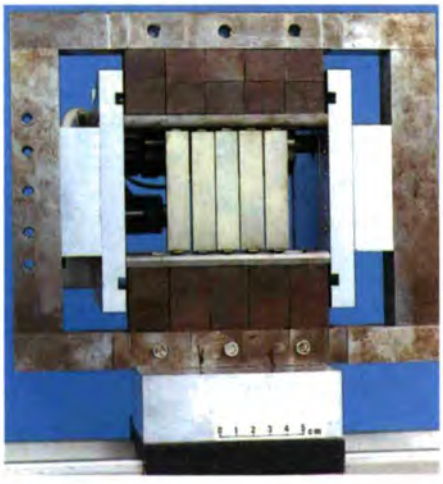

DS - TAS - Fig. 2: The IN14 horizontally focusing Heusler analyser (reflecting area 75 × 75mm²; thickness 3 mm; saturation field 1.3 kOe from Nd_2BFe_{14} permanent magnets).
See report p. 131.

DS - TAS - Fig. 4: View of the IN3 converging guide from sample to monochromator (the top part of the guide has been removed).
See report p. 132.

DS - TAS - blue box - Fig. 2: Photograph of the new IN20 analyser using elastically bent Si 111 crystals. Each of the three stages contains a pack of three silicon plates; the plates in the top and bottom part are skew cut with an inclination angle of 7.5° to provide fixed vertical focusing optimised for $k_f = 2.66$ Å^{-1}.
See report p. 133.

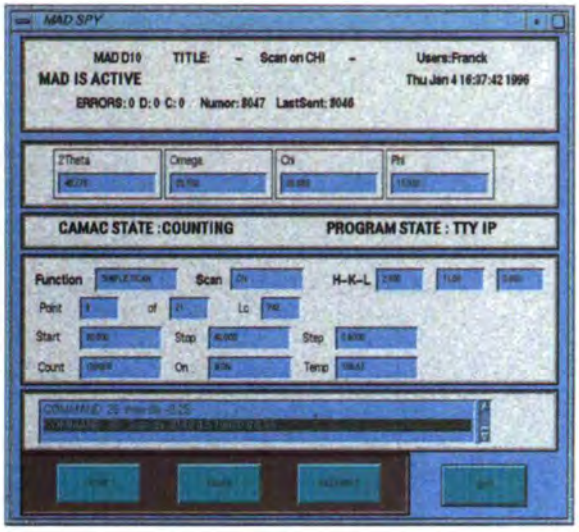

DPT - Fig. 1: Graphic user interface of the instrument control program MAD of D10 based on OSF/MOTIF.
See report p. 151.

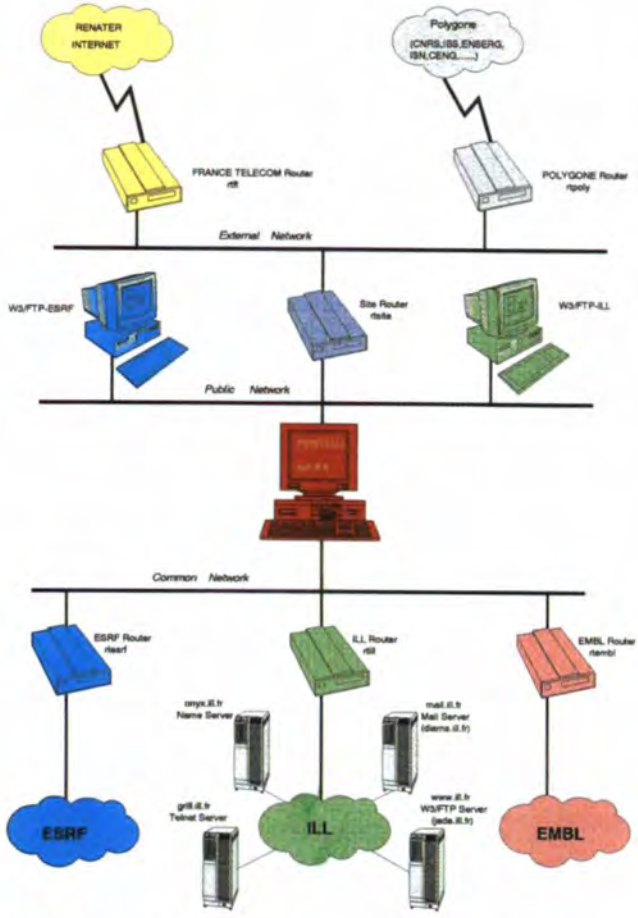

DPT - Fig. 2: General site interconnection diagram.
See report p. 151.

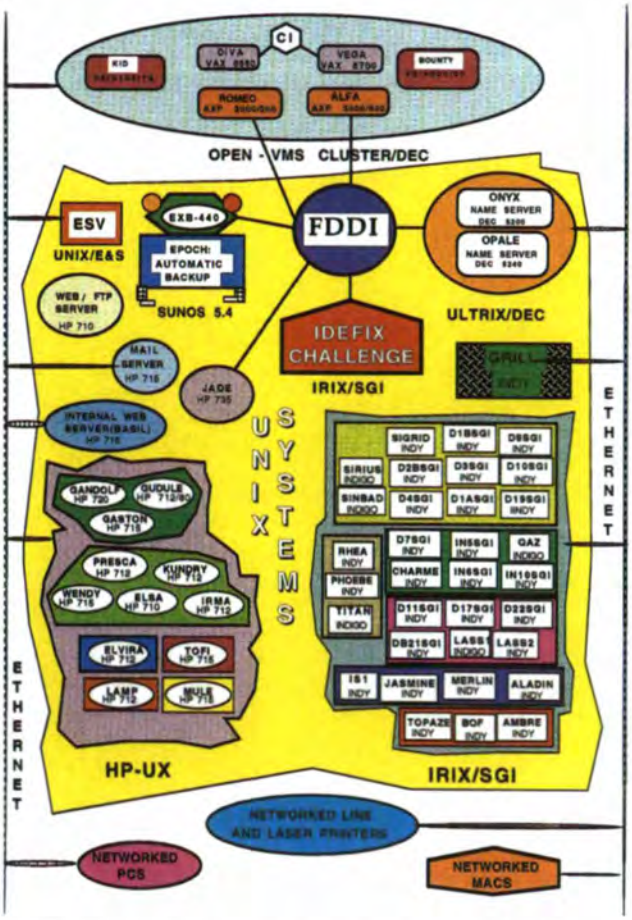

DPT - Fig. 3: The computing infrastructure end of 1995.
See report p. 152.

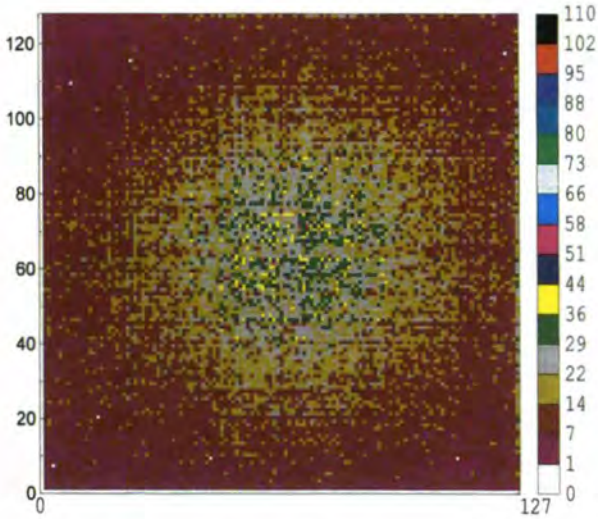

DPT - Fig. 4: Spatial response of the repaired D22 detector measured with a neutron laboratory source.
See report p. 154.

DPT - Fig. 7: The final assembled germanium monochromator for D2B.
See report p. 155.

DPT - Fig. 6: The new hot press developed by B. Guerra and used for bending the Germanium wafers for the D2B monochromator. The design ensures a uniform temperature region of 200 mm hight up to 900 °C, and pressures up to 3.5 bars during a fully automated cycle.
See report p. 155.

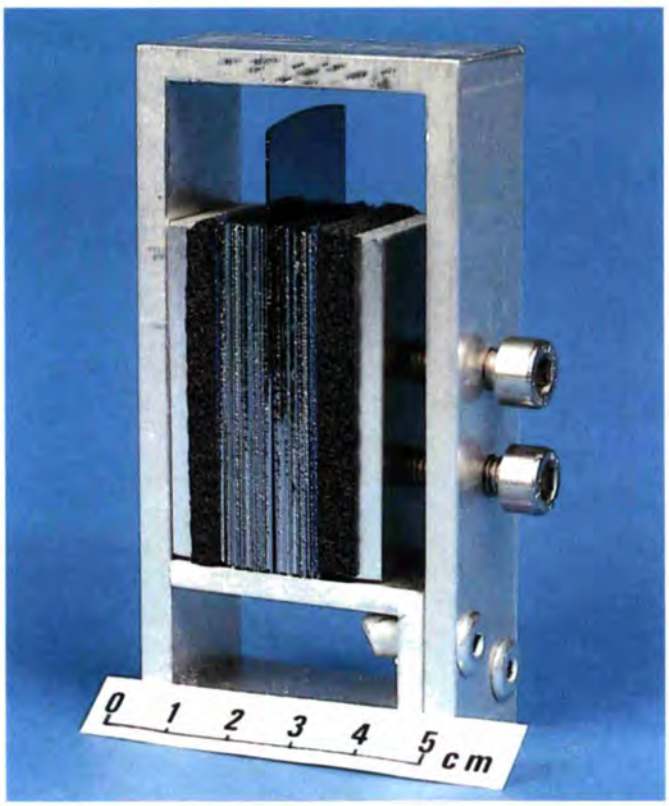

DPT - Fig. 9: The multilayer device used on LADI to select a broad wavelength band (20 % $\Delta\lambda/\lambda$) centered at 3.6 Å. The device consists of 40 silicon wafers, each with 374 Ni/Ti bilayers.
See report p. 156.

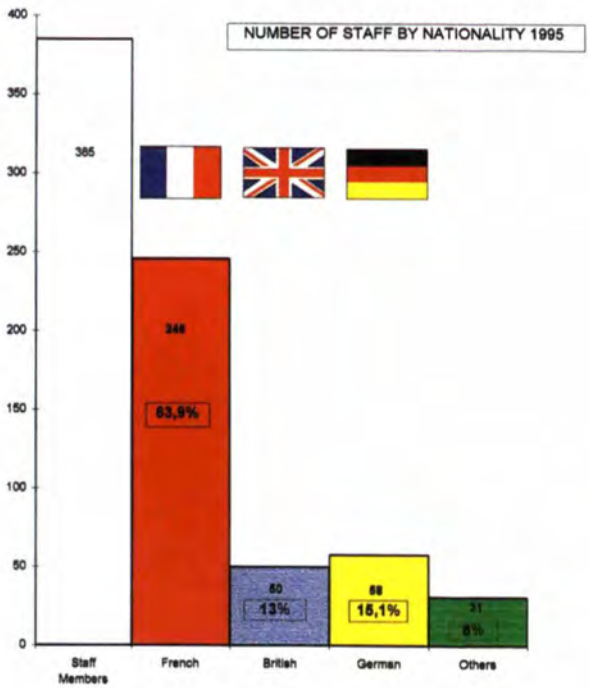

DA - Table 2.
See report p. 171.

REACTOR DIVISION (DR)

Reactor Operation 1995

The 5 operating cycles scheduled for this year were completed.

Start of first cycle: 6 January 1995. The nominal power of 58.3 MW was reached on 7 January at 9.29 p.m.

Although the first cycle of our new reactor was particularly long and interrupted by frequent restarts and shutdowns at various power levels, its 46 equivalent days of full power were completed without any unscheduled shutdowns. According to routine procedure, this cycle ended with the unloading of the fuel element (see Fig. 1).

The first part of the cycle was given over to ILL scientists to allow them to make final adjustments to the instruments and check the effectiveness of the reconstructed radiological shielding.

On 30 January, the reactor resumed continuous operation at nominal power. With the completion of the specific restart programme, reactor operation returned to normal.

Data for 1995

Number of days originally scheduled: 255

Actual number of days of operation: 253

Number of equivalent days of full power: 232

Actual operating time as proportion of year: 70 %

Actual operating time in relation to time scheduled: 99.2 %

Number of fuel elements used: 5

Number of new fuel elements received: 2

Number of unscheduled shutdowns: 2

including: - brief shutdowns: 0

- shutdowns with Xenon poisoning: 2

Cycle 99

The cycle began on 6 January and was completed on the morning of 14 March. Apart from a brief reduction in power on 31 January as a result of the shutdown of a cold source compressor, the schedule was respected.

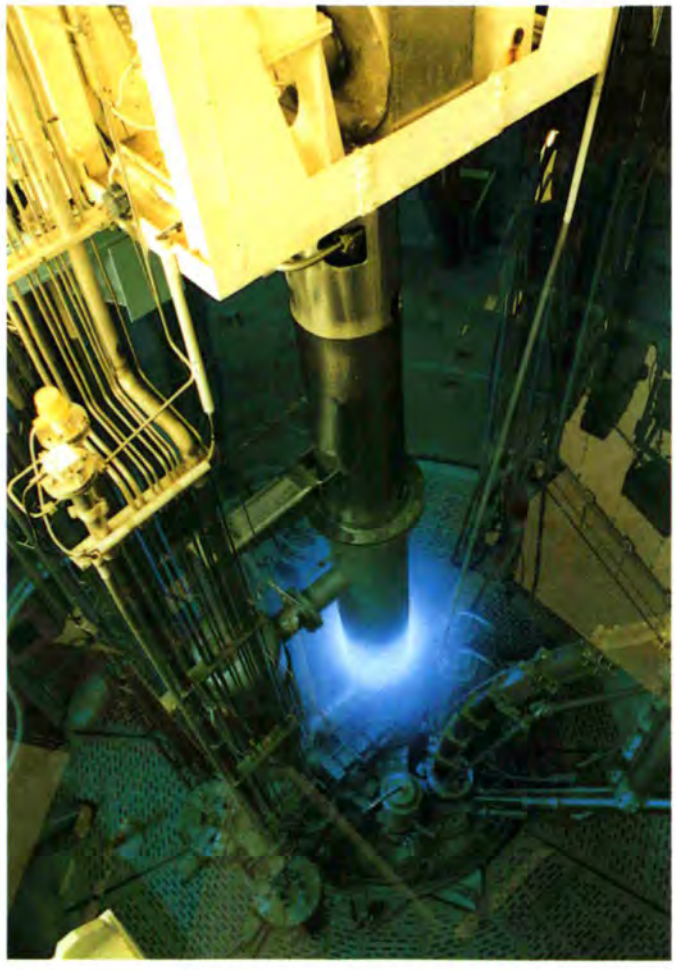

Fig. 1: Unloading the fuel element from cycle 99.

Cycle 100

A power level of 15 MW was established on 3 April to allow flux measurements to be taken on the neutron guides.

The actual cycle began on 4 April and was completed on the morning of 23 May. An unscheduled shutdown of two days occurred on 12 May following a loss of compressed-air

supply which caused the cold source turbines to shut down. To compensate for this delay, the cycle was extended by 2 days.

Cycle 101

The cycle began on 6 June and was completed on the morning of 23 July. Power was cut back for a short time on 22 June in order to inspect an exchanger room after an alarm was triggered.

On 7 July, there was an unscheduled shutdown lasting 2 days due to a voltage drop on the EDF power supply.

Cycle 102

A power level of 15 MW was established on 7 August to allow flux measurements to be taken on the neutron guides.

The actual cycle began on 8 August and was completed on the morning of 24 September.

The cycle was completed without interruption.

Cycle 103

A power level of 15 MW was established on 30 October to allow flux measurements to be taken on the neutron guides.

The actual cycle began on 31 October and was completed on the morning of 17 December.

A brief reduction in power occurred on 29 November following the shutdown of a secondary system cooling pump.

Maintenance

Inspections and maintenance operations are scheduled at regular intervals in order to ensure that the installations continue to operate safely and reliably.

Major work carried out this year included:

– The replacement of an industrial air compressor and two air-start compressors for the diesel generators.

– The diesel generator in the emergency control room was replaced halfway through the year.

– The installation of a temperature control loop for the reactor swimming pool.

– The inspection of the inside and outside of the new reactor block and its «turned-down» grid (see Fig. 2).

– The replacement of four static generators which supply power to the reactor control system and ILL's central computer.

Fig. 2: Preparing the inspection of the new «turned-down» grid.

Under Examination

Now that the beta beam tube has been removed and the flat grid has been replaced by a «turned-down» grid, the reactor cycle can be extended. We have therefore submitted a request to the Safety Authorities to extend the duration of our reactor's operating cycle, which is currently limited to 47 equivalent days of full power.

ADMINISTRATION DIVISION (DA)

Following the restart of the high-flux reactor in January 1995, the Administration Division focused its attention primarily on providing the Institut with optimum service-oriented support as it returned to normal user operations. This involved a broad range of activities, including the procurement of uranium, obtaining contractual guarantees for the production of fuel elements and the provision of spare parts for the reactor, as well as providing administrative support for the necessary investments in instrumentation and logistics support for meeting the administrative needs of visitors and CRGs.

The main priority in 1995 was to keep staff expenditure as low as possible, despite the on-going recruitment of young scientists and technicians (which brought the workforce up to 385 in 1995 compared to 377 in 1994), in order to have sufficient scope in the coming years for urgently needed investments in both existing instruments and new projects.

Generally speaking, efforts were stepped up to review the Institut's cost structures, adapting them, where necessary, to changes in framework conditions. In this context, it was necessary to analyse not only the use of facilities and the general ILL infrastructure, but also the relationship between internal and external services.

Regular budgetary monitoring and cost controls call for the use of state-of-the-art tools for IT and other operations. The first step towards implementing such tools involved creating the necessary hardware and software environment to be able to network the systems. Once this was achieved, the next stage was the overhaul of the Management Information System (MIS). This project was examined from the point of view of existing systems at ESRF and other comparable organisations to ensure that, before going ahead with the acquisition of a new system, all possible options for adopting an existing, tried and tested MIS solution had first of all been thoroughly investigated. Although such an approach meant that the project would fall behind schedule, the delay was accepted in view of the potential cost savings generated by the use of a system which was already operational.

During the period covered by this report, the Administration Division also endeavoured to integrate our CRGs and gained initial experience in the handling of the specific individual contracts concluded with these groups. In certain areas, it is becoming apparent that the cost of supporting CRGs has been underestimated. It is quite possible, therefore, that in the future the range of services provided and their financial repercussions may be reevaluated on the basis of the findings made in 1995.

The Head of Administration has established much closer contacts with his counterparts at ESRF and EMBL, on the one hand, to take account of the increasing need for consultation on matters relating to shared services and, on the other, to improve exchanges of experience between the neighbouring organisations. The regular meetings also serve to discuss, among other things, the possibility of reducing costs through concerted action with regard to suppliers and service-providers. This year, for the first time, the heads of administration of ILL and ESRF attended each other's finance committee meetings as observers.

In the framework of a recently launched initiative for promoting mobility and the exchange of experience in Europe (European Association for Research Managers and Administrators - EARMA), the Head of Administration agreed, at the beginning of 1995, to chair this association, which is supported by ILL, for the first two years of its existence. EARMA seeks to create a comprehensive database of expertise relating to the management of the research process, develop original pilot-projects on research management processes, and make available relevant information to those involved in research management and administration through: networking, publications, audio-visual materials, internet databases, seminars, professional training courses, staff exchanges. Within the context of these activities, ILL has exchanged staff with research institutions from its member countries and set up vocational training periods. EARMA has also successfully organised a training course in Brussels on the management of EU contracts, which attracted 60 participants from more than 10 countries.

Finance and Management Information Systems

Finance

Implementation of the 1995 budget

1995 saw the restart of the reactor and the resumption of experimental activities at ILL - 5 cycles were completed, the first of which served as a test phase for the restart of the instruments. By the end of 1995, ILL was operating the equivalent of 24 instruments, as well as six instruments managed in the context of CRGs.

Expenditure

Total ILL expenditure is expected to amount to 299.9 MF, comprising a normal budget of 295.8 MF and 4.1 MF for the refurbishment of the reactor.

The following table shows the variation in expenditure between 1994 and 1995:

	Expenditure 1994		Estimated expenditure 1995		Change
Expenditure	**kF**	**%**	**kF**	**%**	**%**
1. Staff costs	**182 516**	**57,8**	**178 700**	**59,6**	**-2,1**
2. Fuel elements	**4 687**	**1,5**	**24 480**	**8,2**	**422,3**
Consumables	20 718	6,6	27 249	9,1	31,5
Long term supplies and services	6 690	2,1	10 978	3,7	64,1
Short term supplies and services	14 805	4,7	13 461	4,5	-9,1
Travel	1 974	0,6	1 935	0,6	-2,0
Miscellaneous adm. costs	3 406	1,1	6 696	2,2	96,6
Taxes and fees	1 624	0,5	1 640	0,5	1,0
3. Operation	**49 217**	**15,6**	**61 959**	**20,6**	**25,9**
Buildings	0	0,0	1 200	0,4	NC
Equipment	2 883	0,9	6 914	2,3	139,8
Instruments	12 152	3,8	10 310	3,4	-15,2
Other investments	11 818	3,7	12 238	4,1	3,6
4. Total Investments	**26 853**	**8,5**	**30 662**	**10,2**	**14,2**
5. Normal Budget (1-4)	**263 273**	**83,3**	**295 801**	**98,6**	**12,4**
6. Reactor Refurbishment	**52 711**	**16,7**	**4 058**	**1,4**	**-92,3**
9. Total expenditure (5 + 6)	**315 984**	**100**	**299 859**	**100**	**-5,1**

The normal budget increased by 12.4 %, from 263.3 MF in 1994 to 295.8 MF in 1995.

Staff costs fell by 2.1% compared to 1994, despite average staffing levels of 385, compared to 377 in 1994. This was due primarily to a substantial fall (approximately 4 MF), over 1994 figures, in the amount of funding devoted to the reduction or renewal of permanent positions at ILL in 1995, as well as the injection, as planned, of "young blood" into the staff.

The redundancy programme implemented in 1995 at a cost of 6.3 MF will reduce staff expenditure permanently by an average of 2.5 MF per year.

With the restart of the reactor, fuel costs rose considerably, the major cost items being the purchase of 50 kg of uranium from Nukem at the end of 1995 and the production of two fuel elements (compared with one in 1994). 18 irradiated fuel elements continued to be held in interim storage at Cadarache and the production of cylinders began at the end of 1995.

The other operating costs showed an overall increase of 26% over the previous year. Naturally, this increase corresponds primarily to the expenditure generated by the operation of five reactor cycles (fluids, insurance, etc.) and, where scientific activities are concerned, the cost of welcoming visitors to the Institut starting from the second reactor cycle, as well as providing logistics support for experiments.

Investments rose by 14.2% as a result of the complete overhaul of the roof of ILL 7, at a cost of 3.9 MF. Scientific investments came to 10.3 MF and concerned:

- the high-flux multidetector D20 - 960 KF
- the TOF spectrometer IN4C - 1 600 KF
- the gamma-ray spectrometer GAMS 5 - 890 KF
- the neutron guide H25, - 800 KF
- the polarised ^{3}He filter - 350 KF
- the reflectometer D17 - 300 KF
- LADI - 270 KF
- the development of existing instruments - 5 140 KF

Income

Comparison of 1994 and 1995 Budgets - Income

Income	Income 1994		Estimated Income 1995		Change
	kF	**%**	**kF**	**%**	**%**
Collaboration with ESRF	1 970	0,6	1 900	0,6	-3,6
ILL's own income	3 386	1,1	8 000	2,7	136,3
Spanish contribution	4 240	1,3	4 520	1,5	6,6
Swiss contribution	6 530	2,1	7 900	2,6	21,0
Austrian contribution	5 310	1,7	6 022	2,0	13,4
Associates' contributions	252 839	80,0	260 157	86,8	2,9
Carry forward 94/95	-11 002	-3,5	11 002	3,7	NC
Carry forward 95/96			-3 700	-1,2	NC
Use of reactor reserve	52 711	16,7	4 058	1,4	-92,3
Total	**315 984**	**100,0**	**299 859**	**100,0**	**-5,1**

Expenditure for the refurbishment of the reactor was estimated at 4 MF in 1995 and was financed by reserves set up in previous years, within the limits of the budgetary envelope allocated for the overall project (173.1 MF).

The Associates' contributions amounted to 260.1 MF, which represents 87% of ILL's income. The contributions from the Scientific Members - Austria, Spain and Switzerland - came to an overall total of 18.4 MF, or 6% of ILL's income.

There was a marked increase in other ILL income as a result of the sale of the scientific instruments IN12 to KFA and D15 to the CEA, which from now on will be operated within the framework of CRG contracts.

Finally, the available credits from 1994 (amounting to 11 002 KF) were carried forward to the 1995 budget, while 3 700 KF of the credits generated by the sale of instruments IN12 and D15 will be carried forward to 1996 for scientific investments (image plate detector system, polarising 3He facilities, reflectometer project, etc.).

Outlook for 1996

The 1996 budget was adopted by the Steering Committee on 28 November 1995 for a total of 324.6 MF, an increase of 24.7 MF compared to 1995 (+ 8.2%). This amount comprises 31.7 MF for investments (+ 3%), 14.3 MF to complete the reactor refurbishment programme and 33.3 MF for the supply of fuel elements.

Overall survey: the ILL budget 1997 - 2000

In current prices, the level of the Institut's budget is set to fall in 1997 and 1998 (by 298 MF and 300 MF, respectively) as a result of the suspension of uranium procurement and the completion in 1996 of the reactor refurbishment programme. Investments will amount to 32 MF, i.e. 10% of the budget, a figure which is comparable to investment levels prior to the reactor shutdown. As of 1999, the slight increase in the budget (315.8 MF in 1999 and 312.9 MF in the year 2000) will be due mainly to the production of fuel elements and the resumption of uranium procurement; other operating costs will, on the whole, remain stable.

Management Information Systems

With the expiry of a number of temporary contracts underlining staff shortages in the Management Information Systems group, an audit of our activities was carried out by an external company. As a result of its findings, we decided as of July to subcontract the running of our servers and the hot line to an outside service-provider. Six months later, the benefits of this solution are conclusive: not only do our users get a better service but it also allows the members of the group to focus their efforts more effectively on applications and improvements to architecture and personal computers, in order to enhance interactions and communication.

Hardware

Intensive use has been made of the Novell server (Netware 4.1), which was installed last year in order to simplify sharing in a heterogeneous environment and allow access to common resources. Increased demand has prompted us to extend the server configuration. This extension, which is currently being installed, will provide better performance levels for more users, together with improved operating security.

We have continued work on updating our park of personal computers with hardware upgrades (memory, disk, processor) and by replacing obsolete Macintosh computers, mainly with PCs. We can now reasonably expect all personal computers to use the same software versions, something which was previously impossible due to performance limitations.

Applications

Software support for the most recently added applications has been especially demanding. Much has also been done to improve the consistency of the site database: given the large number of users involved, the validity of the data captured could not be checked correctly and restricted access procedures have been introduced to facilitate the necessary corrections.

The decision to migrate applications to Windows has been taken and the technological choices ratified. All the lists needed by the Scientific Coordination Office (SCO) have therefore been rewritten. These now run under Windows and the performance problems have been resolved. The migration of data capture programmes is starting and will not only include straightforward migration but will also integrate any new functions deemed necessary.

Restructuring of MIS

A number of meetings and preliminary contacts have confirmed the need to overhaul the MIS. The start of the project has been postponed until the beginning of 1996 in order to establish a broad consensus before preparing an initial set of specifications.

Purchasing

The restart of the High Flux Reactor in January 1995 meant a return to normal life for everyone at ILL. The Purchasing Service which had been mainly occupied by the commercial aspects of the reactor refurbishment over the previous four years has now adapted to normal operation again.

Procurement for the fuel cycle

Once the new reactor vessel had been installed our thoughts turned to ensuring the supply of reactor fuel for the forthcoming years. An international invitation to tender for uranium was sent to suppliers in the member states in March;

three offers were received. In May, the Steering Committee authorised the purchase of two lots of Highly Enriched Uranium:

- 9.5 kg from CERCA (F);
- 50 kg from NUKEM/UKAEA (GB).

During the reactor shutdown the production of fuel elements had been slowed down, thus a stock of fuel elements was built up ready for the reactor re-start. This stock is now being consumed and in 1997 fabrication of fuel elements will be raised again. A new contract for supply of fuel elements from 1998 onwards has to be negotiated, and as a first step, we have sent out a call for tender.

Other purchases

Following international calls for tenders important spare parts for the reactor were ordered from

- GEC Alsthom (F), H1-H2 beam tube housing and coupling sleeve,
- NTG (D), anti-siphon valves, and
- GIROD SISA (F), the through-going beam tube H6-H7.

Other major purchases for the reactor include the replacement of neutron flux monitoring equipment for the reactor protection system awarded to SCHNEIDER (F). Schneider also supplied uninterruptable power supplies.

CILAS (F) received a high value contract for the manufacture and installation of a 25m section of the thermal neutron guide H25, which was financed mainly by the CEA.

For the instruments, the highest value order was placed with IMT (CH) for the production of microstrip electrode plates for D20 multidetector. Ten " ILLSEC " temperature controllers were ordered from DUHAMEL (F) for different instruments at ILL. Several calls for tenders were sent out for the different parts of the new instrument IN4C; most of the orders have now been placed.

Other notable purchases in the scientific sector include:

- graphite monochromators for D2B from ATOMGRAPH (USA);
- a polarising analysing station from PETERSBURG NUCLEAR PHYSICS INSTITUTE;
- a magnet power supply for IN20 from DANFYSIK (DK).

For scientific computing, 14 SILICON GRAPHICS Indy workstations as well as four DIGITAL Alpha machines and four HEWLETT PACKARD workstations were bought. For Management Information Services the trend has been to replace Macintoshes by PC's from Hewlett Packard.

Two major building contracts were concluded:

- The construction of a new roof on the experimental hall, building ILL 7;
- The construction of the joint ILL/ESRF coffee bar which enables the restaurant in the Common Building to be extended into the area formerly occupied by the coffee bar.

Distribution of purchases in the member states

Whenever possible, for major purchases, an international call for tenders was carried out; offers were compared on an ex works basis so as not to disadvantage British and German firms compared with local suppliers. This, together with negotiation of discounts from regular suppliers for routine purchases, enabled us to achieve considerable savings.

The distribution of ILL purchases (orders exceeding 50 KF) in 1995 is shown below. Table 1 includes purchases for which a free choice of suppliers was possible excluding therefore the fuel cycle, electricity, and small purchases less than 50 KF.

Customs and transport

The return to normal scientific activity has meant an increase in the volume of temporary imports of samples and apparatus for experiments carried out at ILL. Some of the samples become radioactive after exposure to the neutron beam and consequently, special precautions have to be taken for the packing, transport and formalities for the return to origin.

Stores

A fork-lift truck was bought for use by stores in order to facilitate the transport of heavy items over long distances. Previously the storemen had to share a fork-lift truck with other departments and inevitably problems of availability arose.

An independent inspection of all the machine tools in the raw material stores was carried out with the aim of improving safety and ensuring conformity with current regulations. The continual surveillance, maintenance and upgrading of these machines is essential to the provision of raw materials to ILL's users.

Staff changes have had a profound effect on the service. Following the early retirement of ILL's most experienced buyer, the stock controller transferred to Purchasing. His replacement in stores was recruited internally from the Health Physics Group.

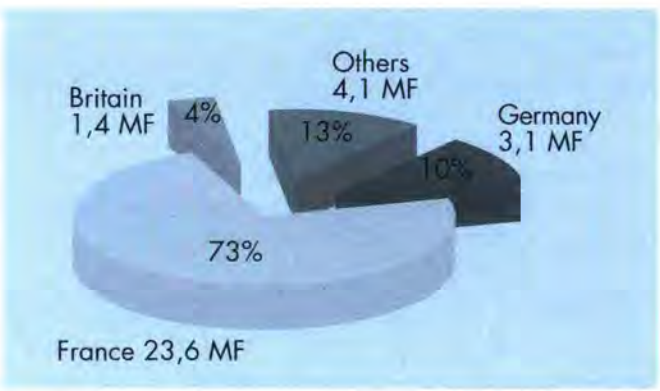

Table 1: Distribution of ILL purchases. (orders > 50 kF)

Personnel and Human Resources

The Personnel and Human Resources Service (SPRH) comprises three groups: Personnel Management, Human Resources Management, and Telecommunications and General Services.

Personnel policy

Personnel policy focused primarily on curbing staff costs by keeping a tighter control on the average earnings of the existing workforce. Among other things, this involved stepping up efforts to "rejuvenate" the workforce through suitable recruitment measures and encouraging some staff members to leave.

Workforce

The authorised workforce increased from 377 in 1994 to 385 in 1995. Compared to 1994, the overall breakdown by nationality (see Table 2 page 163) reveals a noticeable increase in the number of German staff (+ 8), a slight increase in the number of British staff (+ 2), a fall in the number of French staff (- 3) and little change for other nationalities (+ 1).

Following the departures recorded during 1995, a recruitment campaign was launched in the three member countries. For each of the positions advertised, an average of 200 to 250 applications were received from these three countries.

Average age

As a result of this staff rejuvenation policy, the average age of ILL staff has fallen to 43.6 (compared to 44 in 1994 and 44.7 in 1993).

Table 3 below shows a breakdown of the average age by sex and by Division.

Salaries

On 3 May 1995, a wage agreement for 1995 was signed between the Management and the two trade union organisations (CFDT and SAILL), comprising an increase of 1 % on 1 May 1995 and of 0.5 % on 1 August 1995.

Training

Under French law, companies are obliged to devote 1.5 % of their payroll to professional training. A portion of this percentage is paid directly to central government to help fund state-run sandwich courses for the young as well as special training leave ("congé individuel de formation"). The remaining amount is used to fund training provided for ILL personnel. In this context, around 150 members of staff

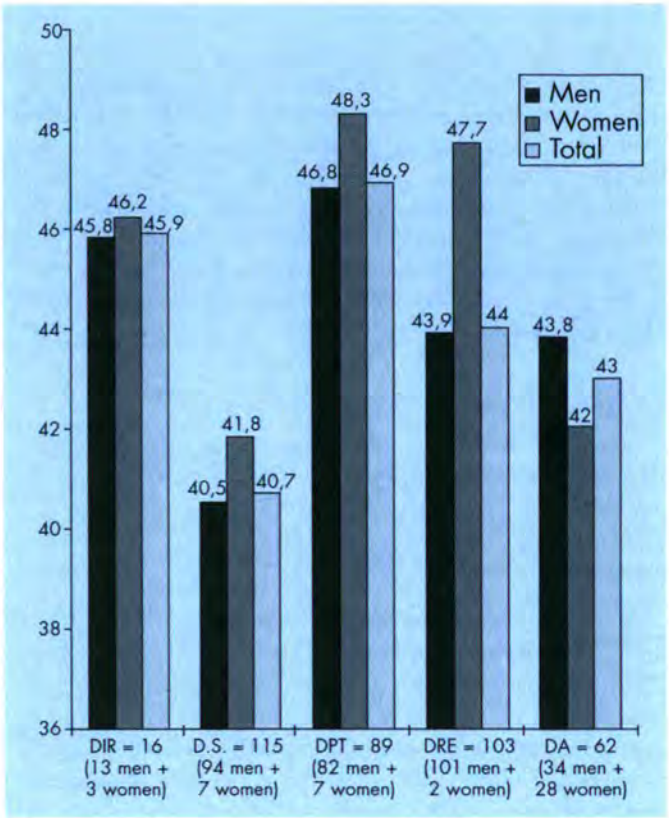

Table 3: Breakdown of average age by sex and by division.

were able to benefit from courses offered in wide variety of areas: management, languages, specific technical subjects, in particular computing.

Student traineeships

The Institut opened its doors to more than a hundred trainees from various schools and universities. Another four sandwich-course students were given "Qualification contracts", allowing them to spend 50 % of their time at ILL and 50 % attending theory classes. Two Qualification contracts are available in each Division in various fields of activity (physical measurements, secretariat, management, CAD).

Measures to encourage staff integration

• *French as a foreign language*

To help foreign members of staff to adapt quickly to life in France, ILL organises French classes, which are also open to ESRF personnel. During the academic year 1994/95, these classes were attended by some 85 people.

• *Accommodation*

Assistance is available to new arrivals who are looking for accommodation. ILL also has nine apartments, which are offered on a temporary basis until suitable permanent accommodation is found. In 1995, ILL helped 133 people to find accommodation.

• *International schooling*

Schooling for children continues to be a key factor in the integration of families. ILL and ESRF are making every effort to develop the system set up in Grenoble. The subject of the charter on international schooling in Grenoble prompted wide-ranging discussions, resulting in a text which outlines the teaching expertise of the staff within the "Sections Internationales" of the "Cité Stendhal". Where school premises and facilities are concerned, however, progress has been brought to a standstill due to the local political climate.

Guest Scientists

The start-up of the reactor has signalled the return of outside users to the Institut. Table 4 below gives the breakdown by nationality of guest scientists funded by ILL.

Telecommunications and General Services

The Joint Telephone Service continued to equip ESRF and ILL with telephone lines. The group also provided a great deal of support in other areas, such as mail, photocopying, messenger services and audio-visual equipment. At the end of 1995, the mail service in particular posed serious problems; a lot of imagination was needed to ensure that urgent mail actually left the Institut.

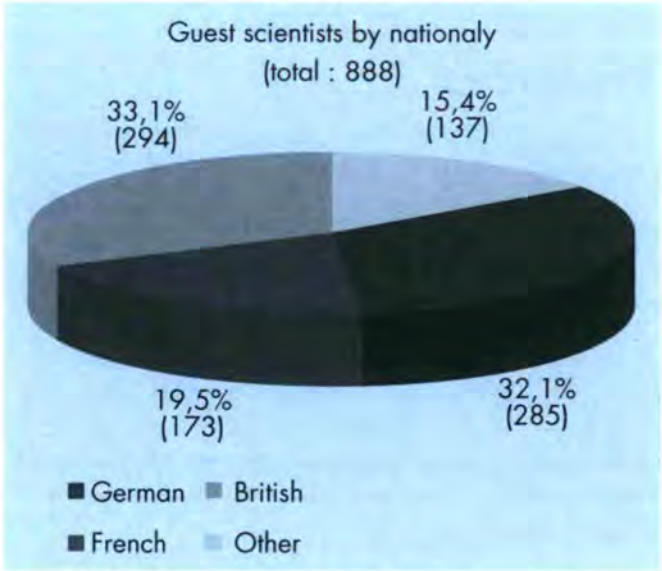

Table 4: Guest scientists by nationality (total: 888).

Building and Site Maintenance

Maintenance, repairs and improvement of the ILL site, buildings and technical installations (except the reactor) are the main activities of the Service. It also provides assistance in its technical fields to the whole Institut, especially to experiments (for shielding, handling and infrastructure).

The Service carries out the necessary interventions with its workshop or by placing external contracts. In 1995, its main tasks were:

• refurbishment of the roof of ILL7 building,

• preparation of experimental positions for CRGs D23 and IN22 on beam H25,

• completion of the primary shielding of IN4C experiment,

• renovation of part of ILL4 toilets,

• studies for " Commission Locaux " in order to optimise the use of offices and laboratories.

The Service is also involved in examining technical problems in relation with other laboratories.

COMMUNICATIONS

Workshops organized or sponsored by the ILL in 1995

Grenoble, France, January 24-27, 1995
Réunion de l'Association Française de Cristallographie - AFC 95
Organisers: EMBL, ESRF, ILL, IBS
Coorganised by Délégation Régionale du CNRS

Les Houches, France, June 06-09, 1995
New Tools for Neutron Instrumentation
Organisers: TASSET F., BÜTTNER H.G.

Seyssins, France, October 04-07, 1995
Quantum Tunnelling of Atoms and Molecules in Solids
Organisers: FILLAUX F., BÜTTNER H.G., KEARLEY G.J., MEINNEL J.

Journal Issue and Book Published

ZACCAI G. [Editor]
Neutrons in biology
Biophysical Chemistry **53** n° 1-2 (1994) (special issue)
Elsevier, 1994
ISSN 0301-4622

JANOT C., MOSSERI R. [Editors]
Quasicrystals - Proceedings of the 5th International Conference
World Scientific, 1995
ISBN 981-02-2418-4

Theses

MURPHY H.M.
Investigation of the structural and magnetic phase transitions in $CeSi_x$ by neutron scattering
A doctoral thesis submitted in partial fulfilment of the requirements for the award of Doctor of Philosophy of the Loughborough University of Technology (July 1993)

WILSON C.
Structure-reactivity relationships through x-ray and neutron diffraction studies
Thesis submitted to the University of Durham for the degree of Ph.D (May 1995)

WUTTKE J.
Dynamische Neutronen- und Lichtstreuung an molekularen Glasbildnern
Dissertation am Fachbereich Physik der Johannes-Gutenberg-Universität Mainz (Dezember 1993)
(Verbesserter Nachdruck Juni 1995)

Seminars

College 2

Theory

"Propriétés de transport et transition métal isolant dans les quasicristaux".
D. MAYOU, LEPES, CNRS, Grenoble, France.

"Fullerènes et autres".
A. RASSAT, Labo de Chimie, ENS, Paris.

"Many body correlations among hard core bosons: basis for a microscopic theory of ^{4}He".
Yi Hong CHEN, University of Madrid, Spain.

"Two-dimensional Hubbard model".
P.W. ANDERSON, Princeton, University USA.

"Fine structure of defects in systems with multi-component order parameters".
I. LUKYANCHUK, Université de Montpellier, France.

"Propriétés dynamiques d'un mélange bosons-fermions".
J.-M. ROBIN, CRTBT-CNRS, Grenoble.

"Supraconductivité sous fort champ magnétique dans les conducteurs quasi-unidimensionnels".
N. DUPUIS, Physique des Solides, Orsay, France.

"Propagation of light in photonic matter".
Ad LAGENDIJK, University of Amsterdam, The Netherlands.

"Structures eutectiques hors d'équilibre".
K. KASSNER, ILL, Grenoble, France.

"The spin-gap in the CuO superconductors".
H. MONIEN, ETH, Zurich, Switzerland.

"Singular surfaces in liquid crystals".
E. KATS, Landau Institute, Moscow and Université Joseph Fourier, Grenoble, France.

"Sliding and relaxation of pinned density waves".
S. BRAZOVSKII, Landau Institute, Moscow and CRTBT-CNRS, Grenoble, France.

"Charge and current conserving a.c. transport in mesoscopic conductors".
M. BUTTIKER, University of Geneva, Switzerland.

"Electromigration et instabilités de surface du silicium".
C. MISBAH, Université Joseph Fourier, Grenoble, France.

"Fracture dirigée".
B. PERRIN, ENS, Paris, France.

"The Mott transition: Basic concepts and results from model calculations".
F. GEBHARD, Phillips Universität, Marburg, Germany.

"Coexistence and two length scales in the critical scattering from systems with long-range disorder".
M. ALTARELLI, ESRF, Grenoble, France.

"Crossover from Bose-Einstein condensation to BCS pairing in dense Fermi systems".
G. ROPKE, Universität Rostock, Germany.

"Une température pour la turbulence développée".
B. CASTAING, CRTBT-CNRS, Grenoble, France.

"Frottement solide et hystérésis".
P. NOZIERES, ILL, Grenoble, France.

"Semiquantum systems: from supertransport to giant opalescence".
E. BASHKIN, Universität Marburg, Germany.

"Heat conductivity in glasses".
Philip B. ALLEN, SUNY-Stony Brook, USA, and Ecole Polytechnique Fédérale de Lausanne, Switzerland.

"Mode-coupling theory for interacting tunnelling defects in KCl:Li".
A. WÜRGER, ILL, Grenoble, France.

"Why is the macroscopic world classical ? The role of nuclear spins".
P. STAMP, University of British Columbia, Vancouver, Canada.

"Resonant Raman scattering in rare earth systems".
M. Van VEENENDAAL, ESRF, Grenoble, France.

"Phase diagram and correlation exponents for interacting electrons in one dimension".
E.B. KOLOMEISKY, Cornell, Ithaca, N.Y., USA.

"Les quasiparticules escamotées: questions récentes en physique des fermions fortement corrélés".
A. GEORGES, Ecole Nationale Supérieure, Paris.

"Magnetic behavior of the cuprate semiconductors".
A. SOKOL, University of Illinois, USA and L.D. Landau Institute, Moscow.

"Van Hove singularity and the related non-Fermi liquid".
I. DZYALOSHINSKI, University of California, Irvine, USA.

"The Hubbard model and the three band CuO_2 model: similarities and dissimilarities".
H. KAGA, Niigata University, Japan.

"Kondo systems in point contacts".
G. ZARAND, Technical University of Budapest, Hungary.

"Radiative transport in magnetic fields".
B. van TIGGELEN, Maison des Magistères, CNRS Grenoble, France.

"On the theory of quantum evaporation".
L. PITAEVSKI, Kapitza Institute, Moscow.

"Accrochage des réseaux de vortex et localisation des bosons en interaction: une théorie variationnelle".
T. GIAMARCHI, Physique des Solides, Orsay, France.

"Nucléation et croissance épitaxiale sur des surfaces à marches".
A. PIMPINELLI, ILL, Grenoble, France.

"Superconductivity in the 2d t-J model at low electron density".
M. KAGAN, Kapitza Institute, Moscow.

"de Haas-van Alphen effect in type II superconductors".
T. MANIV, Technion, Haifa, Israel.

"Polarons et liquides de polarons en dimension infinie".
D. FEINBERG, LEPES-CNRS, Grenoble, France.

"Kirchoff theorem in lattice models of statistical mechanics".
E. KORNILOV, Joint Inst. for Nucl. Research, Dubna, Russia.

"De la convection à la dynamo".
A. TILGNER, Universität Bayreuth, Germany.

"Charged skyrmions in a 2D electron gas under a strong magnetic field".
Y. BYCHKOV, Landau Institute, Moscow.

"The search for marginal, non Fermi liquid behaviour in one and two band Fermi models".
M. KAGAN, Kapitza Institute, Moscow and ILL, Grenoble, France.

"Pouvez-vous monter sur une échelle de spin ?"
L. LEVY, SNCI-CNRS, Grenoble, France.

"From the LDA to low energy hamiltonians for high temperature semiconductors; extended saddle points and interplane coupling".
O. ANDERSEN, Stuttgart, Germany and ESRF Grenoble, France.

"Le bruit grenaille dans les conducteurs mésoscopiques".
T. MARTIN, ILL, Grenoble, France.

"Dynamics of the dissipative two-state system - the anisotropic Kondo model revisited".
T.A. COSTI, ILL, Grenoble, France.

"Theory of photoluminescence at $\nu = 1$: excitons, spin waves and skyrmions".
N. COOPER, ILL, Grenoble, France.

"La transition semiconducteur-métal dans le polyacétylène".
D. BAERISWYL, Université de Fribourg, Switzerland.

College 3

Nuclear and Fundamental physics

"Is it possible to produce next generation of UCN sources with density $10^3 + 10^4$ cm^{-3} ?".
A. SEREBROV, St. Petersburg Nuclear Institute, Gatchina, Russia.

"New measurements of the antineutrino-spin asymmetry in beta decay of the neutron and restriction for mass of M_{wR}".
A. SEREBROV, St. Petersburg Nuclear Institute, Gatchina, Russia.

"Etude des noyaux exotiques par spectroscopie laser".
F. IBRAHIM, Institut de Physique Nucléaire, Orsay, France.

"Realization of a magnetic mirror for cold atoms".
H. ABELE, Universität Heidelberg, Germany.

"Overview of neutron based instrumentation activities at the high flux isotope reactor and the Oak Ridge National Laboratory".
M.C. WRIGHT, Oak Ridge National Laboratory, USA.

"UCN anomalies".
A. STEYERL, University of Rhode Island, Kingston, USA.

"Project of a new 20 MeV electron accelerator for experiments in radiation and nuclear physics".
D. JANSSEN, Forschungszentrum Rossendorf, Germany.

"New techniques for randon progeny monitoring".
S. OBERSTEDT, SCK.CEN, Mol, Belgium.

"Measurement of the asymmetry in the free neutron beta-decay with the spectrometer PERKEO-2 - First results".
T. MÜLLER, Universität Heidelberg, Germany.

"Troitsk experiment on the search for a neutrino mass in the beta-decay of tritium".
V. LOBASHEV, Inst. for Nuclear Research, Troitsk, Russia.

"Polymers studied with nuclear reaction analysis and SANS using dynamic nuclear polarisation".
M.G.D. van der GRINTEN, University of Surrey, UK.

"Transmission neutron tomography".
P. CHIRCO, University of Bologna, Italy.

"The spins of neutron p-wave resonances in ^{238}U and ^{113}Cd".
F. GUNSING, CEA Saclay, France.

"Experiments with UCN - Some practical aspects".
(Lecture on 7th Int. School on Neutron Physics).
V. NESVIZHEVSKI, ILL, Grenoble, France.

"Recent experiments at PNPI (Gatchina)".
1. Studies of UCN production by the solid deuterium.
2. Parity violating spin rotation nearby ^{139}La p-wave resonance.
A. SEREBROV, St. Petersburg Nucl. Physics Inst. Gatchina, Russia.

"High resolution UCN spectrometer for the fundamental investigation in neutron optics".
A.I. FRANK, FLNP, Dubna, Russia.

"New UCN-source at a pulsed reactor".
V.N. SHVETSOV, JINR, Dubna, Russia.

"X-ray and neutron capillar optics and its applications".
M. KUMAKHOV, IRO Institute for Roentgen Optics, Moscow.

College 4

Structural and magnetic excitations

"Structural fluctuations and magnetic correlations in $Bi_2Sr_2(Ca,Pr)Cu_2O_{8+\delta}$ ".
L. VASILIU-DOLOC, Laboratoire Léon Brillouin, CEA-Saclay, Gif-sur-Yvette, France.

"Spin -Peierls transition in $CuGeO_3$".
M. AIN, Laboratoire Léon-Brillouin, CEA-Saclay, Gif-sur-Yvette, France.

"Neutrons and superfluidity in ^4He in vycor and mixtures".
P. SOKOL, Pennsylvania State Univ., USA.

"Spin fluctuations in superconducting $La_{2-x}Sr_xCuO_4$".
S. HAYDEN, H.H. Wills Phys. Lab., Univ. of Bristol, UK.

"Dynamical Chiral fluctuations in magnets and their observation with polarized neutrons".
S.V. MALEYEV, St. Petersburg Nucl. Phys. Inst., Gatchina, St. Petersburg, Russia.

"Changes of phonon dispersion in graphite at high pressure".
A.S. IVANOV, Russian Research Centre Kurchatov Institute, Moscow.

"External phonons and orientational disorder in C_{60}".
S.L. CHAPLOT, Bhabha Atomic Research Centre, Bombay, India.

"A one-megawatt long-pulse spallation source: better or worse than ILL for neutron scattering ?".
R. PYNN, Los Alamos National Laboratory, Los Alamos, USA.

"The concept of internal strains in modelling of crystal lattice instabilities in quartz".
M. SMIRNOV and A. MIRGORODSKY,
Inst. of Silicate Chemistry, St. Petersburg, Russia.

"The magnetic relaxation of liquid ^3He on a paramagnetic crystal surface".
M.S. TAGIROV, Kazan State Univ., Kazan, Russia.

"Experience with the elastically bent silicon monochromator and analyzer on the ILL TAS instruments".
J. KULDA, ILL, Grenoble, France.

"Study of the phase transformation in materials embedded into porous glass".
S. VAKHRUSHEV, A.F. Ioffe Physical - Technical Institute St. Petersburg, Russia.

"Soft modes and phonon interactions in the $Sn_2P_2Se_6$ family studied by inelastic neutron scattering and Raman spectroscopy".
S.H.W. EIJT, Research Inst. for Materials, Univ. of Nijmengen, The Netherlands.

College 5

Crystallography and magnetic structures

"Oxygen vacancies in pyrochlore oxides. Why they matter".
B.J. KENNEDY, School of Chemistry, University of Sydney, Sydney, Australia.

"Giant magnetostriction in compounds with magnetic moment and valence instabilities".
M.R. IBARRA, University of Saragoza, Spain.

"Single-crystal growth and structural characterisation of simple carbocuprates".
F. CINO MATACOTTA, ICTP, Trieste, Italy.

"Developments in internal strain measurement using neutrons".
G. SWALLOWE, Loughborough University of Technology, Loughborough, UK.

"Half a problem: tunnelling spectroscopy of molecular crystals of unknown structure".
M. JOHNSON, ILL, Grenoble, France.

"Structural "tuning" of magnetism in $A_{1-x}A'_xMnO_3$ (A = La, Pr; A' = Ca, Sr, Ba)".
P. RADAELLI, ILL, Grenoble, France.

College 6

Structure and dynamics of liquids and glasses

"Investigations of superionic conductors CuBr, Li_2S, and Ba_2NH by elastic, quasielastic, and inelastic neutron scattering".
W. BÜHRER, Paul Scherrer Institute, Villigen, Switzerland.

"Applications of multilayers to cosmic X-ray studies".
P. GORENSTEIN, Harvard Smithsonian Center for Astrophysics, Cambridge, USA.

"Neutron reflection from rough surfaces analysed in the distorted wave Born approximation".
G. LJUNGDAHL, Rutherford Appleton Laboratory, UK.

"The dynamic structure of liquid alkali metals: results from computer experiments".
G. KAHL, Technische Universität Wien, Austria.

College 7

Material science, surfaces and spectroscopy

"Neutron reflection from Fibonacchi multilayers".
E.I. KORNILOV, Frank Laboratory of Neutron Physics, JINR, Dubna, Russia.

"The lattice dynamics of decagonal quasicrystals".
M. KRAJCI, Technische Universität, Wien, Austria.

"Tethered adsorbing chains: neutron reflectivity and surface pressure of spread diblock copolymer monolayers" and "Toward the solution of the inverse problem in neutron reflectometry".
A.A. VAN WELL, Interfacultair Reactor Instituut, Delft University of Technology, The Netherlands.

"Molecular magnetism: inelastic neutron scattering from magnetic clusters".
H. GUEDEL, Universität Bern, Switzerland.

"The NIST neutron research facility: present and future".
John J. RUSH, National Institute of Standards and Technology, Gaithersburg, USA.

"Rotor phases in alkali-thallium compounds".
D. LONG PRICE, Argonne National Lab., Argonne, USA.

"Neutron scattering from rough interfaces in periodic multilayered structures".
B. TOPERVERG, Petersburg Nuclear Physics Institute, Gatchina, St. Petersburg, Russia, and ILL, Grenoble, France.

College 8

Biology

"Bilayers and the effect of protein coupling: a neutron reflection, NMR and FT-IR study".
Th. BAYERL, University of Würzburg, Germany.

"Determination of deuterium incorporation into RNA and protein components of the E. Coli ribosome by SANS techniques".
I. SERDYUK, Academy of Sciences of Russia, Poustchino, Moscow.

"Crystal structure of the specific membrane channel maltoporin".
T. SCHIRMER, Biozentrum, Universität Basel, Switzerland.

"Analyses of membrane-membrane effectors interaction by solid state NMR".
A. MILON, LPTF-CNRS, Toulouse, France.

College 9

Structure and dynamics of soft-condensed matter.

"Interobject correlations in heterogeneous polymer systems under deformation. A small angle neutron scattering study".
F. BOUE, Laboratoire Léon Brillouin, CEN-Saclay, France.

"The investigation of interfaces between polymers by reflectivity techniques".
M. STAMM, Max-Planck-Institut für Polymerforschung, Mainz, Germany.

"Charge generation and transport in dielectric dispersions".
H.-F. EICKE, Dept. Chemie, Universität Basel, Switzerland.

"Shear-induced changes in the order-disorder transition temperature and the morphology of a triblock copolymer".
A. NAKATANI, Nat. Inst. of Standards and Technology, Gaithersburg, USA.

"Local structure of hard/soft nanocomposites under deformation".
Y. RHARBI, Laboratoire Léon Brillouin, CEN-Saclay, Gif-sur-Yvette, France.

"Shape transformations in the lecithin-bile salt system: from spherical micelles to cylindrical micelles to vesicles".
S.U. EGELHAAF, LSS Group, ILL, Grenoble, France.

"Experiments on the glass transition in polymers".
R. ZORN, IFF/KFA Jülich, Germany.

"Specular reflection of neutrons at the air-water interfaces and small angle scattering by a mixed phospholipid/polymer system".
B. DEMÉ, Service de Chimie Moléculaire, CEN-Saclay, Gif-sur-Yvette, France.

Thursday colloquium

"STM and surface physics".
F. SALVAN, Université de Marseille II, France.

"Conducting linear alkali fulleride polymers".
A. JANOSSY, Inst. of Physics, Technical University of Budapest, Hungary.

"Even-odd symmetry breaking in superconductors"
M. DEVORET, Groupe Quantronique, Service de Physique de l'Etat Condensé, CEN-Saclay, Gif-sur-Yvette, France.

"Electronic Raman scattering as a probe of anisotropic pairing in superconductors".
R. HACKL, Walter Meissner Inst. f. Tieftemperaturforschung, Garching, Germany.

"Ultra-cold atoms".
C. SALOMON, Laboratoire de Spectroscopie Hertzienne, ENS Paris, France.

"Neural networks and biological problems".
ILL-ESRF Joint Colloquium.
G. TOULOUSE, Laboratoire de Physique Théorique, ENS Paris, France.

"Unconventional vortex dynamics in the low-field superconducting phases of UPt_3".
Ana Celia MOTA, Laboratorium für Festkörperphysik, Zurich, Switzerland.

"Two length scales for phase transitions".
ILL-ESRF Joint Colloquium.
R.A. COWLEY, University of Oxford, UK.

"Study of thin films, surface and interfaces using high energy ion beams".
C. COHEN, Groupe de Physique des Solides, Universités Paris VII et VI, Paris.

"IPNS upgrade: a technical feasibility study for a 1-MW pulsed spallation neutron source".
K. CRAWFORD, Argonne Nat. Lab., Illinois, U.S.A.

"The synthesis of the deformed superheavy elements 107 to 111".
ILL-ESRF Joint Colloquium.
P. ARMBRUSTER, G.S.I. Darmstadt, Germany.

"The physics of waste transmutation by neutrons".
M. SALVATORES, CEA Cadarache, France.

"Universalities: from Anderson Loalization to quantum chaos".
ILL-ESRF Joint Colloquium.
B. ALTSHULER, NEC Research Inst. Princeton, N.J. USA and MIT, Cambridge, MA, USA.

"Quantum transport in a mesoscopic superconductor-2DEG quasiparticle interferometer".
B.J. Van WEES, University of Groningen, The Netherlands.

"Industrial application of neutron diffraction".
T. HOLDEN, Chalk River Laboratories, Chalk River, Ontario, Canada.

Conference Contributions

ÅRHUS, Denmark: Symposium in honour of Professor S.E. Rasmussen - 1995/06/08-09

LEHMANN M.S. A large detector for neutron studies: some first results. (Invited talk)

ALP SELLAMATT, Switzerland: Workshop on Composite Germanium Monochromators - 1995/06/12

MAGERL A. The present status of the germanium monochromator development at the ILL.

AVIGNON, France: 5th International Conference on Quasicrystals - 1995/05/22-26

DUGAIN F., SUCK J.B. Temperature dependence of the generalized vibrational density of states of $Al_{70}Co_{15}Ni_{15}$. (Poster)

SCHAUB T.M., BUERGLER D.E., SUCK J.B., AUDIER M., GUENTHERODT H.J. Investigation of the quasicrystalline structure of icosahedral $Al_{68}Pd_{23}Mn_9$ by STM and LEE.

BAD HONNEF, Germany: WE-Heraeus-Seminar: Polymers, Membranes, Soft Matter - 1995/06/12-14

EGELHAAF S.U., PEDERSEN J.S., MUELLER M., SCHURTENBERGER P. Shape transformations in biological mixed surfactant systems: from spheres to cylinder to vesicles.

BALATONFUERED, Hungary: International School on Quasicrystals - 1995/05/13-20

JANOT C. The structure of icosahedral quasicrystals: bases and one example.

BARCELONA, Spain: VIII. European Colloid and Interface Society (ECIS) - 1995/09/17-22

EGELHAAF S.U., BAUER H.H., MERKLE H.P., SCHURTENBERGER P. Bicolloid stability and aggregation: understanding problems from "real life" with complex fluid physics. (Talk)

HOLTHOFF H., EGELHAAF S.U., BORKOVEC M., SCHURTENBERGER P., STICHER H. Simultaneous static and dynamic measurements of coagulation rate constants on a fiber optical set-up. (Poster)

BEIJING, China: International Nuclear Physics Conference -1995/08/21-26

DREXEL W., GELTENBORT P. Ultracold and very cold neutrons for studies of fundamental interactions.

FIONI G., FAUST H. Mass, charge and kinetic energy distributions of fission fragment from $^{245}Cm(n_{th},f)$.

BERLIN, Germany: Verhandlungen der Deutschen Physikalischen Gesellschaft - 1995/03/20-24

BUERGLER D.E., SCHAUB T.M., SUCK J.B., AUDIER M., GUENTHERODT H.-J. Die Oberflaeche eines Quasikristalls - Neue Ergebnisse mit STM und LEED. (Invited talk)

GOMPF F., REICHARDT W., SCHOBER H., RENKER B., BUCHGEISTER M. Gitterschwingungen und Elektron-Phonon Kopplang im supraleitenden YNi_2B_2G (T_c 1 15.6 K) im Vergleich mit nicht supraleitenden $LaNi_2B_2G$ bzw. $Y(Ni_{0.7}Co_{0.3})_2B_2C$. (Talk)

SCHOBER H., RENKER B., GOMPF F., ADELMANN P. Neutron scattering study of low-frequency excitations in Rb_3C_{60} and Rb_6C_{60}.

PYKA N.M., REICHARDT W. Untersuchung des zur Breathing-Mode korrespondierenden Phononensweiges entlang der a-Richtung in $YBa_2Cu_3O_6/0_7$.

SCHAUB T., BUERGLER D., SUCK J.B., AUDIER M., GUENTHERODT H.-J. Untersuchung von ikosaedrischem $Al_{68}Pd_{23}Mn_9$ mittels STM und LEED. (Talk)

BIALOWIEZA, Poland: International School of Condensed Matter Physics - 1995/07/16-25

OULADDIAF B. Determination of magnetic structures by neutron diffraction.

CANCUN, Mexique: ICAM 95 - 1995/08/27-09/01

JANOT C. Advances on quasicrystals and related systems.

CARDIFF, UK.: British Crystallography Association Annual Spring Meeting - 1995/03/27-31

COLE J.M., COLE J.C., CROSS G.H., HOWARD J.A.K., SZABLEWSKI M. Structural studies of organic non-linear optical materials. (Poster)

CHICAGO, USA: 9th International Conference on Liquid and Amorphous Metals - 1995/08/27-09/01

SUCK J.B. Temperature dependence of the total dynamic structure factor of the metallic glass $Ni_{33}Zr_{64}$.

DUGAIN F., MIHALKOVIC M., SUCK J.B. Generalized vibrational density of states of decagonal $Al_{70}Co_{15}Ni_{15}$. (Contributed paper)

CHIEUX P., DUPUY-PHILON J., JAL J.F., SUCK J.B. Temperature dependence of the collective atomic dynamics of liquid Rb.

SUCK J.B., SCHOBER H., GUENTHERODT H.J. The generalised vibrational density of states and total dynamic structure factor of the metallic glass $Zr_{65}Cu_{17.5}Ni_{10}Al_{7.5}$ measured at room temperature.

BENMORE C.J., OLIVIER R.J., SUCK J.B., ROBINSON R.A., EGELSTAFF P.A. A neutron Brillouin scattering study of $Mg_{70}Zn_{30}$.

COL-DE-PORTE, France: Rencontres Franco-Russes - 1995/03/23-26

HENGGELER W., GUILLAUME M., ECCELSTONE R., TROUNOV V., FURRER A. Intermultiplet crystal-field transitions in $SmBa_2Cu_3O_7$.

SUARD E., CAIGNAERT V., MIREBEAU I., BOUREE F., BALAGUROV A.M. Influence of deoxygenation process on magnetic diagram of iron doped $YBa_2Cu_3O_7$ phases.

MUTKA H., PAYEN C., ECCLESTON R.S., BRODY J., JOHNSON J. Susceptibility and magnetization of a spin ladder compound.

DARESBURY, UK.: 4th Annual CCP13/NCD Workshop - 1995/05/09-11

LANGAN P. Neutron fibre diffraction studies.

DARMSTADT, Germany: GSI-Colloquium - 1995/02/07

SCHERM R. ILL - Reaktor wieder in Betrieb.

DUBNA, Russia: VII International School on Neutron Physics - 1995/09/03-22

KEARLEY G.J. Modern chemistry with neutron scattering. (Invited talk)

NESVIZHEVSKY V.V. Use of UCN in experiments (some practical aspects). (Invited talk)

SCHERM R. Methods for condensed matter studies with neutrons.

DURHAM, UK.: The International Meeting in Charge Density Analysis 1995 - 1995/12/14-16

COLE J.M. Non-linear optical effects of organic molecules: Theory and application to charge density studies. (Invited talk)

ERICE, Italy: Workshop on High Tc Superconductors - 1995/07/09-15

HENGGELER W., GUILLAUME M., MESOT J., FURRER A., ADAMS M. Ho^{3+} single ion excitations in $Y_{0.99}Ho_{0.01}Ba_2CuO_7$.

FLORENCE, Italy: Conference on "History of European Scientific and Technological Cooperation" - 1995/11/09-11

SCHERM R. ILL - Present and future challenges.

GARCHY, France: 4th Meeting on "Disorder in Molecular Solids" DISMOS-4 - 1995/05/29-06/01

DIANOUX A.J., SAUVAJOL J.L., KNELLER G.R., SMITH J.C. Inelastic neutron scattering and molecular dynamics simulations of pristine and doped polyacetylene. (Invited talk & Contributed paper)

GIARDINI NAXOS, Italy: XXV Congress of the Italian Association of Crystallography - 1995/09/25-27

RADAELLI P.G., COX D.E., MAREZIO M., CHEONG S.W., SCHIFFER P.E., RAMIREZ A.P. Structural anomalies associated with the magnetic and metal-insulator transitions in $La_{1-x}Ca_xMnO_3$ (x=0.25 and 0.50).

GRENOBLE, France: Réunion de l'Association Française de Cristallographie - 1995/01/24-27

BELLET-AMALRIC E., LEGRAND J.F. Structure cristalline des Polymères Ferroélectriques P(VDF-TsFE) : Effets de la composition. (Talk)

TIMMINS P.A., PEBAY-PEYROULA E., WELTE W. Interactions protéine-détergent dans des monocristaux de protéines membranaires étudiées par cristallographie aux neutrons.

MAY R. D22, un nouvel instrument de diffusion de neutrons aux petits angles à l'ILL.

LEHMANN M.S. L'utilisation des phosphoimageurs sensibles aux neutrons pour un grand multi-détecteur. (Talk)

GRONINGEN, Holland: International Euroconference on Magnetic Correlations, Metal-Insulator Transitions and Superconductivity in Novel Materials - 1995/11/08-13

MUTKA H., PAYEN C., ECCLESTON R.S., BRODY J., JOHNSON J. Analogies in the susceptibility of a spin-ladder compound and a Haldane chain - extracting the intrinsic behaviour.

HABAY-LA-NEUVE, Belgium: Seminar on Fission "Pont d'Oye III" - 1995/05/09-11

FIONI G., FAUST H. and the PIAFE Collaboration. The PIAFE-phase 1 project. (Contributed paper)

HARO, Spain: DYPROSO XXV - 1995/09/23-27

SCHOBER H., RENKER B., GOMPF F. Phonon density-of-states in alkali-metal-intercalated fullerides. (Invited talk)

HIROSHIMA, Japan: 6th International Conference on the Crystallisation of Biological Macromolecules - 1995/11/12-17

VUILLARD L. New agents for protein purification and crystallisation.

KONSTANZ, Germany: Workshop on Colloid Physics - 1995/11/30-12/02

EGELHAAF S.U., PEDERSEN J.S., MUELLER M., SCHURTENBERGER P. Shape transformations in mixed surfactant systems: from spheres to cylinders to vesicles. (Poster)

HOLTHOFF H., EGELHAAF S.U., BORKOVEC M., SCHURTENBERGER P., STICHER H. Simultaneous static and dynamic measurements of coagulation rate constants on a fiber optical set-up. (Poster)

KYOTO, Japan: 'The Outlook for Fundamental Physics with Superlow Energy Neutrons' - 1995/01/11

PENDLEBURY J.M. Fundamental physics with neutrons at the Institut Laue-Langevin. (Invited talk & Contributed paper)

LA PLATA, Argentina: The International School and Workshop in Charge Density Analysis - 1995/05/18-25

COLE J.M., COLE J.C., CROSS G.H., HOWARD J.A.K., SZABLEWSKI M. Zwitterionic TCNQ derivatives: chromophores to organic non-linear optical materials. (Poster)

LES HOUCHES, France: New Tools for Neutron Instrumentation - 1995/06/06-09

LARTIGUE C., COPLEY J.R.D., MEZEI F., SPRINGER T. Focusing of neutron beams using curved mirrors for small angle scattering. (Contributed paper)

ZEYEN M.E., OTAKE Y., FORTE M. Dual polarised beam polarimeter: a highly sensitive tool for the detection of very small neutron spin rotation. (Contributed paper)

MUTKA H., SACCHETTI F. The focussing monochromator of IN4C.

LEHMANN M.S. New tools for neutron instrumentation. (Invited talk)

MAGERL A. Neutron optics with gradient crystals.

ZEYEN C.M.E., KAKURAI K. Spin-echo three-axis spectrometer: a reality. (Contributed paper)

ANDERSON I.S., SCHAERPF O., HØGHØJ P., AGERON P. Multilayers.

CIPRIANI F., CASTAGNA J.C., WILKINSON C., OLEINEK P., LEHMANN M.S. The application of neutron image-plates for a large position-sensitive detector. (Contributed paper)

BROWN P.J. Analysing neutron scattering data with the Cambridge crystallographic subroutine library (CCSL). (Contributed paper)

RICHARD D., FERRAND M., KEARLEY G.J. Analysis and visualisation of neutron scattering data. (Invited talk)

SCHAERPF O., ANDERSON I.S. Classical polarisation analysis. (Contributed paper)

LIVERPOOL, UK.: Condensed Matter and Materials Physics 1995 - 1995/12/19-21

COSTI T.A. Equilibrium dynamics of the dissipative two-state system. (Poster)

LONDON, UK.: "Transport in Porous Media", organised by the SCI Colloid and Surface Chemistry Group - 1995/03/30

DIANOUX A.J. Application of neutron scattering to investigate diffusion in porous media. (Invited talk)

LUND, Sweden: Sixteenth European Crystallographic Meeting - 1995/08/06-11

McINTYRE G.J. Thermal-diffuse-scattering corrections for single-crystal diffraction data from two-dimensional position-sensitive detectors.

SVENSSON S.O., KVICK Å., McINTYRE G.J. Structure refinement of $[Co(NH_3)_6][CuCl_5]$ using synchrotron radiation at $\lambda = 0.160$ Å and large imaging plates.

OLOVSSON I., McINTYRE G.J., PTASIEWICZ-BAK H. Spin and charge density in some hydrates of nickel salts. Bonding and artificial effects.

LEADBETTER A.J. New techniques and new applications of neutron scattering.

LYON, France: International Workshop on MicroStrip Gas Chambers - 1995/11/30-12/02

GELTENBORT P. Performance of passivated and unpassivated glass MSGCs.

GELTENBORT P. A monitor for the carbon and oxygen impurities in the ASDEX-upgrade TOKAMAK.

MANCHESTER, UK.: Neutron Beam Users Meeting - 1995/01/24-27

CIPRIANI F., CASTAGNA J.C., LEHMANN M.S., WILKINSON C. A large image-plate detector for neutron diffractometry. (Poster)

MUTKA H. IN4C - Thermal T-O-F.

MONTPELLIER, France: 5th European Conference on Solid State Chemistry - 1995/09

ALLANCON C., RODRIGUEZ-CARVAJAL J., FERNANDEZ-DIAZ M.T., ODIER P., BASSAT J.M., LOUP J.P., MARTINEZ J.L. Neutron diffraction study of the high temperature tetragonal phase in oxidised $Pr_2NiO_{4+\delta}$.

MONTREAL, Canada: Annual Meeting of the American Crystallographic Association - 1995/07/23-28

McINTYRE G.J. Efficient single-crystal diffractometry with position-sensitive detectors.

PEBAY-PEYROULA E., TIMMINS P.A. Low resolution crystallography on complex systems.

TIMMINS P.A., PEBAY-PEYROULA E., GARAVITO R.M., ROSENBUSCH J., ZULAUF M. Detergent structure in tetragonal crystals of porin from the outer membrane of E.coli.

MORIOKA, Japan: International Symposium: "Frontiers of High Tc Superconductivity" - 1995/10/27-29

KHASANOVA N.R., ISUMI F., TAKAYAMA-MUROMACHI E., HEWAT A.W. Crystal structure of the superconductor $Ca_2Sr_2Cu_3GaO_9$ prepared at high pressure.

OAXTEPEC, Mexico: XVIII Nuclear Physics Symposium - 1995/01/04-07

FAUST H.R., FIONI G., PINSTON J.A. The project of an exotic beam facility in Grenoble (PIAFE). (Contributed paper)

OXFORD, UK.: Polar Solids Discussion Group Meeting - 1995/03/27-29

LEADBETTER A.J. X-ray and neutron scattering.

PARMA, Italy: Quasielastic Neutron Scattering. QENS'95 - 1995/09/07-08

CRISTOFOLINI L., KONSTANTINOS V., KOSMAS P., DIANOUX A.J., KOSAKA M., HIROSAWA I., TANIGAKI K. Molecular dynamics of C_{60} in superconducting Na_2CsC_{60}. (Talk & Contributed paper)

VOGL G. QUENS and quasielastic Mössbauer spectroscopy for studying diffusion.

BEE M., COMBET J., GUILLAUME F., MORELON N.D., FERRAND M., DIANOUX A.J. Neutron scattering studies of linear chains in an organic inclusion compound. (Contributed paper)

GIRARD P., GUILLAUME F., DIANOUX A.J. Molecular dynamics of guest molecules in the channels of urea inclusion compounds investigated by means of IQNS spectroscopy. (Contributed paper)

GIRARD P., GUILLAUME F., DIANOUX A.J. Molecular dynamics of functionalized n-alkane guest molecules in urea inclusion compounds. (Poster)

CHAHID A., McGREEVY R.L., WICKS J., MUTKA H. Critical narrowing of molten $^7Li_{0.62}Na_{0.38}$ alloy. (Contributed paper)

PHILADELPHIA, USA.: MMM95 - 1995/11/06-07

NIRAIMMATHI A.M., GMELIN E., ALLENSPACH P., RITTER C. Magnetic ordering and structure of Nd^{3+} ions in $NdBa_2Cu_{2.5}Ga_{0.5}O_{7-y}$.

PISA, Italy: Workshop on Non Equilibrium Phenomena in Supercooled Fluids, Glasses and Amorphous Materials - 1995/09/25-29

FRICK B. Methyl group dynamics in poly(dimethylsiloxane). (Poster & Contributed paper)

PORT D'ALBRET, France: 4èmes Journées de la Diffusion Neutronique - 1995/05/17-19

GIRARD P., GUILLAUME F., DIANOUX A.J., HARRIS K.D.M. Dynamique réorientationnelle et translationnelle du dioctanoylperoxyde inclus dans l'urée.

SAUVAJOL J.L., PAPANEK P., DIANOUX A.J., FISCHER J.E., McNEILLIS P., MATHIS C., FRANCOIS B. Dynamique des modes de vibration de basse fréquence du polyacétylène dopé au potassium et au sodium.

MIREBEAU I., HENNION M., SUARD E., FERNANDEZ-DIAZ M.T Structure magnétique du composé $ZnMn_2As_2$.

LAFOND A., FRICK B., FISCHER P., MUTKA H. Ordre magnétique dans le composé misfit "$LaCrS_3$".

MARMEGGI J.C. Etudes à basses températures de la diffusion dans l'uranium métal. (Poster)

POZNAN, Poland: 2nd International Seminar on "Neutron Scattering Investigation of Condensed Matter" - 1995/04/19-22

FRICK B. Local dynamics of polymers around the glass transition temperature. (Invited talk)

KULDA J. The ILL reactor reconstruction and restart. (Invited talk)

PRAGUE, Czech Republic: International Workshop on "Neutron Scattering Applications" - 1995/10/04-06

KULDA J., SAROUN J. Elastically bent perfect crystals on a TAS spectrometer. (Invited talk)

REINSTORF, Germany: Deutsche Neutronenstreutagung - 1995/09/18-21

MUTKA H., SACCHETTI F. , BUETTNER H. IN4C - Thermal T-O-F. (Poster)

GUENTHER R. Das Reflekto-Diffraktometer EVA - Spinpolarisierte Neutronenstreuung an Grenzflaechen und Oberflaechen. (Poster & Abstract)

DORNER B., TOPERVERG B.P., SONNTAG A., PETITGRAND D. Excitations in $RbFeCl_3$ in einem äusseren Magnetfeld senkrecht zur Anisotropie-Achse. (Poster)

RICHMOND, USA: International Symposium on the Science & Technology of Atomically Engineered Material - 1995/10/30-11/04

JANOT C. Quasicrystals as self-similar packing of atomic clusters.

ROME, Italy: VI Convegno Annuale di Spettroscopia Neutronica - 1995/05/25-26

LEADBETTER A.J. ILL - Past, present and future.

SAINT-ETIENNE, France: Xe Colloque International "Progrès dans les méthodes d'investigation des métaux et nouveaux matériaux" - 1995/11/15-16

BASTIE P., MANIGUET L., DUPEUX M. Non-destructive detection and localization of straining by gamma-ray diffractometry in a single crystal superalloy submitted to a shear test. (Contributed paper)

SANDANSKI, Bulgaria: Coordination Meeting of Collaborating Scientific Groups in Nuclear Physics - 1995/10/22-26

GELTENBORT P. Current fundamental physics experiments at the ILL.

SANTA FE, USA: Workshop on Future Prospects for Ultra Cold Neutron Research - 1995/12/06-09

GELTENBORT P. Neutron lifetime measurements at ILL. (Invited talk)

STRELKOV A.V., NEKHAEV G.N., SHVETSOV V.N., SEREBROV A.P., KHARITONOV A.G., TAL'DAEV R.R., SAZHIN M.N., VARLAMOV V.E., NESVIZHEVSKY V.V., GELTENBORT P., PENDLEBURY J.M., SCHRECKENBACH K. "Test of conservation of matter with UCN".. or search for the upscattering of UCN to the energy range of VCN. (Invited talk)

PENDLEBURY J.M. Review of present UCN sources. (Invited talk)

PENDLEBURY J.M. The current ILL EDM experiment. (Invited talk)

SAPPORO, Japan: Phonons 95 - 1995/07/24-28

JANOT C., BOISSIEU M. DE Vibrations in quasicrystals: Hierarchies and localization.

SCHOBER H., RENKER B., GOMPF F. Low-energy excitations of A_3C_{60} and A_6C_{60} fullerides. (Talk)

SCHOBER H. Structural phase transitions and the determinant of the dynamical matrix. (Poster)

RANDL O.G., VOGL G., PETRY W. Phonons - A diffusion motor in intermetallics.

SEYSSINS, France: International Workshop on Quantum Tunnelling of Atoms and Molecules in Solids - 1995/10/04-07

KEARLEY G.J., BUETTNER H.G., FILLAUX F., LAUTIE M.F. NH_3 free rotors in Hofman clathrates. (Poster)

ST. PETERSBURG, Russia: European Physical Society - XV Nuclear Physics Divisional Conference "Low Energy Nuclear Dynamics" - 1995/04/18-22

PENDLEBURY J.M. Fundamental physics with neutrons at the Institute Laue-Langevin. (Invited talk & Contributed paper)

ST. PETERSBURG, Russia: Deutsch-Russisches Symposium zum Thema "Physics of Novel Materials" - 1995/09/15

MAGERL A. Magnetic structures and polarized neutron beams.

STRASBOURG, France: E-MRS 95 Symposium - 1995/05/22-26

BUTTARD D., BELLET D., BAUMBACH T. X-ray diffraction investigation of porous silicon superlattices. (Contributed paper)

BASTIE P., HAMELIN B. La méthode de Laue refocalisée à haute énergie : une technique d'étude en volume des monocristaux. (Contributed paper)

STROMBOLI, Italy: Horizons in Small-Angle Scattering from Mesoscopic Systems - 1995/09/27-30

MAY R. New small-angle neutron scattering developments and experiments at the ILL.

TALLAHASSEE, USA: Conference on "Physical Phenomena at High Magnetic Fields - II" - 1995/05/06-09

CHEONG S.W., HWANG H.Y., RADAELLI P.G., COX D.E., MAREZIO M., BATLOGG B., SCHIFFER P., RAMIREZ A.P. Origin and control of the "colossal" magnetoresistance in doped $LaMnO_3$. (Contributed paper)

TOULOUSE, France: Colloque National "Superalliages Monocristallins" - 1995/03/22-24

BASTIE P., ROYER A., BELLET D., LAJZEROWICZ J. Désaccord paramétrique, paramètres de maille et morphologie des précipités. (Contributed paper)

TRIESTE, Italy: The Adriatico Research Conference on "Physics of Sliding Friction" - 1995/06/20-23

CAROLI C., NOZIERES P. Dry friction as a hysteretic elastic response. (Contributed paper)

VILLARS-SUR-OLLON, Switzerland: XVth Moriond Workshop - Dark Matter in Cosmology, Clocks and Tests of Fundamental Law - 1995/01/21-28

PENDLEBURY J.M. Summary talk on precision clocks. (Invited talk & Contributed paper)

PENDLEBURY J.M. The neutron electric dipole moment experiment in preparation at the ILL. (Invited talk & Contributed paper)

VILLINGEN, Switzerland: ICANS XIII - 13th International Conference on Advanced Neutron Sources - 1995/10/11-14

LEADBETTER A.J. The continuing role of neutron scattering in physics and chemistry.

SCHMIDT W., TIETZE-JAENSCH H., GEICK R., WILL G., GRIMM H. Improvements in resolution calculation for triple axis and time-of-flight. (Contributed paper)

ZUOZ, Switzerland: Third Summer School on Neutron Scattering - "Magnetic Neutron Scattering" - 1995/08/20-26

DORNER B. Instruments for neutron scattering. (Contributed paper)

HENGGELER W., CHATTOPADHYAY T., ROESSLI B., FURRER A. Dispersion of the $\Gamma_6^{(1)}$-$\Gamma_6^{(2)}$ Nd crystal field excitation in Nd_2CuO_4.

Publications – ILL-Reports 1995

This list groups publications received during 1995 resulting from the research at the ILL.
ILL-Reports are listed first. They are followed by the list of publications in journals, conference proceedings, books with ILL authors and co-authors and by publications related to experimental work performed by visiting scientists at the ILL but without ILL co-authors.

ILL-Reports

(Code number 1 to 21)

95ED01
EDER K.
Installation of a side deviator at the VCN exit port on PF2
ILL-Report

95KN02
KNELLER G.R., KEINER V., KNELLER M., SCHILLER M.
nMOLDYN: a program package for a neutron scattering oriented analysis of molecular dynamics simulations
ILL-Report

95TH03
THOMAS M.
Etude thermique de la source de "PIAFE"
(ILL/DPT/BI/SCM)
ILL-Report

95MA04
MALBERT P.
IN4C - Spectromètre mobile - Note de calcul
(DPT-BI-95-152PhM)
ILL-Report

95FA05
FAUST H.R.
Calculation of mass and charge distribution in nuclear fission using a Boltzmann formulation (DS/NFP)
ILL-Report

95FA06
FAUST H.R., BAO Z.
Calculation of relative LCP yields in ternary fission by a Boltzmann distribution (DS/NFP)
ILL-Report

95GL07
GLÜCK F., LAST J.
Measurable parameters of neutron decay
ILL-Report

95GU08
GUERRA B.
Four électrique à focalisation de flux "MIRROR FURNACE" 2 KW - 240 V - monophasé équipé d'un thermocouple Pt Rh 30%/Pt Rh 6% pour régulation de température apparente. Notice de mise en service, d'installation, d'exploitation et d'entretien (DTP/BD)
ILL-Report

95GU09
GUERRA B.
Installation de déformation en phase plastique de lames de monocristal Ge (four presse). Notice de mise en service, d'installation, d'exploitation et d'entretien (DTP/BD)
ILL-Report

95TH10
THOMAS M.
Architecture et transferts thermiques de la source de PIAFE (ILL-DPT-BP)
ILL-Report

95TA11
TASSET F., BÜTTNER H.G.
New Tools for Neutron Instrumentation (Abstracts)
Les Houches, June 6-9, 1995
ILL-Report

95SH12
SHOTTON M., LANGAN P.
mcFibre. Software for analysing data collected on D19 in fibre precession geometry
ILL-Report

95RA13
RANDL O.G.
The long-wavelength method or calculating elastic constants from Born-von Karman force constants
ILL-Report

95FI14
FILLAUX F., BÜTTNER H.G., KEARLEY G.J., MEINNEL J.
Quantum Tunnelling of Atoms and Molecules in Solids (Abstracts). Seyssins, France, October 4-7, 1995
ILL-Report

95TH16
THOMAS M.
PIAFE: réaction exothermique due à une entrée d'air - Etude des transferts thermiques
ILL-Report

95BO17
BOISSIEU M. DE, BOUDARD M., LETOUBLON A., FRICK B., JANOT C.
Time relaxation of longwavelength phason fluctuations in the AlPdMn icosahedral phase: high resolution inelastic tests on IN16
ILL-Report

95AN18
ANTONIADIS A., BERRUYER J., CARMONA R., FILHOL A.
ABCstat User's manual and tutorial for the Macintosh
ILL-Report

95TH19
THOMAS M.
Détecteur D22 - Comportement élastique de la membrane précontrainte de séparation des gaz $^3He/^4He$ (DPT)
ILL-Report

95PR20
PRAGER M., HEIDEMANN A.
Rotational tunnelling and neutron spectroscopy: a compilation
ILL-Report

95BO21
BOUVET A., FILHOL A.
PkFit v2.1 for Macintosh user's manual. A tool to fit data from triple axis spectrometers
ILL-Report

Papers published in Scientific Periodicals, Books and Conference Proceedings:

1. With ILL authors and co-authors (Code number from 101 to 350)

95RU101
RUBIN J., PALACIOS E., BARTOLOME J., RODRIGUEZ-CARVAJAL J.
A single-crystal neutron diffraction study of NH_4MnF_3
Journal of Physics Condensed Matter **7**, 563-575 (1995)

95BA102
BAUMBACH G.T., GAILHANOU M.
X-ray diffraction from epitaxial multilayered surface gratings
Journal of Physics D: Applied Physics **28**, 2321-2327 (1995)

95BR103
BRADEN M., SCHNELLE W., SCHWARZ W., PYKA N., HEGER G., FISK Z., GAMAYUNOV K., TANAKA I., KOJIMA H.
Elastic and inelastic neutron scattering studies on the tetragonal to orthorhombic phase transition of $La_{2-x}Sr_xCuO_{4\pm\delta}$
Zeitschrift für Physik B **94**, 29-37 (1994)

95RE104
REICHARDT W., PINTSCHOVIUS L., PYKA N., SCHWEISS P., ERB A., BOURGES P., COLLIN G., ROSSAT-MIGNOD J.M., HENRY I.Y., IVANOV A.S., MITROFANOV N.L., RUMIANTSEV A.Y.
Anharmonicity and electron-phonon coupling in cuprate superconductors studied by inelastic neutron scattering
Journal of Superconductivity **7**, 399-407 (1994)

95KE105
KEARLEY G.J.
A review of the analysis of molecular vibrations using INS
Nuclear Instruments and Methods in Physics Research A **354**, 53-58 (1995)

95TO106
TOMKINSON J., KEARLEY G.J.
The calculation of phonon wing intensities: anisotropic effects
Nuclear Instruments and Methods in Physics Research A **354**, 169-170 (1995)

95NO107
NÖLDEKE C., PRESS W., ASMUSSEN B., DAMAY P., LECLERCQ F., FOUKANI M., DIANOUX A.J.
Ammonia rotations in ytterbiumhexaammine
Journal of Chemical Physics **102**, 1122-1128 (1995)

95SP108
SPILKER H.M., BLOMEYER C.
Advantage of collocating research facilities. The administrator's point of view
Physica B **204**, 8-13 (1995)

95KO109
KOCSIS M., FARAGO B., CERETTI M.
New type of radial collimator for strain measurements by neutron diffraction
Review of Scientific Instruments **66**, 32-37 (1995)

95VU110
VUILLARD L., BRAUN-BRETON C., RABILLOUD T.
Non-detergent sulphobetaines: a new class of mild solubilization agents for protein purification
Biochemical Journal **305**, 337-343 (1995)

95ZO111
ZORN R., ARBE A., COLMENERO J., FRICK B., RICHTER D., BUCHENAU U.
Neutron scattering study of the picosecond dynamics of polybutadiene and polyisoprene
Physical Review E **52**, 781-795 (1995)

95TI112
TIMMINS P.A.
Low resolution neutron crystallography of large biological macromolecular assemblies
Neutron News **6**, 13-18 (1995)

95BO113
BOUDARD M., BOURGEAT-LAMI E., BOISSIEU M. DE, JANOT C., DURAND-CHARRE M., KLEIN H., AUDIER M., HENNION B.
Production and characterization of single quasicrystals of the Al-Pd-Mn icosahedral phase
Philosophical Magazine Letters **71**, 11-19 (1995)

95BO114
BONNETE F., ZACCAI G.
Small angle neutron scattering, total cross-sections and mass density measurements of concentrated NaCl and KCl solutions in H_2O or D_2O
Biophysical Chemistry **53**, 69-76 (1994)

95IB115
IBEL K., MAY R., SANDBERG M., MASCHER E., GREIJER E., LUNDAHL P.
Structure of dodecyl sulfate-protein complexes at subsaturating concentrations of free detergent
Biophysical Chemistry **53**, 77-84 (1994)

95BR116
BRAMWELL S.T., BUCKLEY A.M., ROSSEINSKY M.J., DAY P.
Neutron powder diffraction study of the crystal structure of the layered mineral krautite, $DMnAsO_4.D_2O$
New Journal of Chemistry **18**, 1209-1214 (1994)

95SC117
SCHOBER H., RENKER B., GOMPF F., ADELMANN P.
Inelastic neutron scattering results on Rb_3C_{60} and Rb_6C_{60}
Physica C **235-240**, 2487-2488 (1994)

95GO118
GOGOLIN A.O.
Selected topics in the theory of 1D quantum wires
Annales de Physique **19**, 411-432 (1994)

95MI119
MINEEV V.P.
Superconductivity in UPt_3
Annales de Physique **19**, 367-384 (1994)

95KA120
KATS E.I.
Line liquid crystals
Annales de Physique **19**, 447-458 (1994)

95CH121
CHABRE Y., PANNETIER J.
Structural and electrochemical properties of the proton /γ-MnO_2 system
Progress in Solid State Chemistry **23**, 1-130 (1995)

95RO122
ROSOV N., LYNN J.W., KÄSTNER J., WASSERMANN E.F., CHATTOPADHYAY T., BACH H.
Polarization analysis of the magnetic excitations in $Fe_{72}Pt_{28}$ alloys
Journal of Magnetism and Magnetic Materials **140-144**, 235-236 (1995)

95SU123
SUMARLIN I.W., LYNN J.W., CHATTOPADHYAY T., BARILO S.N., ZHIGUNOV D.I., PENG J.L.
Magnetic structure and spin dynamics of the Pr and Cu in Pr_2CuO_4
Physical Review B **51**, 5824-5839 (1995)

95GO124
GOMPF F., RENKER B., SCHOBER H., ERNST D.
Comparison of the phonon density of states of superconducting $LiTi_{1.92}Al_{.08}O_4$ (T_c=10.5 K) with that of non-superconducting $LiTi_{1.97}Cr_{.03}O_4$
Physica C **235-240**, 1197-1198 (1994)

95RE125
RENKER B., SCHOBER H., ADELMANN P., GOMPF F.
Inelastic neutron scattering study of new mercury based superconductors
Physica C **235-240**, 1199-1200 (1994)

95ST126
STROTHMANN H., SCHAERPF O.
Determination of Bloch wall thickness in Fe (4 at% Si) single crystals by means of neutron refraction close to the Curie point
Journal of Magnetism and Magnetic Materials **140-144**, 1897-1898 (1995)

95KE127
KESSLER M., DEPORTES J., OULADDIAF B., SAYETAT F.
Magnetic properties of $Sc_xTi_{1-x}Fe_2$
Journal of Magnetism and Magnetic Materials **140-144**, 1795-1796 (1995)

95CH128
CHATTOPADHYAY T., BRÜCKEL T., HOHLWEIN D., SONNTAG R.
Magnetic diffuse scattering from the frustrated antiferromagnet MnS_2
Journal of Magnetism and Magnetic Materials **140-144**, 1759-1760 (1995)

95MU129
MUTKA H., PAYEN C., MOLINIE P.
Finite segments in quasi-1D Heisenberg antiferromagnets: comparison of the isostructural systems $AgVP_2S_6$ (S=1) and $AgCrP_2S_6$ (S=3/2)
Journal of Magnetism and Magnetic Materials **140-144**, 1677-1678 (1995)

95PO130
POUGET S., ALBA M., NOGUES M.
Influence of disorder on the static critical behavior in the frustrated ferromagnetic system $CdCr_{2(1-x)}In_{2x}S_4$
Journal of Magnetism and Magnetic Materials **140-144**, 1531-1532 (1995)

95LO131
LOEWENHAUPT M., FABI P., SOSNOWSKA I., FRICK B., ECCLESTON R.S.
Temperature dependence of the magnetic excitation spectrum of $Dy_2Fe_{14}B$
Journal of Magnetism and Magnetic Materials **140-144**, 1053-1054 (1995)

95OU132
OULADDIAF B., BALLOU R., DEPORTES J., LELIEVRE-BERNA E.
Magnetic frustration and instability in $Dy_{1-x}La_xMn_2$
Journal of Magnetism and Magnetic Materials **140-144**, 811-812 (1995)

95BA133
BARES P.A., GEBHARD F.
Asymptotic Bethe-Ansatz results for a Hubbard chain with 1/sinh-hopping
Europhysics Letters **29**, 573-578 (1995)

95CH134
CHATTOPADHYAY T., SIEMENSMEYER K.
Hyperfine induced nuclear polarization in Nd_2CuO_4
Europhysics Letters **29**, 579-584 (1995)

95GA135
GARCIA-MUNOZ J.L., OBRADORS X., RODRIGUEZ-CARVAJAL J.
Magnetic behavior of $R_2Cu_2O_5$ cuprates studied by neutron diffraction
Physical Review B **51**, 6594-6601 (1995)

95RA136
RAINFORD B.D., ADROJA D.T., SEVERING A., GOREMYCHKIN E.A., THOMPSON J.D., FISK Z.
Inelastic neutron scattering study of $U_3Pt_3Sb_4$
Physica B **206-207**, 464-466 (1995)

95MU137
MURANI A.P., PIERRE J.
Low temperature paramagnetic scattering from $YbInAu_2$ and $YbAl_3$
Physica B **206-207**, 329-331 (1995)

95PE138
PEBAY-PEYROULA E., DUFOURC E.J., SZABO A.G.
Location of diphenyl-hexatriene and trimethylammonium-diphenyl-hexatriene in dipalmitoylphosphatidylcholine bilayers by neutron diffraction
Biophysical Chemistry **53**, 45-56 (1994)

95BA139
BARES P.A., GEBHARD F.
Critical behaviour of a one-dimensional Hubbard model with 1/sinh hopping
Journal of Physics Condensed Matter **7**, 2285-2291 (1995)

95RI140
RITTER C., CYWINSKI R., KILCOYNE S.H.
The nature of the Mn moment in Laves phase compounds: evolution of the magnetic order in $Ho_{1-x}Y_xMn_2$
Zeitschrift für Naturforschung A **50**, 191-198 (1995)

95HE141
HENNION B., HENNION M., MIREBEAU I., ALBA M.
Spin-wave anomalies in reentrant spin glasses of $Au_{1-x}Fe_x$ alloys
Physical Review B **51**, 8204-8210 (1995)

95PA142
PACI B., CACIUFFO R., AMORETTI G., MOZE O., BUSCHOW K.H.J., MURANI A.P.
Neutron scattering determination of the crystal field parameters in $ErCu_4Al_8$ and $ErFe_4Al_8$ intermetallics
Solid State Communications **94**, 489-493 (1995)

95BL143
BLANCO J.A., RODRIGUEZ FERNANDEZ J., GOMEZ-SAL J.C., RODRIGUEZ-CARVAJAL J., GIGNOUX D.
Magnetic properties and magnetic structures of $Ho_{1-x}Y_xNi$ compounds
Journal of Physics Condensed Matter **7**, 2843-2853 (1995)

95FR144
FRICK B., RICHTER D.
The microscopic basis of the glass transition in polymers from neutron scattering studies
Science **267**, 1939-1945 (1995)

95BA145
BATESON R.D., BRAMWELL S.T.
Enhanced magnetic x-ray diffraction from a nearly perfect crystal of iron
Journal of Physics Condensed Matter **7**, L175-L180 (1995)

95RI146
RIEGER J., DIPPEL O., HÄDICKE E., LEY G., LINDNER P.
Crystals made of close packed polymeric spheres. A small angle neutron scattering study
In "Colloidal Polymer Particles", GOODWIN J.W. et al. Eds. (Academic Press, 1995) pp. 29-48

95DO147
DORNER B.
Introduction to neutron scattering
In "Neutron Scattering from Hydrogen in Materials. Proceedings of the Second Summer School on Neutron Scattering", Zuoz, Switzerland, 1994-08-14 / 20, FURRER A. Ed. (World Scientific, 1994) pp. 1-18

95PA148
PANNETIER J.
Proton insertion in electrodes studied by neutron powder diffraction
In "Neutron Scattering from Hydrogen in Materials. Proceedings of the Second Summer School on Neutron Scattering", Zuoz, Switzerland, 1994-08-14 / 20, FURRER A. Ed. (World Scientific, 1994) pp. 128-141

95AN149
ANDERSON I.S.
The dynamics of hydrogen in metals studied by inelastic neutron scattering
In "Neutron Scattering from Hydrogen in Materials. Proceedings of the Second Summer School on Neutron Scattering", Zuoz, Switzerland, 1994-08-14 / 20, FURRER A. Ed. (World Scientific, 1994) pp. 142-167

95FI150
FITCH A.N., COCKCROFT J.K.
The structure of solid tribromofluoromethane $CFBr_3$ by powder neutron diffraction
Zeitschrift für Kristallographie **202**, 243-250 (1992)

95LU151
LUKAS P., VRANA M., MIKULA P., KULDA J.
Instrumentation for strain measurements using cylindrically bent perfect crystals
Proceedings SPIE **1738**, 438-446 (1992)

95KA152
KAMBA S., PETZELT J., ZELEZNY V., SMUTNY F., DVORAK V., HLINKA J., QUILICHINI M., VOLKOV A.A., GORSHUNOV B.P., KOZLOV G.V., CURRAT R., LEGRAND J.F.
Dynamical studies of fully deuterated BCCD
Ferroelectrics **159**, 97-102 (1994)

95RO153
RODRIGUEZ-CARVAJAL J.
Neutron powder diffraction for the characterization of structural defects in crystalline solids
In "Defects and Disorder in Crystalline and Amorphous Solids. NATO ASI Series C. Vol 418", CATLOW C.R.A. Ed. (Kluwer Academic Publishers, 1994) pp. 137-156

95HE154
HERNANDEZ-VELASCO J., SAEZ-PUCHE R., RODRIGUEZ-CARVAJAL J., GARCIA-MATRES E., MARTINEZ J.L.
Magnetic properties of novel R_2BaCoO_5 oxides (R=Pr, Nd, Ho)
Journal of Alloys and Compounds **207-208**, 257-262 (1994)

95FA155
FABRIZIO M., GOGOLIN A.O., SCHEIDL S.
Impurity scattering in quantum wires with Coulomb interaction
Journal of Low-Temperature Physics **99**, 583-585 (1995)

95BA156
BARES P.A., GEBHARD F.
Asymptotic Bethe-Ansatz results for a Hubbard chain with 1/sinh-hopping
Journal of Low-Temperature Physics **99**, 565-570 (1995)

95MA157
MAY C., KLIMANEK P., MAGERL A.
Plastic bending of thin beryllium blades for neutron monochromators
Nuclear Instruments and Methods in Physics Research A **357**, 511-518 (1995)

95CA158
CARRA P., FABRIZIO M., THOLE B.T.
High resolution x-ray resonant Raman scattering
Physical Review Letters **74**, 3700-3703 (1995)

95MI159
MILAS M., RINAUDO M., DUPLESSIX R., BORSALI R., LINDNER P.
Small angle neutron scattering from polyelectrolyte solutions: from disordered to ordered xanthan chain conformation
Macromolecules **28**, 3119-3124 (1995)

95CO160
COHEN ADDAD J.P., GUILLERMO A., LARTIGUE C.
NMR approach to the dynamic screening effect in highly entangled polymers: polyethylene oxide
Physical Review Letters **74**, 3820-3823 (1995)

95HO161
HOLY V., BAUMBACH G.T., BESSIERE M.
Interface roughness in surface-sensitive x-ray methods
Journal of Physics D: Applied Physics **28**, A220-A226 (1995)

95GR162
GRAF U., GÖNNENWEIN F., GELTENBORT P.G., SCHRECKENBACH K.
Parity nonconservation and Brosa modes in nuclear fission
Zeitschrift für Physik A **351**, 281-288 (1995)

95VU163
VUILLARD L., MARRET N., RABILLOUD T.
Enhancing protein solubilization with nondetergent sulfobetaines
Electrophoresis **16**, 295-297 (1995)

95JA164
JANOT C.
Quasicrystals
In "Neutron and Synchrotron Radiation for Condensed Matter Studies - Volume II - Applications to Solid State Physics and Chemistry - HERCULES", BARUCHEL J. et al. Eds. (Les Editions de Physique/Springer Verlag, 1994) pp. 197-209

95BO165
BOYSEN H., FREY F., LERCH M., VOGT T.
A neutron powder investigation of the high-temperature phase transition in $NiTiO_3$
Zeitschrift für Kristallographie **210**, 328-337 (1995)

95FA166
FABRIZIO M., GOGOLIN A.O., NOZIERES P.
Crossover from non-Fermi-liquid to Fermi-liquid behavior in the two channel Kondo model with channel anisotropy
Physical Review Letters **74**, 4503-4506 (1995)

95TA167
TASSET F., RESSOUCHE E.
Optimum transmission for a ^{3}He neutron polarizer
Nuclear Instruments and Methods in Physics Research A **359**, 537-541 (1995)

95UD168
UDOVIC T.J., HUANG Q., RUSH J.J., SCHEFER J., ANDERSON I.S.
Neutron-powder-diffraction study of the long-range order in the octahedral sublattice of $LaD_{2.25}$
Physical Review B **51**, 12116-12126 (1995)

95SH169
SHAPIRO L., FANNON A.M., KWONG P.D., THOMPSON A., LEHMANN M.S., GRÜBEL G., LEGRAND J.F., ALS-NIELSEN J., COLMAN D.R., HENDRICKSON W.A.
Structural basis of cell-cell adhesion by cadherins
Nature **374**, 327-337 (1995)

95VE170
VERKHOVSKAYA K.A., FRIDKIN V.M., BUNE A.V., TATIKOLOV A.S., LEGRAND J.F.
The fluorescence of a dye sensitized ferroelectric polymer in an external electric field
Journal of Applied Physics **75**, 663-665 (1994)

95LE171
LEGRAND J.F.
Le PVDF et les copolymères dérivés: des polymères ferroélectriques
In «Initiation à la Chimie et à la Physico-Chimie Macromoléculaire, vol. 9: Introduction aux Propriétés Electriques des Polymères et Applications" (Groupe Français des Polymères, 1995) pp. 255-271

95FR172
FRICK B., BUCHENAU U., RICHTER D.
Boson peak and fast relaxation process near the glass transition in polystyrene
Colloid and Polymer Science **273**, 413-420 (1995)

95WE173
QUE W.,WALKER M.B.
Generalized Frenkel-Kontorova model for structural modulations in bismuth high-T_c superconductors and related compounds
Physical Review B **46**, 14772-14778 (1992)

95KA174
KASSNER K., VALANCE A., MISBAH C., TEMKIN D.E.
New broken-parity state and a transition to anomalous lamellae in eutectic growth
Physical Review E **48**, 1091-1105 (1993)

95KU175
KUROWSKI P., MISBAH C., TCHOURKINE S.
Gravitational instability of a fictitious front during mixing of miscible fluids
Europhysics Letters **29**, 309-314 (1995)

95PE176
PEDERSEN J.S., EGELHAAF S.U., SCHURTENBERGER P.
Formation of polymerlike mixed micelles and vesicles in lecithin-bile salt solutions: a small angle neutron scattering study
Journal of Physical Chemistry **99**, 1299-1305 (1995)

95PI177
PIMPINELLI A., ELKINANI I., KARMA A., MISBAH C., VILLAIN J.
Step motions on high-temperature vicinal surfaces
Journal of Physics Condensed Matter **6**, 2661-2680 (1994)

95TO178
TORRELLES X., BORDAS S., CLAVAGUERA N., CLAVAGUERA-MORA M.T.
Structural relaxation in Ge_xSe_{1-x} glasses
In "Spanish Scientific Research using Neutron Scattering Techniques 1986-1991", GOMEZ SAL J.C. et al. Eds. (Servicio de Publicaciones de la Universidad de Cantabria, 1991) pp. 151-155

95FI179
FIONI G., FAUST H.R.
Review of nuclear charge distribution from (n_{th}, f) experiments at the Lohengrin spectrometer
In "Second International Conference on Dynamical Aspects of Nuclear Fission", Dubna, RUSSIA, 1994, KRISTIAK J. et al. Eds.
Report JINR E7-94-19 pp. 147-159

95KU180
KULDA J., STRAUCH D., ISHII Y.
Refinement of phonon eigenvector phases from intensities of neutron inelastic scattering in Si
In "Proceedings of the Fifth International Symposium on Advanced Nuclear Energy Research. Neutrons as Microscopic Probes"
Report JAERI-M-PP 93-228 Vol.2 pp. 532-539

95PA181
PARLINSKI K., CURRAT R., VETTIER C., ALEKSANDROVA I.P., ECKOLD G.
Neutron diffraction study on rubidium zinc bromide under pressure
Phase Transitions **43**, 183-186 (1993)

95BA182
BARANDIARAN J.M., BLANCO J.A., ESPESO J.I., FERNANDEZ BARQUIN L., GOMEZ SAL J.C., PLAZAOLA F., RODRIGUEZ FERNANDEZ J., SANDONIS J.J.
Neutron scattering studies in some rare-earth compounds
In "Spanish Scientific Research using Neutron Scattering Techniques 1986-1991", GOMEZ SAL J.C. et al. Eds. (Servicio de Publicaciones de la Universidad de Cantabria, 1991) pp. 77-84

95OH183
OHLER M., BARUCHEL J., GALEZ P.
An x-ray diffraction topographic study of highly oriented pyrolytic graphite
Journal of Physics D: Applied Physics **28**, A78-A83 (1995)

95GA184
GABAS M., PALACIO F., RODRIGUEZ-CARVAJAL J., VISSER D.
Magnetic structures of the three-dimensional Heisenberg antiferromagnets $K_2FeCl_5.D_2O$ and $Rb_2FeCl_5.D_2O$
Journal of Physics Condensed Matter **7**, 4725-4738 (1995)

95PO185
POUGET S., ALBA M.
Spin arrangements in $CdCr_{2(1-x)}In_{2x}S_4$-type insulating re-entrant compounds
Journal of Physics Condensed Matter **7**, 4739-4749 (1995)

95BE186
BENMORE C.J., OLIVER B.J., SUCK J.B., ROBINSON R.A., EGELSTAFF P.A.
A neutron Brillouin scattering study of $Mg_{70}Zn_{30}$
Journal of Physics Condensed Matter **7**, 4775-4785 (1995)

95BO187
BOISSIEU M. DE, BOUDARD M., HENNION B., BELLISSENT R., KYCIA S., GOLDMAN A.I., JANOT C., AUDIER M.
Diffuse scattering and phason elasticity in the AlPdMn icosahedral phase
Physical Review Letters **75**, 89-92 (1995)

95GR188
GRIMMER H., BÖNI P., ELSENHANS O., FRIEDLI H.P., LEIFER K., BUFFAT P., ANDERSON I.S.
Growth and structural characterization of Ni/Ti supermirrors for neutrons
In «Physics of X-Ray Multilayer Structures. Summaries of Papers", Optical Society of America Ed. (Optical Society of America, 1994) pp. 87-90

95BR189
BRAMWELL S.T., HOLDSWORTH P.C.W., HUTCHINGS M.T.
Static and dynamic magnetic properties of Rb_2CrCl_4: ideal 2D-*XY* behaviour in a layered magnet
Journal of the Physical Society of Japan **64**, 3066-3071 (1995)

95MI190
MISBAH C., PIERRE-LOUIS O., PIMPINELLI A.
Advacancy-induced step bunching on vicinal surfaces
Physical Review B **51**, 17283-17286 (1995)

95BO191
BOUDARD M., BOISSIEU M. DE, GOLDMAN A.I., HENNION B., BELLISSENT R., QUILICHINI M., CURRAT R., JANOT C.
Dynamics of the AlPdMn icosahedral phase
Physica Scripta **T57**, 84-87 (1995)

95AN192
ANDONOV P., CHIEUX P., KIMURA S.
Local order in the $LiNbO_3$ melt: comparison with the crystalline phases
Physica Scripta **T57**, 36-44 (1995)

95BA193
BAROCCHI F., CHIEUX P., FONTANA R., MAGLI R.
An extended experimental neutron diffraction study on gaseous and liquid Kr
Physica Scripta **T57**, 27-32 (1995)

95DU194
DUPORT C., NOZIERES P., VILLAIN J.
New instability in molecular beam epitaxy
Physical Review Letters **74**, 134-137 (1995)

95RO195
ROLLEY E., BALIBAR S., GUTHMANN C., NOZIERES P.
Adsorption of ^{3}He on ^{4}He crystal surfaces
Physica B **210**, 397-402 (1995)

95AL196
ALEKSEEV P.A., LAZUKOV V.N., ORLOV V.G., SADIKOV I.P., NIZHANKOVSKII V.I., SUCK J.B., SCHMIDT H.
Magnetic properties of amorphous $PrNi_5$
Journal of Magnetism and Magnetic Materials **140-144**, 861-862 (1995)

95PA197
PALMERI J., LEIBLER S.
Fluctuating chains with internal degrees of freedom
In "Dynamical Phenomena at Interfaces, Surfaces and Membranes", BEYSENS D. et al. Eds. (Nova Science Publishers, 1993) pp. 323-330

95FA198
FABRIZIO M., GOGOLIN A.O., NOZIERES P.
Anderson-Yuval approach to the multichannel Kondo problem
Physical Review B **51**, 16088-16097 (1995)

95BA199
BAUMBACH G.T., TIXIER S., PIETSCH U., HOLY V.
Grazing-incidence diffraction from multilayers
Physical Review B **51**, 16848-16859 (1995)

95KI200
KIM H.J., MAGERL A., FISCHER J.E., VAKNIN D., HEITJANS P., SCHIRMER A.
Li diffusion in stage 2 Li-graphite intercalation compounds studied with quasielastic neutron scattering
In "Chemical Physics of Intercalation II", BERNIER P. et al. Eds. (Plenum Press, 1993) pp. 355-359

95RO201
ROSSBERG A., PIECHOTKA M., MAGERL A., KALDIS E.
Mapping of the structural perfection of vapor grown α-HgI_2 crystals by means of γ-ray rocking curves
Journal of Applied Physics **75**, 3371-3376 (1994)

95LI202
LI X.L., FORD G.W., O'CONNELL R.F.
Dissipative effects on the mean square displacement of an oscillator
Physica A **193**, 575-586 (1993)

95TE203
DE TERESA J.M., IBARRA M.R., RITTER C., MARQUINA C., ARNOLD Z., DEL MORAL A.
Magnetic behaviour and magnetostriction of $Tb_xY_{1-x}Mn_2$ intermetallics
Journal of Physics Condensed Matter **7**, 5643-5655 (1995)

95PA204
PASYUK V.V., MCGRATH O.F.K., LAUTER H.J., PETRENKO A.V., LIENARD A., GIVORD D.
Ground state moment reduction in an ultra-thin W(110)/Fe(110)/W(110) film
Journal of Magnetism and Magnetic Materials **148**, 38-39 (1995)

95MA205
MAY R.P.
Small-angle neutron scattering of biological macromolecular complexes consisting of proteins and nucleic acids
In "Modern aspects of small-angle scattering. NATO ASI Serie C Vol. 451", BRUMBERGER H. Ed. (Kluwer Academic Publishers, 1995) pp. 355-370

95RA206
RANDL O.G., VOGL G., PETRY W., HENNION B., SEPIOL B., NEMBACH K.
Lattice dynamics and related diffusion properties of intermetallics: I. Fe_3Si
Journal of Physics Condensed Matter **7**, 5983-5999 (1995)

95RO207
ROBAUT F., MILKULIK P., CHERIEF N., MCGRATH O.F.K., GIVORD D., BAUMBACH G.T., VEUILLEN J.Y.
Epitaxial growth and characterization of Y_2Co_{17}(0001) thin films deposited on W(110)
Journal of Applied Physics **78**, 997-1003 (1995)

95FA208
FABRIZIO M., GOGOLIN A.O.
Interacting one-dimensional electron gas with open boundaries
Physical Review B **51**, 17827-17841 (1995)

95SC209
SCHEIDL S.
Mobility in a one-dimensional disorder potential
Zeitschrift für Physik B **97**, 345-352 (1995)

95FA210
FÅK B., GUCKELSBERGER K., SCHERM R., STUNAULT A.
Spin fluctuations and zero-sound in normal liquid ^{3}He studied by neutron scattering
Journal of Low-Temperature Physics **97**, 445-487 (1994)

95VI211
VISSER D., COLDWELL T.R., MCINTYRE G.J., GRAF H.A., WEISS L., ZEISKE T., PLUMER M.L.
Magnetic ordering in the stacked triangular antiferromagnet $CsMnBr_3$ in the presence of an electric field
Ferroelectrics **162**, 147-152 (1994)

95ME212
MESOT J., MEDARDE M., ROSENKRANZ S., FISCHER P., LACORRE P., GOBRECHT K.
Neutron diffraction study of the metal insulator transition in $PrNiO_3$
High Pressure Research **14**, 35-40 (1995)

95ST213
STEPANOV S.A., PIETSCH U., BAUMBACH G.T.
A matrix approach to grazing-incidence x-ray diffraction in multilayers
Zeitschrift für Physik B **96**, 341-347 (1995)

95MA214
MAGERL A., LISS K.D., HASTINGS J.B., SIDDONS D.P., NEUMANN H.B., POULSEN H.F., RÜTT U., SCHNEIDER J.R., MADAR R.
The local perfection of massive gradient crystals studied by high-energy x-ray diffraction
Europhysics Letters **31**, 329-334 (1995)

95BO215
BOISSIEU M. DE, STEPHENS P., BOUDARD M., JANOT C., CHAPMAN D.L., AUDIER M.
Evidence for random phason disorder in the perfect icosahedral phase of AlPdMn
In "Proceedings of the International Conference on Aperiodic Crystals - Aperiodic '94", CHAPUIS G. et al. Eds. (World Scientific, 1995) pp. 535-540

95JA216
JANOT C., BOISSIEU M. DE, BOUDARD M.
Structure determination of the icosahedral quasicrystals: state of the art and prospect
In "Proceedings of the International Conference on Aperiodic Crystals - Aperiodic '94", CHAPUIS G. et al. Eds. (World Scientific, 1995) pp. 491-504

95SU217
SUORTTI P., BATESON R.D., LIENERT U., BRAMWELL S.T., HONKIMÄKI V.
Energy-dispersive diffraction with synchrotron radiation as a probe of the source and magnetic form factors
Journal of Physics and Chemistry of Solids **10**, 1415-1423 (1995)

95CL218
CLEMENTS B.E., KROTSCHECK E., SAARELA M.
Dynamics of ^{3}He impurities in ^{4}He films - Rapid communication
Journal of Low-Temperature Physics **100**, 175-184 (1995)

95RA219
RAU S., ENSS C., HUNKLINGER S., NEU P., WÜRGER A.
Acoustic properties of oxide glasses at low temperatures
Physical Review B **52**, 7179-7194 (1995)

95CH220
CHAPLOT S.L., REICHARDT W., PINTSCHOVIUS L., PYKA N.
Common interatomic potential model for the lattice dynamics of several cuprates
Physical Review B **52**, 7230-7242 (1995)

95CA221
CARRA P., FABRIZIO M.
X-ray resonant inelastic scattering
In "Core Level Spectroscopies for Magnetic Phenomena. Theory and Experiment. NATO ASI Serie B Vol. 345", BAGUS P.S. et al. Eds. (Plenum Press, 1995) pp. 203-212

95BR222
BROWN P.J., FORSYTH J.B.
Antiferromagnetism in Mn_5Si_3: the magnetic structure of AF_2 phase at 70K
Journal of Physics Condensed Matter **7**, 7619-7628 (1995)

95RA223
RADAELLI P.G., MAREZIO M., THOLENCE J.L., BRION S. DE, SANTORO A., HUANG Q., CAPPONI J.J., CHAILLOUT C., KREKELS T., VAN TENDELOO G.
Crystal structure of the double-Hg-layer copper oxide superconductor $(Hg, Pr)_2Ba_2(Y, Ca)Cu_2O_{8-\delta}$ as a function of doping
Journal of Physics and Chemistry of Solids **56**, 1471-1478 (1995)

95TI224
TIMMINS P.A.
Structural molecular biology: recent results from neutron diffraction
Physica B **213-214**, 26-30 (1995)

95OU225
OULADDIAF B., DEPORTES J., RODRIGUEZ-CARVAJAL J.
Magnetic structures of Er_6Mn_{23} and Dy_6Mn_{23}
Physica B **213-214**, 330-332 (1995)

95KU226
KULDA J., ISHII Y., KATANO S.
Dynamical structure analysis applied to Si and Ge
Physica B **213-214**, 427-429 (1995)

95RO227
ROYER A., BASTIE P., BELLET D., STRUDEL J.L.
Temperature dependence of the lattice mismatch of the AM1 superalloy. Influence of the γ' precipitates' morphology
Philosophical Magazine A **72**, 669-689 (1995)

95BO228
BOUDARD M., BOISSIEU M. DE, KYCIA S., GOLDMAN A.I., HENNION B., BELLISSENT R., QUILICHINI M., CURRAT R., JANOT C.
Optic modes in the AlPdMn icosahedral phase
Journal of Physics Condensed Matter **7**, 7299-7308 (1995)

95GA229
GARCIA-MATRES E., GARCIA-MUNOZ J.L., MARTINEZ J.L., RODRIGUEZ-CARVAJAL J.
Magnetic susceptibility and field-induced transitions in R_2BaNiO_5 compounds (R=Tm, Er, Ho, Dy, Tb, Gd, Sm, Nd, Pr)
Journal of Magnetism and Magnetic Materials **149**, 363-372 (1995)

95UD230
UDOVIC T.J., RUSH J.J., ANDERSON I.S.
Characterization of the vibrational dynamics in the octahedral sublattices of $LaD_{2.25}$ and $LaH_{2.25}$
Journal of Physics Condensed Matter **7**, 7005-7014 (1995)

95SC231
SCHOBER H., MAY T., DORNER B., STRAUCH D., STEIGENBERGER U., MORRII Y.
Lattice dynamics of Cr_2O_3
Zeitschrift für Physik B **98**, 197-205 (1995)

95DI232
DIANOUX A.J., KNELLER G.R., SAUVAJOL J.L., SMITH J.C.
Dynamics of pure and sodium-doped polyacetylene
In "AIP Conference proceedings 330", BERNARDI F. et al. Eds. (American Institute of Physics, 1995) pp. 362-366

95LI233
LINDNER P.
Polymers in solution - Flow techniques
In "Modern Aspects of Small-Angle Scattering. NATO ASI Serie C Vol. 451", BRUMBERGER H. Ed. (Kluwer Academic Publishers, 1995) pp. 409-432

95FO234
FOURCADE B., TREMBLAY A.M.S.
Field theory and second renormalization group for multifractals in percolation
Physical Review E **51**, 4095-4104 (1995)

95YA235
YAMAMURO O., MATSUO T., SUGA H., DAVID W.I.F., IBBERSON R.M., LEADBETTER A.J.
A neutron-diffraction study of tetrahydrofuran and acetone clathrate hydrates
Physica B **213-214**, 405-407 (1995)

95YA236
YAMAMURO O., MATSUO T., SUGA H., DAVID W.I.F., IBBERSON R.M., LEADBETTER A.J.
Critical phenomenon in a molecular-ionic crystal $(CD_3ND_3)_2[SnCl_6]$
Physica B **213-214**, 414-416 (1995)

95AZ237
AZUAH R.T., STIRLING W.G., GUCKELSBERGER K., SCHERM R., GLYDE H.R., BENNINGTON S.M., TAYLOR A.D.
Neutron scattering from liquid ^{3}He at large momentum transfers
Physica B **213-214**, 454-458 (1995)

95BA238
BAROCCHI F., BELLISSENT-FUNEL M.C., CHIEUX P., MAGLI R.
The structure of dilute gaseous N_2 and the intermolecular interaction
Physica B **213-214**, 468-470 (1995)

95BA239
BAROCCHI F., CHIEUX P., FONTANA R., MAGLI R.
The structure of fluid Kr: an experimental study near the liquid-gas transition
Physica B **213-214**, 471-473 (1995)

95FR240
FRICK B., WILLIAMS J., TREVINO S.F., ERWIN R.
Vibrational behaviour of amorphous and crystalline ethylbenzene
Physica B **213-214**, 506-509 (1995)

95CO241
COLOMBAN P., FILLAUX F., TOMKINSON J., KEARLEY G.J.
Proton dynamics in β-alumina
Physica B **213-214**, 634-636 (1995)

95FI242
FILLAUX F., CARLILE C.J., COOK J.C., HEIDEMANN A., KEARLEY G.J., IKEDA S., INABA A.
Relaxation kinetics of the sine-Gordon breather mode in 4-methyl-pyridine crystal at low temperature
Physica B **213-214**, 646-648 (1995)

95KE243
KEARLEY G.J., BÜTTNER H.G., FILLAUX F., IKEDA S., INABA A.
Coupling between phonons and quantum rotors
Physica B **213-214**, 664-666 (1995)

95BU244
BÜTTNER H.G., KEARLEY G.J., FILLAUX F., HOWARD C.J., KAHN R.
The rotational potential of NH_3 groups in metal hexammines
Physica B **213-214**, 669-671 (1995)

95MO245
MONKENBUSCH M., SCHNEIDERS D., RICHTER D., FARAGO B., FETTERS L.J., HUANG J.S.
Dynamics of polymer brushes - What can neutron spin-echo spectroscopy contribute ?
Physica B **213-214**, 707-711 (1995)

95FA246
FARAGO B., MONKENBUSCH M., GOECKING K.D., RICHTER D., HUANG J.S.
Dynamics of microemulsion as seen by neutron spin echo
Physica B **213-214**, 712-717 (1995)

95FI247
FILLAUX F., BARON M.H., LEYGUE N., TOMKINSON J., KEARLEY G.J.
Proton transfer dynamics in polyglycine
Physica B **213-214**, 766-768 (1995)

95LA248
LANGAN P., FORSYTH V.T., MAHENDRASINGAM A., GIESEN U., DAUVERGNE M.T., MASON S.A., WILSON C.C., FULLER W.
Neutron fibre diffraction studies of DNA hydration
Physica B **213-214**, 783-785 (1995)

95TA249
TAKEDA T., KOMURA S., SETO H., NAGAI M., KOBAYASHI H., YOKOI E., EBISAWA T., TASAKI S., ZEYEN C.M.E., ITO Y., TAKAHASHI S., YOSHIZAWA H.
Neutron spin-echo spectrometer at JRR-3M
Physica B **213-214**, 863-865 (1995)

95MA250
MAGERL A.
Towards still better monochromators
Physica B **213-214**, 917-921 (1995)

95MI251
MIKULA P., LUKAS P., SAROUN J., WAGNER V., KULDA J.
Cylindrically bent perfect crystals as neutron monochromators
Physica B **213-214**, 922-925 (1995)

95KU252
KULDA J.
Towards ideal focusing monochromators
Physica B **213-214**, 926-928 (1995)

95TA253
TASSET F.
Towards helium-3 neutron polarizers
Physica B **213-214**, 935-938 (1995)

95CL254
CLEMENS D., BÖNI P., FRIEDLI H.P., GÖTTEL R., FERMON C., GRIMMER H., VAN SWYGENHOVEN H., ARCHER J., KLOSE F., KRIST T., MEZEI F., THOMAS P.
Polarizing $Ti_{1-u}X_u/Fe_xCo_yV_z$ supermirrors
Physica B **213-214**, 942-944 (1995)

95CI255
CIPRIANI F., CASTAGNA J.C., LEHMANN M.S., WILKINSON C.
A large image-plate detector for neutrons
Physica B **213-214**, 975-977 (1995)

95ME256
MEDARDE M., MESOT J., ROSENKRANZ S., LACORRE P., GOBRECHT K., FISCHER P.
Pressure dependence (internal and external) of the metallization process and the magnetic ordering of $PrNiO_3$: a neutron powder diffraction study
Physica B **213-214**, 1025-1027 (1995)

95CA257
CACIUFFO R., AMORETTI G., BUSCHOW K.H.J., MOZE O., MURANI A.P., PACI B.
Neutron spectroscopy studies of the crystal-field interaction in RET_4Al_8 compounds (RE=Tb, Ho or Er; T=Mn, Fe or Cu)
Journal of Physics Condensed Matter **7**, 7981-7989 (1995)

95WU258
WÜRGER A.
Collective low-energy excitations of two-level tunnelling defects in mixed crystals
Zeitschrift für Physik B **98**, 561-573 (1995)

95PE259
PEBAY-PEYROULA E., GARAVITO R.M., ROSENBUSCH J.P., ZULAUF M., TIMMINS P.A.
Detergent structure in tetragonal crystals of OmpF porin
Structure **3**, 1051-1059 (1995)

95ME260
MEDARDE M., MESOT J., LACORRE P., ROSENKRANZ S., FISCHER P., GOBRECHT K.
High-pressure neutron-diffraction study of the metallization process in $PrNiO_3$
Physical Review B **52**, 9248-9258 (1995)

95FO261
FOLOPPE N., FERRAND M., BRETON J., SMITH J.C.
Structural model of the photosynthetic reaction center of *Rhodobacter capsulatus*
Proteins: Structure, Function and Genetics **22**, 226-244 (1995)

95BE262
BERRET J.F., ROUX D.C., PORTE G., LINDNER P.
Tumbling behaviour of nematic worm-like micelles under shear flow
Europhysics Letters **32**, 137-142 (1995)

95TA263
TAKEDA T., KOMURA S., SETO H., NAGAI M., KOBAYASHI H., YOKOI E., ZEYEN C.M.E., EBISAWA T., TASAKI S., ITO Y., TAKAHASHI S., YOSHIZAWA H.
A neutron spin echo spectrometer with two optimal field shape coils for neutron spin precession
Nuclear Instruments and Methods in Physics Research A **364**, 186-192 (1995)

95SC264
SCHRECKENBACH K., LIAUD P., KOSSAKOWSKI R., NASTOLL H., BUSSIERE A., GUILLAUD J.P.
A new measurement of the beta emission asymmetry in the free decay of polarized neutrons
Physics Letters B **349**, 427-432 (1995)

95BO265
BOUCHERLE J.X., BURLET P., GIVORD F., ISIKAWA Y., NEUDERT R., SCHMITT D., SCHOBER H.
Magnetic behaviour of the compound $CeNi_2Al_5$: double- κ magnetic structure
Journal of Physics Condensed Matter **7**, 8337-8350 (1995)

95RO266
ROSSBERG A., PIECHOTKA M., MAGERL A., STEICHELE E., WETZEL G., KALDIS E.
A study of structural defects in vapour grown α-HgI_2 single crystals by γ-ray diffraction
Journal of Crystal Growth **146**, 112-118 (1995)

95AS267
ASMUSSEN B., BALSZUNAT D., PRAGER M., PRESS W., CARLILE C.J., BÜTTNER H.G.
Rotational excitations of a symmetric top in cubic orientational potentials: CH_3D matrix-isolated in argon and krypton
Journal of Chemical Physics **103**, 6880-6890 (1995)

95LO268
LORENZEN M., FERRERO C., DIAT O., RIEKEL C., MAYERHOFER U.
A program package for preprocessing of two-dimensional detector data
Journal of Applied Crystallography **28**, 630-632 (1995)

95PA269
PAPANEK P., FISCHER J.E., SAUVAJOL J.L., DIANOUX A.J., MCNEILLIS P.M., MATHIS C., FRANCOIS B.
Inelastic neutron scattering by pristine and doped phases of polyacetylene
In "Neutron Scattering in Materials Science II. Materials Research Society Proceedings 376", NEUMANN D.A. et al. Eds. (MRS, 1995) pp. 763-767

95CH270
CHATTOPADHYAY T., SCOTT C.A., VON LÖHNEYSEN H.
μSR investigation of the magnetic ordering in $CeCu_{5.5}Au_{0.5}$
Journal of Magnetism and Magnetic Materials **140-144**, 1259-1260 (1995)

95SC271
SCHEIDL S., FEINBERG D.
Dynamics of strongly pinned vortices
Physica C **235-240**, 3109-3110 (1994)

95BO272
BÖRNER H.G., PENDLEBURY J.M.
New developments for the nuclear and fundamental physics facilities at the high flux reactor of the ILL Grenoble
In "Proceedings of the 8th International Symposium on Capture Gamma-Ray Spectroscopy and Related Phenomena", KERN J. Ed. (World Scientific, 1994) pp. 823-837

95GE273
GELTENBORT P.G.
Recent results with microstrip gas chambers
Nuclear Instruments and Methods in Physics Research A **353**, 168 (1994)

95JU274
JUNGCLAUS A.
The gamma-ray induced Doppler (GRID) broadening method: a status report
In "Proceedings of the 8th International Symposium on Capture Gamma-Ray Spectroscopy and Related Phenomena", KERN J. Ed. (World Scientific, 1994) pp. 888-899

95FA275
FABRIZIO M., GOGOLIN A.O.
Toulouse limit for the overscreened four-channel Kondo problem
Physical Review B **50**, 17732-17735 (1994)

95PI276
PILLIERE H., SOUBEYROUX J.L., BEGUIN F.
Influence of critical temperature on the phases formed during the intercalation of methane in CsC_{24}
Phase Transitions **46**, 27-39 (1993)

95NA277
NAVARRO A., LOPEZ GONZALEZ J.J., KEARLEY G.J., TOMKINSON J., PARKER S.F., SIVIA D.S.
Vibrational analysis of the inelastic neutron scattering spectrum of s-triazine and trichloro-s-triazine
Chemical Physics **200**, 395-403 (1995)

95SO278
SOKOLOV A.P., BUCHENAU U., STEFFEN W., FRICK B., WISCHNEWSKI A.
Comparison of Raman- and neutron-scattering data for glass-forming systems
Physical Review B **52**, R9815-R9818 (1995) - Rapid Communications

95NO279
NOZIERES P.
Some comments on Bose-Einstein condensation
In "Bose-Einstein Condensation", GRIFFIN A. et al. Eds. (Cambridge University Press, 1995) pp. 15-30

95PO280
POUGET S., ALBA M., NOGUES M.
Static critical properties of disordered ferromagnets studied by superconducting quantum interference device magnetometry and small-angle neutron-scattering techniques
Journal of Applied Physics **75**, 5826-5828 (1994)

95RE281
REJMANKOVA P., BARUCHEL J., KULDA J., CALEMCZUK R., SALCE B.
An x-ray topographic investigation of α-$LiIO_3$ under a direct or alternating current electric field
Journal of Physics D: Applied Physics **28**, A69-A73 (1995)

95GI282
GISLER T., RÜGER H., EGELHAAF S.U., TSCHUMI J., SCHURTENBERGER P., RICKA J.
Mode-selective dynamic light scattering: theory versus experimental realization
Applied Optics **34**, 3546-3553 (1995)

95EG283
EGELHAAF S.U., PEDERSEN J.S., SCHURTENBERGER P.
Shape transformations in biological mixed surfactant systems: from spheres to cylinders to vesicles
Progress in Colloid and Polymer Science **98**, 224-227 (1995)

95HE284
HENGGELER W., CUNTZE G., MESOT J., KLAUDA M., SAEMANN-ISCHENKO G., FURRER A.
Neutron spectroscopic evidence for cluster formation and percolative superconductivity in $Pr_{2-x}Ce_xCuO_{4-\delta}$ ($0 \leq x \leq 0.2$)
Europhysics Letters **29**, 233-238 (1995)

95MU285
MUTKA H., PAYEN C., MOLINIE P., ECCLESTON R.S.
Quasi-1D antiferromagnets with S=1 and S=3/2: the isostructural compounds $AgVP_2S_6$ and $AgCrP_2S_6$
Physica B **213-214**, 170-172 (1995)

95NO286
NOWOTNY P., RÜHL M., NOWOTNY V., MAY R.P., BURKHARDT N., VOSS H., NIERHAUS K.H.
Direct shape determination of ribosomal proteins in solution and within the ribosome by means of neutron scattering
Biophysical Chemistry **53**, 115-122 (1994)

95KU287
KURONEN A., KEINONEN J., BÖRNER H.G., JOLIE J.
Slowing down of 3-eV ions in Eu compounds
Physical Review B **52**, 12640-12643 (1995)

95SO288
SOUAILLE M., SMITH J.C., DIANOUX A.J., GUILLAUME F.
Dynamics of n-nonadecane chains in urea inclusion compounds as seen by incoherent quasielastic neutron scattering and computer simulations
In "Observation, Prediction and Simulation of Phase Transitions in Complex Fluids", BAUS M. et al. Eds. (Kluwer Academic Publishers, 1995) pp. 609-624

95SA289
SAUVAJOL J.L., PAPANEK P., FISCHER J.E., DIANOUX A.J., MAO G., WINOKUR M.J., KARASZ F.E.
Densités d'états des modes de vibration de basse fréquence du poly-(p-phénylène vinylène). Une étude par diffusion inélastique des neutrons
Journal de Chimie Physique **92**, 955-958 (1995)

95FI290
FIONI G. and the PIAFE Collaboration
The PIAFE project and its possible implications in r-process studies
In "Nuclei in the Cosmos III - AIP Conference Proceedings 327", BUSSO M. et al. Eds. (American Institute of Physics, 1995) pp. 153-156

95VU291
VUILLARD L., MADERN D., FRANZETTI B., RABILLOUD T.
Halophilic protein stabilization by the mild solubilizing agents nondetergent sulfobetaines
Analytical Biochemistry **230**, 290-294 (1995)

95MA292
MARTINEZ J.L., FERNANDEZ-DIAZ M.T., CHEN Q., PRIETO C., DE ANDRES A., SAEZ-PUCHE R., ROMERO J.
Bulk magnetic characterization of $RCaCrO_4$ (R=Y, Pr, Sm) oxides
Journal of Magnetism and Magnetic Materials **140-144**, 1179-1180 (1995)

95MA293
MARTINEZ J.L., ALONSO J., FERNANDEZ-DIAZ M.T., RODRIGUEZ-CARVAJAL J., VALLET-REGI M., GONZALEZ-CALBET J.M.
Magnetic properties of $Nd_{2-x}Sr_xNiO_{4+\delta}$ oxides
Physica C **235-240**, 1561-1562 (1994)

95FI294
FIONI G., FAUST H.R., FRIEDRICHS T., GROSS M., KOESTER U.
Thermal neutron induced fission of ^{245}Cm
In "Proceedings of the Seminar on Fission 'Pont d'Oye III'", Habay-La-Neuve, BELGIUM, 1995-05-09 / 11, WAGEMANS C. Ed. (Institute for Reference Materials and Measurements, 1995), Report EUR 16295 EN pp. 42-47

95KA295
KASSNER K.
Morphological instability: dendrites, seaweed, and fractals
In "Science and Technology of Crystal Growth", VAN DER EERDEN J. et al. Eds. (Kluwer Academic Publishers, 1995) pp. 193

95GR296
GRISHKIN Y.L., MARTEMYANOV A.N., AKINDINOV A., CHUMAKOV M.M., POGORELKO O.I., POSDNYAKOV S., SHISKOV P.N., USHAKOV V.I., KROSS B., MAJEWSKI S., WEISENBERGER A., WOJCIK R., BAKER O.K., HWANG I., LYONS D., NICULESCU G., NICULESCU I.M., SMITH G., GELTENBORT P.G., OED A.
Preliminary study of a new type of gas microstrip chamber on a sapphire substrate
Nuclear Instruments and Methods in Physics Research A **354**, 309-317 (1995)

95BI297
BISHAI M.R., GERNDT E.K.E., SHIPSEY I.P.J., WANG P.N., BAGULYA A.V., GRISHIN V.M., NEGODAEV M.A., GELTENBORT P.G.
Performance of microstrip gas chambers passivated by thin semiconducting glass and plastic films
Nuclear Instruments and Methods in Physics Research A **365**, 54-58 (1995)

95PO298
POLICARPO A.P.L., CHEPEL V., LOPES M.I., PESKOV V., GELTENBORT P.G., FERREIRA MARQUES R., ARAUJO H., FRAGA F., ALVES M.A., FONTE P., LIMA E.P., FRAGA M.M., SALETE LEITE M., SILANDER K., ONOFRE A., PINHAO J.M.
Observation of electron multiplication in liquid xenon with a microstrip plate. Letter to the editor
Nuclear Instruments and Methods in Physics Research A **365**, 568-571 (1995)

95CH299
CHIBANE Y., LAMOREAUX S.K., PENDLEBURY J.M., SMITH K.F.
Minimum variance of frequency estimations for a sinusoidal signal with low noise
Measurement Science and Technology **6**, 1671-1678 (1995)

95PE300
PENDLEBURY J.M.
Opportunities from the restart of the ILL reactor and fundamental physics with neutrons at the ILL
In "Proceedings of a One Day Meeting: the Outlook for Fundamental Physics with Super-Low Energy Neutrons", Kyoto, Japan, 1995-01-03, MASIAKE A. Ed. (University of Kyoto, 1995) pp. 1-15

95RE301
REEHUIS M., RODRIGUEZ-CARVAJAL J., DANEBROCK M.E., JEITSCHKO W.
Magnetic properties of the carbides Y_2ReC_2, Tb_2ReC_2, Er_2ReC_2 and Lu_2ReC_2
Journal of Magnetism and Magnetic Materials **151**, 273-282 (1995)

95RI302
RITTER C., MARQUINA C., IBARRA M.R.
On the stability of the magnetic ground state of Mn in $Dy_{1-x}Y_xMn_2$ intermetallics
Journal of Magnetism and Magnetic Materials **151**, 59-66 (1995)

95HW303
HWANG H.Y., CHEONG S.W., RADAELLI P.G., MAREZIO M., BATLOGG B.
Lattice effects on the magnetoresistance in doped $LaMnO_3$
Physical Review Letters **75**, 914-917 (1995)

95RA304
RADAELLI P.G., COX D.E., MAREZIO M., CHEONG S.W., SCHIFFER P.E., RAMIREZ A.P.
Structural anomalies associated with the magnetic and metal-insulator transitions in $La_{1-x}Ca_xMnO_3$ (x=0.25 and 0.50)
In "XXV Congresso Nazionale della Societa' Italiana di Cristallografia", Giardini Naxos, Italy, 1995 pp. 21

95RA305
RADAELLI P.G., COX D.E., MAREZIO M., CHEONG S.W., SCHIFFER P.E., RAMIREZ A.P.
Simultaneous structural, magnetic and electronic transitions in $La_{1-x}Ca_xMnO_3$ with x = 0.25 and 0.50
Physical Review Letters **75**, 4488-4491 (1995)

95MA306
MAREZIO M., ALEXANDRE E.T., BORDET P., CAPPONI J.J., CHAILLOUT C., KOPNIN E.M., LOUREIRO S.M., RADAELLI P.G., VAN TENDELOO G.
Cation and anion disorder in $HgBa_2Ca_{n-1}Cu_nO_{2n+2+\delta}$
Journal of Superconductivity **8**, 507 (1995)

95AZ307
AZUAH R.T., STIRLING W.G., GUCKELSBERGER K., SCHERM R., BENNINGTON S.M., YATES M.L., TAYLOR A.D.
Neutron scattering from liquid ^3He at intermediate to large wavevectors
Journal of Low-Temperature Physics **101**, 951-969 (1995)

95LE308
LEGRAND J.F., DAUDIN B., BELLET-AMALRIC E.
Dipolar glass behaviour of a ferroelectric polymer after irradiation
Nuclear Instruments and Methods in Physics Research B **105**, 225-228 (1995)

95LO309
LOEFFEN P.W., PETTIFER R.F., FILLAUX F., KEARLEY G.J.
Vibrational force field of solid imidazole from inelastic neutron scattering
Journal of Chemical Physics **103**, 8444-8455 (1995)

95NO310
NOZIERES P.
Some comments on the Mott transition in metal and semiconductors
Annales de Physique **20**, C2/417-C2/423 (1995)

95VI311
VILLAIN J., DUPORT C., NOZIERES P.
Elastic instabilities in crystal growth
In "25 Years of Non-Equilibrium Statistical Mechanics - Proceeding of the 13th Sitges Conference", Lecture Notes in Physics 445. - BREY J. Ed. (Springer Velag, 1995) pp. 177-188

95VO312
VOIT J.
One-dimensional Fermi liquids
Reports on Progress in Physics **58**, 977-1116 (1995)

95BO313
BONNETE F., MADERN D., ZACCAI G.
Stability against denaturation mechanisms in halophilic malate dehydrogenase "adapt" to solvent conditions
Journal of Molecular Biology **244**, 436-447 (1994)

95SA314
SAMATEY F.A., ZACCAI G., ENGELMAN D.M., ETCHEBEST C., POPOT J.L.
Rotational orientation of transmembrane α-helices in bacteriorhodopsin. A neutron diffraction study
Journal of Molecular Biology **236**, 1093-1104 (1994)

95SE315
SERDYUK I.N., PAVLOV M.Y., RUBLEVSKAYA I.N., ZACCAI G., LEBERMAN R.
The triple isotopic substitution method in small angle neutron scattering. Application to the study of the ternary complex EF-Tu.GTP.aminoacyl-tRNA
Biophysical Chemistry **53**, 123-130 (1994)

95ZA316
ZACCAI G.
Neutrons in biology - Complementarity with x-rays
In "Synchrotron Radiation in the Biosciences", CHANCE B. et al. Eds. (Clarendon Press, 1994) pp. 215-220

95MA317
MADERN D., PFISTER C., ZACCAI G.
Mutation at a single acidic amino acid enhances the halophilic behaviour of malate dehydrogenase from *Haloarcula marismortui* in physiological salts
European Journal of Biochemistry **230**, 1088-1095 (1995)

95FI318
FILLAUX F., FONTAINE J.P., BARON M.H., LEYGUE N., KEARLEY G.J., TOMKINSON J.
Inelastic neutron-scattering study of the proton transfer dynamics in polyglycine I at 20K
Biophysical Chemistry **53**, 155-168 (1994)

95CE319
CENDRIN F., JOUVE H.M., GAILLARD J., THIBAULT P., ZACCAI G.
Purification and properties of a halophilic catalase-peroxidase from *Haloarcula marismortui*
Biochimica et Biophysica Acta **1209**, 1-9 (1994)

95EB320
EBEL C., ALTEKAR W., LANGOWSKI J., URBANKE C., FOREST E., ZACCAI G.
Solution structure of glyceraldehyde-3-phosphate dehydrogenase from *Haloarcula vallismortis*
Biophysical Chemistry **54**, 219-227 (1995)

95RI321
RICHARD S., BONNETE F., DYM O., ZACCAI G.
The MPD-NaCl-H_2O system for the crystallization of halophilic proteins
In "Archaea, a Laboratory manual" (Cold Spring Harbor Laboratory Press, 1995) pp. 149-154

95SC322
SCHRECKENBACH K.
Fundamental physics with slow neutrons
Acta Physica Hungarica **75**, 25-30 (1994)

95SC323
SCHRECKENBACH K.
Free neutron decay
In "Astro - Particle Physics. Proceedings of a Workshop", Ringberg Castle, GERMANY, 1995-03-06 / 10, WEISS A. et al. Eds. (Technische Universität Muenchen - Ludwig-Maximilian-Universität , MPI, 1995) pp. 52-58
Report SFB 375

95SU324
SUCK J.B.
Mode softening in rapidly quenched supersaturated $Al_{96.5}Si_{3.5}$
Materials Science Forum **179-181**, 735-740 (1995)

95SC325
SCHAUB T.M., BÜRGLER D.E., SUCK J.B., AUDIER M., GÜNTHERODT H.J.
Investigation of the quasicrystalline structure of icosahedral $Al_{68}Pd_{23}Mn_9$ by STM and LEED
In "Proceedings of the 5th International Conference on Quasicrystals", JANOT C. et al. Eds. (World Scientific, 1995) pp. 132-138

95JO326
JOENSEN K.D., GORENSTEIN P., HØGHØJ P., CHRISTENSEN F.E.
X-ray supermirrors: novel multilayer structures for broad band hard x-ray applications
In "Physics of X-Ray Multilayer Structures. Summaries of Papers. Postconference Edition" (Optical Society of America, 1994) pp. 159-162

95HO327
HØGHØJ P., ZIEGLER E., SUSINI J., FREUND A.K., JOENSEN K.D., GORENSTEIN P.
Broad-band focusing of hard x-rays using a supermirror
In "Physics of X-Ray Multilayer Structures. Summaries of Papers. Postconference Edition" (Optical Society of America, 1994) pp. 142-145

95JO328
JOENSEN K.D., GORENSTEIN P., HØGHØJ P., STEENSTRUP S.
Deconvolution of energy-dispersive reflection data using the maximum entropy principle
In "Physics of X-Ray Multilayer Structures. Summaries of Papers. Postconference Edition" (Optical Society of America, 1994) pp. 95-98

95CH329
CHRISTENSEN F.E., HORNSTRUP A., JOENSEN K.D., ABDALI S., HØGHØJ P., JOENSEN K.D., SLANE P., ROMAINE S.E.
High resolution x-ray scatter studies from single films and multilayers
In "Physics of X-Ray Multilayer Structures. Summaries of Papers. Postconference Edition" (Optical Society of America, 1994) pp. 68-69

95LU330
LÜKEN E., ZIEGLER E., HØGHØJ P., FREUND A.K., GERDAU E., FONTAINE A.
In Situ growth studies of nanometer thin-film multilayers using grazing x-ray reflectivity and ellipsometry
In "Physics of X-Ray Multilayer Structures. Summaries of Papers. Postconference Edition" (Optical Society of America, 1994) pp. 12-15

95BO331
BOUE F., LINDNER P.
Small angle neutron scattering from sheared semidilute solutions: butterfly effect
In "Flow-Induced Structure in Polymers. ACS Symposium Series 597", NAKATANI A. et al. Eds. (American Chemical Society, 1995) pp. 48-60

95ST332
STÖLKEN S., BARTSCH E., SILLESCU H., LINDNER P.
Spherical polymer micronetwork colloids - A small-angle scattering study
Progress in Colloid and Polymer Science **98**, 155-159 (1995)

95RO333
ROUX D.C., BERRET J.F., PORTE G., PEUVREL-DISDIER E., LINDNER P.
Shear-induced orientations and textures of nematic wormlike micelles
Macromolecules **28**, 1681-1687 (1995)

95GO334
GODFRIN H., LAUTER H.J.
Experimental properties of ^{3}He adsorbed on graphite
In "Progress in Low Temperature Physics. Vol. XIV",
HALPERIN W.P. Ed. (Elsevier, 1995) pp. 213-320

95BY335
BYCHKOV Y.A., MANIV T., VAGNER I.D.
Charged skyrmions in a system of 2D spin excitons
in the Hartree-Fock approximation
JETP Letters **62**, 727-732 (1995)

95GY336
GYGAX F.N., AMATO A., FEYERHERM R.,
SCHENCK A., ANDERSON I.S., UDOVIC T.J., SOLT G.
Dynamics of μ^+ in Sc and ScH_x
Journal of Alloys and Compounds **231**, 248-251 (1995)

95BA337
BARTSCH E., FUJARA F., LEGRAND J.F., PETRY W.,
SILLESCU H., WUTTKE J.
Dynamics in viscous orthoterphenyl: results from coherent
neutron scattering
Physical Review E **52**, 738-745 (1995)

95HU338
HUANG Q., UDOVIC T.J., RUSH J.J., SCHEFER J.,
ANDERSON I.S.
Characterization of the structure of $TbD_{2.25}$ at 70 K
by neutron powder diffraction
Journal of Alloys and Compounds **231**, 95-98 (1995)

95UD339
UDOVIC T.J., RUSH J.J., ANDERSON I.S.
Neutron spectroscopic comparison of β-phase rare
earth hydrides
Journal of Alloys and Compounds **231**, 138-143 (1995)

95AS340
ASIF M., HAVILL R.L., TITMAN J.M., FRICK B.
Neutron quasi-elastic scattering measurements of hydrogen
diffusion in the $NiZr_2$ intermetallic phase
Journal of Alloys and Compounds **231**, 243-247 (1995)

95LA341
LATROCHE M., PERCHERON-GUEGAN A., CHABRE Y.,
BOUET J., PANNETIER J., RESSOUCHE E.
Intrinsic behaviour analysis of substituted $LaNi_5$-type
electrodes by means of in-situ neutron diffraction
Journal of Alloys and Compounds **231**, 537-545 (1995)

95FA342
FAUST H.R., FIONI G., PINSTON J.A.
The project of an exotic beam facility in Grenoble (PIAFE)
Revista Mexicana de Fisica **41**, 168-177 (1995)

95OE343
OED A.
Properties of micro-strip gas chambers (MSGC)
and recent developments
Nuclear Instruments and Methods in Physics Research A
367, 34-40 (1995)

95GA344
GABRYS B., SCHAERPF O., PEIFFER D.G.
Model ionomers studied with spin-polarized neutrons using
spin-polarization analysis
In "Ionomers. Characterization, Theory, and Applications",
SCHLICK S. Ed. (CRC Press, 1996) pp. 57-81

95FI345
FISCHER C., KRÜGER J.K., BOHN K-P., VOGT U.,
SCHREIBER J., JIMENEZ R., WOLF D., LEGRAND J.F.,
ALNOT P., SERVET B.
About the microstructure of PCVD prepared crystal mats
of statistical oligo-vinylidene-fluoride-trifluoroethylene
in relation to other fluorinated polymers
Journal of Polymer Science B **33**, 237-246 (1995)

95LE346
LEIFER K., BUFFAT P., BÖNI P., CLEMENS D.,
FRIEDLI H.P., GRIMMER H., ANDERSON I.S.
Structural and chemical characterization of nickel titanium
multilayers with T.E.M.
In "Materials Research Society Symposium Proceedings
382" (Materials Research Society, 1995) pp. 173-178

95WA347
WAGEMANS C., GELTENBORT P.G.
Fission of isomers: a simulation of stellar conditions
In "Proceedings of the Seminar on Fission 'Pont d'Oye III'",
Habay-La-Neuve, BELGIUM, 1995-05-09 / 11,
WAGEMANS C. Ed. (Institute for Reference Materials and
Measurements, 1995), Report EUR 16295 EN pp. 19-21

95ST348
STUMPF P., DENSCHLAG H.O., FAUST H.R.
Odd-even effects in the fission of the odd compound nucleus
^{243}Am (Z=95)
In "Proceedings of the Seminar on Fission 'Pont d'Oye III'",
Habay-La-Neuve, BELGIUM, 1995-05-09 / 11,
WAGEMANS C. Ed. (Institute for Reference Materials and
Measurements, 1995), Report EUR 16295 EN pp. 196-203

95FA349
FAUST H.R.
Calculation of mass and charge distribution in nuclear
fission using a Boltzmann formulation
In "Proceedings of the Seminar on Fission 'Pont d'Oye III'",
Habay-La-Neuve, BELGIUM, 1995-05-09 / 11,
WAGEMANS C. Ed. (Institute for Reference Materials and
Measurements, 1995), Report EUR 16295 EN pp. 211-219

95FA350
FAUST H.R., BAO Z.
Calculation of relative LCP yields in ternary fission by a Boltzmann distribution
In "Proceedings of the Seminar on Fission 'Pont d'Oye III'", Habay-La-Neuve, BELGIUM, 1995-05-09 / 11, WAGEMANS C. Ed. (Institute for Reference Materials and Measurements, 1995), Report EUR 16295 EN pp. 220-231

2. Without ILL authors and co-authors (Code number from 1001 to 1016)

95AB1001
ABOLFATHI E., MODLEN G.F., WEBSTER P.J., MILLS G.
The effect of residual stresses on the properties of hoist chains
In "Residual Stresses", HANK V. et al. Ed. (DGM Informationsgesellschaft mbh, 1993) pp. 457-466

95RU1002
RUDKINS N.T., MODLEN G.F., WEBSTER P.J.
Residual stresses in cold extrusion and cold drawing: a finite element and neutron diffraction study
Journal of Materials Processing Technology **45**, 287-292 (1994)

95MO1003
MODLEN G.F., WEBSTER P.J., WANG X., MILLS G.
An investigation of residual stresses in cold-extruded and in cold-drawn rods using neutron diffraction
In "Sheet Metal" SHIRVANI B. et al. Eds. (IOP, 1992) pp. 171-179

95DO1004
DOSCH H.
The EVA diffractometer: merging Snell's law into Bragg's law
Neutron News **6**, 19-25 (1995)

95KA1005
KARTINI E., MEZEI F.
Quasielastic neutron scattering in liquid $Ca_{0.4}K_{0.6}(NO_3)_{1.4}$
Physica B **213-214**, 486-489 (1995)

95FR1006
FRÖBA G., KALUS J.
Structure of the isotropic, nematic, and lamellar phase of a solution of tetramethylammonium perfluorononanoate in D_2O
Journal of Physical Chemistry **99**, 14450-14467 (1995)

95HO1007
HORSEWILL A.J., IKRAM A., TOMSAH I.B.I.
Hydrogen bond dynamics in tetrafluoroterephthalic acid studied by NMR and INS
Molecular Physics **84**, 1257-1272 (1995)

95KR1008
KRÜGER E., NISTLER W., WEIRAUCH W.
Determination of the fine-structure constant by measuring the quotient of the Planck constant and the neutron mass
IEEE Transactions on Instrumentation and Measurement **44**, 514-517 (1995)

95KR1009
KRÜGER E., NISTLER W., WEIRAUCH W.
Determination of the fine-structure constant by a precise measurement of h/m_n
Metrologia **32**, 117-128 (1995)

95ME1010
MEYER D.F., NEALIS A.S., BRUCKDORFER K.R., PERKINS S.J.
Characterization of the structure of polydisperse human low-density lipoprotein by neutron scattering
Biochemical Journal **310**, 407-415 (1995)

95VI1011
VISSER D., MONTEITH A.R., HARRISON A., PETITGRAND D.
Magnetic excitations and magnetic ordering in the hexagonal perovskites $AFeX_3$ under hydrostatic pressure
High Pressure Research **14**, 29-34 (1995)

95BE1012
BELLITTO C., DAY P.
Organic-intercalated halogenochromates(II): low-dimensional magnets
Journal of Materials Chemistry **2**, 265-271 (1992)

95HO1013
HORKAY F., HECHT A.M., GEISSLER E.
Thermodynamic interaction parameters in polymer solutions and gels
Journal of Polymer Science B **33**, 1641-1646 (1995)

95HO1014
HORKAY F., HECHT A.M., GEISSLER E.
Small angle neutron scattering in poly(vinyl alcohol) hydrogels
Macromolecules **27**, 1795-1798 (1994)

95MA1015
MANIGUET L., BASTIE P., BELLET D., DUPEUX M.
Non-destructive bulk detection of localized straining by γ-ray diffractometry. Application to a sheared single crystal of CMSX-2 superalloy
Physica Status Solidi (a) **148**, 389-406 (1995)

95DA1016
DAWIDOWSKI J., CHAHID A., BERMEJO F.J., ENCISO E., ALMARZA N.G.
Dynamic correlations in a dense dipolar liquid
Physical Review E **52**, 2787-2796 (1995)

Author Index

Publications and ILL reports 1995

Papers accepted for Publication

1. Neutron Instruments and Methods

ANDERSEN K.H.
Resolution function of the neutron time-of-flight spectrometer MARI.
Nuclear Instruments and Methods (95AN5100).

ANDERSON I.S., SCHAERPF O., HØGHØJ P., AGERON P.
Multilayers.
Journal of Neutron Research (Proceedings of the Workshop on "New Tools for neutron Instrumentation", Les Houches, France, June 6-9, 1995) (95AN5065).

BASTIE P., HAMELIN B.
La méthode de Laue refocalisée à haute énergie : une technique d'étude en volume des monocristaux.
Journal de Physique (Proceedings of the Colloque Rayons X et Matière, Strasbourg, France, November 6-10, 1995 (95BA5105).

BROWN P.J.
Analysing neutron scattering data with the Cambridge crystallographic subroutine library (CCSL).
Journal of Neutron Research (Proceedings of the Workshop on "New Tools for neutron Instrumentation", Les Houches, France, June 6-9, 1995) (95BR5069).

CIPRIANI F., CASTAGNA J.C., WILKINSON C., OLEINEK P., LEHMANN M.S.
Cold neutron protein crystallography using a large position-sensitive detector based on image-plate technology.
Journal of Neutron Research (95CI5058).

EGELHAAF S., SCHURTENBERGER P.
A fiber-optics based light scattering instrument for time-resolved simultaneous static and dynamic measurements.
Review of Scientific Instruments (95EG5074).

LANGAN P., DENNY R.C., MAHENDRASINGAM A., MASON S.A.
Collecting and processing neutron fibre diffraction data from a single crystal diffractometer.
Journal of Applied Crystallography (95LA5045).

LARTIGUE C., COPLEY J.R.D., MEZEI F., SPRINGER T.
Focusing of neutron beams using curved mirrors for small angle scattering.
Journal of Neutron Research (95LA5038).

MUTKA H., SACHETTI F.
The focussing monochromator of IN4C.
Journal of Neutron Research (Proceedings of the Workshop on "New Tools for neutron Instrumentation", Les Houches, France, June 6-9, 1995) (95MU5083).

RICHARD D., FERRAND M., KEARLEY G.J.
Analysis and visualisation of neutron-scattering data.
Journal of Neutron Research (Proceedings of the Workshop on "New Tools for neutron Instrumentation", Les Houches, France, June 6-9, 1995) (95RI5079).

SCHAERPF O., ANDERSON I.S.
New tools for neutron instrumentation.
Journal of Neutron Research (95SC5040).

SCHMIDT W., TIETZE-JAENSCH H., GEICK R., WILL G., GRIMM H.
Improvements in resolution calculation for triple axis and time-of-flight.
Proceedings of the Conference "ICANS-XIII" 13th Meeting of the International Collaboration on Advanced Neutron Sources, Villigen, Switzerland, October 11-14, 1995 (95SC5086).

ZEYEN C.M.E., KAKURAI K.
Spin-echo three-axis spectrometer: a reality.
Journal of Neutron Research (Proceedings of the Workshop on "New Tools for neutron Instrumentation", Les Houches, France, June 6-9, 1995) (95ZE5064).

ZEYEN C.M.E., OTAKE Y., FORTE M.
Dual polarised beam polarimeter: a highly sensitive tool for the detection of very small neutron spin rotation.
Journal of Neutron Research (Proceedings of the Workshop on "New Tools for Neutron Instrumentation", Les Houches, June 6-9, 1995) (95ZE5072).

ZEYEN C.M.E., REM P.C.
Optimal Larmor precession magnetic field shapes: application to neutron spin echo three axis spectrometry.
Measurement Science & Technology (95ZE5094).

2. Theory

CAROLI C., NOZIERES P.
Dry friction as an hysteretic elastic response.
Proceedings of the Adriatico Research Conference on "Physics of Sliding Friction" (NATO Series), Trieste, Italy, June 20-25,1995 (95NO5052).

DZYALOSHINSKII I.
Extended van-Hove singularity and related non-Fermi liquids.
Journal de Physique I (95DZ5039).

HOBBS A.K., METZENER P., KASSNER K.
Dynamical patterns in directional solidification.
Physica D (95HO5025).

3. Nuclear and Fundamental Physics

ALTEREV I.S., BORISOV Yu.V., CHIBANE Y., DREXEL W., HECKEL B.R., GREEN K., IAYDJIEV P., GELTENBORT P., HARRIS P.G., IVANOV S.N., KILVINGTON I., LAMOREAUX S.K., LOBASHEV V.M., MAY D.J., PENDLEBURY J.M., RAMSEY N.F., SMITH K.F.
The neutron electric dipole moment experiment in preparation at the ILL.
Proceedings of the XVth Moriond Workshop on "Dark Matter in Cosmology, Clocks and Tests of Fundamental Laws", Villars-sur-Ollon, Switzerland, January 21-28, 1995 (95AL5007).

JENTSCHEL M., HEINIG K.H., BOERNER H.G., JOLIE J., KESSLER E.G.
Atomic collision cascades studied with the crystal-GRID method.
Nuclear Instruments and Methods B (95JE5087).

PENDLEBURY J.M.
Fundamental physics with neutrons at the Institut Laue-Langevin.
Proceedings of "The Outlook for Fundamental Physics with Superlow Energy Neutrons", Kyoto, Japan, January 21-28, 1995 (95PE5009).

PENDLEBURY J.M.
Summary talk on precision clocks.
Proceedings of the XVth Moriond Workshop on "Dark Matter in Cosmology, Clocks and Tests of Fundamental Laws", Villars-sur-Ollon, Switzerland, January 21-28, 1995 (95PE5018).

PENDLEBURY J.M.
Fundamental physics with neutrons at the Institut Laue-Langevin.
Proceedings of European Physical Society - XV Nuclear Physics Division Conference "Low Energy Nuclear Dynamics", St. Petersburg, Russia, April 1995 (95PE5022).

4. Structural and Magnetic Excitations

DORNER B., SCHMID B., KAKURAI K., PETITGRAND D.
The phase diagram of $RbFeCl_3$ in a magnetic field perpendicular to the chain direction.
Canadian Journal of Physics (95DO5017).

HENGGELER W., CHATTOPADHYAY T., ROESSLI B., ZHIGUNOV D.I., BARILO S.N., FURRER A.
Dispersion of the $\Gamma_6^{(1)}$-$\Gamma_6^{(2)}$ Nd crystal field excitation in Nd_2CuO_4.
Zeitschrift für Physik B (95HE5076).

JANOT C., DE BOISSIEU M.
Vibrations in quasicrystals: hierarchies and localization.
Physica B (Proceedings of "Phonons 95" Conference, Sapporo, Japan, July 24-28, 1995) (95JA5029).

JANOT C.
Conductivity in quasicrystals via hierarchically variable range hopping.
Physical Review B: Condensed Matter (95JA5030).

LORENZO J.E., CURRAT R., DIANOUX A.J., MONCEAU P., LEVY F.
Phonon density of states and low temperature specific heat of quasi-one dimensional $(TaSe_4)_2I$ and $(NbSe_4)_3I$.
Physical Review B (95LO5023).

RANDL O.G., VOGL G., PETRY W.
Phonons - a diffusion motor in intermetallics ?
Physica B (95RA5077).

REQUARDT H., KALNING M., BURANDT B., PRESS W., CURRAT R.
Critical X-ray scattering at the Peierls-transition in the quasi-one-dimensional system $(TaSe_4)_2I$.
Journal of Physics: Condensed Matter (95RE5104).

SCHOBER H., RENKER B., GOMPF F.
Low-frequency excitations in Rb_3C_{60} and Rb_6C_{60}.
Physica B (95SC5092).

5. Crystallography and Magnetic Structures

5a - Crystallography

ALLANCON C., RODRIGUEZ-CARVAJAL J., FERNANDEZ-DIAZ M.T., ODIER P., BASSAT J.M., LOUP J.P., MARTINEZ J.L.
Crystal structure of the high temperature phase of oxidised $Pr_2NiO_{4+\delta}$.
Zeitschrift für Physik B (95AL5089).

BASTIE P., HAMELIN B.
La méthode de Laue refocalisée à haute énergie : une technique d'étude en volume des monocristaux.
Journal de Physique (Proceedings of the Colloque Rayons X et Matière, Strasbourg, France, November 6-10, 1995 (95BA5105).

BROWN P.J.
Analysing neutron scattering data with the Cambridge crystallographic subroutine library (CCSL).
Journal of Neutron Research (Proceedings of the Workshop on "New Tools for neutron Instrumentation", Les Houches, France, June 6-9, 1995) (95BR5069).

CHEONG S.W., HWANG H.Y., RADAELLI P.G., COX D.E., MAREZIO M., BATLOGG B., SCHIFFER P., RAMIREZ P.
Origin and control of the "colossal" magnetoresistance in doped $LaMnO_3$.
Proceedings of the Conference on "Physical Phenomena at High Magnetic Fields - II", Tallahassee, Florida, USA, May 6-9, 1995 (95CH5033).

JANOT C.
Conductivity in quasicrystals via hierarchically variable range hopping.
Physical Review B: Condensed Matter (95JA5030).

JANOT C.
Quasicrystals as self-similar packing of atomic clusters.
Proceedings of the International Symposium on the Science and Technology of Atomically Engineered Material, Ed. Khanna S., Singapore (World Scientific Publ. Co., 1995), Richmond, Virginia,USA, October 30-November 4, 1995 (95JA5066).

KHASANOVA N.R., IZUMI F., TAKAYAMA-MUROMACHI E., HEWAT A.W.
Crystal structure of the superconductor $Ca_2Sr_2Cu_3GaO_9$ prepared at high pressure.
Physica C (95KH5070).

LOUREIRO S.M., RADAELLI P.G., ANTIPOV E.V., CAPPONI J.J., SOULETIE B., BRUNNER M., MAREZIO M.
The replacement of Hg by the tetrahedral sulfate oxyanion in the Hg-1201 superconductor.
Journal of Solid State Chemistry (95LO5050).

PAASCH M., WINTERLICH M., BÖHMER R., SONNTAG R., McINTYRE G., LOIDL A.
The phase diagram of $(NH_4I)_x(KI)_{1-x}$.
Zeitschrift für Physik B (95PA5004).

PAASCH M., McINTYRE G., REEHUIS M., SONNTAG R., LOIDL A.
Neutron diffraction study of $(NH_4I)_{0.73}(KI)_{0.27}$.
Zeitschrift für Physik B (95PA5005).

RADAELLI P.G., MAREZIO M., HWANG H.Y., CHEONG S.W.
Structural phase diagram of perovskite $A_{0.7}A'_{0.3}MnO_3$ (A = La, Pr; A' = Ca, Sr, Ba): a new Imma allotype.
Journal of Solid State Chemistry (95RA5106).

SCHOBER H.
Structural phase transitions and the determinant of the dynamical matrix.
Physica B (95SC5081).

5b - Magnetism

CAIGNAERT V., SUARD E., MAIGNAN A., SIMON C., RAVEAU B.
Neutron diffraction evidence for an antiferromagnetic ordering in the CMR manganites $Pr_{0.7}Ca_{0.3-x}Sr_xMnO_3$.
Journal of Magnetism and Magnetic Materials (95CA5061).

CHEONG S.W., HWANG H.Y., RADAELLI P.G., COX D.E., MAREZIO M., BATLOGG B., SCHIFFER P., RAMIREZ P.
Origin and control of the "colossal" magnetoresistance in doped $LaMnO_3$.
Proceedings of the Conference on "Physical Phenomena at High Magnetic Fields - II", Tallahassee, Florida, USA, May 6-9, 1995 (95CH5033).

GUZIK A., PIERRE J., KACZMARSKA K., LAMBERT-ANDRON B., OULADDIAF B.
Kondo properties of the new compounds $Ce(Ag_xCu_{1-x})_{2-\delta}Sb_2$.
Journal of Magnetism and Magnetic Materials (95GU5080).

KRAEMER K., ROMSTEDT H., GUEDEL H.U., FISCHER P., MURASIK A., FERNANDEZ-DIAZ M.T.
3-D magnetic structure of ErF_3.
Journal of Solid State Inorganic Chemistry (95KR5090).

6. Structure and Dynamics of Liquids and Glasses

ALEKSEEV P.A., KCHLOPKIN M.N., LAZUKOV V.N., ORLOV V.G., SADIKOV I.P., SUCK J.B., SCHMIDT H.
Magnetic excitation spectra and thermodynamics of amorphous $PrNi_5$.
Physical Review B (95AL5049).

BERMEJO F.J., CRIADO A., DE ANDRES A., ENCISO E., SCHOBER H.
Microscopic dynamics of glycerol in its crystalline and glassy states.
Physical Review B (95BE5093).

CHAHID A., McGREEVY R.L., WICKS J., MUTKA H.
Critical narrowing of molten $^7Li_{0.62}Na_{0.38}$ alloy.
Physica B (Proceedings of the International Conference on "Quasielastic Neutron Scattering" QEN'S 95, Parma, Italy, September 7-8,1995 (95CH5084).

CHIEUX P., DUPUY-PHILON J., JAL J.F., SUCK J.B.
Temperature dependence of the collective atomic dynamics of liquid Rubidium.
Journal of Non-Crystalline Solids (95CH5107).

SUCK J.B.
Temperature dependence of the total dynamic structure factor of the metallic glass $Ni_{33}Zr_{67}$.
Journal of Non-Crystalline Solids (95SU5108).

SUCK J.B., SCHOBER H., GUENTHERODT H.
The generalised vibrational density of states and total dynamic structure factor of the metallic glass $Zr_{65}Cu_{17.5}Ni_{10}Al_{7.5}$ measured at room temperature.
Journal of Non-Crystalline Solids (95SU5109).

7. Material Science, Surfaces and Spectroscopy

BASTIE P., ROYER A., BELLET D., LAJZEROWICZ J.
Désaccord paramétrique, paramètres de maille et morphologie des précipités.
Proceedings of the Colloque National Superalloys Monocristallins, Toulouse, France, March 22-24, 1995 (95BA5101).

BASTIE P., MANIGUET L., DUPEUX M.
Non-destructive detection and localization of straining by γ-ray diffractometry in a single crystal superalloy submitted to a shear test.
Bulletin du Cercle d'Etudes des Métaux, Tome XVI, n° 11, p 15.1-15.10 (95BA5102).

BEE M., COMBET J., GUILLAUME F., MORELON N.D., FERRAND M., DJURADO D., DIANOUX A.J.
Neutron scattering studies of linear chains in an organic inclusion compound.
Physica B (Proceedings of the International Conference on "Quasielastic Neutron Scattering" QEN'S 95, Parma, Italy, September 7-8,1995) (95BE5063).

BUTTARD D., BELLET D., BAUMBACH T.
X-ray diffraction investigation of porous silicon superlattices.
Thin Solid Films (Proceedings of the EMRS 1995 Spring Meeting, Strasbourg, France, May 22-26, 1995) (95BU5078).

CRISTOFOLINI L., KONSTANTINO V., PRASSIDES K., DIANOUX A.J., KOSAKA M., HIROSAWA I., TANIGAKI K.
Molecular dynamics of C_{60} in superconducting Na_2CsC_{60}.
Physica B (Proceedings of the International Conference on "Quasielastic Neutron Scattering" QEN'S 95, Parma, Italy, September 7-8, 1995) (95CR5071).

DIANOUX A.J., SAUVAJOL J.L., KNELLER G.R., SMITH J.C.
Inelastic neutron scattering and molecular dynamics simulations of pristine and doped polyacetylene.
Proceedings of the 4th Meeting on "Disorder in Molecular Solids", Garchy, France, May 29-June 1, 1995 (95DI5015).

DIANOUX A.J.
Application of neutron scattering to investigate diffusion in porous media.
Extended abstract for the Meeting "Transport in Porous Media", organised by the Colloid and Surface Chemistry Group of the Society of Chemical Industry, London, U.K., March 30, 1995 (95DI5021).

FILLAUX F., KEARLEY G.J., CARLILE C.J.
Inelastic neutron scattering study of isotopic mixtures of lithium acetate with partially deuterated CH_2D groups and sine-Gordon dynamics.
Physica B (95FI5085).

GIRARD P., GUILLAUME F., DIANOUX A.J.
Molecular dynamics of guest molecules in the channels of urea inclusion compounds investigated by means of IQNS spectroscopy.
Physica B (Proceedings of the International Conference on "Quasielastic Neutron Scattering" QEN'S95, Parma, Italy, September 7-8, 1995) (95GI5073).

JONES M.J., GUILLAUME F., HARRIS K.D.M., DIANOUX A.J.
Molecular dynamics of tetrakis(trimethylsilyl)silane in the solid state: an incoherent quasielastic neutron scattering investigation.
Proceedings of the Royal Society (95JO5024).

KEARLEY G.J., BUETTNER H.G., FILLAUX F., LAUTIE M.F.
NH_3 free rotors in Hofmann clathrates.
Physica B (95KE5062).

MIHALKOVIC M., DUGAIN F., SUCK J.B.
Vibrational density of states of decagonal $Al_{70}Co_{15}Ni_{15}$.
Journal of Non-Crystalline Solids (95MI5110).

SKRIPOV A.V., COOK J.C., KARMONIK C., HEMPELMANN R.
Localized motion of hydrogen in C15-type TaV_2: a quasielastic neutron scattering study.
Journal of Physics: Condensed Matter (95GE5099).

8. Biology

CIPRIANI F., CASTAGNA J.C., WILKINSON C., OLEINEK P., LEHMANN M.S.
Cold neutron protein crystallography using a large position-sensitive detector based on image-plate technology.
Journal of Neutron Research (95CI5058).

GOLDBERG M.E., EXPERT-BEZANCON N., VUILLARD L., RABILLOUD T.
Non-detergent sulphobetaines: a new class of molecules that facilitate *in vitro* protein renaturation.
Protein Folding and Design (95GO5095).

LANGAN P., DENNY R.C., MAHENDRASINGAM A., MASON S.A.
Collecting and processing neutron fibre diffraction data from a single crystal diffractometer.
Journal of Applied Crystallography (95LA5045).

TIMMINS P.A., PEBAY-PEYROULA E.
Protein-detergent interactions in single crystals of membrane proteins studied by neutron crystallography.
"Neutrons in Biology", Plenum Press 1996 (Schoenborn & Knott, Eds) (95TI5034).

VUILLARD L., BAALBAKI B., LEHMANN M.S., NORAGER S., LEGRAND P., ROTH M.
Protein crystallography with non detergent sulfobetaines.
Journal of Crystal Growth (95LV5055).

9. Structure and Dynamics of Soft-Condensed Matter

DUX C., VERSMOLD H., REUS V., ZEMB T., LINDNER P.
Neutron diffraction from shear ordered colloidal dispersions.
Journal of Chemical Physics (95DU5053).

EGELHAAF S., SCHURTENBERGER P.
A fiber-optics based light scattering instrument for time-resolved simultaneous static and dynamic measurements.
Review of Scientific Instruments (95EG5074).

FRICK B.
Methyl group dynamics in poly(dimethylsiloxane).
World Scientific Publishing Co. (Proceedings of the Workshop on "Non Equilibrium Phenomena in Supercooled Fluids, Glasses and Amorphous Materials", Pisa, Italy, September 25-29, 1995) (95FR5103).

MILAS M., LINDNER P., RINAUDO M., BORSALI R.
Influence of shear rate on small angle neutron scattering pattern of polyelectrolyte solutions: the xanthan example.
Europhysics Letters (95MI5011).

RICHTERING W., SCHMIDT G., LINDNER P.
Small-angle neutron scattering from a hexagonal phase under shear.
Colloid and Polymer Science (95RI5048).

WEIGEL R., LAUGER J., RICHTERING W., LINDNER P.
Anisotropic small angle scattering from a lyotropic lamellar phase under shear.
Journal de Physique II (95WE5056).

Acknowledgement

The Scientific Secretary, Bruno Dorner, editor of this report, wishes to thank all those who have contributed.

Layout and typesetting by Idra

Cover layout and printing by Technic Color

Photography by
J.L. Baudet (ILL), S. Claisse (ILL), J. Italia (ILL).

Other publications available

- Guide to Neutron Research Facilities, Edition 1994
- General Information and Regulations, Edition 1990.

The Scientific Secretary
Institut Max von Laue - Paul Langevin
BP 156
38042 Grenoble Cedex 9
France
Telephone: 76 20 72 93 – Telefax: 76 48 39 06 – Telex: 320621

Institut Max von Laue
Paul Langevin
Grenoble - France

BP 156 - 38042 Grenoble Cedex 9 - France - Tél. 76 20 71 11 - Fax 76 48 39 06 - Télex 320 621